



## Task 425.013

# Non-PFOS/non-PFAS Photoacid Generators: Environmentally Friendly Candidates for Next Generation Lithography

*Victor M Gamez<sup>1</sup>, Ramakrishan Ayothi<sup>2</sup>, Yi Yi<sup>2</sup>, James A Field<sup>1</sup>,  
Chris K Ober<sup>2</sup>, Reyes Sierra<sup>1</sup>*

*<sup>1</sup> Department of Chemical & Environmental Engineering, University of Arizona*

*<sup>2</sup> Department of Materials Science and Engineering, Cornell University*

# Project Background and Objectives

- This project aims to develop novel PFOS-free PAGs that meet the stringent performance demands required by semiconductor manufacturing and do not pose a risk to public health or the environment.
- Work on the development of the novel non-PFOS/non-PFAS PAGS is conducted at Cornell University. Environmental studies of these new materials are in progress at the University of Arizona.
- Studies undertaken to evaluate the inhibitory potential of the new chemistries are presented here.

# **ESH Metrics and Impact**

- *Reduction in emission of ESH-problematic materials to environment: 100% removal of PFOS utilized as PAG in photolithography.*

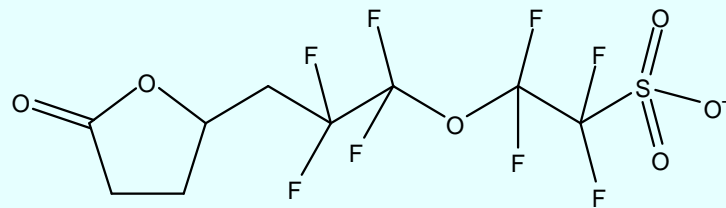
## Results and Discussion

The inhibitory potential of several non-PFOS PAGs and their counter ions, diphenyl iodonium (DPI) and triphenyl sulfonium (TPS), (Fig. 1) was evaluated using three different bioassays and a modeling software:

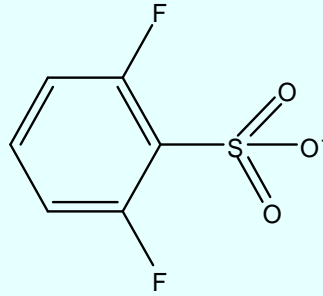
- the Mitochondrial Toxicity Test (MTT);
- Microtox<sup>®</sup>,
- the methanogenic inhibition test,
- and the EPA PBT profiler.

PFBS and PFOS, were included in the bioassay as a reference.

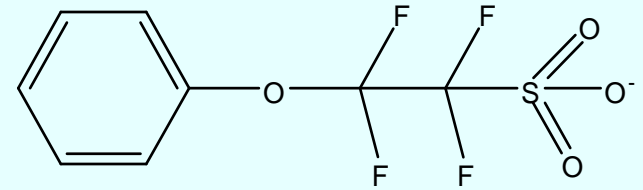




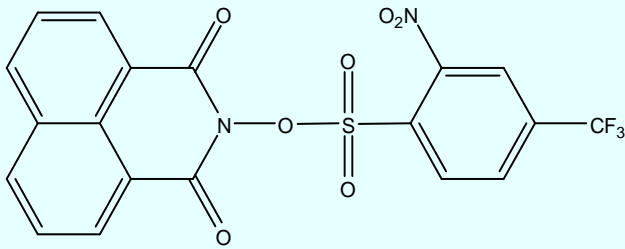
**Lactone**



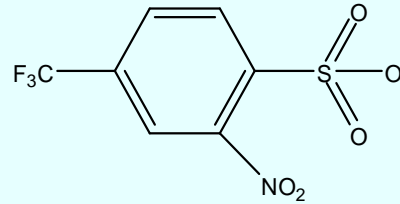
**SF Sulfonate 1**



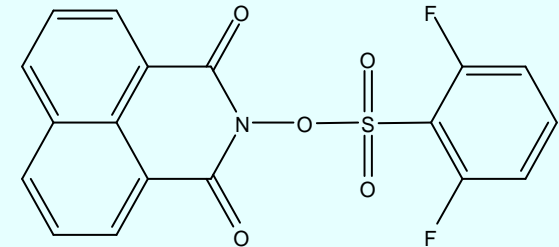
**PF Sulfonate 1**



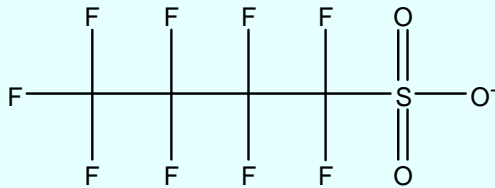
**SF 3**



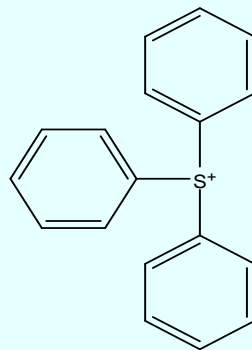
**SF Sulfonate 2**



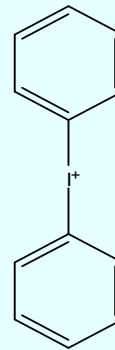
**SF 4**



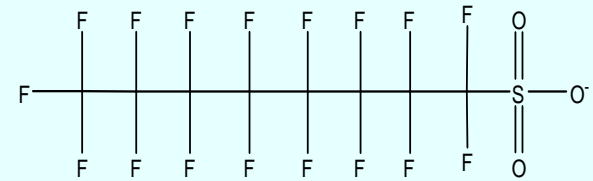
**PFBS**



**Triphenylsulfonium**



**Diphenyliodonium**

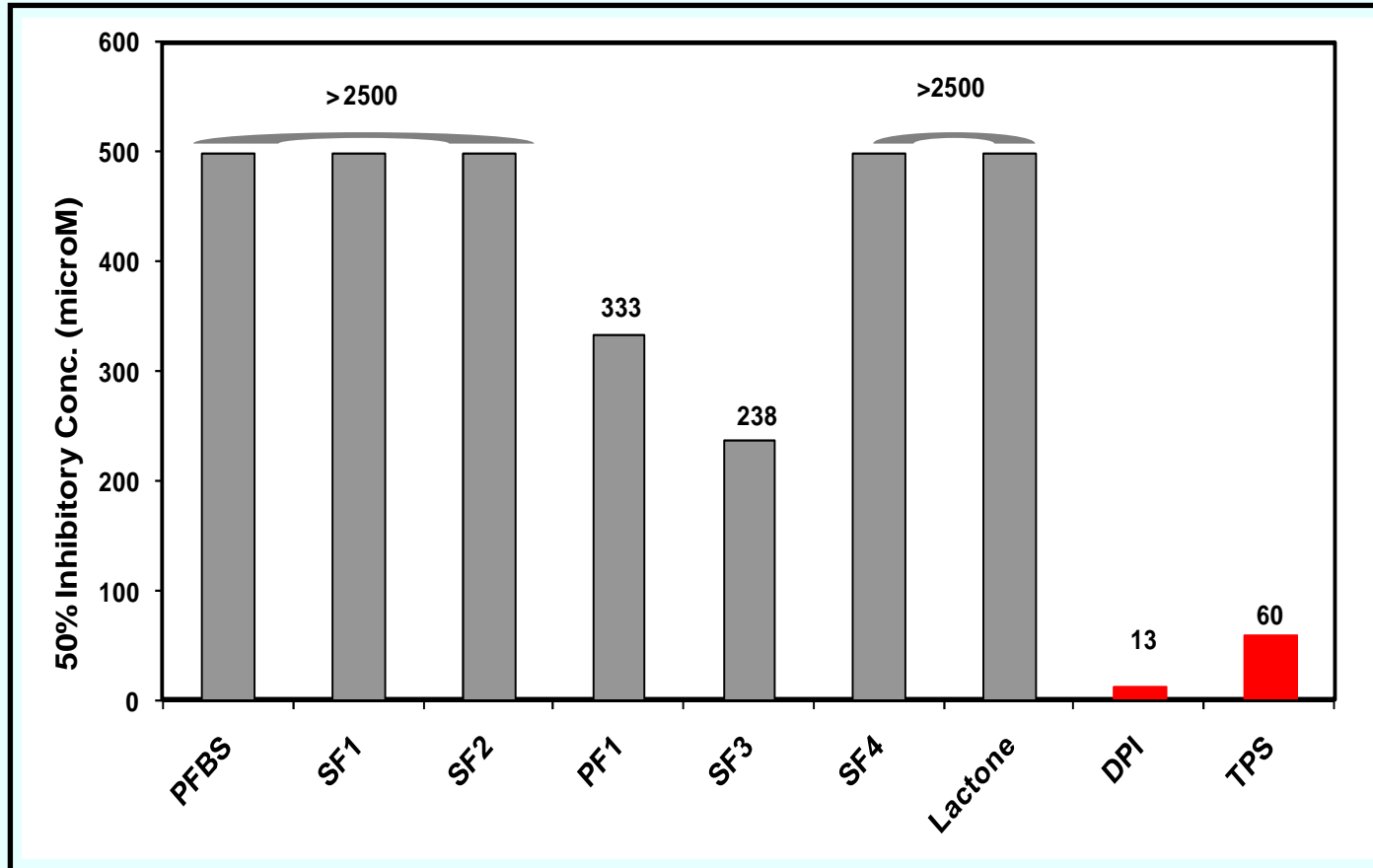


**PFOS**

**Fig. 1- Non-PFOS PAGs and counter ions studied.**

# MTT Assay

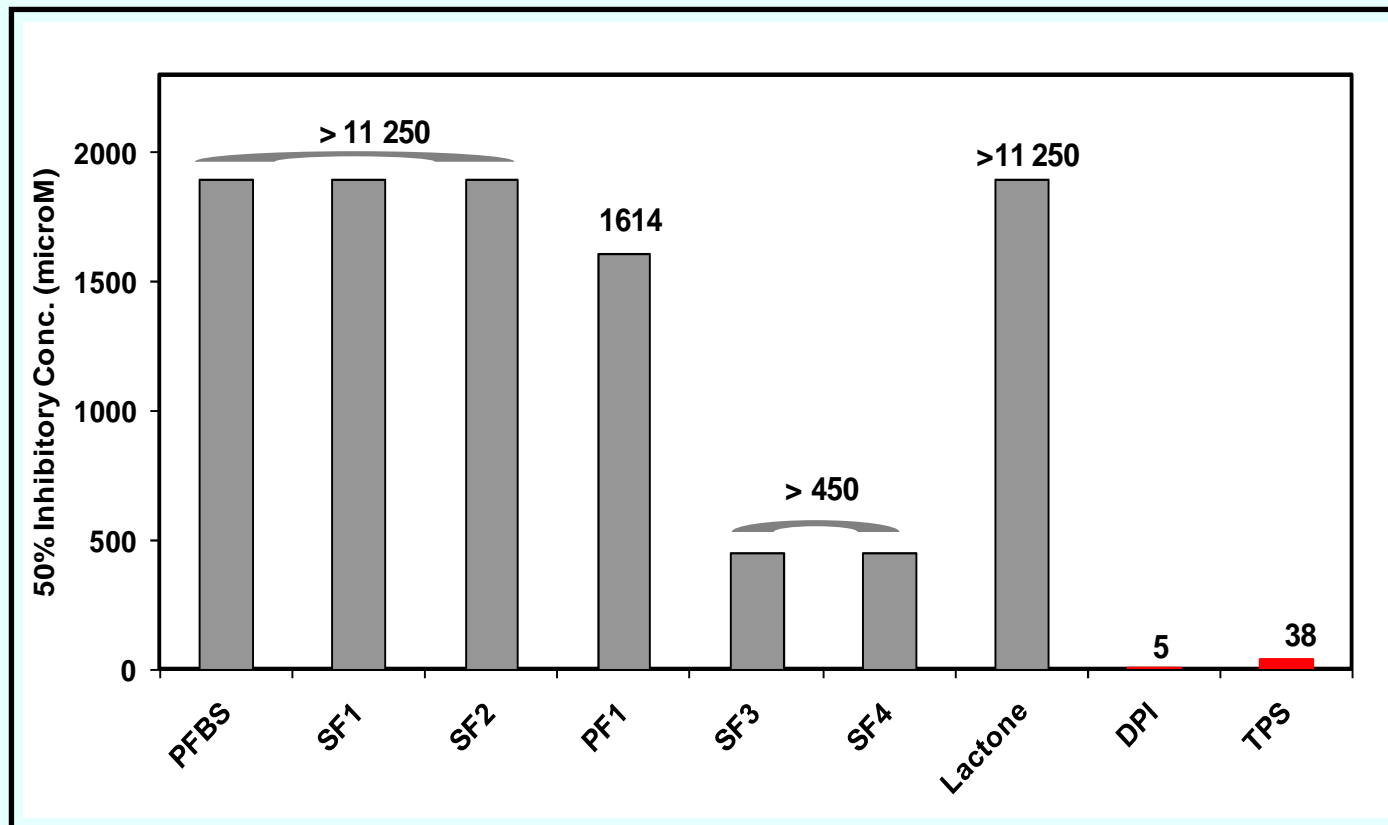
The PAG counter ions, DPI and TPS, showed the highest toxic effects in the MTT assay (Fig. 2). PF1 was the only PAG displaying toxicity in this bioassay.



**Fig. 2-** Inhibitory effect of the new non-PFOS PAGs and the PAG counter ions in the MTT bioassay.

# Microtox Assay

In agreement with the findings of the MTT assay, the PAG counter ions were also the most inhibitory compounds in the Microtox assay (Fig 3). PF1 also displayed microbial inhibition, albeit at relatively high concentrations (50% inhibitory concn. (IC50)= 1.6 mM).



**Fig. 3-** Inhibitory effect of the new PAGs and their counter ions in the Microtox bioassay.

# Methanogenic Inhibition

The counter ions displayed inhibition towards H<sub>2</sub> and acetate-utilizing methanogens (Fig. 4). In contrast, the PAGs were generally not toxic. SF2 was an exception, with an IC<sub>50</sub> value of 1,470 μM. Methanogens are an important microbial population in anaerobic sludge digestors. Severe methanogenic inhibition can result in process failure.

NAME	Acetotoclastic		Hydrogen-utilizing	
	Concentration (μM)	Inhibition	Concentration (μM)	Inhibition
SF Sulfonate 1	2589	7% ± 1%	2589	3% ± 3%
SF Sulfonate 2	1850	63% ± 3%	1850	4% ± 5%
PF Sulfonate 1	1830	43% ± 4%	1830	-2% ± 1%
Lactone	1600	56% ± 1%	1600	0% ± 2%
Perfluorobutane sulfonate	1672	15% ± 1%	1672	7% ± 2%
Triphenylsulfonium	1519	31% ± 3%	1519	51% ± 21%
Diphenyliodonium	1779	56% ± 1%	711	28% ± 5%

**Fig. 4-** Inhibitory effect (IC<sub>50</sub>) of the new non-PFOS PAGs and counter ions in (A) autotrophic methanogens and (B) acetoclastic methanogens in anaerobic sludge. \*NT= Not toxic at the highest concn. tested: SF1 (2,589 μM); SF2 (1,851 μM), PF1 (1,830 μM), PFBS (1,672 μM).

# PBT Profiler

The EPA PBT (Persistence-Bioaccumulation-Toxicity) Profiler (available at <http://www.pbtprofiler.net/>) was utilized to estimate the persistence, bioaccumulation, and chronic fish toxicity potential of the various PAGs. The applicability of the PBT Profiler to surfactants, highly fluorinated compounds and reactive compounds is known to be very limited. Predictions obtained using this screening method should be used with caution.

PAG/Counter-ions	PBT Color code	Persistence	Bioaccumulation	Fish- Chronic Toxicity
SF1	PBT	+	—	—
SF2	PBT	+	—	—
PF1	PBT	+	—	—
Lactone	PBT	+	—	—
PFBS	PBT	+	—	—
PFOS	PBT	+	—	—
SF3	PBT	++	—	Not calculated
SF4	PBT	++	—	Not calculated
Diphenyliodonium (K <sup>+</sup> )	PBT	+	--	+
Triphenylsulfonium (K <sup>+</sup> )	PBT	+	+	++

**Green:** no criteria have been exceeded (no environmental concern)

**Orange:** EPA criteria have been exceeded (environmental concern)

**Red:** EPA criteria have been exceeded (High environmental concern)

## Conclusions

- The counter ions, diphenyliodonium (DPI) and triphenylsulfonium (TPS), showed the highest toxic effects in all three tests.
- The new PAGs, SF1 and SF2, were not inhibitory, or only at very high concentrations. PF1 displayed inhibition in the MTT and Microtox assays but the IC50 levels were 1-2 orders of magnitude higher compared to those determined for the counter ions.
- The PBT Profiler presented good correlation with the results obtained for all the toxicity tests.

## Future Work

- Evaluate the environmental compatibility of new generation PAGs.
- Continue the evaluation of the treatability of the most promising PAGs using conventional physico-chemical and biological methods.
- Evaluate the environmental fate properties of the new PAGs using a commercial prediction engine (CATABOL)\* known to be suited for fluorinated compounds. The applicability of the EPA PBT profiler for these compounds is limited.

\* Dimitrov et al. (2004) Predicting the biodegradation products of perfluorinated chemicals using CATABOL. SAR QSAR Environ Res. 15(1):69-82).

# Environmentally Benign Electrochemically-Assisted Chemical- Mechanical Planarization (E-CMP)

*(Task Number: 425.014)*

## Experimental Investigation of Cu and Ta E-CMP Processes

### PI:

- **Srini Raghavan, Department of Materials Science and Engineering, UA**

### Graduate Student:

- **Ashok Muthukumaran: PhD candidate, Department of Materials Science and Engineering, UA**

### Undergraduate Student:

- **Raymond Lee, Department of Materials Science and Engineering, UA**

### Cost Share (other than core ERC funding):

- **In-kind donation (patterned wafers) from Intel :\$10,000**

SRC/SEMATECH Engineering Research Center for Environmentally Benign Semiconductor Manufacturing

# Objectives

- Optimize dihydroxybenzene sulfonic acid (DBSA) based chemical system for electrochemical mechanical **removal of Ta with a 1:1 selectivity with respect to copper**
- Evaluate DBSA based chemical system for the removal of TaN under ECMP conditions
- Working with an industrial partner (Intel), fabricate a test structure for additional evaluation



# ESH Metrics and Impact

➤ ECMP Electrolyte

- Requires very low solid content (~ 0.1 wt%) as compared to ~ 10 wt% solids in conventional Ta CMP slurry

➤ Low toxicity of DBSA

Compound	LD <sub>50</sub> (rat)	Carcinogenic
DBSA	> 5000 mg/kg	NO
Catechol	260 mg/kg	YES
Benzotriazole	965 mg/kg	NO

➤ EHS Impact

Goals	Usage Reduction		Waste Reduction	
	Chemicals	Abrasives	Solid	Liquid
Using full sequence ECMP	N/A	> 90%	> 99%	N/A

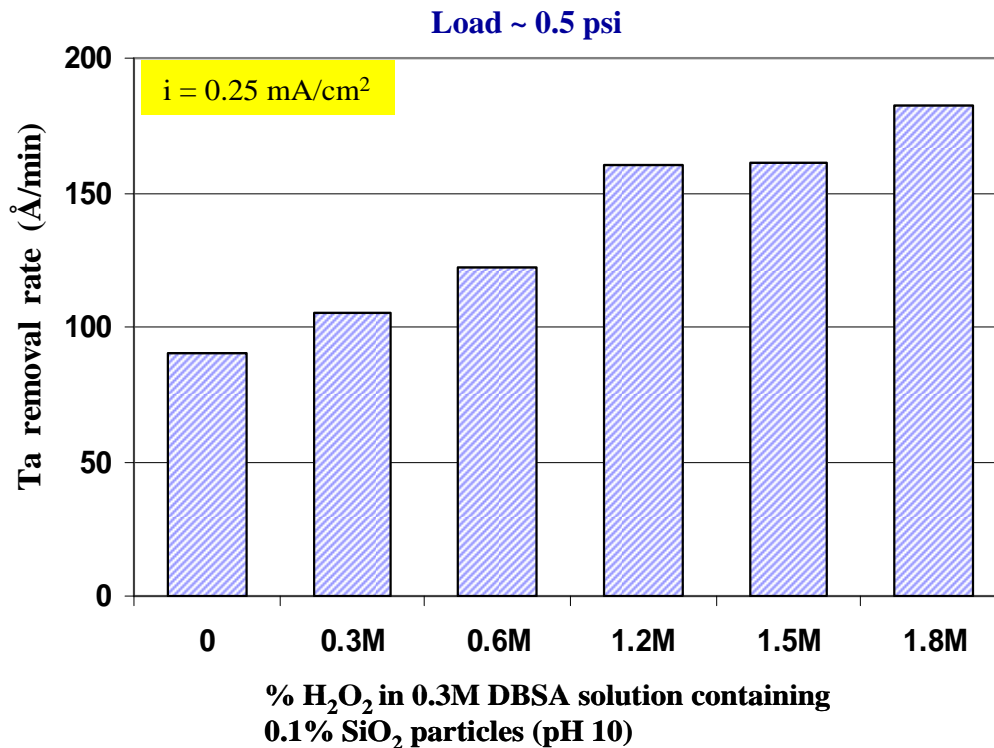
# Current Year Activities

➤ During the last contract year, Di-hydroxybenzene Sulfonic acid (DBSA) was shown to have promise as a chemical agent suitable for ECMP of Ta

In the current contract year, optimization of DBSA based chemical system has been done to obtain a Ta removal rate of  $\sim 200 \text{ \AA}/\text{min}$  with a 1:1 selectivity with respect to Cu

- Variables Optimized: Peroxide Concentration, pH, Current density
- Used optimized formulation for the removal of TaN
- Fabricated a patterned test structure and conducted experiments to verify blanket wafer results

# Effect of Peroxide Concentration on Ta Removal



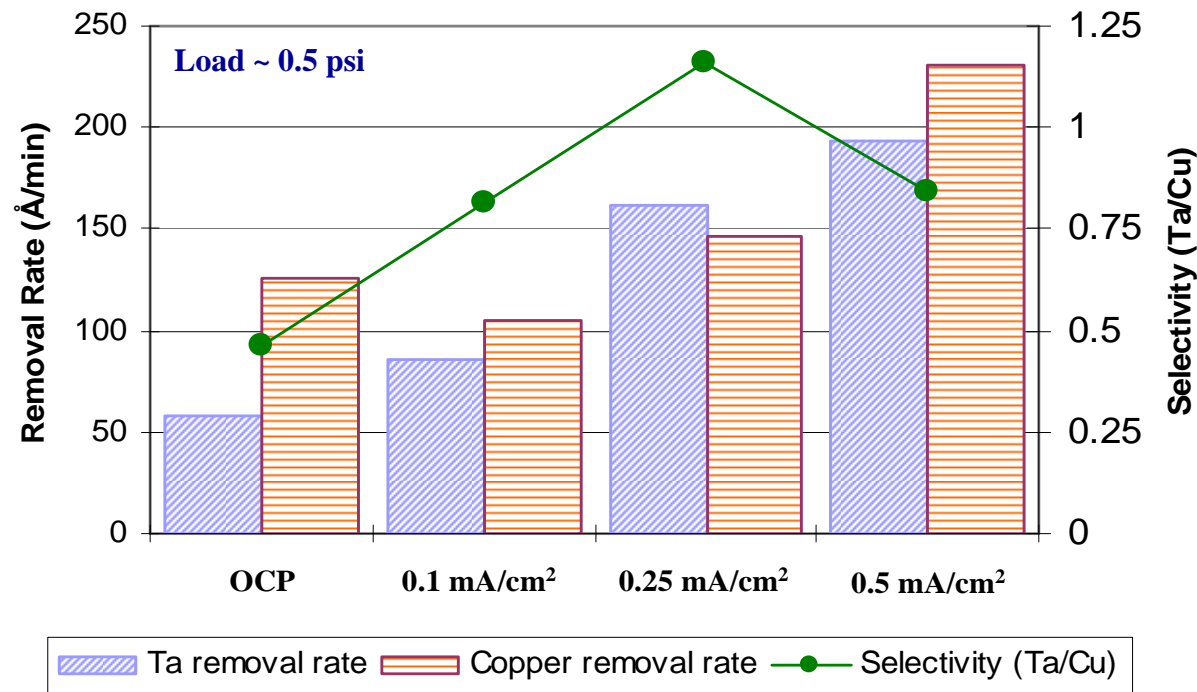
➤ 0.3M DBSA solution (pH 10) containing 0.1% of 80 nm SiO<sub>2</sub> particles ; current density = **0.25 mA/cm<sup>2</sup>**

➤ Removal rate of tantalum is 90 Å/min in the absence of peroxide

➤ **Addition of 1.2M peroxide, increases the removal rate to 160 Å/min**

➤ Peroxide concentration greater than 1.2M increases the removal rate only marginally

# Effect of Current Density on Removal Rate and Selectivity (Ta/Cu)



$$\text{Selectivity} = \frac{\text{Removal rate of Ta}}{\text{Removal rate of Cu}}$$

- 0.3 M DBSA solution + **1.2M H<sub>2</sub>O<sub>2</sub>** + 0.1 % SiO<sub>2</sub> (**pH 10**)
- Ta removal rate of **~ 200 Å/min** at 0.5 mA/cm<sup>2</sup> (corresponding to 1 V overpotential)
- Selectivity (Ta/Cu) of **1.2:1** and **0.85:1** at 0.25 and 0.5 mA/cm<sup>2</sup>, respectively

# Proposed Mechanism and Current Efficiency

## ➤ MECHANISM OF Ta REMOVAL

- Ta undergoes an **interfacial 2 e<sup>-</sup> transfer reaction** forming TaO on the surface



- TaO is further oxidized and dissolved by H<sub>2</sub>O<sub>2</sub> and DBSA in the bulk solution to form complexes of the type,

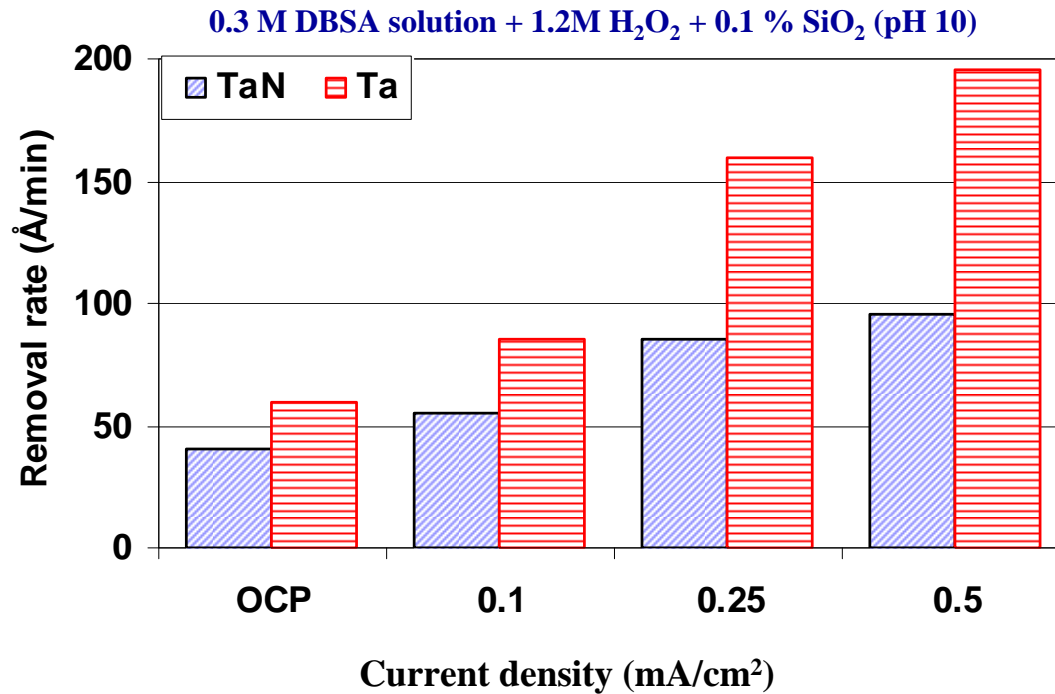


where  $x = \{1,2,3\}$  with corresponding  $y = \{6,4,2\}$  and **L represents one ionized DBSA molecule**

Applied current density (mA/cm <sup>2</sup> )	Estimated removal rate (Å/min) of tantalum based on 2e <sup>-</sup> transfer	Actual removal rate of tantalum (Å/min) in 0.3M DBSA + 1.2M H <sub>2</sub> O <sub>2</sub> + 0.1% SiO <sub>2</sub> (pH 10)	Calculating current efficiency (%) after correcting for OCP removal rate
OCP	-	60	-
0.1	34	85	80
0.25	85	160	109*
0.5	169	195	81

Note: \* Current efficiency greater than 100% most likely due to analytical error

# Evaluation of DBSA for TaN Removal

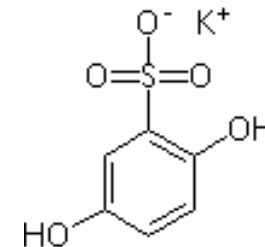


*Schematic representation of barrier stack*



➤ At  $i = 0.5 \text{ mA/cm}^2$

- TaN removal rate  $\sim 100 \text{ \AA/min}$
- Ta removal rate  $\sim 200 \text{ \AA/min}$

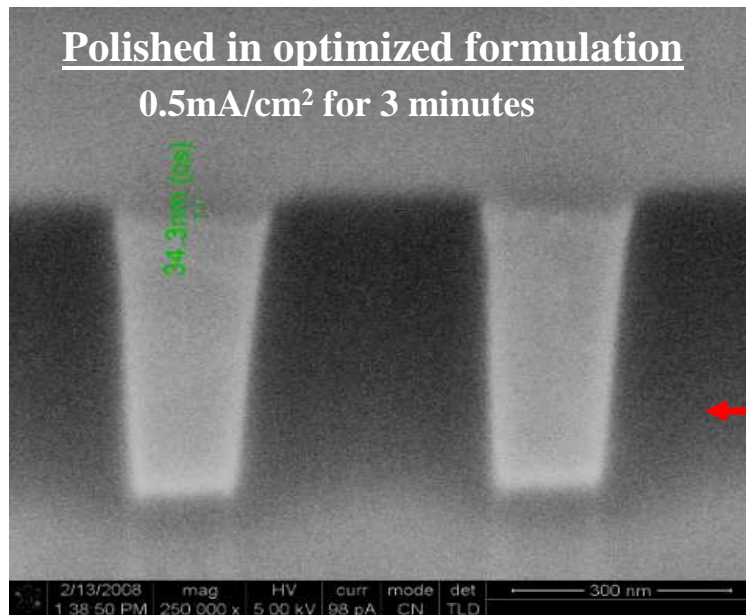
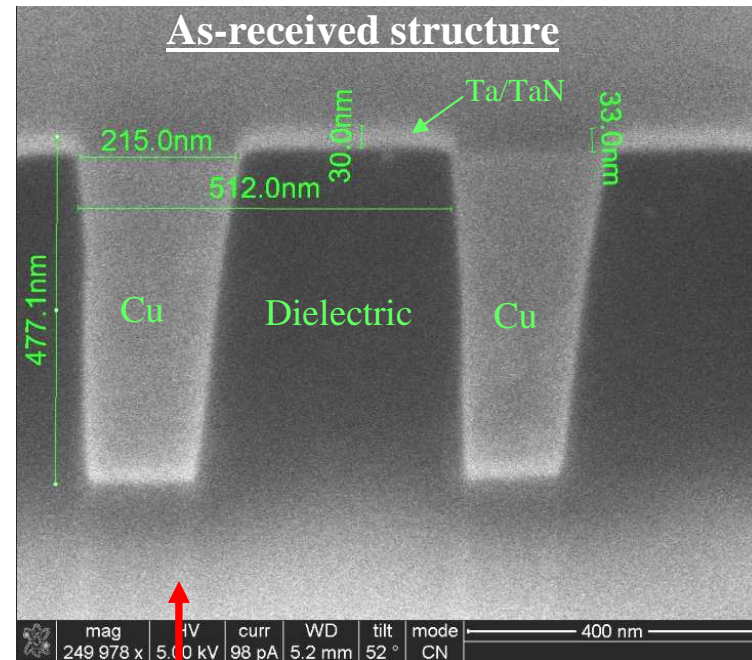
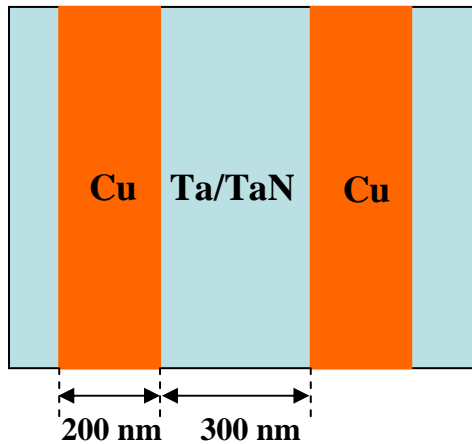


*Potassium salt of dihydroxy benzene sulfonic acid*

DBSA is not as effective for TaN as it is for Ta

# ECMP of Patterned Structure in Optimized Formulation

*Schematic of patterned structure*



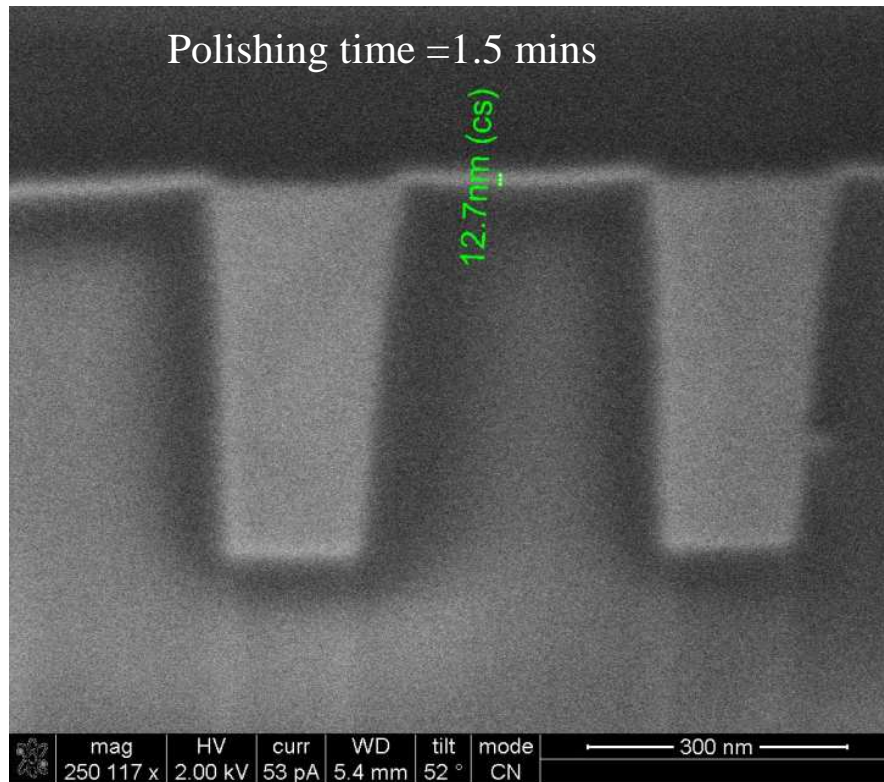
➤ As received test structure : Cu removed on platen 1 and 2 stopping on Ta.

**Note ~ 30 nm Cu recess**

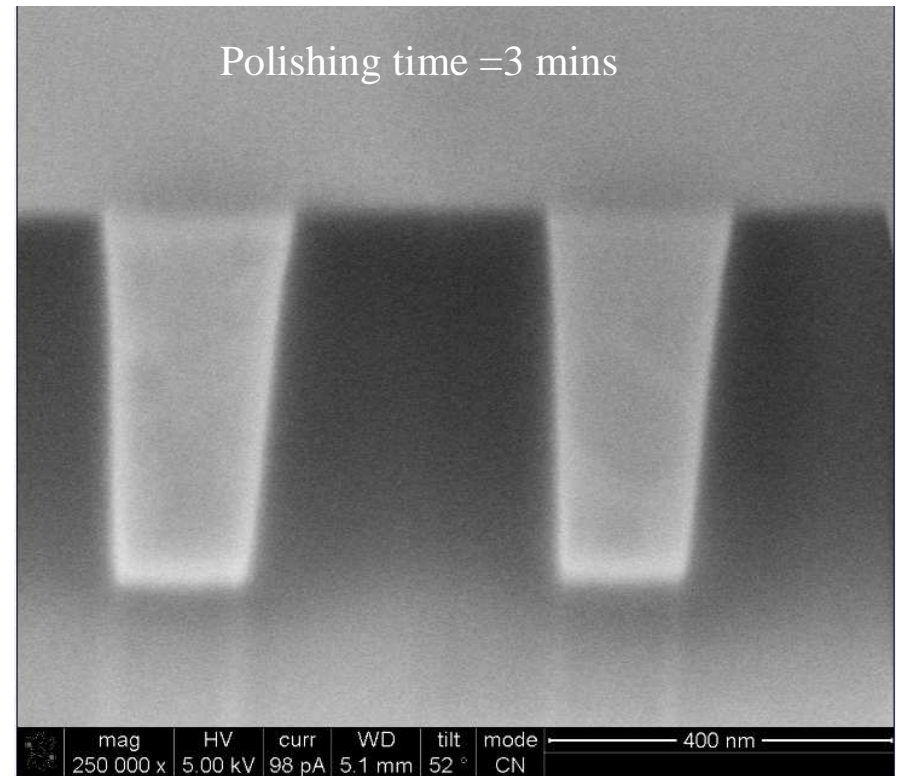
➤ Barrier layer is removed; however surface planarity **NOT** achieved (step height between the dielectric and Cu ~ 34nm)



# ECMP of Patterned Structure in Optimized Formulation with BTA



➤ Barrier layer thickness and step height reduced to ~ 13 nm



➤ Barrier film is completely removed and the surface appears to be *planar*

Note: Test structure polished in 0.3M DBSA solution containing 1.2M H<sub>2</sub>O<sub>2</sub>, 0.1% SiO<sub>2</sub> and **0.01M BTA** (pH 10) at 0.5 mA/cm<sup>2</sup>

*SRC/SEMATECH Engineering Research Center for Environmentally Benign Semiconductor Manufacturing*



# Summary

- Ta removal rate of ~ **200Å/min** obtained in 0.3 M DBSA solution containing 1.2M H<sub>2</sub>O<sub>2</sub> and 0.1% SiO<sub>2</sub> (pH 10) at  $i = 0.5 \text{ mA/cm}^2$
- Ta/Cu selectivity of ~ **1:1** observed at pH 10 at a current density of 0.5 mA/cm<sup>2</sup> (oxide removal rate in the formulation ~ 30 Å/min)
- DBSA is not as effective for TaN as it is for Ta
- Patterned test structure
  - Complete removal of barrier layer and surface planarity achieved by polishing in optimized solution containing **0.01M BTA**

# Industrial Interactions and Technology Transfer

- Work on Ta ECMP was presented at **Applied Materials** in August 2007; the seminar was hosted by Dr. Tom Osterheld
- Technical discussions with Dr. Renhe Jia of **Applied Materials**
- Interacted with Dr. Liming Zhang, Dr. Raghu Gorantla, Dr. Michael Ru and Dr. Zhen Guo of **Intel Corporation**, Santa Clara (to design test structures)

## Publications/Presentations

- A.Muthukumaran, N. Venkataraman and S. Raghavan, "Evaluation of Sulfonic Acid Based Solutions for Electrochemical Mechanical Removal of Tantalum," *J. Electrochem. Soc.*, 155 (3), pp. H184-87 (2008).
- A.Muthukumaran, N. Venkataraman, S. Tamilmani and S. Raghavan, "Anodic Dissolution of Copper in Hydroxylamine Based Solutions with Special Reference to Electrochemical Planarization (ECMP)," *Proceedings of The Corrosion Control 007 Conference*, Australia, Paper 105, 8 pp (2007).
- A.Muthukumaran and S. Raghavan, "Sulfonic Acid Based Chemistries for Electrochemical Mechanical Removal of Tantalum," *TECHCON*, Texas, Sep 10-12 (2007).
- A.Muthukumaran, N. Venkataraman, V. Lowalekar and S. Raghavan, "Sulfonic Acid Based Chemistries for Electrochemical Mechanical Removal of Tantalum," *Proceedings of the ECS - The 6<sup>th</sup> International Semiconductor Technology Conference (ISTC)*, China, 273-80 (2007).

# Future Plans

## Next Year Plans

- Find methods to improve TaN removal rate
  - Use of a different oxidant (ex.  $\text{KIO}_3$ )
  - Use DBSA with  $-\text{OH}$  groups in the ortho position
- Extend the studies to tungsten nitride barrier layer
- Preliminary studies on removal of self forming barrier materials such as Cu-Mn alloys

# Future Plans

## Long-Term Plans

- Develop chemical systems for one step removal of Cu and barrier layer
- Design of pads for ECMP
  - Electrical contacts: metal vs. other conductive layer coatings
  - Placement of contacts for controlling electric field distribution : Modeling effort (with MIT/ Boning)
  - Pad Surface and Mechanical Property Optimization for ECMP (with Philipposian and Boning)

# **Environmentally Benign Electrochemically-Assisted Chemical Mechanical Planarization (E-CMP)**

*(Task 425.014)*

## **Subtask 2: Modeling, Optimization and Control of E-CMP Processes**

### **PI:**

- **Duane Boning, Electrical Engineering and Computer Science, MIT**

### **Graduate Students:**

- **Daniel Truque, EECS, MIT, graduated with M.S. in June 2007**
- **Wei Fan, EECS, MIT Ph.D. candidate, started Sept. 2007**
- **Joy Johnson, EECS, MIT M.S. candidate, started Sept. 2007**

### **Undergraduate Students:**

- **Zhipeng Li, EECS, MIT**

### **Other Researchers:**

- **Ed Paul, Visiting Professor, Stockton College**

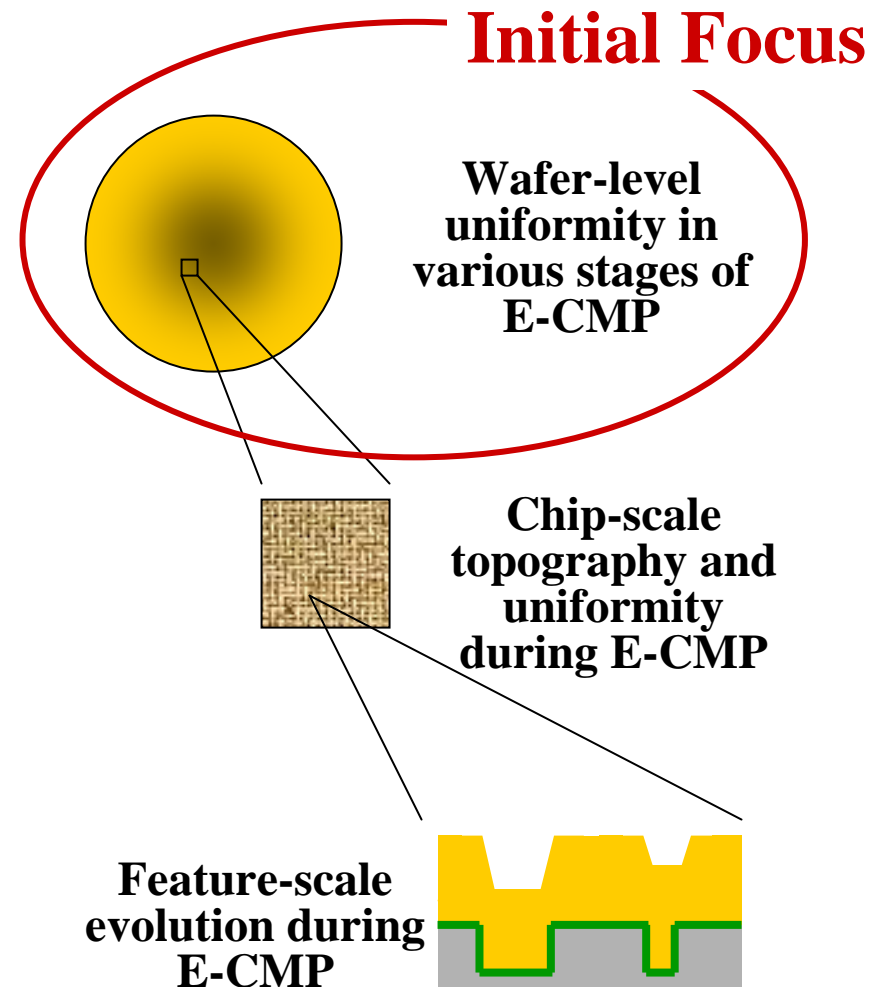
### **Cost Share & Industrial Interactions:**

- **Chris Borst, ECMP experimental support, Albany Nanotech**

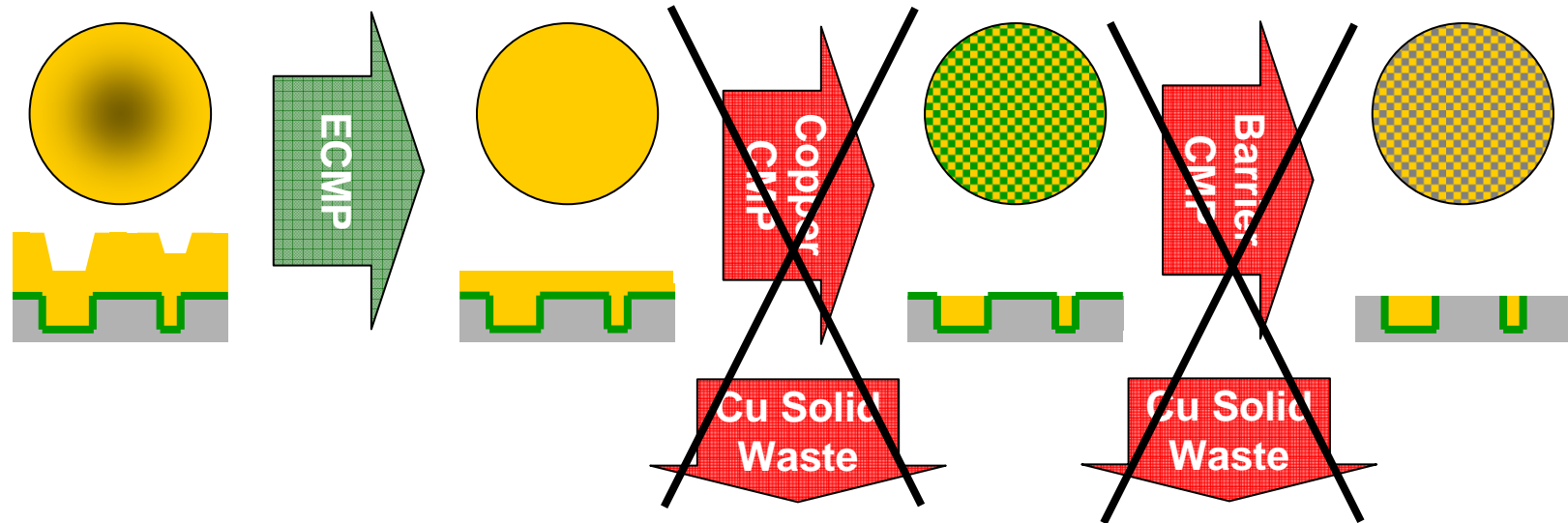
*SRC/SEMATECH Engineering Research Center for Environmentally Benign Semiconductor Manufacturing*

# Objectives

- **Develop models for ECMP (bulk copper, full copper, and barrier removal steps) at the:**
  - wafer-scale
  - chip-scale
  - feature-scale
- **Develop control and optimization strategies utilizing integrated models**
  - minimize process time, consumables usage
  - maximize uniformity, yield



# ESH Metrics and Impact



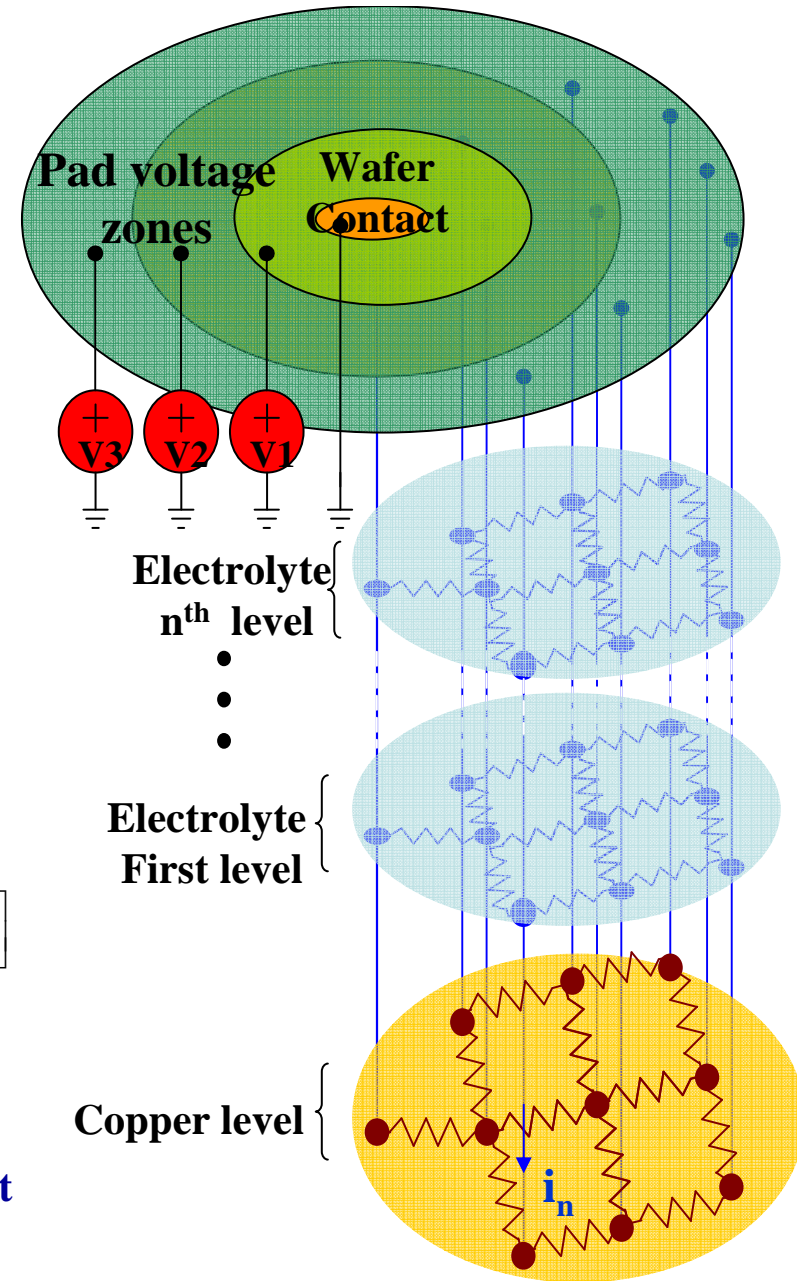
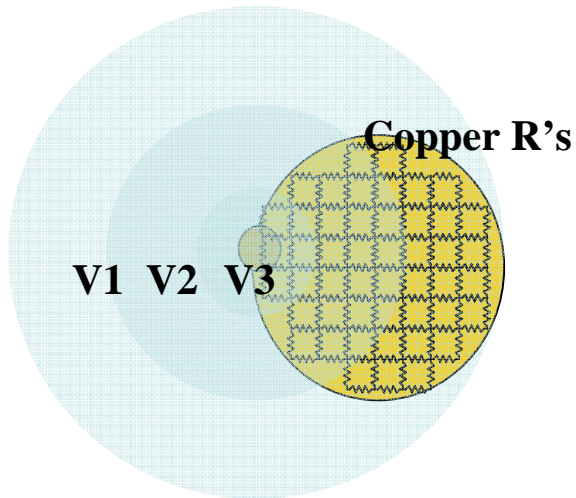
- 1. Reduction in the use or replacement of ESH-problematic materials**
- 2. Reduction in emission of ESH-problematic material to environment**
  - **Reduce or eliminate solid slurry particle waste**
    - Eliminate copper touch-down CMP (eliminate ~20% of planarization cycle)
    - Lower solid content barrier ECMP (~80% solids reduction in this step)
- 3. Reduction in the use of natural resources (water and energy)**
  - **Shorten process cycle time by ~20%**
  - **Increase in pad lifetime (5X)**
- 4. Reduction in the use of chemicals**
  - **Replace CMP slurry with more benign ECMP electrolyte**

# **ECMP – Wafer Scale Modeling Approach**

- **Cu removal rate across wafer as function of:**
  - Initial copper thickness (e.g. nonuniform plating profile)
  - Applied voltages in multiple zones in ECMP tool
  - Tool/process parameters: geometry of electrical contact to wafer, velocity, pressure
- **Semi-physical model**
  - Model structure based on physics of process
  - Fit to experimental characterization data
- **Two models considered:**
  1. **Ohmic:** voltage drops vertically/laterally in electrolyte
  2. **Nonlinear:** focus on electrochemical dependence at electrode (ignore lateral voltage drop in electrolyte)



# 1. Ohmic ECMP Model



## Ohmic ECMP Model Approach:

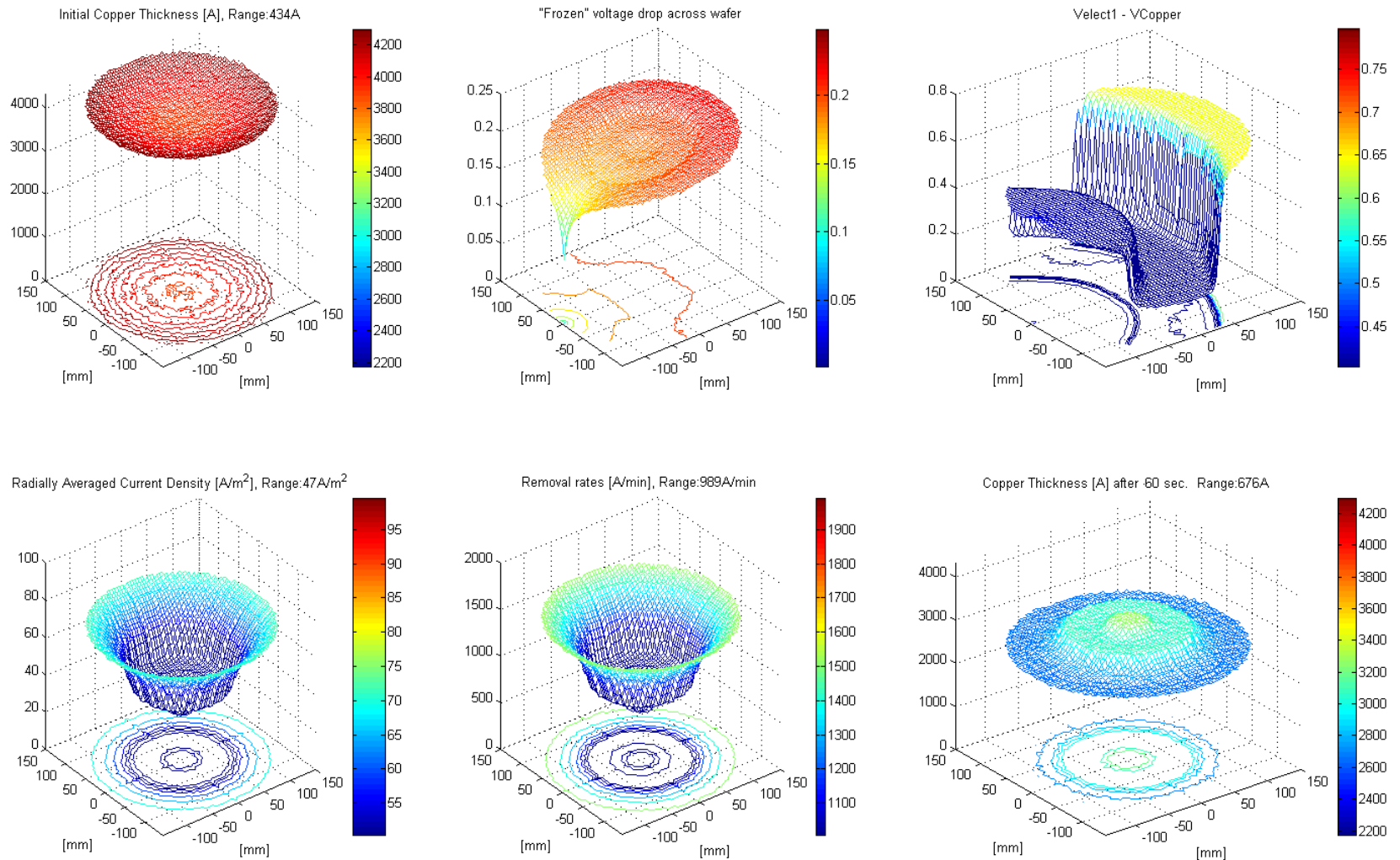
- Calculate static current density to calculate removal

$$I \left[ \frac{C}{sec} \right] \cdot \frac{1}{area [cm^2]} \cdot \frac{1 atom_{Cu}}{2e^- [C]} \cdot \frac{1 mole_{Cu}}{N_A atoms_{Cu}} \cdot \frac{63.546 g_{Cu}}{1 mole_{Cu}} \cdot \frac{1 cm^3}{8.941 g_{Cu}} \cdot \frac{10^7 nm}{1 cm} \cdot \frac{60 sec}{1 min} = RR \left[ \frac{nm}{min} \right]$$

$$area_{wafer} = 683.4 cm^2 \rightarrow \frac{RR}{I} = 31.02 \frac{nm}{A \cdot min}$$

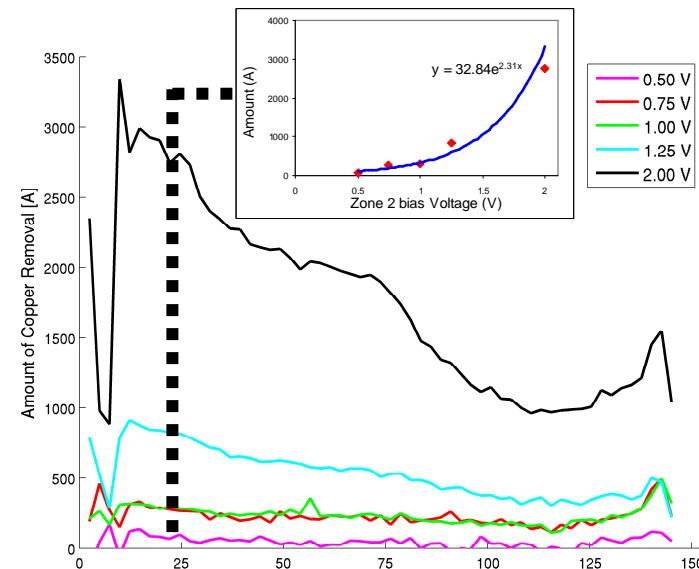
- Average radially and calculate removal rate
- Add static etch rate and calculate time interval's amount removed
- Update thickness and iterate

# Ohmic ECMP Model Results: $t = 10$ sec



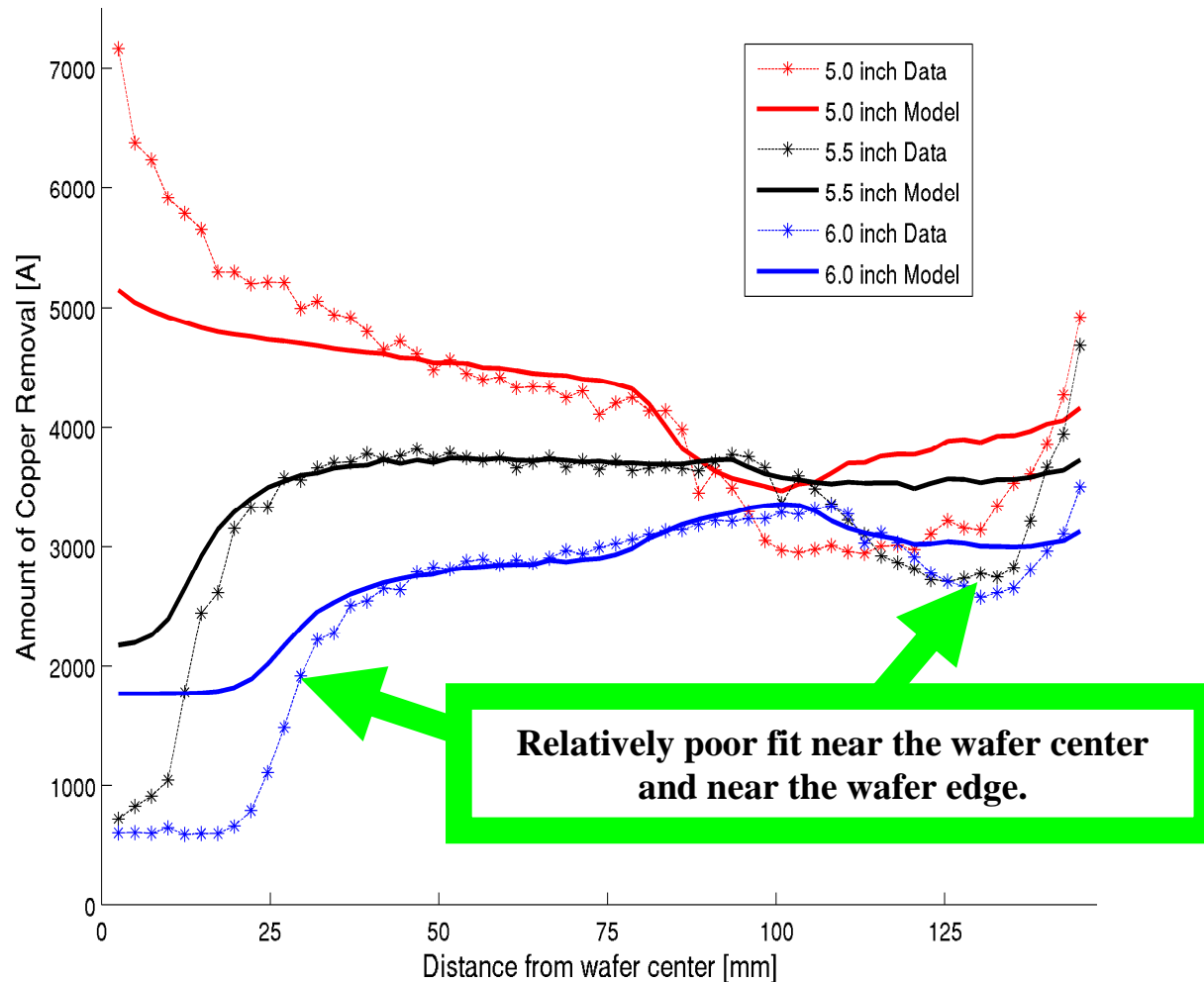
# Ohmic ECMP Model Experiments & Results

- **Collaboration with Albany Nanotech**
- **Experiment:**
  - Different voltages on different zones – intentionally introduce nonuniformity to aid in modeling
  - Measure Cu thicknesses on blanket films before and after
  - With and without head sweep (to better localize kinematics)
- **Revised numerical implementation of model**
  - Better handling of zero-current boundary conditions
- **Results: Model accuracy limitations**
  - Nonlinear voltage dependence
  - Does not fit well near center of wafer
  - Edge region – difficult to fit



Experimentally measured copper removal for five different values of  $V_2$  (with  $V_1 = V_3 = 0V$ ,  $L = 6.0$  inch). Figure inset shows the observed nonlinear relationship between  $V_2$  and the removal amount (current density) for one selected wafer radius.

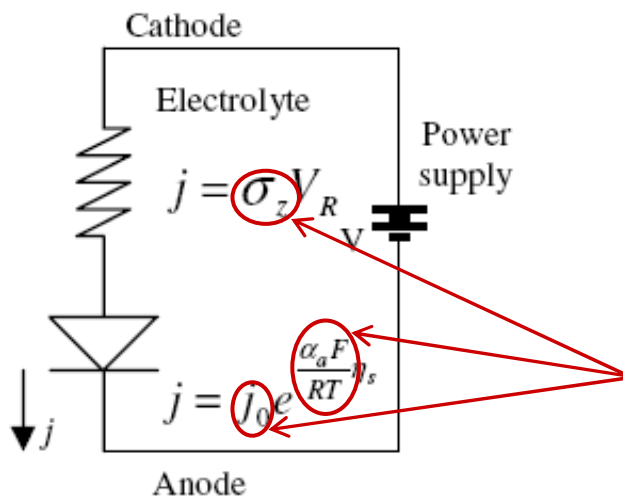
# Ohmic ECMP Model Results – Different Voltages in Each Zone



**Amount of copper removal for head position L of 5.0, 5.5, and 6.0 inches, and voltage zone settings of  $V1, V2, V3 = 2, 1, 3$  V. Basic ohmic model versus data. The RMS error of this fit is 531 Å.**

## 2. Non-Ohmic ECMP Model

- Account for nonlinear (exponential) Butler-Volmer electrochemical dependence at the wafer surface using a simple equivalent diode electrical model
- 1D implementation
  - Neglect voltage drop across wafer (highly conductive copper film)
  - Neglect lateral coupling and current flow in the electrolyte



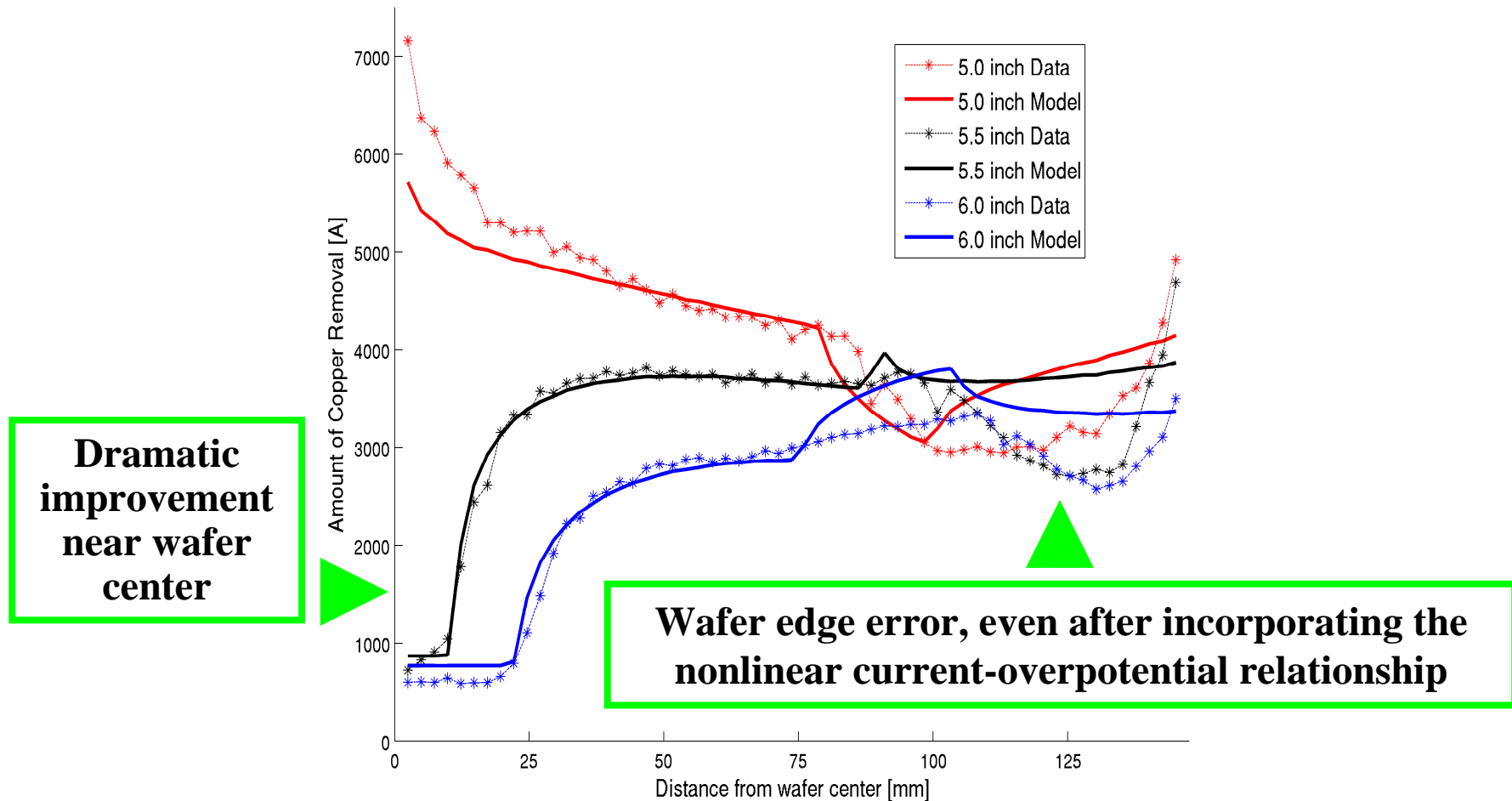
Assumptions:

1. Conduction and Faradaic current are equal
2. Instantaneous /complete removal of surface layer
3. Removal of passivation layer by zone
4. "Best fit" values for  $V_o$ ,  $J_o$ , &  $\sigma$
5. Only anodic reaction contribution

Removal Rate (J,t )

$$t \cdot \frac{J \cdot C}{s \cdot cm^2} \cdot \frac{1Cu}{2e^-} \cdot \frac{1molCu}{N_A \cdot Cu} \cdot \frac{63.54gCu}{1mols} \cdot \frac{cm^3}{8.96g} \cdot \frac{1e^-}{1.67 \times 10^{-19}C} \cdot \frac{10^7 nm}{1cm} = nm$$

# Non-Ohmic Model Results

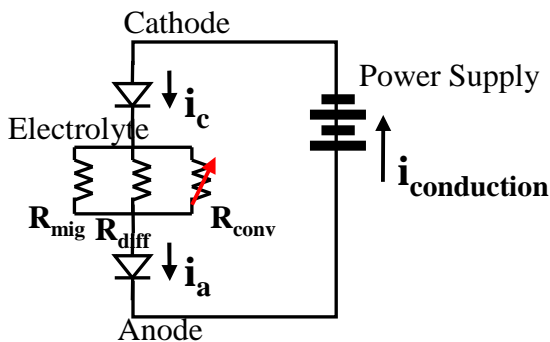


Amount of copper removal for  $L = 5.0, 5.5, 6.0$  inch, and voltage zone settings of  $V1, V2, V3 = 2, 1, 3$  V. Non-ohmic model versus data. The RMS error of this fit is  $412 \text{ \AA}$ , a 22% improvement.

# 3. Full Electrochemical Non-Ohmic ECMP Model

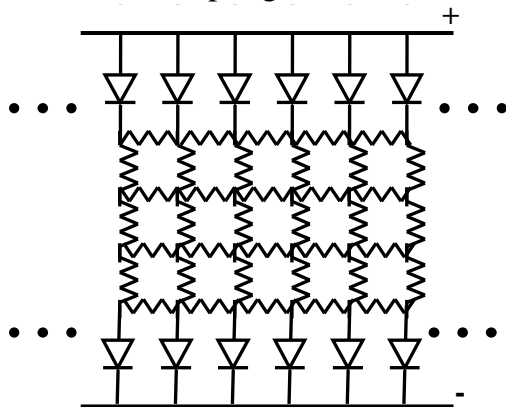
1-D View:

[without lateral coupling current]



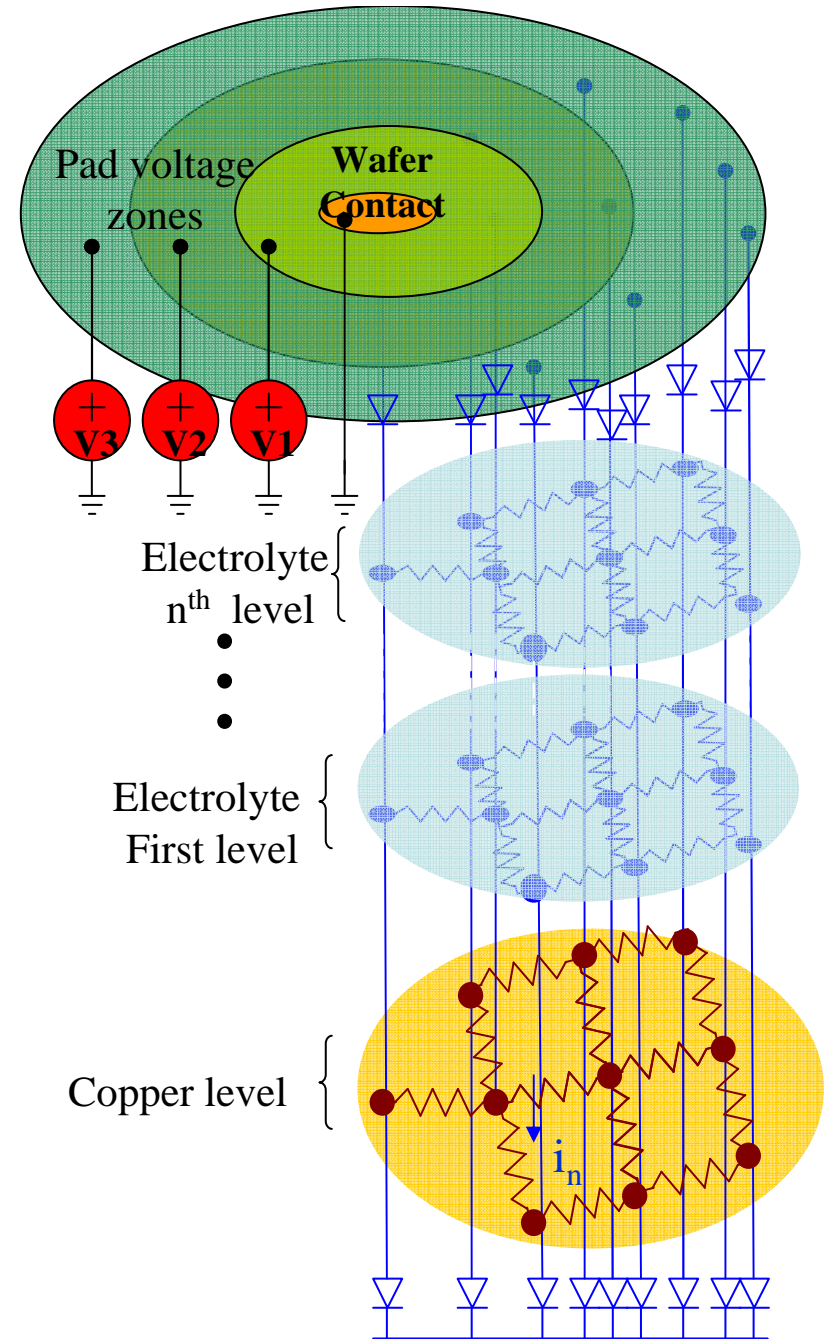
2-D View:

[with lateral coupling current]



Assumptions:

1. Anodic & cathodic electrochemical current contributions
2. \*Lateral coupling current contributions
3. Faradaic current and conduction not always equivalent
4. Instantaneous and complete removal of surface layer
5. Neglect voltage drop across the wafer (highly conductive copper film)
6. \*Passivation layer formation and removal effects on the time-averaged voltage





# Future Plans

## Next Year Plans

- Improve wafer scale ECMP model physics
  - Two electrode model with electrochemistry
  - Consider dynamics of protective film formation/removal
- Implement 2D/3D version of wafer scale model
  - Cross-coupling in electrolyte; thin film resistance for full copper removal
- Analysis of conductive pad configuration
- Begin feature/chip-scale ECMP model development

## Long Term Plans

- Integrated feature, chip and wafer-scale ECMP model
  - Incorporate electrochemical effects for new metal/barrier electrolytes (Raghavan, West)
- Design of pads for ECMP (with Raghavan, Philipossian)
  - Electrical contact modeling: metal vs. other conduction layers
  - Placement of contacts for e-field distribution and uniformity
  - Pad property optimization: for feature/chip/wafer performance and uniformity
- Optimization and control strategies for maximized uniformity and minimized process consumption/time



# **ESH Impact of Electrochemical Mechanical Planarization Technologies**

*(Task Number: 425.016)*

## **PI:**

- Alan West, Chemical Engineering, Columbia University

## **Graduate Student:**

- Kristin Shattuck: PhD candidate, Chemical Engineering, Columbia University

## **Undergraduate Student:**

- Neha Solanki, Chemical Engineering, Columbia University

## **Other Researcher:**

- Jeng-Yu Lin, PhD candidate, Chemical Engineering, National Tsing-Hua University

# Objectives

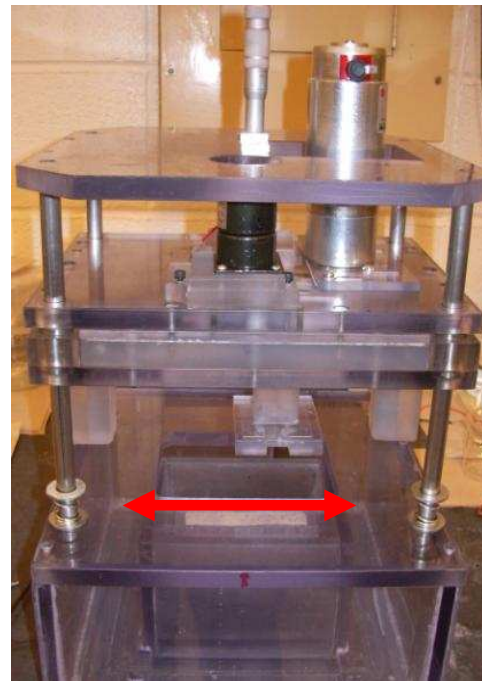
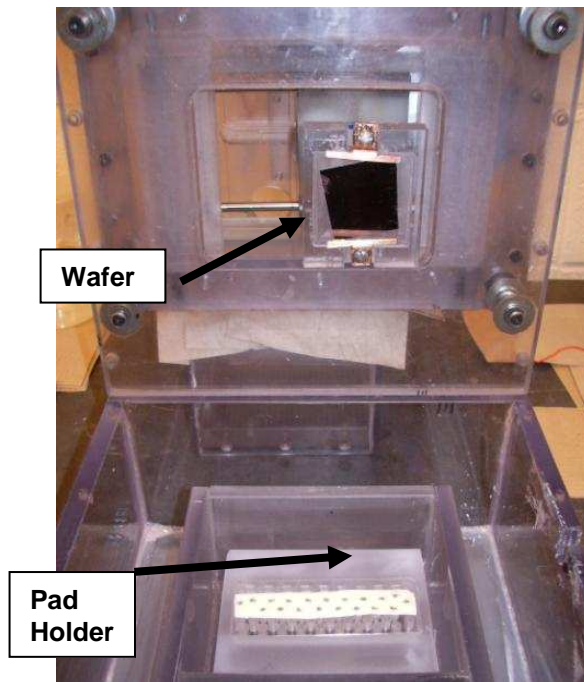
- Develop methods for planarization that optimize the use of electrochemistry and improve aspects of current technologies
- Develop a method to predict feature scale planarization through the use of planarization factors
- Test planarization capabilities of novel ECMP electrolytes using patterned structures
  - Phosphate based electrolytes containing BTA inhibitors
- Develop electrolytes for polishing liner materials
  - Ruthenium
- Study galvanic corrosion between Cu and Ru
  - Potentially utilizing microfluidics

# ESH Metrics and Impact

- Development of a more environmentally benign polishing electrolyte
  - Improve process yield
  - Potential elimination of slurry particles
  - Reduction or elimination of complexing agents and oxidizers in solution, facilitating waste treatment
- Potential reduction in electrolyte volume
  - Reduce waste generation
- Extend lifetime of consumables
  - Polishing pads

# Method

- Screen ECMP electrolytes using an RDE
  - Potassium phosphate based electrolytes investigated
- Use custom built ECMP tool to evaluate electrolytes for their planarization capabilities
  - Compare results with RDE predictions to develop a potential screening technique and model for planarization



## Design features:

- **2D linear motion**
- **Apply and control low downforces (<1 psi)**
- **Ease of changing between various electrolytes and pads**
- **Operate in contact and non-contact modes**

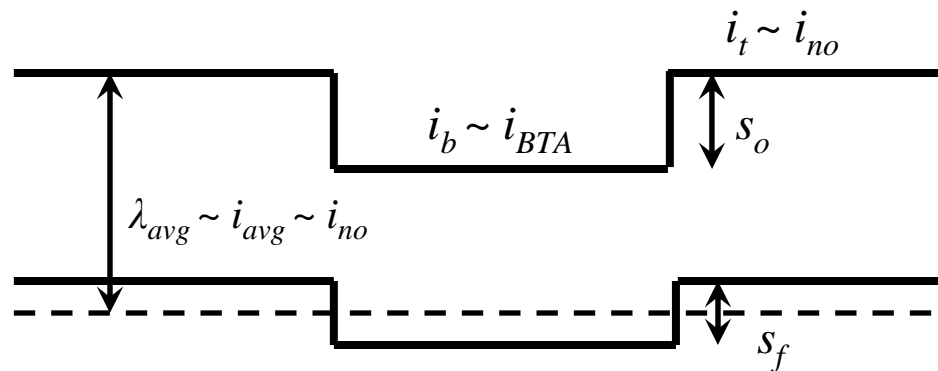
# Method

- To screen potential ECMP electrolytes
  - Relate removal rate to current density

$$\mathcal{E} = \frac{s_o - s_f}{\lambda_{avg}} \sim \frac{i_t - i_b}{i_{avg}}$$

For Experiments Using RDE

$$\mathcal{E}_{RDE} = \frac{i_{no} - i_{BTA}}{i_{no}}$$



For Experiments using Tool with Blanket Wafers

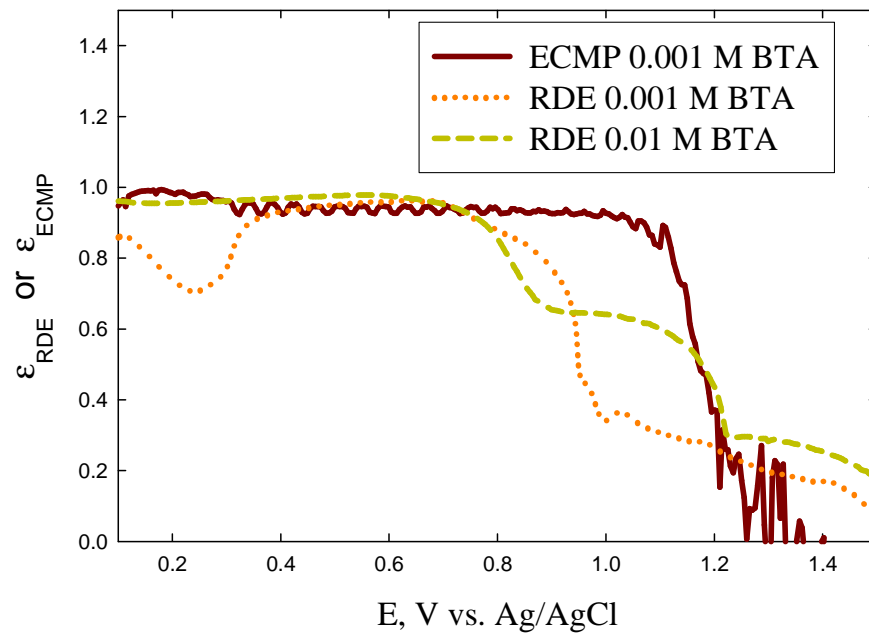
$$\mathcal{E}_{ECMP} = \frac{i_{pad} - i_{no-pad}}{i_{pad}}$$

# Results

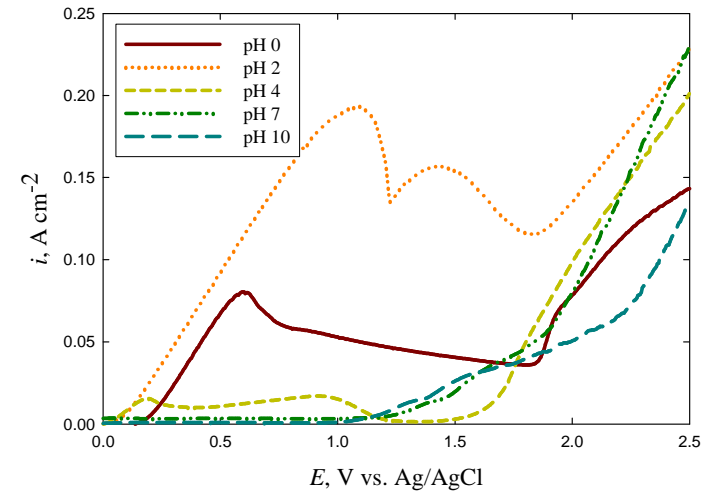
## Theoretical Planarization Factors

### RDE & ECMP

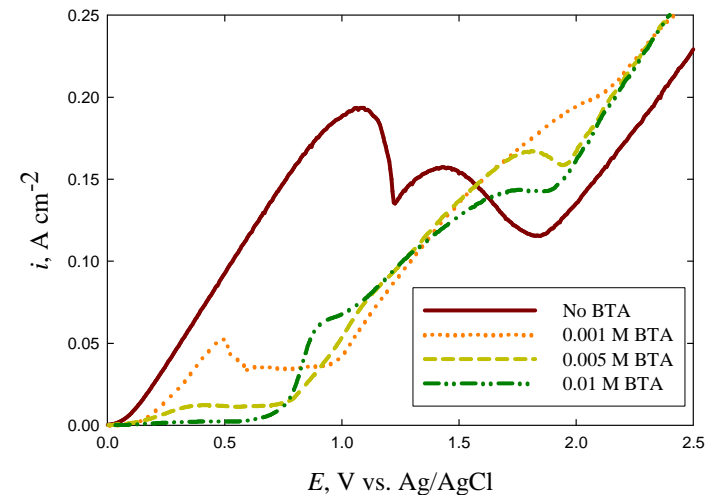
- pH 2
- 0.001 or 0.01 M BTA



pH values 0 to 10  $\rightarrow$  No BTA



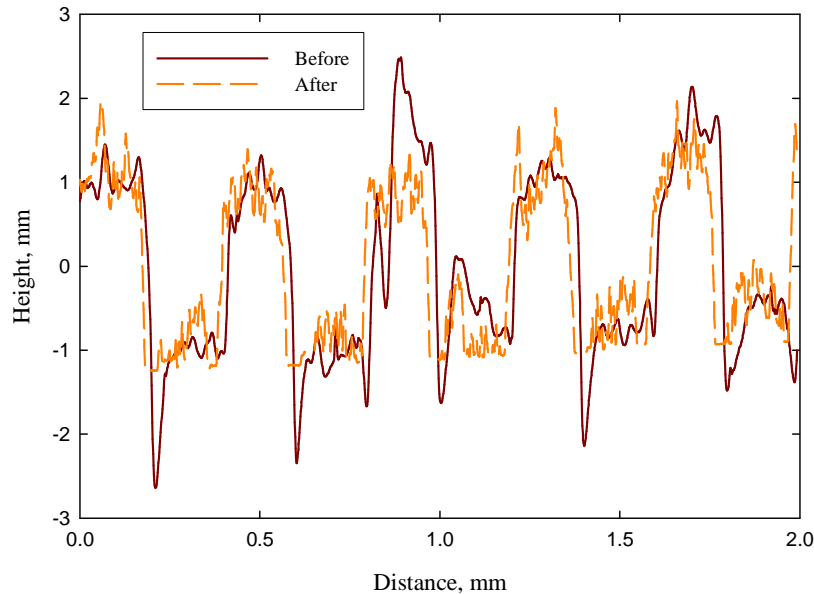
pH 2  $\rightarrow$  0 to 0.01 M BTA



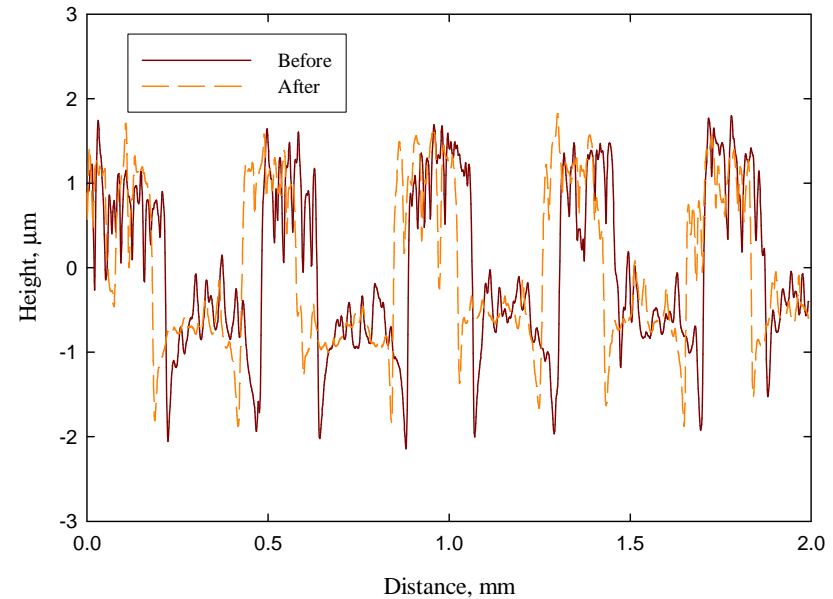
# Results

- All planarization experiments were performed at:
  - 0.5 V vs. Ag/AgCl
  - Downforce ~ 1 psi

## No Contact – No BTA



## Contact – No BTA



➤ **No BTA – No Planarization Achieved**

# Results

- Planarization Results

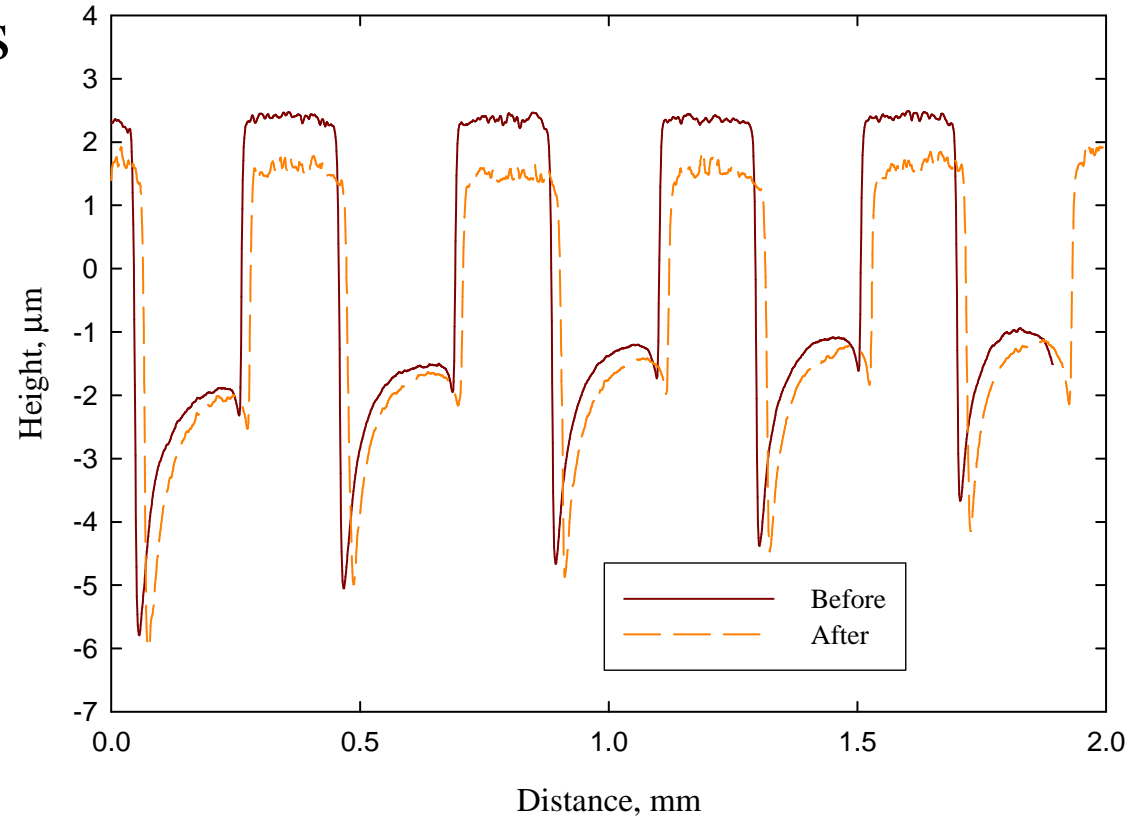
- *IC1000 Pad* – 40 s

Step Height Reduction

- $\sim 0.74 \mu\text{m}$

- Similar results achieved on:

- D100 Cabot Pad
- Suba Pad



$$\varepsilon = \frac{s_o - s_f}{\lambda_{avg}} \sim \frac{4.4 - 3.7}{0.34} \sim 2.1$$

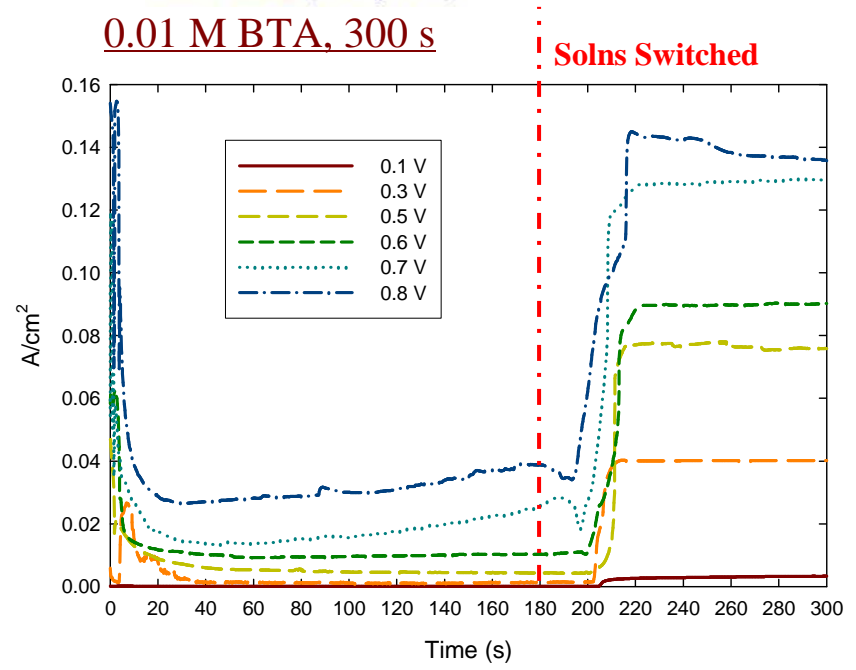
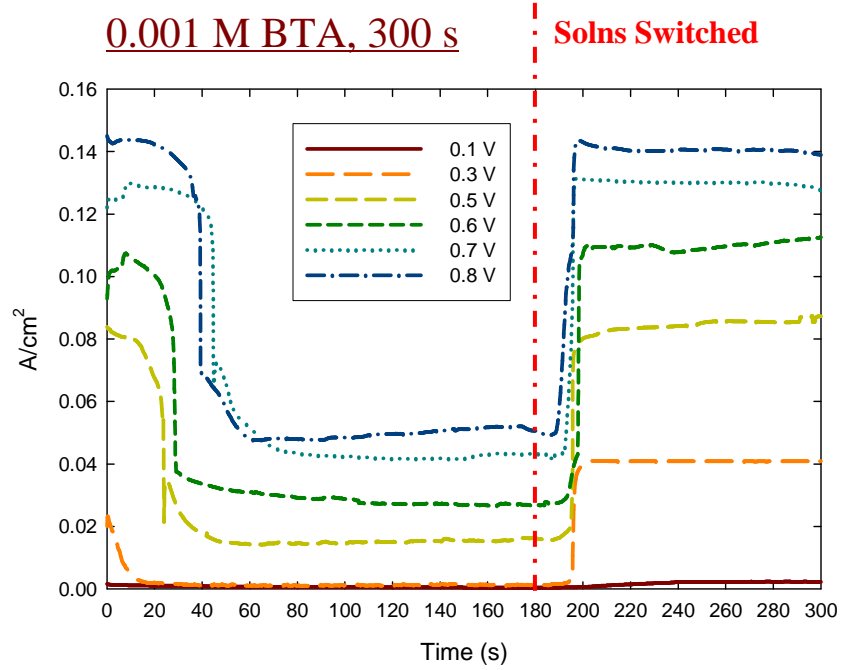
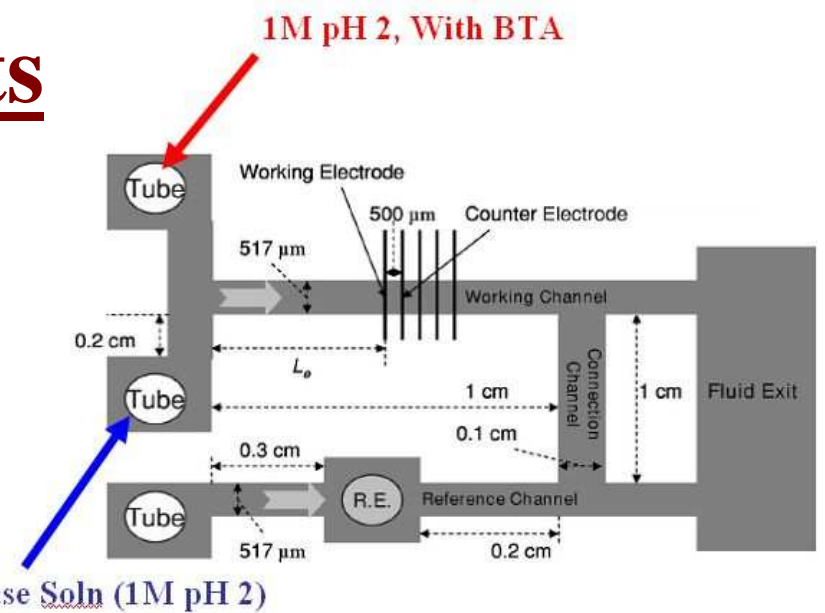
**Predicted By RDE:**

**$\sim 1.9$**



# Results

- BTA adsorption and desorption studies
  - For CMP and cleaning applications
  - 0 – 180 s**, BTA electrolyte (1M pH 2, 0.001 & 0.01 M BTA)
  - 180 – 300 s**, Base Solution (1M pH 2)



<sup>1</sup> Willey, M. J., A.C. West, A Microfluidic Device to Measure Electrode Response to Changes in Electrolyte Composition. *Electrochemical and Solid-State Letters*, 9 7 E17-E21 2006

# Industrial Interactions and Technology Transfer

- **Industry mentors/contacts**
  - **Intel**
  - **Novellus**
  - **Texas Instruments**
- **Polishing Pads**
  - **Cabot**
  - **Rohm & Haas**
- **Wafers**
  - **IBM**
  - **Novellus**

# Future Plans

## Next Year Plans

- **Finish planarization studies on Cu ECMP**
  - **Establish appropriate model to predict planarization**
- **Continue investigation of polishing liner materials**
  - **Ru**
- **Begin microfluidic studies to investigate galvanic corrosion between Ru and Cu**

## Long-Term Plans

- **Optimize pad / chemistry**
- **Demonstrate on Cu/Ru/Ta structures**
- **Collaborate with industry/university to perform wafer-scale ECMP tool experiments**

# Publications, Presentations, and Recognitions/Awards

## Presentations:

- ECS May 2008
- SRC Teleconference Oct 2007

## Papers:

- K. G. Shattuck, J. Y. Lin, and A. C. West, Characterization of Phosphate Electrolytes for use in Cu Electrochemical Mechanical Planarization, *Electrochimica Acta*, (*Submitted*)
- K. G. Shattuck, J. Y. Lin, and A. C. West, Planarization Studies of Phosphate Based Electrolytes for use in Cu ECMP, (*Pending*)
- J. Y. Lin, A. C. West, and C. C. Wan, Adsorption and Desorption Studies of Glycine and Benzotriazole during Cu Oxidation in a Chemical Mechanical Polishing Bath, *Journal of the Electrochemical Society*, (*Submitted*)
- J. Y. Lin, A. C. West, and C. C. Wan, Evaluation of Post-Cu CMP Cleaning of Organic Residuals Using a Microfluidic Device, *Electrochemistry Communication*, (*Submitted*)

# **Environmentally Benign Vapor Phase** **and Supercritical CO<sub>2</sub> Processes for** **Patterned Low k Dielectrics** *(Task Number: 425.017)*

## **PIs:**

- **Karen K. Gleason, Department of Chemical Engineering, MIT**

## **Graduate Students:**

- **Salaman Baxamusa: PhD Candidate, Department of Chemical Engineering, MIT (NSF Fellow)**
- **Shannan O'Shaughnessy, PhD: Department of Chemical Engineering, MIT (Graduated 5/07)**
- **Nathan J. Trujillo: PhDCEP Candidate, Department of Chemical Engineering, MIT (Started 9/07)**

## **Cost Share (other than core ERC funding):**

- **\$70,000 (NSF Fellowship for Sal Baxamusa)**

# Objectives

- **Develop new methods to deposit, pattern, and process low k materials**
  1. **Additive polymer patterning using self assembled mask (no traditional lithography)**
  2. **Resistless patterning**
- **Process step reduction results from EHS focused approach**

# ESH Metrics and Impact

1. *Resist-free photolithography would eliminate use of photoresist. Approximately 25,000 liters of photoresist materials is used annually in typical semiconductor foundries, at a cost of about \$1,600 per liter. Through spin-on process approximately 95% of resist is wasted and disposed as toxic material [1] .*
2. *Common positive tone resist developer tetramethyl ammonium hydroxide poses health hazards when handled[2] . Acute aquatic toxicity testing of neutralized solution has been shown to be highly toxic to organisms. High resolution features were developed using IPA which is biodegradable, not likely to bioconcentrate, and has low potential to affect organisms.*
3. *Typical iCVD process requires between .02-.12 W/cm<sup>2</sup> [3] for polymer deposition compared to conventional PECVD which uses 0.4-2.1 W/cm<sup>2</sup>[4,5] . No plasma etch eliminates additional >7.1 W/cm<sup>2</sup>[6] power requirement.*

[1] Percin et al., IEEE Transactions on Semiconductor Manufacturing (2003) 16 (3)

[2] Lee et al., J. Micromech. Microeng. (2005) 15

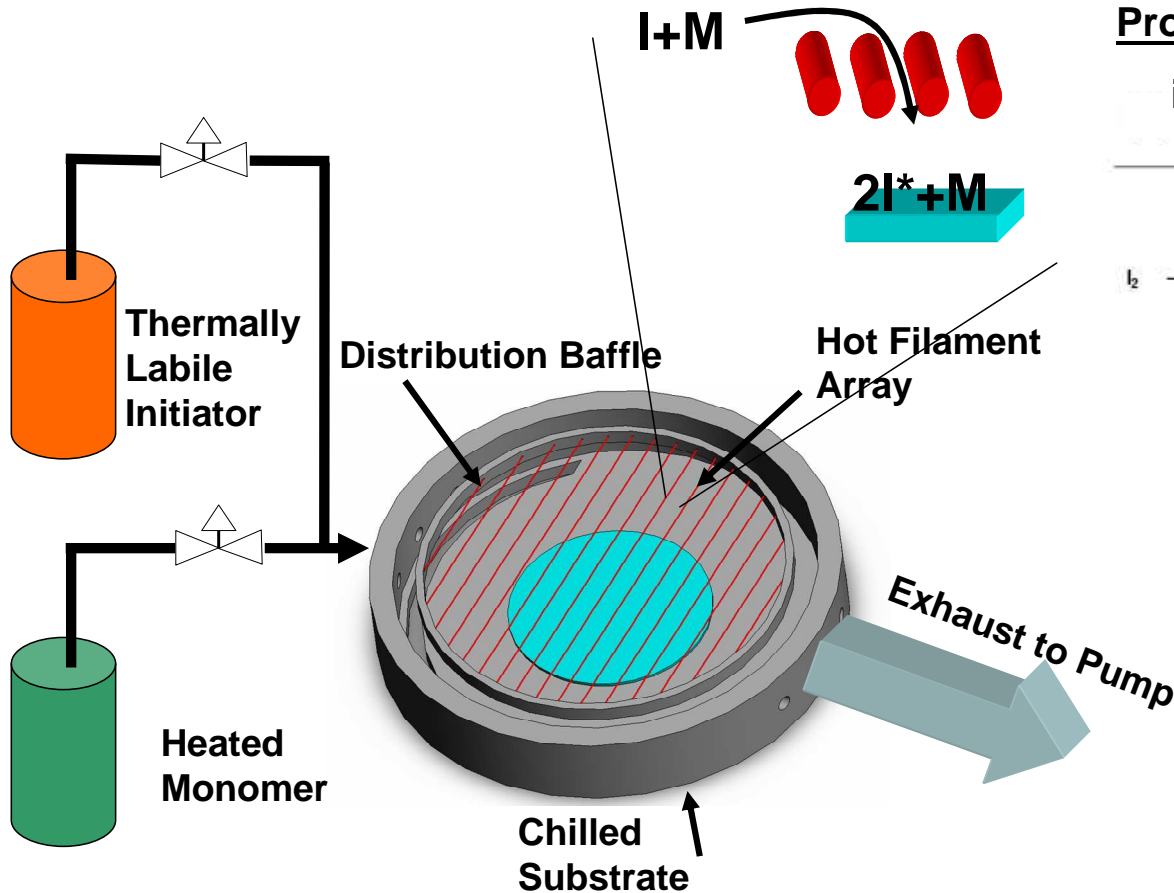
[3] Martin et al. Surf. Coating Tech. (2007) 201

[4] Castex et al. Microelec. Eng. (2005) 82

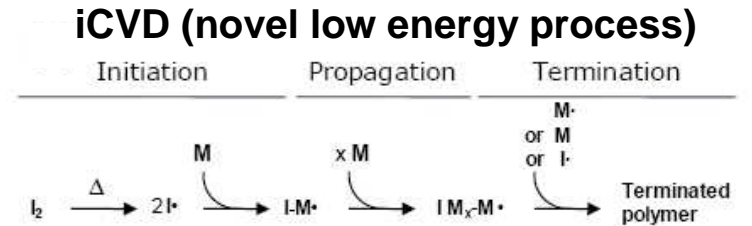
[5] Wong et al. Thin Sol. Films 462–463 (2004)

[6] Berruyer et al. J. Vac. Sci. Technol. A. 16.3 (1998)

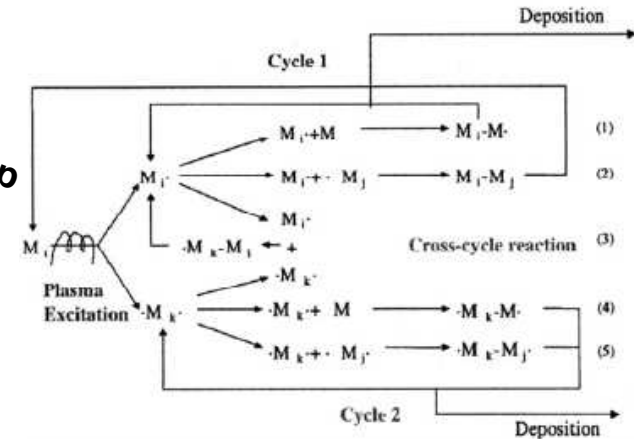
# iCVD Process Chemistry



## Proposed Polymerization Mechanisms



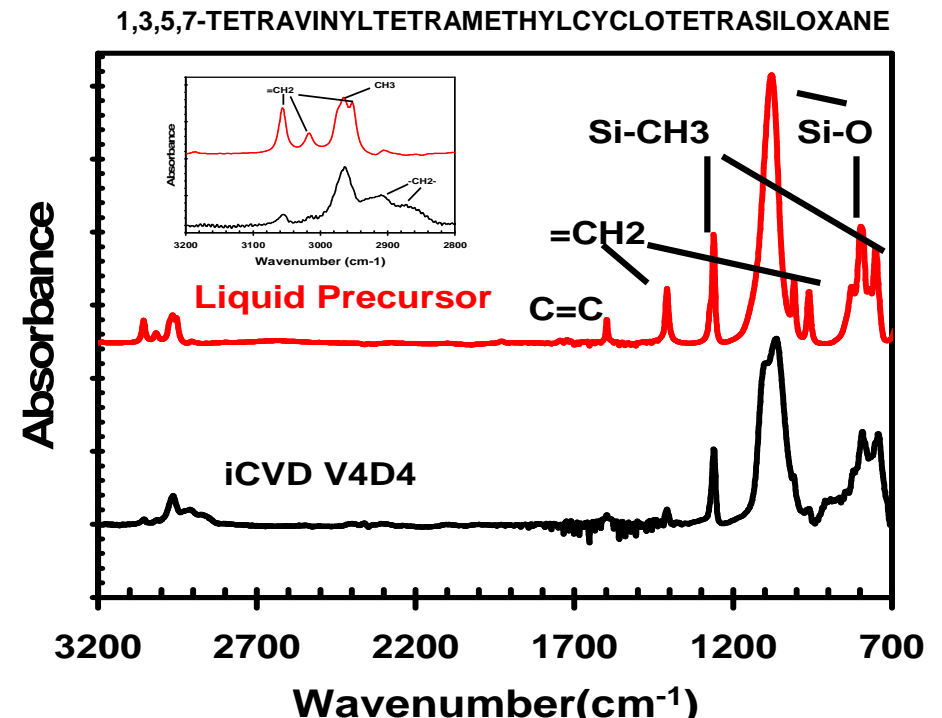
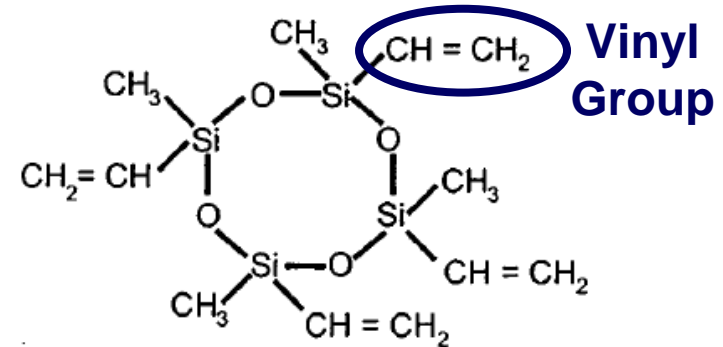
## **PECVD (conventional process)**



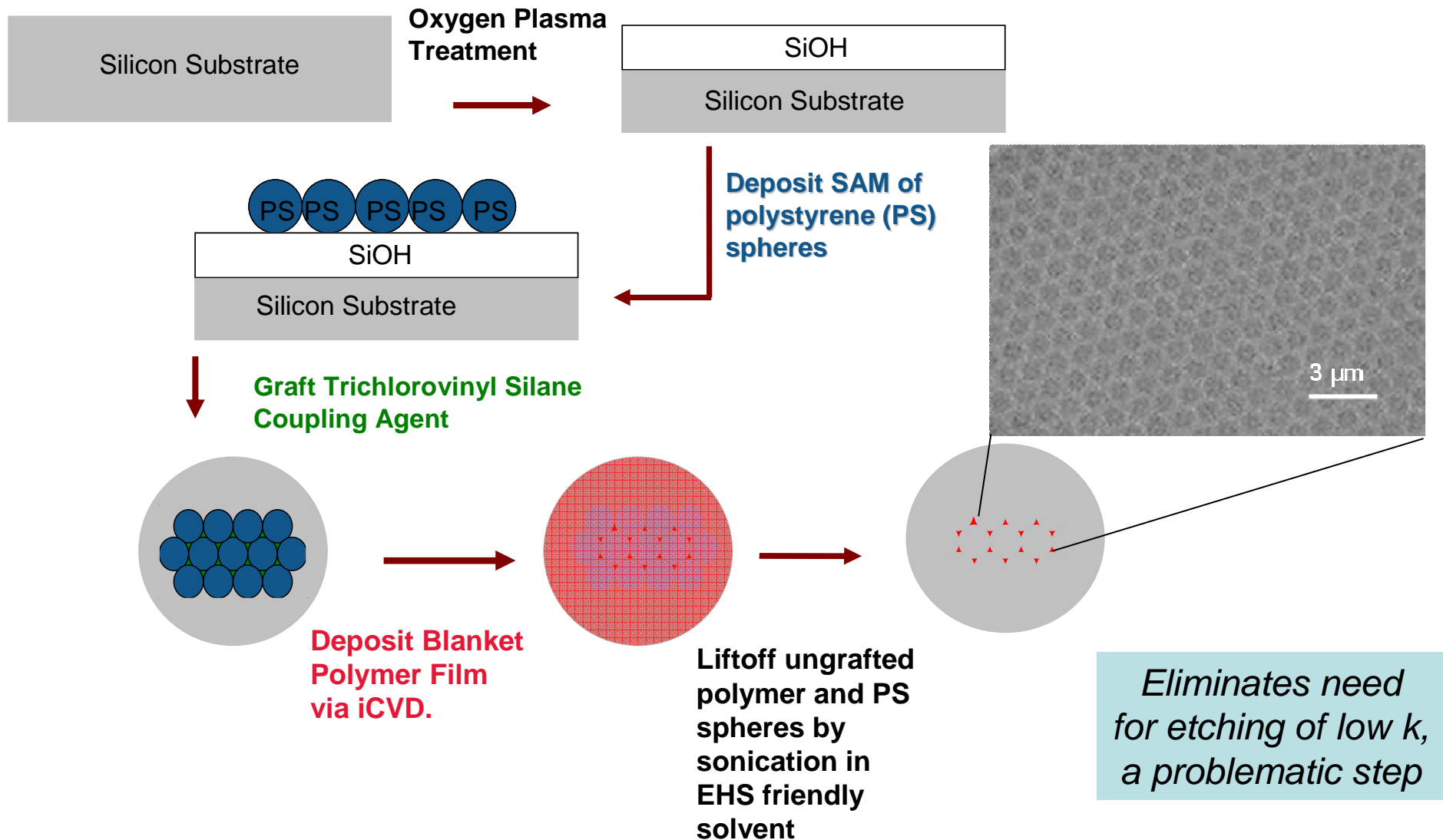


# New Low-k iCVD Precursor V4D4

- Free volume of siloxane ring for low-k
- Chemical structure analogous to commercially used low k organosilicate glass (OSG) precursors such as TOMCATS
- Four vinyl groups make ideal for free radical polymerization via iCVD
- No need for cross linker
- 3-D network from “puckered” ring
- k-value of 2.7 measured at Novellus for dense film, typical for OSG. Last year, reduced k of iCVD V3D3 by incorporating novel porogens provided by Cornell

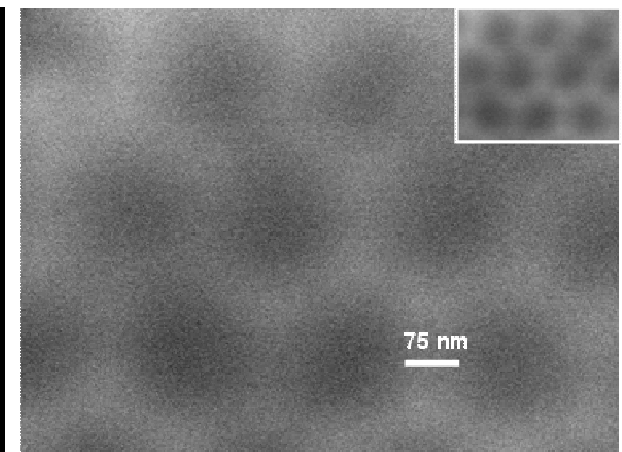
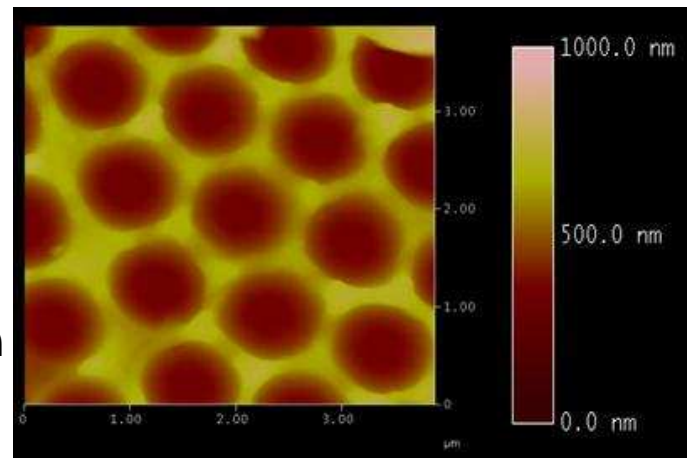
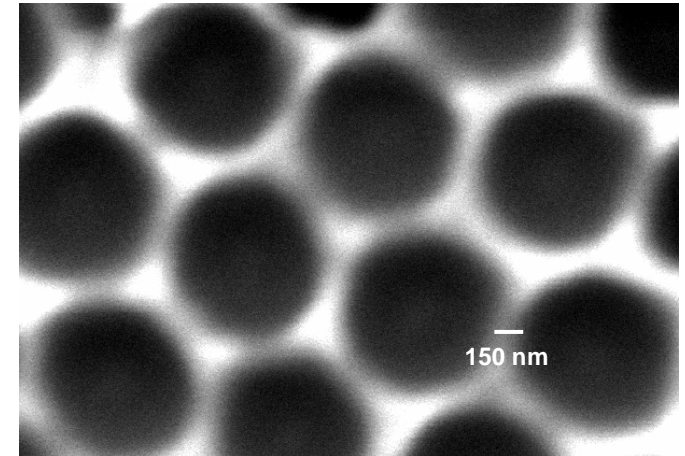
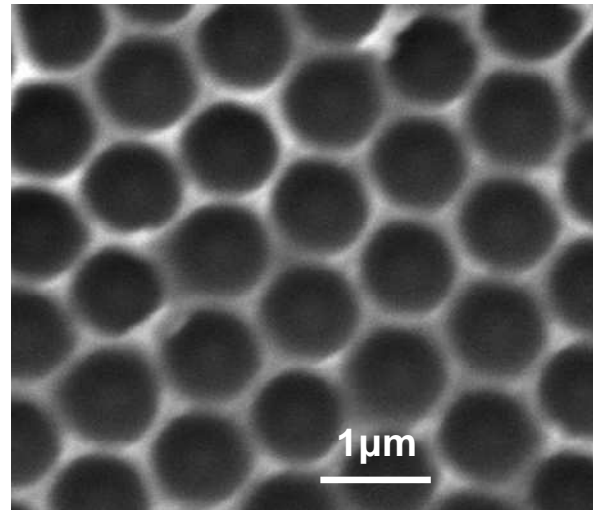


# Additive Polymer Patterning Using Self Assembled Mask (no traditional lithography)

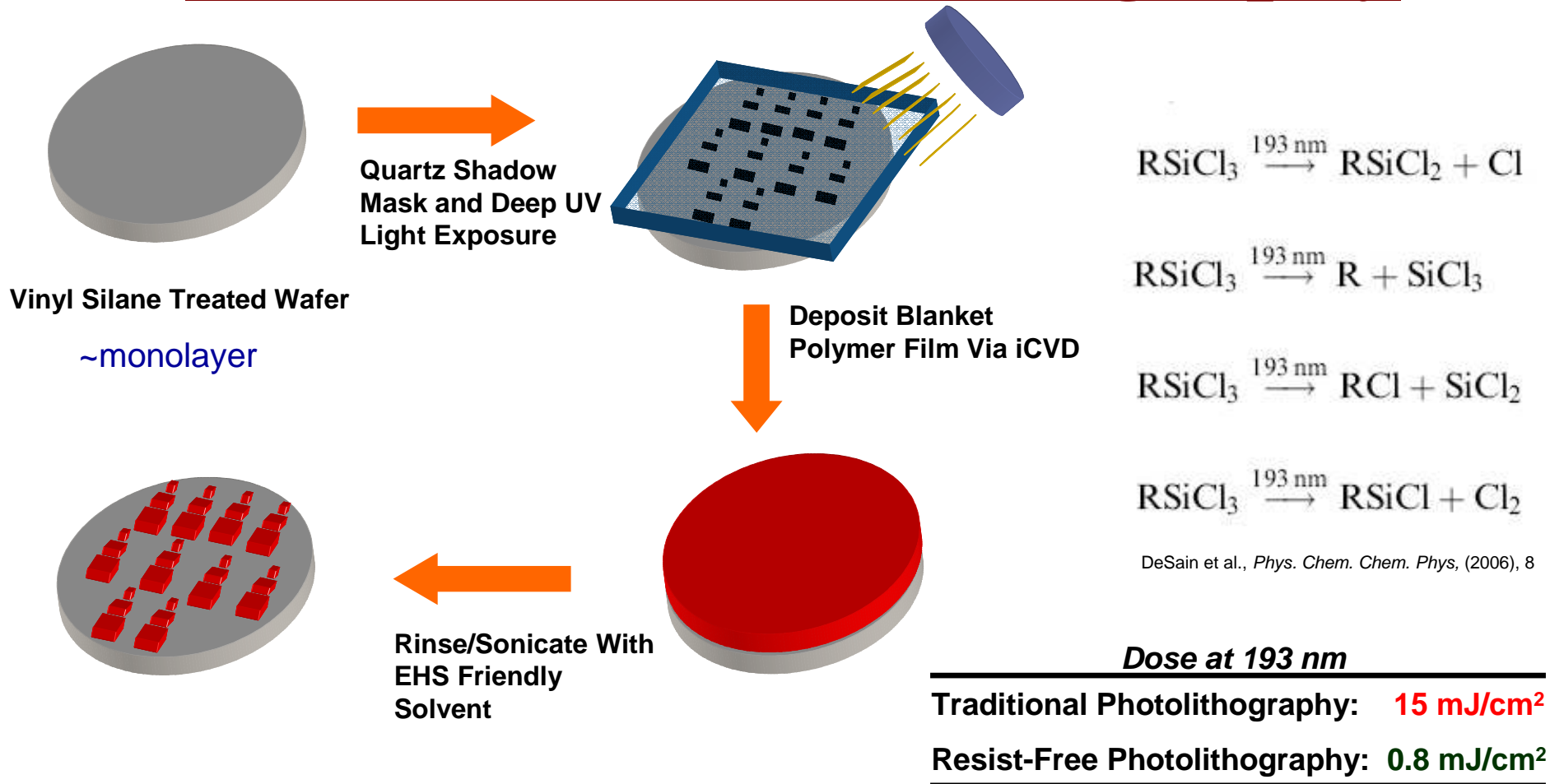


# Low-k iCVD V4D4 Patterns: No Traditional Lithography

- Low k templating with 1  $\mu\text{m}$  and 200 nm diameter spheres
- Very well-ordered patterns achieved after sonicating in environmentally friendly IPA for 1 hr
- Large features up to 700 nm in height and smallest about 75 nm wide and about 100 nm in height
- Excellent substrate adhesion: survives >10 minute sonication in THF



# Resist-Free Photolithography

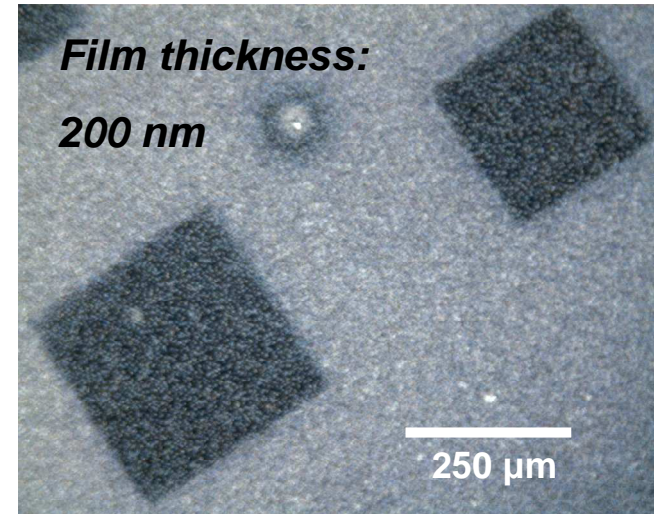
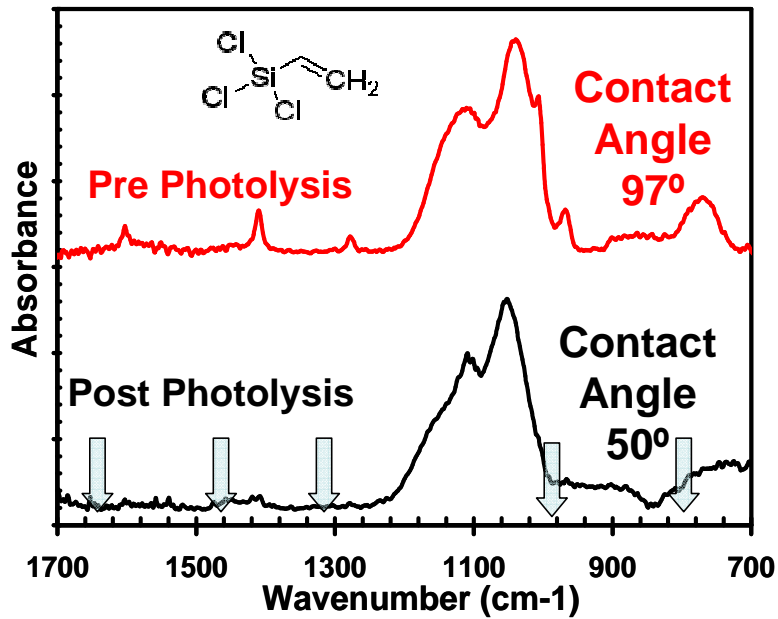


- Exposing grafted vinyl silane monolayer to 193 nm light photolyzes vinyl bonds and removes ability to tether iCVD polymer. Could use commercial steppers for irradiation and lithography masks to define exposure pattern.

SRC/SEMATECH Engineering Research Center for Environmentally Benign Semiconductor Manufacturing

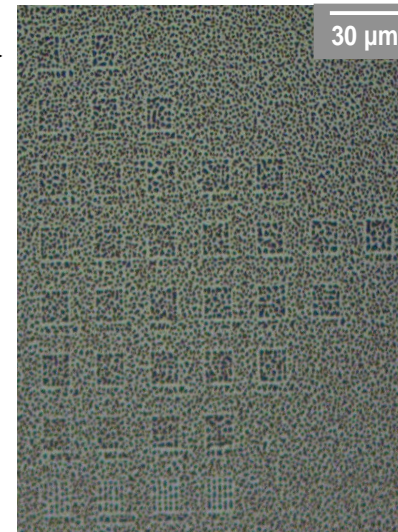
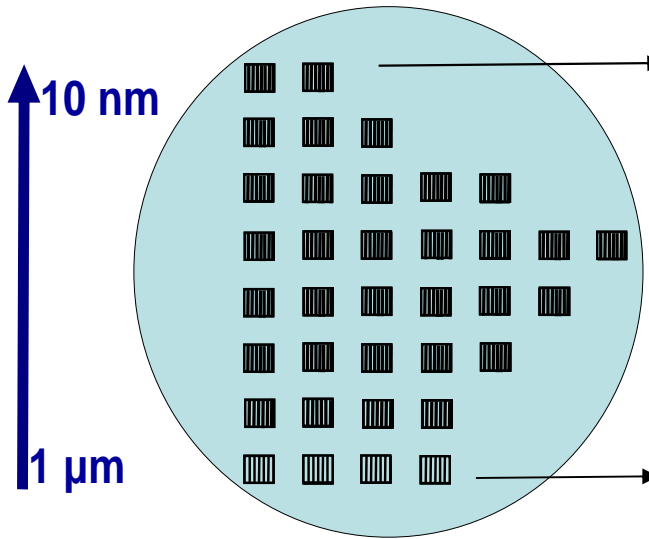
# Resist-Free Patterning

193 nm  
UV



e-beam  
(Ober,  
Cornell)

Decreasing  
Line Width



After lift-off  
polymer should  
and does remain  
everywhere but  
in between the  
lines



# Industrial Interactions and Technology Transfer

- **Harry Levinson, Manager Strategic Lithography Technology and Senior Fellow: AMD**
- **Qingguo Wu, Technologist: Novellus Systems Inc.**
- **Dorel Toma, Director: US Technology Development Center, Tokyo Electron Limited.**
- **Robert Miller, Manager: Advanced Organic Materials Almaden Research Center, IBM**

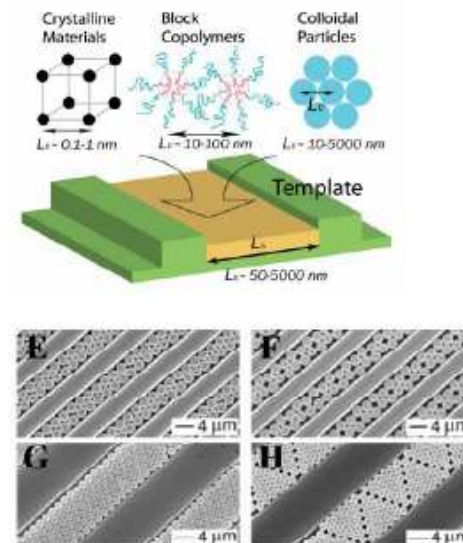
# Future Plans

## Next Year Plans

- Incorporate porogens into additively patterned low k material to reduce k value.
- Achieve resolution of additively patterned low k to sub 50 nm using smaller self assembled polymeric beads
- Optimize iCVD process for resist free patterning using a trichlorovinyl silane surface treatment, patterned by e-beam lithography at Cornell, to achieve sub 50 nm resolution

## Long-Term Plans

Demonstrate the hierarchical use of conventional lithography to define large features which template low defect self assembled iCVD low k



Cheng et al., *Adv. Mater.* (2006), 18

# Publications, Presentations, and Recognitions/Awards

## **PUBLICATIONS**

- W. Shannan O'Shaughnessy, Sal Baxamusa, Karen K. Gleason, "Additively Patterned Polymer Thin Films by Photo-Initiated Chemical Vapor Deposition (piCVD)", Chem. Mater. 19, 5836–5838 (2007).
- W. S. O'Shaughnessy, S. K. Murthy, D. J. Edell, and K. K. Gleason; Stable Insulation Synthesized by Initiated Chemical Vapor Deposition of Poly(1,3,5-trivinyltrimethylcyclotrisiloxane) Biomacromolecules, 8, 2564-2570 (2007).
- O'Shaughnessy, W.S.; Mari-Buye, N.; Borros, S.; and Gleason, K.K.; Initiated Chemical Vapor Deposition (iCVD) of a surface modifiable copolymer for covalent attachment and patterning. Macromol. Rapid Commun. 28, 1877–1882 (2007).
- Tyler P. Martin, Kenneth K.S. Lau, Kelvin Chan, Yu Mao, Malancha Gupta, W. Shannan O'Shaughnessy, Karen K. Gleason, Initiated chemical vapor deposition (iCVD) of polymeric nanocoatings, Surface And Coatings Technology, 201, 9400-9405 (2007).
- O'Shaughnessy, W.S.; Edell, D.J.; Gleason, K.K.; Thin Solid Films, Initiated chemical vapor deposition of biopassivation coatings, Thin Solid Films 516, 684-686 (2008).
- Ph.D. Thesis, W. Shannan O'Shaughnessy, Dept. of Chemical Engineering, MIT

## **PRESENTATIONS**

- K.K. Gleason, Polymeric Nanocoatings by Chemical Vapor Deposition, Pall Corporation, 2/6/2007
- K.K. Gleason, Design of CVD processes for low k dielectrics and air gap formation, 2007 MRS Spring Meeting:Symp. B, San Francisco, CA 4/11/2007 (invited)
- K.K. Gleason, Initiated chemical vapor deposition (iCVD) of polymeric nanocoatings, 16th European Conference on Chemical Vapor Deposition, Den Haag, Netherlands, 9/20/2007 (invited).
- K.K. Gleason, Chemical Vapor Deposition of Polymeric Nanocoatings, U. Calgary, Dept. Chemical Engineering, 10/5/2007 (invited).
- K.K. Gleason, Conformal Polymeric Thin Films via Initiated Chemical Vapor Deposition, AVS Seattle, WA, 10/15/2007 (invited)
- K.K. Gleason, Engineering Polymeric Nanocoatings by Vapor Deposition 31th Annual Symposium of the Macromolecular Science and Engineering Program at the University of Michigan., Ann Arbor, MI, 10/25/2007 (invited).
- Nathan J. Trujillo and Karen K. Gleason, ERC TeleSeminar, "Additive Patterning of Low Dielectric Constant Polymer Using iCVD", December 13, 2007

*SRC/SEMATECH Engineering Research Center for Environmentally Benign Semiconductor Manufacturing*



# Synthesis of Low-k Films in CO<sub>2</sub>: High Mechanical Strength and Direct Patterning

---



Alvin Romang, Sivakumar Nagarajan, Tom Russell and Jim Watkins  
Polymer Science and Engineering, University of Massachusetts-Amherst  
Collaborators: Chris Ober, Cornell University and Karen Gleason, MIT  
*Task Number: 425.017; Watkins sub-task*

*SRC/Sematech Engineering Research Center for Environmentally Benign Semiconductor Manufacturing*

# ULK Films Synthesis in CO<sub>2</sub>

---

## First Generation Films:

- $k < 2.2$  demonstrated
- Rapid processing time and survives CMP
- Low stress and high crack threshold

## Film Improvements:

- POSS addition for mechanical properties
- Bridged silsesquioxanes for  $k$  and mechanical properties

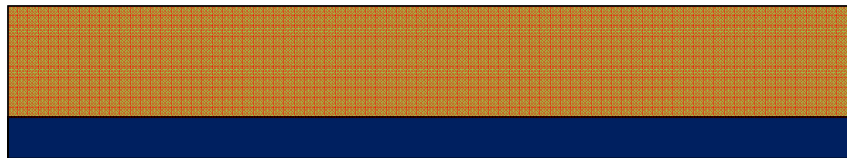
## Direct Patterning:

- Direct implementation into current process
- Patterned low- $k$  films without etching

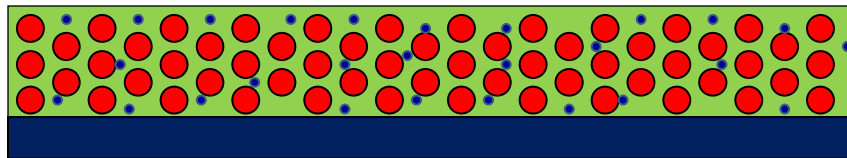


# ULK Synthesis Route

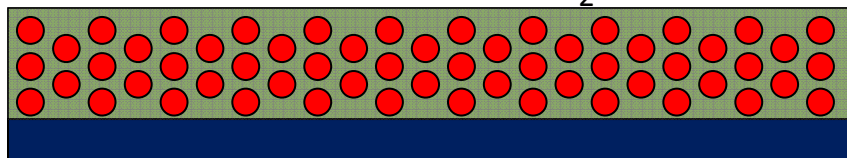
Block copolymer template/POSS and acid catalyst, spin coat



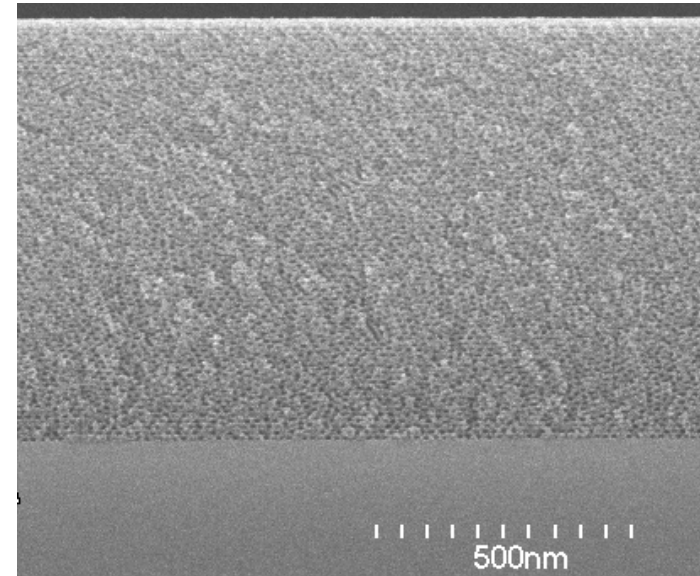
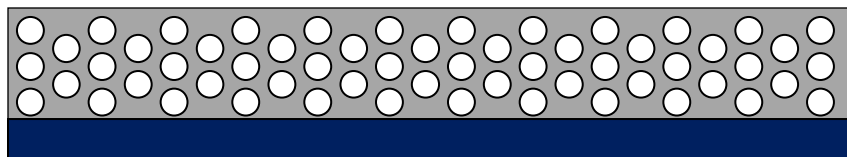
Anneal/order/orient



$M(OR)_x$  infusion in humidified  $CO_2$



400 °C calcination

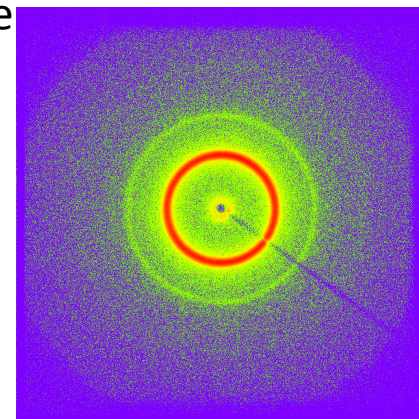
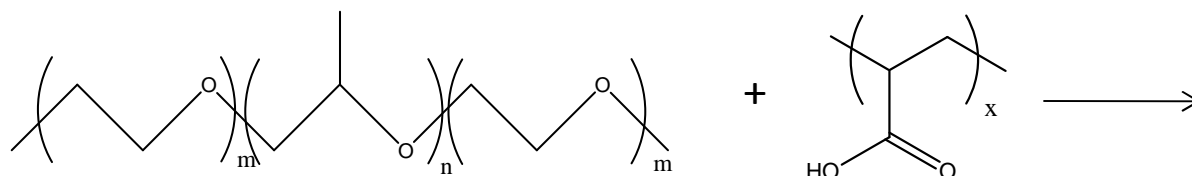


- Alkoxide condensation separate from template ordering
- Preservation of BCP detail structure in the silica replication
- High degree of silica condensation
- Rapid processing cycle

*Pai et al., Science, 303, 507, 2004*

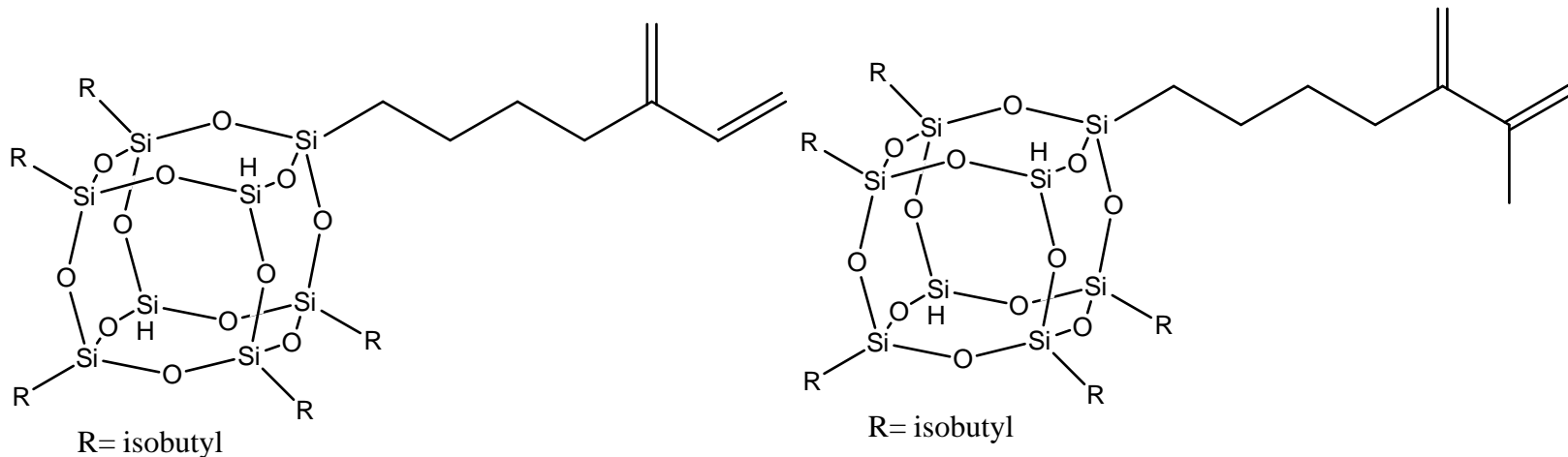
# POSS-PAA and Pluronic Blends

PAA/Pluronic blends yield highly ordered phase separated template



*Tirumala, V.R. et al. Adv. Mater. accepted*

Free radical copolymerization of AA with POSS monomer



R= isobutyl

Acryloisobutyl POSS (Mw = 929.61)

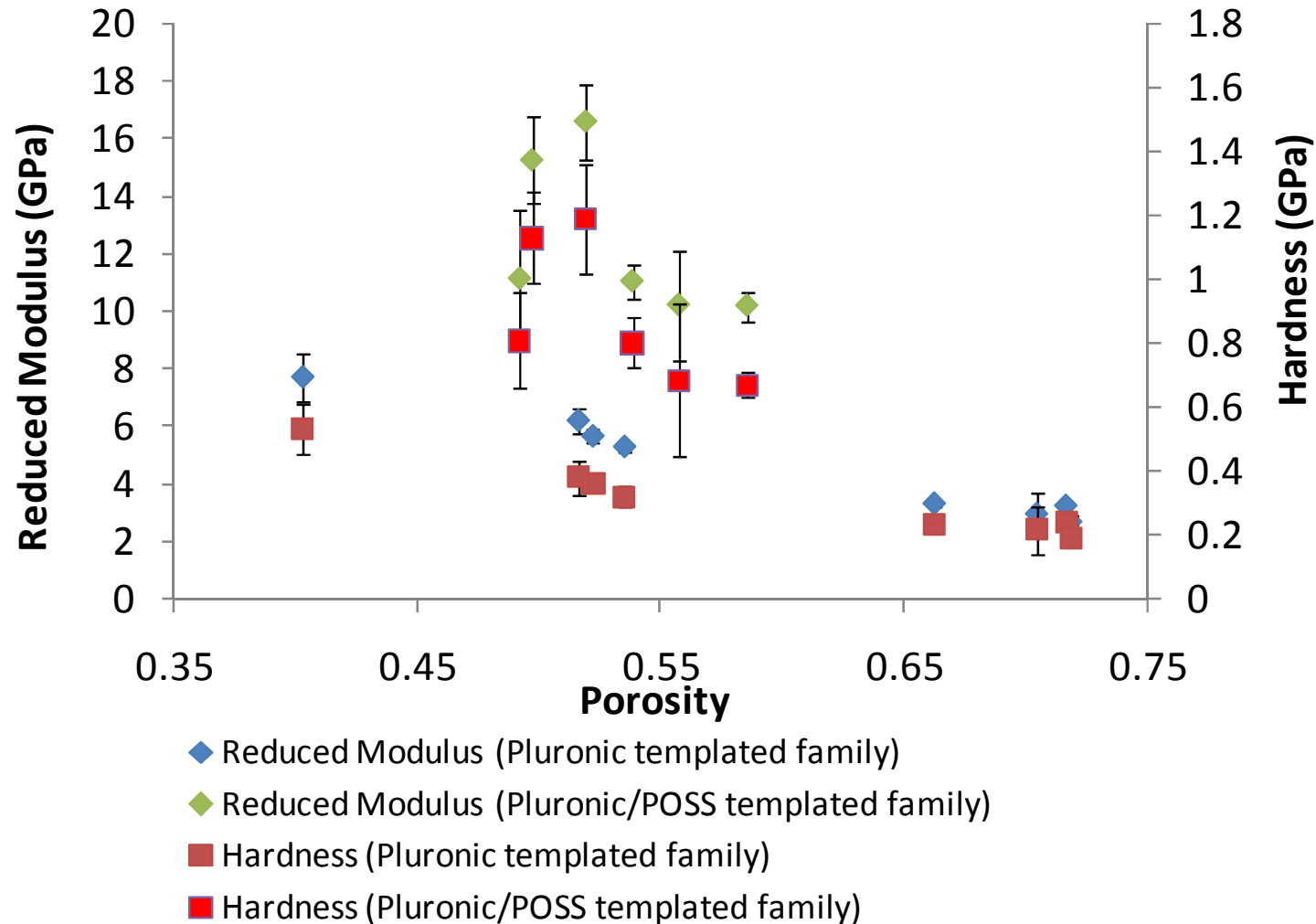
ACPOSS

R= isobutyl

Methacrylisobutyl POSS (Mw = 943.61)

MIBPOSS

# Mechanical Strength Increase with POSS



Higher modulus and hardness of POSS doped films for given porosities measured by nanoindentation. Porosities were measured by spectroscopic ellipsometry

*SRC/Sematech Engineering Research Center for Environmentally Benign Semiconductor Manufacturing*

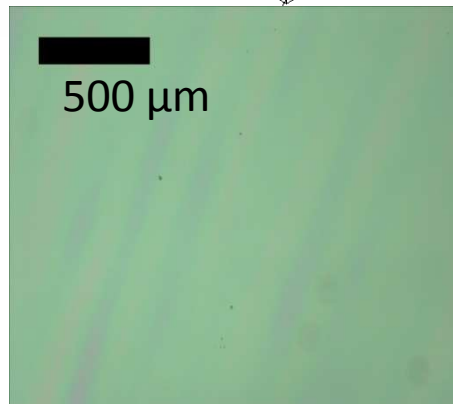
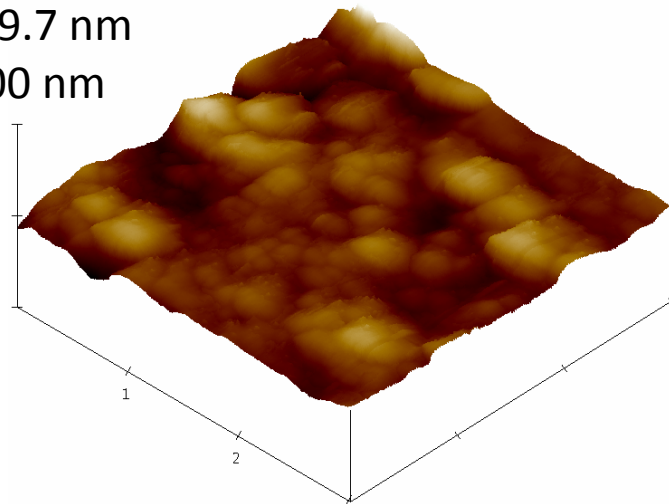


# Smooth Films Throughout the Substrate

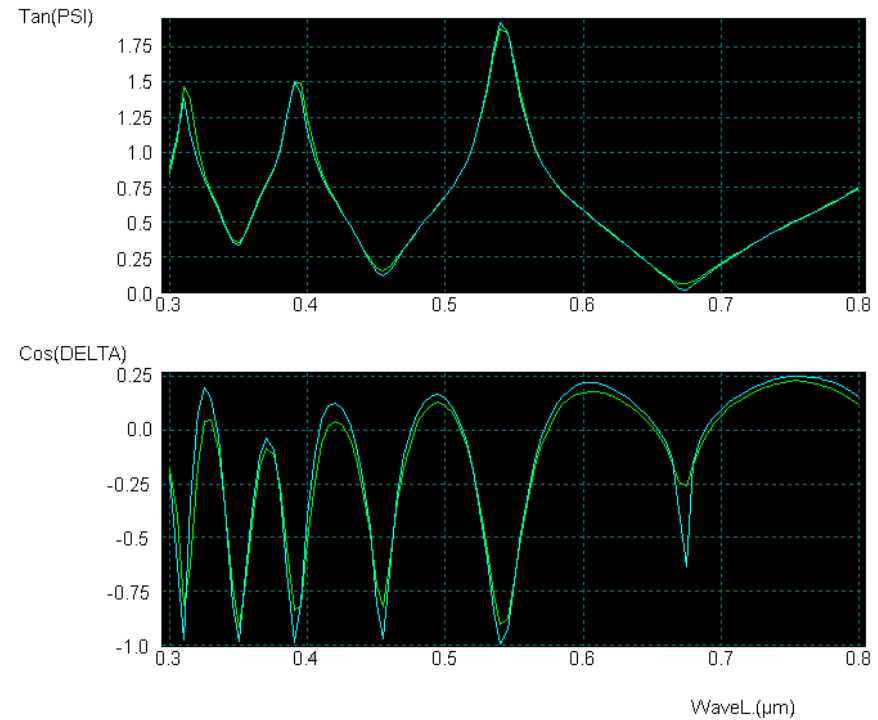
RMS Roughness: 5.7 nm

Z range: 49.7 nm

Z scale: 100 nm



Optical micrograph showing long-range film smoothness



Ellipsometry fit for porosity

Film details:

Calcined silica film

F108/Poly(ACPOSS-co-AA (2:1)) blend at 7:3 by wt.

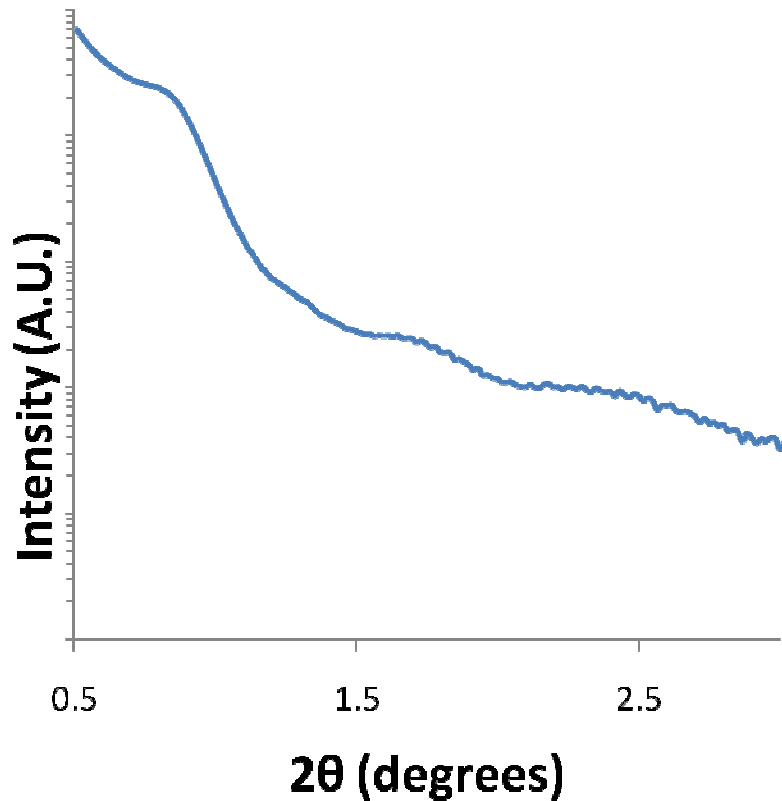
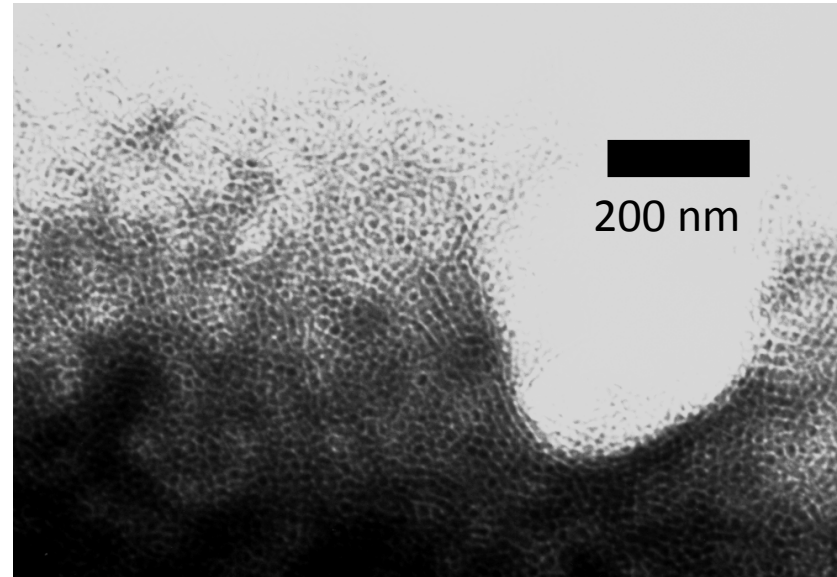
Thickness: 920 nm, Porosity: 52%

TEOS precursor in CO<sub>2</sub> at 60 °C



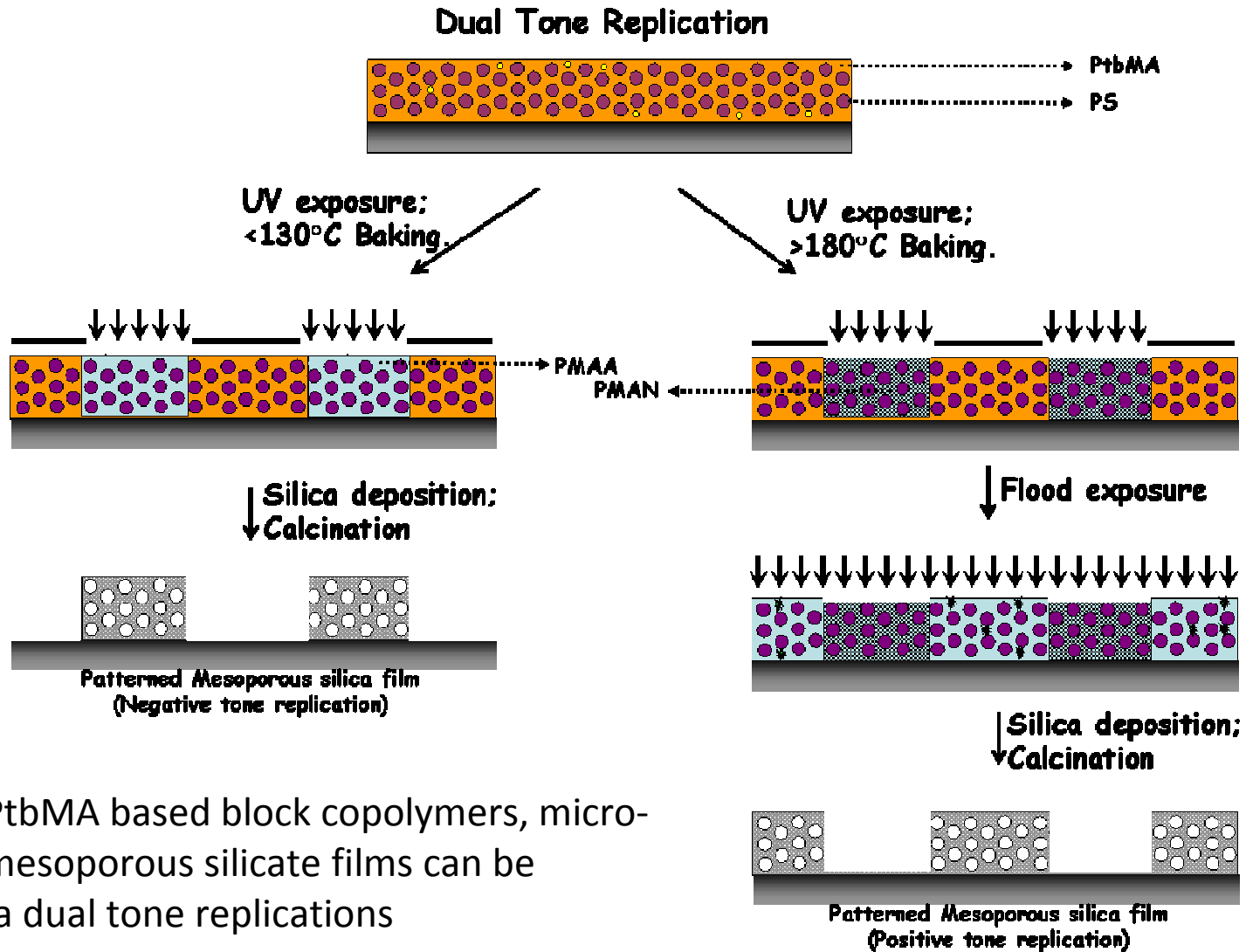
# Domain Level Porosity

TEM image shows ordered porous structure at the domain level



Small angle XRD of the film shows correlation peaks of the film porosity

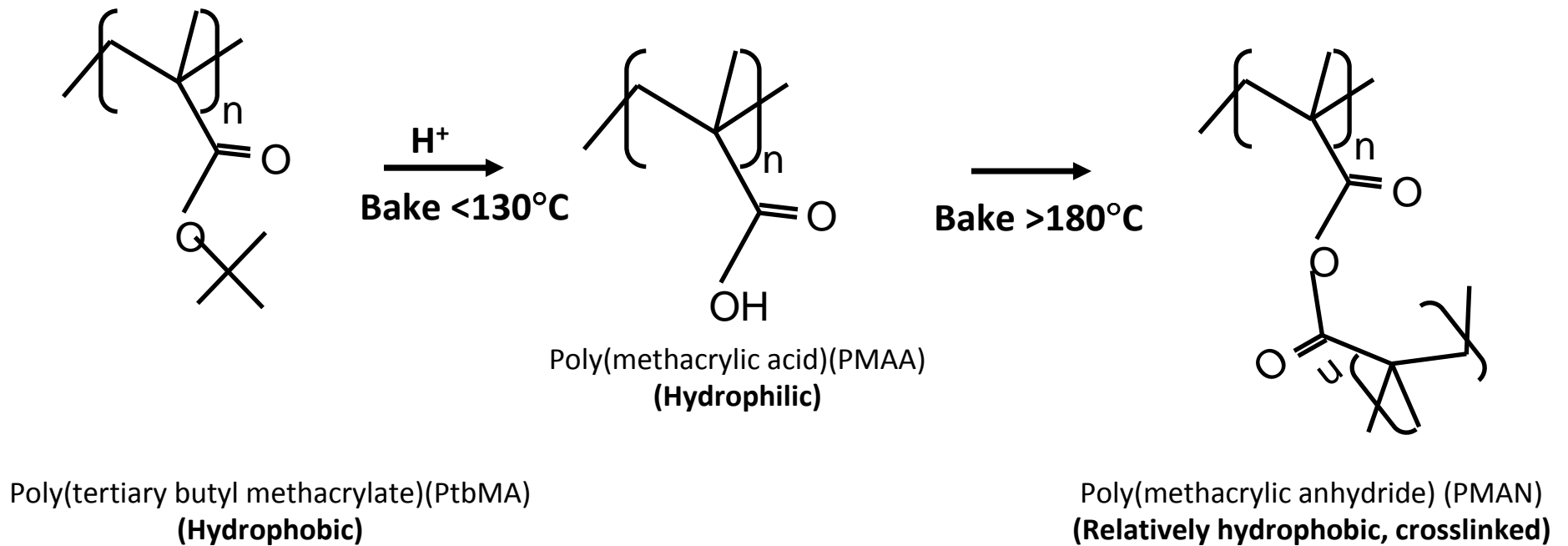
# Schematic of Direct Patterning



By using a PtBMA based block copolymers, micro-patterned mesoporous silicate films can be obtained via dual tone replications



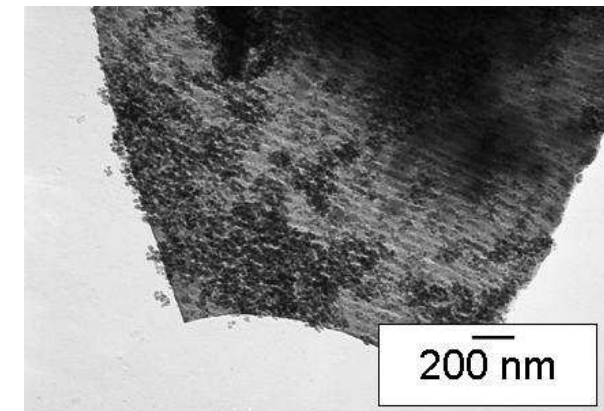
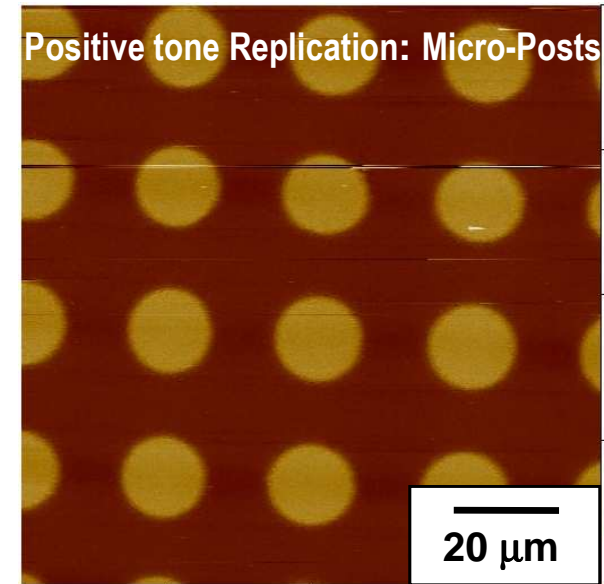
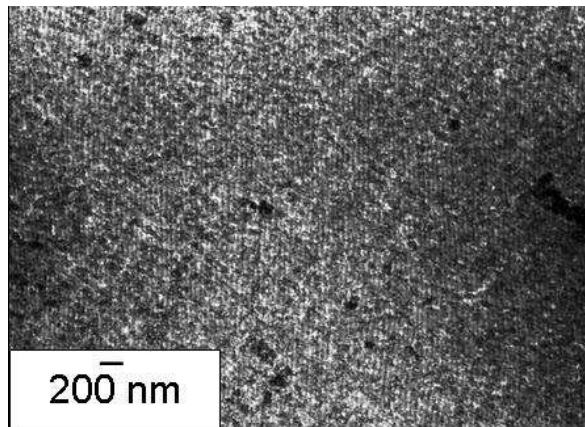
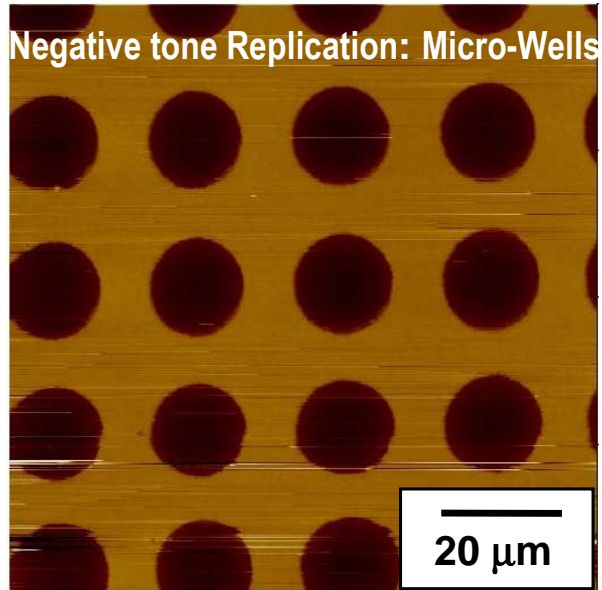
# Chemical Amplification PtbMA for 193 nm line



*Ito H et al., Macromolecules 1988*



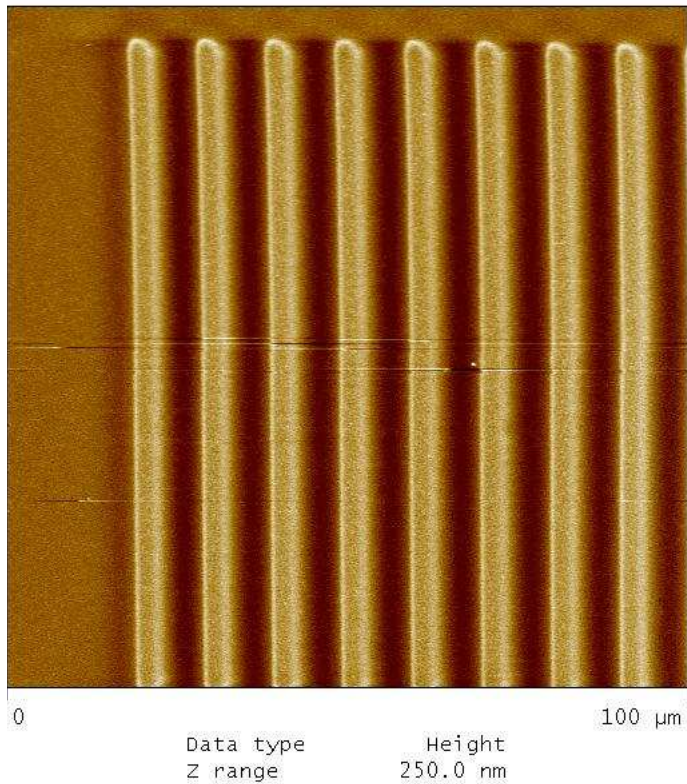
# Device and Domain Levels Replication



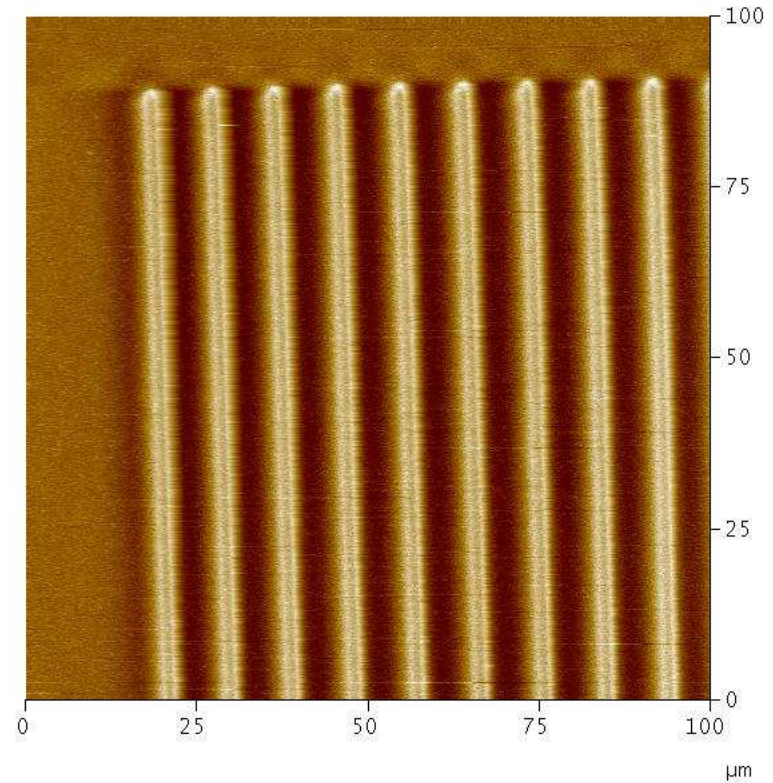
Crude contact mask photolithography

# Lines and Spaces Pattern with Sharp Boundaries

Lines: ~ 4  $\mu\text{m}$  ; Space: ~ 6 $\mu\text{m}$



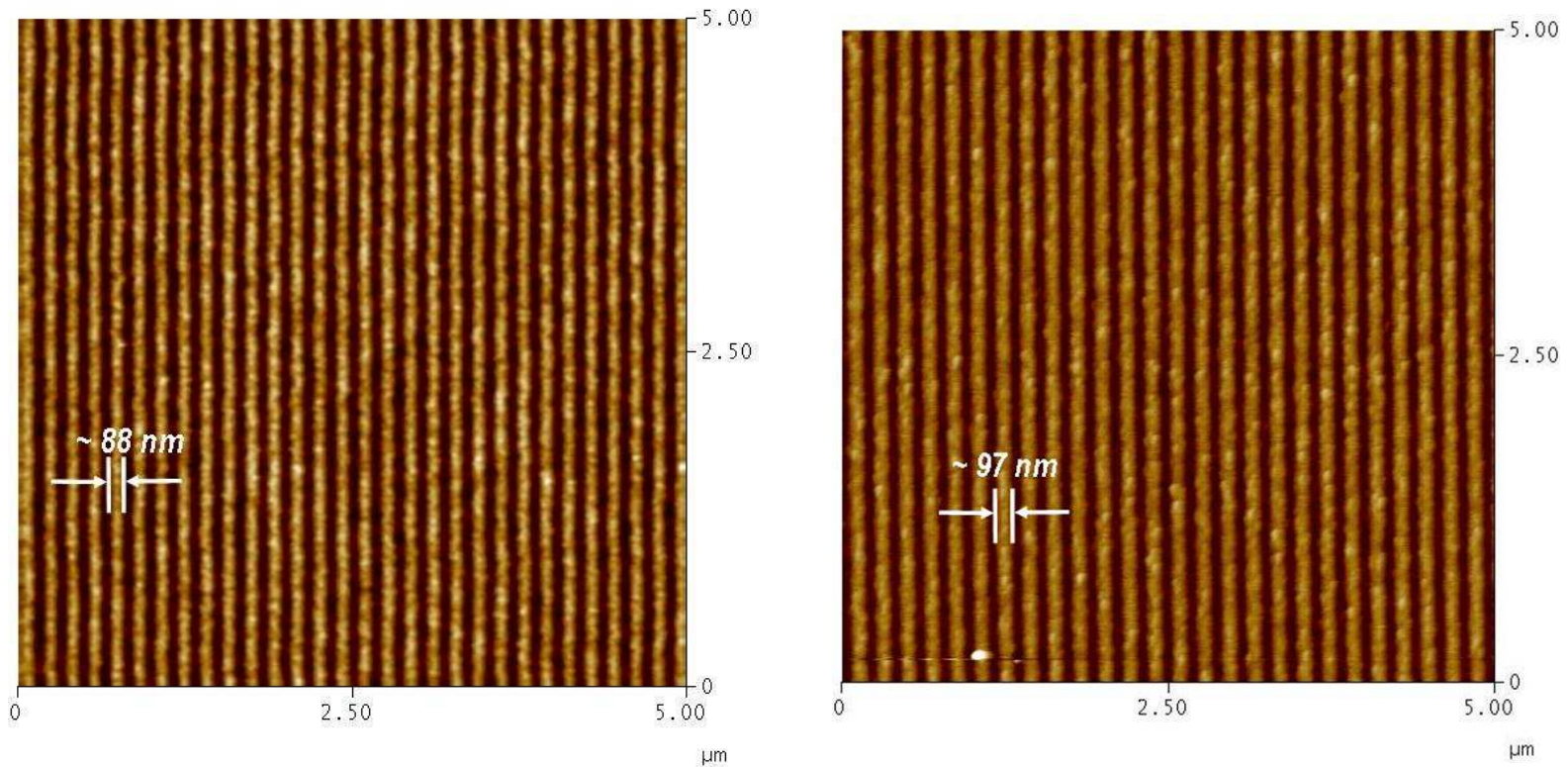
Lines: ~ 2.5  $\mu\text{m}$  ; Space: ~ 6 $\mu\text{m}$



Limitation on photolithography, not the direct patterning process



# Sub-100 nm silica patterning



In collaboration with industrial partner:

- Sub 100 nm direct patterning was demonstrated
- First attempt using off-the-shelf photo resist
- **Bypassing the etching step**

Potential for cost savings and streamlined process integration

# Conclusions and Future Work

---

## High Mechanical Strength Films

- Achieved higher hardness and modulus with long-range film uniformity
- POSS-PAA copolymers increase POSS compatibility with the Pluronic templates

## Directly Patterning Dielectrics

- Direct patterning on 248 and 193 nm resists
- Sub-100 nm patterning without etch

## Future Work

- Optimize the template and precursor chemistry for high hardness and low k films
- Optimize resists and resolution of the directly patterned template
- Explore NIL of new monomers with Gleason

## Additional Funding

- NSF Center for Hierarchical Manufacturing at UMass Amherst
- NSF NIRT



# Destruction of Perfluoroalkyl Surfactants (PFAS) in Semiconductor Process Waters using Boron Doped Diamond Film Electrodes

**Task # 425.018 / Thrust C**

Kimberly Carter, James Farrell, Valeria Ochoa, Reyes Sierra  
Department of Chemical and Environmental Engineering  
The University of Arizona

# Research Objectives

- Determine the feasibility of oxidative destruction of PFOS and PFBS using BDD electrodes.
- Determine the reaction products.
- Determine the reaction mechanisms and rate limiting steps.
- Develop a multi-step concentration and destruction treatment technology.
- Pilot test treatment technology at a semiconductor facility.

# ESH Impact / ESH Metrics

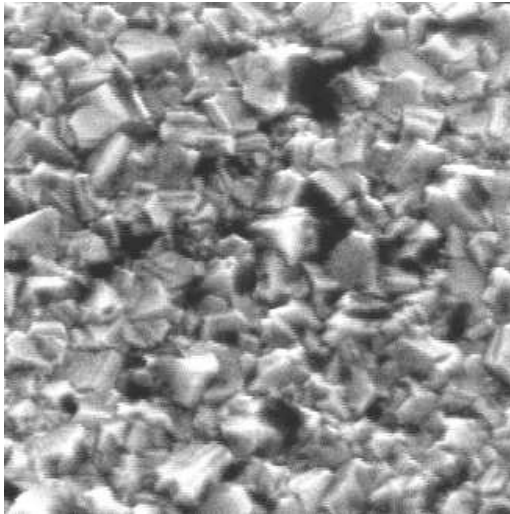
- PFAS are used in photoresist developers and antireflective coatings.
- Most PFAS waste is contained in organic solvents and destroyed by incineration.
- There is a need to treat dilute aqueous waste streams containing PFAS.
- Ion exchange, carbon adsorption, UV/peroxide, sonolysis & biodegradation treatments are impractical or ineffective.
- An effective method for removing PFAS from aqueous waste streams is needed in order to secure a limited use exemption from the U.S. Environmental Protection Agency.

<b>Goal/Possibilities</b>	<b>Energy</b>	<b>PFCs</b>
Remove PFAS from aqueous waste streams	Elimination of costly reverse osmosis treatments	>99% removal from disposed wastewaters



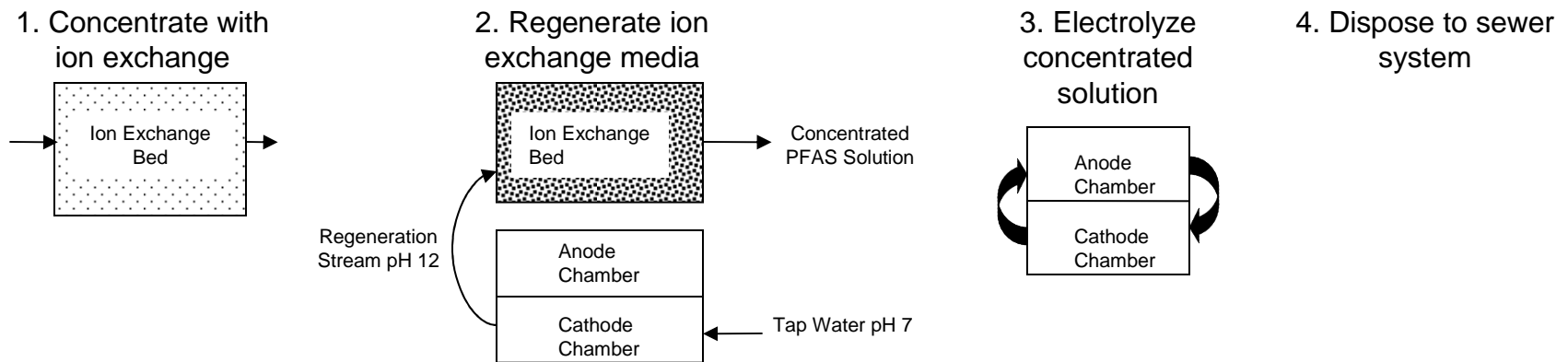
# Boron-Doped Diamond Film (BDD) Electrodes

- Diamond film grown on p-silicon substrate using CVD
- Boron doping provides electrical conductivity
- Highly stable under anodic polarization
- No catalyst to foul or leach from electrode
- Emerging technology being adopted for water disinfection



Scanning electron micrograph of BDD electrode. The individual diamond crystals are  $\sim 0.5 \mu\text{m}$  in size.

# Proposed Treatment Scheme



## Multi-step treatment scheme:

1. Concentrate PFAS from dilute aqueous solutions using ion exchange resin.
2. Regenerate ion exchange resin using cathodically generated high pH solution.
3. Recirculate concentrated PFAS solution through a BDD electrode reactor.
4. Dispose of treated solution containing electrolysis products ( $\text{CO}_2$  &  $\text{F}^-$ ) into sanitary sewer system.

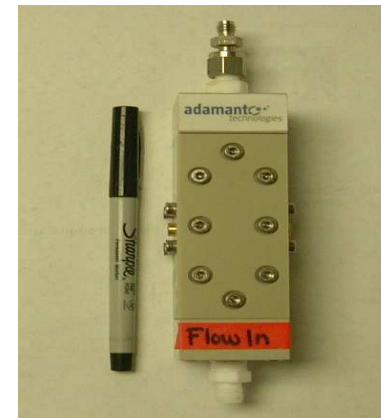
# Experimental Systems



- No mass transfer limitations
- Electrode surface area = 1 cm<sup>2</sup>
- Solution volume = 350 mL
- $a_s = 0.00286 \text{ cm}^2/\text{mL}$

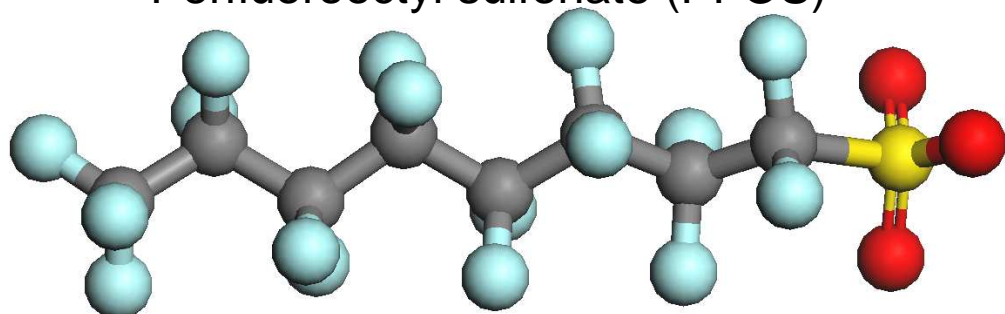
- Rates similar to real treatment process
- Electrode surface area = 25 cm<sup>2</sup>
- Solution volume = 15 mL
- $a_s = 1.67 \text{ cm}^2/\text{mL}$

Parallel plate flow-cell.



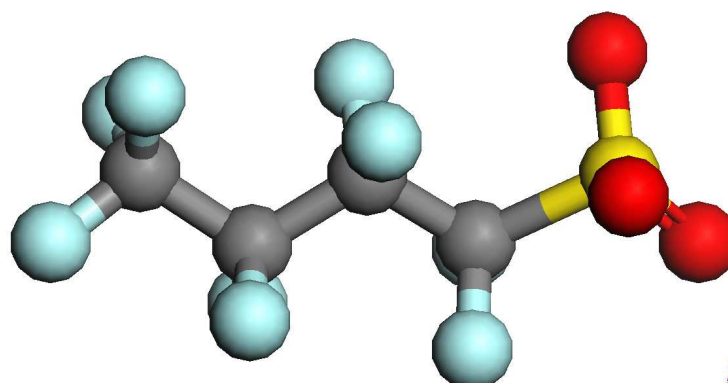
# Target Compounds: Perfluorooctyl sulfonate & Perfluorobutyl sulfonate

Perfluorooctyl sulfonate (PFOS)



Most widely used PFAS.

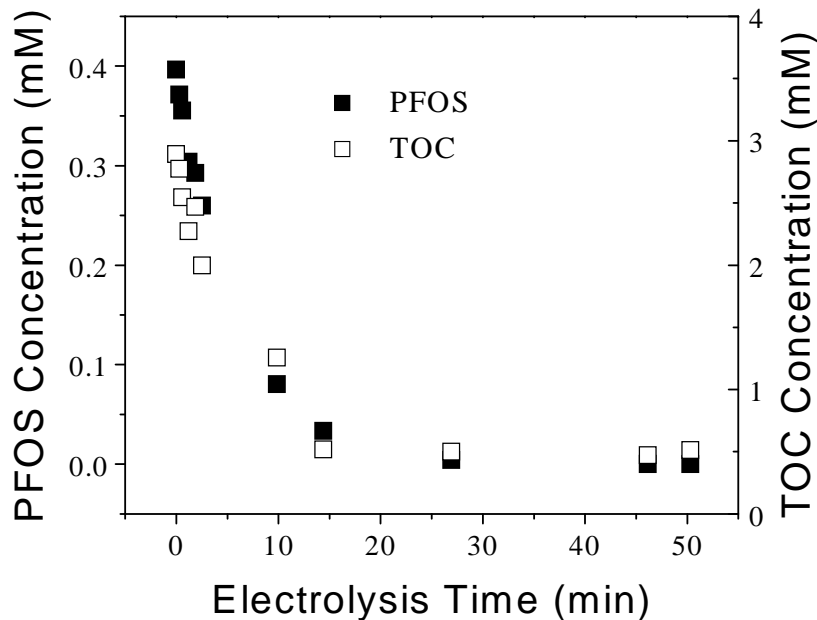
Perfluorobutyl sulfonate (PFBS)



Suggested replacement for PFOS.

- Used in semiconductor for electroplating and electronic etching baths, photographic emulsifiers, and surface treatment agents for photolithography.
- Does not biodegrade in wastewater treatment plants or in the environment.
- Does not react with conventional advanced oxidation processes.
- Worldwide average human blood serum concentrations of 164  $\mu\text{g/L}$ .
- Accumulates in the liver with a half-life in the human body ~ 4 to 20 years.

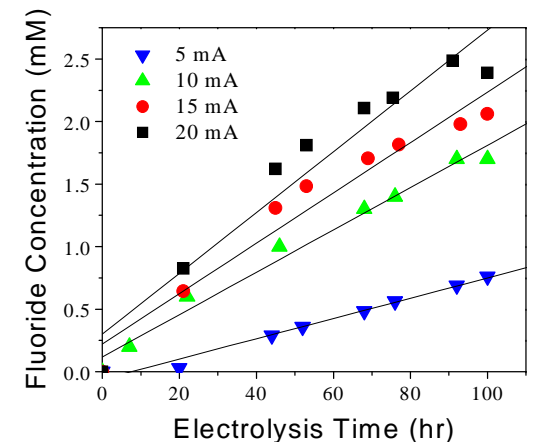
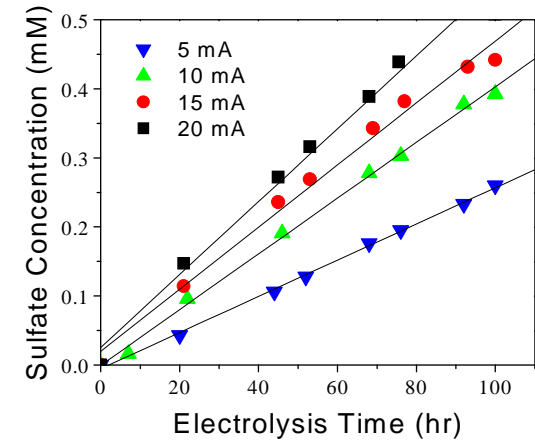
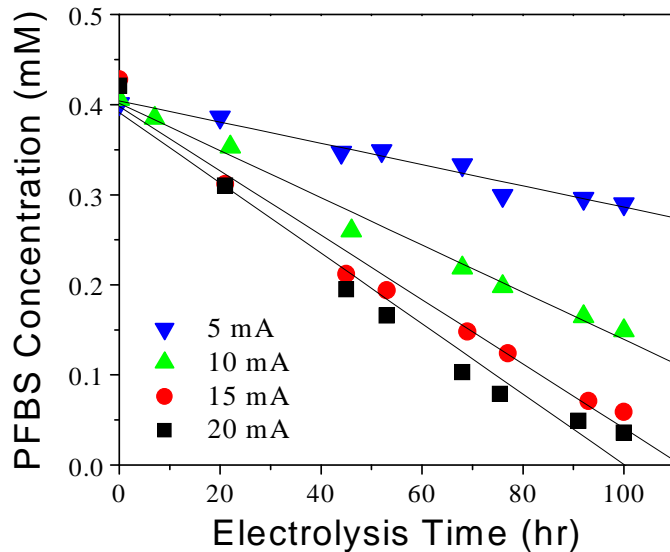
# Experimental Results: Flow Through Reactor



PFOS & total organic carbon (TOC) concentrations as a function of electrolysis time for the flow-cell operated at a current density of 20 mA/cm<sup>2</sup>.

- PFOS can be rapidly removed from water with a half-life ~7 min.
- Reaction rates are first order in PFOS concentration.
- No build-up of fluorinated organic reaction products.
- Similar results observed for PFBS.

# Experimental Results: Rotating Disk Reactor

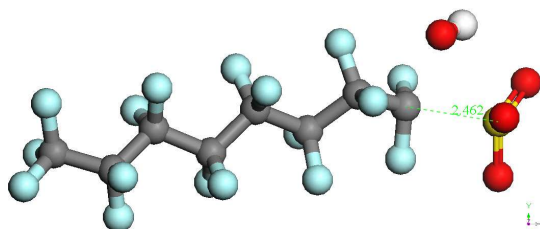


- Reaction rates are 0<sup>th</sup> order in PFBS concentration.
- 1 sulfate ion produced per PFBS degraded.
- 7.5 out of 9 fluoride ions per PFBS degraded.
- 14 out of 17 fluoride ions per PFOS degraded.
- Some fluoride loss via HOF volatilization.

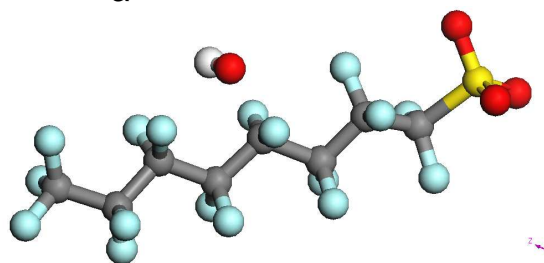
# Quantum Chemistry Modeling: Activation Energies for HO• Attack

## Transition State Structures

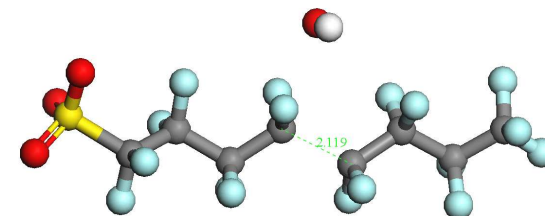
$E_a = 123$  kJ/mol



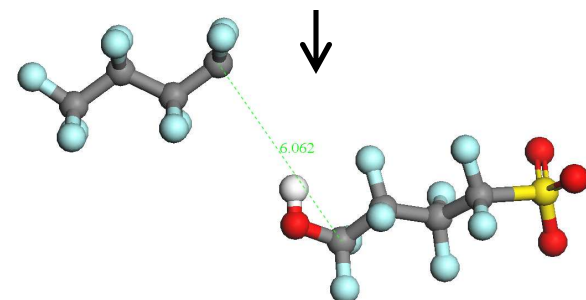
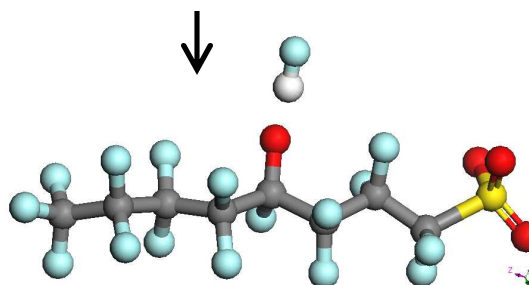
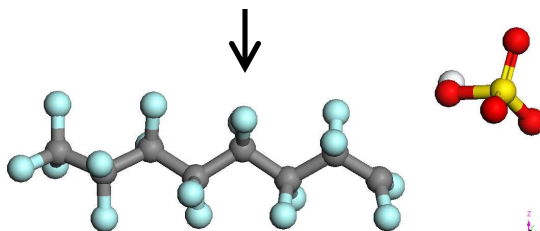
$E_a = 241$  kJ/mol



$E_a = 169$  kJ/mol



## Final Products



- Activation energies are much higher than those observed for compounds that readily react at room temperature.
- PCBs are unreactive with HO• at room temperature:  $E_a = 71-93$  kJ/mol.
- Phenol readily reacts with HO• at room temperature:  $E_a = 4-25$  kJ/mol.

# Reaction Mechanisms

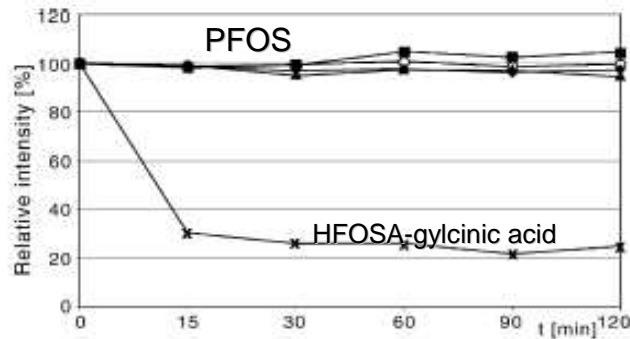


Fig. 1. Graphs of elimination for PFOS and HFOSA-glycinic acid under AOP treatment over a period of 120 min applying different AOP reagents (PFOS treated with:  $O_3$  ▲;  $O_3/UV$  ■;  $O_3/H_2O_2$  ◆; Fenton ○; HFOSA-glycinic acid treated with:  $O_3/UV$  x).

PFOS unreactive with:

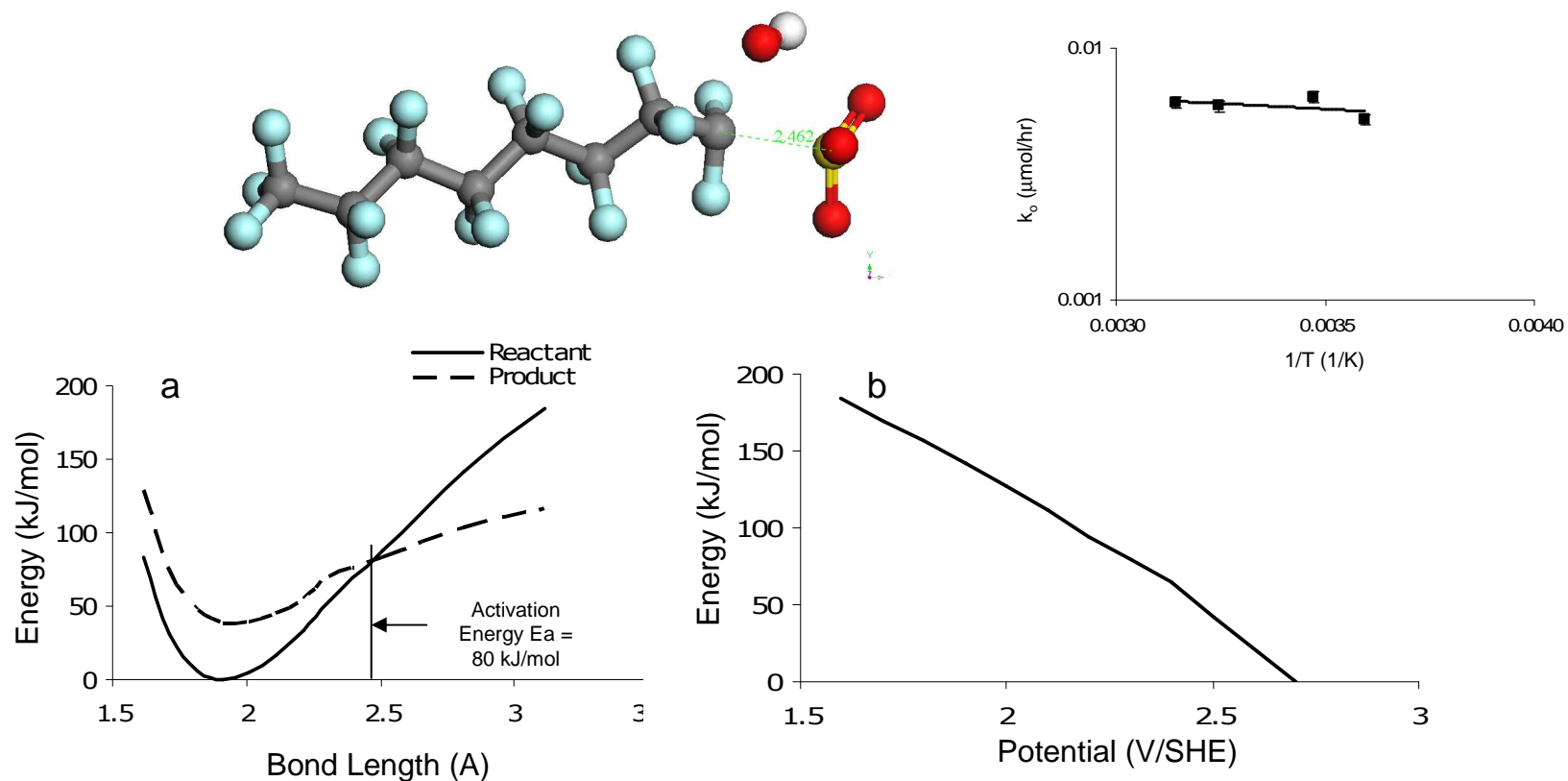
1.  $O_3$
2.  $O_3/UV$
3.  $H_2O_2/O_3$
4.  $H_2O_2/Fenton (Fe^{2+}/Fe^{3+})$

Schroder and Meesters, *J. Chromatog. A.*, 2005.

High activation energies for oxidation by  $HO^\bullet$  is consistent with absence of reactivity with  $H_2O_2$  based AOPs.

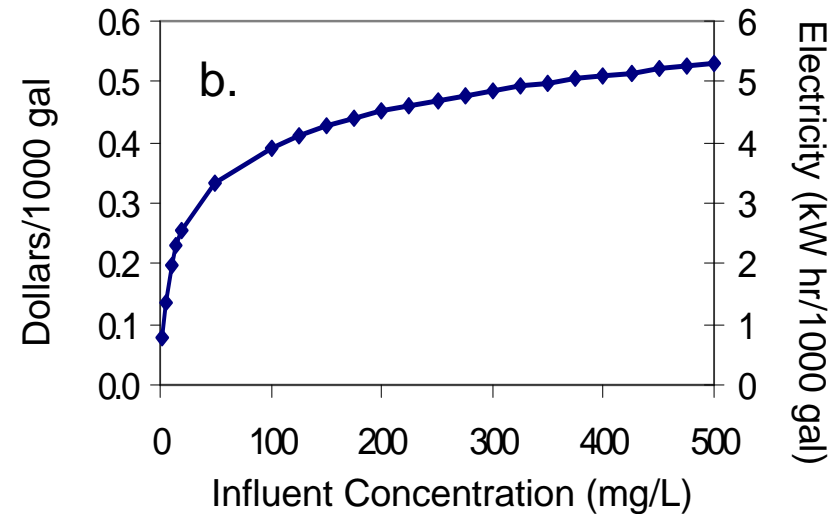
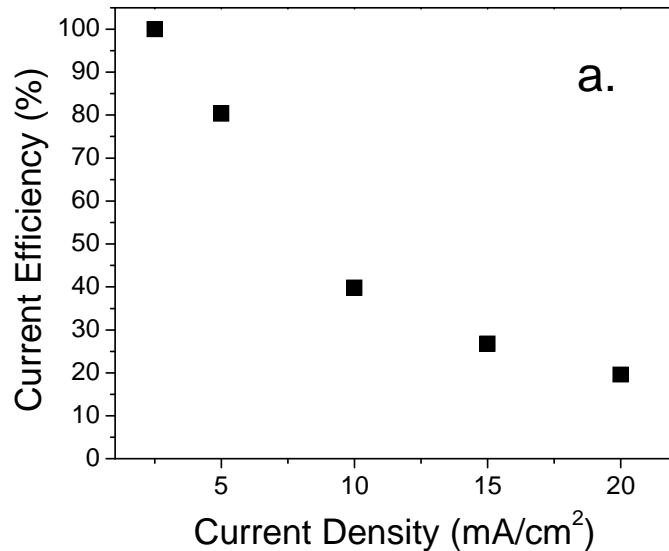


# Quantum Chemistry Modeling: $E_a$ for Direct Electron Transfer



a) Energy profiles for reactant (C<sub>8</sub>F<sub>17</sub>SO<sub>3</sub><sup>-</sup>) and products (C<sub>8</sub>F<sub>17</sub>SO<sub>3</sub> + e<sup>-</sup>) for vertical electron transfer as a function of the C-S bond length at an electrode potential of 2.5 V/SHE. b) Activation energies as a function of electrode potential for a direct electron transfer reaction.

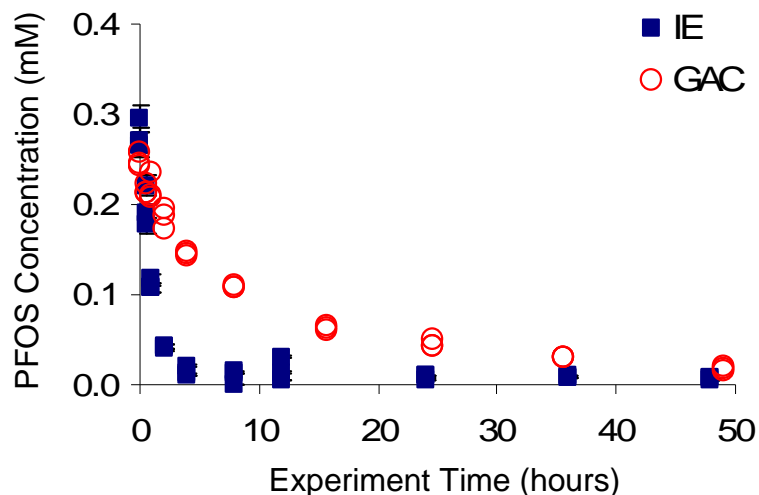
# Current Efficiencies and Treatment Costs



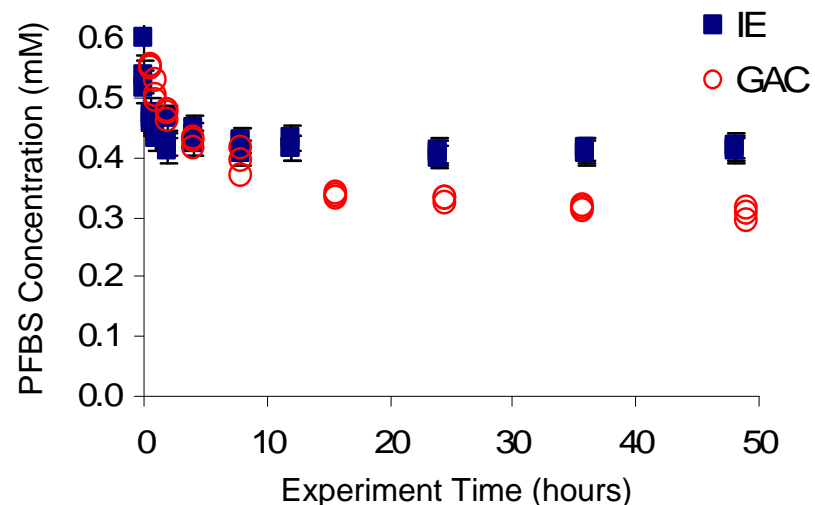
- Faradic current efficiencies for PFOS oxidation based on 34 mol e<sup>-</sup> per mol of PFOS.
- Electrical power requirements and costs required to reach a final PFOS concentration of 1 mg/L (2.5 μM) as a function of the influent PFOS concentration. Costs based on flow-cell operated at a current density of 20 mA/cm<sup>2</sup> and an energy cost of \$0.10/kWhr.

- Electrical power costs are small compared to other treatment methods.
- Capital costs for a 10 liter per minute flow-cell are ~\$2500.

# Batch Testing of Ion Exchange (IE) and Granular Activated Carbon (GAC) Equilibrium & Kinetics



10 g of ion exchange resin or 10 g of GAC into  
6 L of 0.3 mM PFOS solution



10 g of ion exchange resin or 10 g of GAC into  
6 L of 0.6 mM PFBS solution

- 5 hours of equilibrium time is needed for ion exchange
- PFOS more effectively removed than PFBS

# Conclusions

- Demonstrated that PFOS and PFBS can be rapidly oxidized to CO<sub>2</sub> and F<sup>-</sup> at BDD electrodes.
- Determined the rate-limiting step involves direct electron transfer in the activationless overpotential region.
- Demonstrated that PFOS and PFBS can be removed from aqueous solution using Amberlite<sup>®</sup> IRA 458 ion exchange resin.

# Future Plans

- Perform column tests to optimize the concentration and regeneration steps in the four-step process.
- Pilot test treatment scheme on real process wastewaters.

# Acknowledgements

- Lily Liao and Arpad Somogyi
- NSF/SRC ERC 2001MC425
- NSF Chemical and Transport Systems CTS-0522790
- Petroleum Research Fund 43535-AC5

# Industrial Collaboration

- |                     |                         |
|---------------------|-------------------------|
| • Tim Yeakley       | Texas Instruments       |
| • Thomas P. Diamond | IBM                     |
| • Jim Jewett        | Intel                   |
| • Laura Mendicino   | Freescale Semiconductor |

# **Low Environmental Impact Processing of Sub-50 nm Interconnect Structures**

*(Task Number: 425.019)*

## **PIs:**

- **Karen K. Gleason, Department of Chemical Engineering, MIT**

## **Graduate Students:**

- **Chia-Hua Lee: PhD Candidate, Department of Material Science and Engineering, MIT**
- **Wyatt Tenhaeff, Ph.D Candidate, Department of Chemical Engineering, MIT (NSF Fellow)**

## **Cost Share (other than core ERC funding):**

- **\$70k (NSF Fellowship for Wyatt Tenhaeff)**

# Objectives

- **Develop new methods to deposit patterns at resolution of 50 nm and below without conventional UV or ebeam lithography**
  - **Using Dip-Pen Nanolithography (DPN) and microcontact stamping to create surface quantum dot patterns on the polymer substrate.**
  - **Using carbon nanotubes (CNTs) as the etching masks to create high resolution functional polymer patterns**
- **Use EHS focused design approach to minimize process steps in the novel patterning processes**
- **Use low energy iCVD method as the process platform technology.**
- **Develop integration methods for quantum dots (QDs), allowing integration of high performance devices onto flexible substrates, relying on the naturally small dimensions of the QDs to achieve high resolution.**

# ESH Metrics and Impact

1. *Resist-free lithography would eliminate use of photoresist. Approximately 25,000 liters of photoresist materials is used annually in typical semiconductor foundries, at a cost of about \$1,600 per liter. Through spin-on process approximately 95% of resist is wasted and disposed as toxic material <sup>[1]</sup>. In contrast, the cost of CNTs is about \$ 10 per gram. For typical 4 inch wafer,(assuming 50% masking area), only 0.124mg of CNTs are needed. Hence, the cost of CNT needed for obtaining patterns on a 4-inch diameter wafer is about 1 cent.*
2. *Typical iCVD process requires between 0.02-0.12 W/cm<sup>2</sup> <sup>[3]</sup> for polymer deposition compared to conventional PECVD which uses 0.4-2.1 W/cm<sup>2</sup><sup>[4,5]</sup>. No plasma etch eliminates additional >7.1 W/cm<sup>2</sup><sup>[6]</sup> power requirement.*

[1] Percin et al., IEEE Transactions on Semiconductor Manufacturing (2003) 16 (3)

[2] Lee et al., J. Micromech. Microeng. (2005) 15

[3] Martin et al. Surf. Coating Tech. (2007) 201

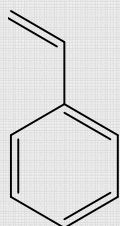
[4]Castex et al. Microelec. Eng. (2005) 82

[5]Wong et al. Thin Sol. Films 462–463 (2004)

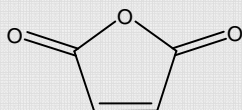
[6]Berruyer et al. J. Vac. Sci. Technol. A. 16.3 (1998)



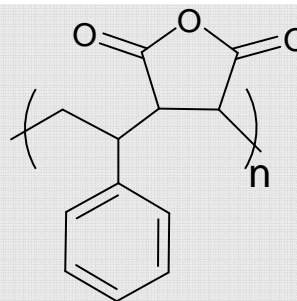
# iCVD poly(styrene-alt-maleic anhydride)



Styrene



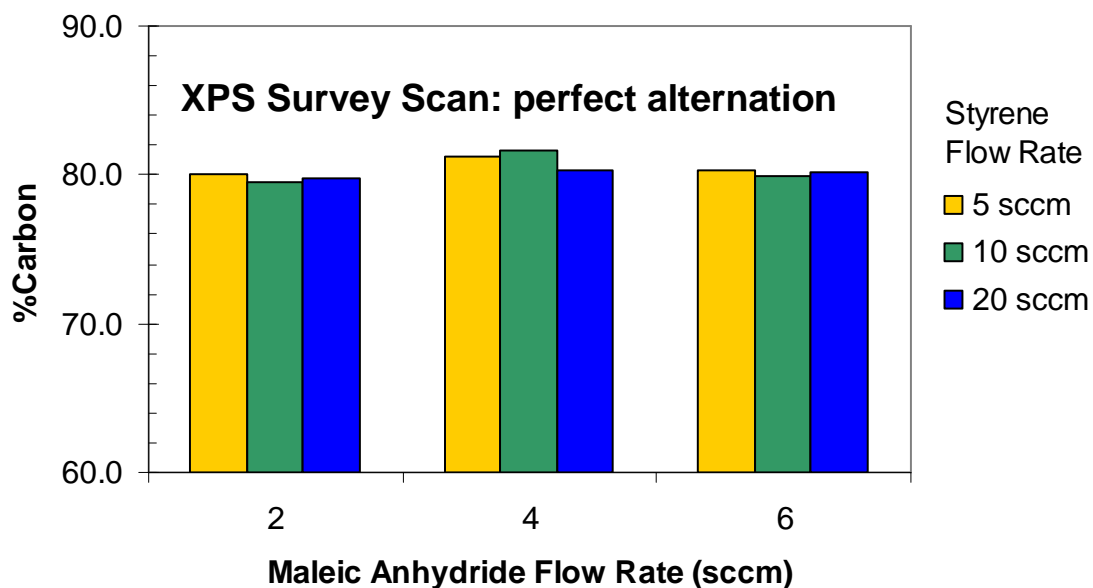
Maleic Anhydride



Poly(styrene-alt-maleic anhydride) (PSMa)

*\*used to coat oral ingested drugs\**

12 C: 3 O  
per unit  
(80%  
carbon)



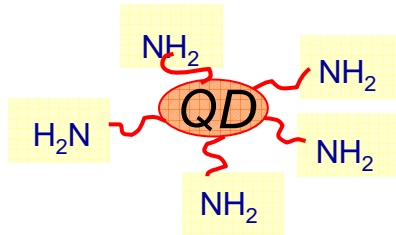
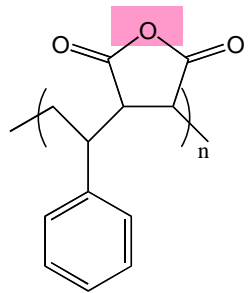
**<sup>13</sup>C NMR :**

**Only alternating  
triads: M-S-M**

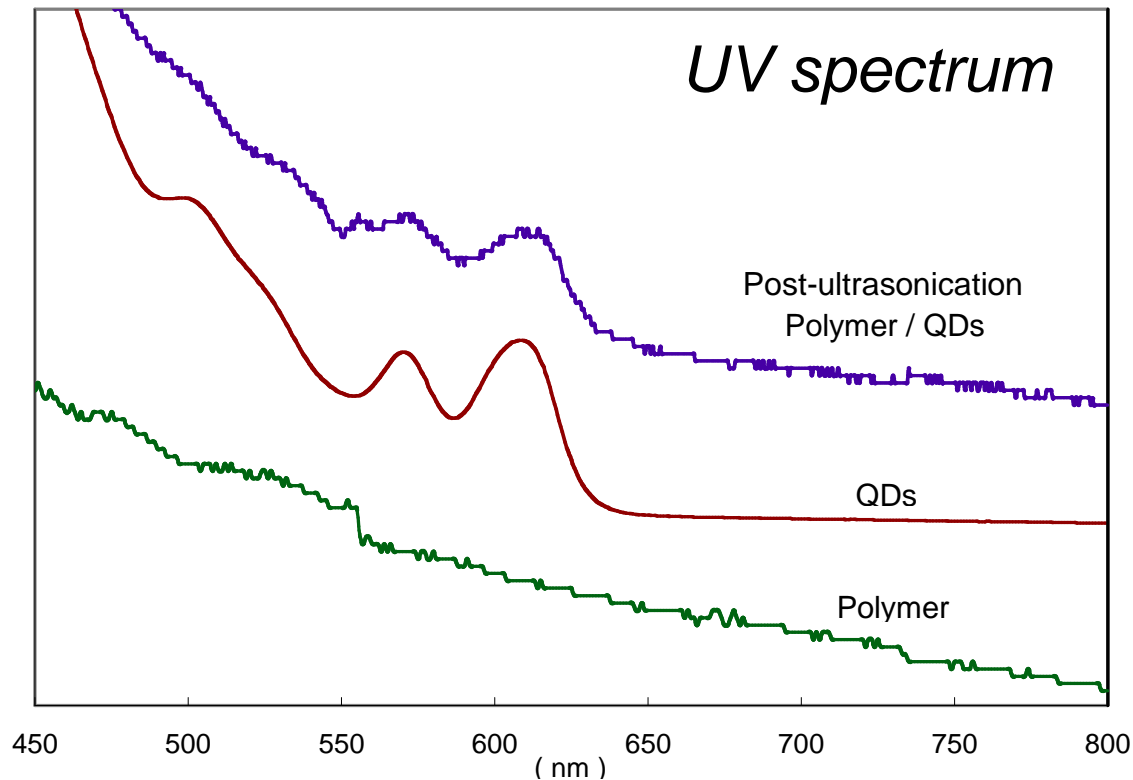
**No M-S-S or S-S-S  
detected**

W.E. Tenhaeff and K.K. Gleason  
Langmuir 23, 6624 (2007).

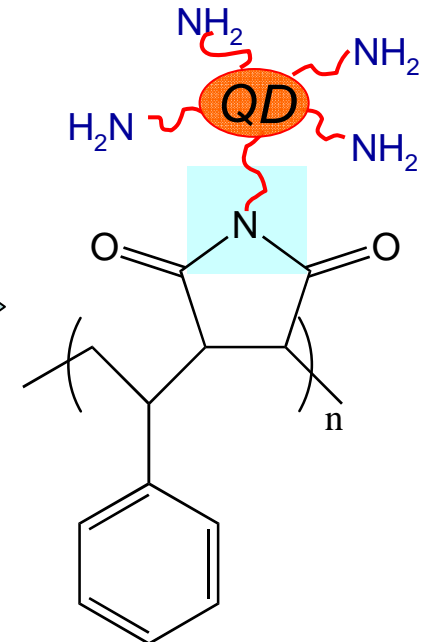
# Covalent attachment of QDs to iCVD PSMa



- Poly(styrene-alt-maleic anhydride) (PSMa)
- CdSe quantum dots (QD)  
capped bifunctional ligands -NH<sub>2</sub>

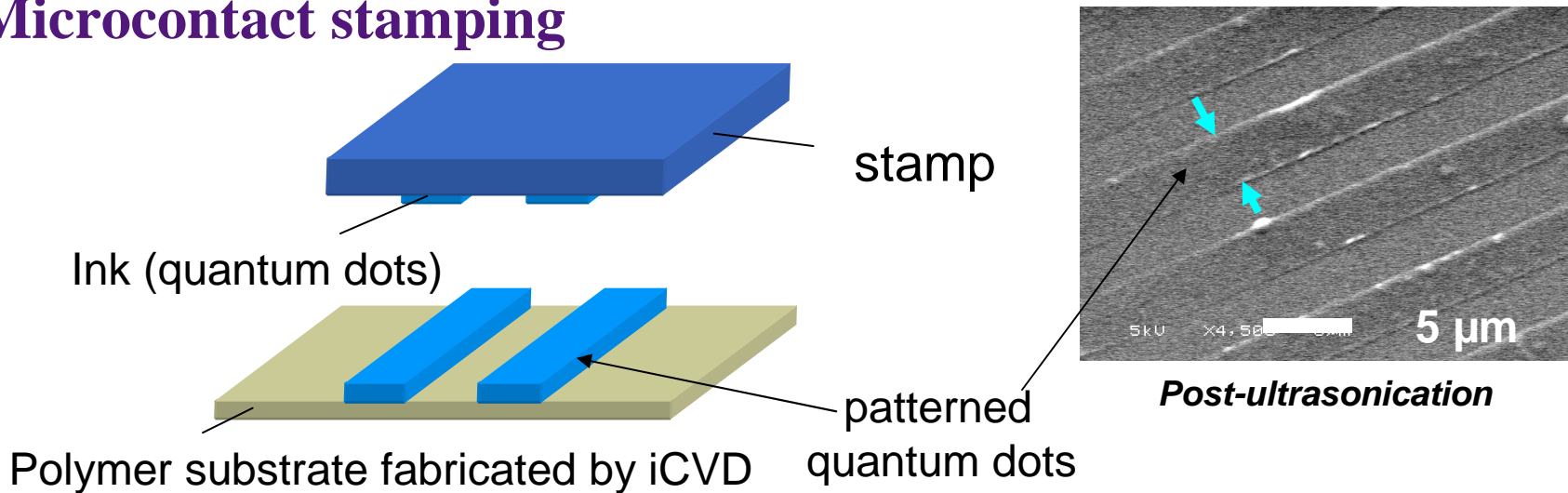


**QD Size ~ 5 nm**

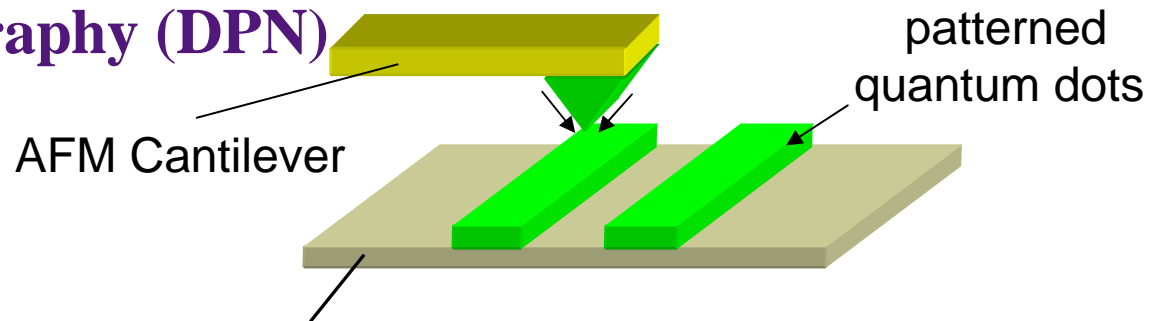


# Direct writing with QD ink on iCVD PSMa

## Microcontact stamping



## Dip-pen Nanolithography (DPN)

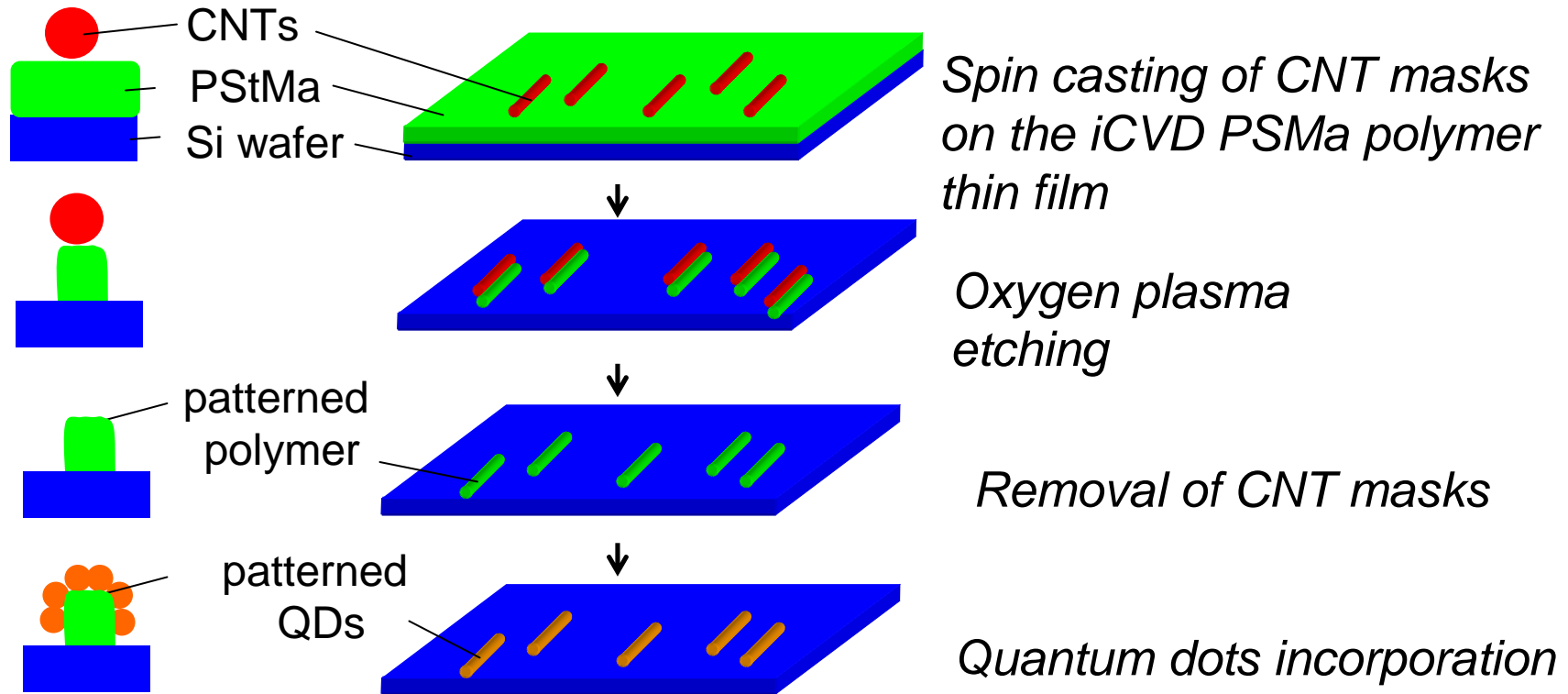


Polymer substrate fabricated by iCVD

**Writing speed can be increased by using multiple cantilevers in parallel**

*SRC/SEMATECH Engineering Research Center for Environmentally Benign Semiconductor Manufacturing*

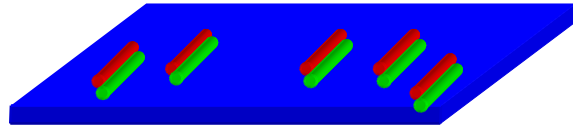
# CNT masks for patterning iCVD PSMa



*Use of semiconducting QDs removes the need for substrates to be high quality substrates.*

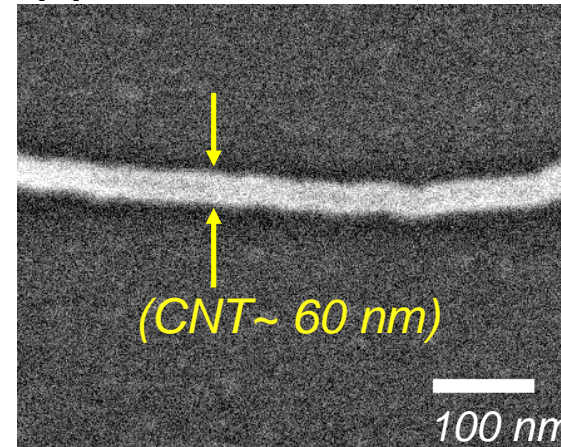
*Inexpensive, lightweight flexible substrates possible. Avoids energy intensive fabrication of high purity silicon wafers.*

# Carbon Nanotube (CNT) masking results

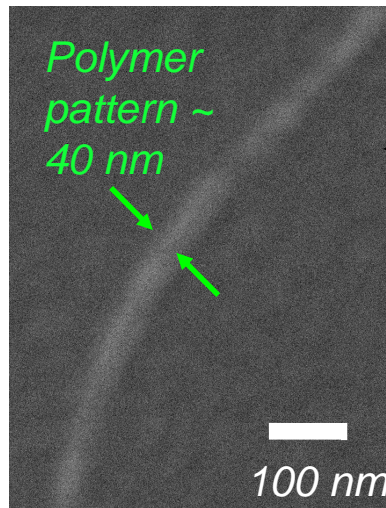


After spin-casting of CNTs

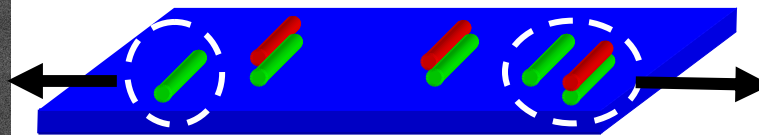
(1)



(2)



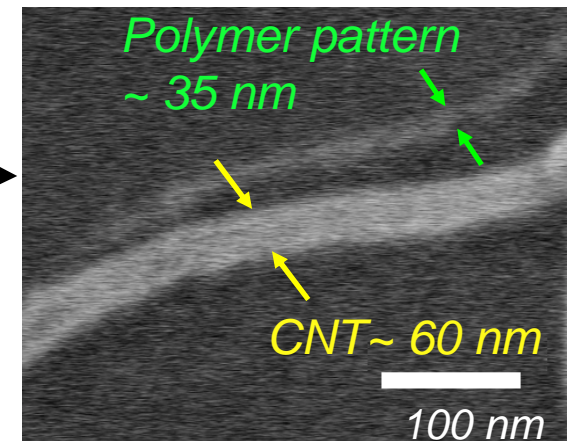
(Etching time: 30 s)



After etching and partial removal of the CNTs

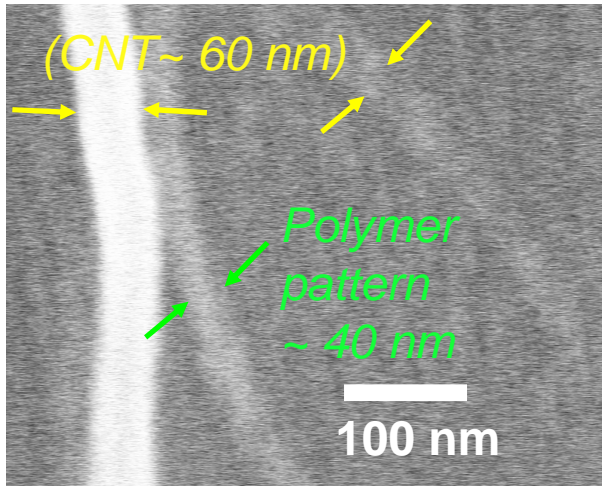
Pattern in polymer is smaller than CNT diameter

(3)

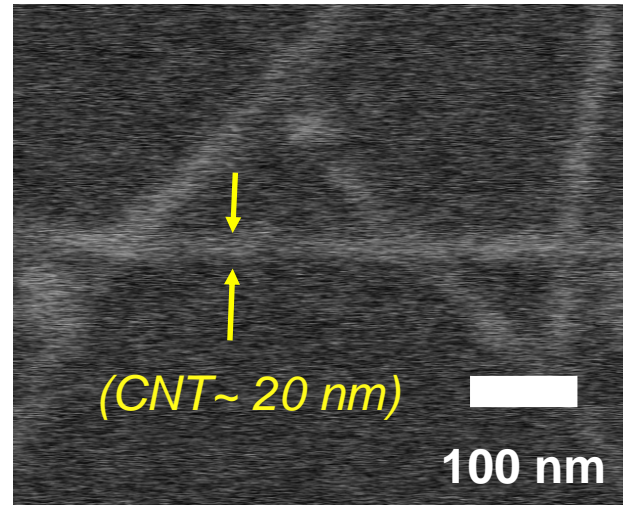


(Etching time: 40 s)

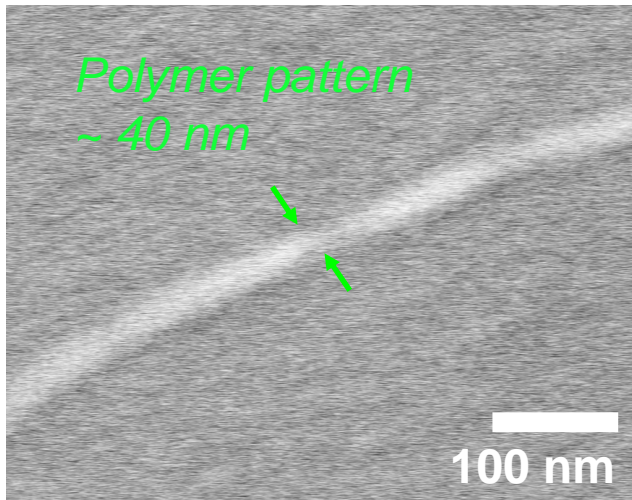




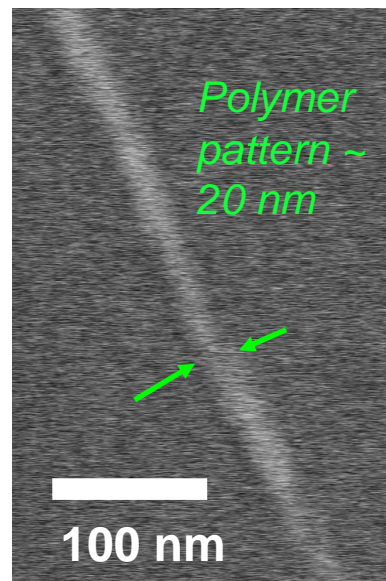
(Etching time: 30 s)



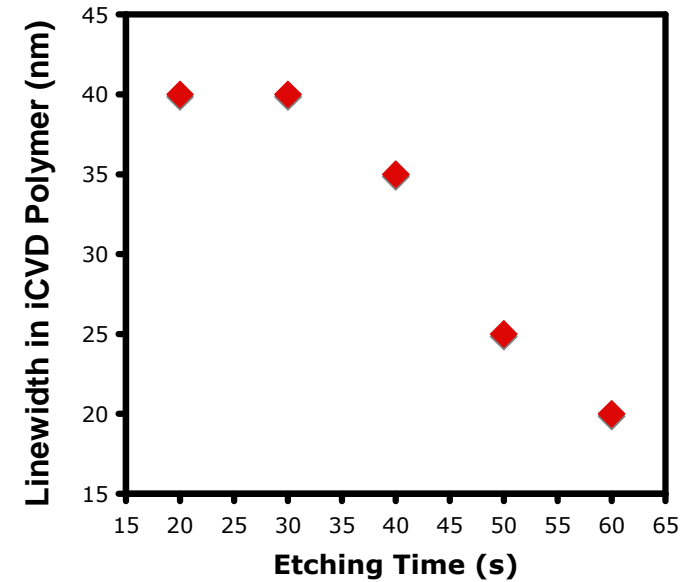
Pattern sizes depend on **the CNT diameters** and **the etching time**



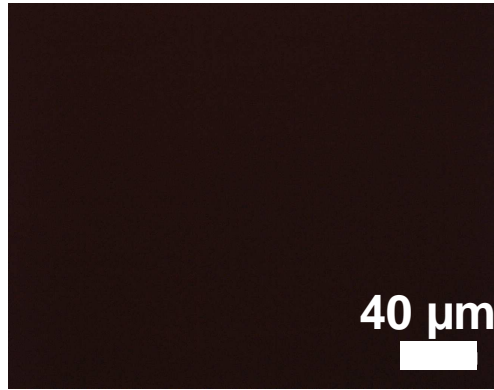
(Etching time: 60 s)



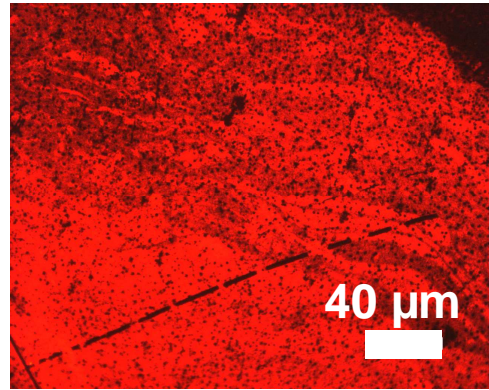
(Etching time: 60 s)



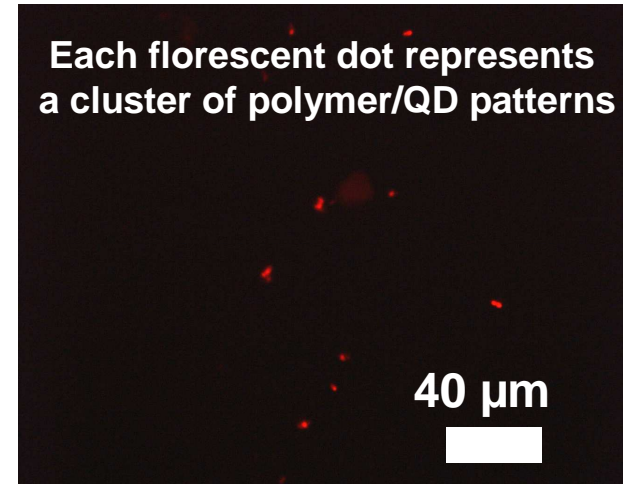
# Fluorescence Microscope



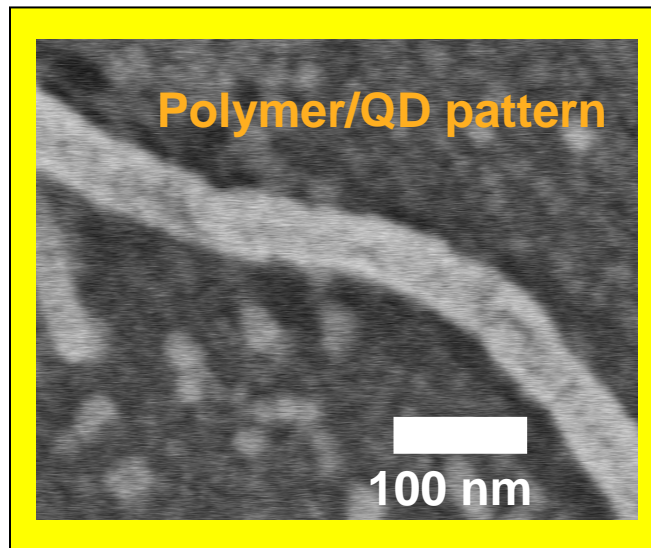
P(SMa) iCVD polymer film



P(SMa) /QD blanket film



P(SMa) /QD patterned film



SEM images of polymer/QD pattern

# Future Plans

## Next Year Plans

- **Optimize the incorporation of the monodisperse and functionalized quantum dots in collaboration with Prof. Muscat's group**
- **Use functional iCVD polymers to align the carbon nanotubes**
- **Fabricate simple quantum dot devices using the novel patterning strategies**

## Long-Term Plans

- **Demonstrate the performance of high resolution devices on flexible, low cost, light weight substrates.**



# Publications, Presentations, and Recognitions/Awards

## **PUBLICATIONS**

- W.E. Tenhaeff, K.K. Gleason, Initiated Chemical Vapor Deposition of Alternating Copolymers of Styrene and Maleic Anhydride, Langmuir 23(12), 6624-6630 (2007).
- Wyatt E. Tenhaeff and Karen K. Gleason, Initiated chemical vapor deposition of perfectly alternating poly(styrene-alt-maleic anhydride), Surface And Coatings Technology 201,9417-9421 (2007)

## **PRESENTATIONS**

- K.K. Gleason, Polymeric Nanocoatings by Chemical Vapor Deposition, Pall Corporation, 2/6/2007
- K.K. Gleason, Design of CVD processes for low k dielectrics and air gap formation, 2007 MRS Spring Meeting: Symp. B, San Francisco, CA 4/11/2007 (invited)
- K.K. Gleason, Initiated chemical vapor deposition (iCVD) of polymeric nanocoatings, 16th European Conference on Chemical Vapor Deposition, Den Haag, Netherlands, 9/20/2007 (invited).
- W. Tenhaeff and K.K. Gleason, Initiated chemical vapor deposition of perfectly alternating Poly(styrene-alt-maleic anhydride), 16th European Conference on Chemical Vapor Deposition, Den Haag, Netherlands, 9/20/2007
- K.K. Gleason, Chemical Vapor Deposition of Polymeric Nanocoatings, U. Calgary, Dept. Chemical Engineering, 10/5/2007 (invited).
- K.K. Gleason, Conformal Polymeric Thin Films via Initiated Chemical Vapor Deposition, AVS Seattle, WA, 10/15/2007 (invited)
- K.K. Gleason, Engineering Polymeric Nanocoatings by Vapor Deposition 31th Annual Symposium of the Macromolecular Science and Engineering Program at the University of Michigan., Ann Arbor, MI, 10/25/2007 (invited).
- W.E. Tenhaeff and K.K. Gleason, Initiated Chemical Vapor Deposition of Functional Thin Hydrogel Films to Incorporate Quantum Dots, MRS Fall Conference, Boston, MA, 11/30/2007

*SRC/SEMATECH Engineering Research Center for Environmentally Benign Semiconductor Manufacturing*

# Low Environmental Impact Processing of sub-50 nm Interconnect Structures

*(Task Number: 425.019)*

## PIs:

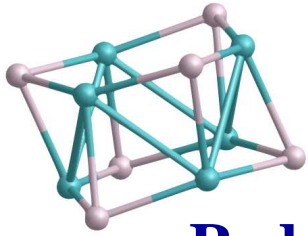
- Anthony Muscat, Chemical and Environmental Engineering, UA
- Masud Mansuripur, College of Optical Sciences, UA (added 2008)

## Other Researchers:

- Zhengtao Deng, Postdoctoral Fellow, ChEE & Optical Sciences, UA

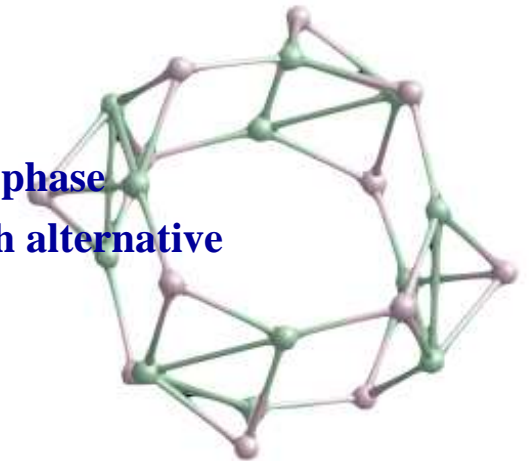
## Cost Share (other than core ERC funding):

- \$85k from Arizona TRIF


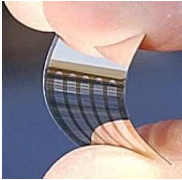

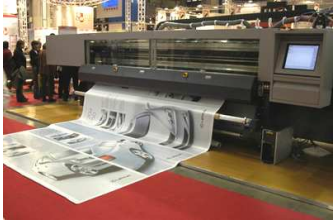


## Objectives

- **Reduce the power required for switching and to transmit signals on a chip and between chips by using light**
- **Reduce the water, energy, and materials required to fabricate interconnect wiring**
- **Use clusters of crystalline semiconductors (quantum dots) to build interconnect structures**
  - **Inherently small 1-5 nm q-dots  $\Rightarrow$  scaling**
  - **Tunable band gap and photosensitivity  $\Rightarrow$  optical switching or signal transmission**
- **Develop processes to**
  - **(1) grow crystalline quantum dots in water and in a gas phase**
  - **(2) pattern quantum dots on surfaces and thin films with alternative lithographic processes**
  - **(3) use materials that have low ESH impact**

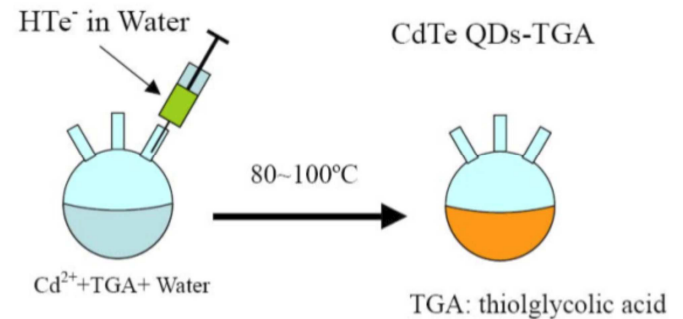


# ESH Metrics and Impact

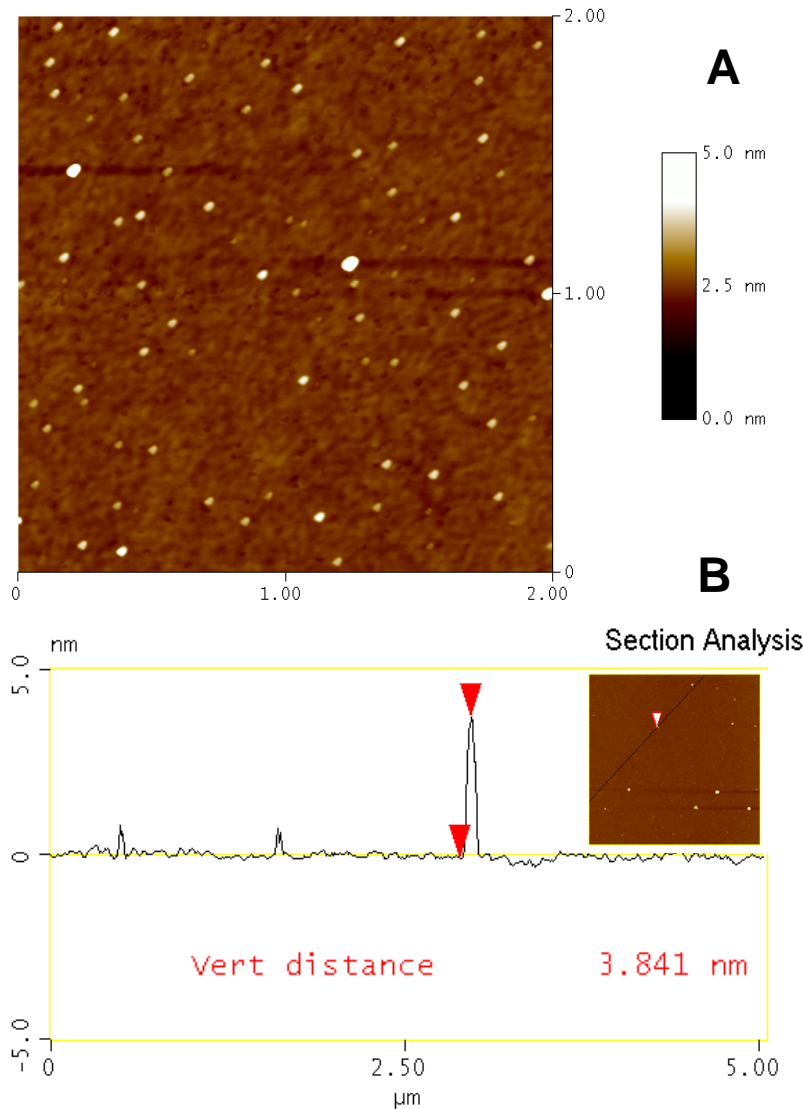
Sustainability Metrics		
Attribute	Si wafer	QD on plastic
Cost per cm <sup>2</sup>	\$50-120	< \$100
Energy used per cm <sup>2</sup> in fabrication	>1KWh	<1KWh
Flexible?	No 	Yes 
Processing	batch 	batch or semi-continuous (roll to roll) 
Optical	not directly	yes
Lithography	traditional/e-beam	hierarchical assembly of carbon nanotubes

# Methods and Approach

- **Develop fast, simple, reproducible, cost-efficient, and environmentally friendly routes to fabricate highly luminescent quantum dots with tunable photoluminescence (PL) peaks**
- **Water based and gas phase synthesis routes that are scaleable to commercial applications**
- **Deposit on Si and dielectric surfaces by tuning ligand**
  - Thiol ligands with different chain lengths and chemistries
- **Validate properties of quantum dots in solution and on surfaces**
  - Bleaching
  - Fluorescence intensity intermittency (blinking) and frequency shift



# AFM of QDs Deposited on Si Surface

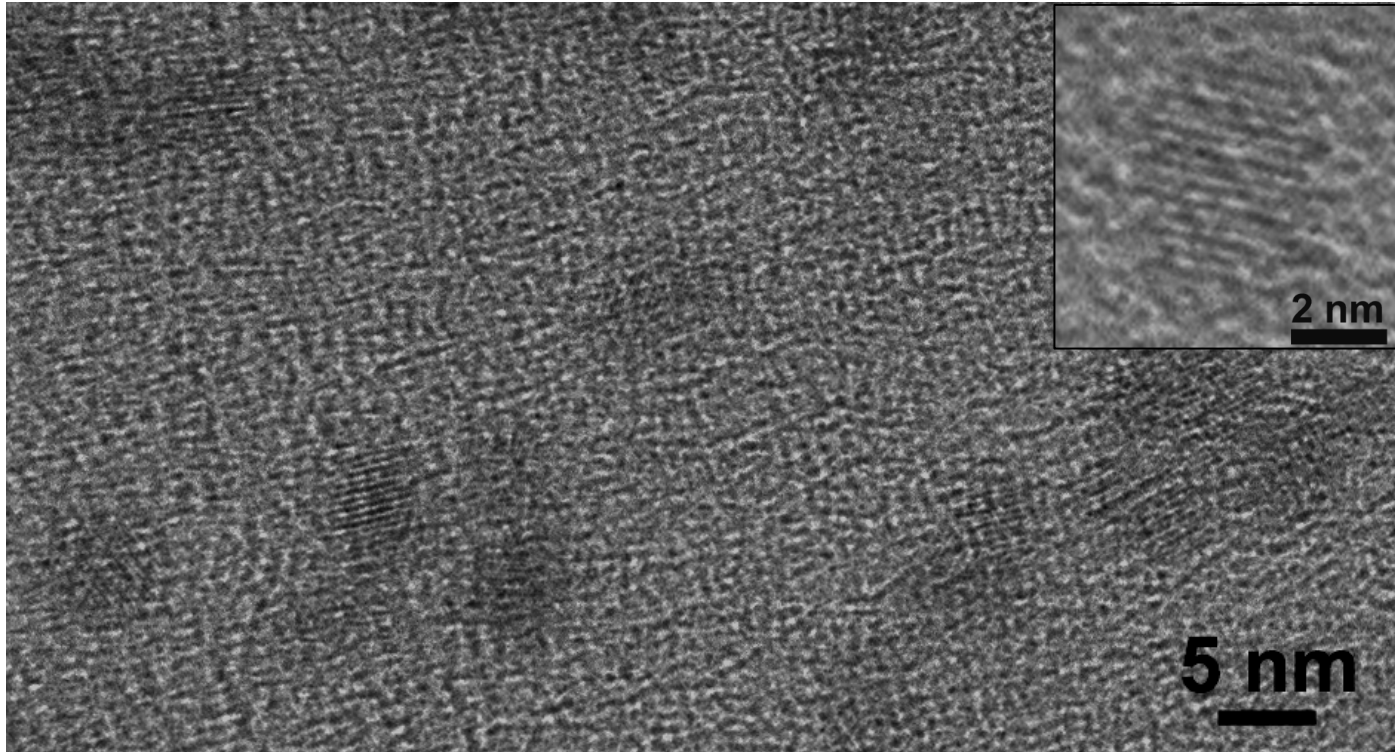


**A** AFM topography image of TGA-capped quantum dots with maximum emission at 590 nm on hydrophilic silicon wafer substrate

**B** Height profile of AFM line scan in the image shown in the inset. Red arrows define dimensions of one typical quantum dot with a diameter close to 3.8 nm.

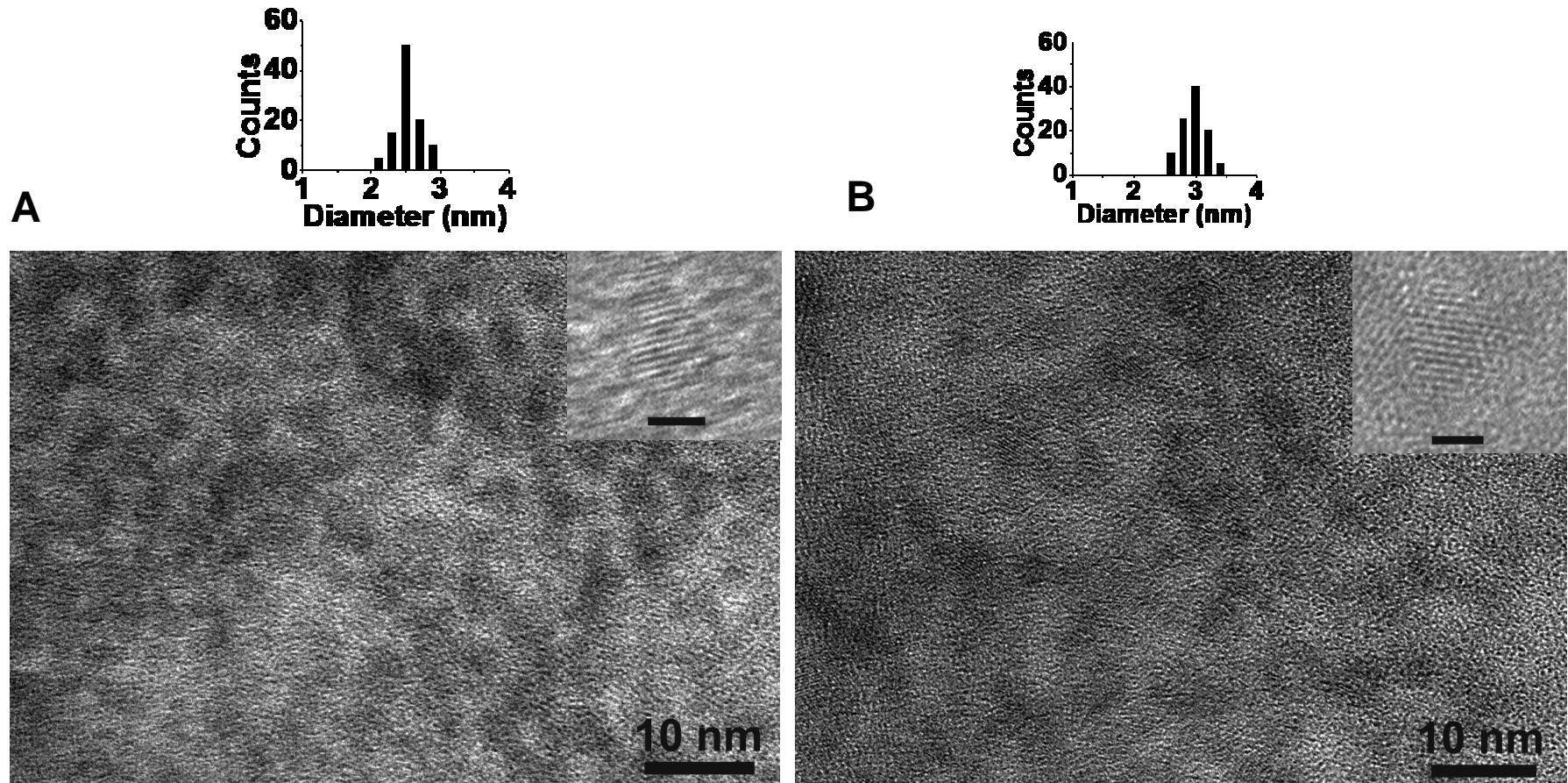


# TEM study of CdTe QDs



Transmission electron microscopy image of thioglycolic acid capped CdTe quantum dots deposited on TEM grid

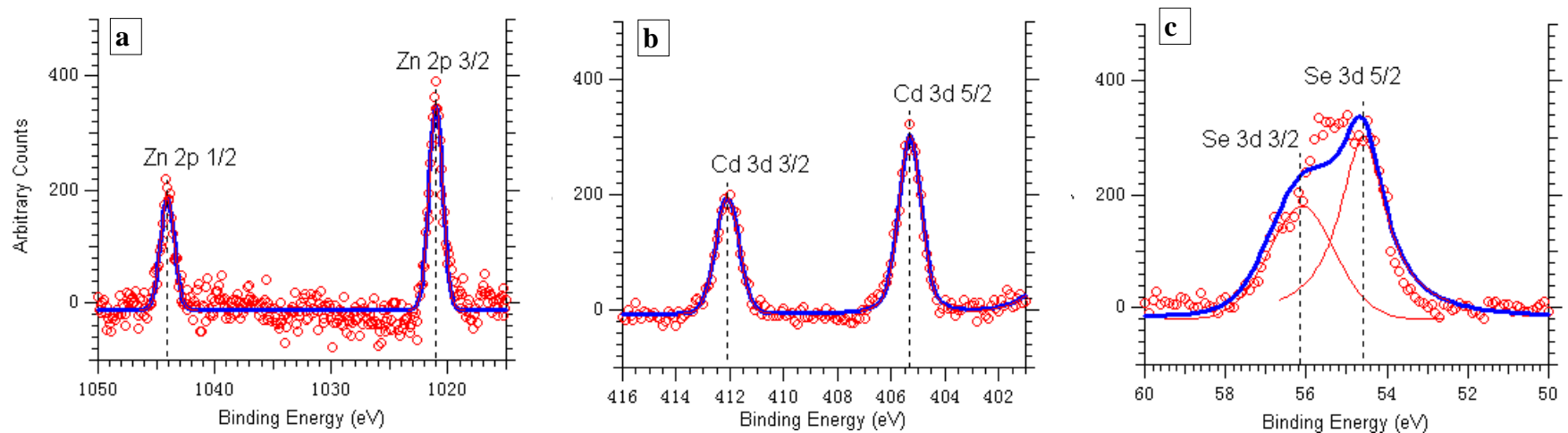
# TEM study of ZnSe and $Zn_xCd_{1-x}Se$ QDs



TEM images of TGA-capped ZnSe (A) and  $Zn_xCd_{1-x}Se$  QDs samples (B). Inset is the enlarged images of single QDs, scale bar 2 nm.

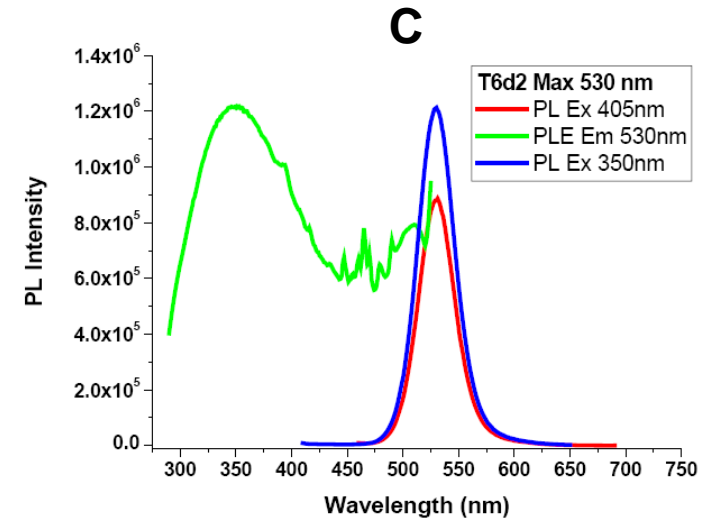
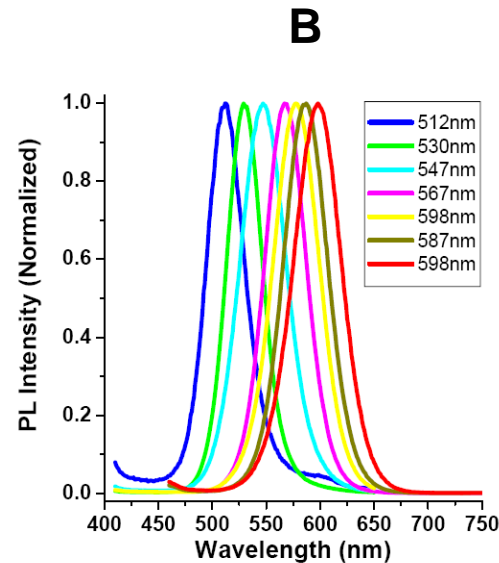
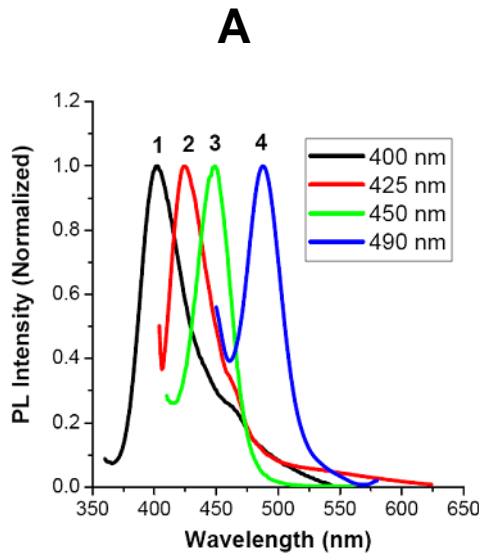


# XPS study of $Zn_xCd_{1-x}Se$ QDs



High-resolution x-ray photoelectron spectra of  $Zn_xCd_{1-x}Se$  QDs samples with near bandgap emission peak at 490 nm: (a) Zn 2p<sub>3/2</sub> and Zn 2p<sub>1/2</sub> spectral lines; (b) Cd 3d<sub>3/2</sub> and Cd 3d<sub>5/2</sub> spectral lines; (c) Se 3d<sub>5/2</sub> and Se 3d<sub>3/2</sub> spectral lines.

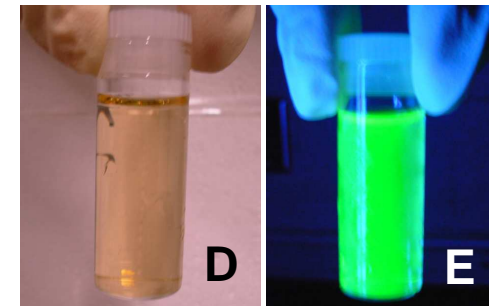
# Optical Properties



**A** photoluminescence (PL) spectra of a series of thioglycolic acid capped  $Zn_xCd_{1-x}Se$  QD samples

**B** PL spectra of a series of thioglycolic acid capped CdTe QD samples

**C** PL and PLE spectra of one typical thioglycolic acid capped CdTe QD samples

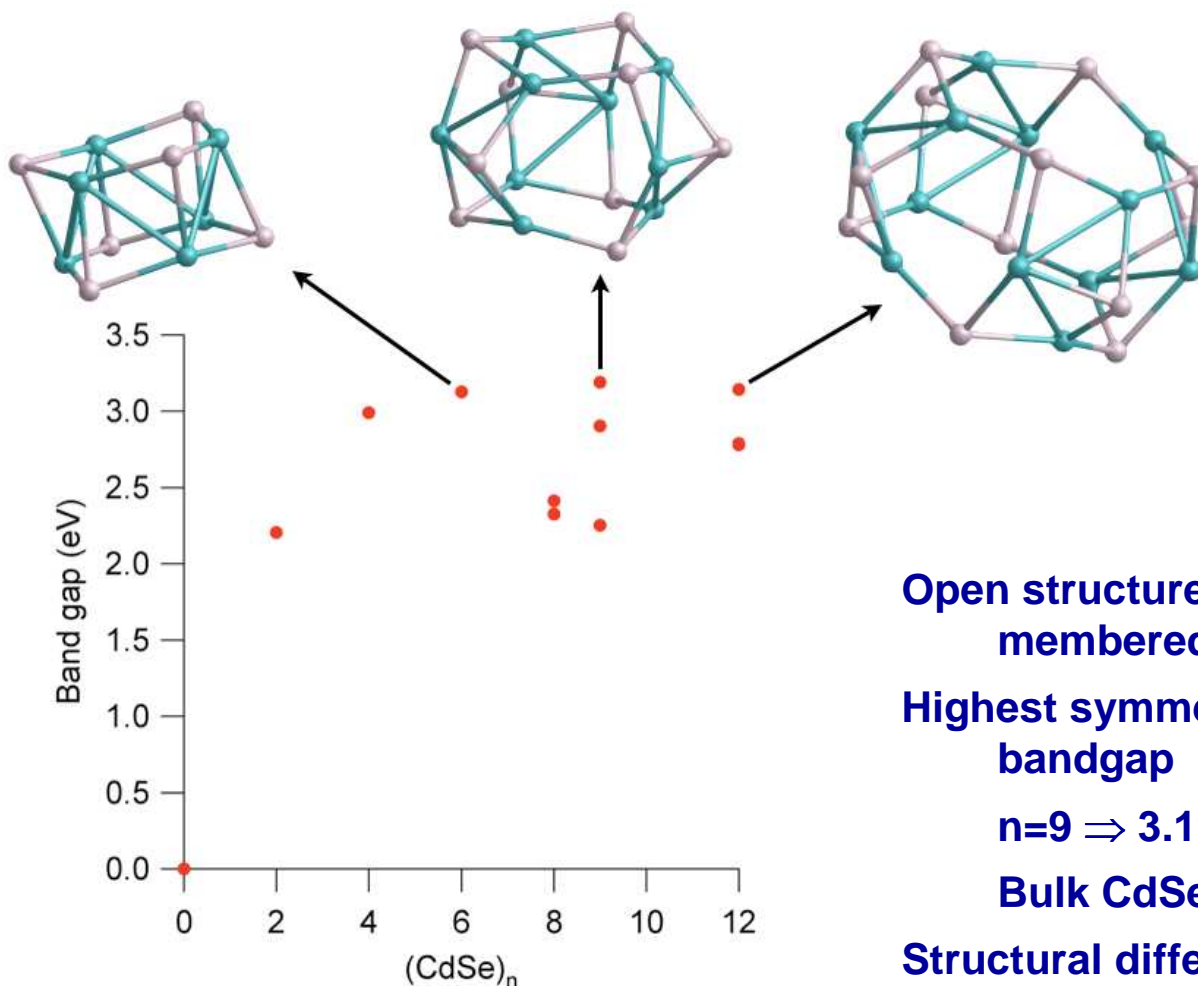


Pictures of typical TGA-capped CdTe QDs samples under

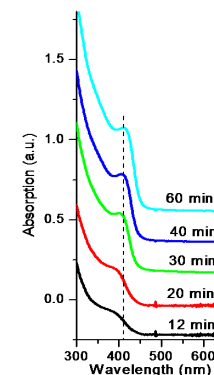
**D** room light

**E** 365 nm UV light

# Band Gap of QD Clusters Computed by Molecular Modeling



Density Functional Theory  
B3LYP exchange-correlation functional  
LANLD2Z effective core potential/basis set  
Gamess code



**Open structures containing 6-membered (CdSe)<sub>3</sub> rings**  
**Highest symmetry produces largest bandgap**  
**n=9 ⇒ 3.19 eV (389 nm)**  
**Bulk CdSe band gap = 1.74eV**  
**Structural differences affect band gap**

# Future Plans

## Next Year Plans

- Investigate replacing the reproductive toxin Cd with Cu or Mn
- Model q-dot structure and properties with computational chemistry
- Deposit q-dots on semiconductor and dielectric surfaces by varying ligand chemistry
- Define prototype devices
- Assess costs of introducing new processing technology

## Long-Term Plans

- Work with Prof. Karen Gleason's group at MIT to selectively deposit q-dots on surfaces patterned using iCVD
- Build a prototype device based on q-dots



# Students on Task 425.019



- **Current students and anticipated grad date**
  - **Rachel Morrish, December 2009**

# **An Integrated, Multi-Scale Framework for Designing Environmentally Benign Copper, Tantalum and Ruthenium Planarization Processes**

*(Task Number: 425.020)*

## **Subtask 2: Real-Time Detection and Modeling of Pattern Evolution**

### **PI:**

- Ara Philipossian, Chemical and Environmental Engineering, UA

### **Graduate Students:**

- Yasa Sampurno: Ph. D. candidate, Chemical and Environmental Engineering, UA

### **Other Researchers:**

- Yun Zhuang, Research Associate, Chemical and Environmental Engineering, UA
- Fransisca Sudargho, Research Technician, Chemical and Environmental Engineering, UA

### **Cost Share (other than core ERC funding):**

- In-kind donation (pads) from Neopad Technologies Corporation
- In-kind support from Araca, Inc.

# Objectives & ESH Metrics and Impact

## **Objectives:**

- Investigate the effects of break-in time and in-situ conditioning duty cycle on coefficient of friction, removal rate, and variance of shear force.
- Explore shear force spectral fingerprints to understand the effect of break-in time and in-situ pad conditioning duty cycle during copper CMP.

## **ESH Metrics and Impact:**

- Reduce diamond disc and pad consumption by 25% by reducing pad break-in and conditioning time.

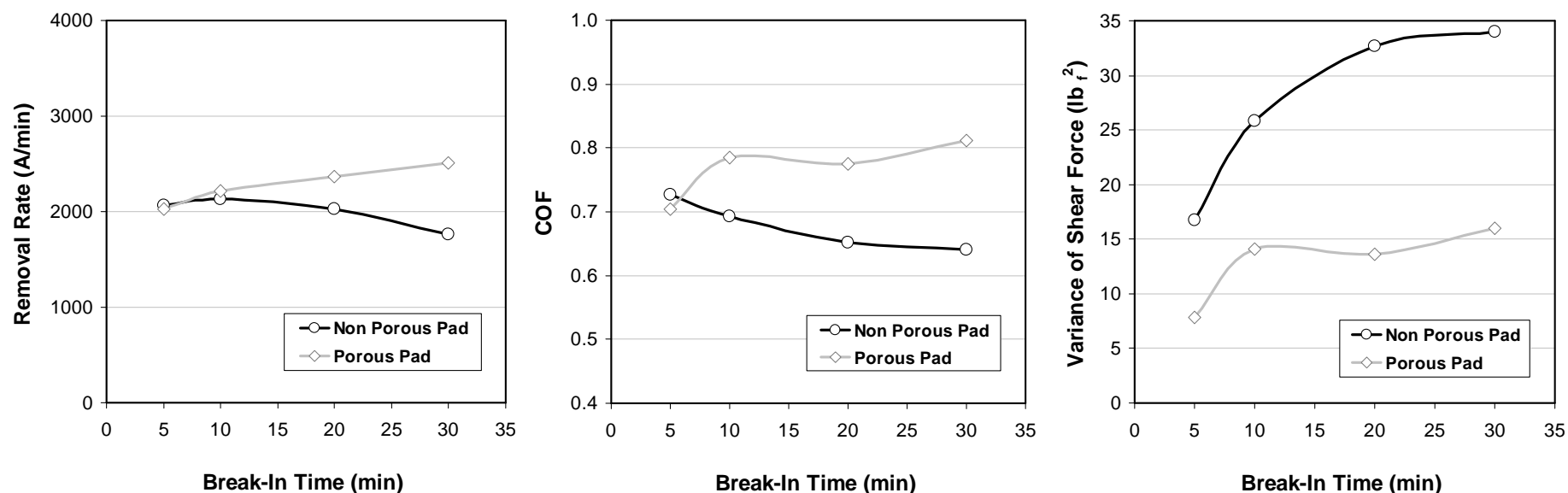
# **Experimental Conditions**

## **Pad Break-in Time Study**

- **Diamond disc: 2-inch 100-grit TBW Industries**
- **Conditioning pressure: 0.5 PSI**
- **Conditioning : *In-situ* at 30 RPM disc speed and 10 times per minute sweep frequency**
- **Break-in time: 5, 10, 20 and 30 minutes**
- **Wafers: 100-mm blanket CVD copper**
- **Wafer pressure: 3 PSI**
- **Sliding velocity: 0.7 m/s**
- **Slurry flow rate: 60 ml/min**
- **Slurry: Cabot Microelectronics Corporation iCue 600Y75**
- **Pad: Porous and non-porous pads**
- **Polishing time: 60 seconds**



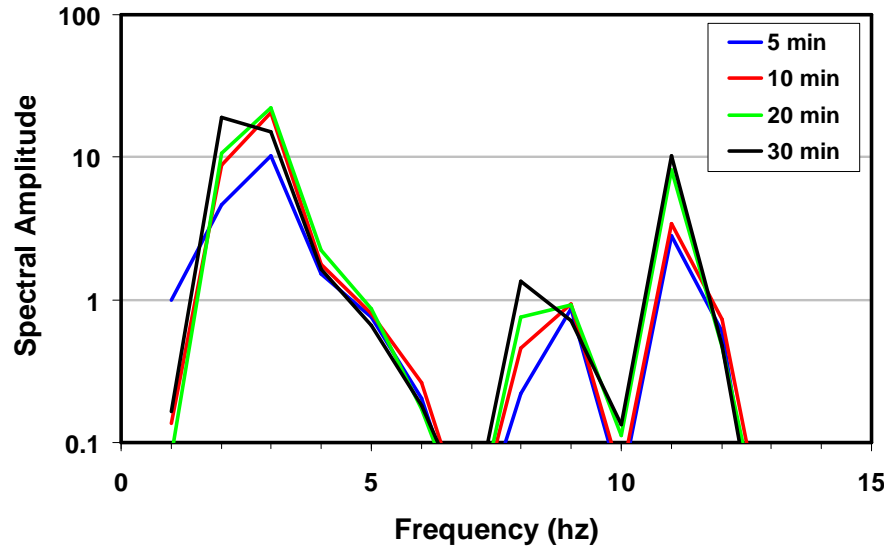
# Removal Rate, COF, and Variance of Shear Force



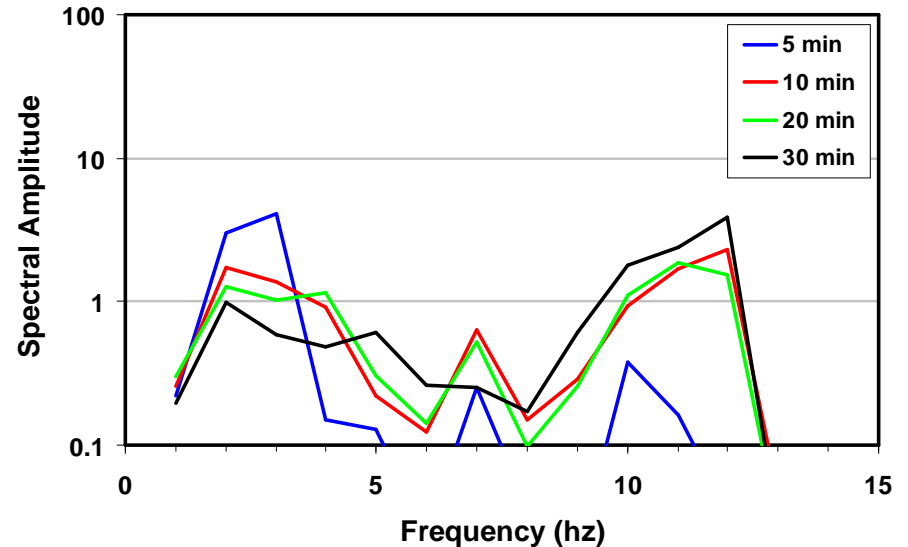
**Pad break-in time has opposite effects on removal rate and COF for porous and non-porous pads.**

**The variance of shear force initially increases with the pad break-in time and then reaches a plateau for both porous and non-porous pads.**

# Spectral Analysis



Non-porous pad



Porous pad

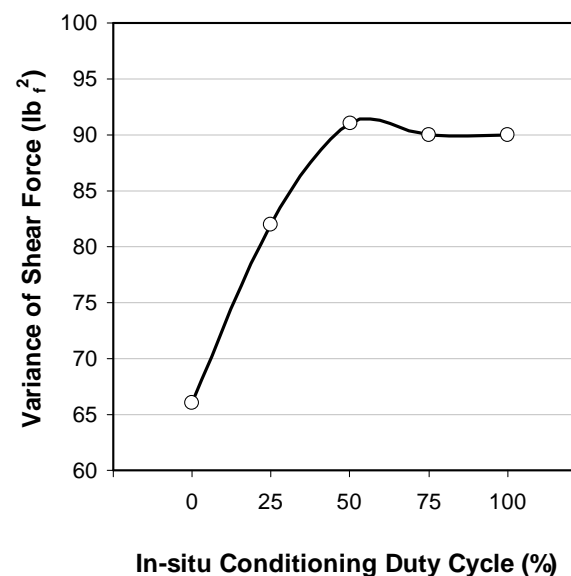
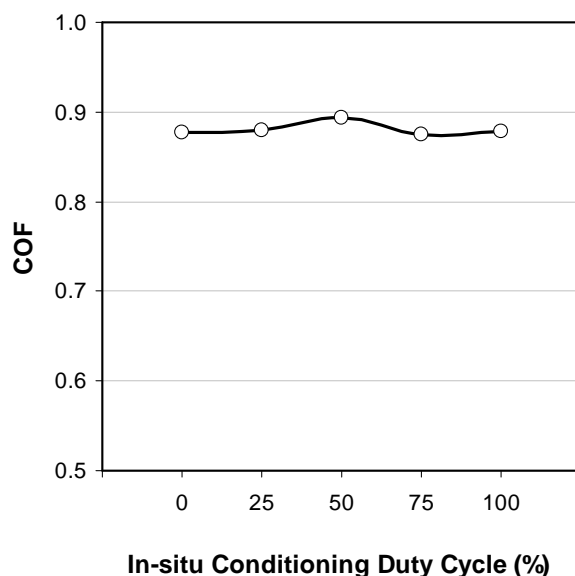
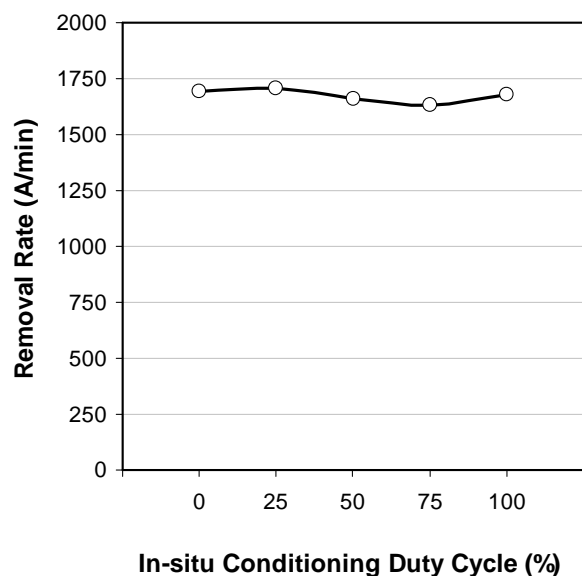
**The non-porous pad shows consistent spectra under different pad break-in time.**

# **Experimental Conditions**

## **In-situ Conditioning Duty Cycle Study**

- **Diamond disc conditioner: 2-inch 100-grit TBW Industries**
- **Conditioning pressure: 0.5 PSI**
- **Conditioning : *In-situ* at 30 RPM disc speed and 10 times per minute sweep frequency**
- **In-situ conditioning duty cycle: 0, 25, 50, 75 and 100 percent**
- **Wafers: 100-mm blanket CVD copper**
- **Wafer pressure: 2 PSI**
- **Sliding velocity: 0.62 m/s**
- **Slurry flow rate : 80 ml/min**
- **Slurry: Cabot Microelectronics Corporation iCue 600Y75**
- **Pad : Non-porous pad**
- **Polishing time: 60 seconds**

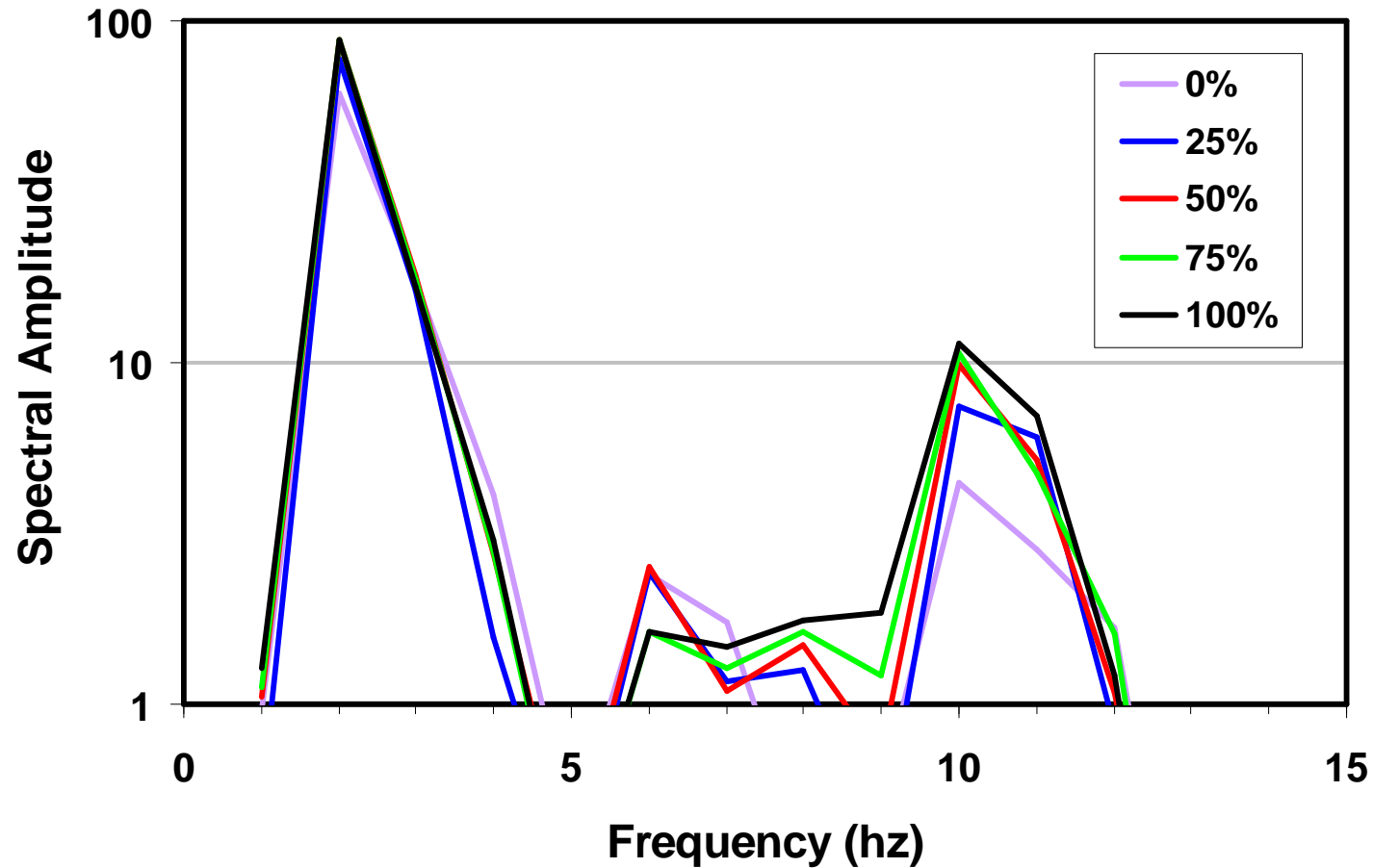
# Removal Rate, COF, and Variance of Shear Force



**Removal rate and COF are not affected by the conditioning duty cycle.**

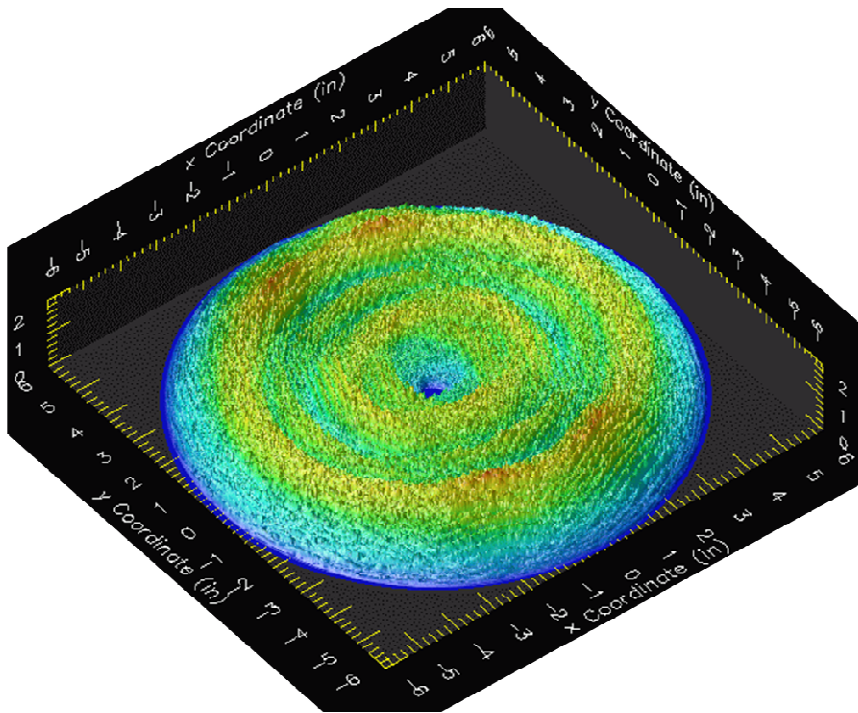
**The variance of shear force initially increases with the conditioning duty cycle and then reaches a plateau.**

# Shear Force Spectral Analysis

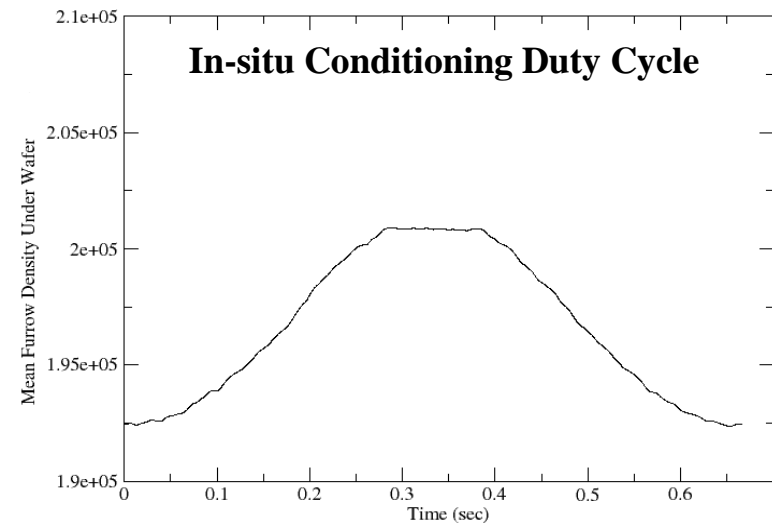
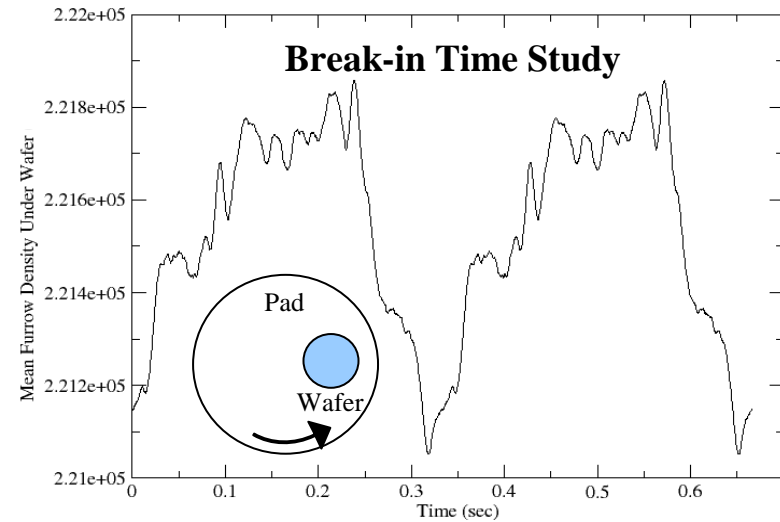


**High duty cycles result in similar spectral amplitude distributions.**

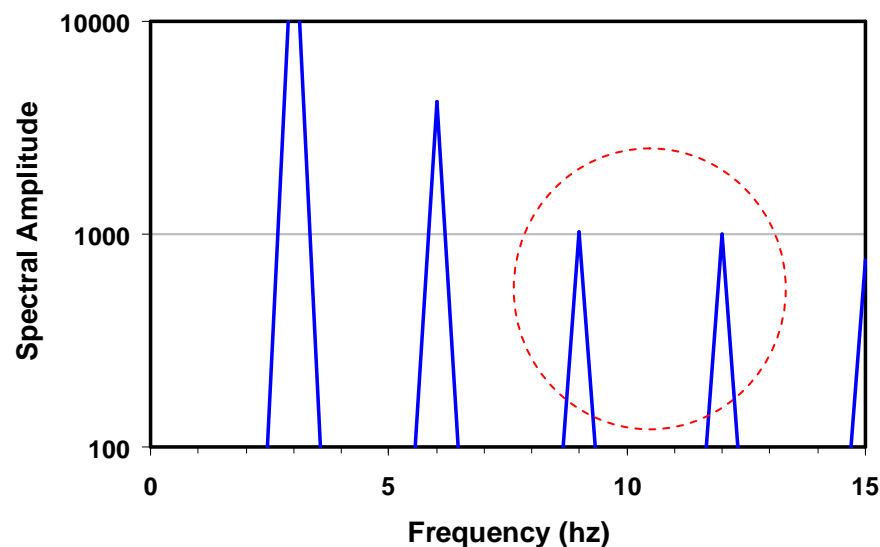
# Mean Furrow Density Under Wafer



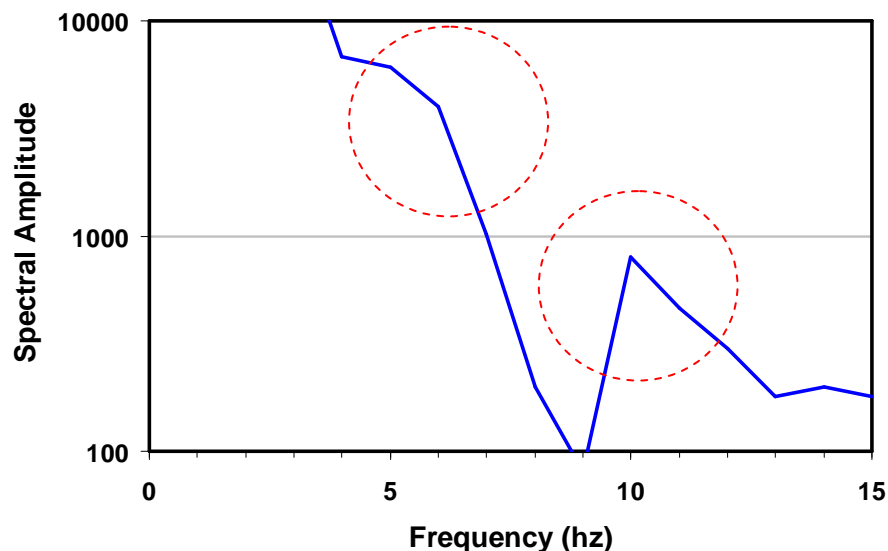
Monte Carlo simulation of pad topography with the microscopic furrows generated by the pad conditioner.



# Spectral Analysis of Furrow Density Under Wafer



Pad Break-in Time Study



In-situ Conditioning Duty Cycle Study

**The simulated furrow density spectrums show similar spectral distributions to the shear force spectrums, suggesting some specific peaks are associated with pad conditioning.**

# **Industrial Interactions and Future Plans**

## **Industrial mentors / contacts:**

- **Sudhanshu Misra (Neopad Technologies Corporation)**
- **Karey Holland (Neopad Technologies Corporation)**
- **Leonard Borucki (Araca, Inc.)**

## **Next year plan:**

- **Investigate the effect of pad break-in and conditioning duty cycle on Rohm and Haas IC pads during copper CMP process.**

## **Long term plan:**

- **Investigate the effect of pad break-in time and in-situ conditioning duty cycle on various industrially-relevant pads for metal CMP processes.**



# Publications and Presentations

## Publication:

- **Effect of Pad Break-in Time and In-Situ Pad Conditioning Duty Cycle for Porous and on-Porous Pads in CMP. Y. Sampurno, L. Borucki, S. Misra, K. Holland, Y. Zhuang and A. Philipossian. 13th International Conference on Chemical-Mechanical Polish (CMP) Planarization for ULSI Multilevel Interconnection Proceedings, to be published.**

## Presentation:

- **Effect of Pad Break-in Time and In-Situ Pad Conditioning Duty Cycle for Porous and on-Porous Pads in CMP. Y. Sampurno, L. Borucki, S. Misra, K. Holland, Y. Zhuang and A. Philipossian. To be presented at the 13th International Conference on Chemical-Mechanical Polish (CMP) Planarization for ULSI Multilevel Interconnection Proceedings, Fremont, California, March 3-6 (2008).**

# **An Integrated, Multi-Scale Framework for Designing Environmentally Benign Copper, Tantalum and Ruthenium Planarization Processes**

*(Task Number: 425.020)*

## **Subtask 1: Wear Phenomena and Their Effect on Process Performance**

### **PI:**

- Ara Philipossian, Chemical and Environmental Engineering, UA

### **Graduate Students:**

- Xiaomin Wei: Ph. D. candidate, Chemical and Environmental Engineering, UA
- Anand Meled: Ph. D. candidate, Chemical and Environmental Engineering, UA

### **Undergraduate Students:**

- Geoff Steward, Chemical and Environmental Engineering, UA
- Roy Dittler, Chemical and Environmental Engineering, UA

### **Other Researchers:**

- Yun Zhuang, Research Associate, Chemical and Environmental Engineering, UA
- Jiang Cheng, Visiting Scholar, Chemical and Environmental Engineering, UA

### **Cost Share (other than core ERC funding):**

- In-kind donation (diamond discs) from Mitsubishi Materials Corporation
- In-kind support from Araca, Inc.

*SRC/SEMATECH Engineering Research Center for Environmentally Benign Semiconductor Manufacturing*

# Objectives & ESH Metrics and Impact

## **Objectives:**

- Identify active and aggressive diamonds that make contacts with pad surface and create cutting furrows during pad conditioning.
- Investigate diamond wear during copper CMP process.
- Investigate diamond disc substrate wear during copper CMP process.

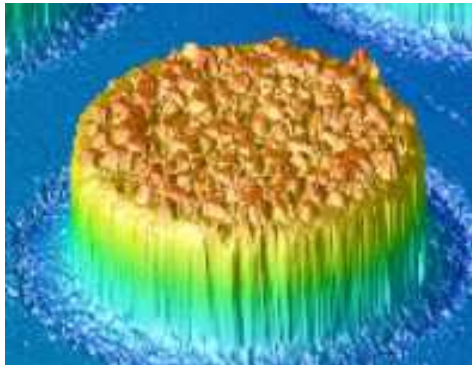
## **ESH Metrics and Impact:**

- Reduce diamond disc consumption by 20% through a better understanding of diamond and diamond disc substrate wear mechanism.

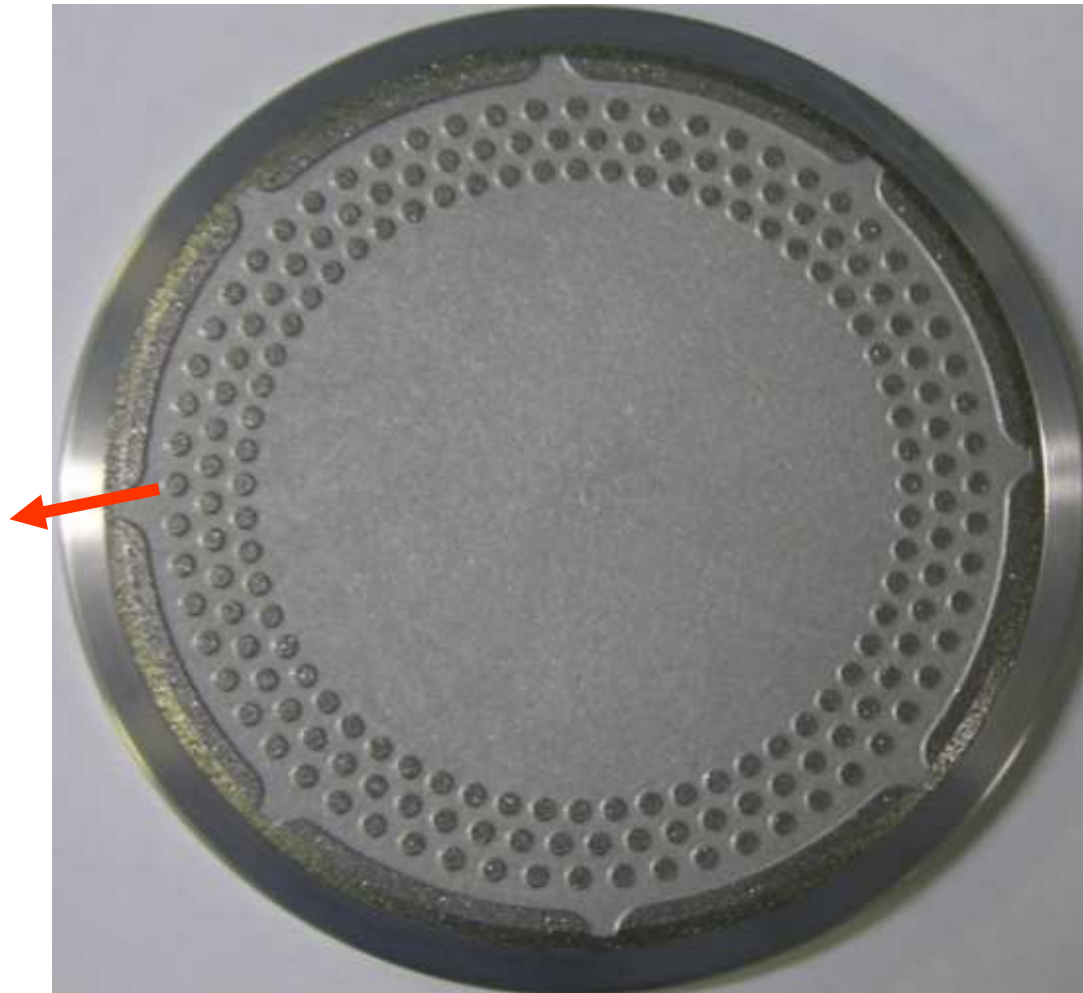
# Diamond Disc with Triple Ring Dot Design

**4.25-inch diameter**

**35 /mm<sup>2</sup> at 100 grit  
~60,000 diamonds**



**Raised 2 mm dots**



# Active Diamonds

**Active diamonds**, are defined as those diamonds that modify a pad surface by cutting furrows.

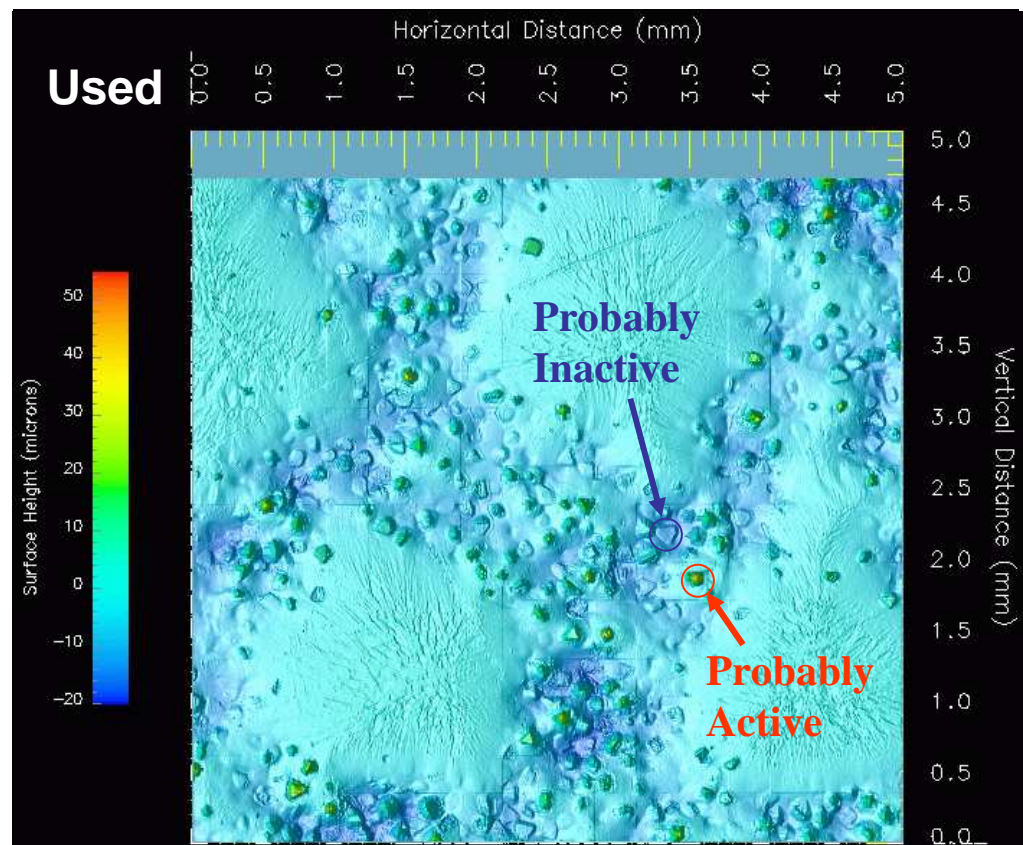
All diamonds that cut should wear

*but*

wear by itself is not proof of cutting.

For example, the metallization wears but does not cut.

Interferometry of an MMC Mosaic disc with a Teflon coating

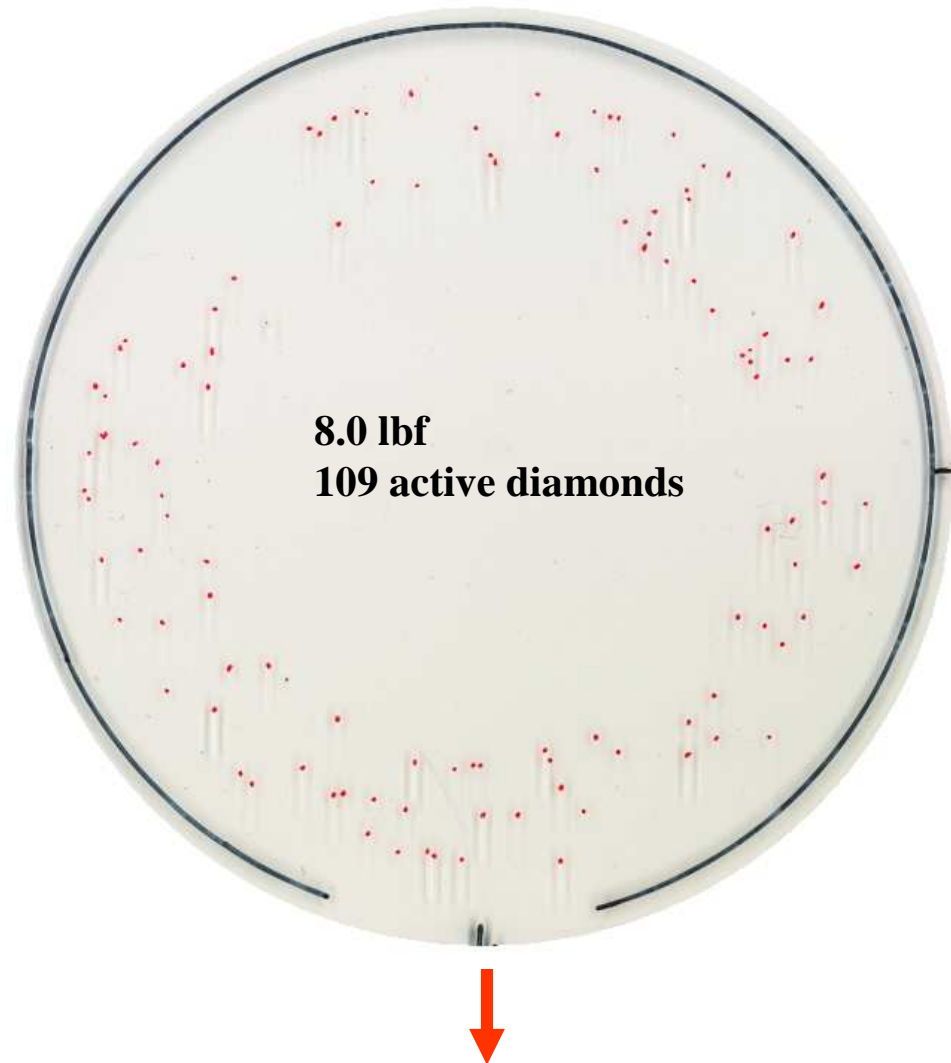


## Identify Active Diamonds - Short Draw Test



**Conditioner is pulled  
only about 1/4 inch.**

**Scratch origins are marked.**

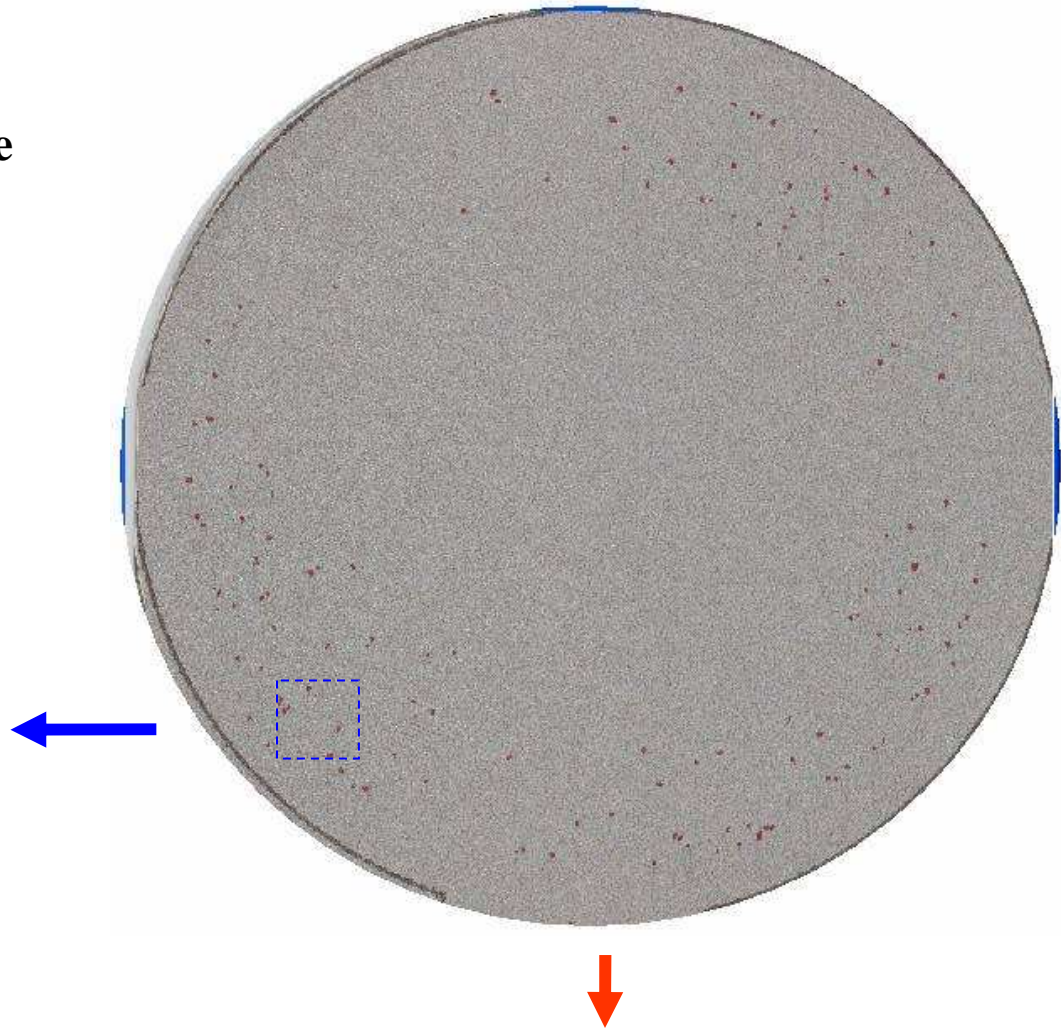




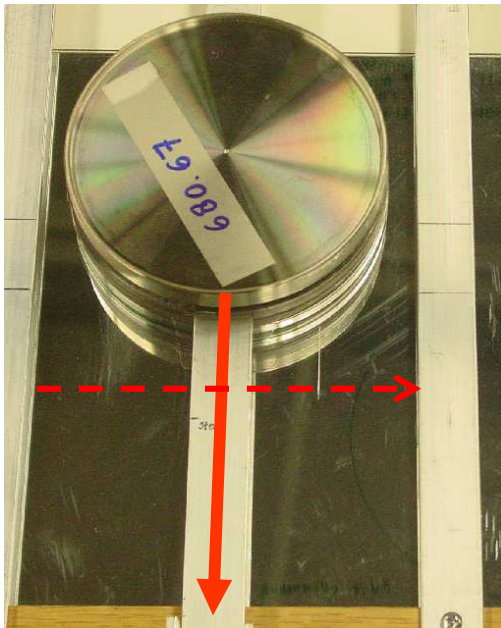
## Active Diamonds on IC1000 Pad

**IC1000 pad**  
**No grooves**  
**Mounted on polycarbonate**

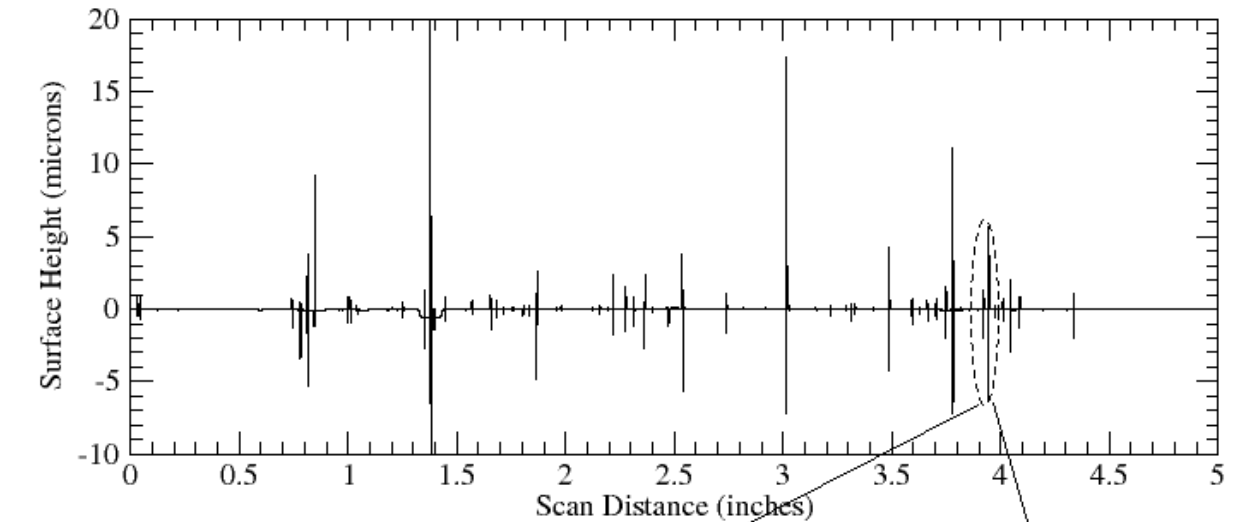
**80 nm Cr layer**  
**Deposited at 70 °C**



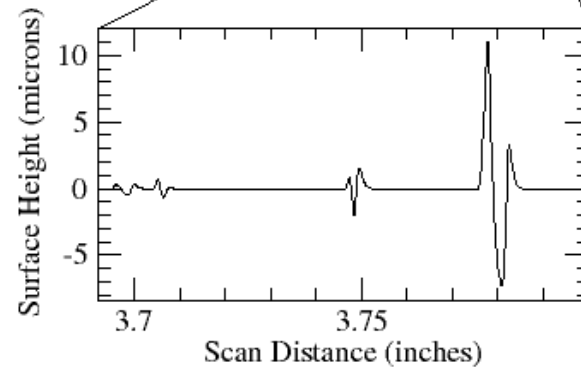
# Identify Aggressive Diamonds - Long Draw Test



**Conditioner is pulled  
more than one diameter  
of the disc.**

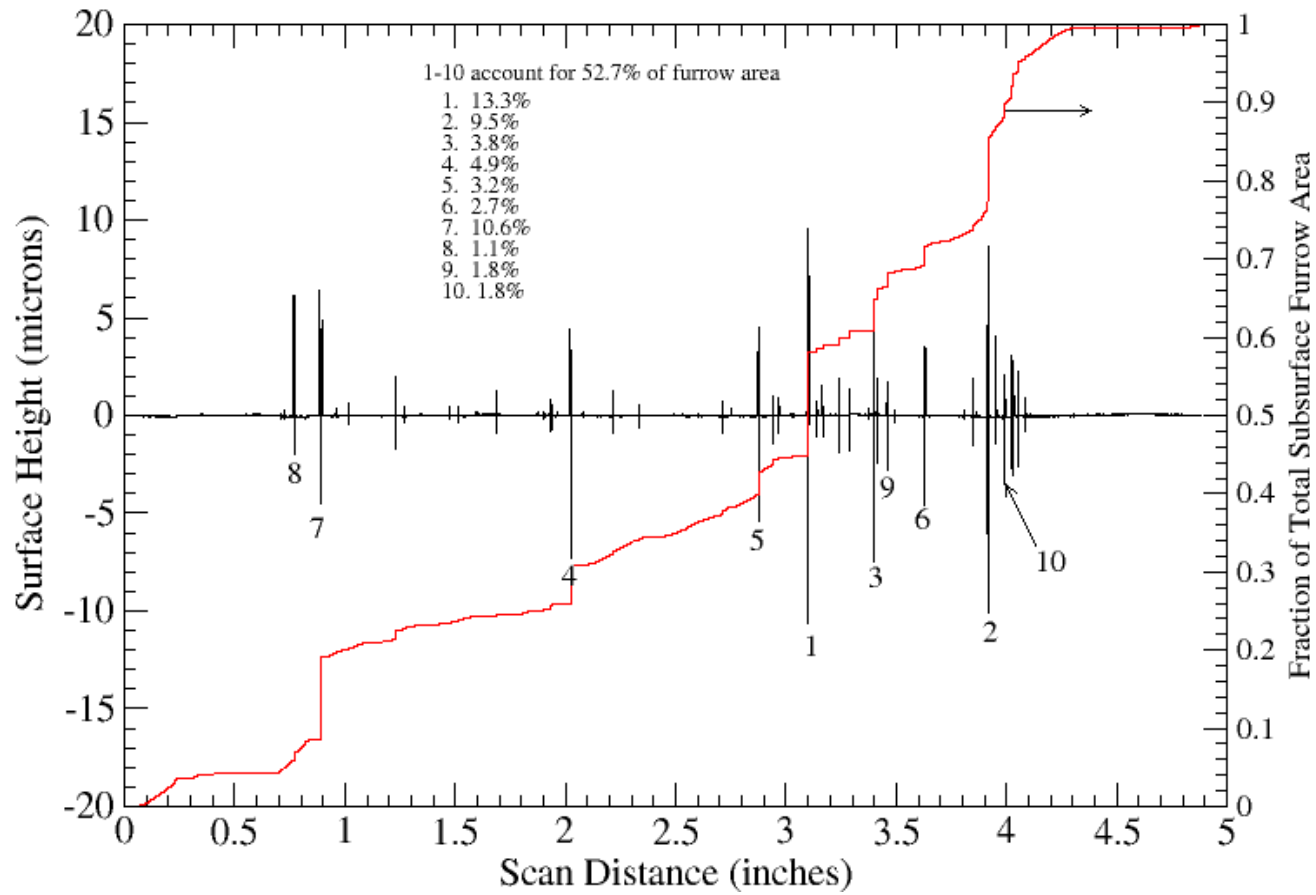


**Polycarbonate  
surface is profiled.**



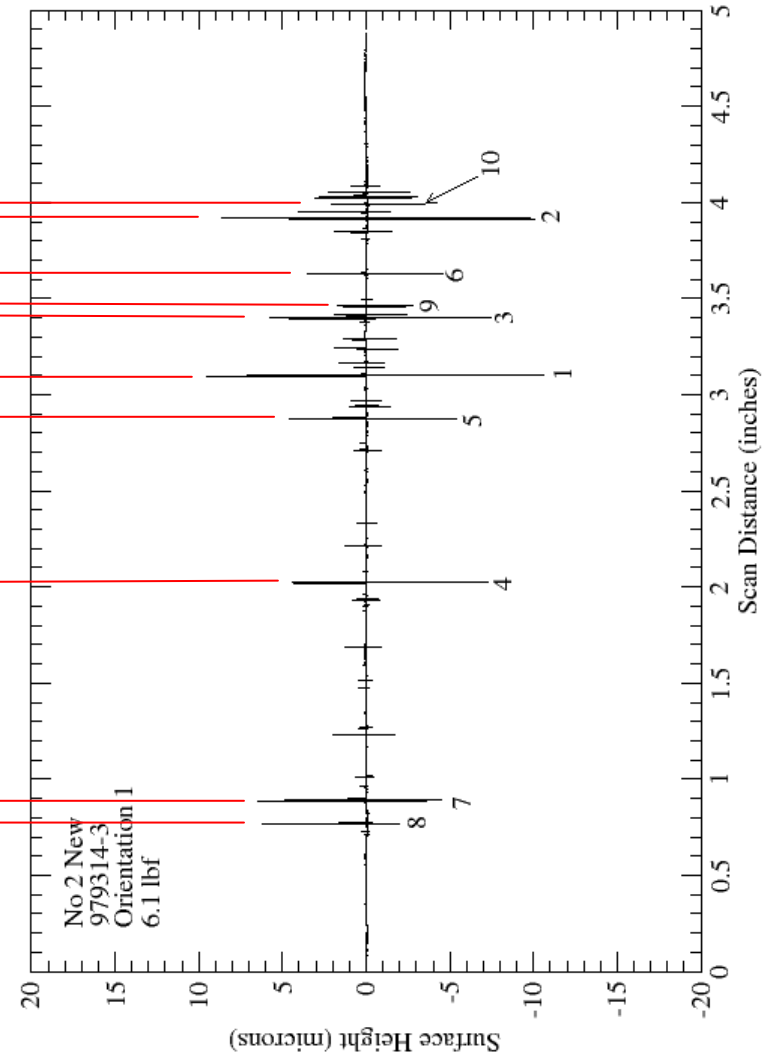
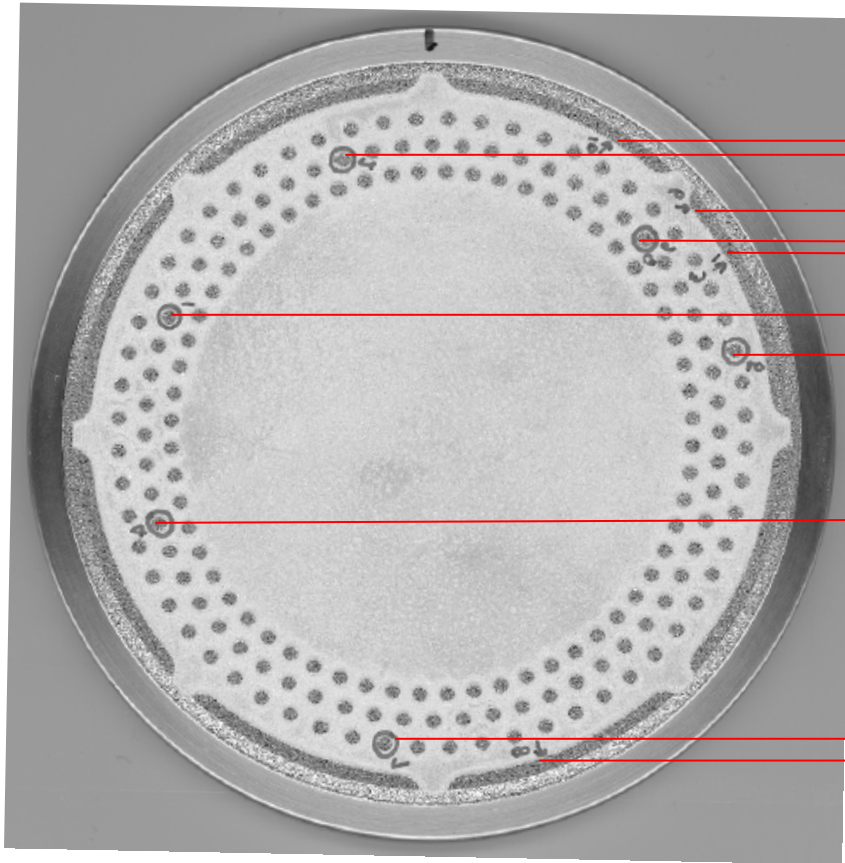


# Furrow Surface Area Analysis

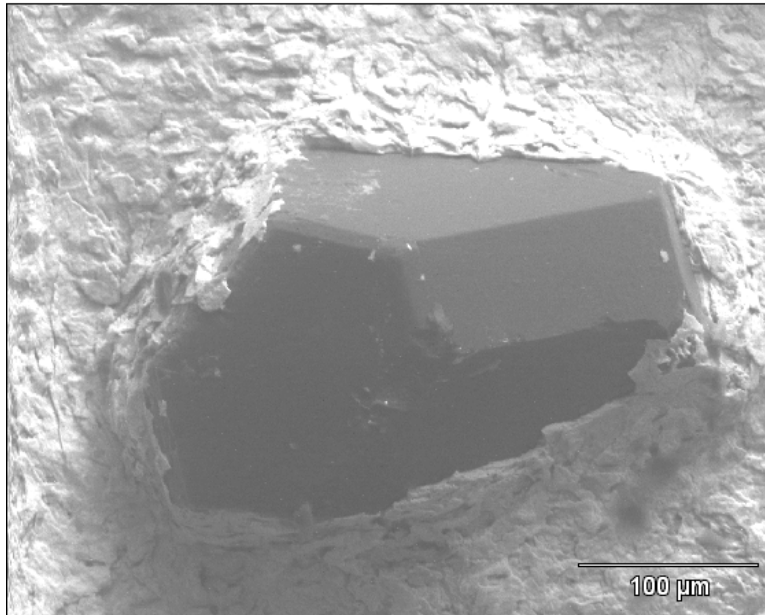


**The ten most aggressive diamonds account for more than 50% of pad cut rate during conditioning.**

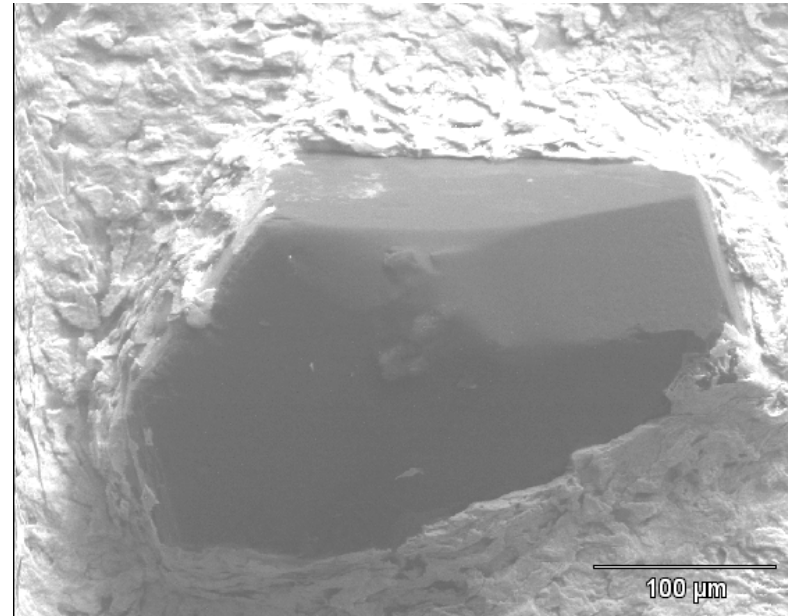
# Locate Aggressive Diamonds



## Diamond Wear



New aggressive diamond



Same diamond after wear test

**Normally there is no bulk wear on the diamond and micro wear occurs on the cutting edges of the diamond.**

# Industrial Interactions and Future Plans

## **Industrial mentors / contacts:**

- **Naoki Rikita (Mitsubishi Materials Corporation)**
- **Leonard Borucki (Araca, Inc.)**

## **Next year plan:**

- **Perform static etch tests and wear tests on diamond discs and quantify the extent of diamond micro-wear and diamond disc substrate wear at multiple temperatures through marathon conditioning tests (in copper slurries), static etch rate tests (in copper slurries) and white light interferometry.**

## **Long term plan:**

- **Obtain fundamental understanding of diamond and diamond disc substrate wear mechanism and extend diamond disc life.**

# Publications and Presentations

## Publications:

- **Diamond Conditioner Wear Characterization for a Copper CMP Process. L. Borucki, Y. Zhuang, A. Philipossian, R. Kikuma, R. Rikita, T. Yamashita, K. Nagasawa, H. Lee, T. Sun, D. Rosales-Yeomans and T. Stout. Transactions on Electrical and Electronic Materials, 8(1), 15-20 (2007).**
- **CMP Active Diamond Characterization and Conditioner Wear. L. Borucki, R. Zhuang, Y. Zhuang, A. Philipossian and N. Rikita. Materials Research Society Symposium Proceedings, Vol. 991, C01-01 (2007).**

## Presentation:

- **CMP Active Diamond Characterization and Conditioner Wear. L. Borucki, R. Zhuang, Y. Zhuang, A. Philipossian and N. Rikita. 2007 Materials Research Society Spring Meeting, San Francisco, California, April 9-13 (2007).**

# **An Integrated, Multi-Scale Framework for Designing Environmentally Benign Copper, Tantalum and Ruthenium Planarization Processes**

*(Task Number: 425.020)*

## **Subtask 1: Wear Phenomena and Their Effect on Process Performance**

### **PI:**

- Ara Philipossian, Chemical and Environmental Engineering, UA

### **Graduate Student:**

- Ting Sun: Ph. D. candidate, Chemical and Environmental Engineering, UA

### **Undergraduate Student:**

- Roy Dittler, Chemical and Environmental Engineering, UA

### **Other Researcher:**

- Yun Zhuang, Research Associate, Chemical and Environmental Engineering, UA

### **Cost Share (other than core ERC funding):**

- In-kind donation (pads and slurries) from Cabot Microelectronics Corporation
- In-kind support from Araca, Inc.

*SRC/SEMATECH Engineering Research Center for Environmentally Benign Semiconductor Manufacturing*

# Objectives & ESH Metrics and Impact

## **Objectives:**

- Investigate the effect of conditioning on pad topography through white light interferometry and incremental loading analysis.
- Investigate the effect of conditioning on pad surface contact area through confocal microscopy analysis.
- Investigate the effect of pad conditioning on slurry film thickness in pad-wafer interface area through dual emission UV enhanced fluorescence (DEUVEF) technique.

## **ESH Metrics and Impact:**

- Reduce diamond disc consumption by 20% and reduce pad consumption by 33% through a better understanding of the conditioning effect during CMP processes.

## Relevance of Pad Surface Abruptness ( $\lambda$ )

Profilometry analysis: **surface roughness** (top pad asperities to pad valleys), **no consistent correlation with material removal rates**.

White light interferometry and incremental loading analysis: **surface abruptness** (top 20 - 30  $\mu\text{m}$  pad asperities), **closely correlated with material removal rates**.

Two-step modified Langmuir-Hinshelwood removal rate model:

$$\text{Removal rate} \quad RR = \frac{M_w}{\rho} \frac{k_2 k_1}{k_2 + k_1}$$

$$\text{Chemical rate constant} \quad k_1 = A \cdot e^{-E/k\bar{T}}$$

$$\text{Mechanical rate constant} \quad k_2 = c_p \mu_k pV$$

$$\text{Wafer surface reaction temperature} \quad \bar{T} = \bar{T}_p + \frac{\beta_1 \kappa_s^{3/4} \lambda^{-1/4} \eta_s^{-1/2}}{V^{1/2+e}} \mu_k pV$$

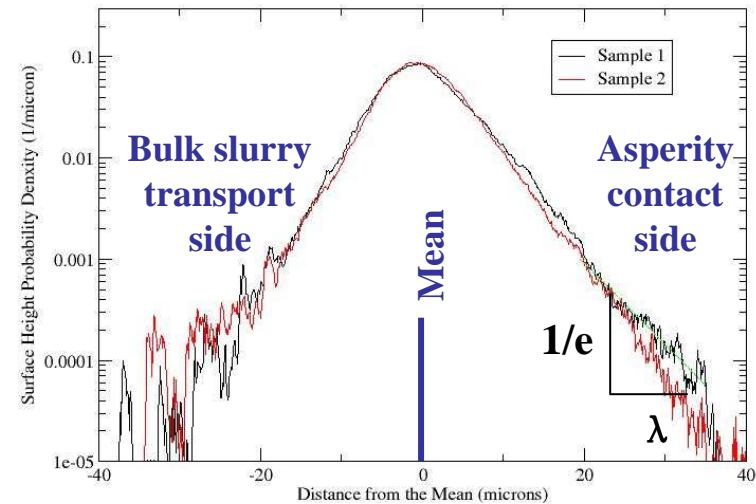
$$\text{COF} \quad \mu_k = \mu_{pa} + \mu_{visc}^1 \kappa_s^{0.19} \lambda^{-0.17}$$



# Pad Surface Abruptness Measurement

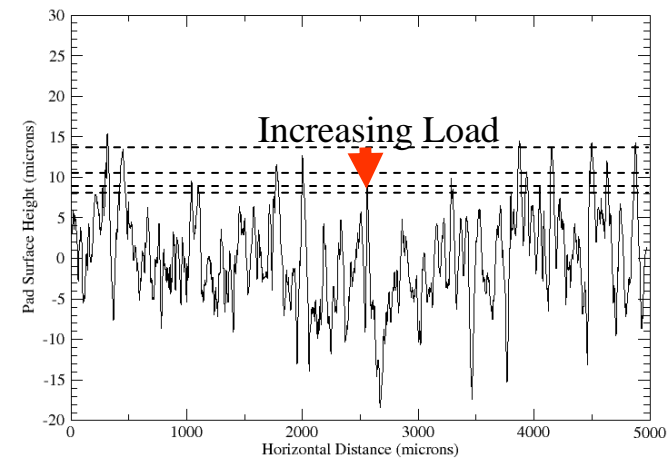
## Extracted from white light interferometry

$\lambda$  - For PDFs with an exponential tail,  $\lambda$  is the distance over which the tail drops by a factor of  $1/e$ .

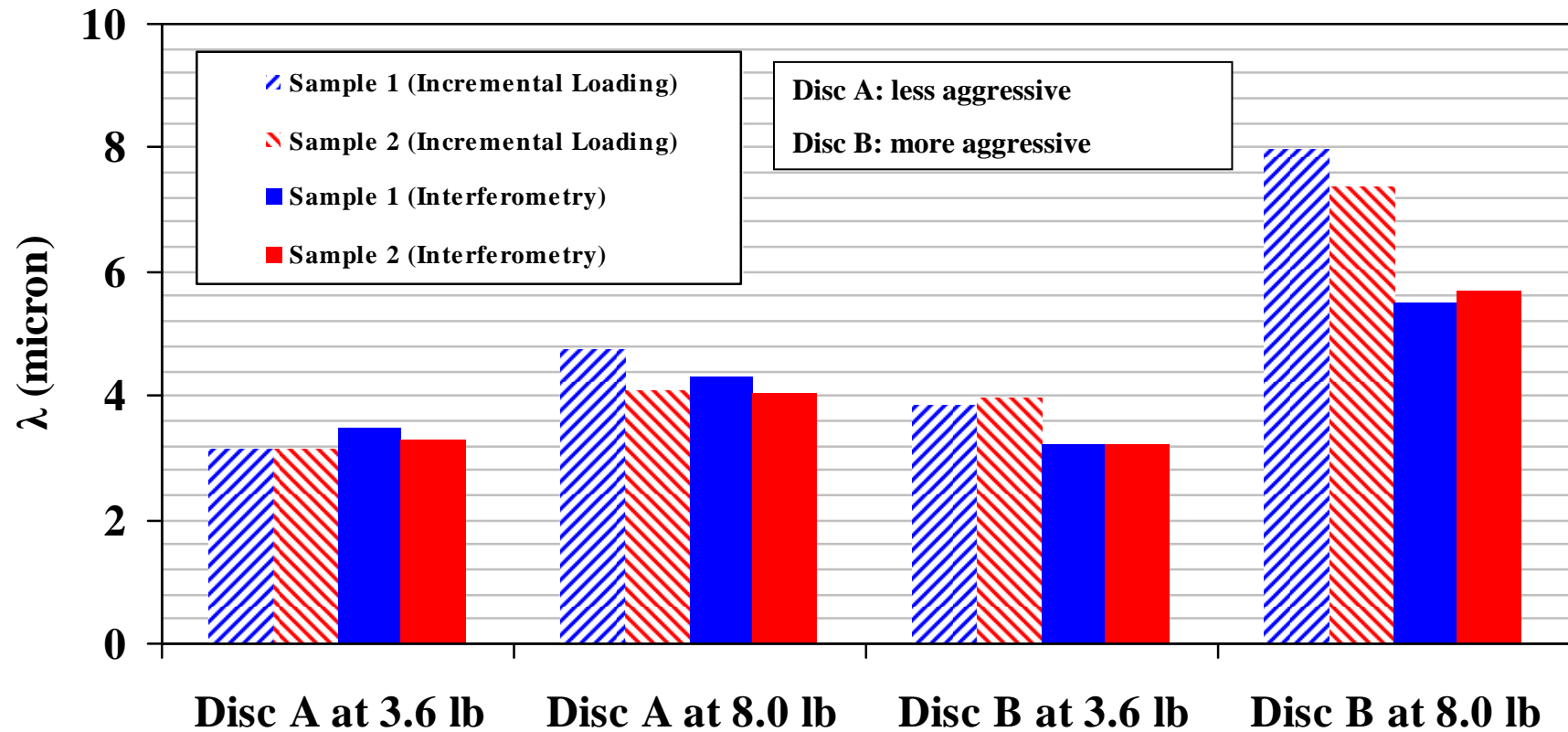


## Extracted from incremental loading analysis

$\lambda$  is the increment in pad surface displacement that occurs when the applied pressure is increased or decreased by a factor of  $e$ .

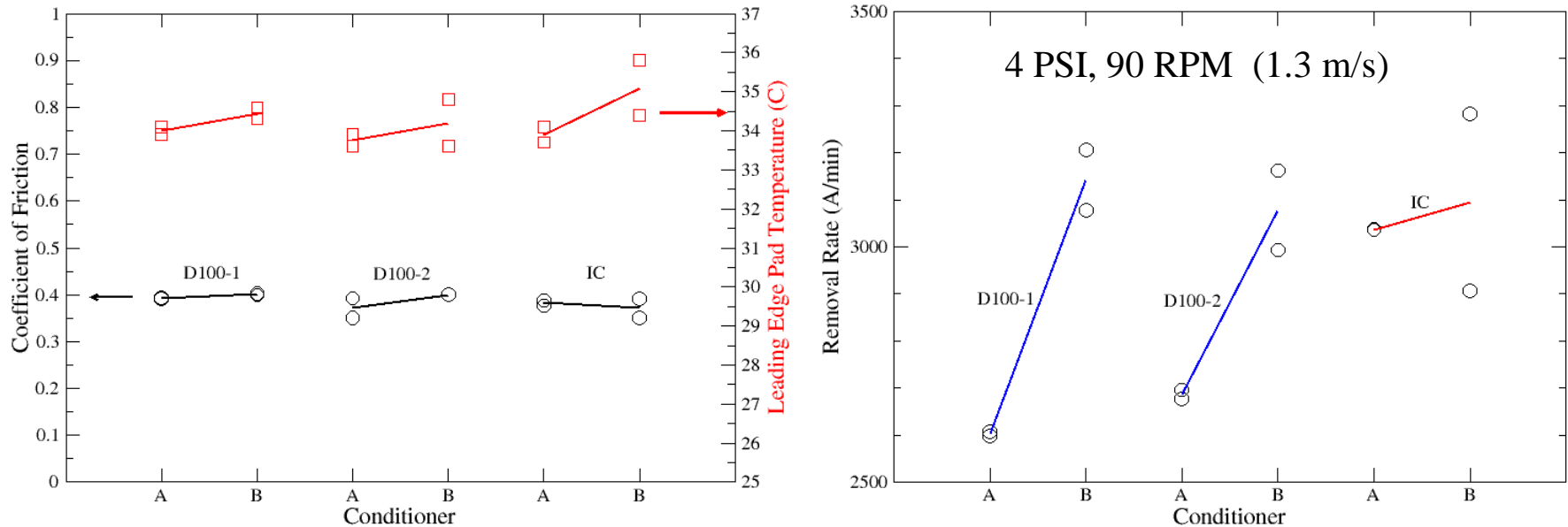


# Effect of Conditioning on Pad Surface Abruptness



**The surface abruptness extracted from the incremental loading analysis and interferometry is consistent. A more aggressive diamond disc generates a more abrupt pad surface under a higher conditioning force.**

# Effect of Conditioning on COF, Pad Temperature, and Oxide Removal Rate

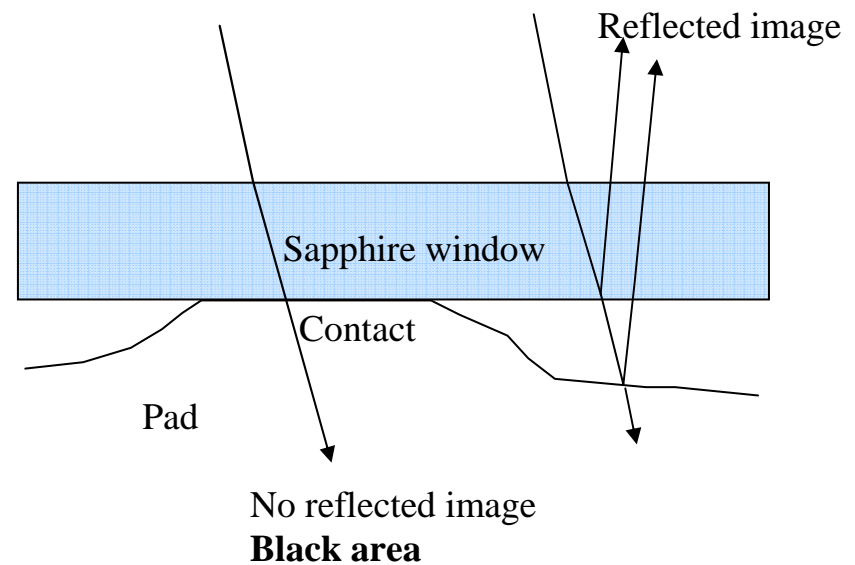


**A more aggressive diamond disc generates higher pad temperatures and higher oxide removal rates.**

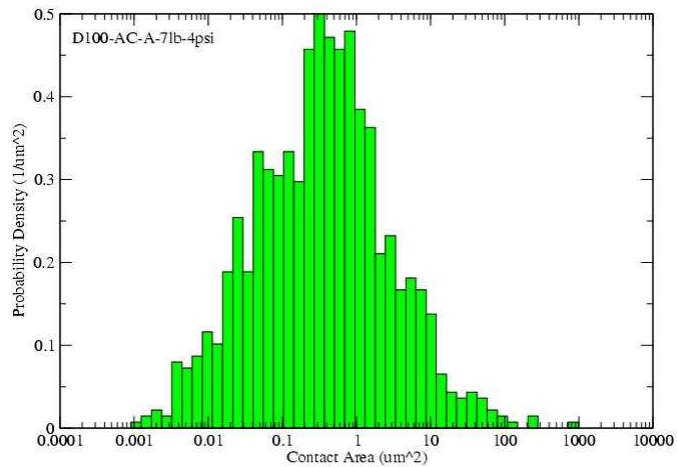
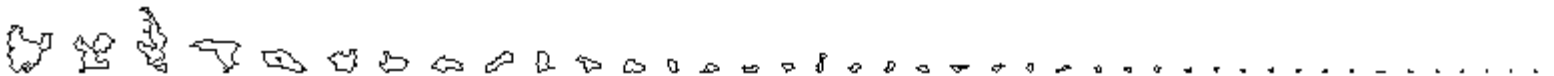
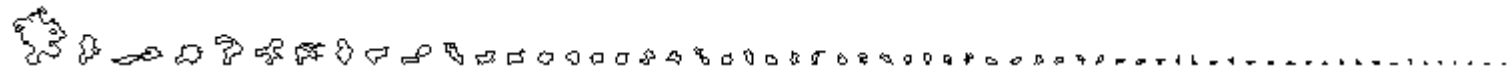
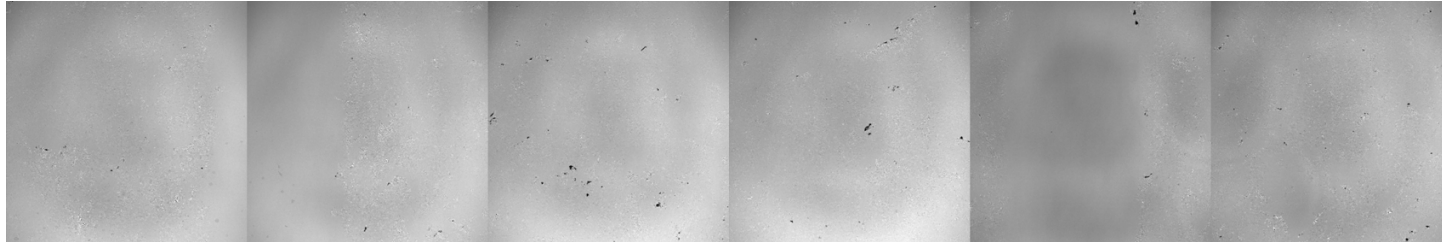
# Pad Surface Contact Area Measurement through Laser Confocal Microscopy



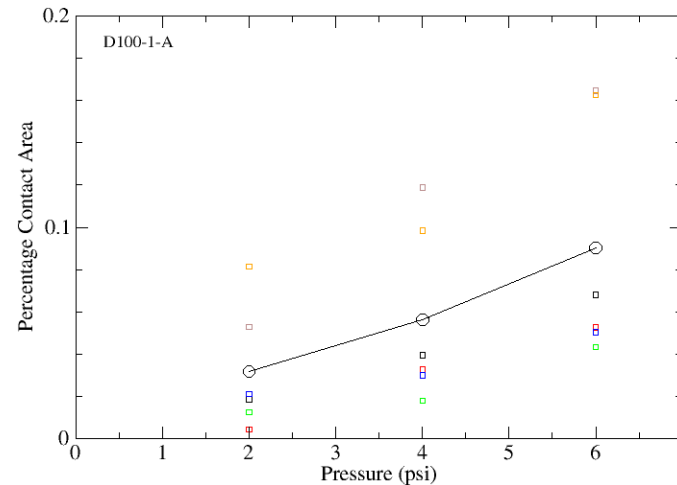
**Zeiss LSM 510 Meta NLO**  
488 nm wavelength laser



# Pad Surface Contact Area Analysis

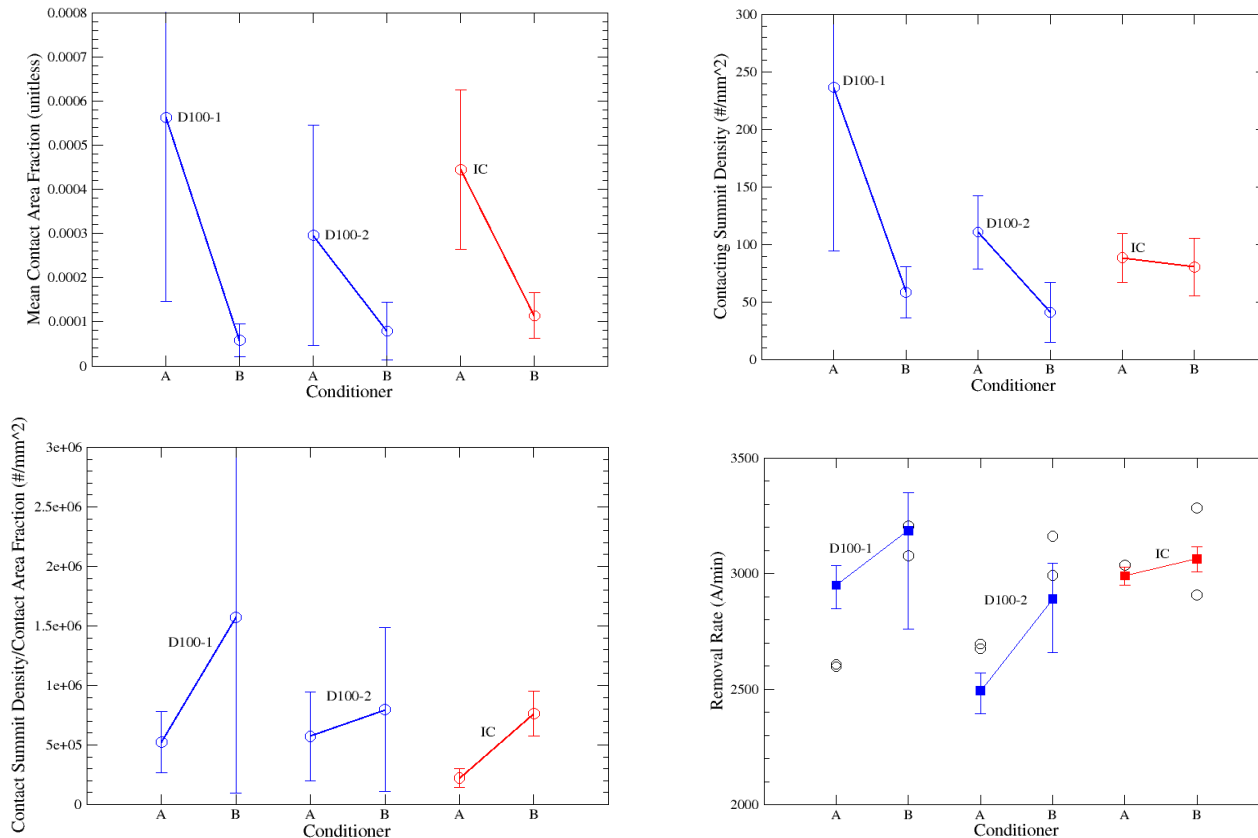


Pad contact area histogram



Pad contact area vs. Pressure

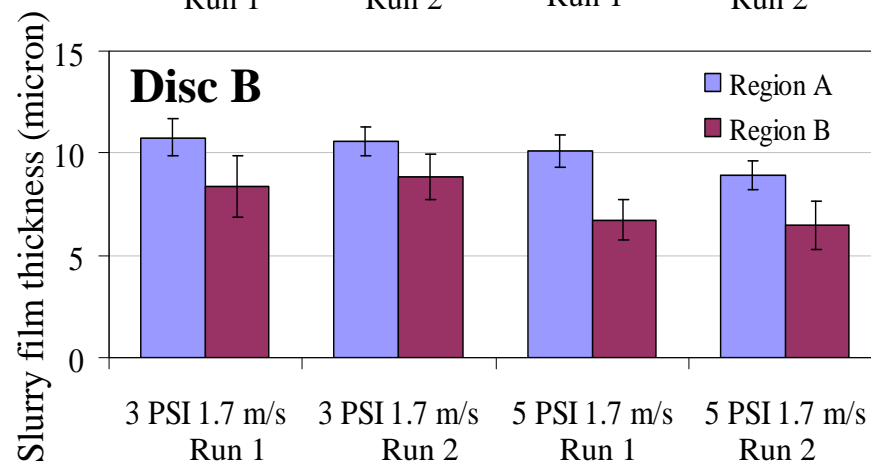
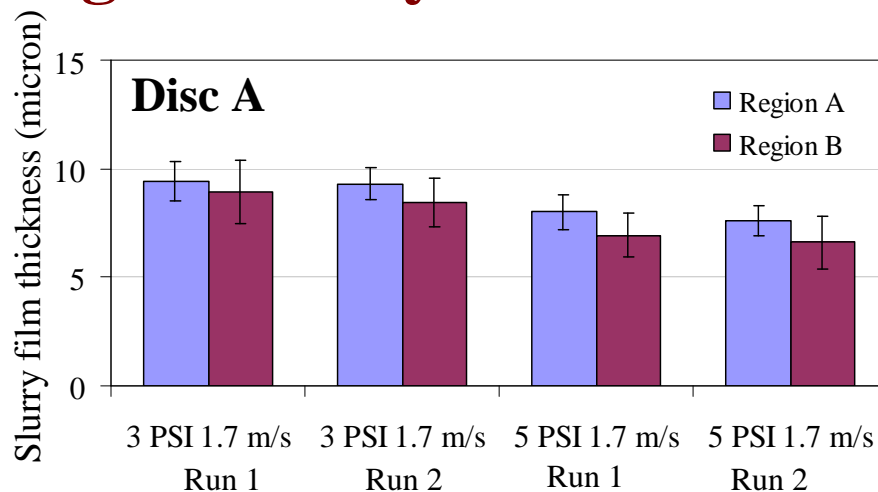
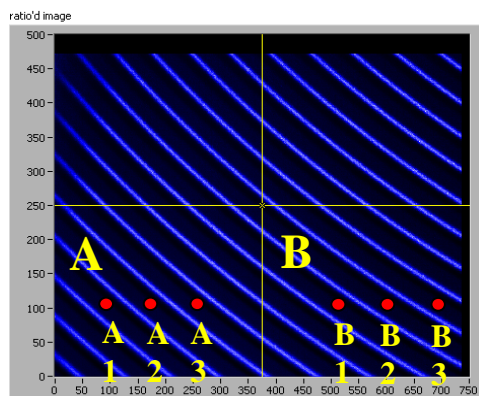
# Effect of Conditioning on Contact Area



**The ratio of the contacting summit density to the contact area fraction is more important than either measured separately since the ratio determines the mean real contact pressure.**

**Removal rate simulation indicates that the conditioning effect arises from the influence of the mean real contact pressure on the chemical rate of the polishing process.**

# Effect of Conditioning on Slurry Film Thickness



**A more aggressive disc generates a more abrupt pad surface, leading to a thicker slurry film in the pad-wafer interface area.**

# Industrial Interactions and Future Plans

## **Industrial mentors / contacts:**

- **Sriram Anjur (Cabot Microelectronics Corporation)**
- **Abaneshwar Prasad (Cabot Microelectronics Corporation)**
- **Ananth Naman (Cabot Microelectronics Corporation)**
- **Cliff Spiro (Cabot Microelectronics Corporation)**
- **Leonard Borucki (Araca, Inc.)**

## **Next year plan:**

- **Investigate the effect of conditioning on pad topography for metal CMP processes.**

## **Long term plan:**

- **Achieve fundamental understanding of the effect of conditioning on pad topography and polishing performance for CMP processes.**



## **Publications and Presentations**

### **Publication:**

- **Investigation of Diamond Grit Size and Conditioning Force Effect on CMP Pads Topography. T. Sun, L. Borucki, Y. Zhuang and A. Philipossian. Materials Research Society Symposium Proceedings, Vol. 991, C01-07 (2007).**

### **Presentations:**

- **On the Relationship between Contact Area Data and Polishing. L. Borucki, T. Sun, Y. Sampurno, F. Sudargho, X. Wei, Y. Zhuang, S. Anjur and A. Philipossian. 12th International Symposium on Chemical-Mechanical Planarization, Lake Placid, New York, August 12-15 (2007).**
- **The Effect of Conditioning on Pad Topography and Shear-Induced Flow Resistance during CMP. T. Sun, L. Borucki, R. Zhuang, Y. Zhuang and A. Philipossian. 2007 Materials Research Society Spring Meeting, San Francisco, California, April 9-13 (2007).**

# **An Integrated, Multi-Scale Framework for Designing Environmentally Benign Copper, Tantalum and Ruthenium Planarization Processes**

*(Task Number: 425.020)*

## **Subtask 1: Wear Phenomena and Their Effect on Process Performance**

### **PI:**

- **Ara Philipossian, Chemical and Environmental Engineering, UA**

### **Graduate Students:**

- **Xiaomin Wei: Ph. D. candidate, Chemical and Environmental Engineering, UA**
- **Yasa Sampurno: Ph. D. candidate, Chemical and Environmental Engineering, UA**

### **Other Researchers:**

- **Yun Zhuang, Research Associate, Chemical and Environmental Engineering, UA**
- **Francisca Sudargho, Research Technician, Chemical and Environmental Engineering, UA**

### **Cost Share (other than core ERC funding):**

- **In-kind donation (retaining rings) from Entegris, Inc.**
- **In-kind support from Araca, Inc.**

*SRC/SEMATECH Engineering Research Center for Environmentally Benign Semiconductor Manufacturing*

# Objectives & ESH Metrics and Impact

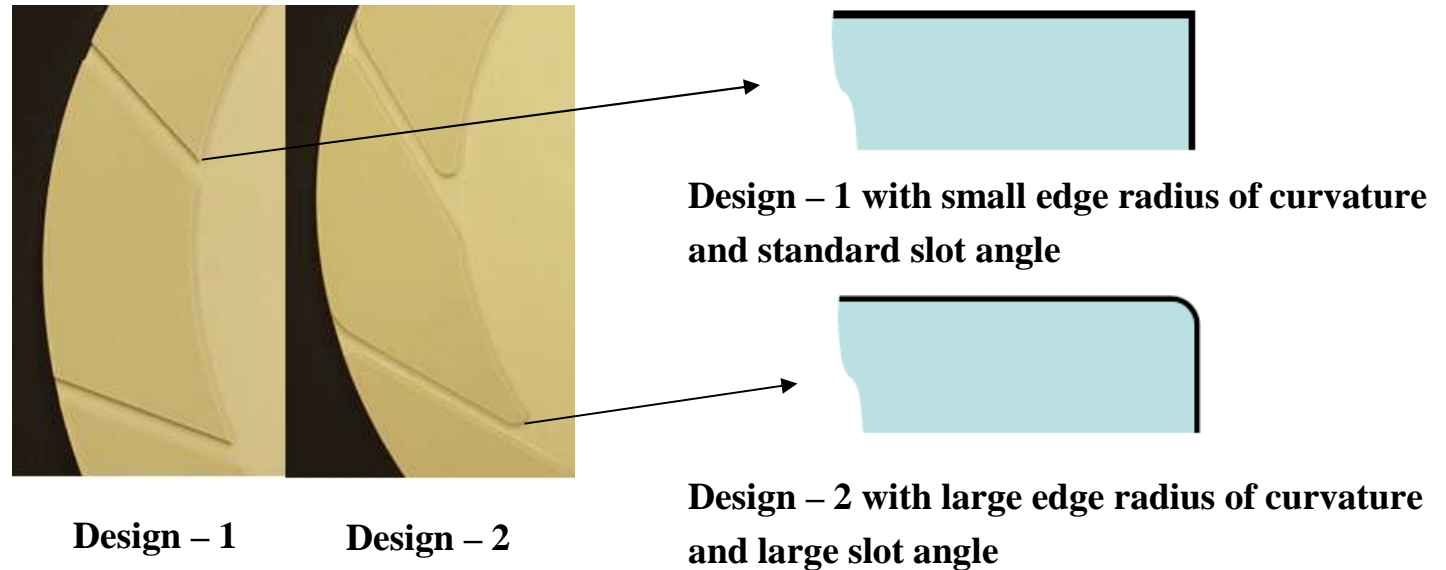
## **Objectives:**

- Develop methodology to accurately measure retaining ring local wear rate.
- Investigate how retaining ring material and design affect:
  - Retaining ring wear rate
  - Average shear force and variance of shear force
  - Pad temperature
  - Pad micro-texture
  - Slurry mean residence time

## **ESH Metrics and Impact:**

- Reduce retaining ring consumption by 33% and slurry consumption by 20% through a better understanding of retaining ring wear mechanism and the effect of retaining ring design on slurry flow during CMP processes.

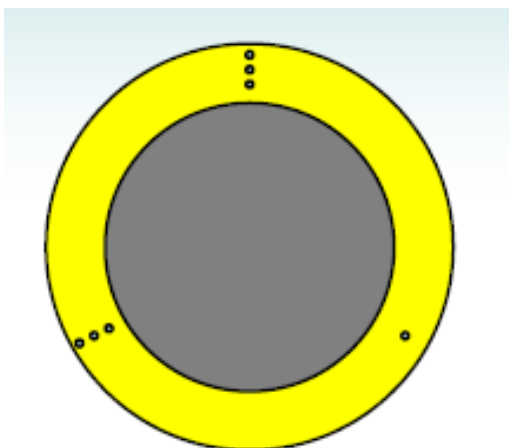
## Retaining Ring Material and Design



**Three retaining rings were investigated:**

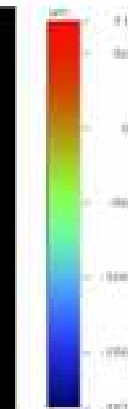
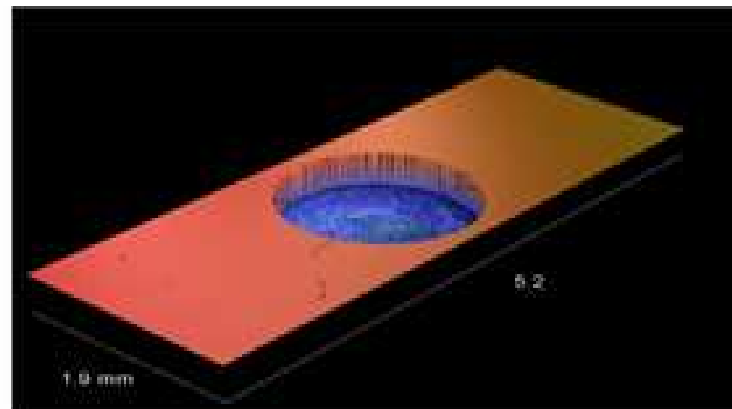
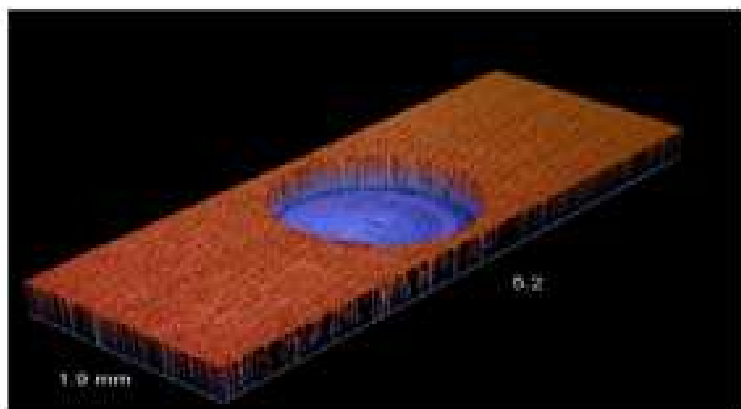
- **PPS - 1:** made of PPS (polyphenylene sulfide) with **Design - 1**
- **PEEK - 1:** made of PEEK (polyetherenterketone) with **Design - 1**
- **PEEK - 2:** made of PEEK (polyetherenterketone) with **Design - 2**

# White Light Interferometry Measurement



Seven shallow trenches (1.5 mm in diameter and 0.2 mm in depth) were precision-machined into the land areas of each retaining ring.

Interferometry analysis was then performed on the trenches before and after a 4-hour wear test to calculate the local and average retaining ring wear rate.



Trench interferometry image before wear test

Trench interferometry image after a 4-hour wear test

## Retaining Ring Wear Rate

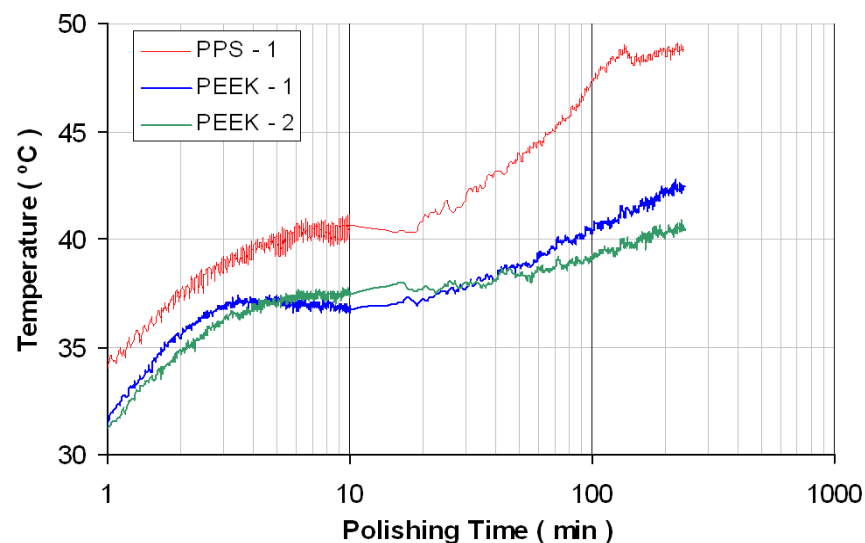
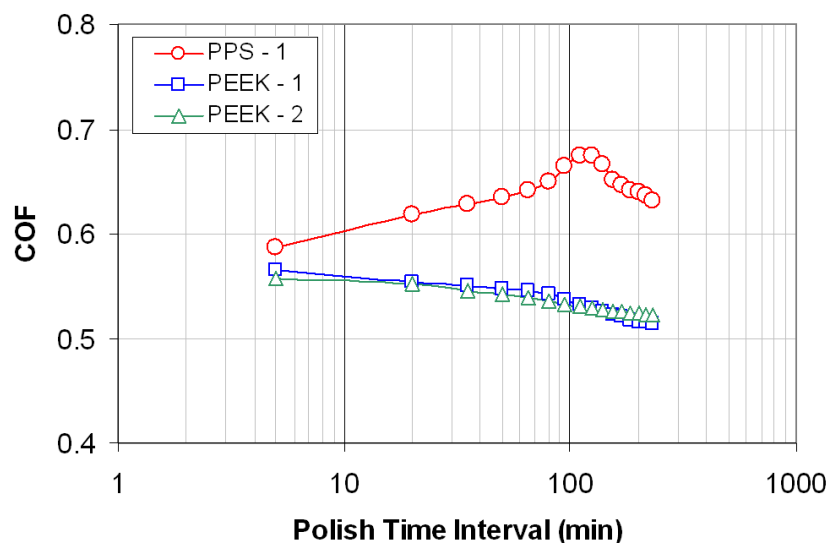
Pre and post interferometry results from the micro-machined trenches indicate the following wear rates:

- PPS – 1 ring: 28.2  $\mu\text{m}/\text{hour}$
- PEEK – 1 ring: 24.0  $\mu\text{m}/\text{hour}$
- PEEK – 2 ring: 23.5  $\mu\text{m}/\text{hour}$

This indicates that the retaining ring material, not design, is the main factor influencing the wear rate.

Micrometry results (taken from areas adjacent to the micro-machined trenches) indicate a difference of  $\pm 13$  percent compared to interferometry results.

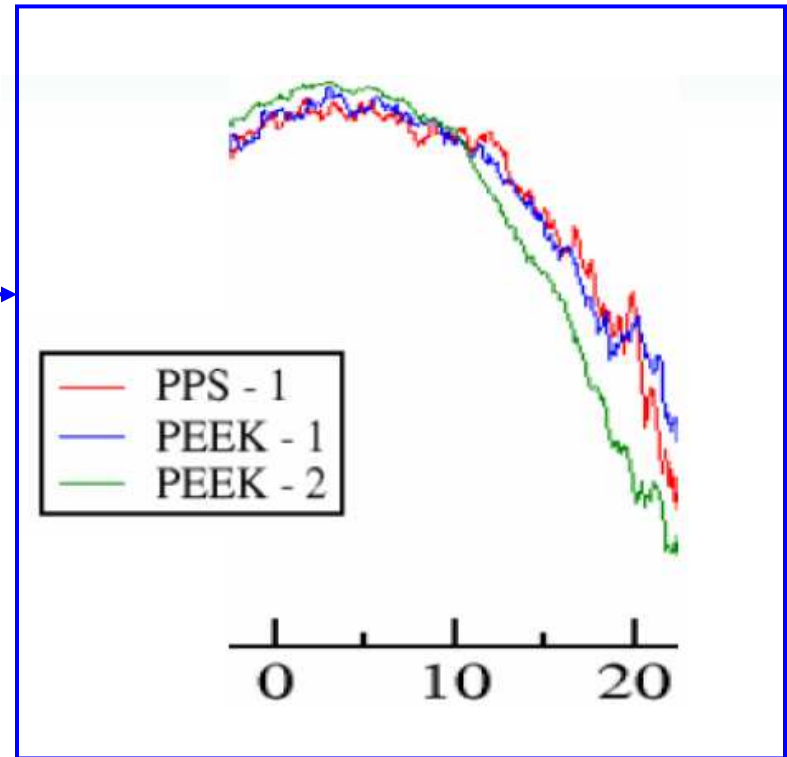
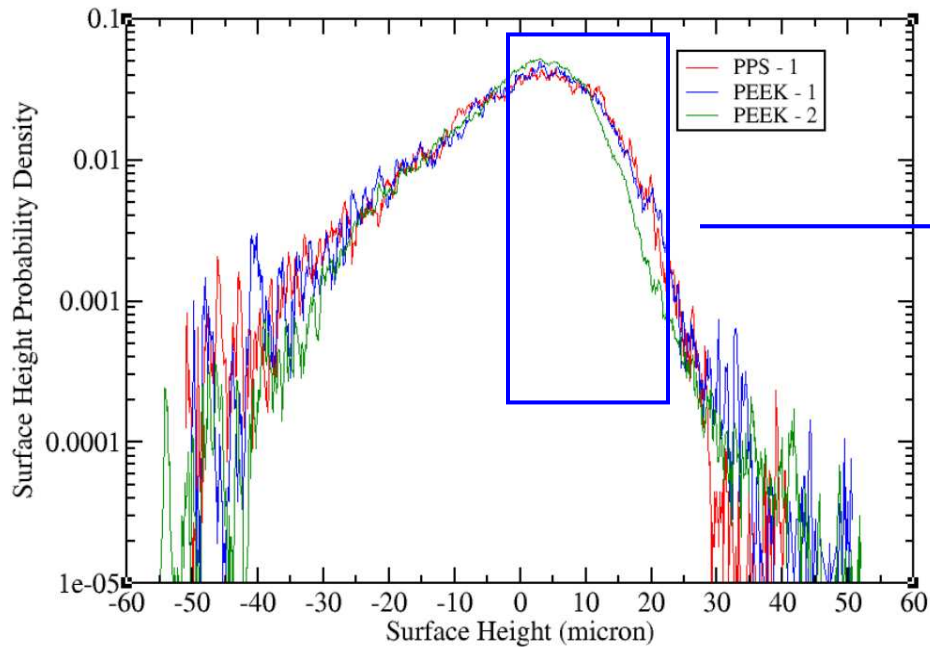
## COF and Pad Temperature



The PEEK rings achieve better lubricity and COF stability than the PPS ring.

Higher temperatures associated with the PPS ring can cause higher material removal rates, thus indicating that thermal effects need to be taken into account when qualifying rings made of new materials.

# Pad Surface Interferometry Analysis

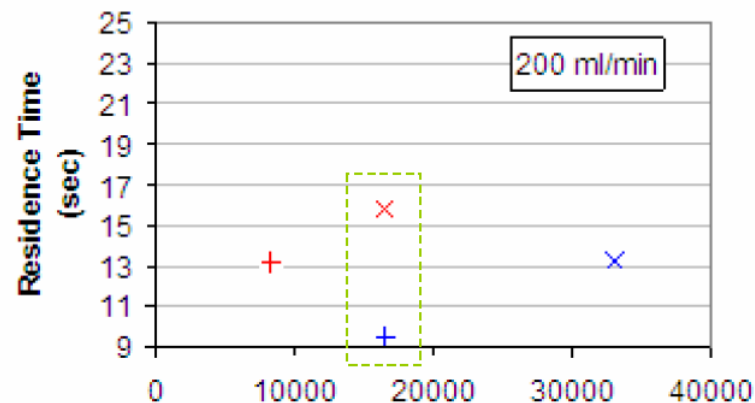
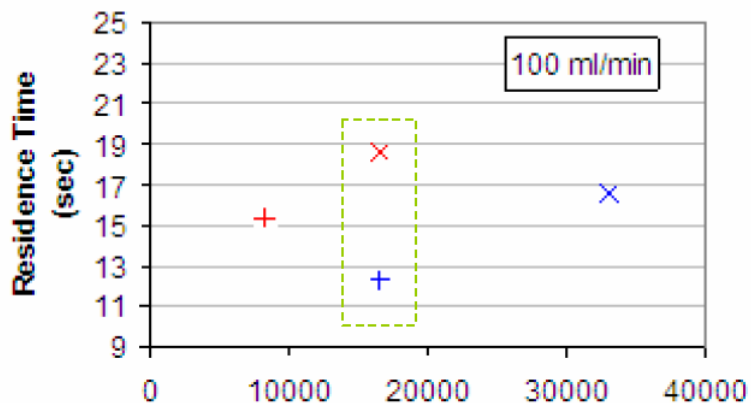


The PEEK – 2 ring achieves a narrower pad surface height distribution than the PPS – 1 and PEEK – 1 rings, suggesting that the slot design and the edge rounding play significant roles in shaping the pad micro texture.

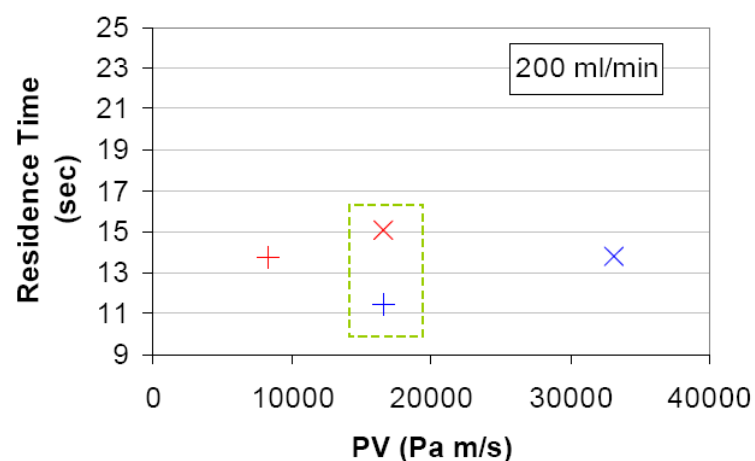
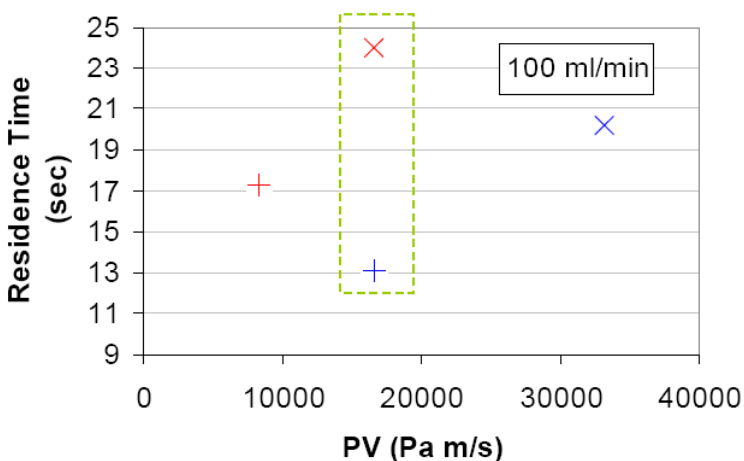


# Slurry Mean Residence Time

**PEEK - 1**



**PEEK - 2**

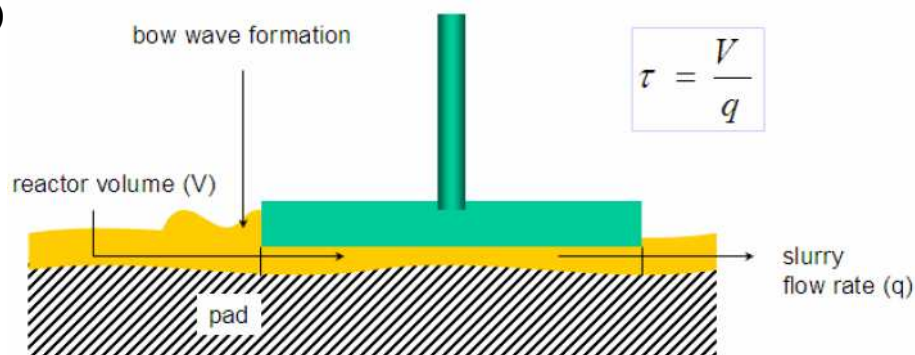


**Design - 1 is 10 - 20 percent more efficient in getting slurry in and out the wafer-pad interface.**

# Mean Residence Time Trend Analysis

- **Effect of Flow Rate**

- Higher flow rates decrease MRT (on average, a 2X increase in flow causes MRT to decrease by only 25 percent)
- CMP is an open system with plenty of slurry being wasted



- **Effect of Sliding Velocity**

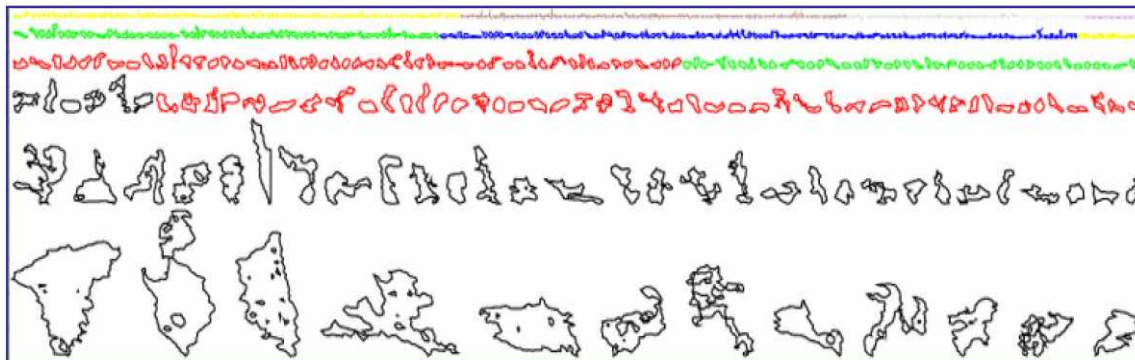
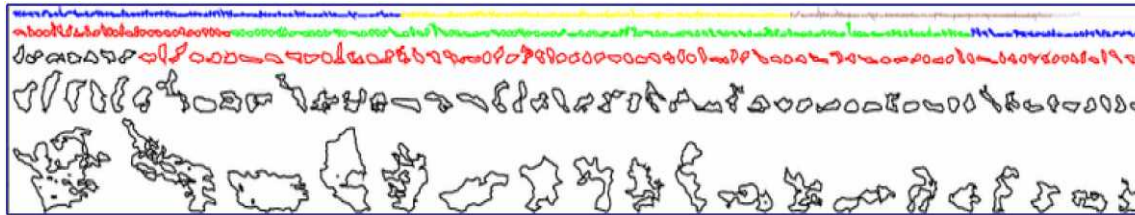
- Higher sliding velocities increase MRT (on average, a 2X increase in sliding velocity causes MRT to increase by 30 percent)
- DEUVEF images examples at low velocity (left) and high velocity (right)



# Mean Residence Time Trend Analysis

## Effect of Pressure

- Higher pressures decrease MRT (on average, a 2X increase in pressure causes MRT to decrease by 15 percent)
- Laser Confocal Microscopy examples of pad contacting features at low (top) and high (bottom) pressures



$$\tau = \frac{V}{q}$$

# Industrial Interactions and Future Plans

## **Industrial mentors / contacts:**

- **Christopher Wargo (Entegris, Inc.)**
- **Leonard Borucki (Araca, Inc.)**

## **Next year plan:**

- **Perform DEUVEF (dual emission UV enhanced fluorescence) tests to investigate the effects of retaining ring design, slurry flow rate, sliding velocity, and wafer pressure on slurry film thickness in the pad-wafer interface.**

## **Long term plan:**

- **Extend retaining ring life and improve retaining ring design to achieve better slurry utilization efficiency.**

## **Publications and Presentations**

### **Publication:**

- **Tribological, Kinetic, Thermal and Flow Characteristics of PPS and PEEK Retaining Rings. A. Philipossian, X. Wei, Y. Sampurno, F. Sudargho, Y. Zhuang, C. Wargo and L. Borucki. International Conference on Planarization/CMP Technology Proceedings, 31-35 (2007).**

### **Presentation:**

- **Tribological, Kinetic, Thermal and Flow Characteristics of PPS and PEEK Retaining Rings. A. Philipossian, X. Wei, Y. Sampurno, F. Sudargho, Y. Zhuang, C. Wargo and L. Borucki. International Conference on Planarization/CMP Technology, Dresen, Germany, October 25-27 (2007).**

# **An Integrated, Multi-Scale Framework for Designing Environmentally Benign Copper, Tantalum and Ruthenium Planarization Processes**

*(Task Number: 425.020)*

## **Subtask 2: Real-Time Detection and Modeling of Pattern Evolution**

### **PI:**

- Ara Philipossian, Chemical and Environmental Engineering, UA

### **Graduate Students:**

- Yasa Sampurno: Ph. D. candidate, Chemical and Environmental Engineering, UA

### **Other Researchers:**

- Yun Zhuang, Research Associate, Chemical and Environmental Engineering, UA
- Fransisca Sudargho, Research Technician, Chemical and Environmental Engineering, UA
- Siannie Theng, Research Technician, Chemical and Mechanical Engineering, UA

### **Cost Share (other than core ERC funding):**

- In-kind donation (slurries) from Hitachi Chemical Co., Ltd.
- In-kind support from Araca, Inc.

*SRC/SEMATECH Engineering Research Center for Environmentally Benign Semiconductor Manufacturing*

# Objectives & ESH Metrics and Impact

## **Objective:**

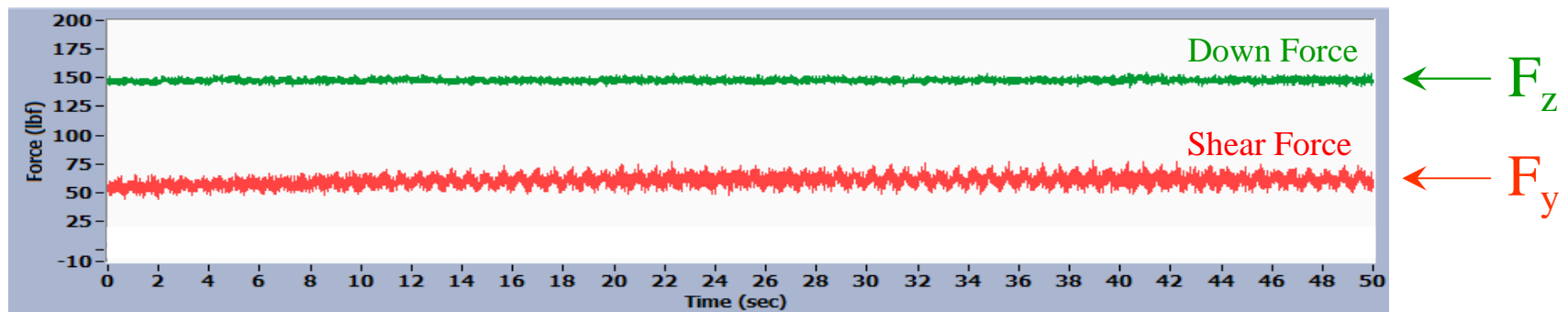
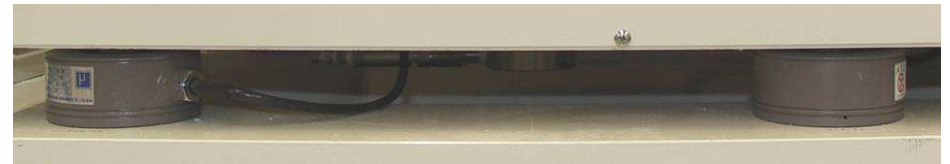
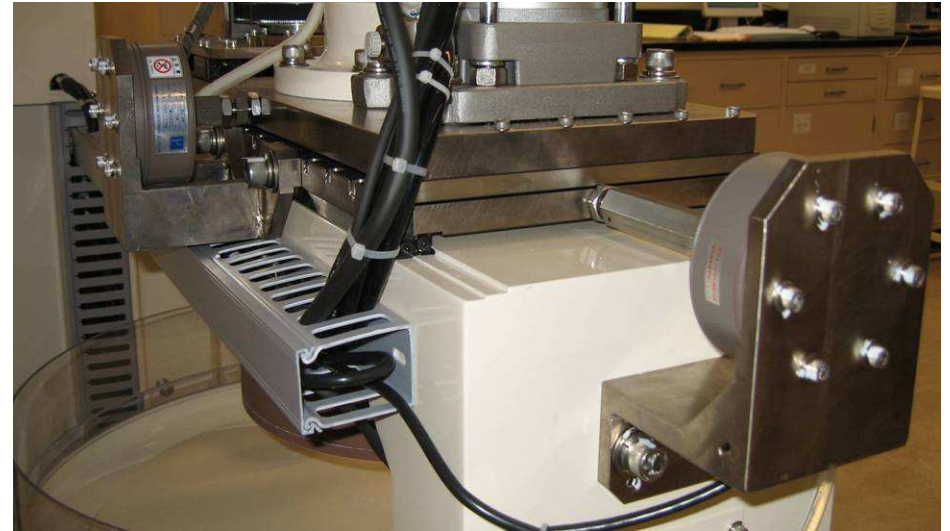
Determine whether shear force and down force spectral analysis can generate unique spectral fingerprints before, during, and after transition from oxide to  $\text{Si}_3\text{N}_4$  layer during STI patterned wafer polishing.

## **ESH Metrics and Impact:**

Reduce slurry, diamond disc, and pad consumption by 25% by establishing end-point detection through shear force and down force spectral analysis.

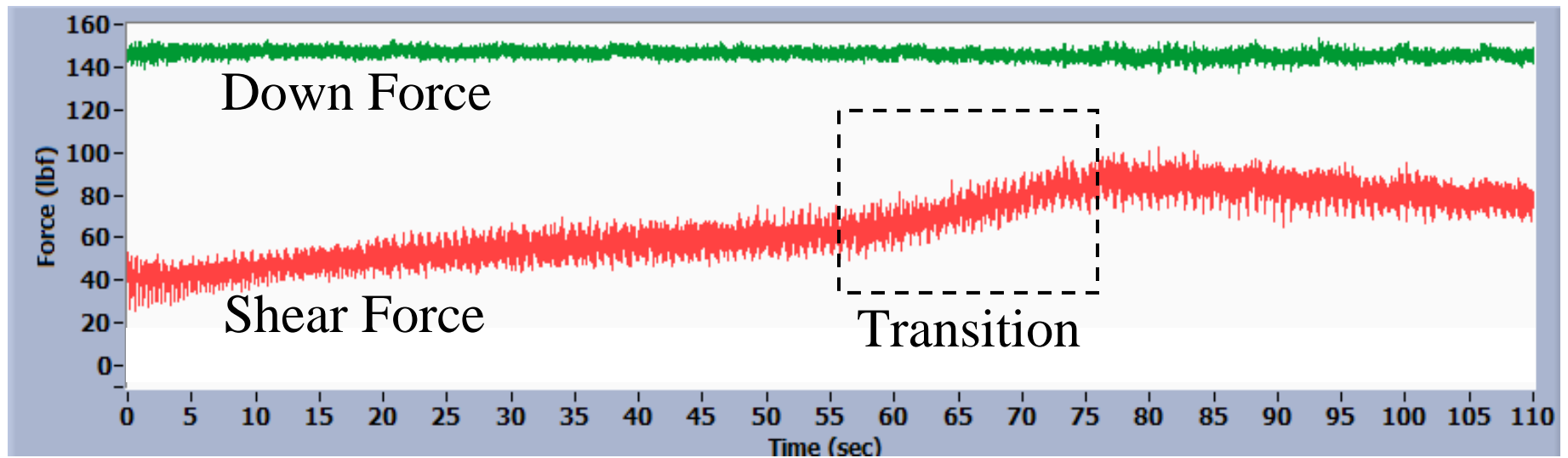
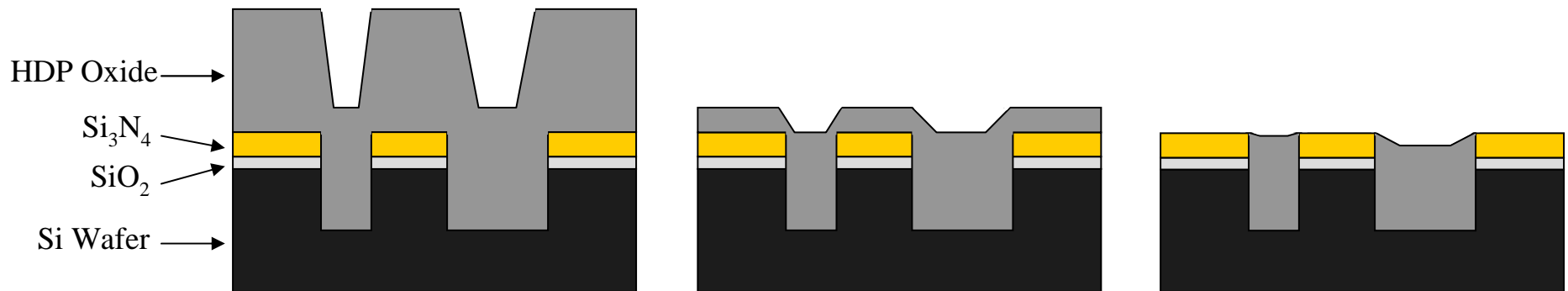


# APD – 500 Polisher & Tribometer

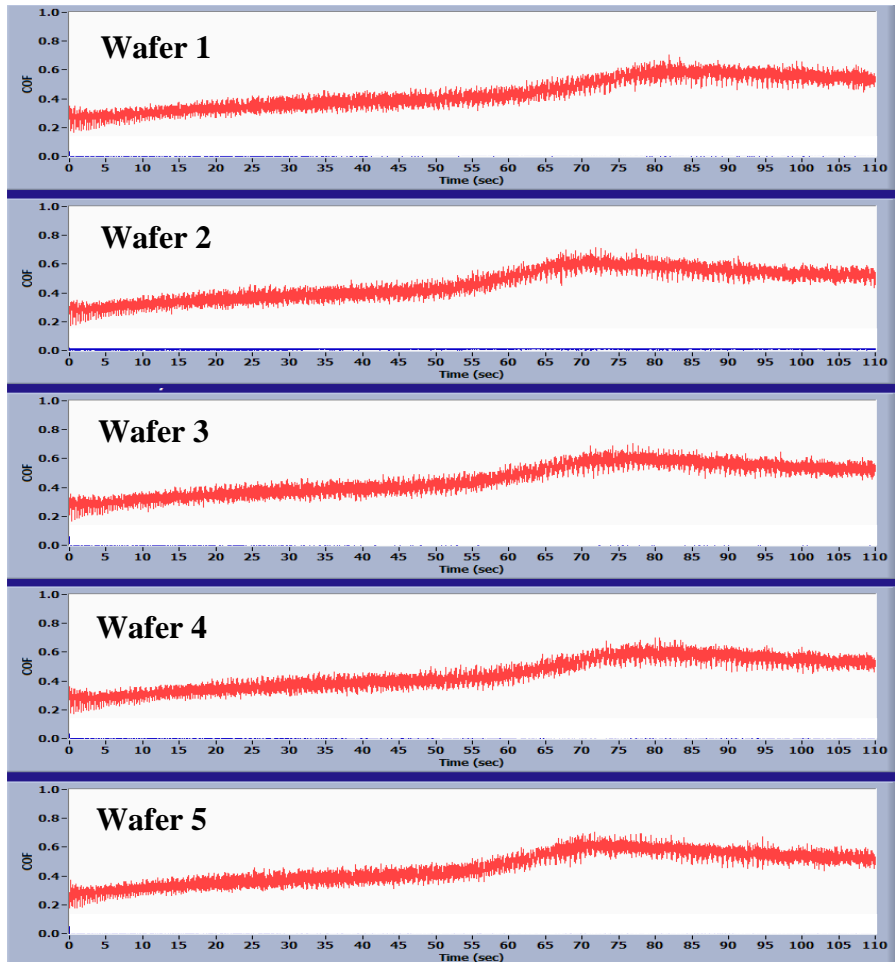




# Shear Force and Down Force Measurement



# COF Transients



## Polish Time

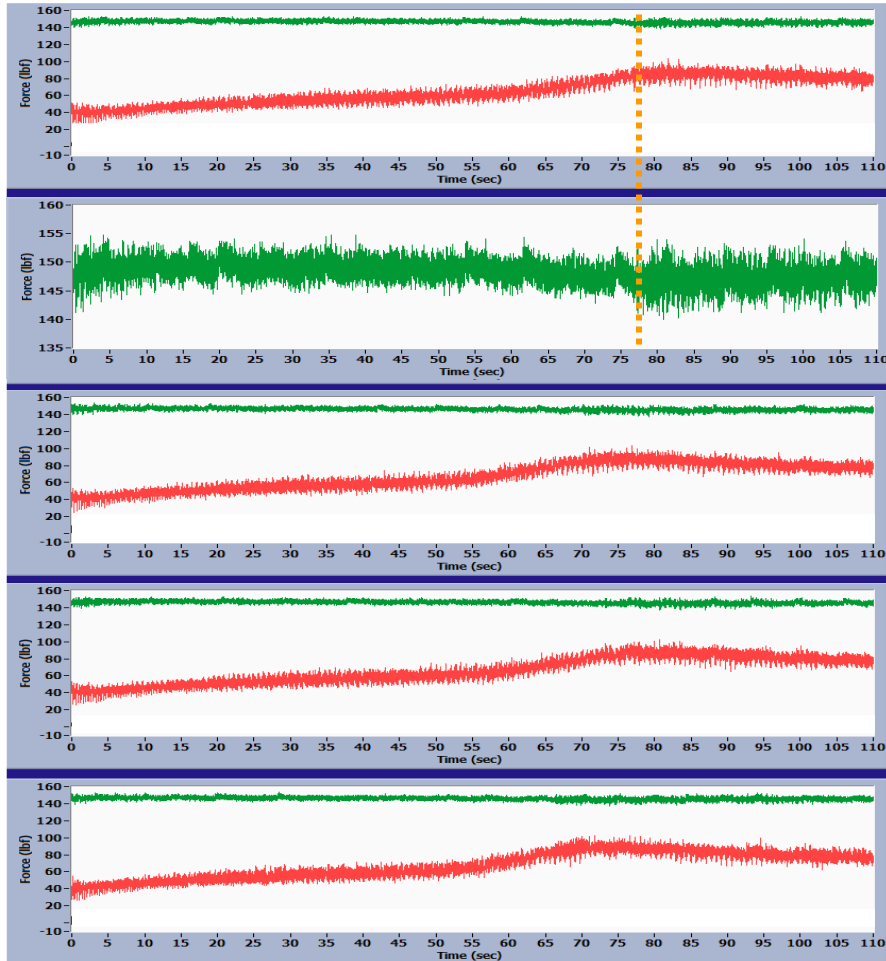
	Transition Start (s)	Transition End (s)
<b>Average</b>	<b>56.4</b>	<b>71.4</b>
<b>SD</b>	<b>3.4</b>	<b>4.5</b>
<b>RSD</b>	<b>6.1%</b>	<b>6.3%</b>

## Coefficient of Friction

	Before Transition	During Transition	After Transition
<b>Average</b>	<b>0.361</b>	<b>0.510</b>	<b>0.566</b>
<b>SD</b>	<b>0.004</b>	<b>0.006</b>	<b>0.008</b>
<b>RSD</b>	<b>0.1%</b>	<b>0.3%</b>	<b>0.5%</b>

**The COF shows consistent transition during STI patterned wafer polishing.**

# Force Transients



## Polish Time

	Transition Start (s)	Transition End (s)
Average	56.4	71.4
SD	3.4	4.5
RSD	6.1%	6.3%

## Variance of Shear Force ( $\sigma^2$ )

	Before Transition ( $lb_f^2$ )	During Transition ( $lb_f^2$ )	After Transition ( $lb_f^2$ )
Average	58.7	57.8	33.6
SD	2.8	7.7	9.2
RSD	4.7%	13.3%	27.4%

## Variance of Down Force ( $\sigma^2$ )

	Before Transition ( $lb_f^2$ )	During Transition ( $lb_f^2$ )	After Transition ( $lb_f^2$ )
Average	2.3	2.2	3.4
SD	0.03	0.22	0.19
RSD	1.3%	10%	5.5%

The variances of shear force and down force show consistent transition during STI patterned wafer polishing.

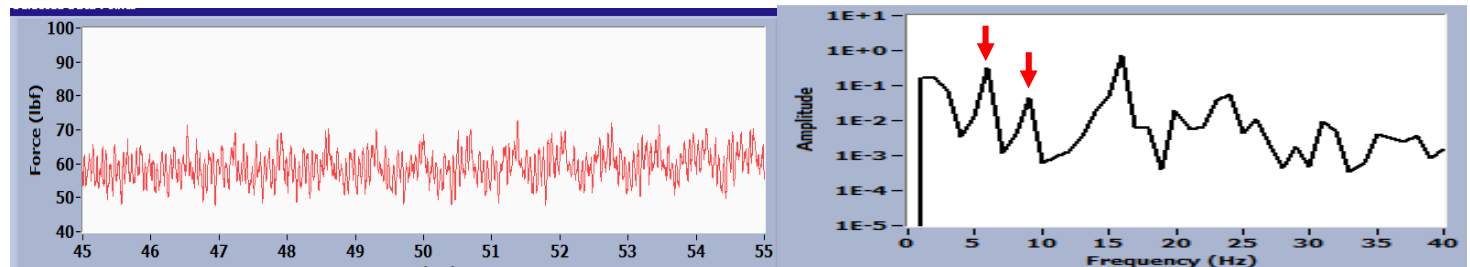
# Shear Force Spectral Analysis

## Wafer #1

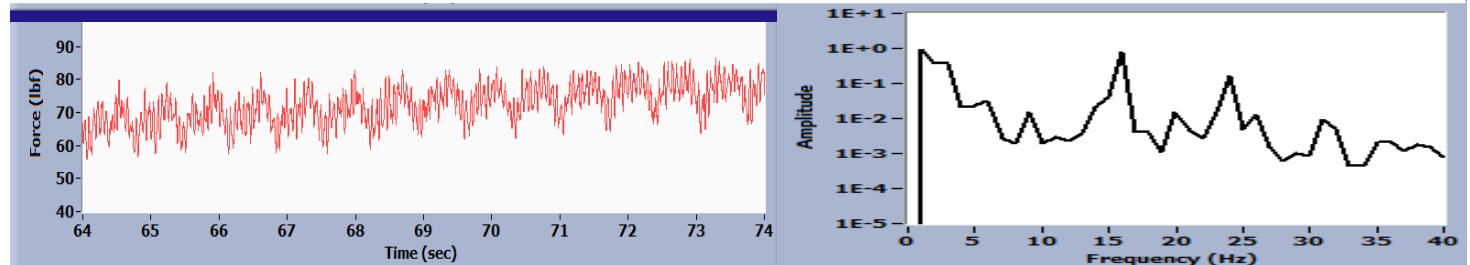
### Raw Shear Force Data

### Shear Force Spectral Analysis

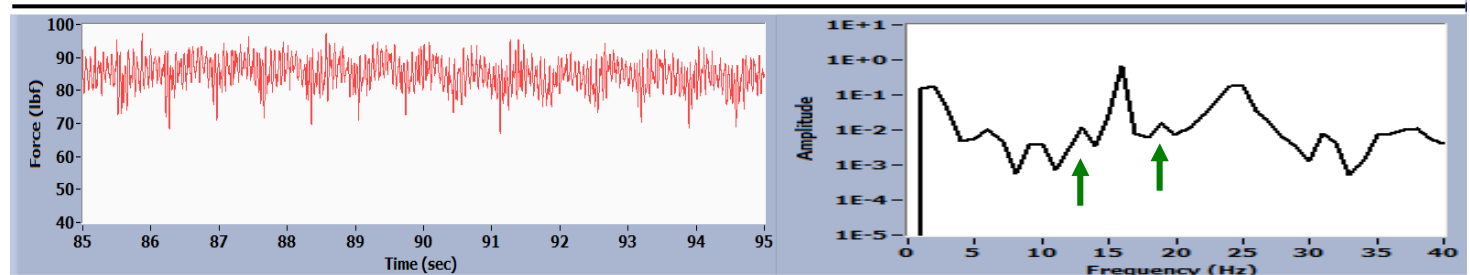
Before Transition



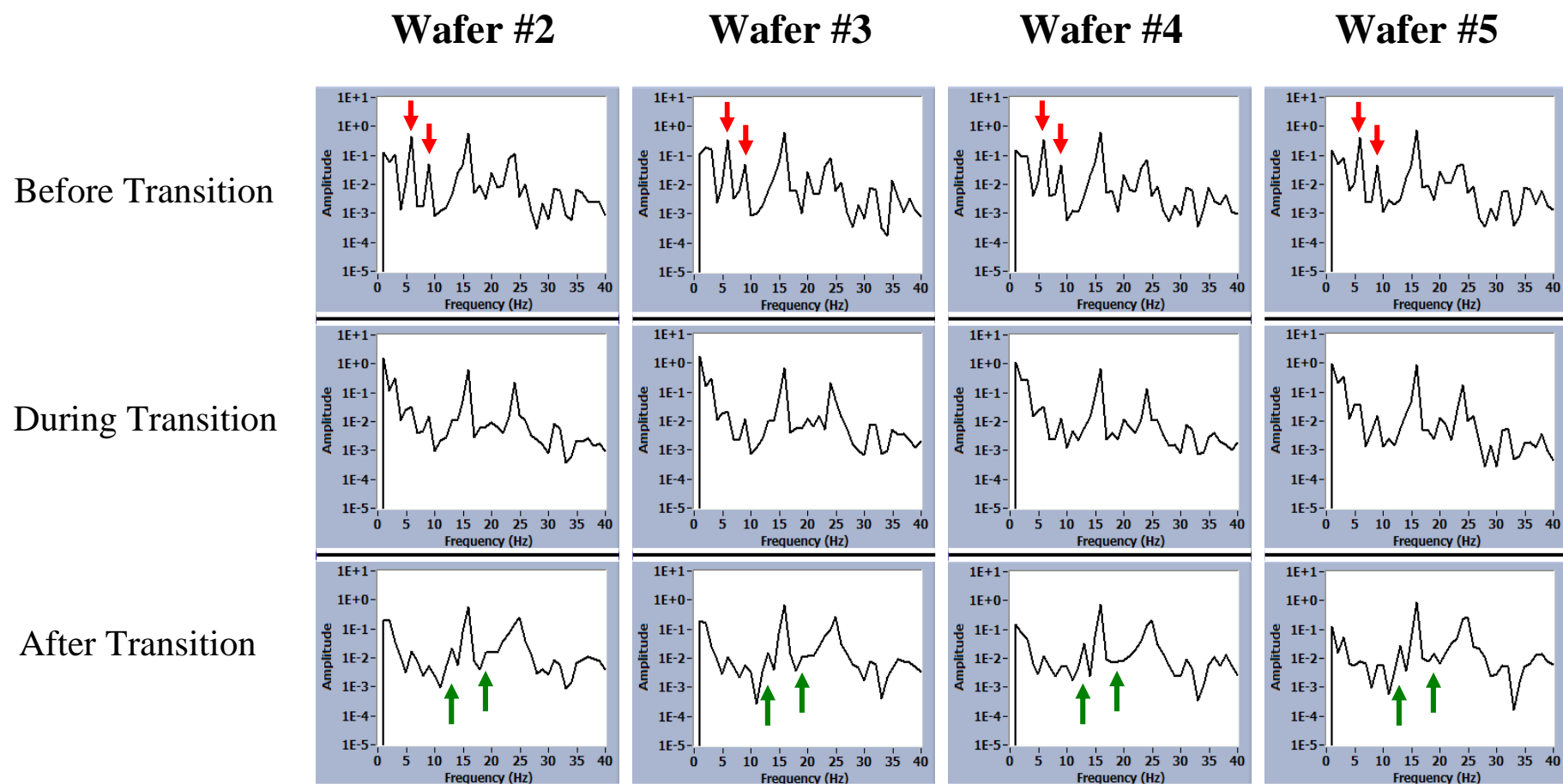
During Transition



After Transition



# Shear Force Spectral Analysis



**The shear force spectral analysis shows consistent spectral transition during STI patterned wafer polishing.**

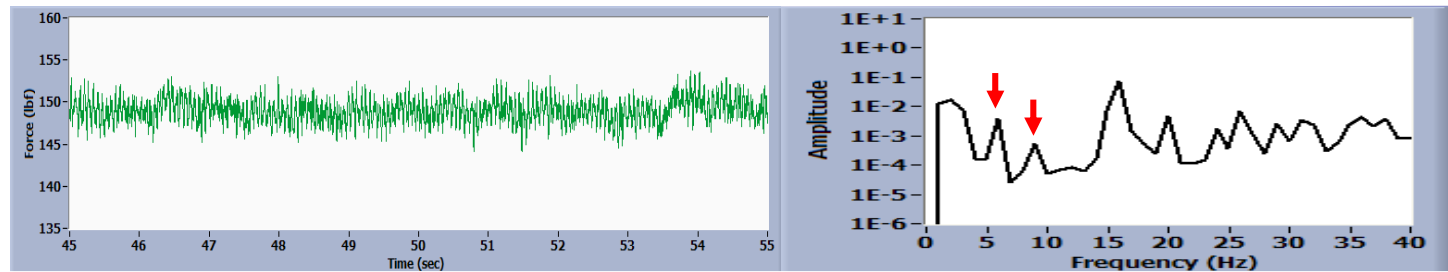
# Down Force Spectral Analysis

## Wafer #1

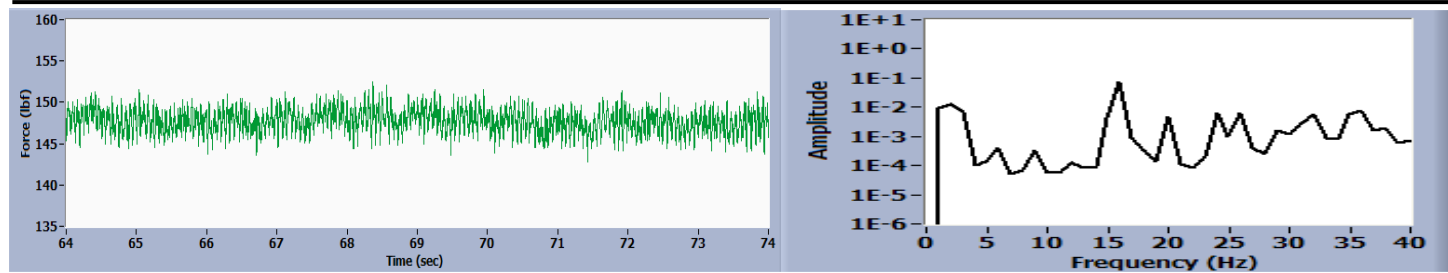
### Raw Down Force Data

### Down Force Spectral Analysis

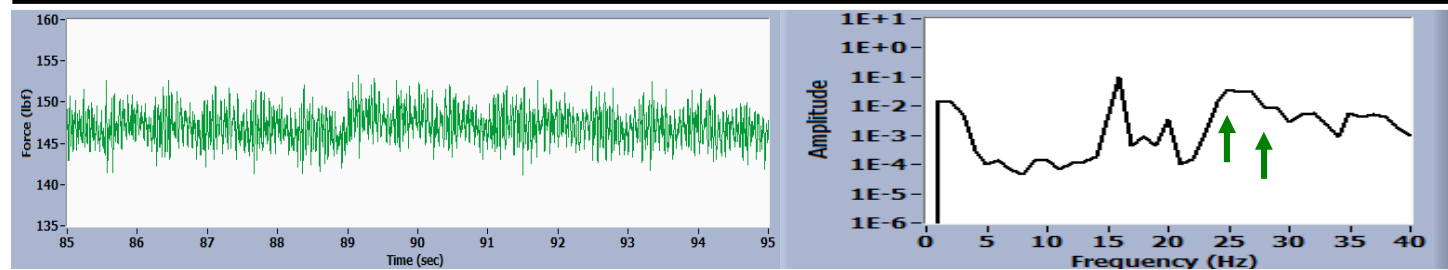
Before Transition



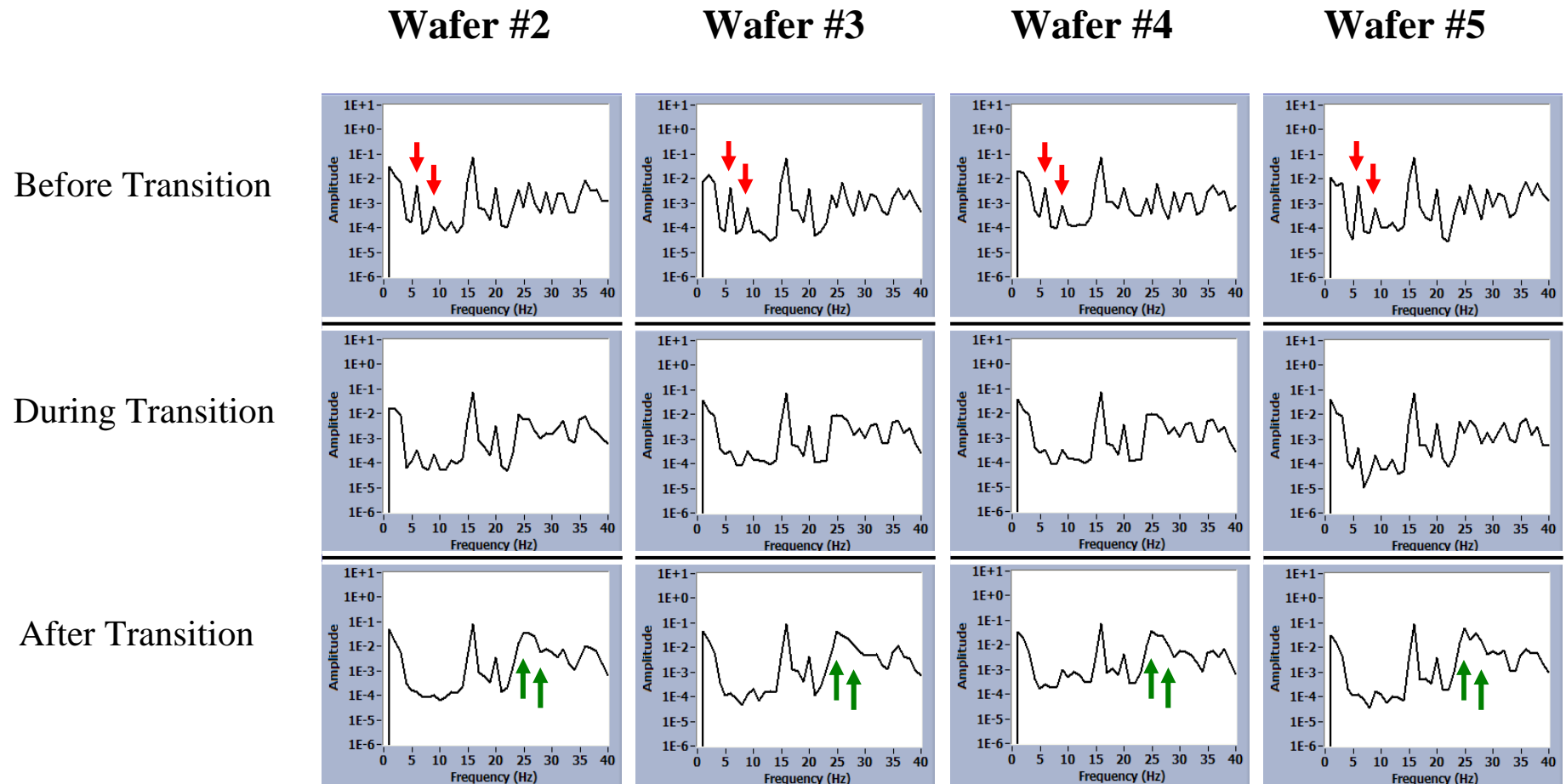
During Transition



After Transition



# Down Force Spectral Analysis



**The down force spectral analysis shows consistent spectral transition during STI patterned wafer polishing.**

# Industrial Interactions and Future Plans

## **Industrial mentors / contacts:**

- **Toranosuke Ashizawa (Hitachi Chemical Co., Ltd.)**
- **Hiroyuki Morishima (Hitachi Chemical Co., Ltd.)**

## **Next year plan:**

- **Investigate the shear force and down force transition during early evolution of wafer topography for STI CMP.**

## **Long term plan:**

- **Investigate the shear force and down force transition during evolution of wafer topography for metal CMP.**



## **Publications and Presentations**

### **Publication:**

- **Applications of Shear Force Spectral Analysis in STI CMP. Y. Sampurno, F. Sudargho, Y. Zhuang, T. Ashizawa, H. Morishima and A. Philipossian. International Conference on Planarization/CMP Technology Proceedings, 129-133 (2007).**

### **Presentation:**

- **Applications of Shear Force Spectral Analysis in STI CMP. Y. Sampurno, F. Sudargho, Y. Zhuang, T. Ashizawa, H. Morishima and A. Philipossian. International Conference on Planarization/CMP Technology, Dresen, Germany, October 25-27 (2007).**

# **An Integrated, Multi-Scale Framework for Designing Environmentally-Benign Copper, Tantalum and Ruthenium Planarization Processes**

*(Task Number: 425.020)*

**ERC Thrust A / Subtask 1.2**

## **Task Leaders:**

- Ara Philipossian, Univ. of Arizona
- ***Stephen Beaudoin*, Purdue University**
- Duane Boning, MIT
- Vincent Manno, Tufts University
- Chris Rogers, Tufts University
- Robert White, Tufts University

## **Graduate Students from Purdue University:**

- ***Bum Soo Kim***, PhD candidate, Chemical Engineering
- Caitlin M. Kilroy, PhD student, Chemical Engineering

# Objectives

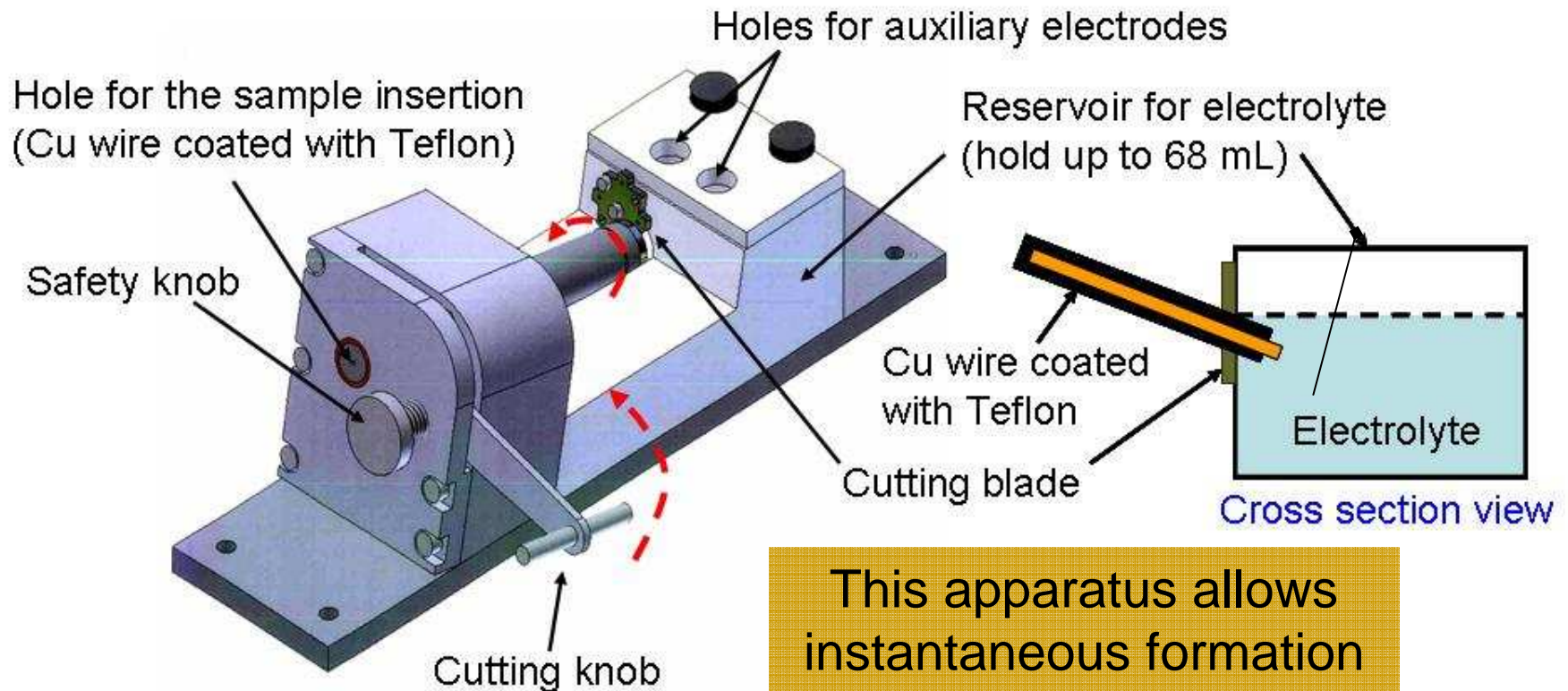
- Evaluate electrochemical processes occurring on Cu surfaces in slurry
  - CMP-relevant timeframes
  - Provides information on surface film on Cu surface
- Develop, validate models for Cu removal based on dissolution, abrasion
  - Including sub-models for particle interactions with Cu surface

# ESH Metrics and Impact

- Comparison
  - Existing Cu CMP process
- Envisioned process
  - Optimized slurry pH, ionic strength, additive composition
  - Optimized abrasive size and composition
- Envisioned process
  - Extend pad life by up to 15% by reducing aggressiveness of required conditioning
  - Reduce slurry demand by 20% by enhancing interactions between abrasive particles and Cu surface

# Guillotined Electrode

## Apparatus for Exposing Fresh Cu

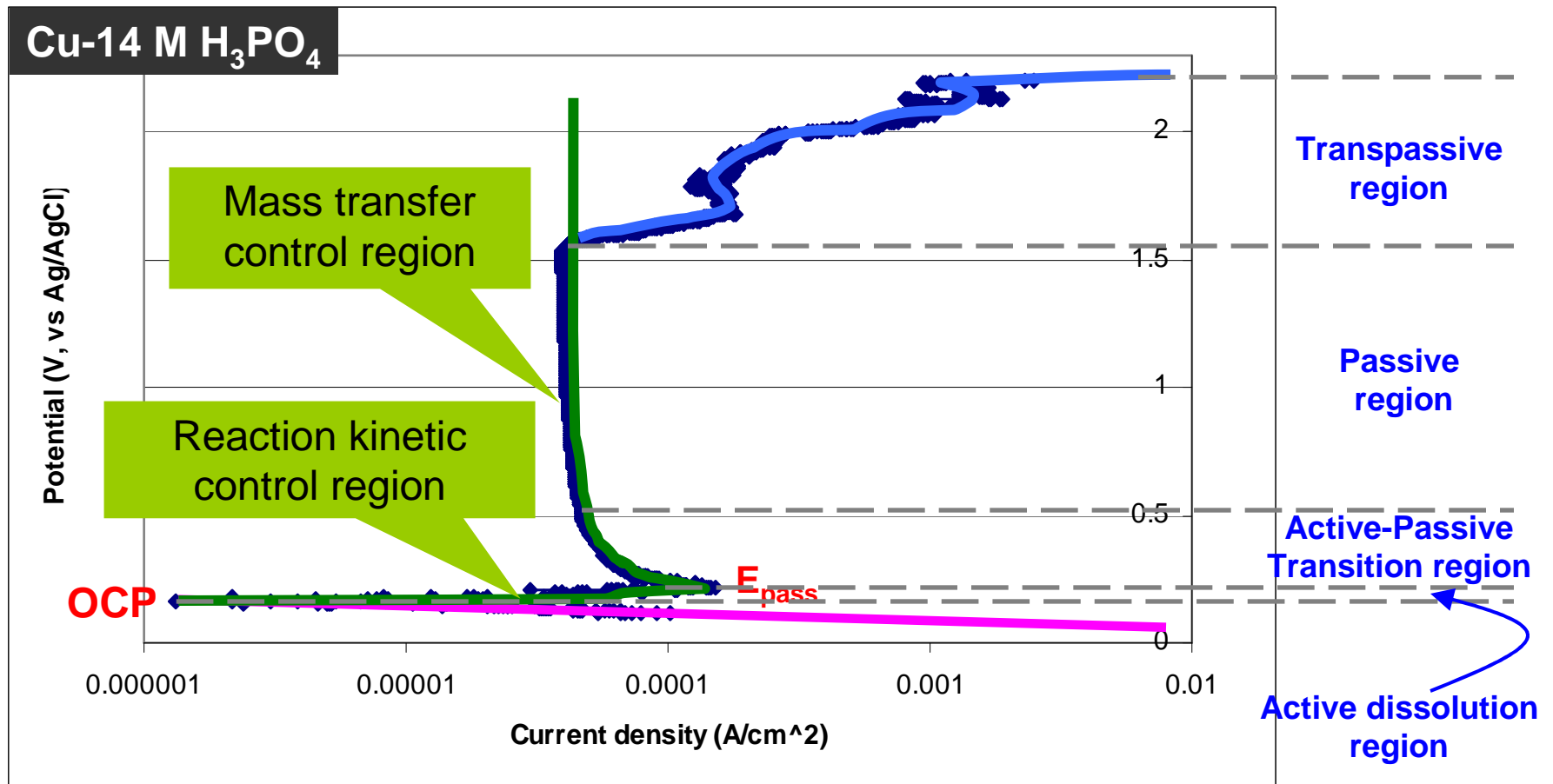


**Exposed Cu surface: 0.0052 cm<sup>2</sup>**

This apparatus allows instantaneous formation of fresh Cu for study of surface reactions at different slurry conditions

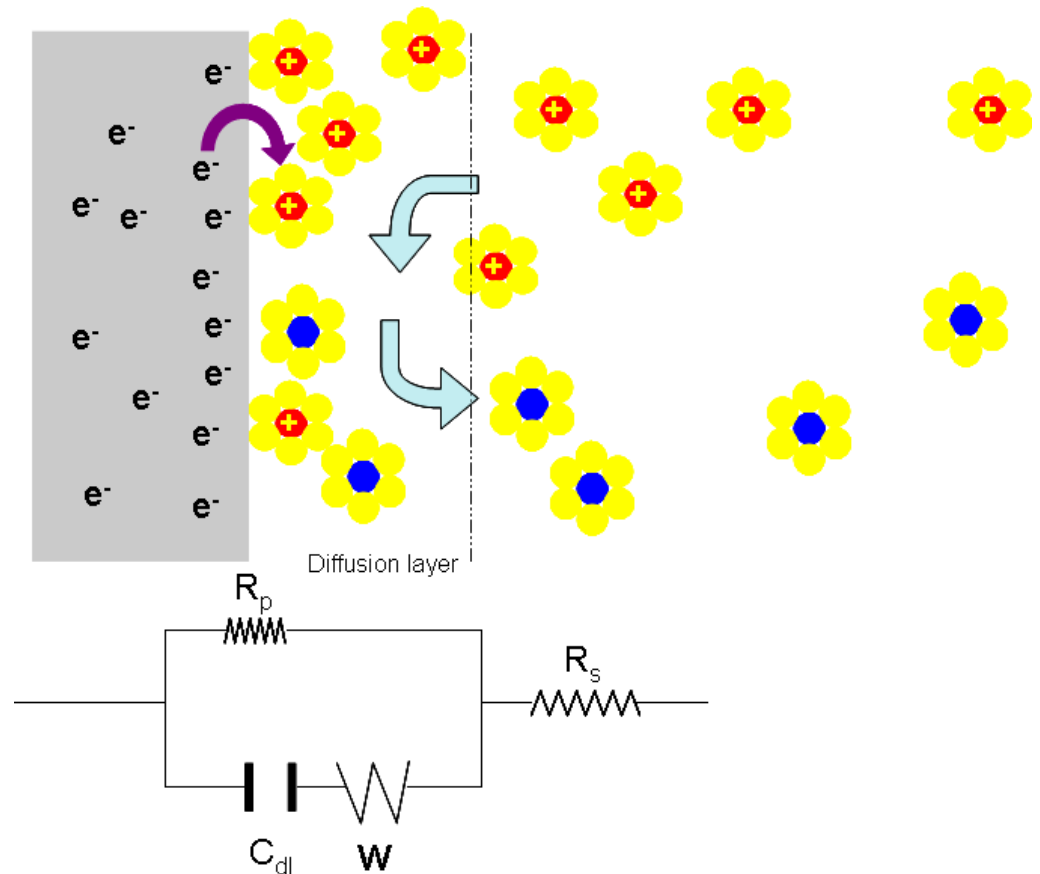
# Active/Passive Behavior

- When a compact passive film is formed, this causes a drop in current
  - Due to the resistance of the film and its effect as a barrier to charge transfer



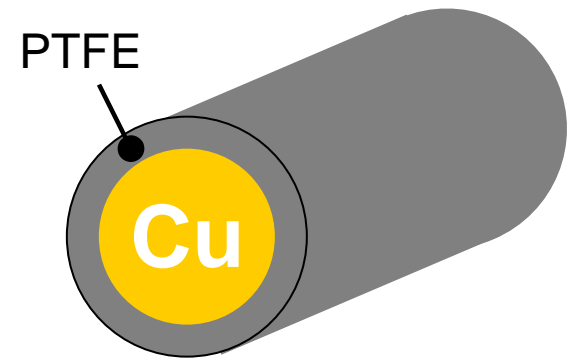
# Electrochemical Impedance Spectroscopy (EIS)

- Impedance
  - Generalized complex resistance
  - Frequency dependent
- Info from Nyquist plot
  - $R_s = R_m + R_e + R_f$
  - $R_p$
- $R_f$  is the resistance of the porous salt/viscous liquid film
- Increase in  $R_s$  (Impedance at high limit frequency)
  - Formation of porous salt or viscous liquid layer
- Resistance of compact solid film can be detected by changes in  $R_p$



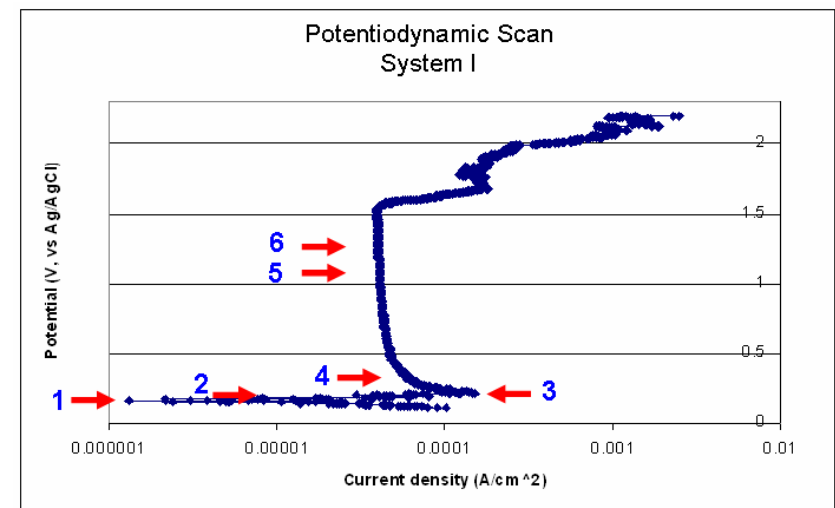
# Systems and Conditions

- Sample
  - Teflon coated Cu wire (0.0052 cm<sup>2</sup>)
- Systems
  - For surface film study
    - 1) Cu - 1 wt% HNO<sub>3</sub>
    - 2) Cu - 1 wt% HNO<sub>3</sub>+ 0.02 M BTA
    - 3) Cu - 1 wt% HNO<sub>3</sub>+ 0.02 M BTA+5 wt% H<sub>2</sub>O<sub>2</sub>
- Ag/AgCl reference electrode (0.197 V vs. SHE)
- Superimposed AC: 5 mV



# Experiments

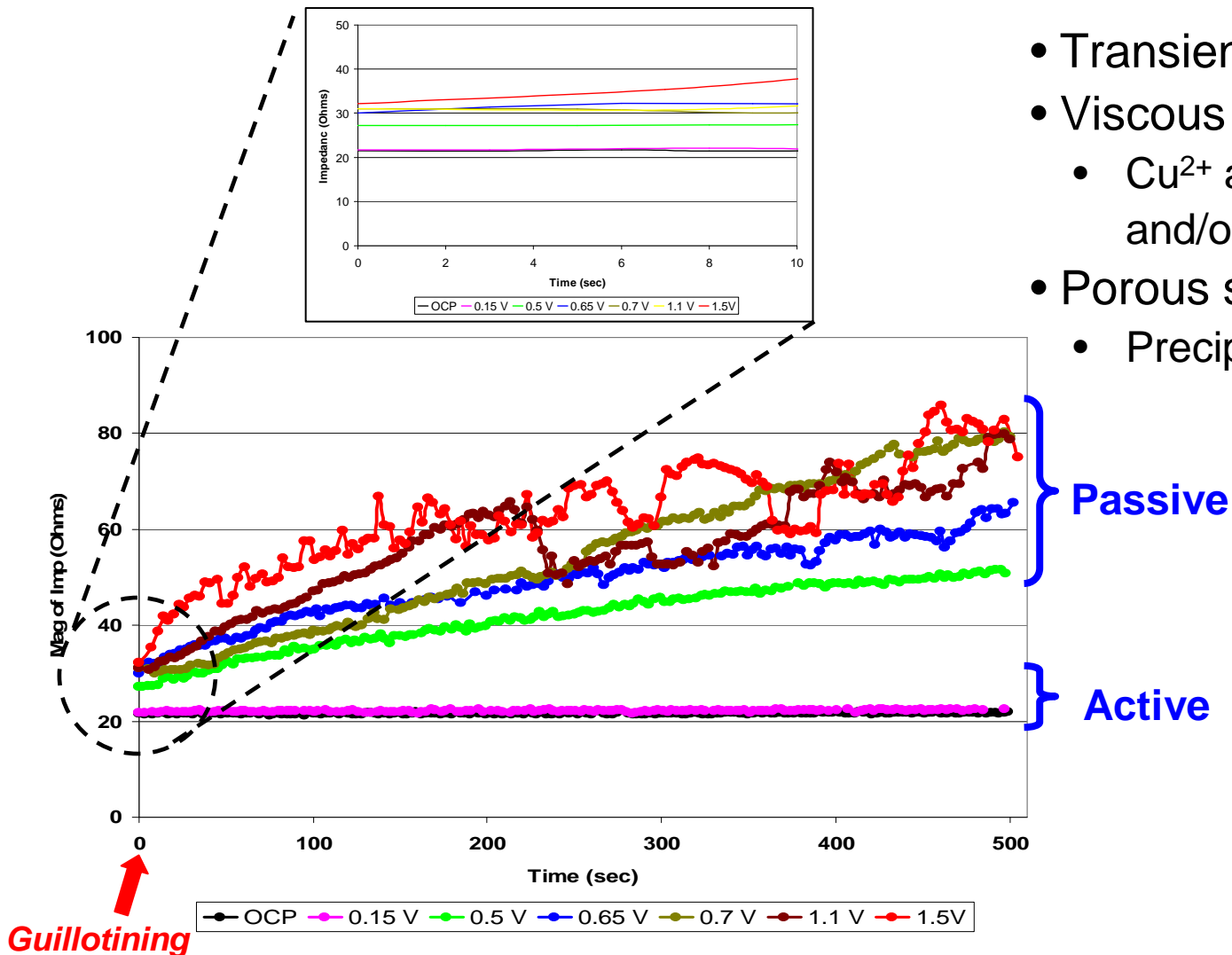
- PD scans
  - Active/passive behavior
- $|Z|$  vs. time
  - DC potential selection for  $|Z|$  measurements
    - OCP,  $E_{\text{pass}}$ , and potentials from active/passive region in a PD scan
    - DC potential holds the system at corresponding potential (region)
- Record  $|Z|(t)$  at 100 kHz ( $R_s$ ) for each system after guillotining (cutting) the Cu wire





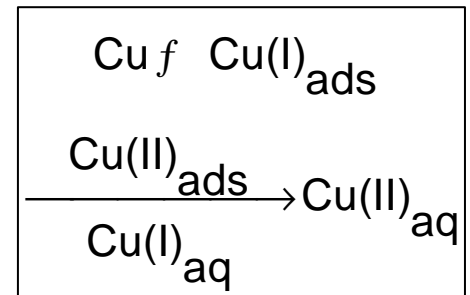
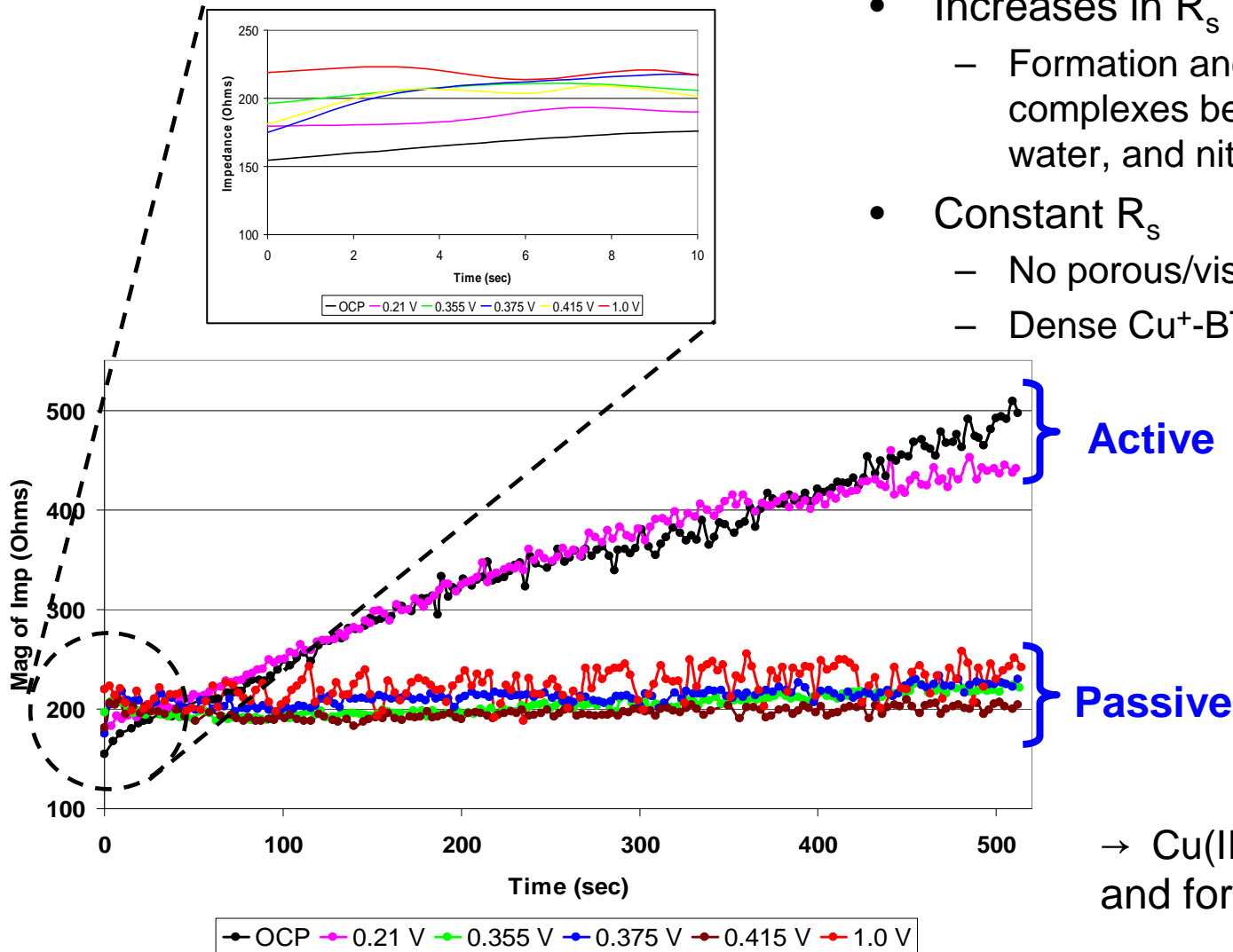
# Cu - 1 wt% HNO<sub>3</sub>

- Transient oxide film
- Viscous liquid layer
  - Cu<sup>2+</sup> and its salt (water and/or NO<sub>3</sub><sup>-</sup>)
- Porous salt film
  - Precipitation of complexes



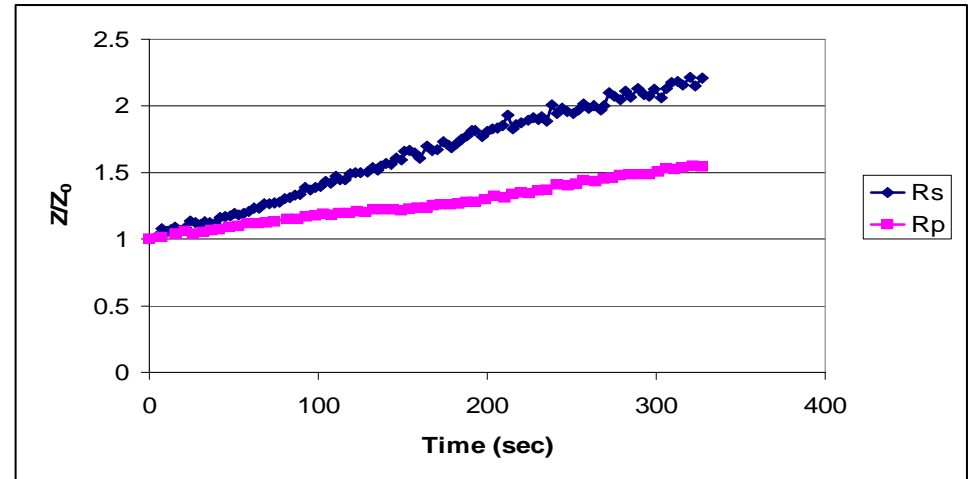
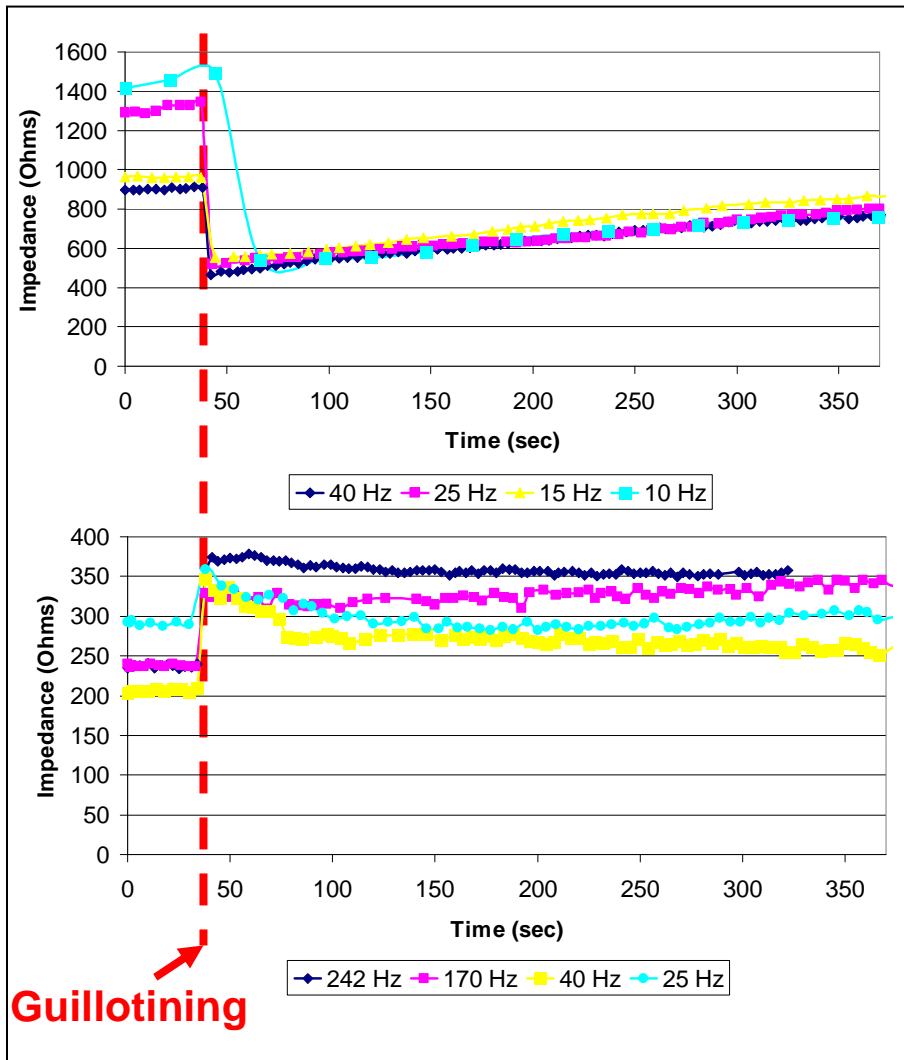
# Cu - 1 wt% HNO<sub>3</sub>+ 0.02 M BTA

- Increases in  $R_s$ 
  - Formation and precipitation of the complexes between  $\text{Cu}^{2+}$  and BTA, water, and nitrate
- Constant  $R_s$ 
  - No porous/viscous film
  - Dense  $\text{Cu}^+$ -BTA film



→  $\text{Cu(II)}_{\text{ads}}$  is an intermediate and formed for the dissolution

# $R_p$ Measurement for BTA System



- $R_p$  (Polarization resistance)
  - Compact  $\text{Cu}^+$ -BTA film
  - Low frequency region
- Active region (0.21 V, Top)
  - $R_p$  drop with cut
  - Slow increase
    - Slow  $\text{Cu}^+$ -BTA film formation
- Passive region (0.375V, Bottom)
  - $R_p$  jump with cut
  - Almost constant
    - Instant  $\text{Cu(I)}$ -BTA film formation

# Conclusion

- Impedance at high-limit frequency
  - Porous salt/viscous liquid film formation
  - Cu - 1 wt% HNO<sub>3</sub>
  - Cu - 1 wt% HNO<sub>3</sub>+ 0.02 M BTA
  - Aforementioned explanation
- Comparison the rate of formation between R<sub>p</sub> and R<sub>s</sub>
  - First protection by porous salt film
- Leads to better understanding of CMP surface reactions
  - Will be combined with particle-surface interaction studies

# Industrial Interactions and Technology Transfer

- Multiple meetings with industry CMP council
  - Intel, Cabot

## Future Plans

Project has been completed and sunsetted

## Recent Presentation and Publication

- *Electrochemical impedance studies of copper surface reactions during chemical mechanical planarization*, 2007 AIChE Annual meeting, Salt Lake City, UT
- *Electrochemical Analysis of Surface Films on Copper in Phosphoric Acid, with a Focus on Microelectronics Processing*, Journal of the Electrochemical Society (In review), 2008

[SRC/SEMATECH Engineering Research Center for Environmentally Benign Semiconductor Manufacturing](#)

# An Integrated, Multi-Scale Framework for Designing Environmentally-Benign Copper, Tantalum and Ruthenium Planarization Processes

*(Task Number: 425.020)*

## Subtask: Slurry Thickness and Flow Measurement using *in-situ* Optical Techniques

### PIs:

- C. B. Rogers, Mechanical Engineering, Tufts University
- V. P. Manno, Mechanical Engineering, Tufts University
- R. D. White, Mechanical Engineering, Tufts University

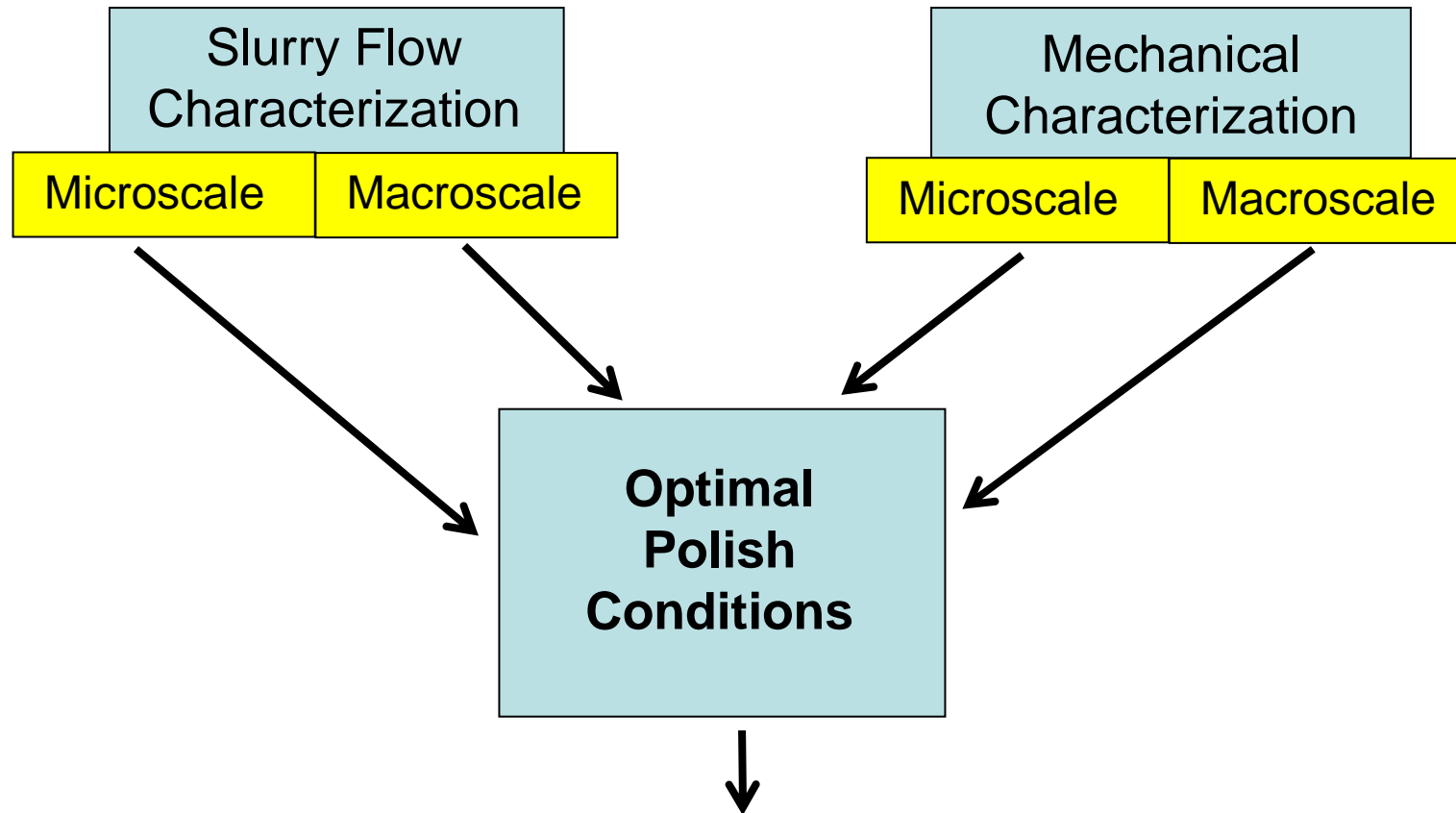
### Graduate Students:

- Caprice Gray: PhD candidate, Tufts Mechanical Engineering, May 2008
- Nicole Braun: MS candidate, Tufts Mechanical Engineering, May 2008

# Objective

- Use Dual Emission Laser Induced Fluorescence (DELIF) to obtain in-situ images of the slurry layer thickness during CMP and quantify wafer-pad contact during polishing – Caprice Gray (PhD Student)
- (Seed Project) Investigate the feasibility of using particle image velocimetry (PIV) to quantitatively measure particle-slurry flow in-situ. – Nicole Braun (MS Student)

# ESH Metrics and Impact



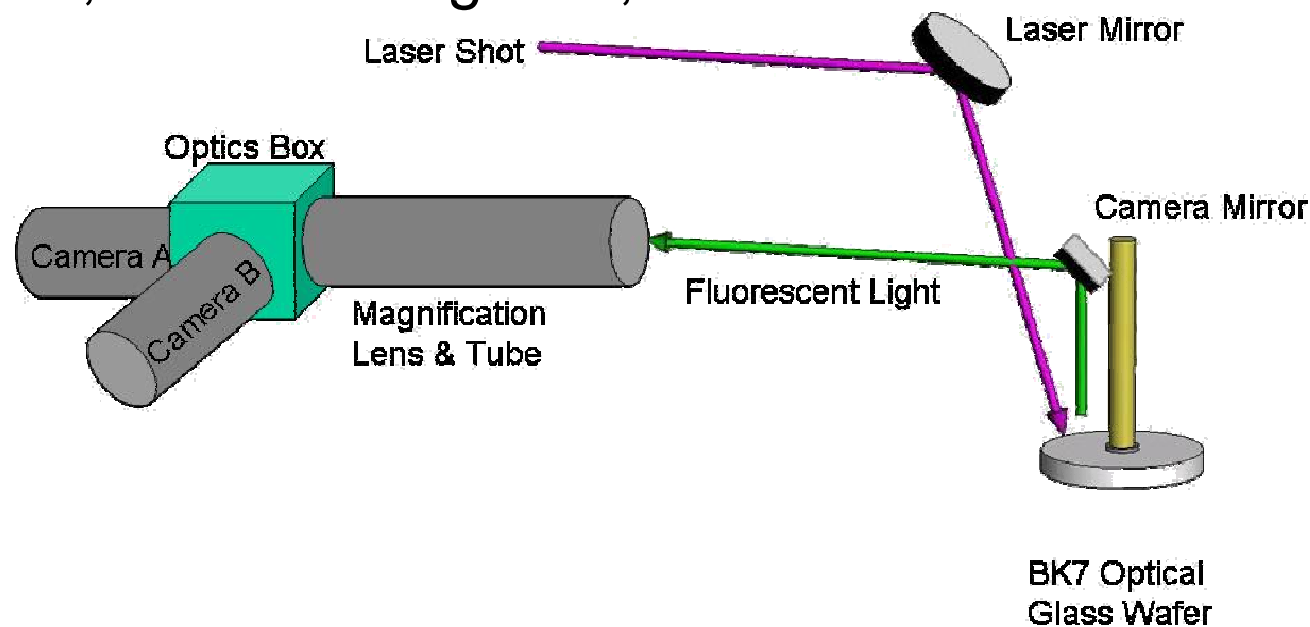
- Reduced time to polish (energy and cost savings)
- Reduced consumables (waste and cost reduction)



# Dual Emission Laser Induced Fluorescence

## Dual Emission Laser Induced Fluorescence (DELIF)

- In-situ contact images
- 6 ns time integration, 2 images/sec
- ~3 micron/pixel to resolve asperity sized features
- Pads (all polyurethane based): CMC D100, CMC D200, Fruedenburg FX9, IC1000



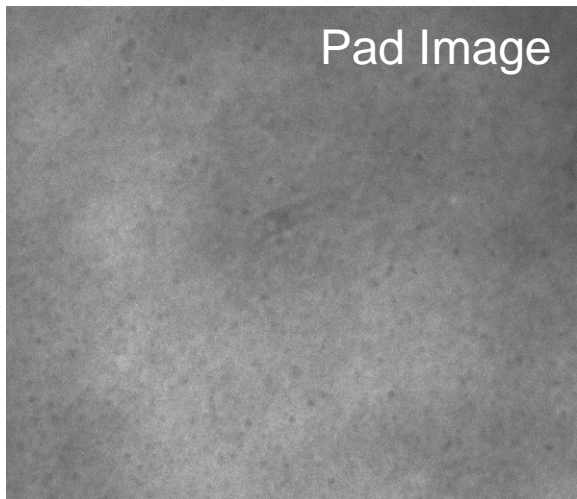
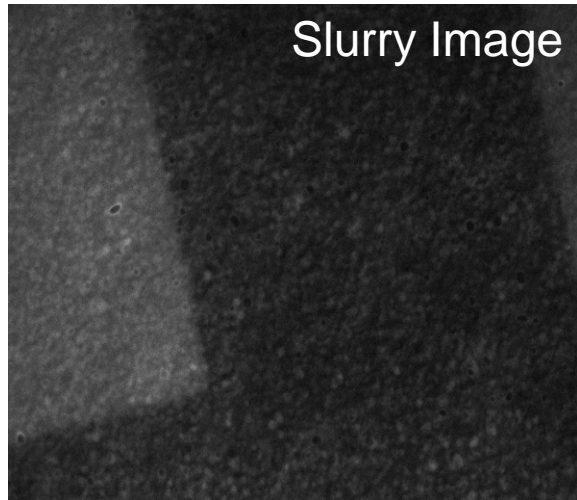
# DELIF: Film Thickness

Two cameras:

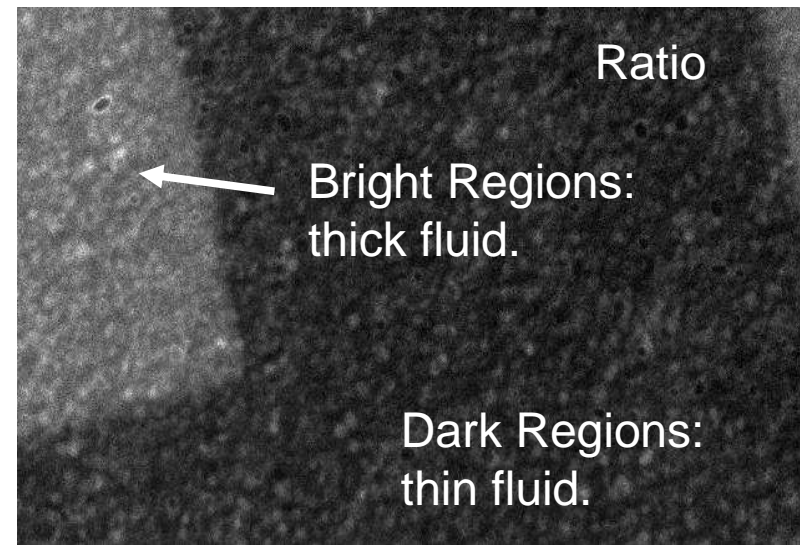
(1) wavelength of slurry dye

(2) wavelength of pad fluorescence

Image ratio cancels source intensity variation



=

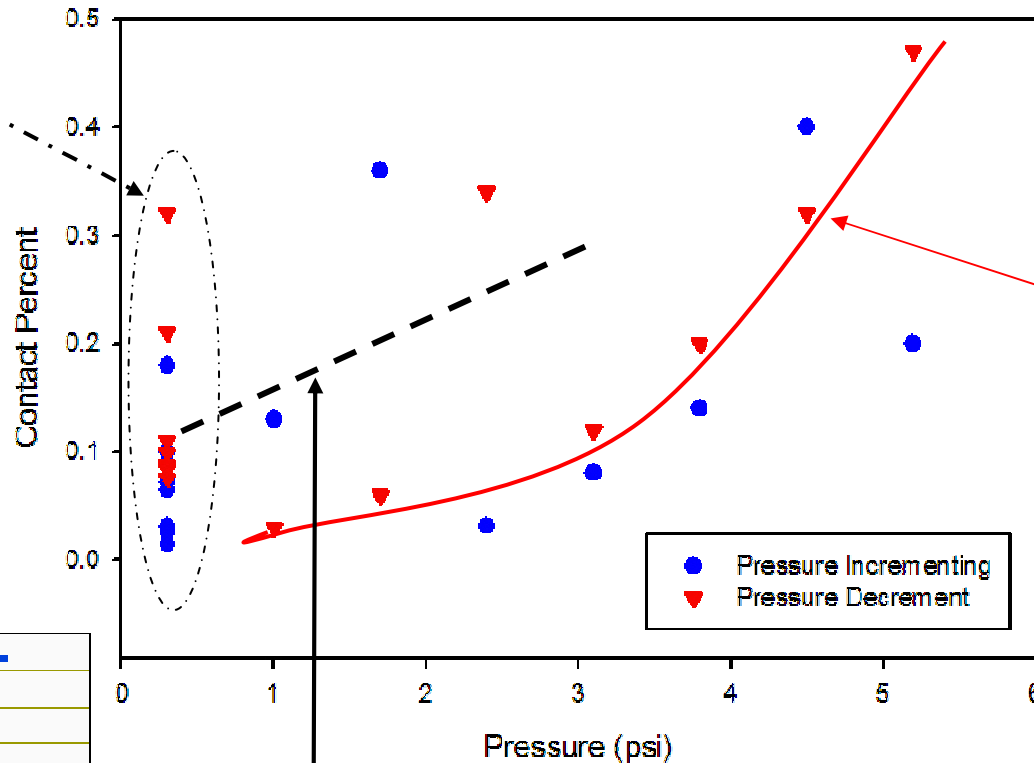


Brighter regions are thicker fluid layers.

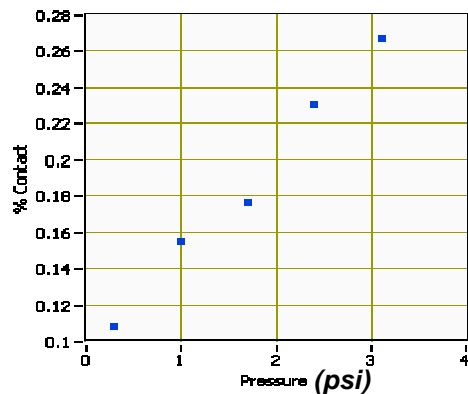
# DELIF: Static Contact

CMC D100 AC grooved pad, BK7 glass wafer, 3:2 Cab-o-sperse SC1 slurry (fumed silica, 22 wt% at this dilution)

Variability is observed in the measurement for grooved pads with low downforce.



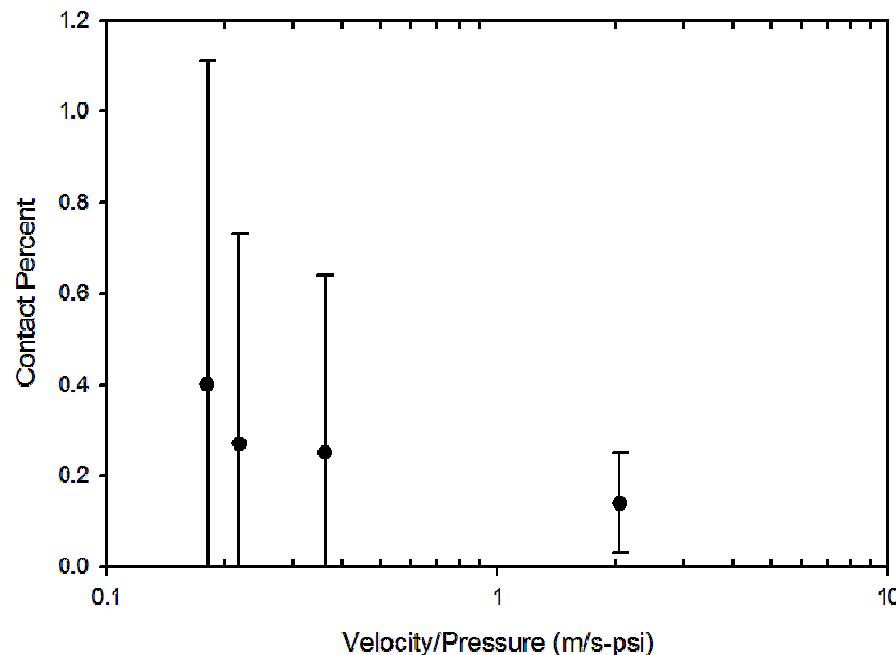
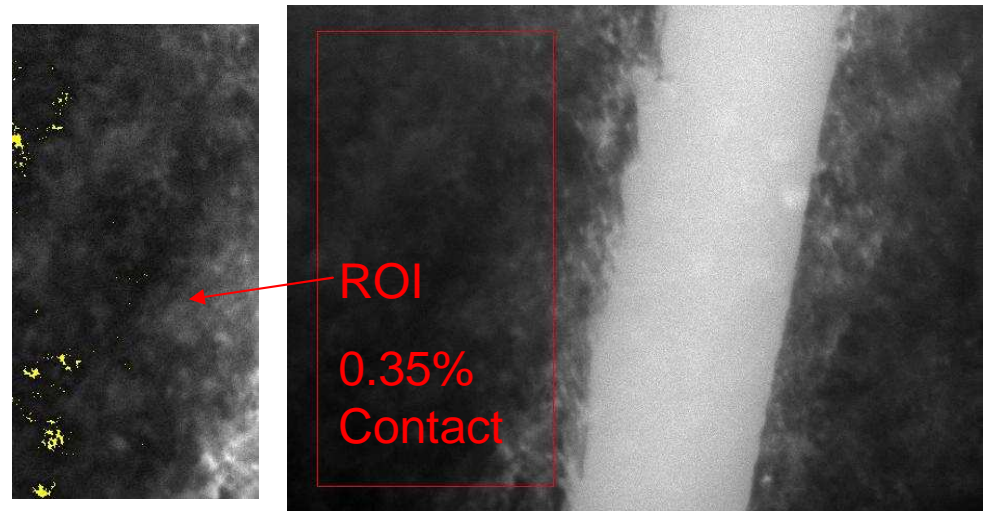
Grooved pad: shows increasing contact with pressure, but less contact than ungrooved case. This may be due to missed contact at the groove edges.



Ungrooved pad: shows a linear trend between downforce and contact percentage

# DELIF: Dynamic Contact

- Contact regions on a soaked pad appear away from the grooves.
- Contact percentages in the dynamic case on the same order of magnitude as the static case.
- The majority of images show contact < 1%.

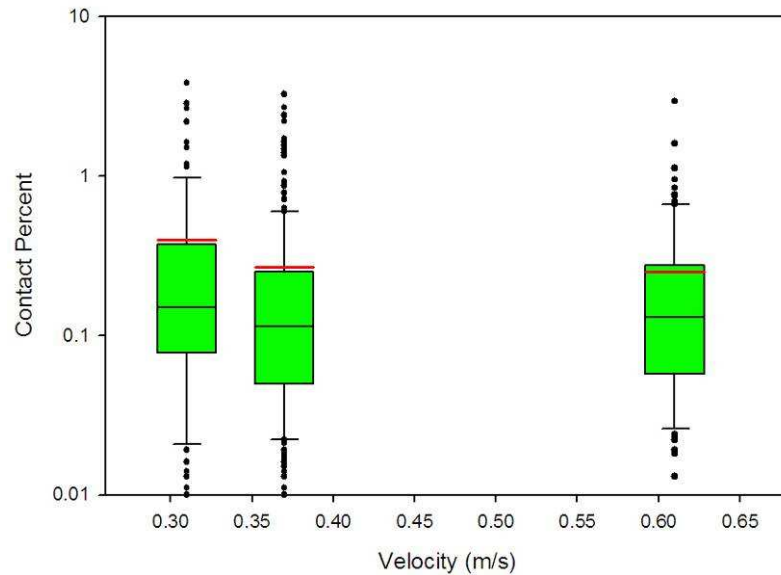


Contact means follows a Stribeck-type curve, suggesting a boundary lubrication regime.

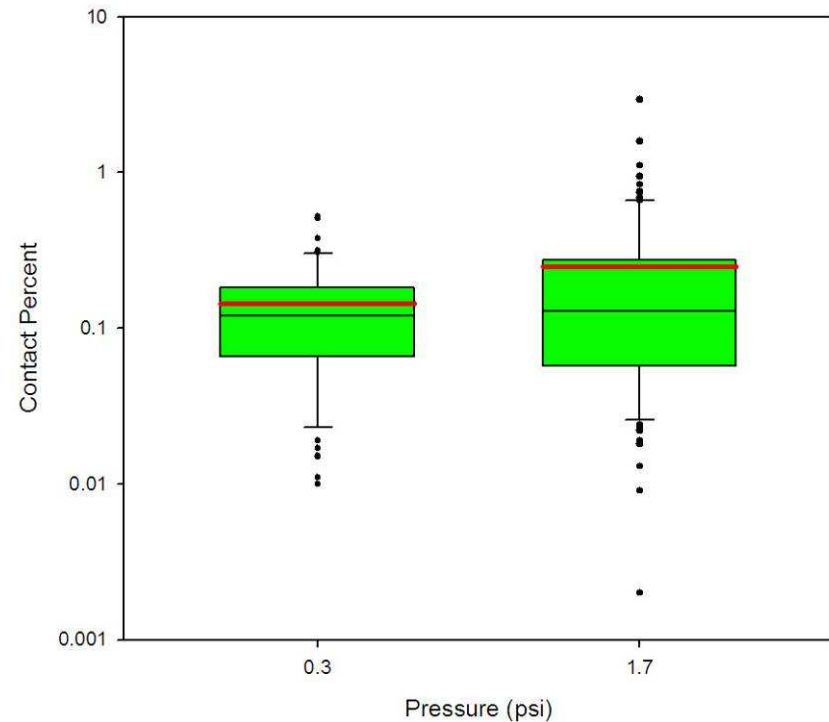
CMC D100 pad, AC grooves,  
3:2 Cab-o-sperse SC1 (22 wt%)

# DELIF: Dynamic Contact

Contact increases with decreasing velocity



Contact increases with increasing pressure



## Box Plot

Box Bounds – 25% to 75%

Black Line = Median

Red Line = Mean

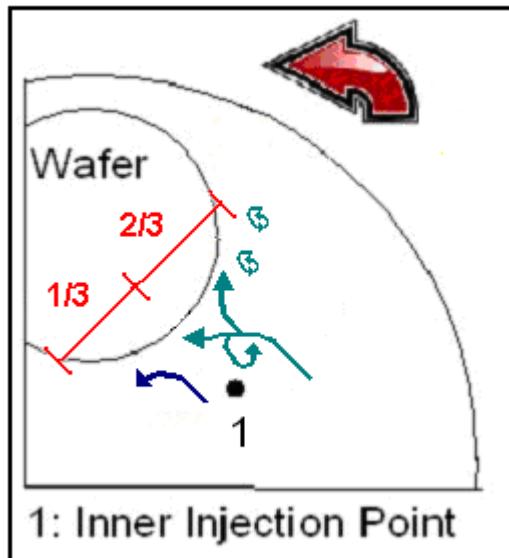
Error Bars – 10% & 90%

Points – outlying data

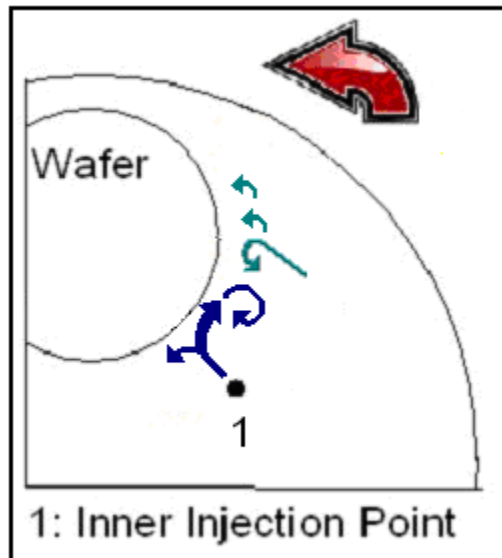
CMC D100 pad, AC grooves, 3:2 Cab-o-sperse SC1 (22 wt%)

# Flow Visualization – Initial Results

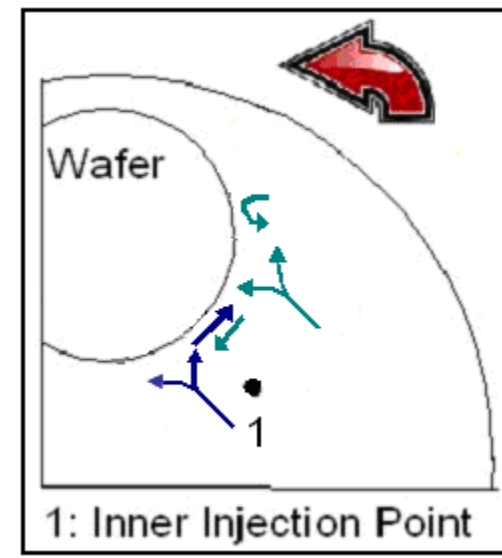
**Example Result:** Pad grooving is observed to have a major impact on slurry flow patterns around the wafer.



Ungrooved FX9 pad:  
Old slurry dominates wafer bow wave.



XY Grooved FX9 Pad:  
New slurry dominates wafer bow wave.



AC Grooved D100 Pad:  
Shearing of old and new slurry, mixing at bow wave.

## Flow visualization using particle tracers:

1. **Vorticity, shearing and structure of bow wave.**
2. **Global slurry flow path and residence.**

For inner injection point, 35 rpm, conditioning, 22% wt fumed silica slurry.

**All data is available at:**

[http://docs.google.com/Doc?id=dc9dhbdb\\_13fphfz7dp](http://docs.google.com/Doc?id=dc9dhbdb_13fphfz7dp)

*SRC/SEMATECH Engineering Research Center for Environmentally Benign Semiconductor Manufacturing*

# Industrial Interactions and Technology Transfer

- Close collaboration with industry partners – Cabot Microelectronics and Intel
  - Monthly telecons – secure website for information exchange
  - Semi-annual face-to-face meetings
  - Thesis committees and joint publication authorship
  - Metrology and analysis methodology technology transfer
  - In-kind support – specialized supplies and equipment
  - Student internships (e.g. C. Gray at Intel during Summer 2005)
- Close coordination with A. Philipossian research group at U of Arizona
- Information and results exchange with MIT (D. Boning, G. McKinley), Stockton College (E. Paul), Harvard University (H. Stone).
  - Monthly joint meetings of PIs and research students



# Future Plans

## Next Year Plans

- All current students complete theses and graduate:
  - C. Gray, PhD : DELIF for pad-wafer contact and slurry thickness
  - J. Vlahakis, PhD : Wafer-scale characterization of CMP mechanics
  - N. Braun, MS : Particle image velocimetry for CMP slurry flow
  - D. Gauthier, MS : MEMS for asperity scale force measurement in CMP

## Long-Term Plans

- Deploy the newly demonstrated *in situ* measurement technologies (DELIF, wafer attitude, PIV, MEMS force sensing) to a 200 mm polisher.
- Characterize polishing of patterned tantalum/copper and oxide substrates using the suite of new measurement technologies on the 200 mm platform.
- Apply results of the experimental study to optimize polish conditions, pad geometry/type, conditioner geometry/type for improved polish quality and reduced consumables.



# Publications, Presentations, and Recognitions/Awards

- Gray, C., White, R. D., Manno, V. P., and Rogers, C. B. “*Simulated Effects of Measurement Noise on Contact Measurements between Rough and Smooth Surfaces*”, **Tribology Letters**, In Press, Accepted Manuscript, December 27, 2007.
- N. Braun, C. Gray, A. Mueller, J. Vlahakis, D. Gauthier, V. P. Manno, C. Rogers, R. White, S. Anjur, M. Moinpour. “*In-Situ Investigation of Wafer-Slurry-Pad Interactions during CMP*” in the **Proceedings of the International Conference on Planarization/CMP Technology**, Dresden, Germany, October 25-27, 2007.
- Gray, C., Rogers, C. Manno, V., White, R., Moinpour, M., Anjur S.. “*Determining Pad-Wafer Contact using Dual Emission Laser Induced Fluorescence*”, in the **Proceedings of the Material Research Society**, Vol. 991, Symposium C, Advances and Challenges in Chemical Mechanical Planarization, 2007.

# **An Integrated, Multi-Scale Framework for Designing Environmentally-Benign Copper, Tantalum and Ruthenium Planarization Processes**

*(Task Number: 425.020)*

## **Subtask: Pad-Wafer Mechanical Characterization using *in-situ* Force and Position Measurements**

### **PIs:**

- **C. B. Rogers, Mechanical Engineering, Tufts University**
- **V. P. Manno, Mechanical Engineering, Tufts University**
- **R. D. White, Mechanical Engineering, Tufts University**

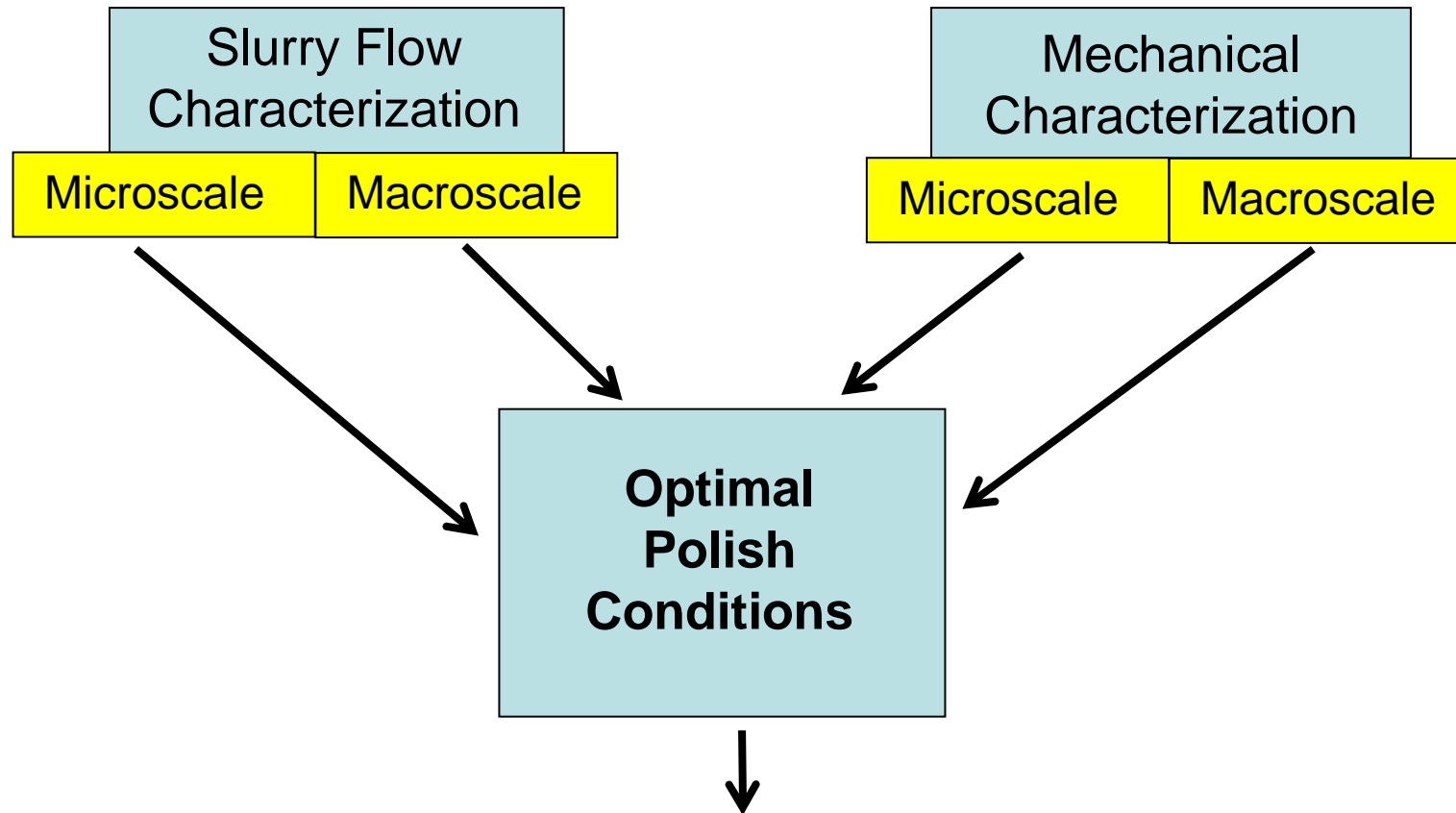
### **Graduate Students:**

- **James Vlahakis: PhD candidate, Mechanical Engineering, August 2008**
- **Douglas Gauthier: MS candidate, Mechanical Engineering, August 2008**
- **Andrew Mueller: MS, Mechanical Engineering, August 2007**

# Objectives

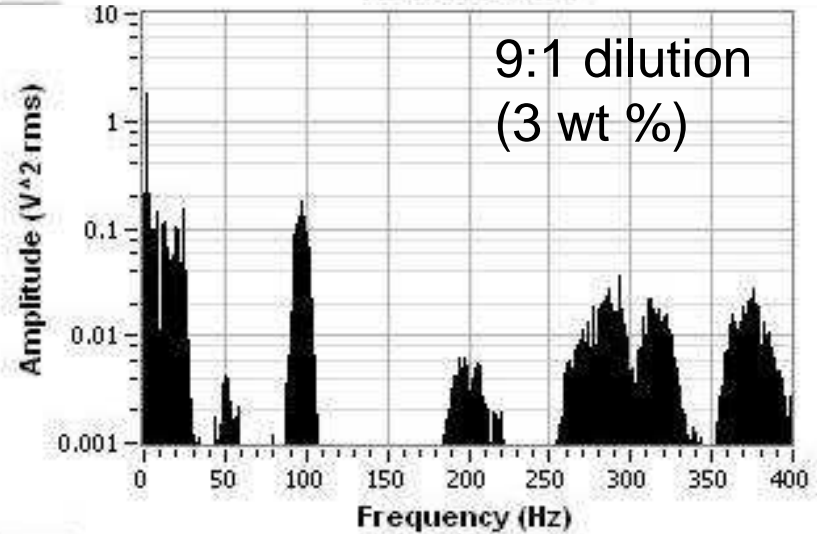
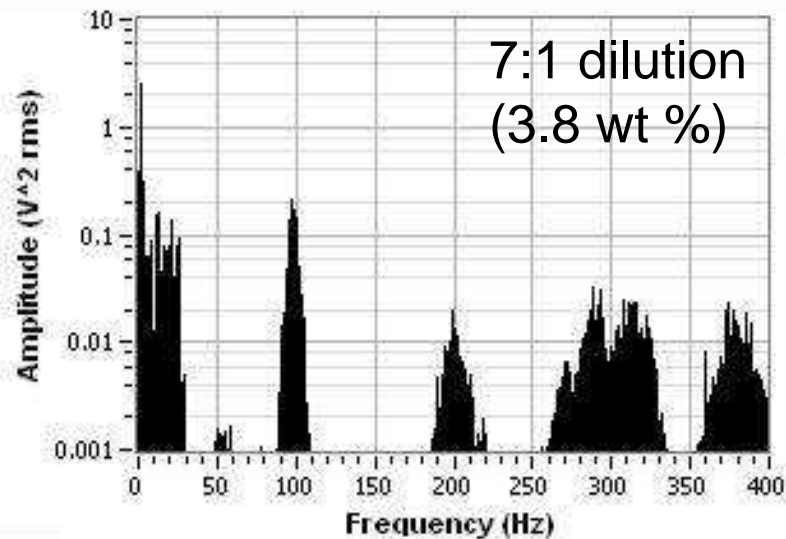
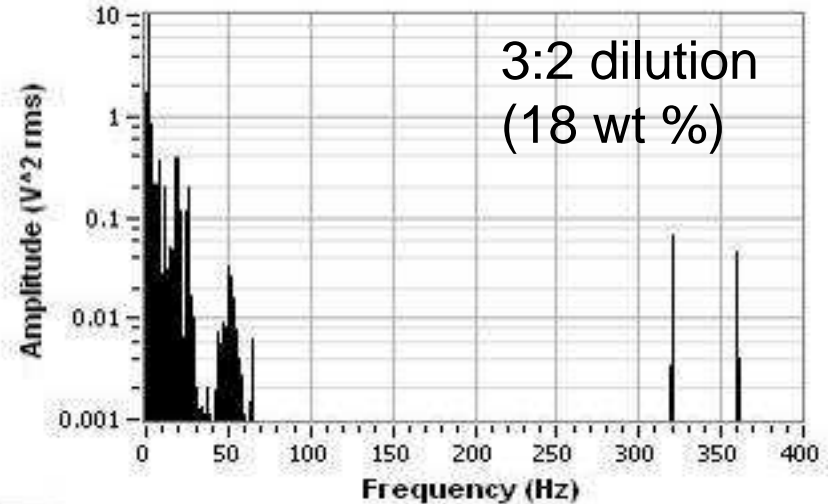
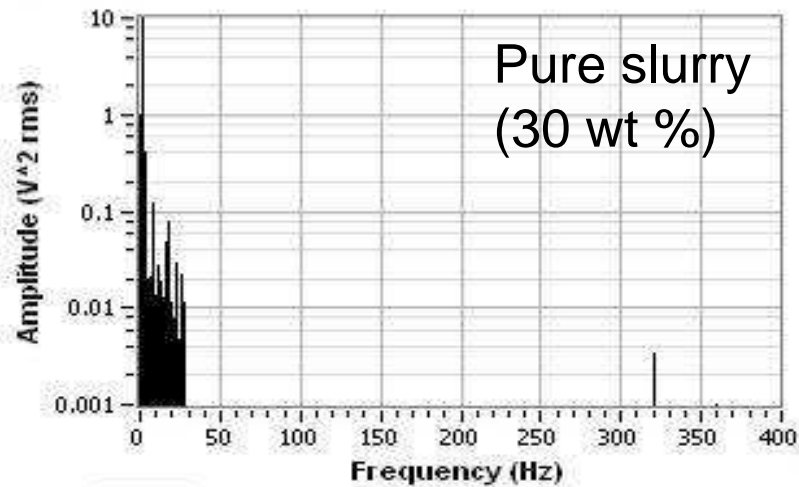
- Concurrent measurement of spatially averaged force (3-axis, COF, moments), force spectra, wafer attitude, and material removal rate under a variety of polishing conditions – James Vlahakis (PhD Student)
- Use custom micromachined sensors to measure local (100  $\mu\text{m}$  scale), high sample rate (0.1 ms) asperity scale forces at the pad-wafer interface during CMP - Douglas Gauthier (MS Student)

# ESH Metrics and Impact



- Reduced time to polish (energy and cost savings)
- Reduced consumables (waste and cost reduction)

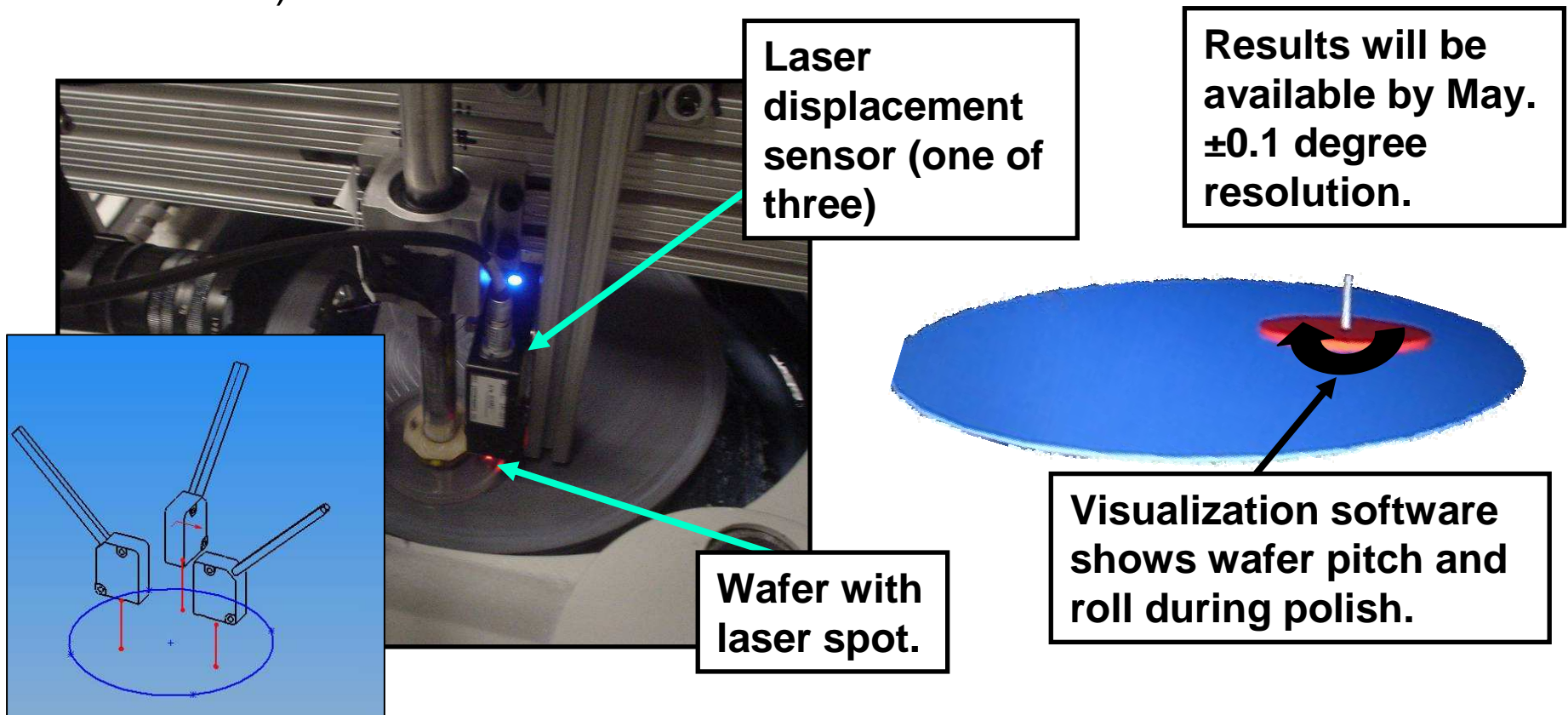
# In-Plane Force Spectra



Spectral signatures vary with slurry concentration. 30 wt % slurry (fumed silica slurry) exhibits the least high frequency force content.

# Wafer Attitude

- Three laser displacement sensors are mounted in the rig to measure the wafer pitch, roll, and bounce during polishing.
- Wafer displacement is correlated to pad angular position (measured with an encoder).

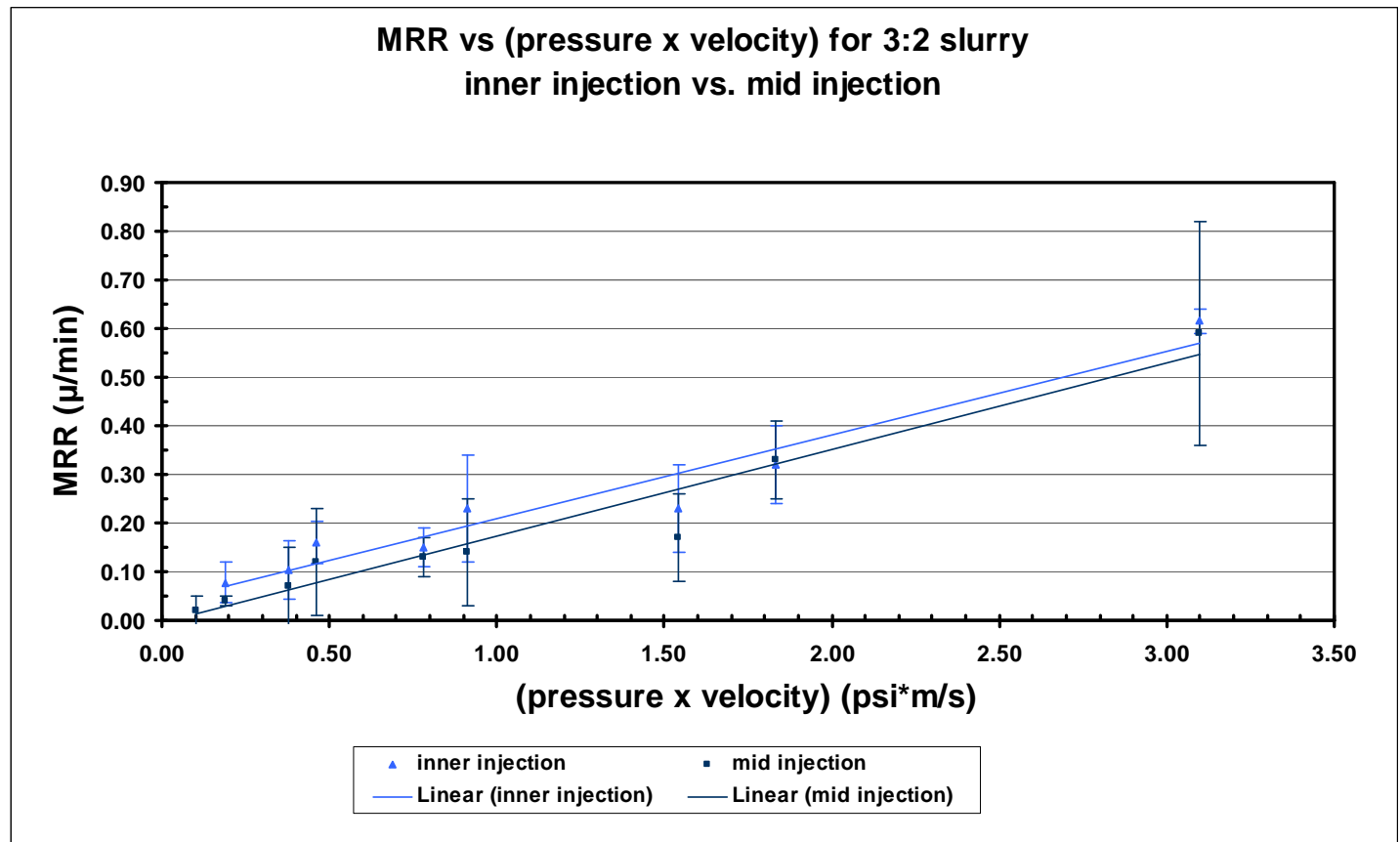


# Material Removal Rate

- Material removal rate (MRR) is Prestonian for oxide polishing using 22% by weight fumed silica slurry.

- MRR is 50-600 nm/min over the 0.1 to 3.1 psi-m/s range.

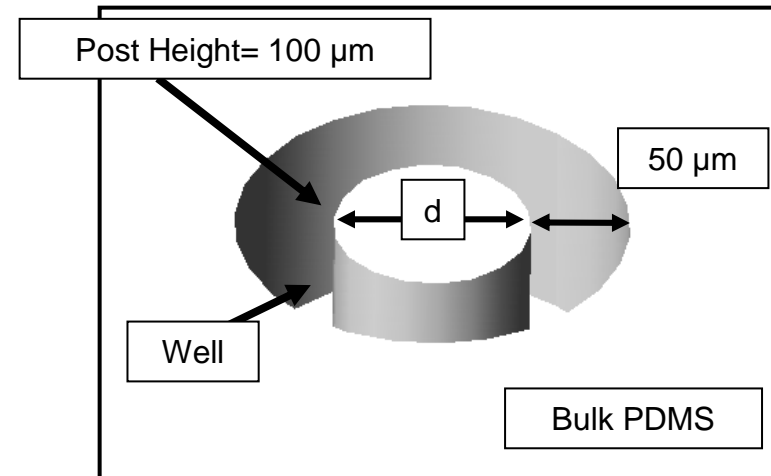
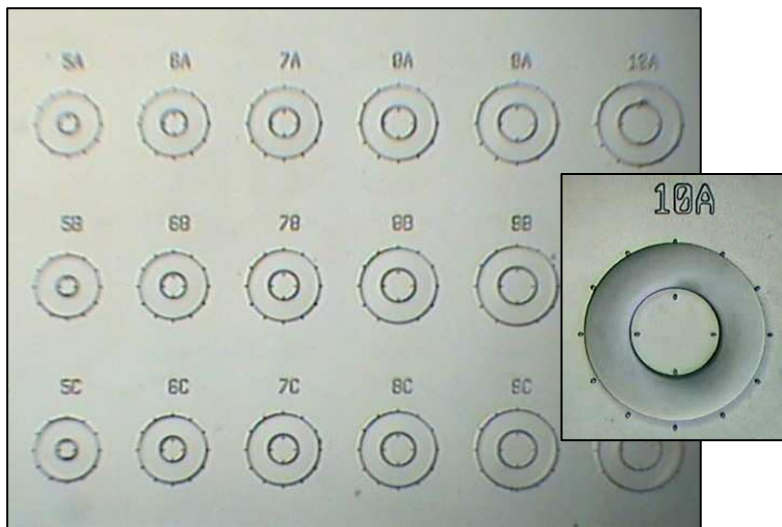
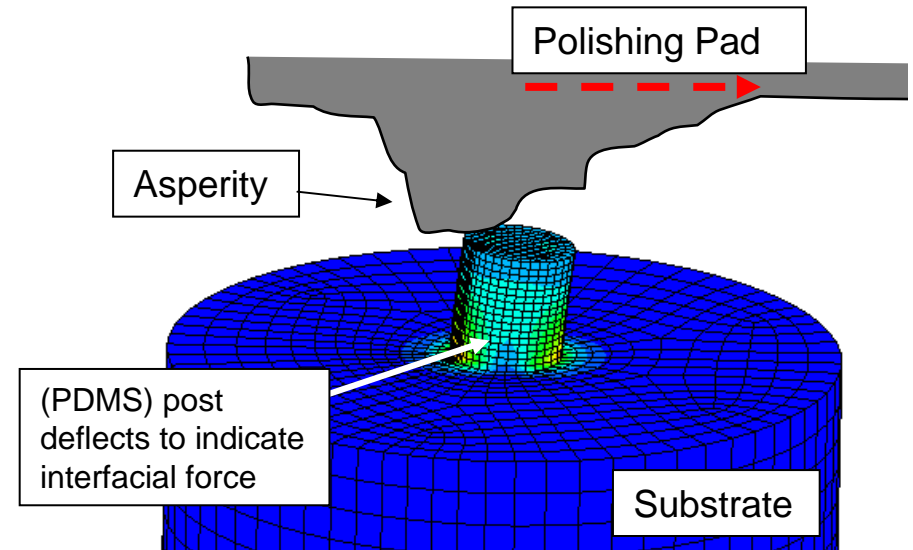
- For the saturated flow rates used, no dependence on slurry injection point is observed.





# MEMS Force Sensors

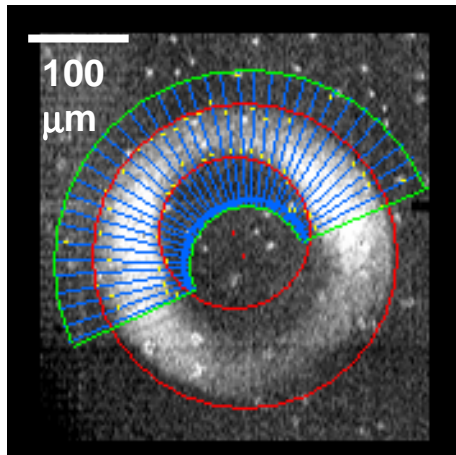
- Cylindrical PDMS posts:
  - 100  $\mu\text{m}$  tall, 30-100  $\mu\text{m}$  diameter.
  - Deflect due to shear force.
  - Recessed in wells.
- Calibrated sensitivity is linear:
  - 200  $\text{nm}/\mu\text{N}$  for 100  $\mu\text{m}$  diameter



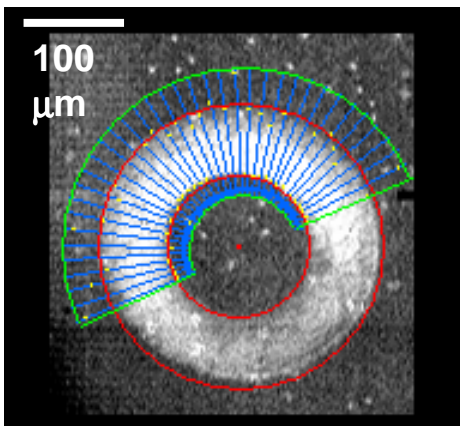


# Asperity Level Forces

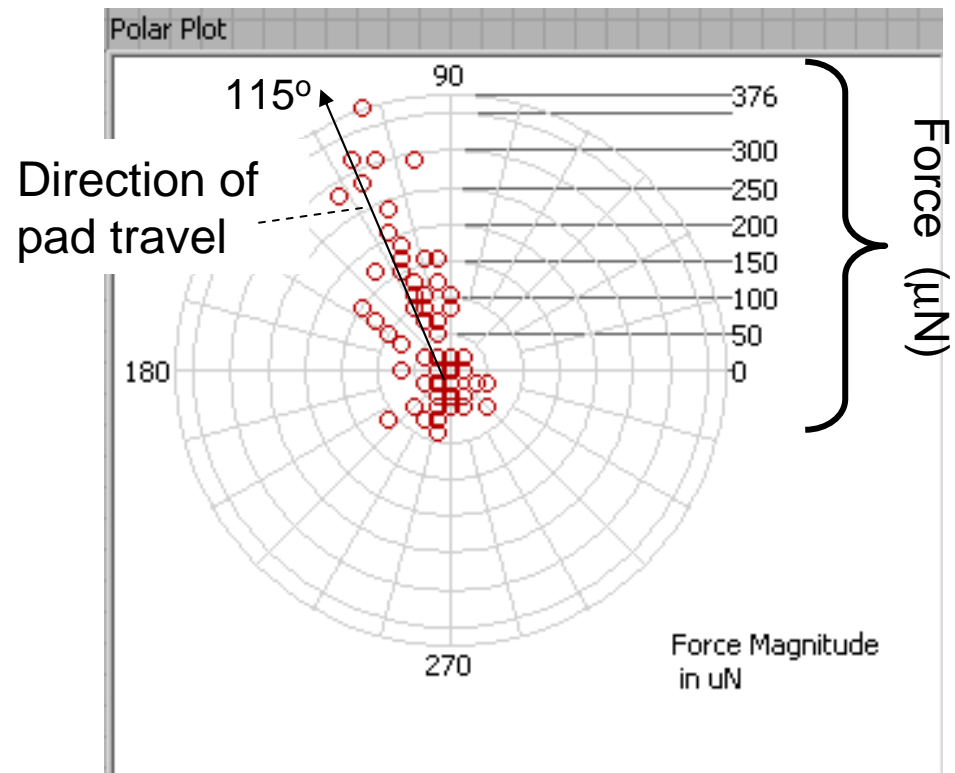
Image processing extracts motion of the post from high-speed (10,000 fps) video.



**Deflected**



**Not deflected**

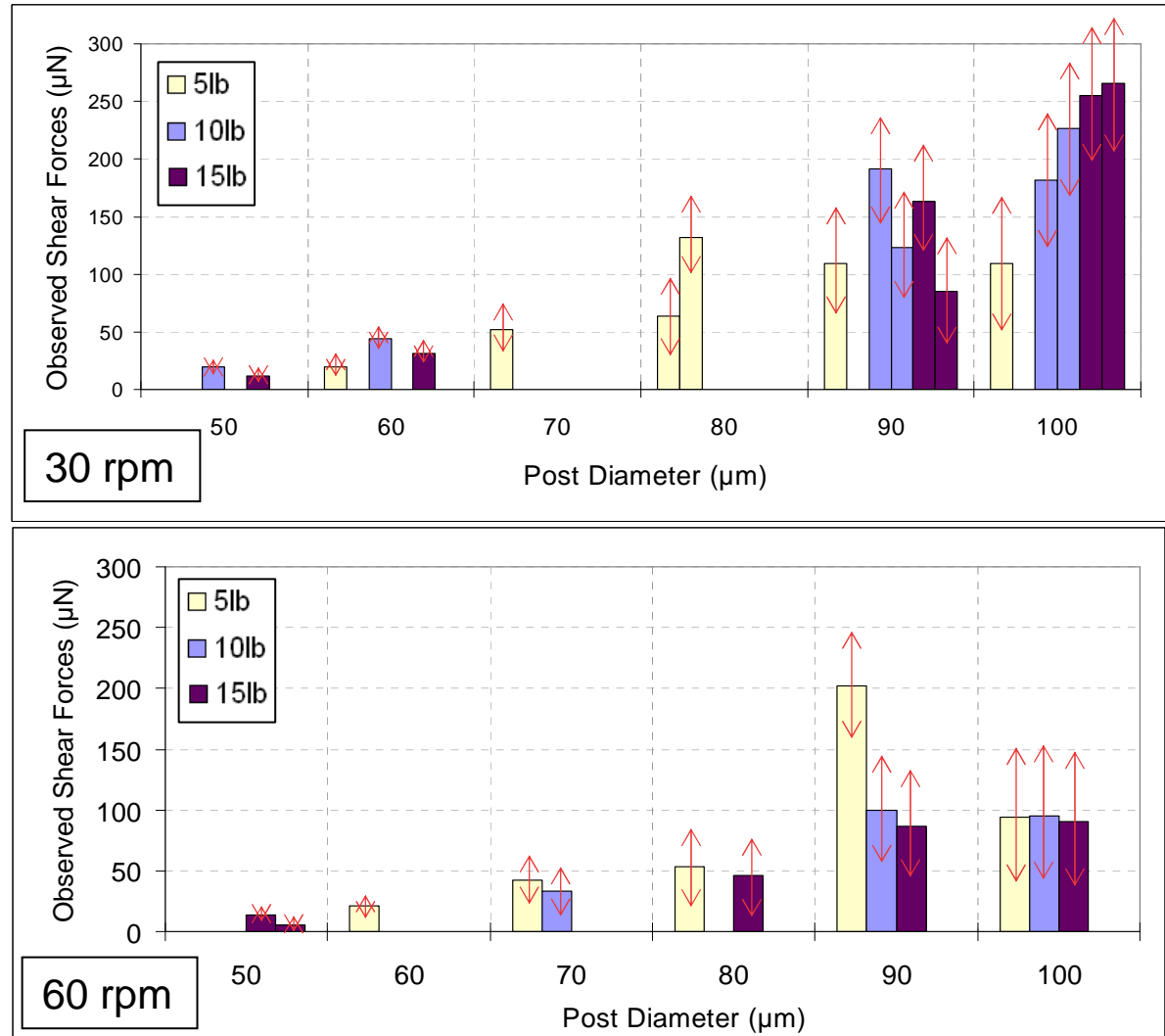


Each point corresponds to the force (direction and magnitude) measured at each 100 microsecond time step. The average force direction aligns with the direction of pad travel.

# Asperity Level Forces: Trends

Plots show peak shear forces for maximum force events.

- **Increase** in pad rotation leads to a **decrease** in local shear force.
- **Increase** in structure size leads to an **increase** in local shear force.
- Increase in downforce leads to an increase in local shear force only at lower speeds.
- Maximum shear forces for 100  $\mu\text{m}$  structures are approximately 300  $\mu\text{N}$ .



# Industrial Interactions and Technology Transfer

- Close collaboration with industry partners – Cabot Microelectronics and Intel
  - Monthly telecons – secure website for information exchange
  - Semi-annual face-to-face meetings
  - Thesis committees and joint publication authorship
  - Metrology and analysis methodology technology transfer
  - In-kind support – specialized supplies and equipment
  - Student internships (e.g. C. Gray at Intel during Summer 2005)
- Close coordination with A. Philipossian research group at U of Arizona
- Information and results exchange with MIT (D. Boning, G. McKinley), Stockton College (E. Paul), Harvard University (H. Stone).
  - Monthly joint meetings of PIs and research students

# Future Plans

## Next Year Plans

- All current students complete theses and graduate:
  - C. Gray, PhD : DELIF for pad-wafer contact and slurry thickness
  - J. Vlahakis, PhD : Wafer-scale characterization of CMP mechanics
  - N. Braun, MS : Particle image velocimetry for CMP slurry flow
  - D. Gauthier, MS : MEMS for asperity scale force measurement in CMP

## Long-Term Plans

- Deploy the newly demonstrated *in situ* measurement technologies (DELIF, wafer attitude, PIV, MEMS force sensing) to a 200 mm polisher.
- Characterize polishing of patterned tantalum/copper and oxide substrates using the suite of new measurement technologies on the 200 mm platform.
- Apply results of the experimental study to optimize polish conditions, pad geometry/type, conditioner geometry/type for improved polish quality and reduced consumables.

# Publications, Presentations, and Recognitions/Awards

- N. Braun, C. Gray, A. Mueller, J. Vlahakis, D. Gauthier, V. P. Manno, C. Rogers, R. White, S. Anjur, M. Moinpour. “*In-Situ Investigation of Wafer-Slurry-Pad Interactions during CMP*” in the **Proceedings of the International Conference on Planarization/CMP Technology**, Dresden, Germany, October 25-27, 2007.
- Mueller, A. White, R. D., Manno, V., Rogers, C., Barns, C. E., Anjur, S., and Moinpour, M. “*Micromachined Shear Stress Sensors for Characterization of Surface Forces During Chemical Mechanical Polishing*” in the **Proceedings of the Material Research Society**, Vol. 991, Symposium C, Advances and Challenges in Chemical Mechanical Planarization, 2007.

# An Integrated, Multi-Scale Framework for Designing Environmentally Benign Copper, Tantalum and Ruthenium Planarization Processes

*(Task 425.020)*

## Subtask 1: Modeling of Planarization Performance

### PI:

- Duane Boning, Electrical Engineering and Computer Science, MIT

### Graduate Students:

- Hong Cai, Materials Science, MIT, graduate with Ph.D. in June 2007
- Xiaolin Xie, Physics, MIT, graduate with Ph.D. in June 2007
- Wei Fan, Ph.D. candidate, EECS, MIT, started Sept. 2007

### Undergraduate Student:

- Zhipeng Li, EECS, MIT

### Other Researcher:

- Ed Paul, Visiting Professor, Stockton College

### Cost Share (other than core ERC funding):

- Experimental support, JSR Micro

*SRC/SEMATECH Engineering Research Center for Environmentally Benign Semiconductor Manufacturing*

# Objectives

- Focus on *chip-* and *feature-scale* performance of CMP processes
  - Connect with physical investigations by team members
  - Connect with metrology and wafer level for control
- Understand how pad properties relate to the *planarization* capability of CMP processes
  - Pad bulk: chip-scale uniformity (pattern density)
  - Pad surface: step-height removal dependencies (dishing)
- Joint optimization of pad properties to achieve processes with reduced time, consumables, and waste, *as well as* reduced dishing, erosion, and within die nonuniformity

# ESH Metrics and Impact

**Driving principle: Joint improvement in CMP performance and ESH performance**

- 1. Reduction in the use or replacement of ESH-problematic materials***
- 2. Reduction in emission of ESH-problematic material to environment***
  - Reduce slurry particle use and Cu solid waste by 20-50%**
- 3. Reduction in the use of natural resources (water and energy)***
  - Shorten CMP polish times (copper, barrier) by 20-50%**
  - Improve yield (multiplication over all inputs/outputs) by 1-2%**
- 4. Reduction in the use of chemicals***
  - Reduced plated copper thickness by 25%**
  - reduced slurry usage by 20%**
  - Improved pad lifetime by 20-50%**

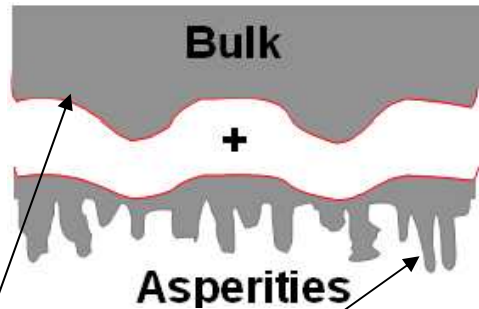


# Pad/Planarization Modeling Approach

- **Previous CMP chip-scale model:**
  - “planarization length” concept for pattern density effect on amount removed uniformity within die
  - “critical step height” concept for feature-scale step height removal
- **New CMP chip-scale model:**
  - More directly physically based
  - Effective pad bulk modulus
    - Explicit long range pad bending (replaces planarization length)
  - Asperity height distribution
    - Probabilities on asperity heights replaces critical step height
- **Application/Verification**
  - Alternative CMP water-soluble particle (WSP) pad, JSR Micro

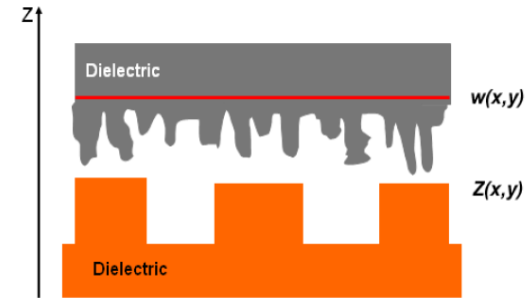
# Physical CMP Chip-Scale Model

## Parameters



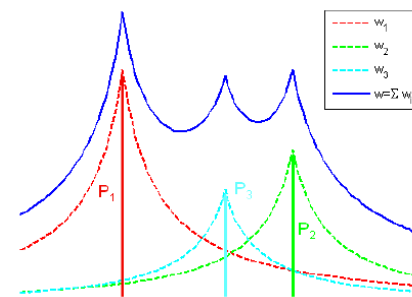
- $E$  = Effective Young's Modulus (Property of pad bulk)
- $\lambda$  = Characteristic Asperity Height (Property of pad asperities)
- $K$  = Blanket Removal Rate at reference pressure (Scaling factor of the system)

## Pad Bulk: Contact Mechanics



Contact Mechanics describes the relationship between pad displacement  $w(x,y)$  and pad pressure  $P(x,y)$

- Point pressure,  $w(r) \sim 1/r$
- Linear superposition

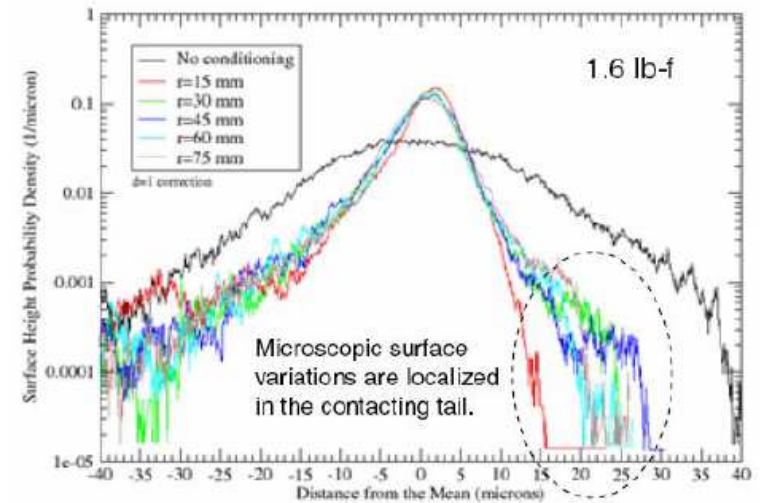


$$w(x, y) - w_0 = \frac{1 - \nu^2}{\pi E_p} \int d\xi \int d\eta \frac{P(\xi, \eta)}{\sqrt{(x - \xi)^2 + (y - \eta)^2}}$$

# Pad Asperities

## Assumptions:

1. Negligible width
2. Exponential distribution of height, mean  $\lambda$
3. Hooke's law: force proportional to compressed amount



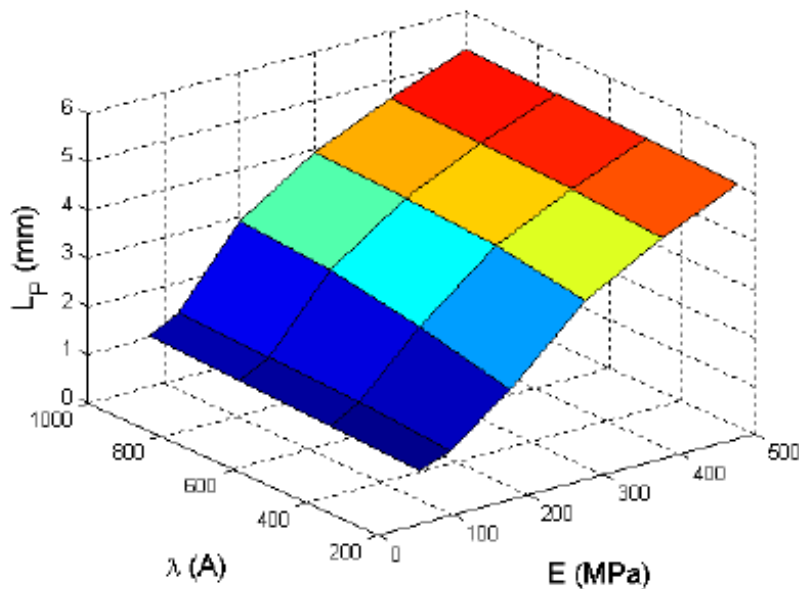
Surface Height Distribution

L. Borucki, 2006, ICPT

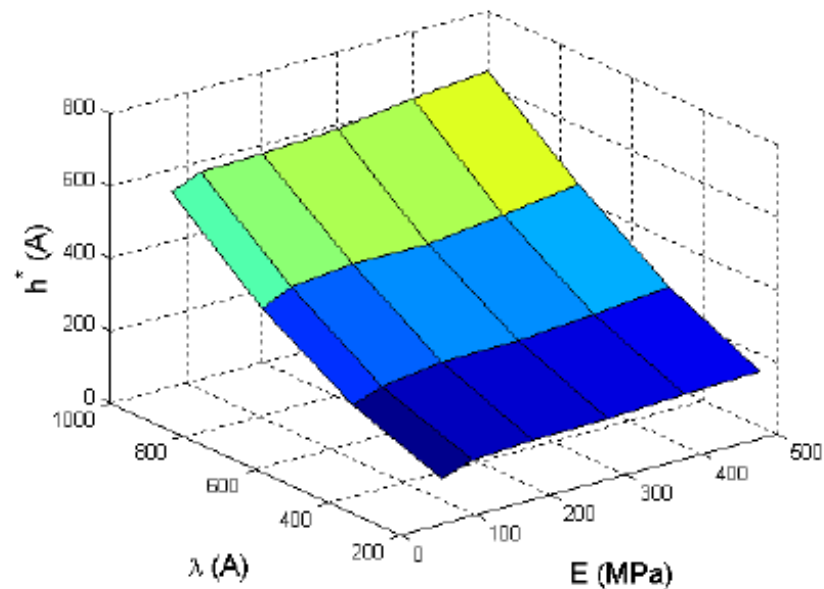
$$\left\{ \begin{array}{l} P_d = \frac{1}{1 + \rho(e^{h/\lambda} - 1)} P \\ P_u = \frac{e^{h/\lambda}}{1 + \rho(e^{h/\lambda} - 1)} P \end{array} \right. \Rightarrow \left\{ \begin{array}{l} K_d = \frac{1}{1 + \rho(e^{h/\lambda} - 1)} K \\ K_u = \frac{e^{h/\lambda}}{1 + \rho(e^{h/\lambda} - 1)} K \end{array} \right.$$

# Interpreting Pattern-Density/ Step-Height Parameters

- Planarization length  $L_P$ 
  - $z_u$  (across chip)
  - increases with  $E$
  - insensitive to asperity height distribution

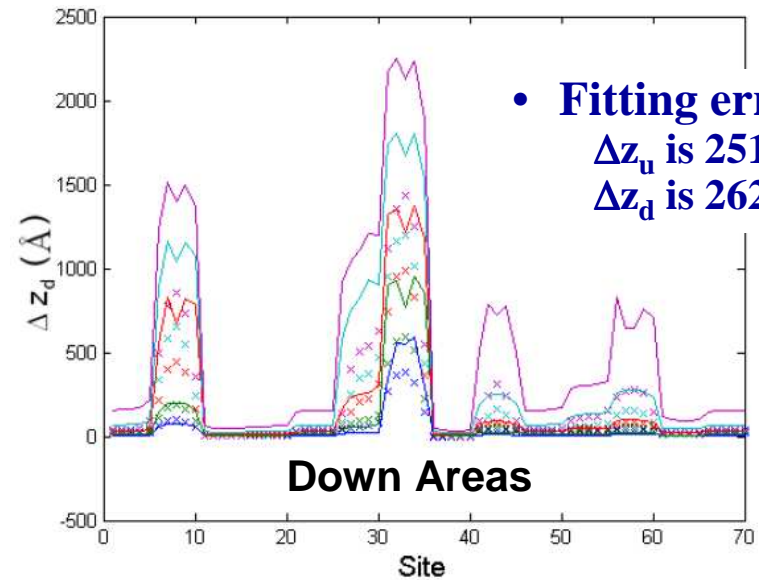
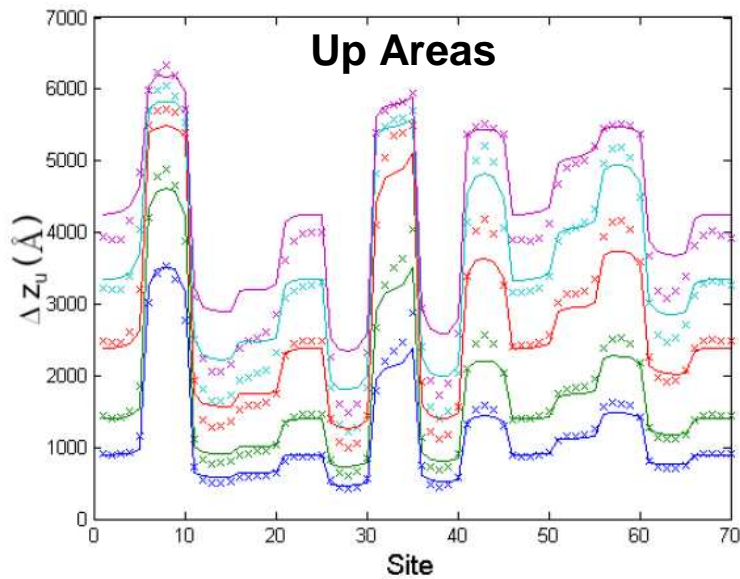
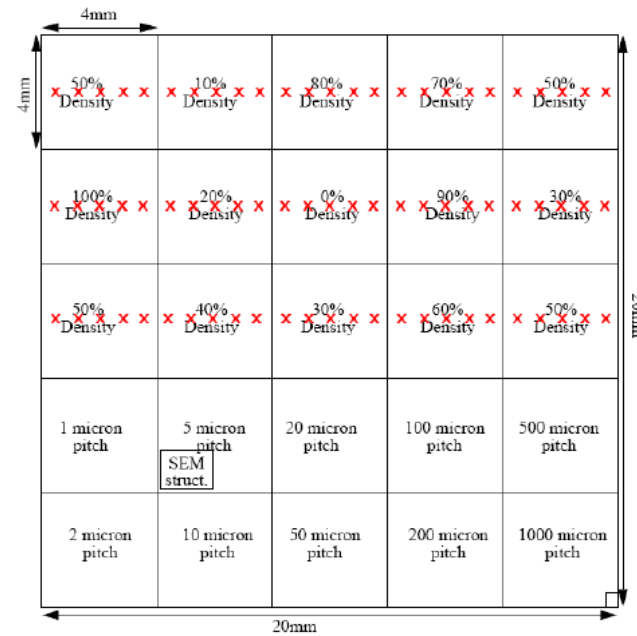


- Characteristic step-height  $h^*$ 
  - step height evolution
  - depends strongly on asperity height distribution
  - insensitive to  $E$



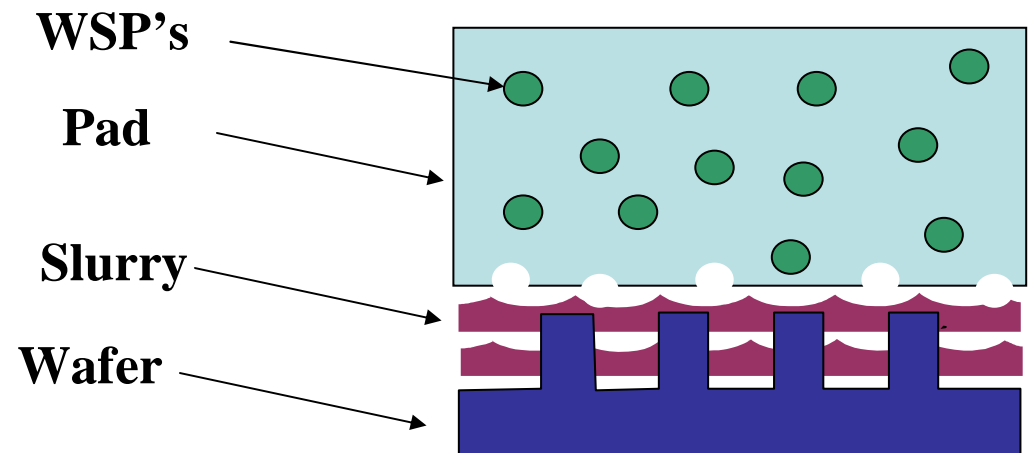
# Experimental Verification of Model

- STI CMP experiment
- STI CMP test mask
- IC-1400 pad
- SS-25 slurry
- Polishing time splits:
  - 5, 10, 15, 30, 40 seconds
- Optical thickness measurements
  - at “x” marks
  - both raised and trench areas

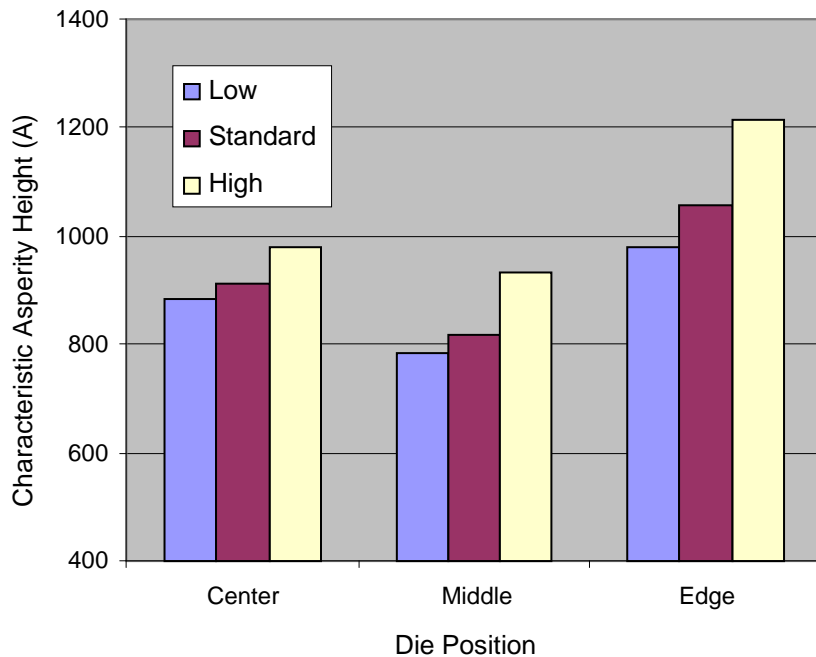


# Model Application: Study of Pad/Planarization Dependencies

- **Pad with water soluble particles (WSP's)**
  - Keeps pad bulk rigid (increased bulk stiffness)
  - Pores aid in slurry transport
  - Modifies/controls pad surface/asperity structure
- **Goal of study**
  - Extract chip-scale model parameters for different WSP pad designs
  - Understand chip-scale performance as function of pad parameters
- **Experiments**
  1. Vary WSP size (fixed concentration)
  2. Vary WSP concentration (fixed size)

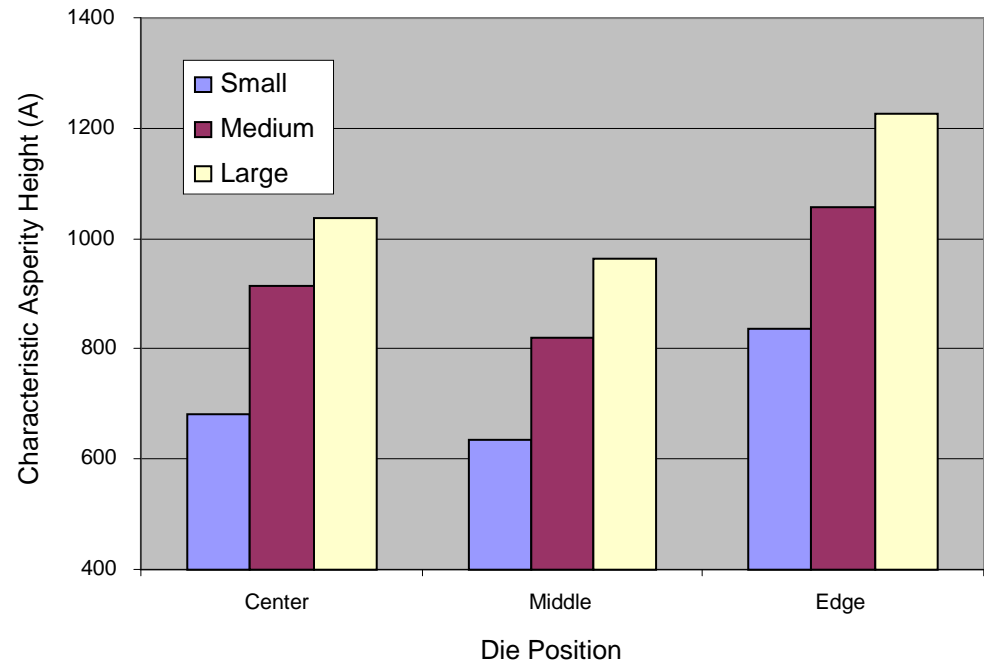


# Effect of WSP Concentration



- Higher concentration → more porous surface when particles dissolve in slurry → a larger mean asperity height
- Asperities longer at wafer edge, effect of different conditioning?

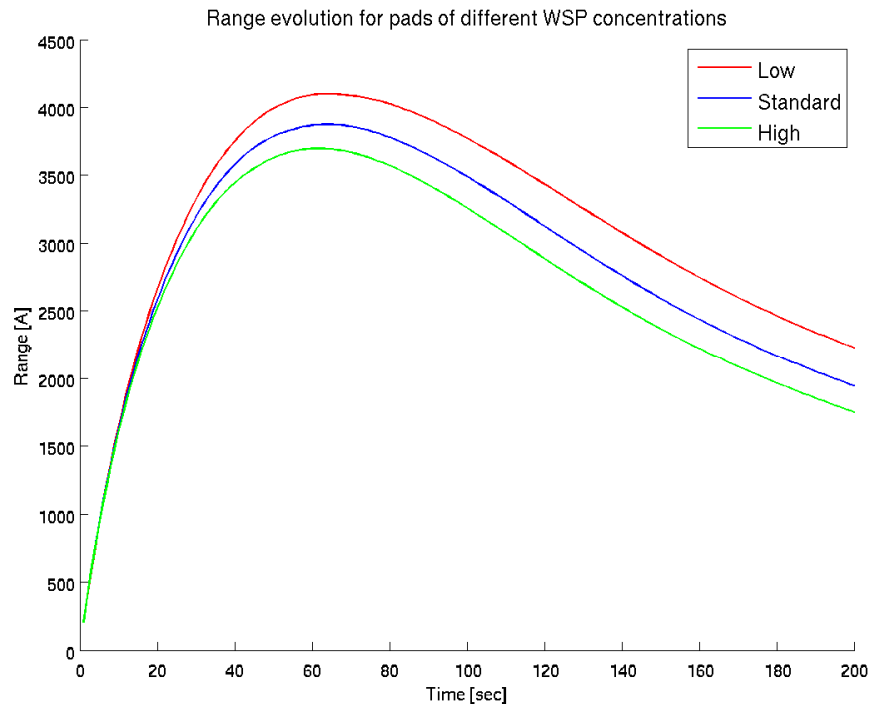
# Effect of WSP Size



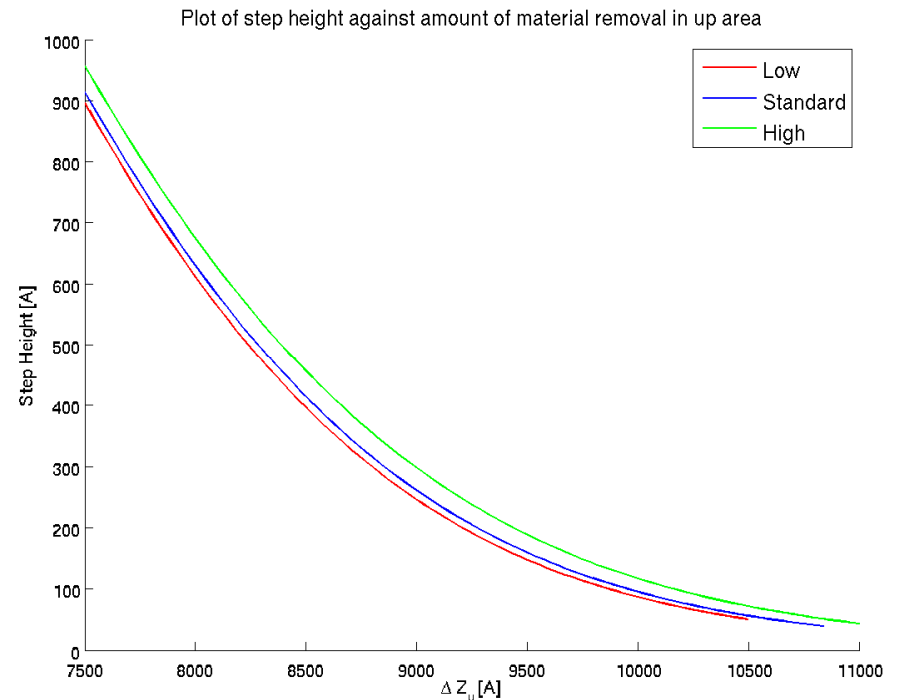
- Large WSP size → bigger pores → extract a larger mean asperity height

# Performance Metrics

## Up-Area Range (Max-Min) Across Chip



## Planarization Efficiency



- **Enables exploration of trade-off or joint optimization between**
  - **Chip-scale (within-die) uniformity**
  - **Feature-scale planarization (dishing)**



# Future Plans

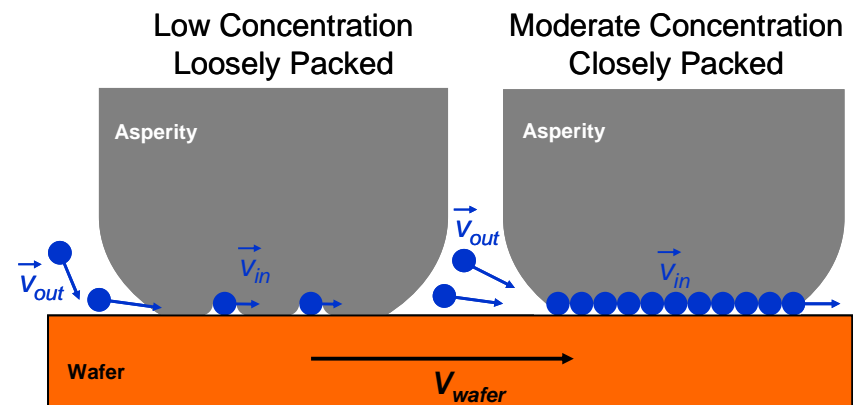
## Next Year Plans

- Modeling & verification experiments
  - Pad bulk modulus and surface distribution experiments for improved planarization and step-height reduction (range of polymer stiffness)
  - Measurement of pad asperity vs. bulk mechanical properties using nanoindentation
  - Mechanical modeling of force distribution: asperities vs. pad bulk
- Experimental exploration of slurry particle density on pad asperities (with Tufts)
  - Establish whether model assumption of dense pack is correct; potential implications for slurry particle concentration (solid waste reduction)

## Extension Program Plans

- Integrate feature, chip and wafer-scale CMP model with sensor models
  - Based on in-situ sensor signals, identify stage of planarization, dishing, erosion, across chip and wafer
- Develop CMP physical model improvements and interfaces
  - In-situ studies of pad/wafer contact, pad topography, slurry/particle flow (UA, Tufts)
  - Apply to process optimization and waste reduction

## **Pad-Abrasive-Wafer Interaction**



# **Environmentally-Friendly Cleaning of New Materials and Structures for Future Micro and Nano Electronics Manufacturing** *(Task Number: 425.022)*

## **Post Etch Residue Removal in Copper Damascene Structures**

### **PI:**

- **Srini Raghavan, Materials Science and Engineering, University of Arizona**

### **Graduate Student:**

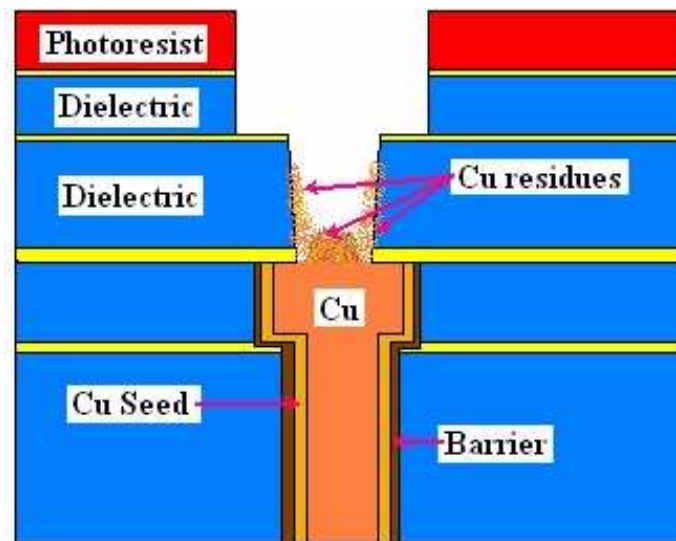
- **Nandini Venkataraman, PhD candidate, Materials Science and Engineering, University of Arizona**

### **Undergraduate Student:**

- **Alex Luce, Engineering Physics, University of Arizona**

# Objectives

- Evaluate and optimize chemical systems having low solvent and fluoride content, for the selective removal of copper oxides ( $\text{CuO}_x$ ) and post-etch residues from copper and dielectric surfaces
- Develop an electrochemical impedance spectroscopy based end point technique for the removal from copper surfaces



# ESH Metrics and Impact

- *ESH objective:* Reduction of solvent content in semi aqueous fluoride (SAF) based solutions for removal of post etch residue

Solution components	Weight % in typical formulations	Weight % in best formulation in this study	% Reduction
Solvent	> 60%	29%	> 50%
Water	< 40%	71%	- 35% (increase)
Fluoride	~ 1-2%	1%	0 – 50%

Typical Solvents	LD <sub>50</sub> (Oral Rat) mg/kg
Dimethyl Sulfoxide	<b>14500</b>
N-Methyl Pyrrolidone	3900
Sulfolane	2000

# Experimental Approach

## Blanket CuO<sub>x</sub> Films

- Formed by thermal oxidation of Cu films at 300°C

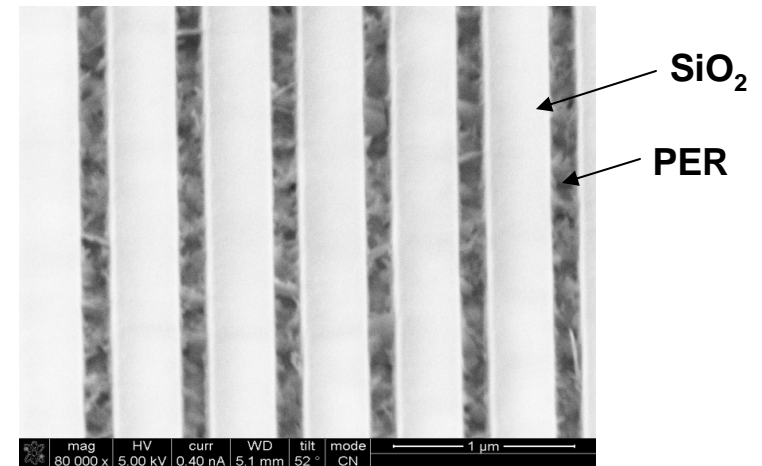
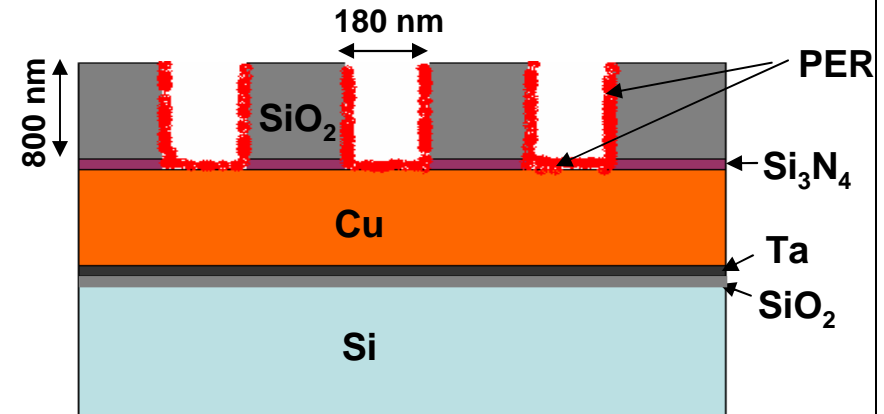
## Solutions

- Water (30-100%), Dimethyl Sulfoxide (0-69%), NH<sub>4</sub>F and oxalic acid (pH ~ 4-6)

## Methods

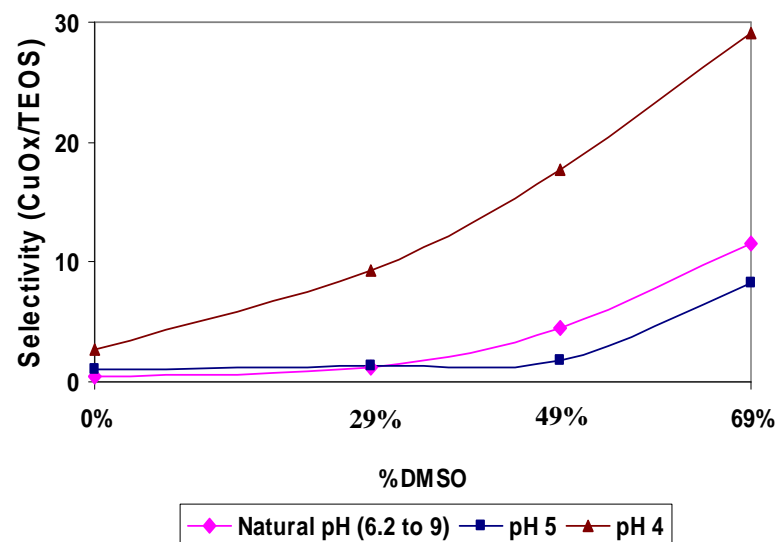
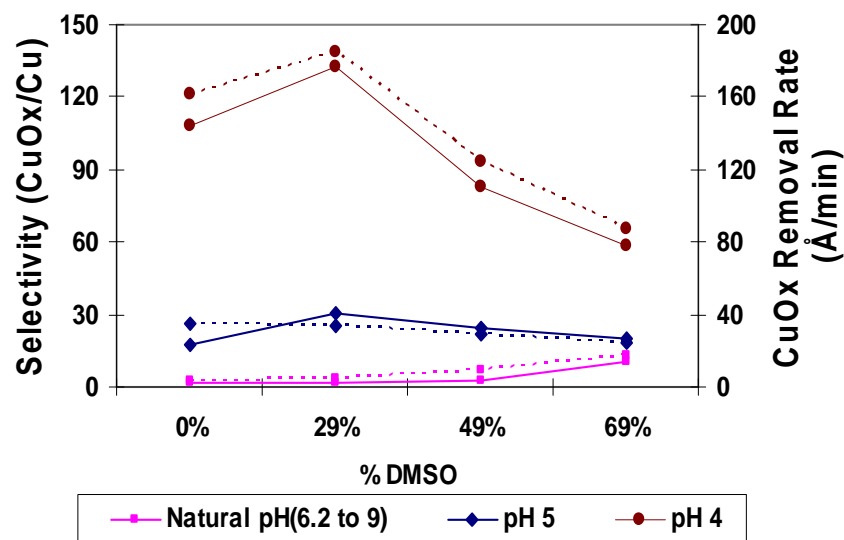
- CuO<sub>x</sub> removal rate by solution analysis using Atomic Absorption Spectrophotometry
- CuO<sub>x</sub> film/residue dissolution followed using multi-sine Electrochemical Impedance Spectroscopy and data fitting using ZView software

## Patterned Wafers



Thickness of post etch residue layer on copper  
~ 5-8 nm from FIB-TEM measurements

# Selective Removal of $\text{CuO}_x$ over Cu and TEOS

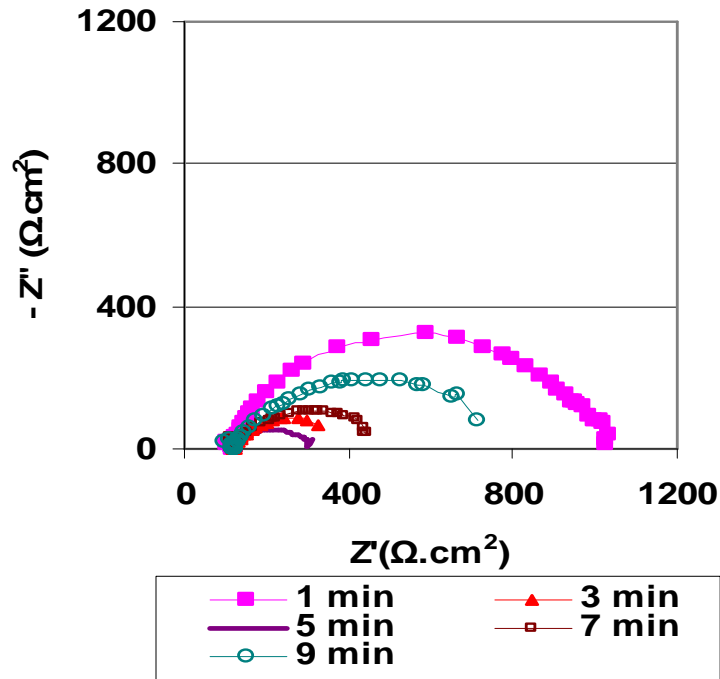


----- Removal Rates of  $\text{CuO}_x$   
 ———— Selectivity ( $\text{CuO}_x/\text{Cu}$ )

**29% DMSO, 1%  $\text{NH}_4\text{F}$ , 70%  $\text{H}_2\text{O}$  (pH 4)**

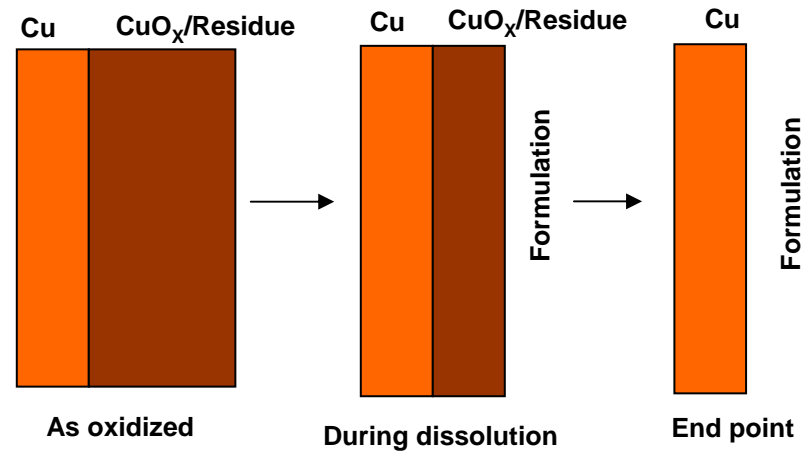
- $\text{CuO}_x$  removal rate  $\sim 180 \text{ \AA}/\text{min}$
- $\text{CuO}_x/\text{Cu}$  selectivity  $\sim 130:1$
- $\text{CuO}_x/\text{TEOS}$  selectivity  $\sim 10:1$

# Electrochemical Impedance Spectroscopy

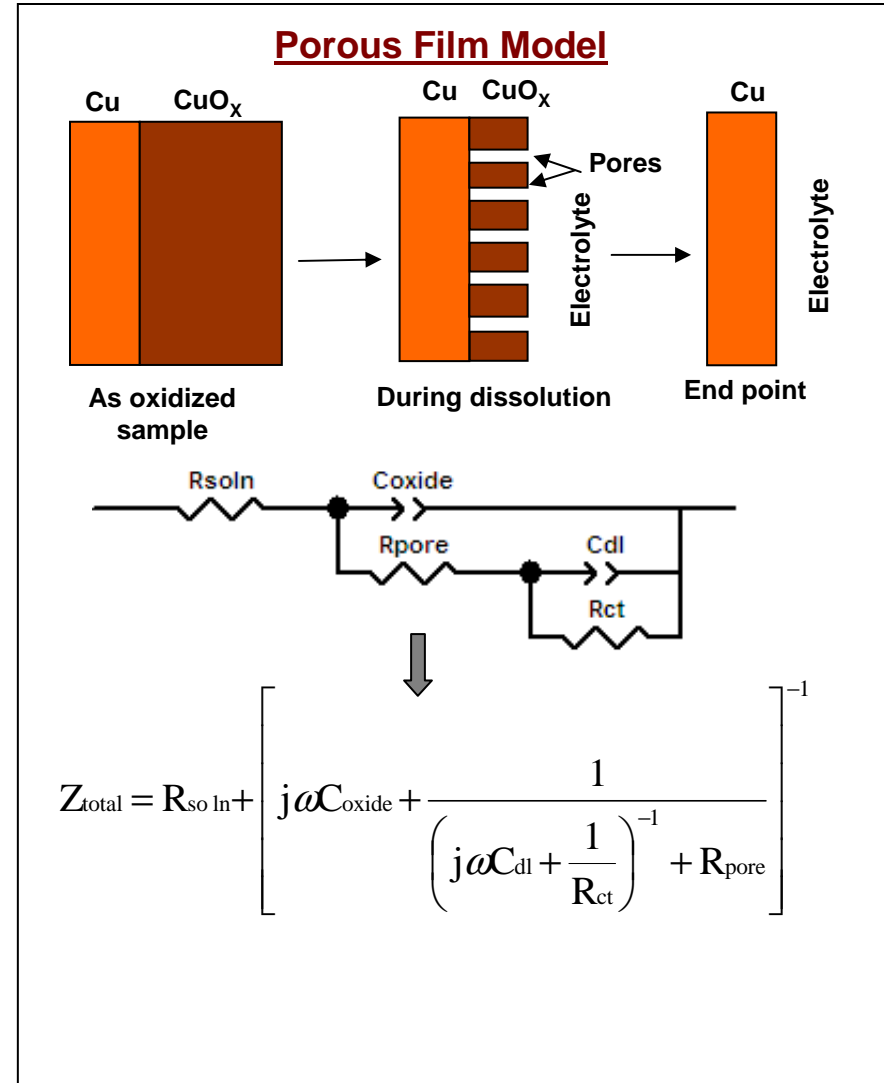
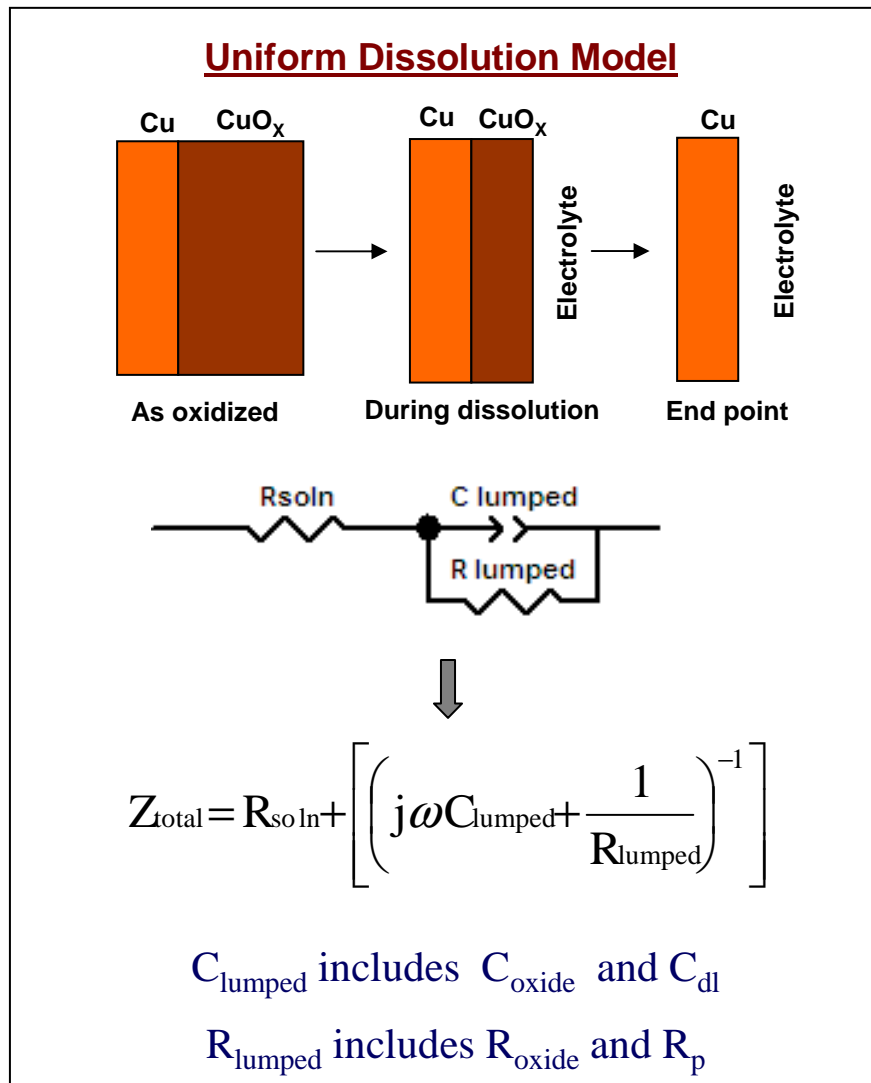


*Impedance Spectra of  $\text{CuO}_x$  film as a function of time in solution containing 49% DMSO, 1%  $\text{NH}_4\text{F}$  and 50%  $\text{H}_2\text{O}$  (pH 4)*

- Follow  $\text{CuO}_x$  dissolution using EIS
- **Sample:**  $\text{CuO}_x$  film of thickness  $\sim 55$  nm
- Measured data at different times form a depressed semicircle



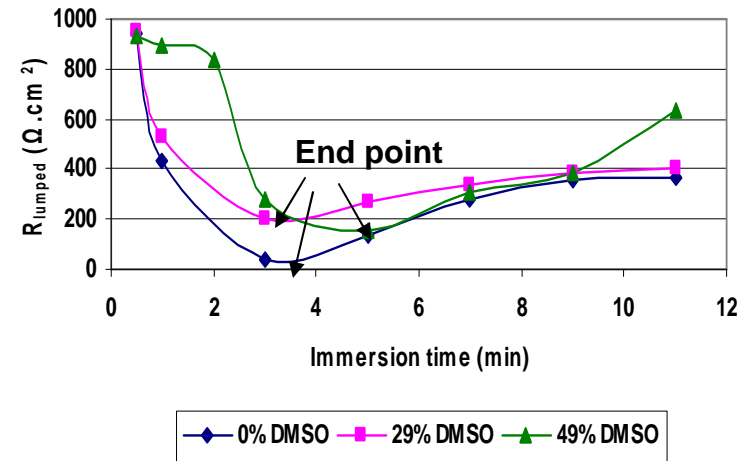
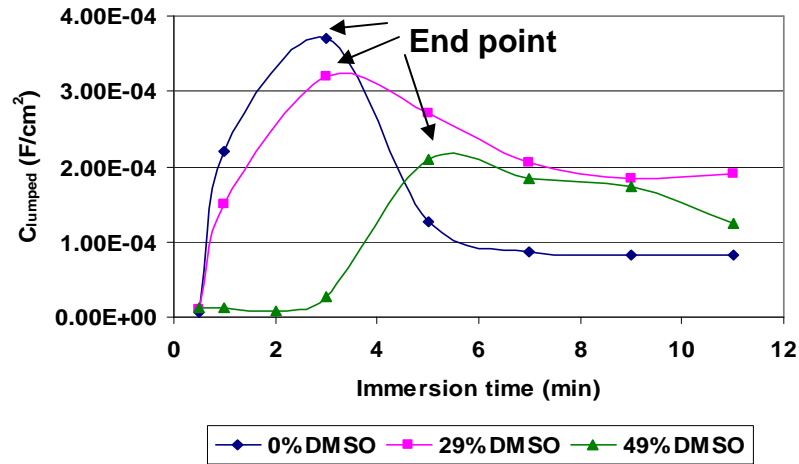
# Equivalent Circuit Modeling for CuO<sub>x</sub> dissolution



**Both models provide good fit to data**



# Uniform Dissolution Model



- **During dissolution**

- $\uparrow C_{lumped}$  due to  $\uparrow C_{oxide}$

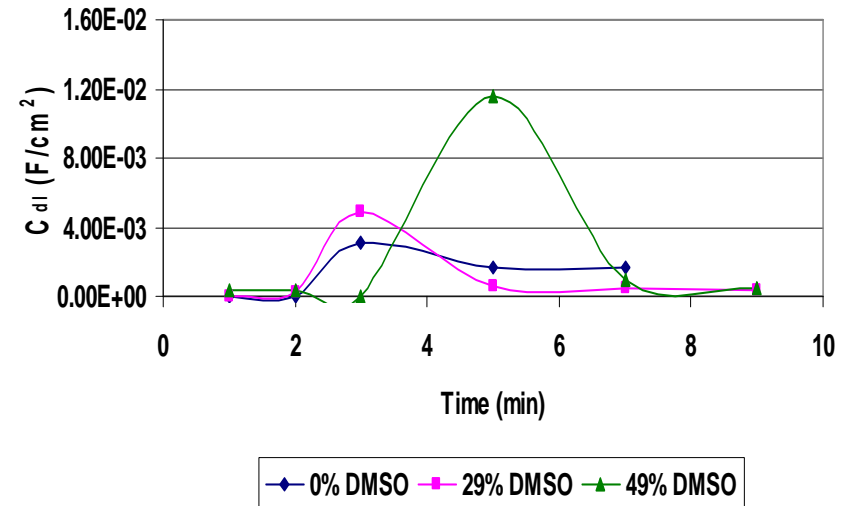
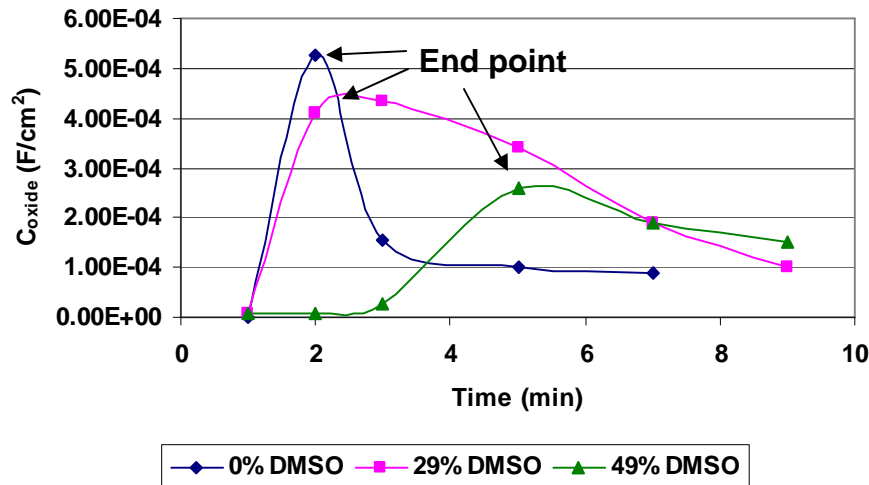
- $\downarrow R_{lumped}$  due to  $\downarrow R_{oxide}$

- **At end point**

- $C_{lumped} \rightarrow C_{dl}$  (Cu/electrolyte)

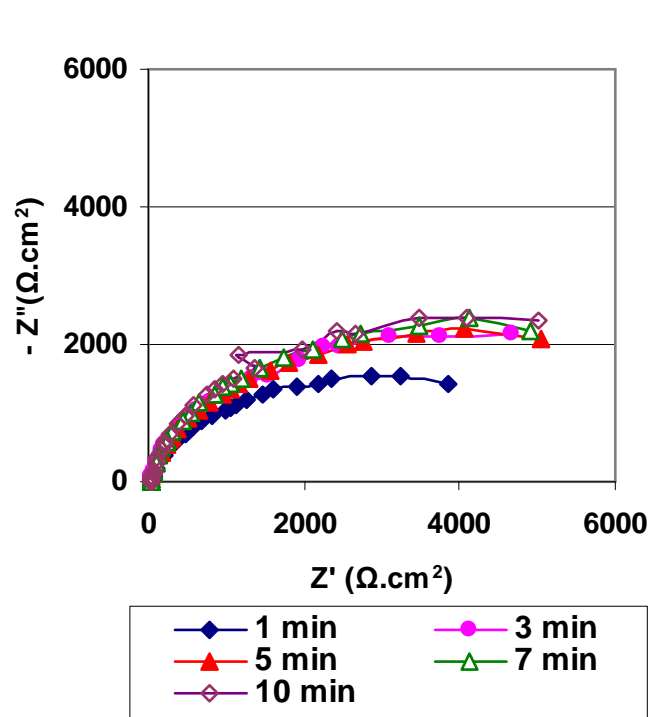
- $R_{lumped} \rightarrow R_{ct}$  at Cu/electrolyte interface

# Porous Film Model

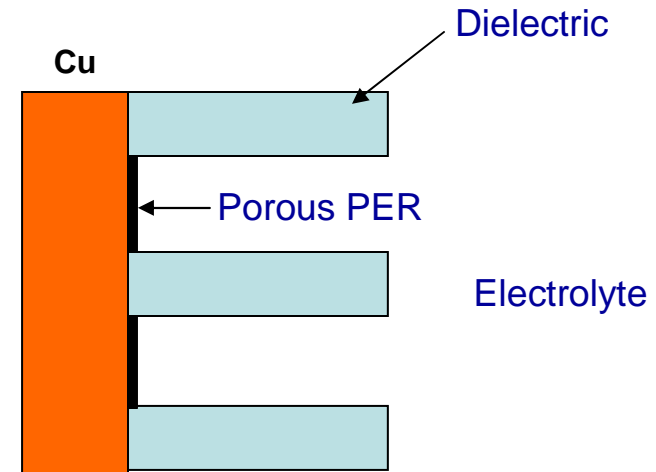


- **During dissolution**
  - $\uparrow C_{oxide}$  due to loss of oxide
  - $\uparrow C_{dl}$  due to  $\uparrow$  Cu surface area
- **After end point,**
  - $\downarrow C_{oxide}$  due to repassivation
- **Values of  $C_{dl}$  too high to represent double layer capacitance alone** – reasons are being investigated

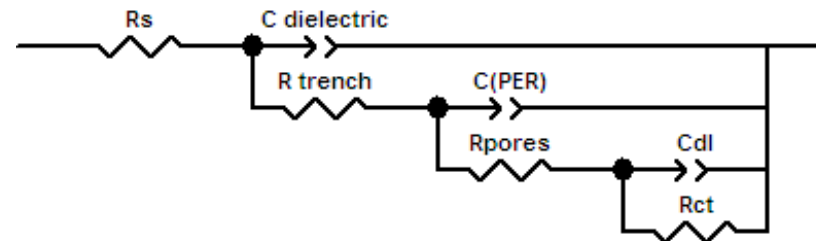
# EIS in Patterned Wafers



*Impedance Spectra of Patterned test structure as a function of time in solution containing 49% DMSO, 1%  $\text{NH}_4\text{F}$  (pH 4)*



## Equivalent circuit under consideration



- Magnitude of impedance for PER higher than controlled  $\text{CuO}_x$  films
- Values of  $C_{\text{PER}}$  to be followed as a function of time to determine end point

# Summary

- Selective removal of  $\text{CuO}_x$  over copper and dielectric in water, DMSO,  $\text{NH}_4\text{F}$  based chemical systems systematically investigated
- Better  $\text{CuO}_x/\text{Cu}$  and  $\text{CuO}_x/\text{TEOS}$  selectivity in  $\text{NH}_4\text{F}$  based formulations than HF based formulations reported last year
- $\text{CuO}_x$  removal rate  $\sim 180 \text{ \AA}/\text{min}$  with  $\text{CuO}_x/\text{Cu}$  selectivity  $\sim 130:1$  and  $\text{CuO}_x/\text{TEOS}$  selectivity  $\sim 10:1$  obtained in 1%  $\text{NH}_4\text{F}$  solutions, 29% DMSO solutions (pH 4).
- Reasonable selectivity over TEOS requires some amount of DMSO
- Electrochemical Impedance spectroscopy and equivalent circuit modeling used to detect  $\text{CuO}_x$  and residue removal end point

# Industrial Interactions

- Patterned test structures were developed at *Intel Corp., Santa Clara* with the assistance of Dr. Liming Zhang, Dr. Zhen Guo and Dr. Michael Ru
- Many discussions with Dr. Liming Zhang, Dr. Zhen Guo and Dr. Michael Ru, *Intel Corp., Santa Clara*, during the fabrication of test structures
- Discussions with Dr. Robert Small, *R.S. Associates, Tucson*

# Future Plans

## Next Year Plans

- Improve selectivity towards oxide based dielectrics (FSG, TEOS) in solutions with very low or no solvent content
  - Use of suitable buffers to control pH in the range of 6 to 7
- Continue Electrochemical Impedance Spectroscopy investigations on patterned test structures; determine if signals at specific frequencies can be used for rapid end point detection
- Characterize rinsing steps using Electrochemical Impedance Spectroscopy

# Future Plans

## Long-Term Plans

- Identify and investigate novel aqueous chemical systems (eg. Phosphate/multifunctional carboxylic acid based solutions) based on the chemical properties of low k materials and post etch residues; improve models developed by Weber at Sematech
- Address the challenge of via/trench penetration with all-aqueous formulations
  - Residues are hydrophobic with low critical surface tension of wetting ( $\gamma_c$ )
  - Requirement of wetting agents in formulation

# Publications, Presentations, and Recognitions/Awards

## **Publications**

- N. Venkataraman, A. Muthukumar, S. Raghavan, "Evaluation of Copper Oxide to Copper Selectivity of Chemical Systems for BEOL Cleaning Through Electrochemical Investigations", **Mater. Res. Soc. Symp. Proc.** Volume 990, Paper # 0990-B08-25, p.197-201 (2007)

## **Awards**

- **AMAT Graduate Fellowship** awarded to Nandini Venkataraman by Applied Materials, Santa Clara, for 2007-2008



# **Post-Planarization Waste Minimization**

## **PI:**

- **Ara Philipossian, Chemical and Environmental Engineering, UA**

## **Graduate Student:**

- **Ting Sun: Ph. D. candidate, Chemical and Environmental Engineering, UA**

## **Other Researcher:**

- **Yun Zhuang, Research Associate, Chemical and Environmental Engineering, UA**

## **Cost Share (other than core ERC funding):**

- **In kind donation (PVA brushes) from ITW Rippey Corporation**

# Objectives & ESH Metrics and Impact

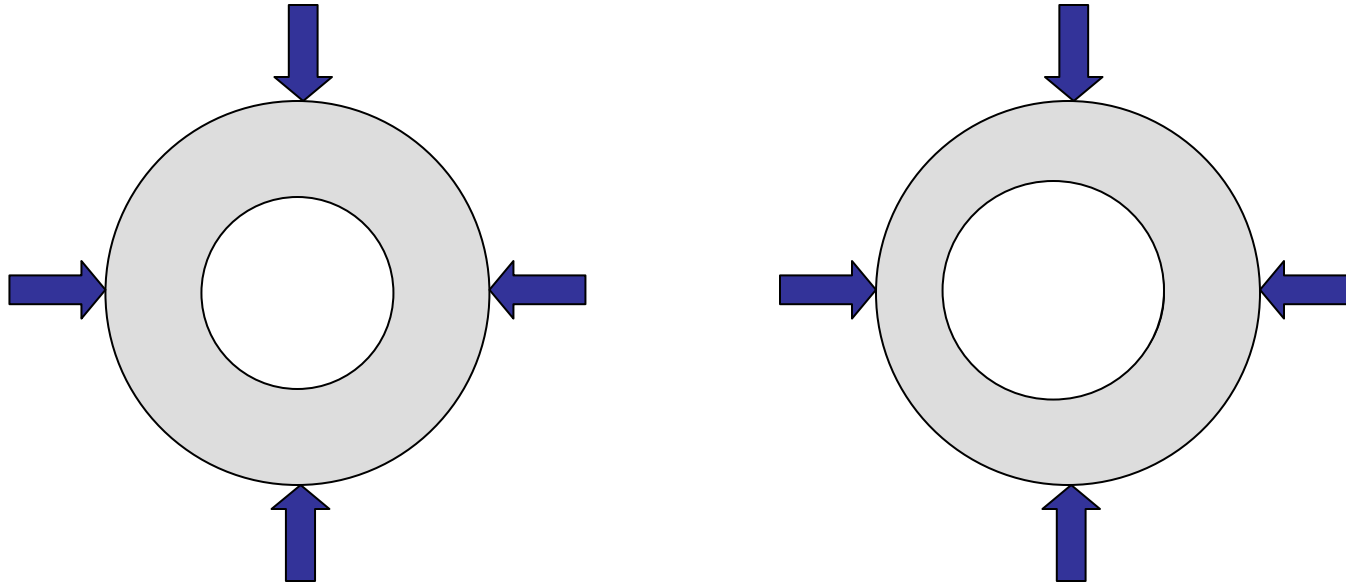
## **Objective:**

- Investigate how eccentric PVA brushes behave differently during post-CMP cleaning process in terms of brush contact pressure, contact area, variance of shear force, and shear force spectrum.

## **ESH Metrics and Impact:**

- Eliminates chemical, water, and energy consumption associated with qualifying PVA brushes that are eccentric for post-CMP cleaning processes.

## Method and Approach



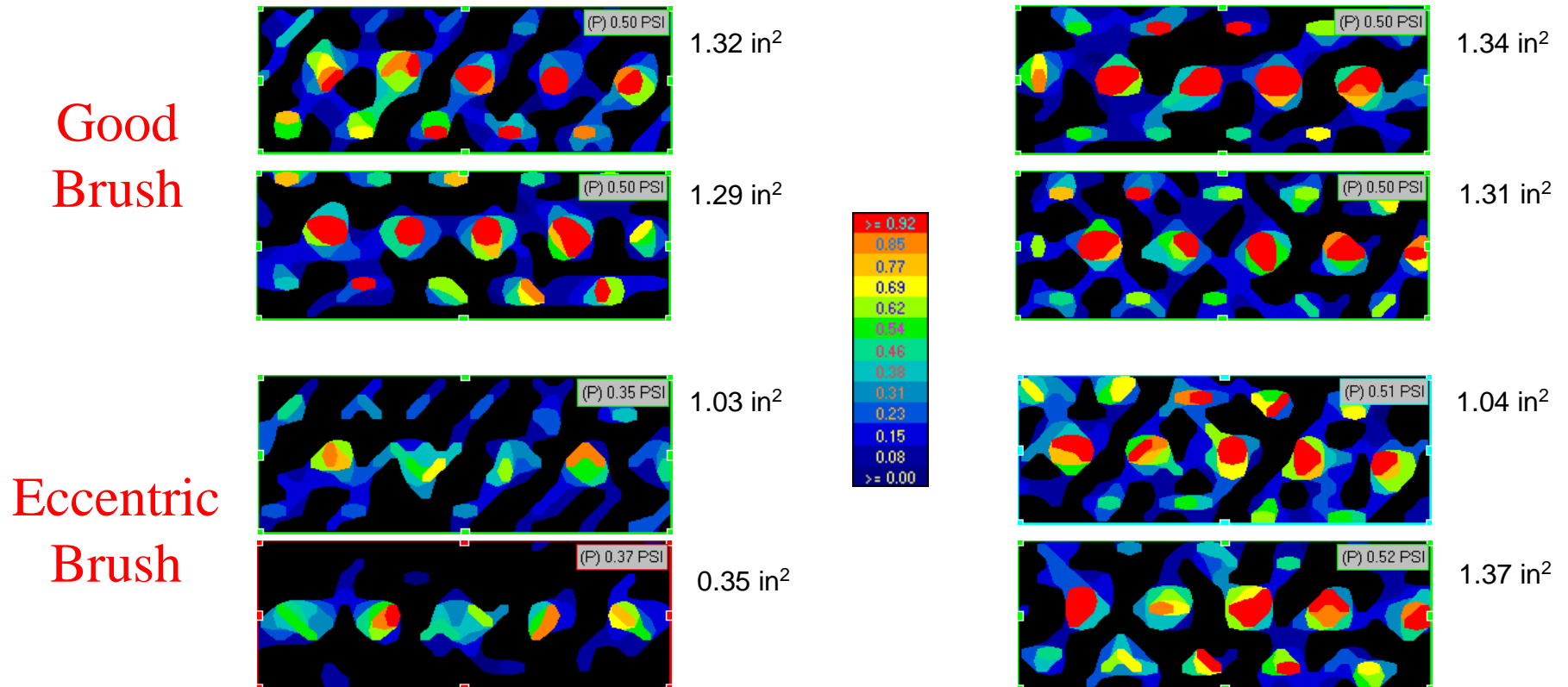
Good (i.e. perfectly concentric) Brush

Eccentric Brush

Good brushes were tested and compared with eccentric brushes when scrubbing under the same compression distance, *i.e.*, all brushes were compressed to the same point to generate a pressure of 0.5 PSI for the good brushes.

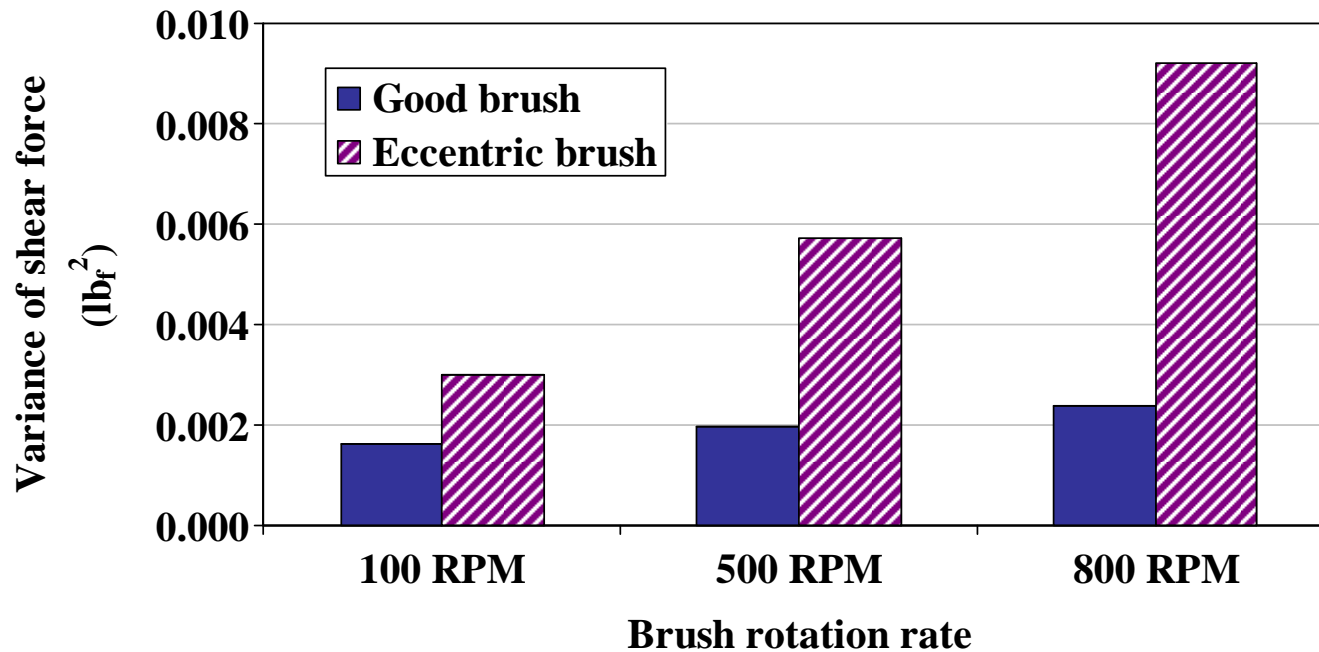
Multiple contact pressure and area measurements were performed by rotating brushes under four different orientations to investigate the effect of eccentricity.

# Pressure Contour Map and Contact Area



**For the good brush, the contact pressure and contact area were consistent when rotating the brush. In comparison, for the eccentric brush, both the contact pressure and contact area varied significantly when rotating the brush.**

## Variance of Shear Force

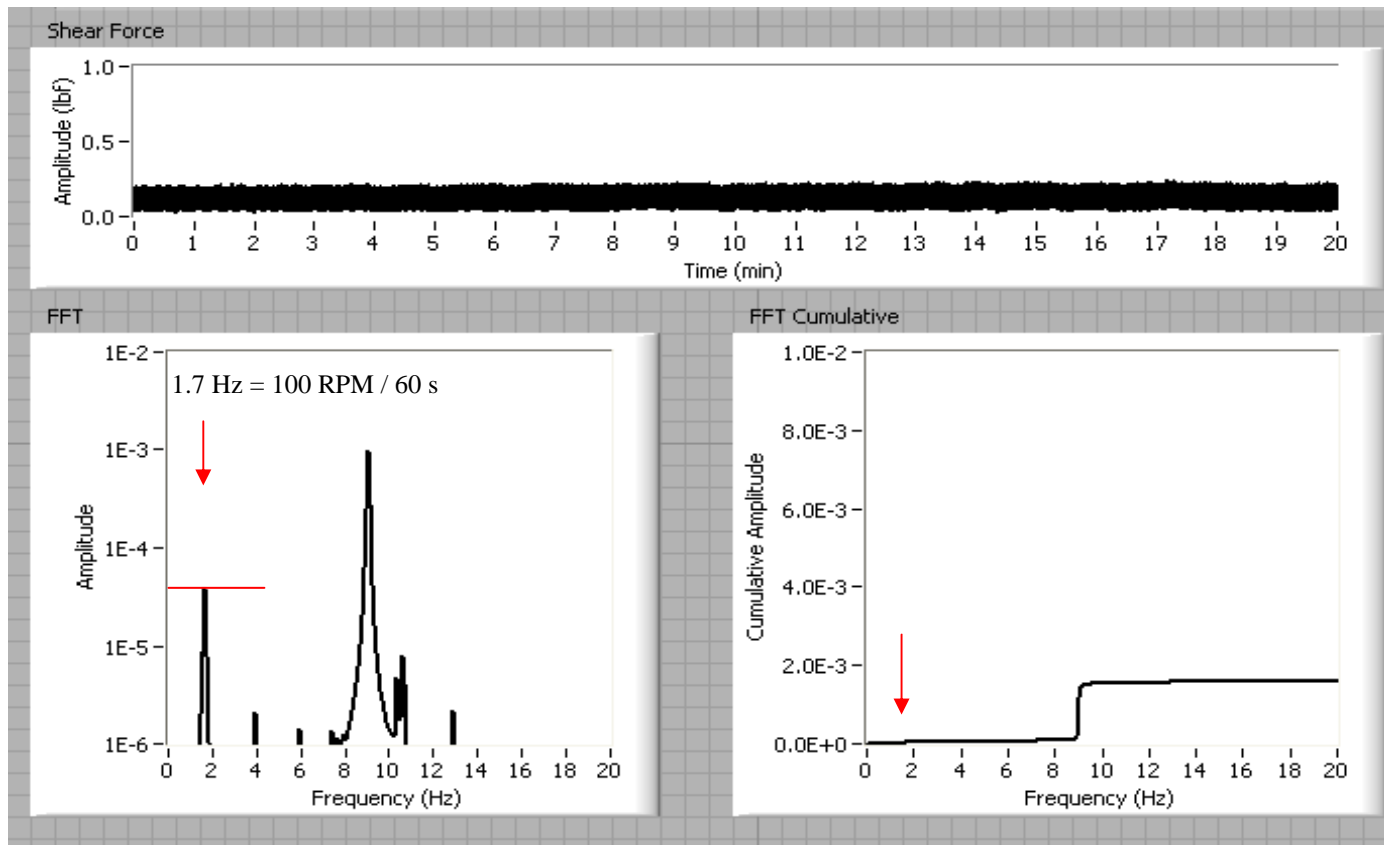


**For both good and eccentric brushes, the variance of shear force increased with the brush rotation rate.**

**Under the same brush rotation rate, the eccentric brush had a significantly higher variance of shear force than the good brush.**

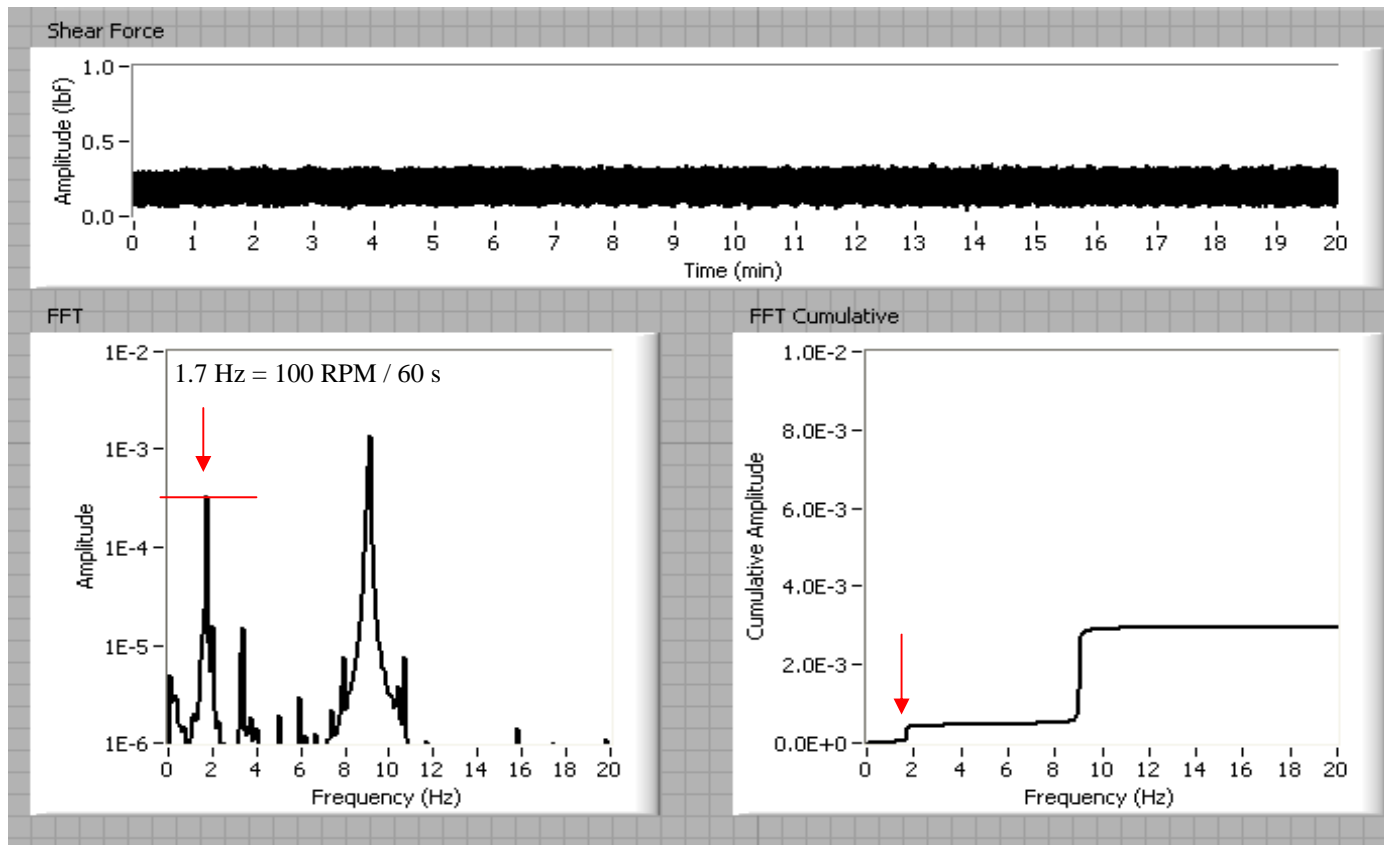
# Shear Force Spectral Analysis

## Good Brush, 100 RPM



# Shear Force Spectral Analysis

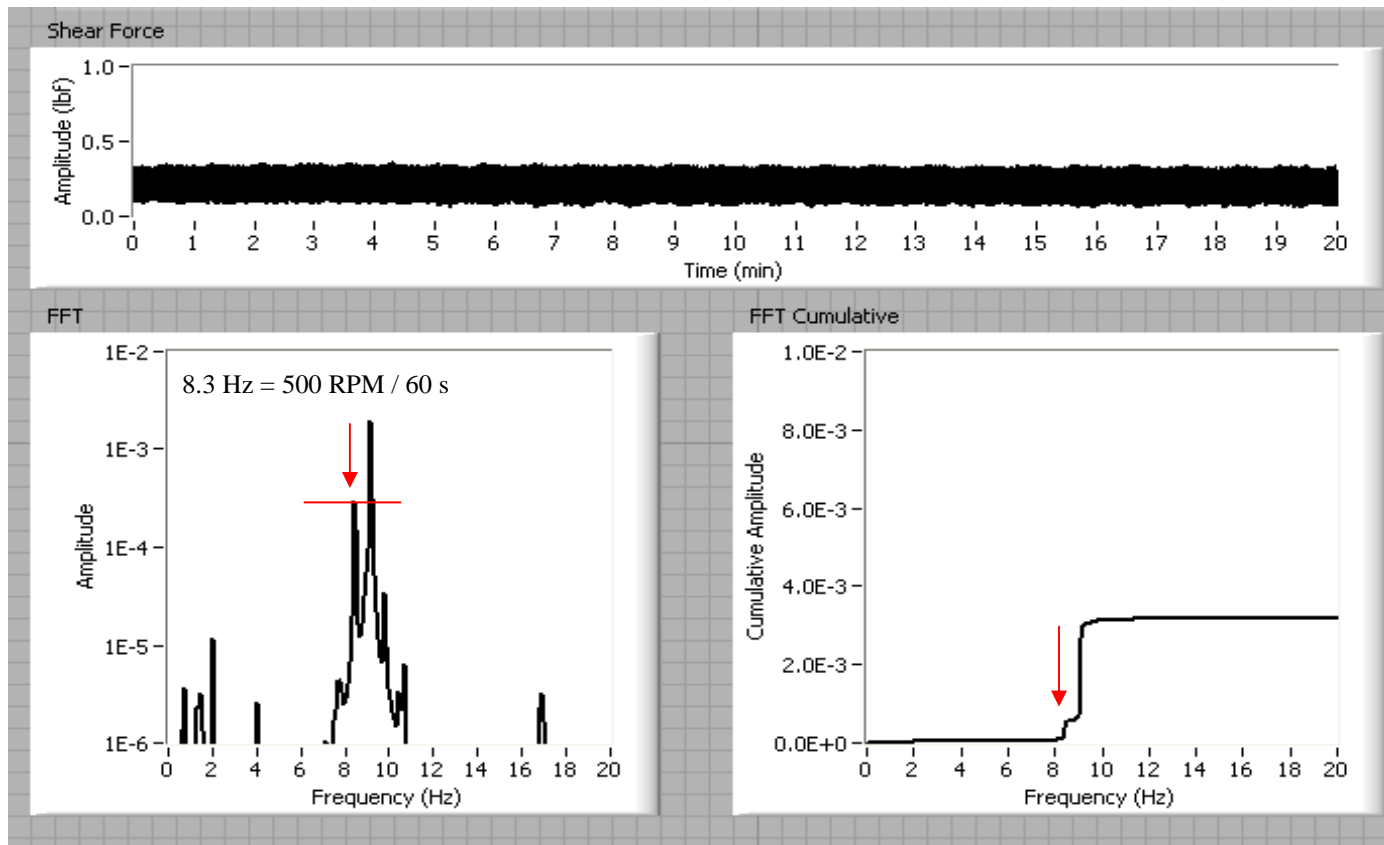
## Eccentric Brush, 100 RPM



At 100 RPM, the eccentric brush showed higher spectral amplitudes at the frequency of 1.7 Hz.

# Shear Force Spectral Analysis

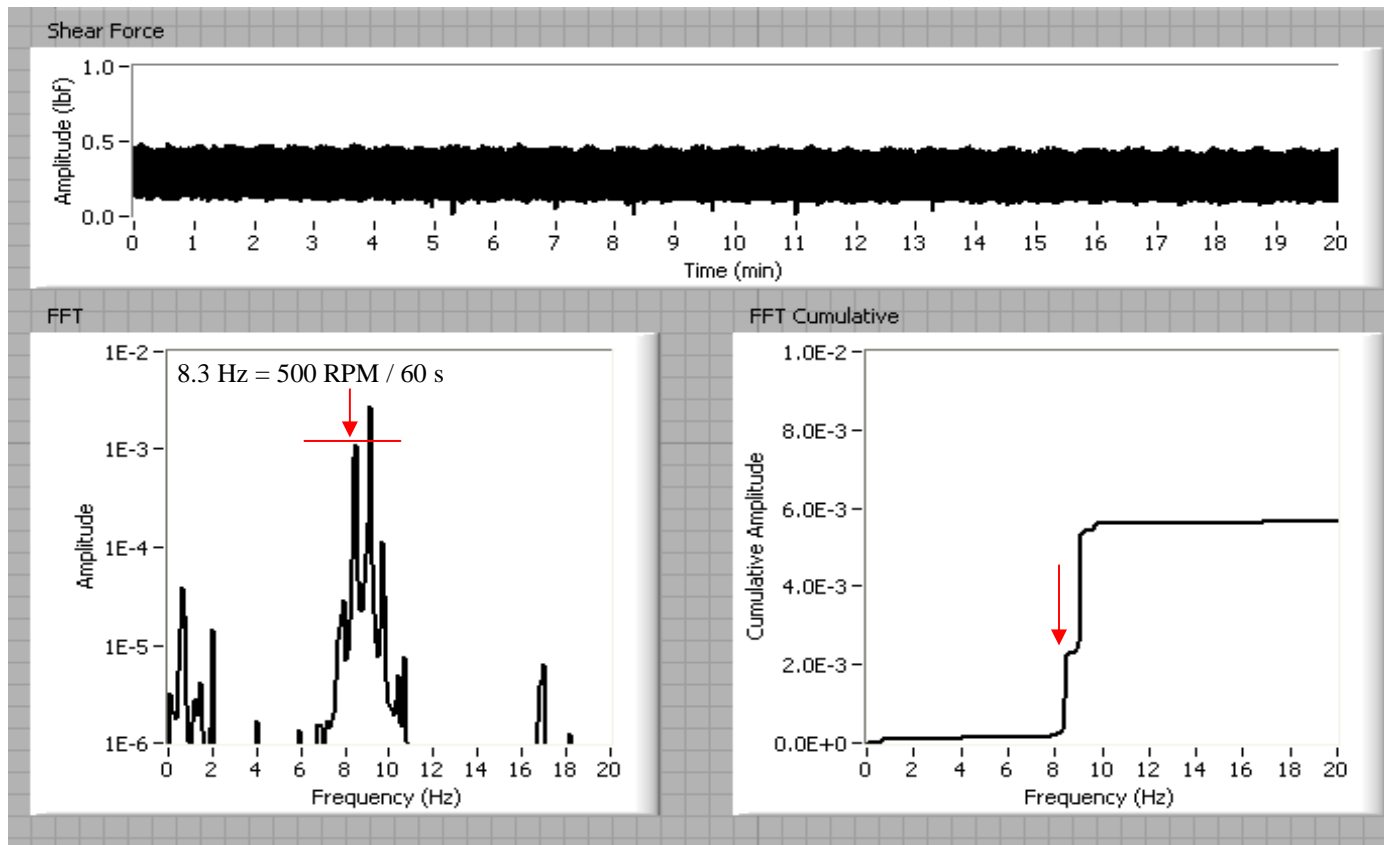
## Good Brush, 500 RPM





# Shear Force Spectral Analysis

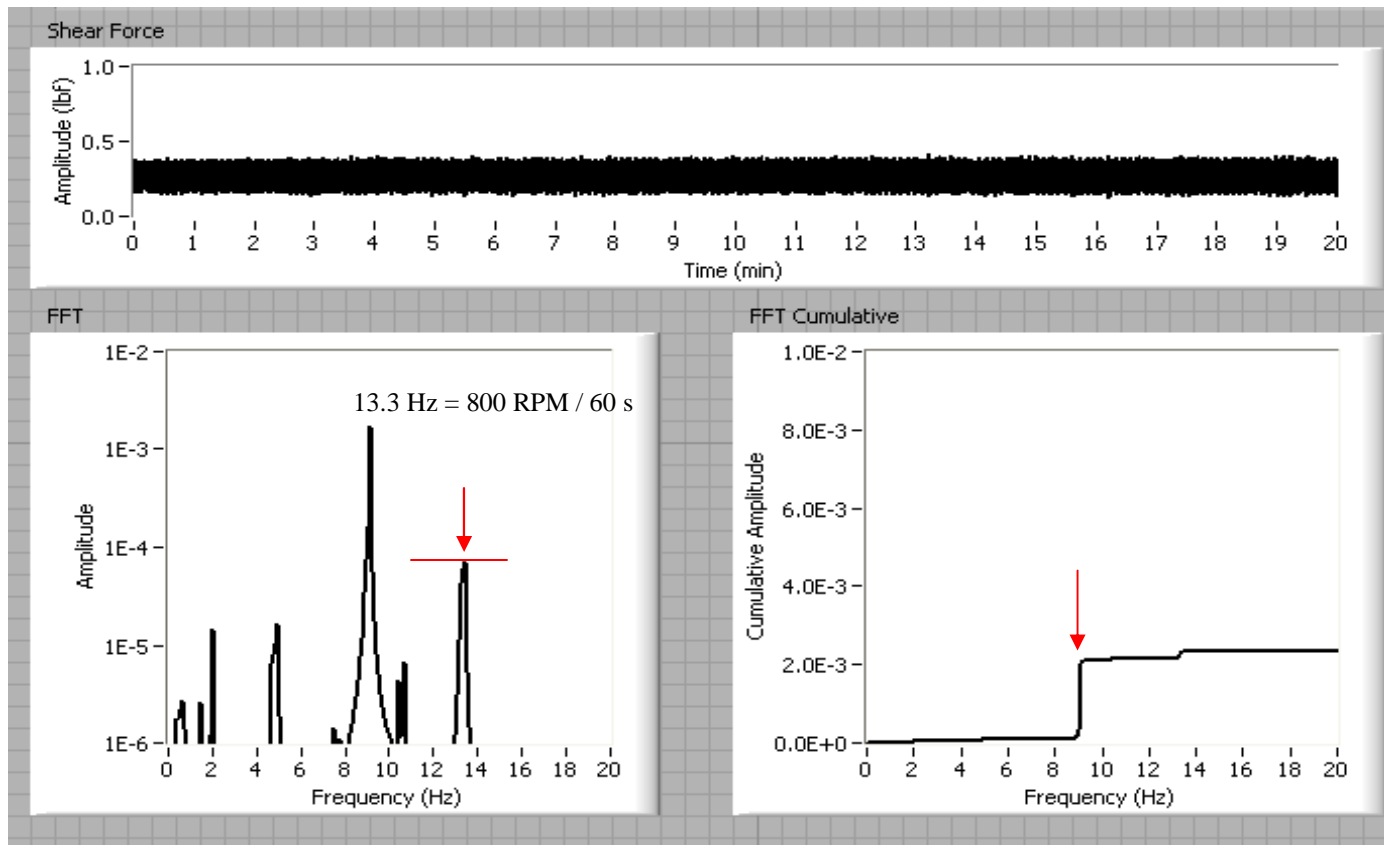
## **Eccentric Brush, 500 RPM**



**At 500 RPM, the eccentric brush showed higher spectral amplitudes at the frequency of 8.3 Hz.**

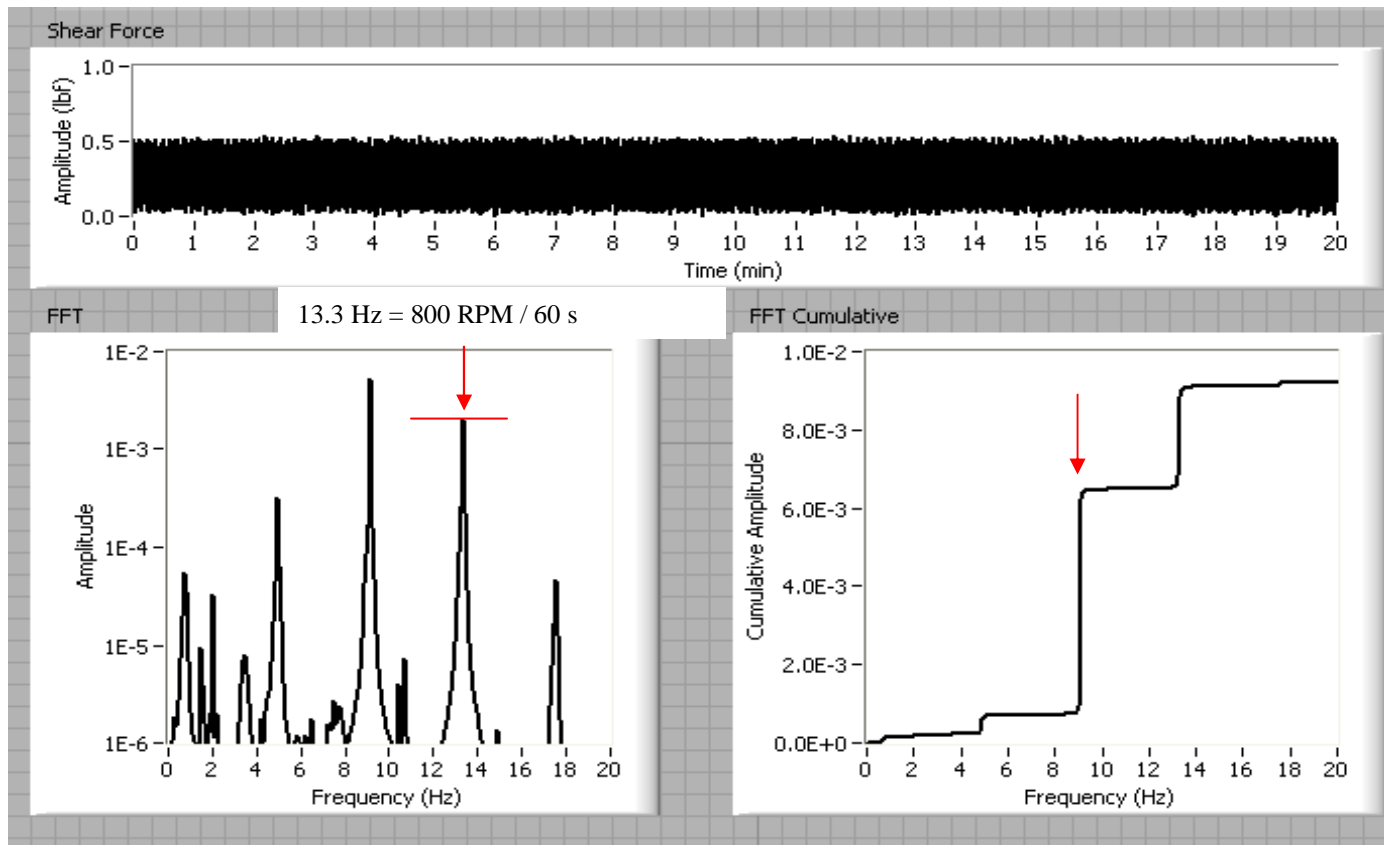
# Shear Force Spectral Analysis

## Good Brush, 800 RPM



# Shear Force Spectral Analysis

## Eccentric Brush, 800 RPM



**At 800 RPM, the eccentric brush showed higher spectral amplitudes at the frequency of 13.3 Hz.**

# Industrial Interactions and Future Plans

## **Industrial mentor / contact:**

- **Weijin Li (ITW Rippey Corporation)**

## **Next year plan:**

- **Investigate the effect of brush physical properties on the tribological behavior during post-CMP cleaning processes.**
- **Design, construct and qualify an incremental loading tool to investigate brush nodule deformation as a function of applied load and extended use.**

## **Long term plan:**

- **Extend PVA brush life by achieving a better understanding of the brush wear mechanism.**

# **Simulation of Pad Stain Formation during Copper CMP**

## **PI:**

- **Ara Philipossian, Chemical and Environmental Engineering, UA**

## **Graduate Student:**

- **Hyosang Lee: Ph. D. candidate, Chemical and Environmental Engineering, UA**

## **Other Researcher:**

- **Yun Zhuang, Research Associate, Chemical and Environmental Engineering, UA**

## **Cost Share (other than core ERC funding):**

- **In-kind support from Araca, Inc.**

# Objectives & ESH Metrics and Impact

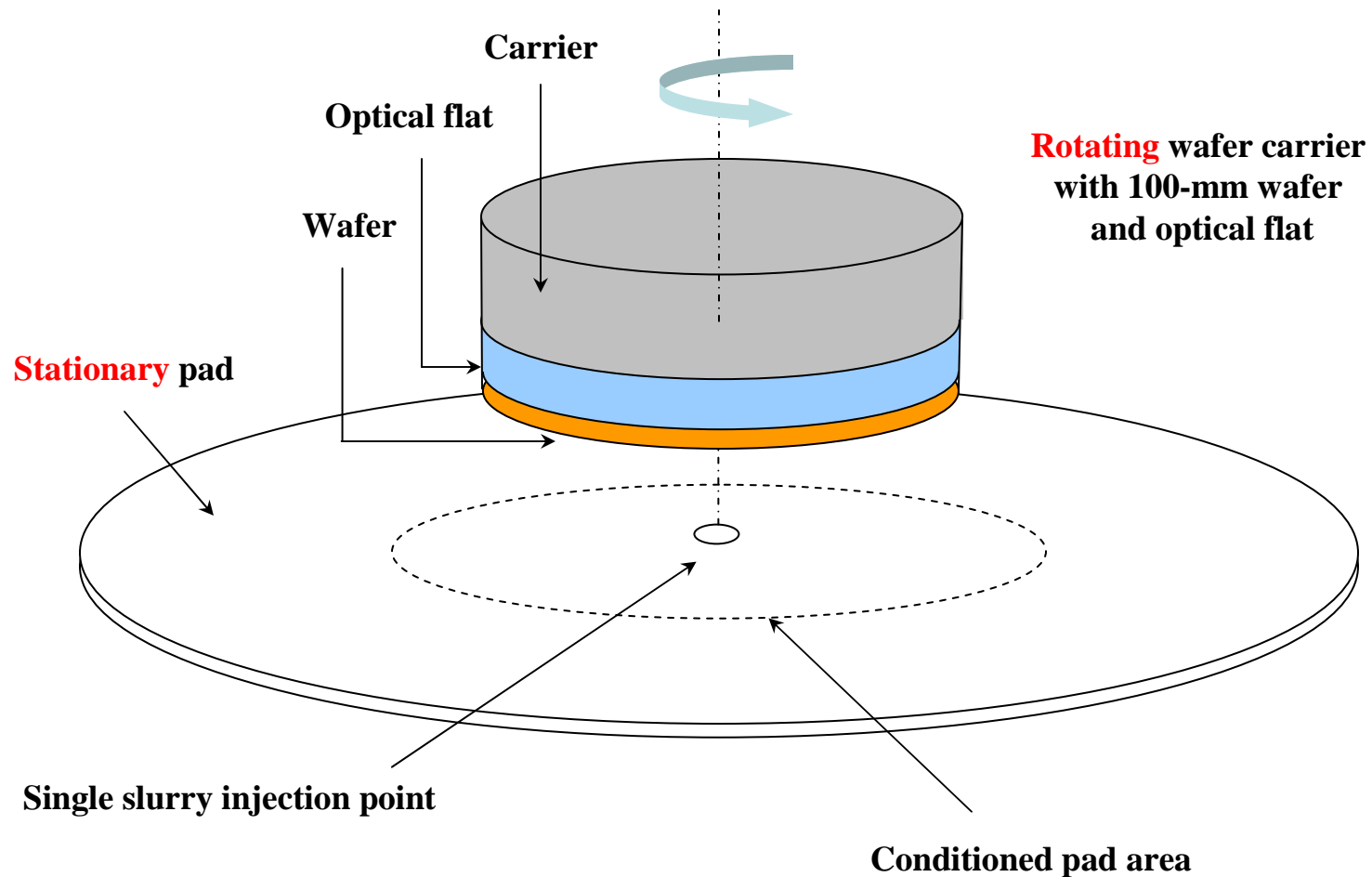
## **Objective:**

- Develop 3-D fluid transport, thermal and kinetic models to simulate pad stains formed during copper CMP process.

## **ESH Metrics and Impact:**

- Reduce pad and pad cleaning solution consumption by 25% through a better understanding of stain formation mechanism during copper CMP process.

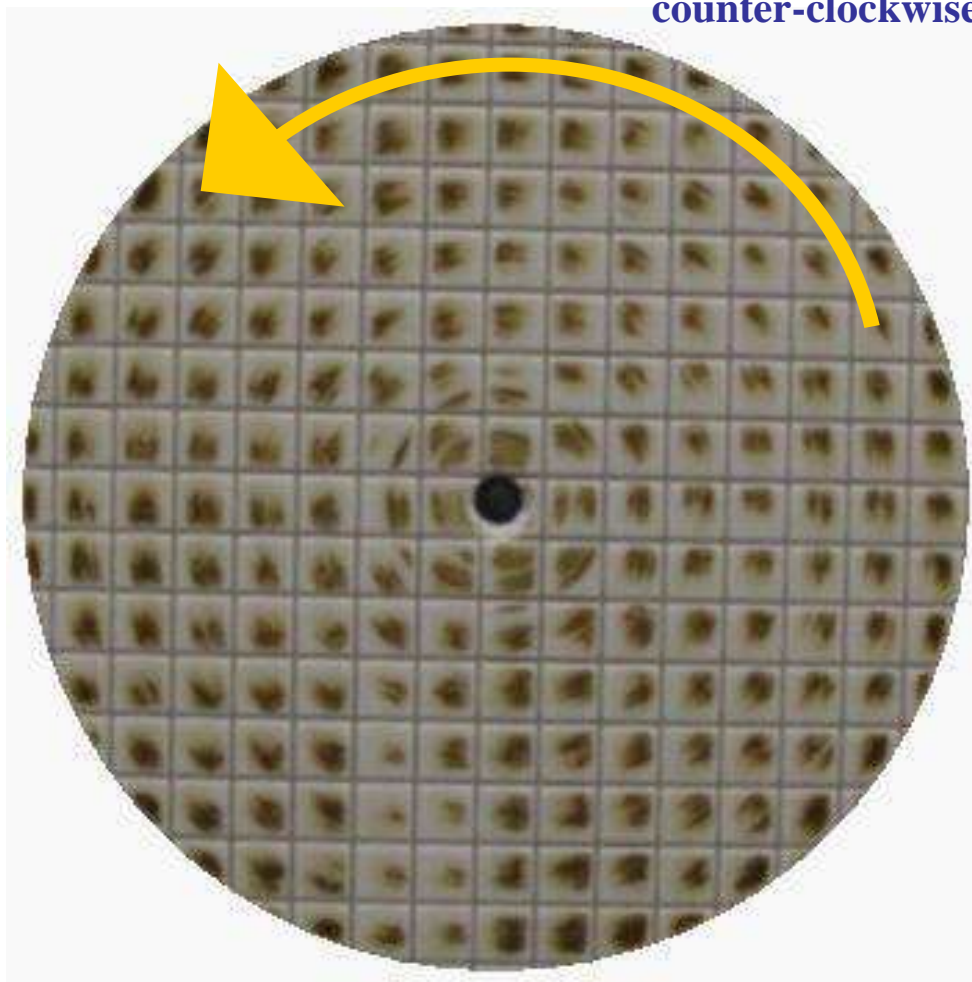
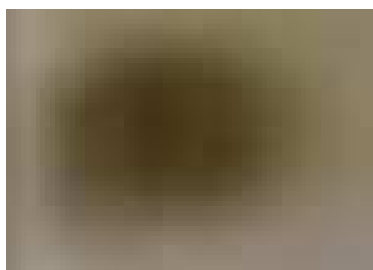
# Axisymmetric Polishing System



## Stain Advection

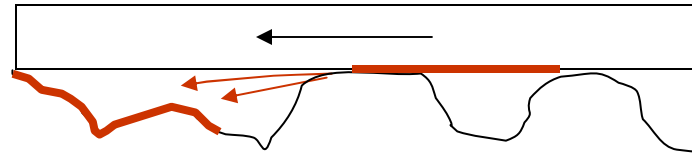
Pad was rotating counter-clockwise.

The generated pad stain on each land area was darker following the direction of wafer rotation, suggesting the stain was affected by slurry advection.





# Simulation of By-Product Concentration on Pad Surface



Governing equation:

$$\frac{\partial c_s}{\partial t} + \underbrace{\bar{V}}_{\substack{\uparrow \\ \text{Advection by the fluid with a velocity}}} \cdot \bar{\nabla} c_s = \bar{\nabla} \cdot (D \bar{\nabla} c_s)$$

Advection by the fluid with a velocity

$C_s$ : Concentration of by-product

B.C. at wafer surface:

$$D \bar{\nabla} C_s \cdot \bar{n} = \frac{k_2 k_1}{k_1 + k_2}$$

$$k_1 = A_1 \cdot \exp\left(\frac{-E_1}{kT}\right)$$

T: extracted from copper surface

$$k_2 = c_p \times \mu_k \times p_s \times V$$

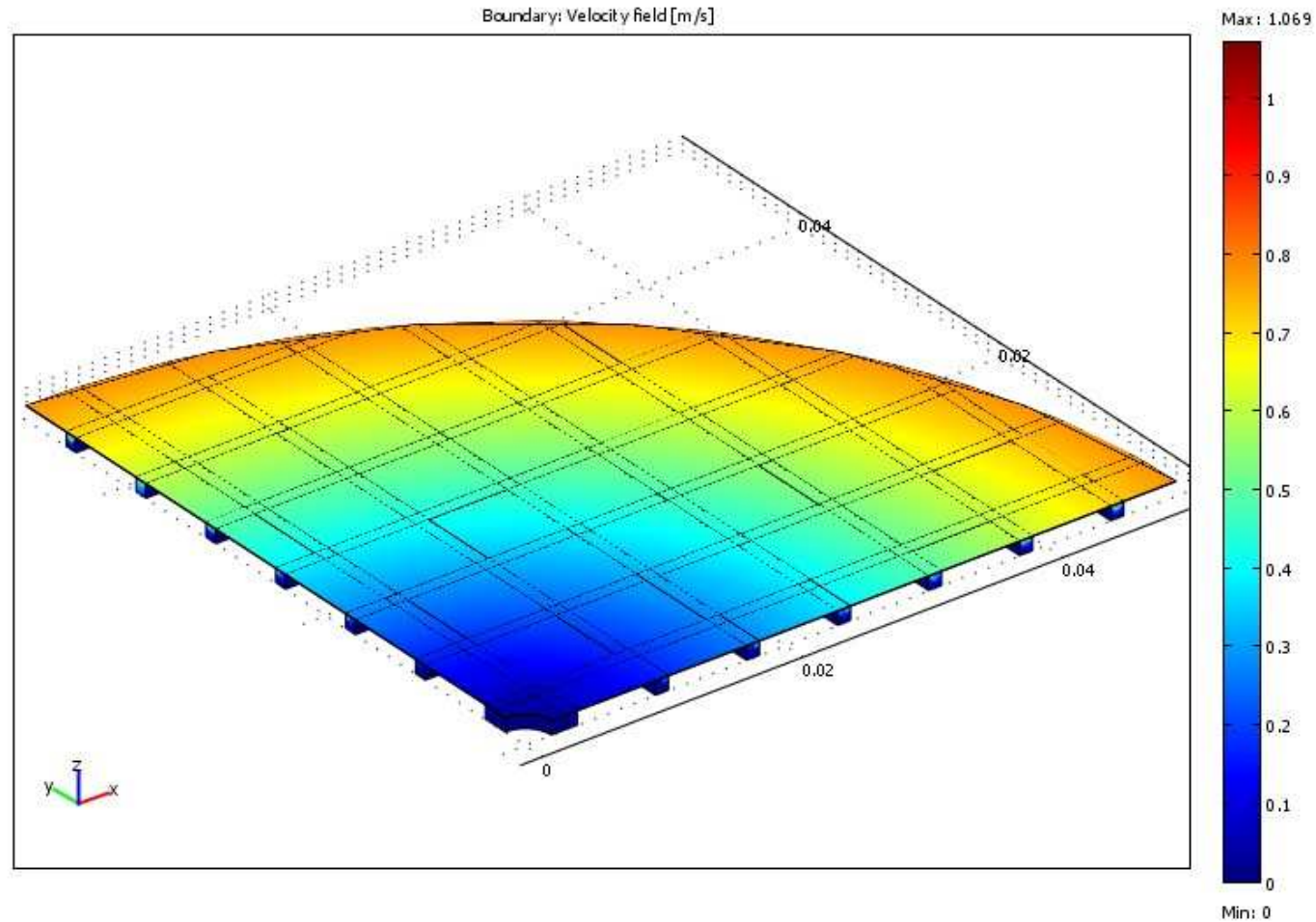
B.C. at pad surface:

$$-D \bar{\nabla} C_s \cdot \bar{n} = k_4 C_s$$

$$k_4 = A_4 \cdot \exp\left(\frac{-E_4}{kT}\right)$$

T: extracted from pad surface

# Simulated Slurry Velocity on Wafer Surface



**Slurry velocity increased gradually on wafer surface in the radial direction due to wafer rotation, thus affecting slurry velocity in the grooves.**



# Thermal Model

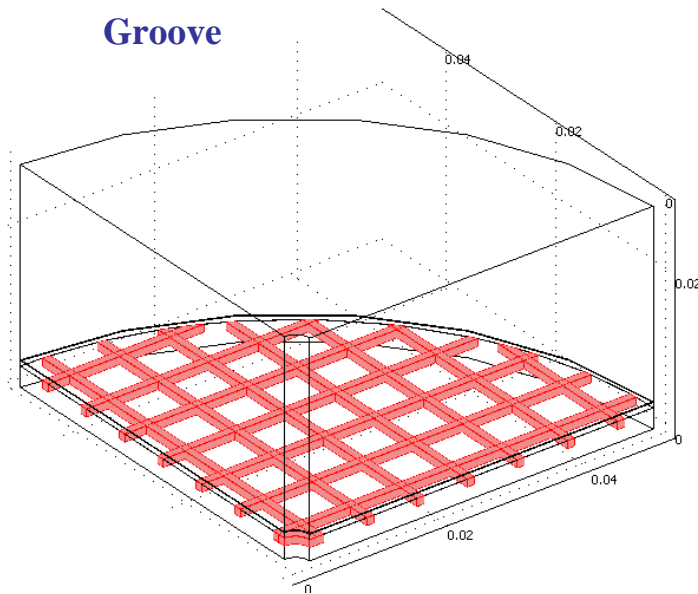
Heat equation

$$\rho C_p \left( \frac{\partial T}{\partial t} + \vec{V} \cdot \vec{\nabla} T \right) = \vec{\nabla} \cdot (\kappa \vec{\nabla} T) + Q$$

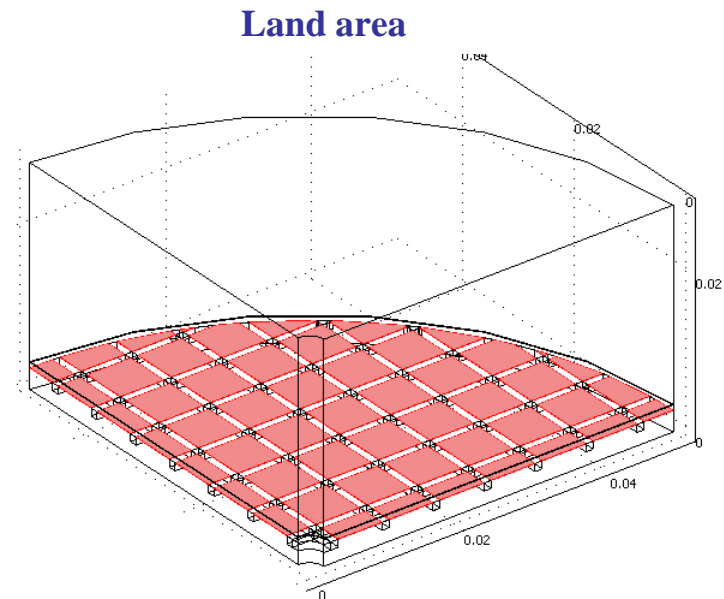
- $\vec{V}$  :
- From Navier-Stokes in slurry layer
  - Rigid body in wafer and above
  - 0 in pad

$Q$  :  $\frac{\mu_k p_s V_s}{h}$  in slurry layer

$\mu_k$  : COF



$$\rho C_p \left( \frac{\partial T}{\partial t} + \vec{V} \cdot \vec{\nabla} T \right) = \vec{\nabla} \cdot (\kappa \vec{\nabla} T)$$

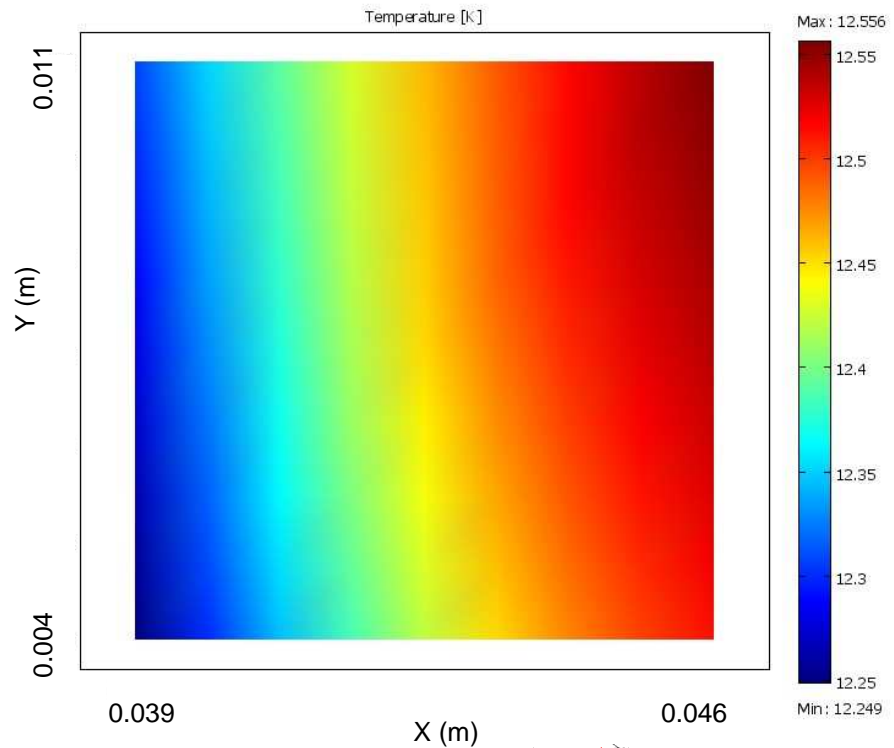
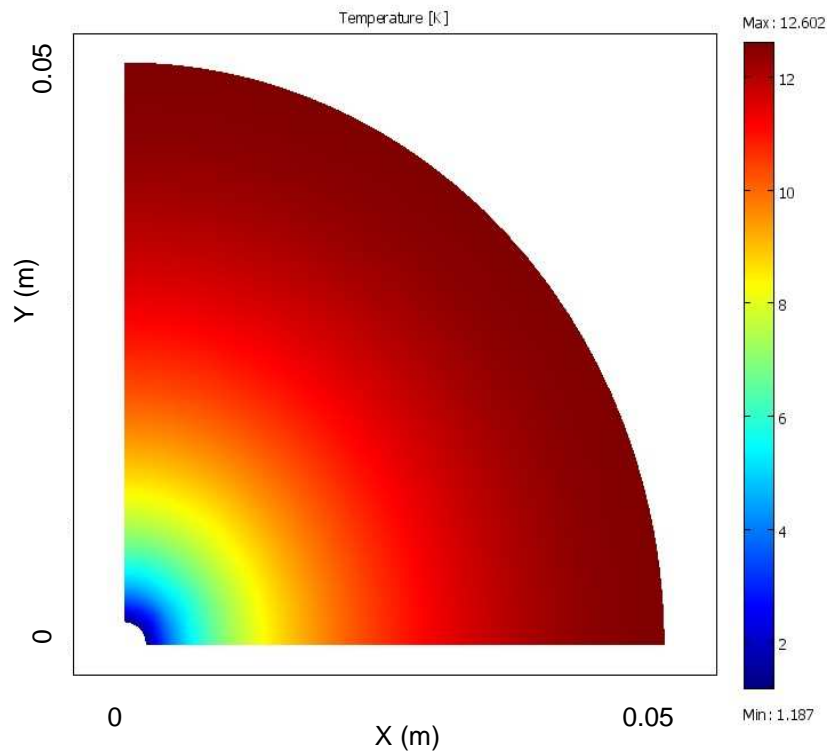


$$\rho C_p \left( \frac{\partial T}{\partial t} + \vec{V} \cdot \vec{\nabla} T \right) = \vec{\nabla} \cdot (\kappa \vec{\nabla} T) + \frac{\mu_k p_s V_s}{h}$$

# Simulated Temperature Profile

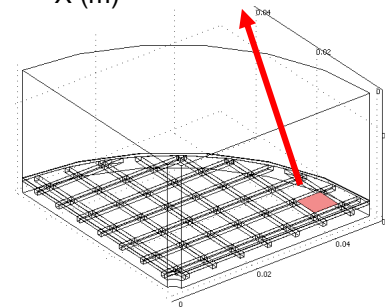
Copper surface

Pad land area



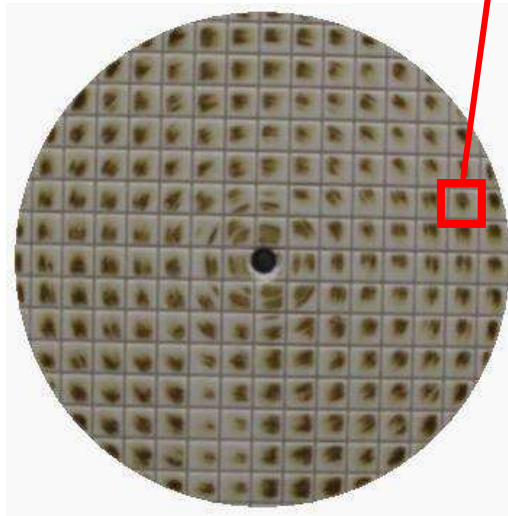
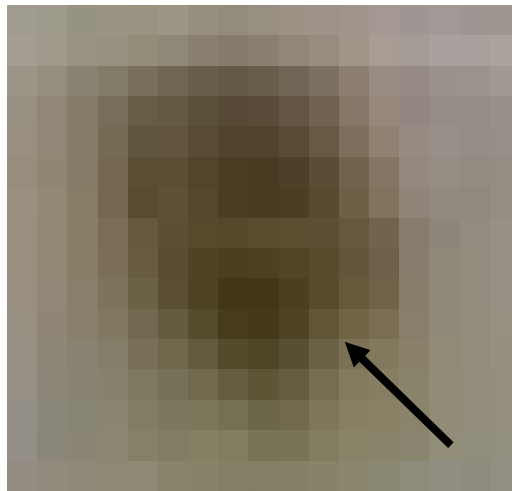
**Simulated wafer and pad temperatures increased in the radial direction.**

**There was a 12 °C temperature rise at the wafer edge.**

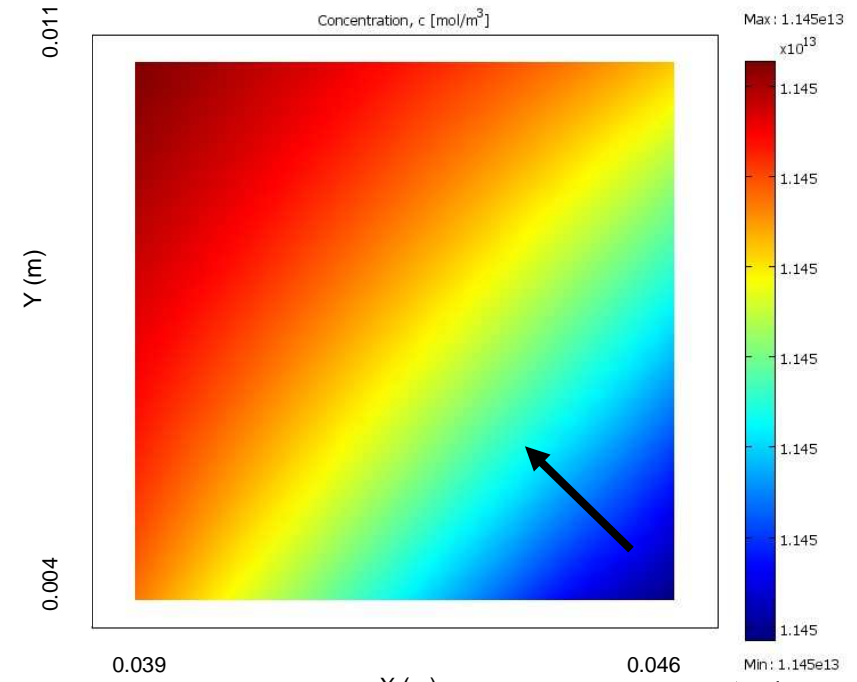


# Simulated Stain Formation

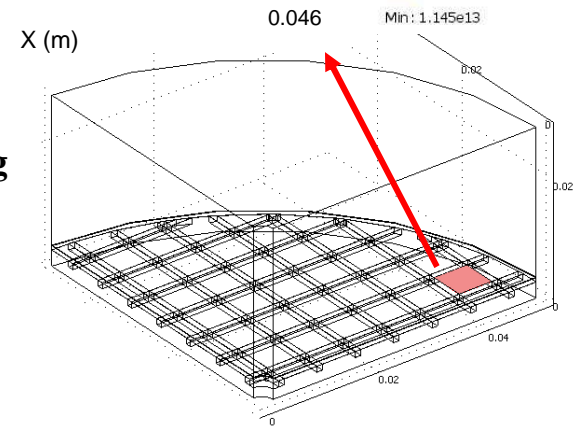
Pad stain picture



Simulated pad stain



The simulated pad stain was darker following the direction of wafer rotation (black arrows indicated the direction of wafer rotation).



# Industrial Interactions

## **Industrial mentors / contacts:**

- **Fergal O'Moore (Novellus Systems, Inc.)**
- **Sooyun Joh (Novellus Systems, Inc.)**
- **Brian Brown (Novellus Systems, Inc.)**
- **Leonard Borucki (Araca, Inc.)**



## **Publications and Presentations**

### **Publication:**

- **Experimental Investigation and Numerical Simulation of Pad Stain Formation during Copper CMP. H. Lee, Y. Zhuang, L. Borucki, F. O'Moore, S. Joh and A. Philipossian. Materials Research Society Symposium Proceedings, Vol. 991, C06-02 (2007).**

### **Presentation:**

- **Experimental Investigation and Numerical Simulation of Pad Stain Formation during Copper CMP. H. Lee, L. Borucki, Y. Zhuang, F. O'Moore, S. Schultz, S. Joh and A. Philipossian. 2007 Materials Research Society Spring Meeting, San Francisco, California, April 9-13 (2007).**



# **Effect of Concentric Slanted Groove Patterns on Slurry Flow during Copper CMP**

## **PI:**

- **Ara Philipossian, Chemical and Environmental Engineering, UA**

## **Graduate Students:**

- **Daniel Rosales-Yeomans: Chemical and Environmental Engineering, UA, graduated with Ph. D. degree in December 2007**
- **Hyosang Lee: Ph. D. candidate, Chemical and Environmental Engineering, UA**

## **Cost Share (other than core ERC funding):**

- **In-kind support (pad grooving service) from Toho Engineering**

# Objectives & ESH Metrics and Impact

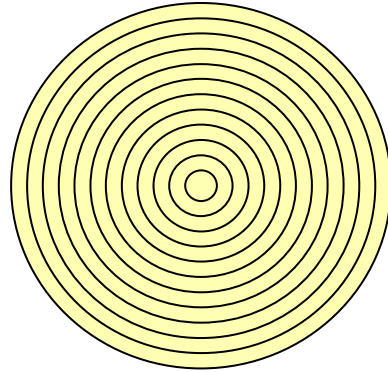
## **Objective:**

- Determine the effects of concentric slanted groove design, wafer pressure, sliding velocity, and slurry flow rate on slurry film thickness between pad and wafer interface.

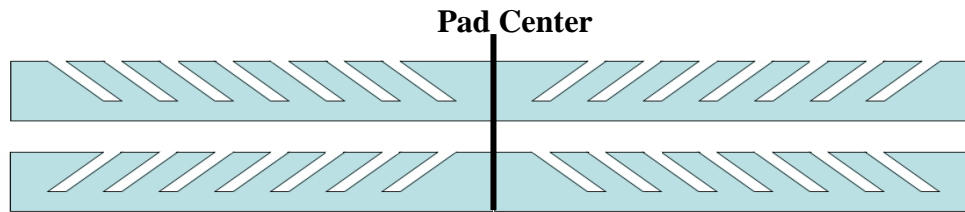
## **ESH Metrics and Impact:**

- Reduce slurry and pad consumption by 33% through novel pad groove design.

# Concentric Slanted Groove Design

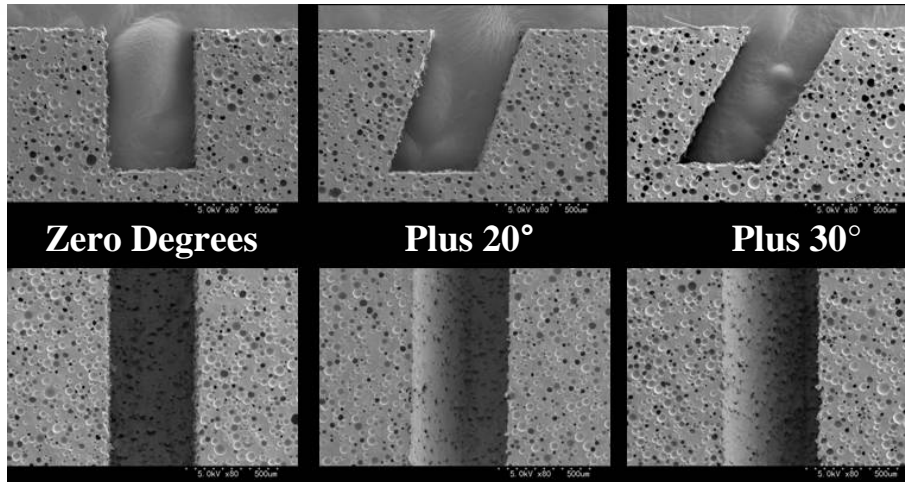


Wafer and pad rotate **counter – clockwise.**



**Positive Direction**

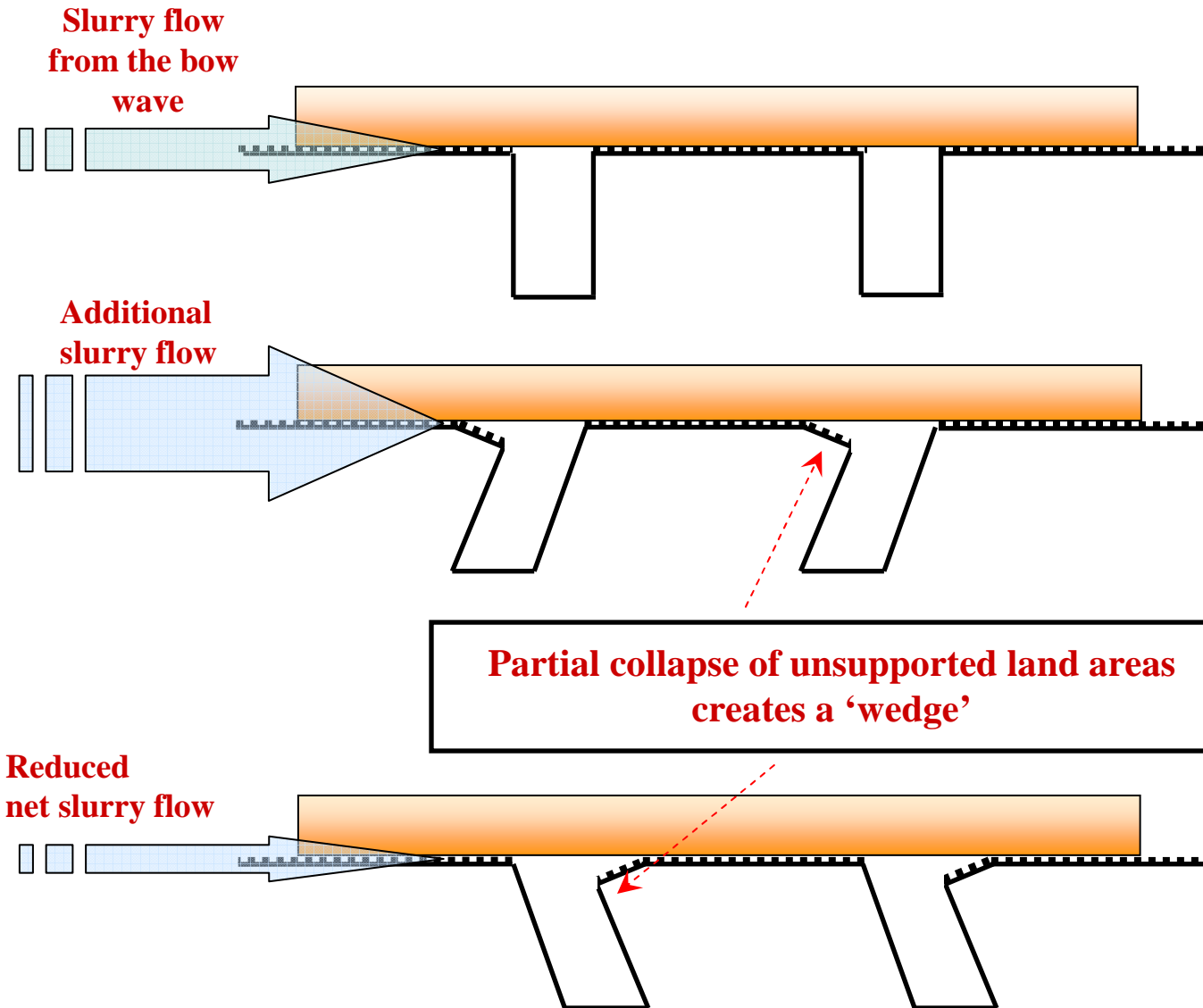
**Negative Direction**



**Side View**

**Top View**

# The Effect of Slanted Grooves on Slurry Flow

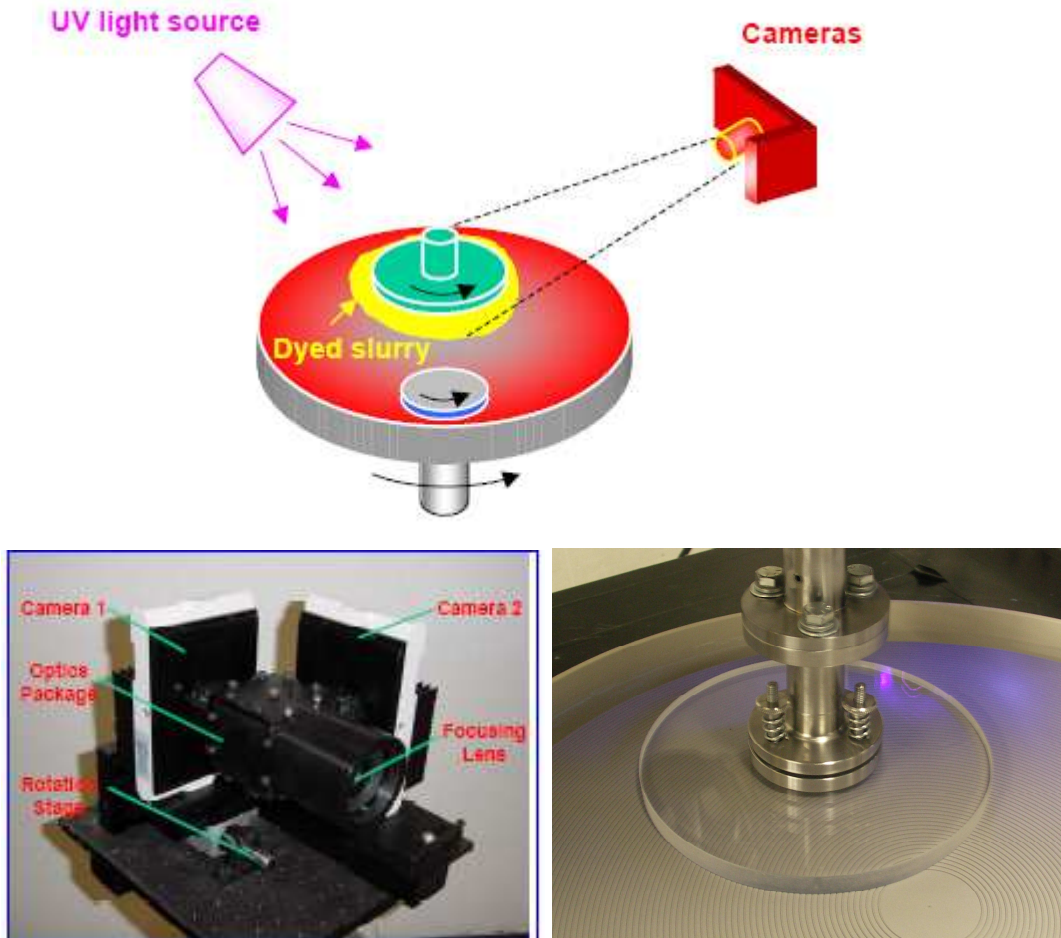


Wafer load is supported by **pad land areas**.

Wafer load is partially supported by **pad land areas** and by the **slurry**.

Slurry must flow continuously **INTO** the wedge of the 'land area' to balance hydrodynamic forces.

# 200-mm Polisher Equipped with DEUVEF



**Two CCD cameras are aligned orthogonally and rotationally.**

**The optics configuration allows each camera to record the exact same spatial image, but in a different color (i.e. different ranges of wave lengths).**

*SRC/SEMATECH Engineering Research Center for Environmentally Benign Semiconductor Manufacturing*

# Experimental Conditions

- **Constants:**

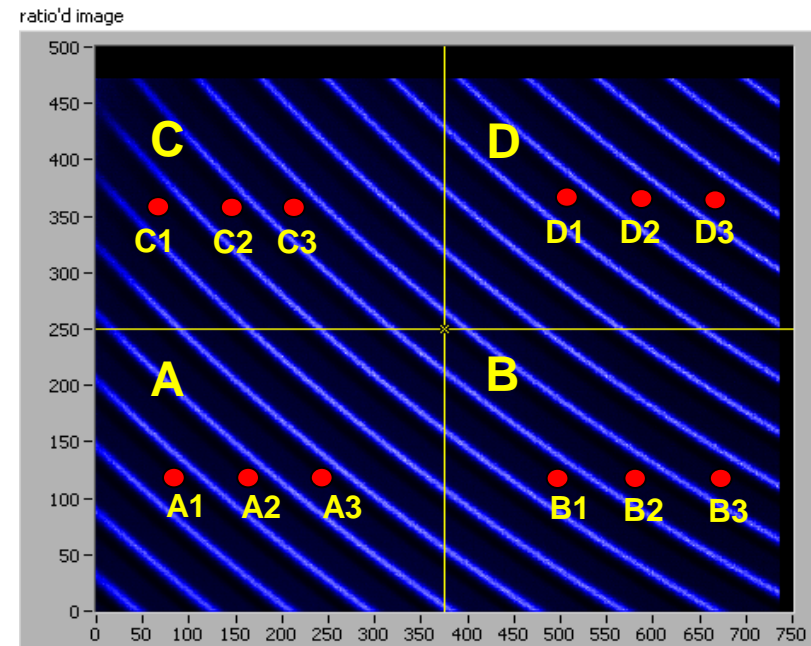
- **Pad break-in**
  - 100-grit TBW diamond disc conditioner
  - 30 min with UPW at 30 rpm disc speed and 20 times per min sweep frequency
- **Slurry**
  - Fujimi PL-7102 slurry with coumarin and calcein dyes
- **Wafer**
  - 200-mm quartz wafer

- **Variables:**

- **Sliding velocity (m/s)**
  - 0.30
  - 1.20
- **Wafer pressure**
  - 1.0 PSI (6,894 Pa)
  - 2.0 PSI (13,780 Pa)
  - 3.0 PSI (20,684 Pa)
- **Slurry flow rate**
  - 220 cc/min
  - 165 cc/min
  - 110 cc/min
- **Pad groove design**
  - Concentric Slanted (Minus 30°, Minus 20°, Plus 20° and Plus 30°)
  - Concentric (0°)



# Slurry Film Thickness Measurement Area



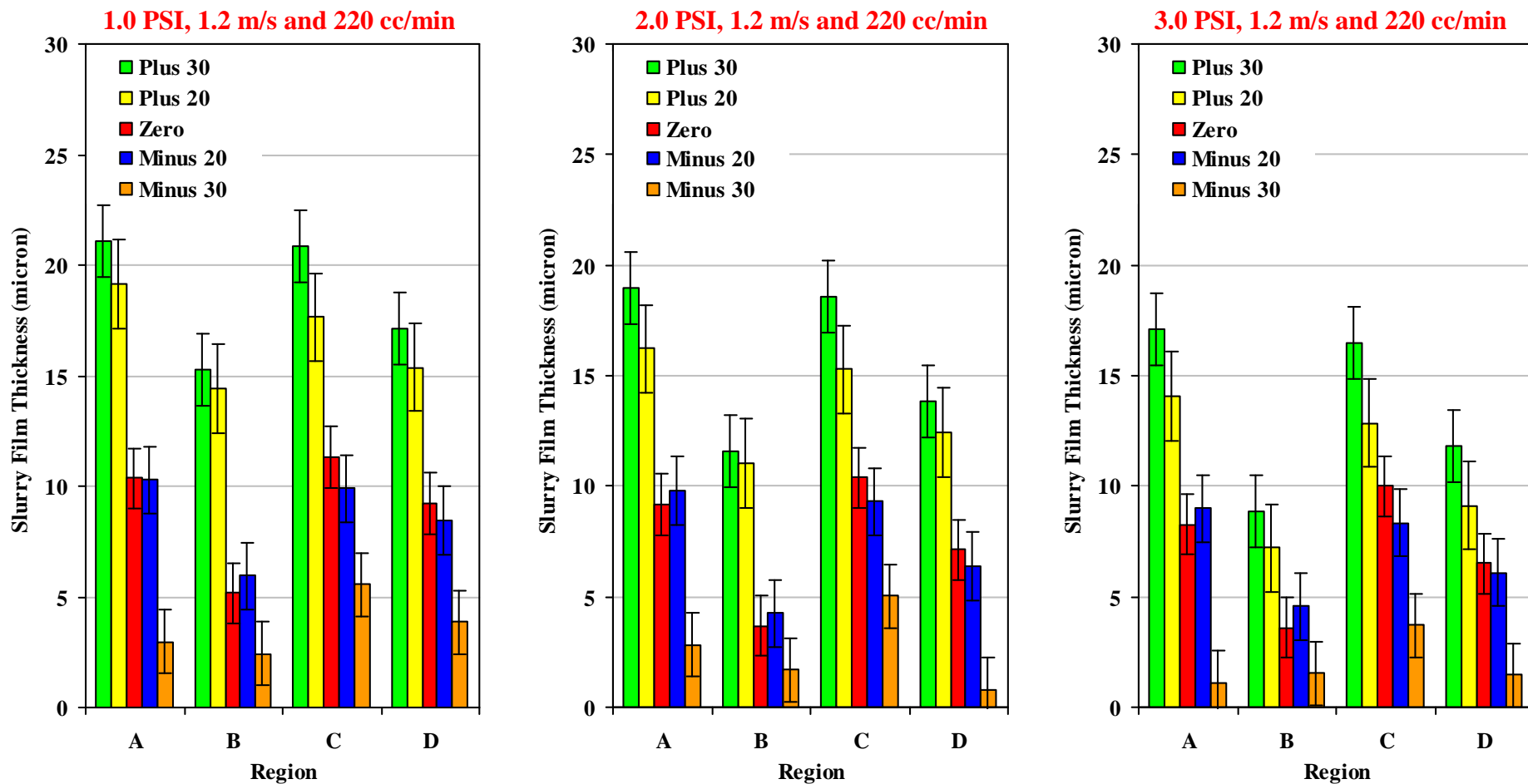
The area analyzed under the wafer is divided into four smaller regions: A, B, C and D.

**Regions A & C are close to the wafer edge; Regions B & D are close to the wafer center.**

In each region, three sub land areas are analyzed.

Values reported for each region (A, B, C and D) are an average of the three sub land areas.

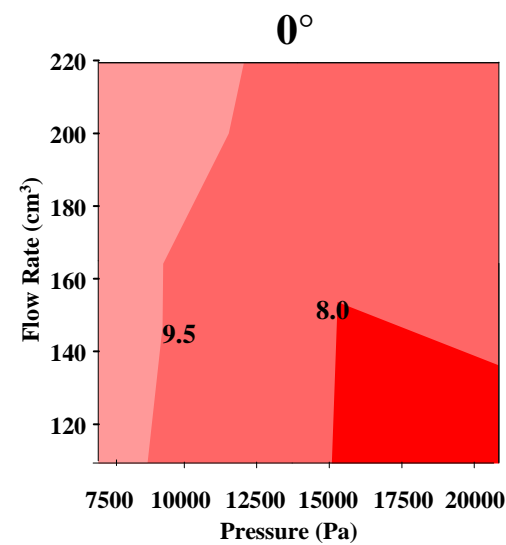
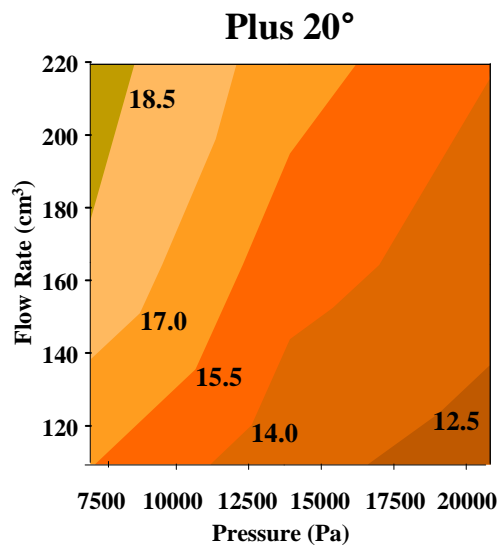
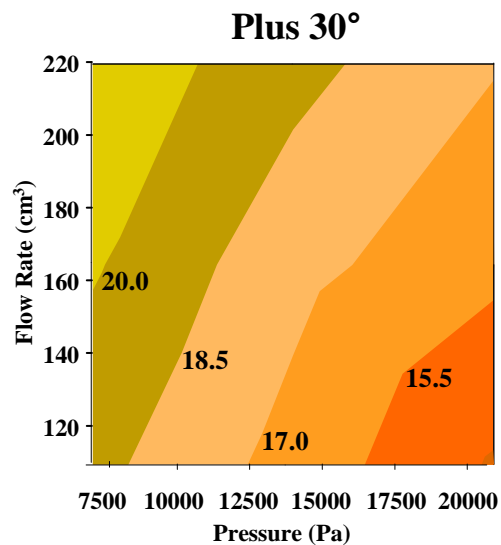
# Effect of Groove Slanting on Slurry Film Thickness



Slanting the grooves towards the edge of the pad (i.e. positive direction) facilitates slurry flow into the pad-wafer interface area.  
 Slanting the grooves towards the center of the pad (i.e. negative direction) reduces slurry flow into the pad-wafer interface area.



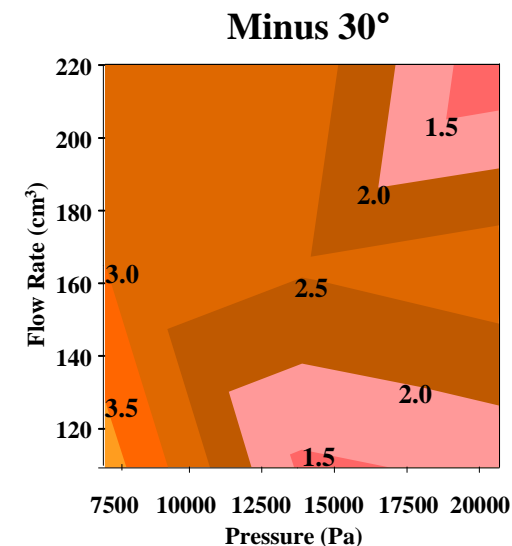
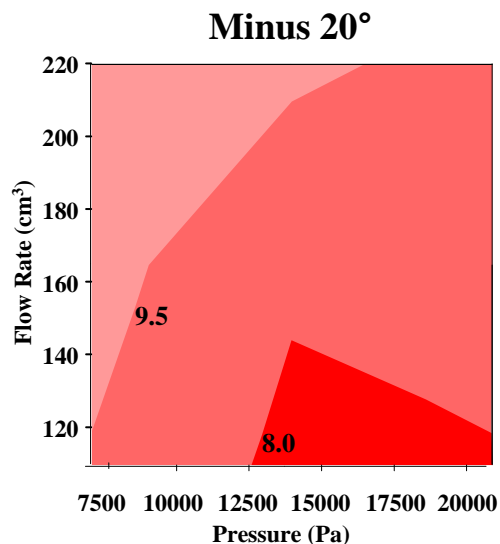
# Slurry Film Thickness Contour Plot



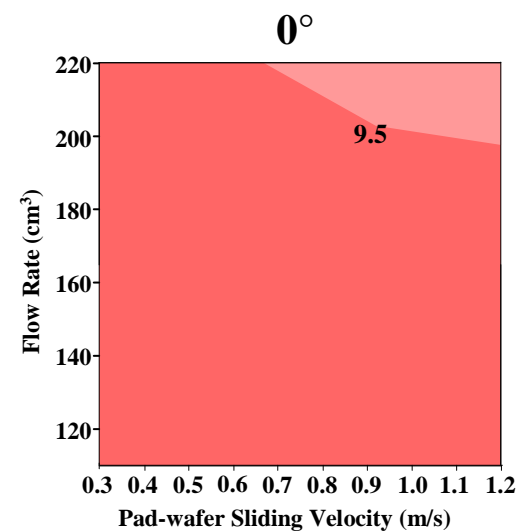
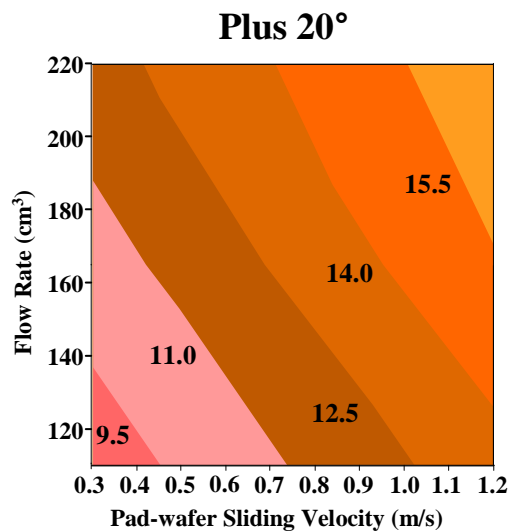
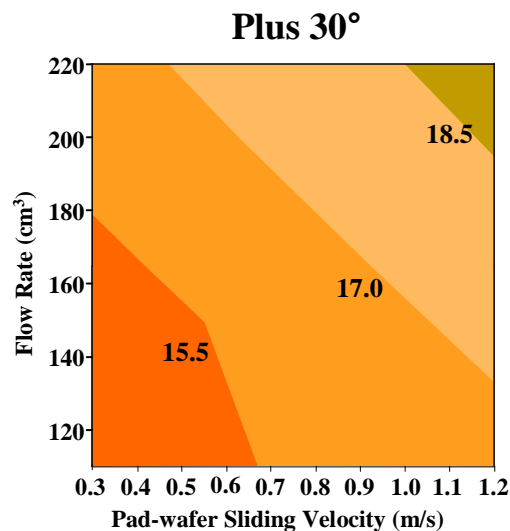
**Sliding Velocity = 1.2 m/s**

The slurry film thickness generally increases with the flow rate, showing evidence of saturation at higher flow rates.

Higher wafer pressures further compress pad asperities thereby diminishing the slurry flow into the pad-wafer interface area.



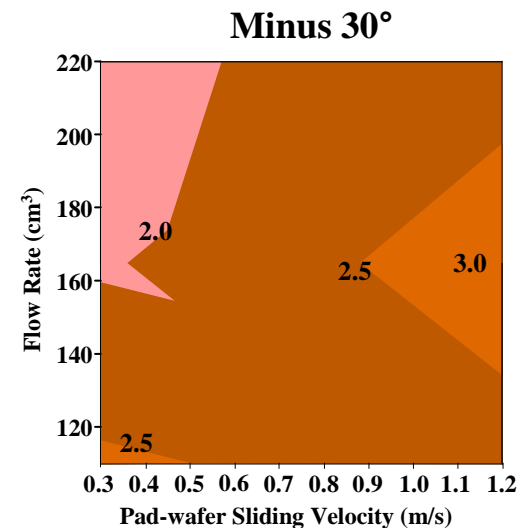
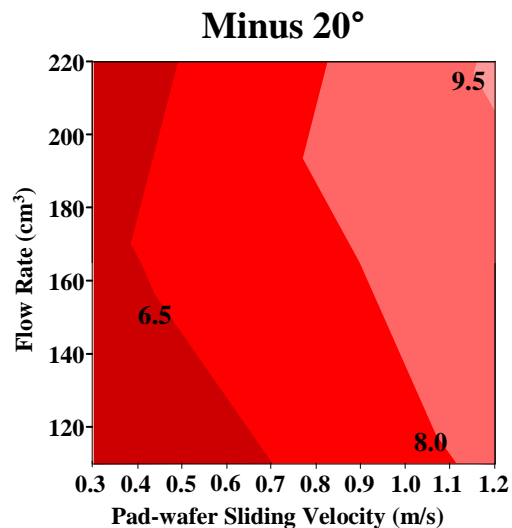
# Slurry Film Thickness Contour Plot



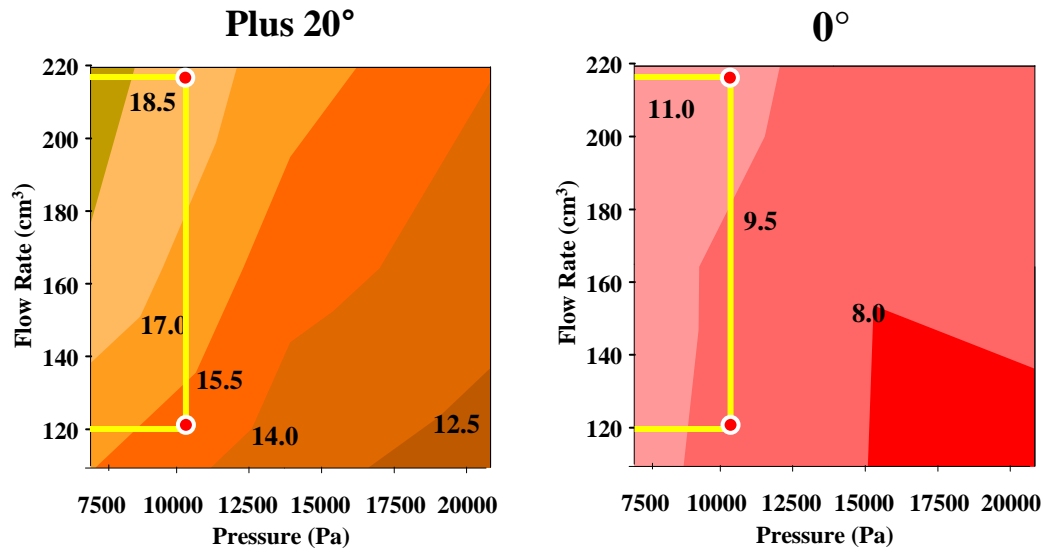
**Pressure = 3 PSI**

The slurry film thickness generally increases with the flow rate, showing evidence of saturation at higher flow rates.

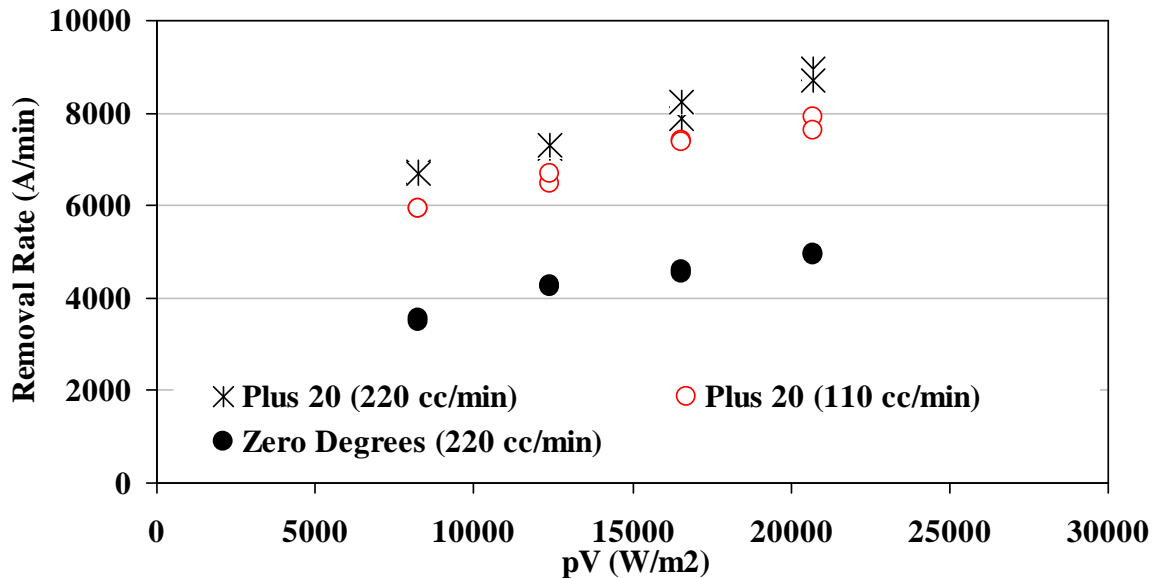
The slurry film thickness generally increases with the sliding velocity.



# Effect of Groove Slanting on Removal Rate



At any given sliding velocity, pressure, and flow rate, the Plus 20° pad shows a higher slurry film thickness at the pad land area compared to the 0° pad. This can have significant pad-wafer contact area ramifications that affect removal rate and defectivity.



Removal rate slightly decreases as the flow rate is cut by 2X for the Plus 20° pad. However, even at this lower flow rate (110 cc/min), the Plus 20° pad has a significantly higher removal rate than the 0° pad at 220 cc/min.

# Industrial Interactions and Presentation

## **Industrial mentor / contact:**

- Tatsutoshi Suzuki (Toho Engineering)

## **Presentation:**

- Effect of Concentric Slanted Groove Patterns on Slurry Flow during Copper CMP. D. Rosales-Yeomans, H. Lee, T. Suzuki and A. Philipossian. SRC 9th Premier TECHCON, September 10-12, Austin, Texas, 2007.

# **Biologically Inspired Nano-Manufacturing**

## **(BIN-M): Characterization**

### **PIs:**

- Anthony Muscat, Chemical and Environmental Engineering, UA
- Megan McEvoy, Biochemistry and Molecular Biophysics, BIO5 Institute, UA
- Masud Mansuripur, College of Optical Sciences, UA

### **Graduate Students:**

- Amber Young, PhD candidate, College of Optical Sciences, UA
- Sam Jayakanthan, PhD candidate, Biochemistry and Molecular Biophysics, UA
- Shawn Miller, PhD candidate, College of Optical Sciences, UA
- Rahul Jain, PhD candidate, Chemical and Environmental Engineering, UA

### **Undergraduate Student:**

- Ben Mills, Chemical and Environmental Engineering, UA

### **Other Researchers:**

- Zhengtao Deng, Postdoctoral Fellow, ChEE & Optical Sciences, UA
- Babak Imangholi, Postdoctoral Fellow, ChEE & Optical Sciences, UA
- Gary Fleming, Postdoctoral Fellow, Chemical and Environmental Engineering, UA

### **Cost Share (other than core ERC funding):**

- \$825k Science Foundation Arizona, ASM, SEZ, Arizona TRIF

# Project Objectives

- Minimize costs of materials, energy, and water to fabricate nanoscale devices using bio-based strategy
- Exploit homogeneity, mild reaction conditions, and specificity of active biological molecules
- Grow 3D structures to achieve scalable architecture
- Employ additive, bottom up patterning methods

## ESH Metrics and Impact

Sustainability metrics			
Process	Water l/bit/masking layer	Energy J/bit/masking layer	Materials g/bit/masking layer
Subtractive 32 nm*	$3.3 \times 10^{-10}$	$1.5 \times 10^{-12}$ EUV	$2.9 \times 10^{-16}$
Additive	$3.6 \times 10^{-13}$	$9.2 \times 10^{-17}$	$1.8 \times 10^{-19}$

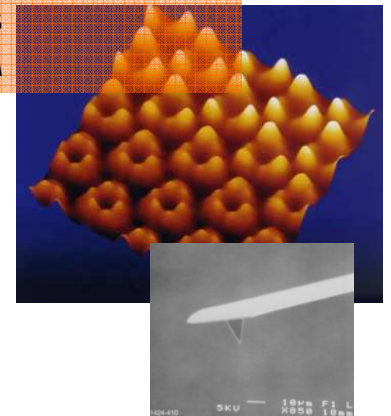
\*D. Herr, Extending Charge-based Technology to its Ultimate Limits: Selected Research Challenges for Novel Materials and Assembly Methods. Presentation at the NSF/SRC EBSM Engineering Research Center Review Meeting: February 24, 2006.

# Process Goal: Deposit Array of Metal Dots

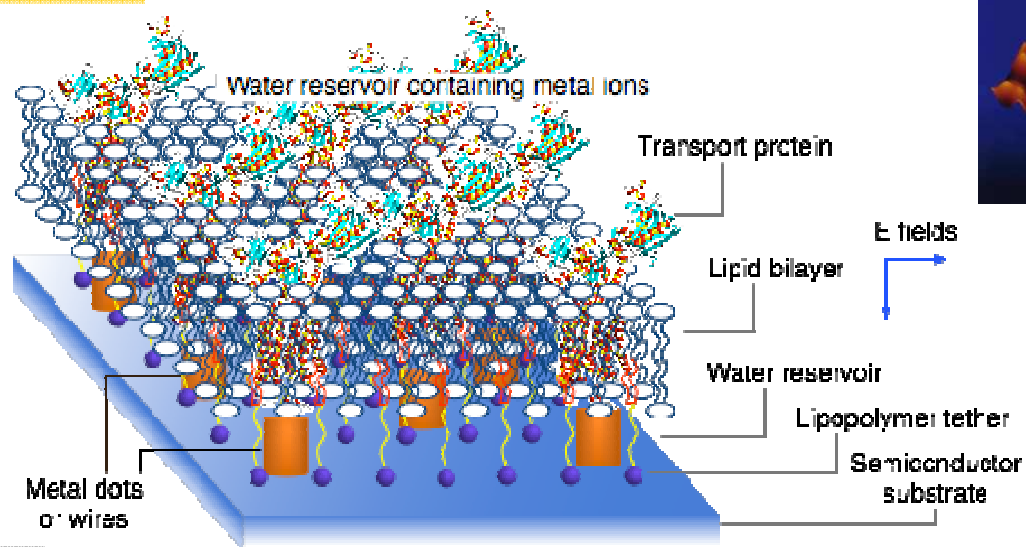
Biochemistry of metal transport proteins  
*Megan McEvoy/UA*



Characterize bio & inorganic structures using scanning probe and optical techniques  
*Masud Mansuripur/UA*



Selective deposition  
*Glen Wilk, Eric Shero, Christophe Pomarede, Steve Marcus/ASM*



Pattern surfaces and build structures  
*Anthony Muscat/UA*



Semiconductor surface preparation  
*Harald Okorn-Schmidt, Zach Hatcher, Jeremy Klitzke/SEZ*

# Characterization

## **Lipid Bilayer**

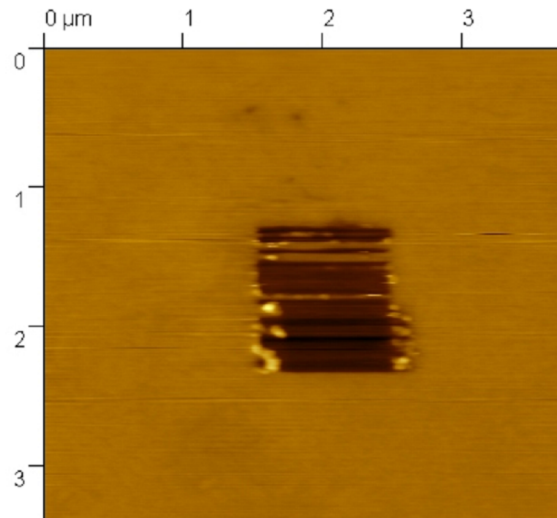
- **Verify lipid membrane is a bilayer using patchclamp, AFM, impedance measurements and ellipsometry**
- **Examine large area coverage**
- **Investigate surface uniformity**

## **Proteins**

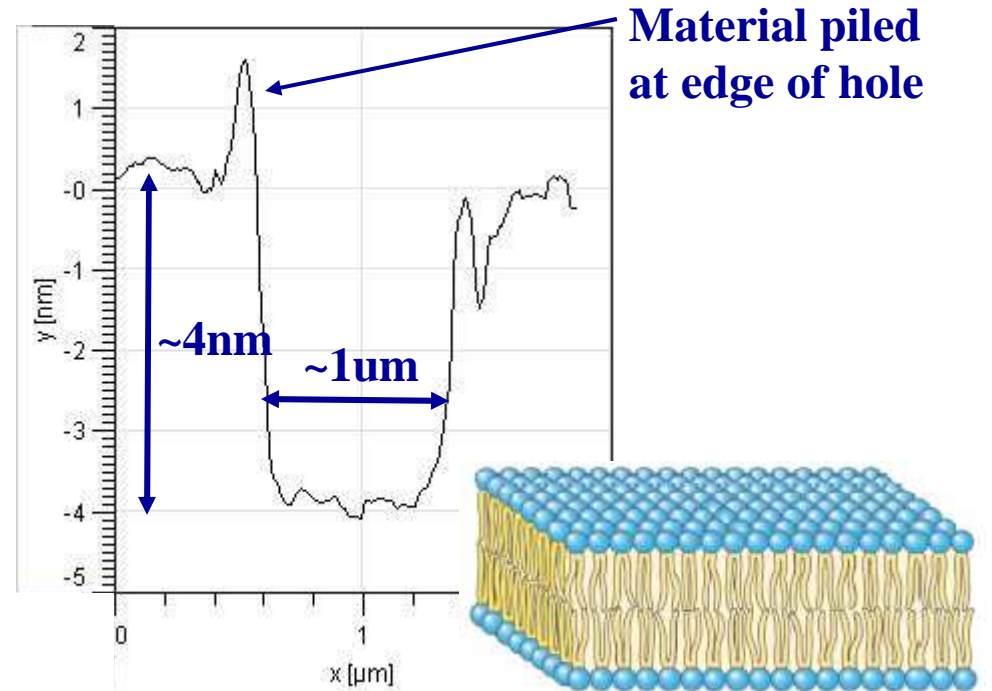
- **Explore fluorescence microscopy, fluorescence spectrometry and AFM as tools to characterize quantum-dot-tagged proteins**
- **Determine multi-color resolution of quantum-dot-tagged proteins in a lipid bilayer**



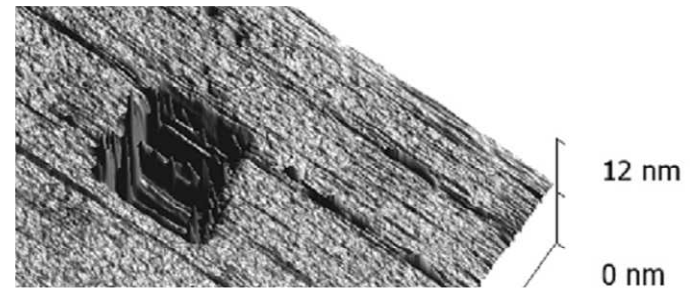
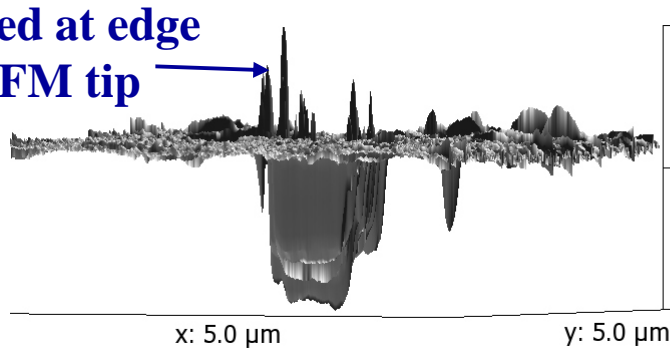
# AFM Characterization of Bilayer



**1 μm square hole dug in lipid membrane. Observe smooth bilayer surface. Note excess material piled at edge of hole.**

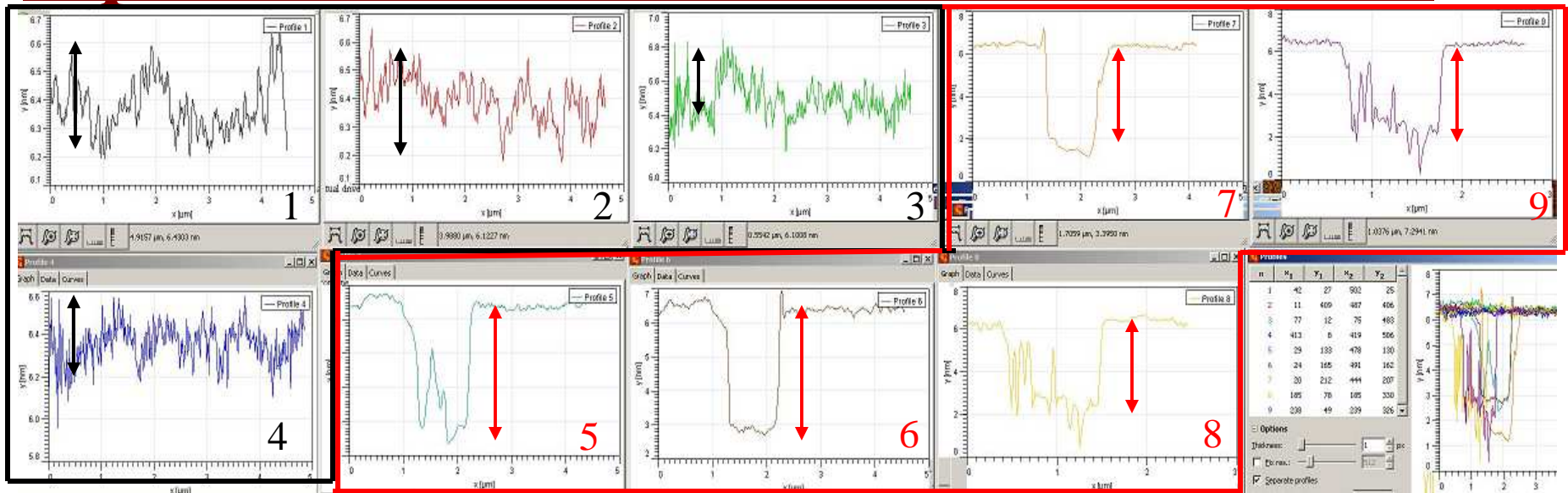


**Material piled at edge of hole by AFM tip**



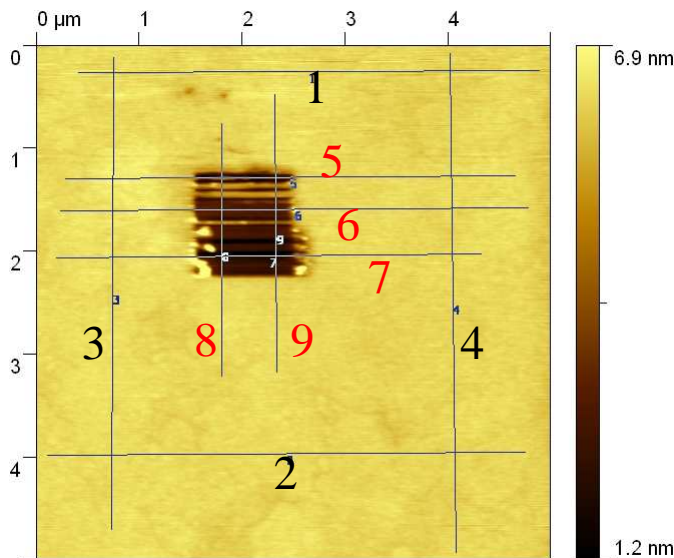
**3D representations of hole dug in bilayer**

# Lipid Membrane Surface Cross-Sections



↕ Represents 0.4nm variation

↕ Represents 4nm variation



## Observations:

- Some material remains in hole, but fairly uniform depth
- 3.5 nm depth is consistent with expected lipid bilayer thickness
- Variation in bilayer surface in regions far from hole  $\leq 0.4\text{nm}$

# Bilayer Electrical Properties

## **Challenge**

- Large area characterization of lipid membrane
- Patch clamp technique is limited to small areas

## **Conventional Solution**

- Impedance spectroscopy on conductive substrates is used to characterize large area lipid membranes
  - Insulating native oxide on the semiconductor impairs impedance measurement
  - Frequency dependence of semiconductor electrical property complicate impedance measurement

## **Our Novel Solution**

- Phase Sensitive Measurements with a Lock-in amplifier

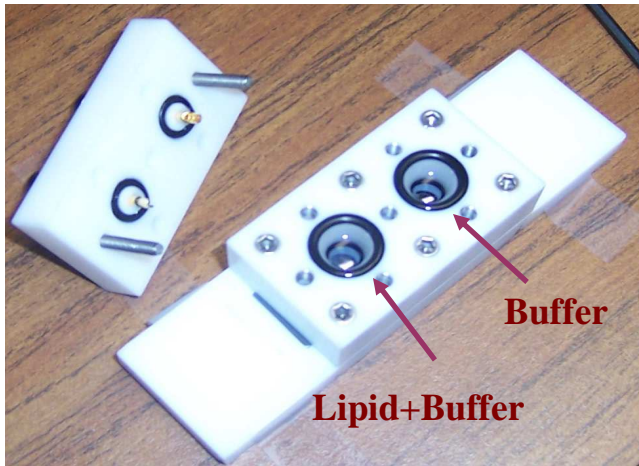
# Phase Sensitive Detection

## Basic Theory

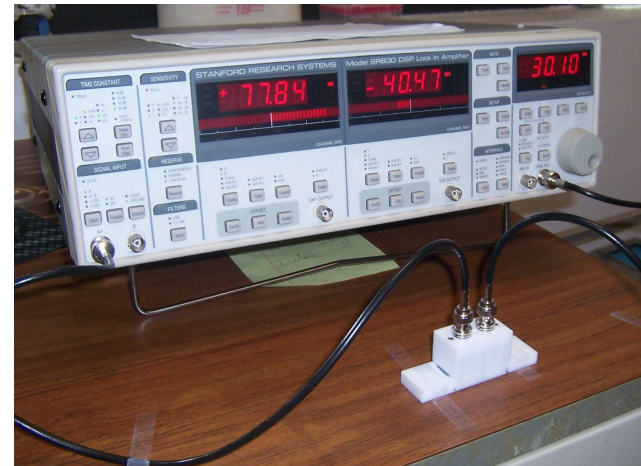
Phase vs. frequency of lipid bilayer is measured independent of semiconductor properties via differential phase measurement

$$\Delta\varphi = -\text{ArcTan}\left[\frac{R_L^2 X_C}{R R_L^2 + (R + R_L) X_C^2}\right]$$

$R_L$  &  $X_C$  represent lipid resistance and impedance,  $R$  is Lock-in input impedance



Test chambers



Labview controlled Lock-in amplifier

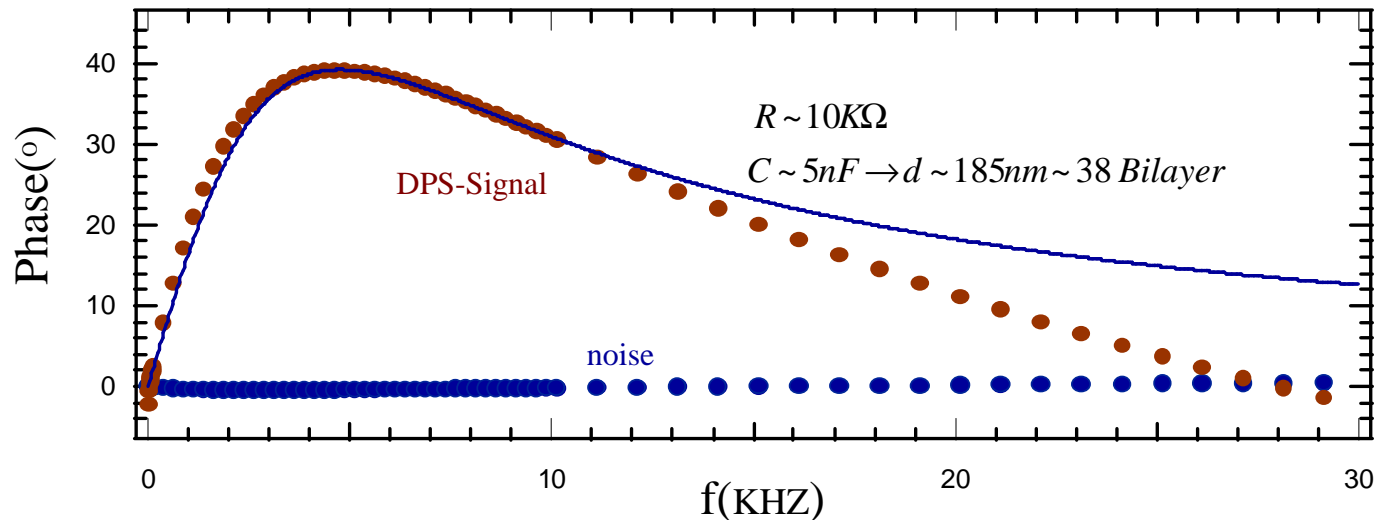
# Data Analysis and Discussion

## Calibration

Lock-in system is calibrated using electronic component

## Measurement

Phase change due to resistance and capacitance of Lipid is measured



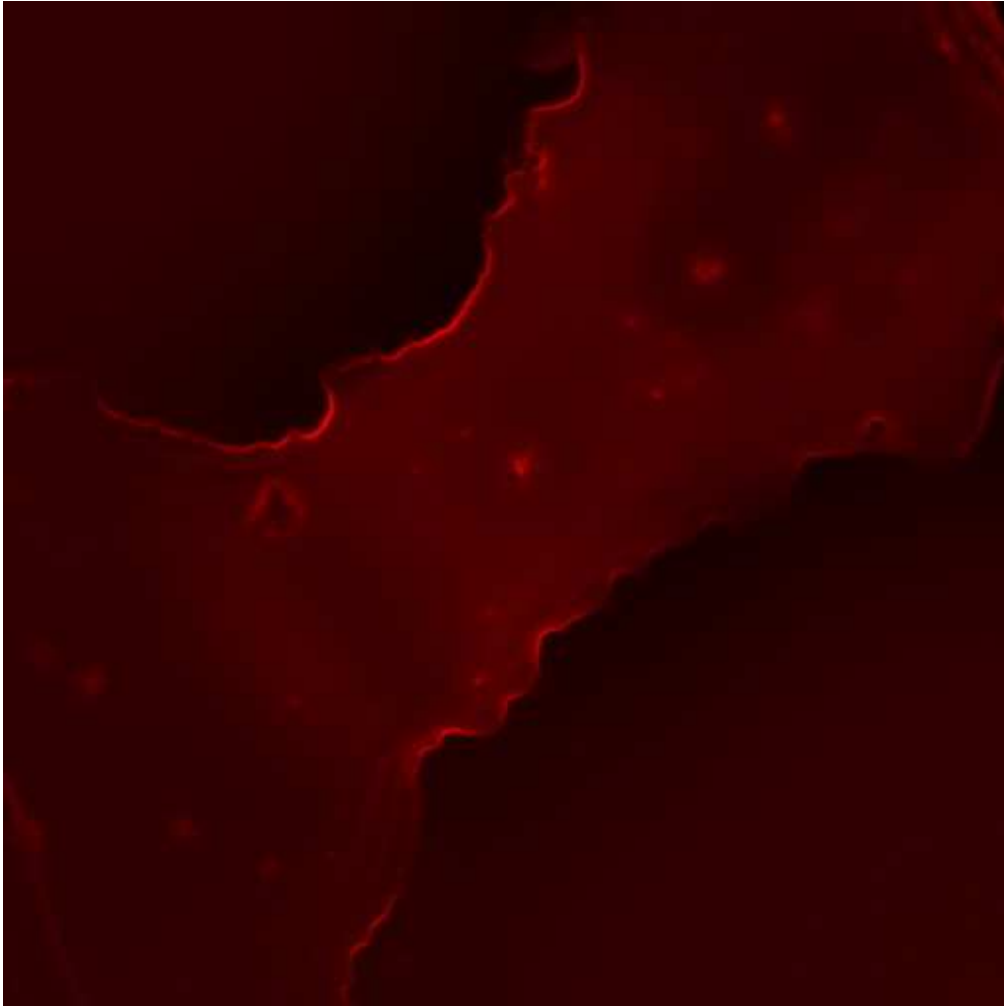
## Goal

Lipid resistance describes impermeability of the lipid membrane

Lipid capacitance describes thickness and uniformity of the Lipid

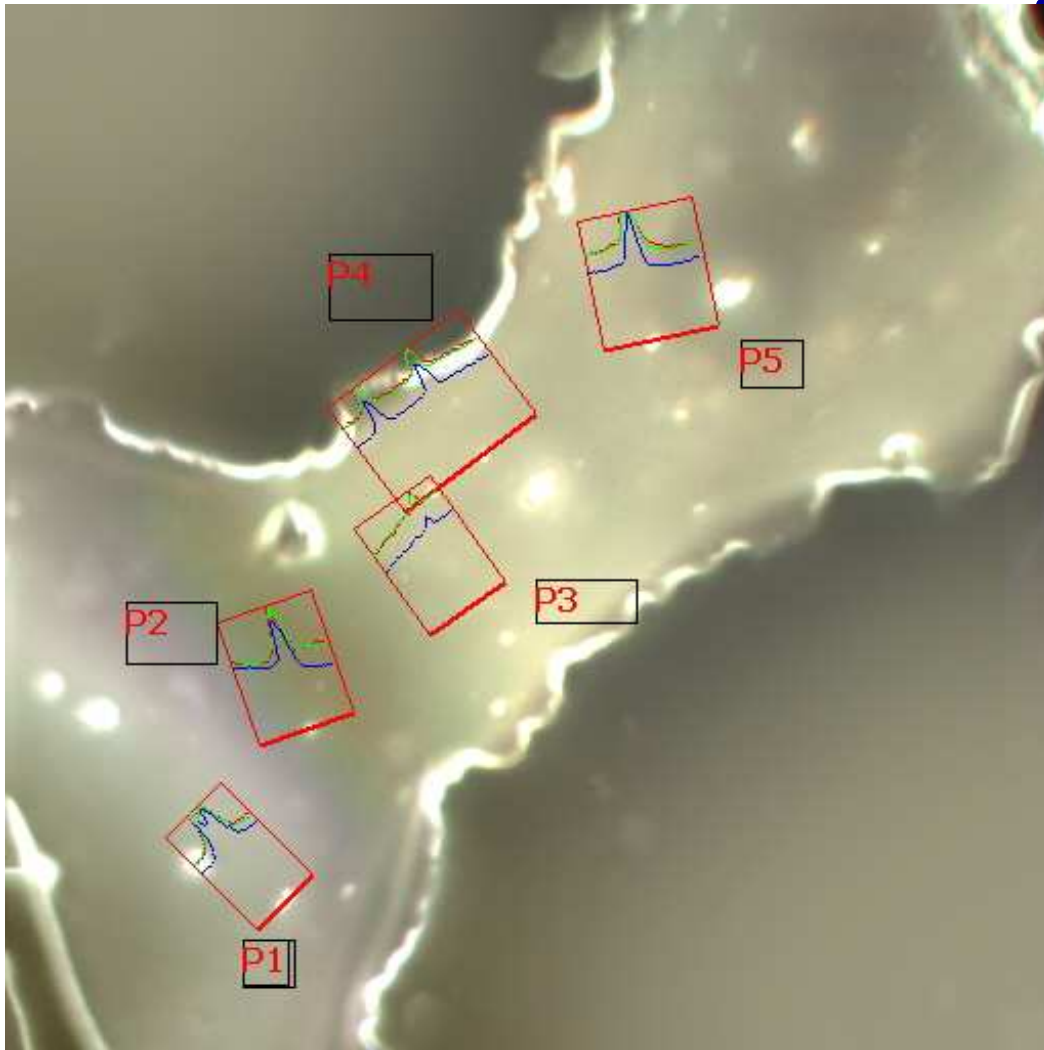


# Single Filter Fluorescence Image



- **Sample: Red (605nm) and Green (540nm) Quantum dots on glass substrate**
- **Excitation: HBO filtered by 365nm filter with 20nm FWHM**
- **Emission Filter: 525nm**

# Combined Image



**Sample: Red (605nm)  
and Green (540nm)  
Quantum dots on glass  
substrate**

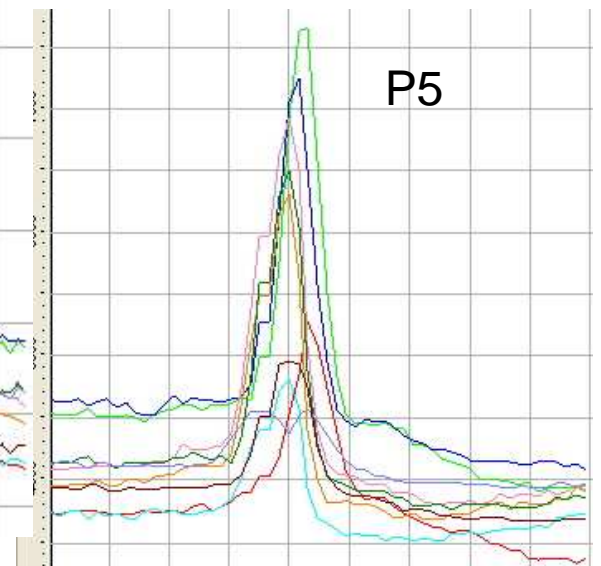
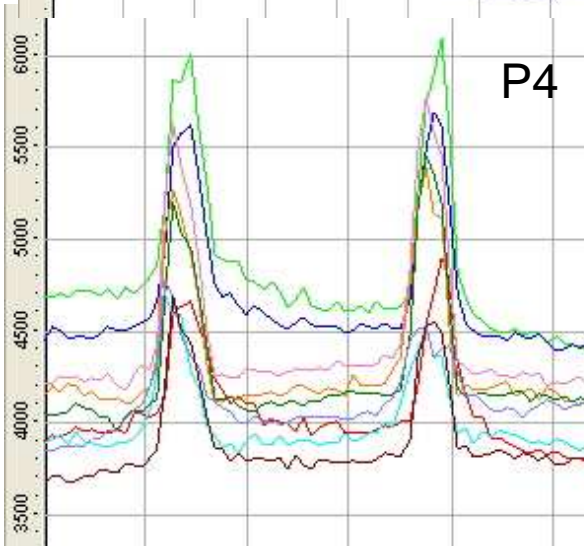
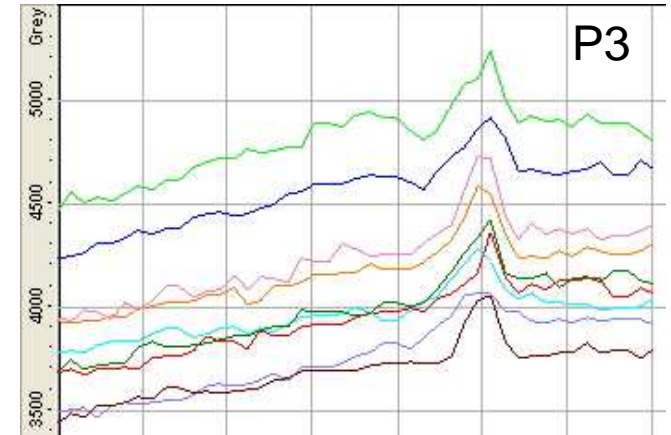
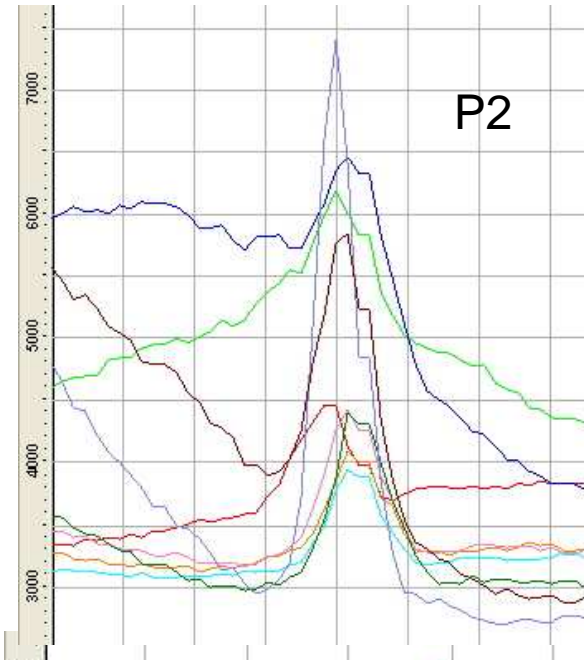
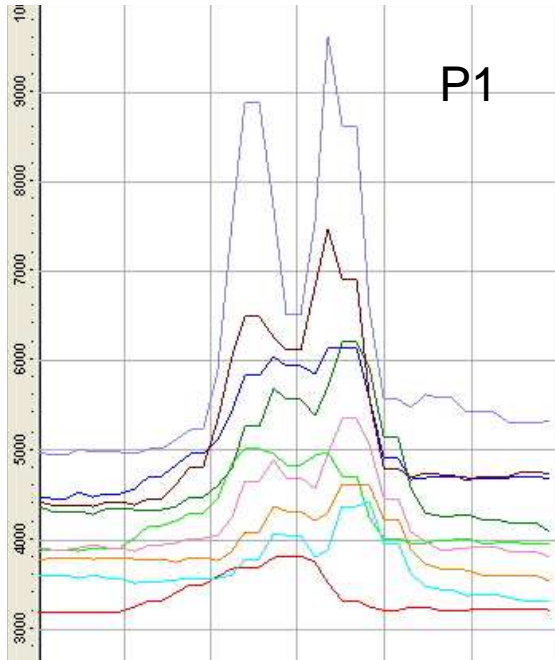
**Excitation: HBO  
filtered by 365nm filter  
with 20nm FWHM**

**9 Emission Filters**

- **525, 565, 595, 605,  
655, 705, 755, 800,  
850 nm (20 nm  
FWHM)**

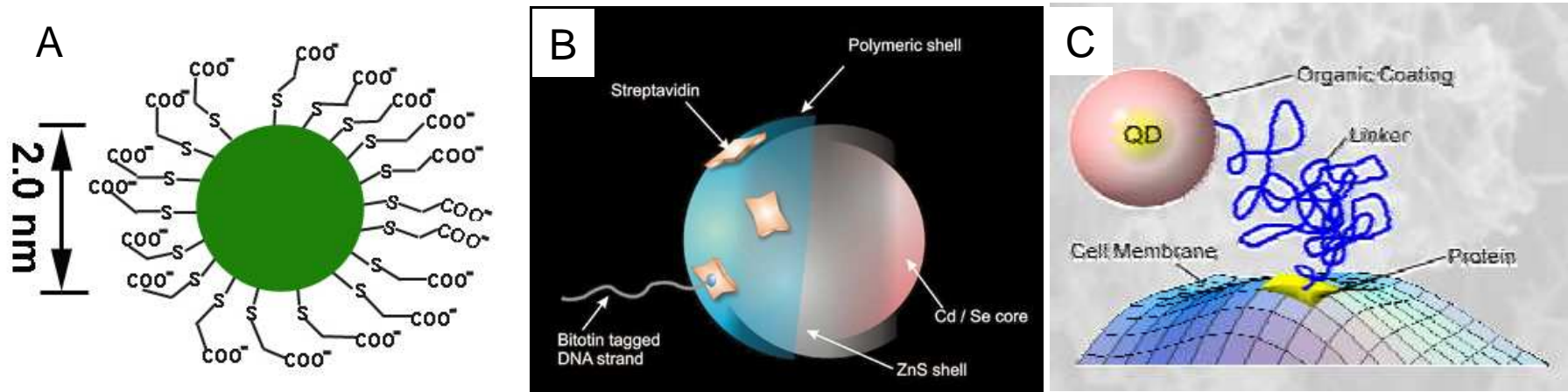
**Profiles drawn across  
points of interest**

# Profiles Referenced on Combined Image



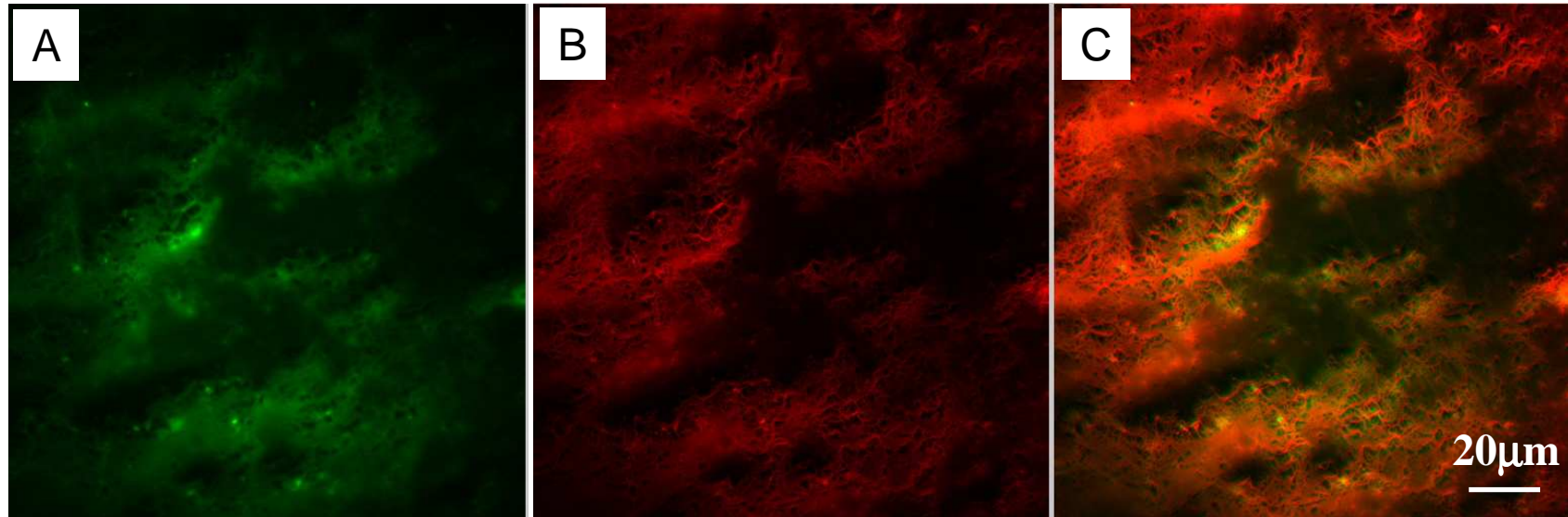


# Imaging of Proteins with Quantum Dots



- (A) Single quantum dot terminated with COOH groups
- (B) Functionalized quantum dot
- (C) Quantum dot attached to protein with linker

# Fluorescent Microscopy Study of Red CdTe QDs Labeled YFP



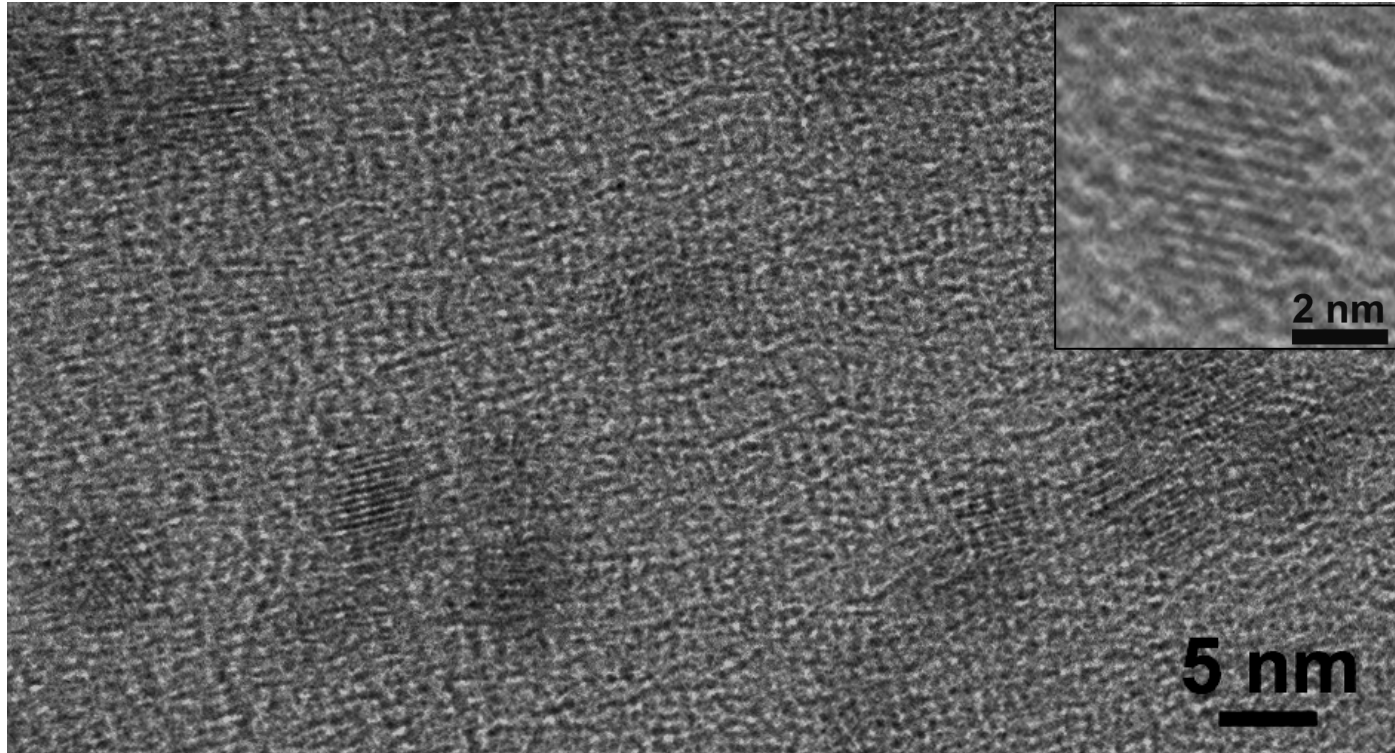
**(A) Image with filter  $525 \pm 10$  nm;**

**(B) Image with filter  $605 \pm 10$  nm;**

**(C) Combined image of A and B.**

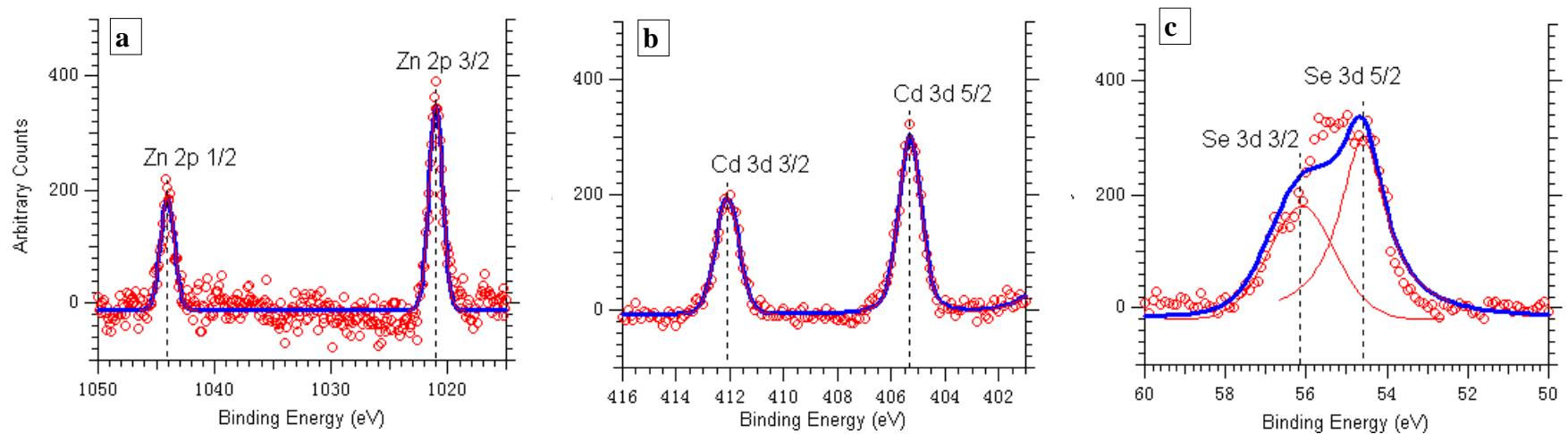
**Note: Pure CdTe QDs with emission peak at 600 nm;  
Pure YFP with emission peak at 528 nm**

# TEM of QDs



Transmission electron microscopy image of thioglycolic acid capped CdTe quantum dots deposited on TEM grid

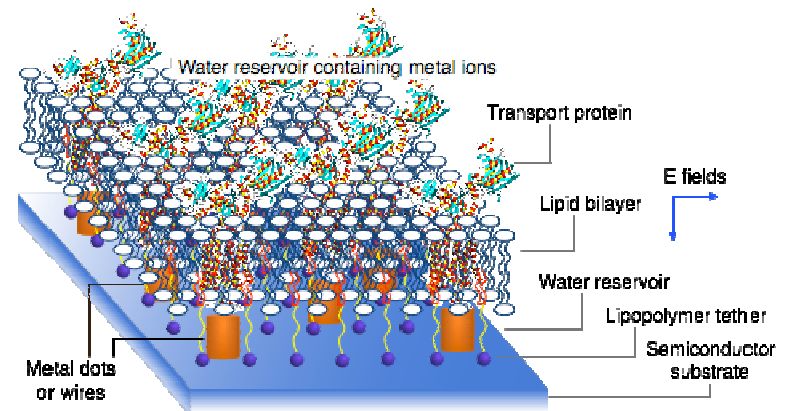
# XPS study of $Zn_xCd_{1-x}Se$ QDs



**High-resolution x-ray photoelectron spectra of  $Zn_xCd_{1-x}Se$  QDs samples with near bandgap emission peak at 490 nm: (a) Zn 2p<sub>3/2</sub> and Zn 2p<sub>1/2</sub> spectral lines; (b) Cd 3d<sub>3/2</sub> and Cd 3d<sub>5/2</sub> spectral lines; (c) Se 3d<sub>5/2</sub> and Se 3d<sub>3/2</sub> spectral lines.**

# Future Characterization Efforts

- Incorporate proteins in lipid bilayer
  - Verify presence of proteins in lipid bilayer with AFM, PSD and other imaging techniques including fluorescence microscopy
- Characterize protein-quantum dot pairs
- Activate and control quantum-dot-tagged-transport proteins in lipid bilayer
- Experiment with additive, bottom up patterning methods using quantum-dot-tagged proteins in lipid bilayer





# Biologically Inspired Nano-Manufacturing (BIN-M): Fabrication

## PIs:

- Anthony Muscat, Chemical and Environmental Engineering, UA
- Megan McEvoy, Biochemistry and Molecular Biophysics, BIO5 Institute, UA
- Masud Mansuripur, College of Optical Sciences, UA

## Graduate Students:

- Amber Young, PhD candidate, College of Optical Sciences, UA
- Sam Jayakanthan, PhD candidate, Biochemistry and Molecular Biophysics, UA
- Shawn Miller, PhD candidate, College of Optical Sciences, UA
- Rahul Jain, PhD candidate, Chemical and Environmental Engineering, UA

## Undergraduate Student:

- Ben Mills, Chemical and Environmental Engineering, UA

## Other Researchers:

- Zhengtao Deng, Postdoctoral Fellow, ChEE & Optical Sciences, UA
- Babak Imangholi, Postdoctoral Fellow, ChEE & Optical Sciences, UA
- Gary Fleming, Postdoctoral Fellow, Chemical and Environmental Engineering, UA

## Cost Share (other than core ERC funding):

- \$825k Science Foundation Arizona, ASM, SEZ, Arizona TRIF

# Fabrication

Four phase process to incorporate transporter proteins into lipid bilayer on semiconductor surfaces:

## Lipid Preparation

- Process organic molecules, lipids, for deposition onto semiconductor

## Surface Preparation

- Process semiconductor surface to have favorable interactions with lipids

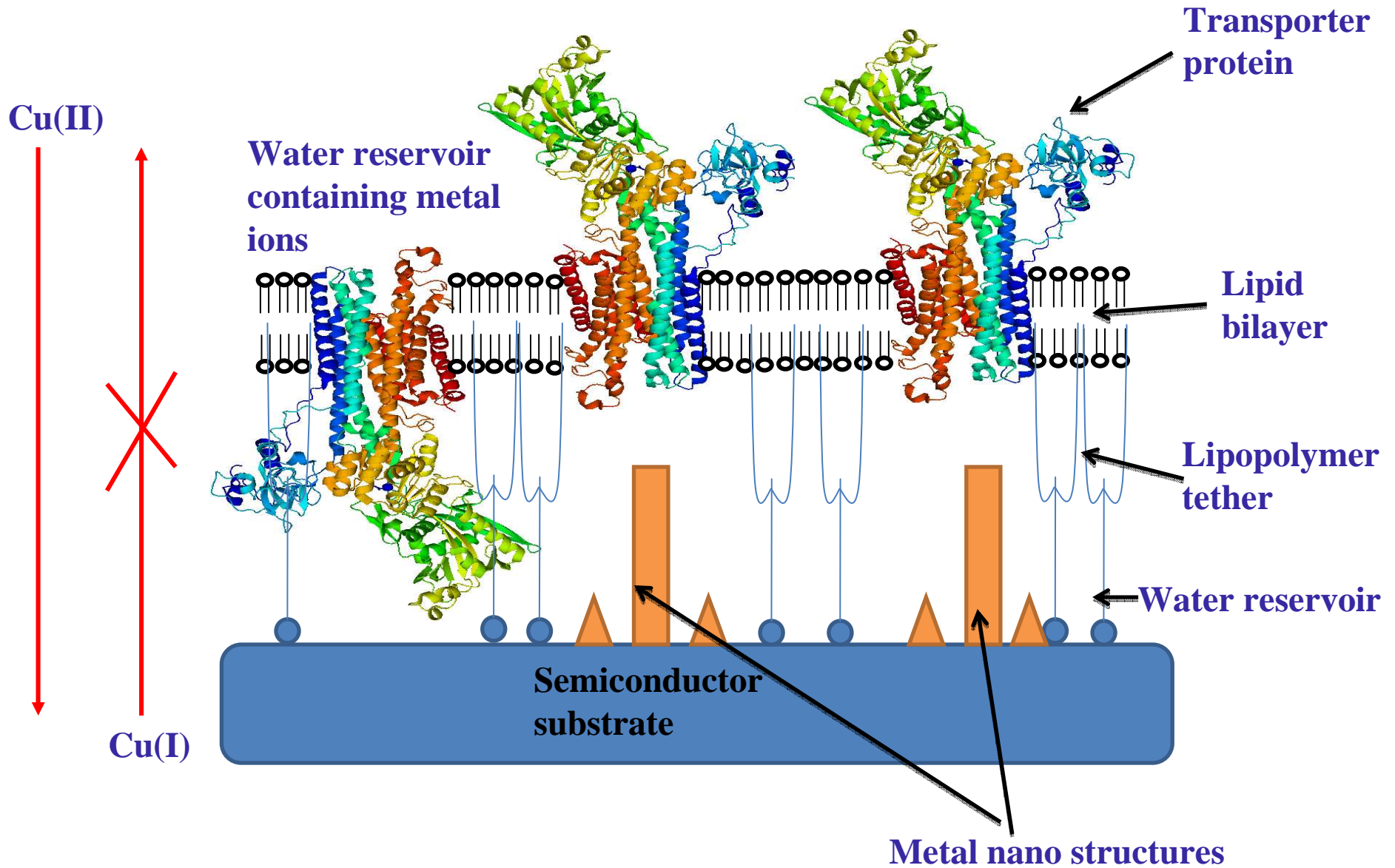
## Vesicle Deposition

- Allow natural and favorable interactions to form continuous bilayer on semiconductor surface.

## Protein Expression and purification

- Cloning, expression and purification of Cu(II) transporting ATPase – CopB.

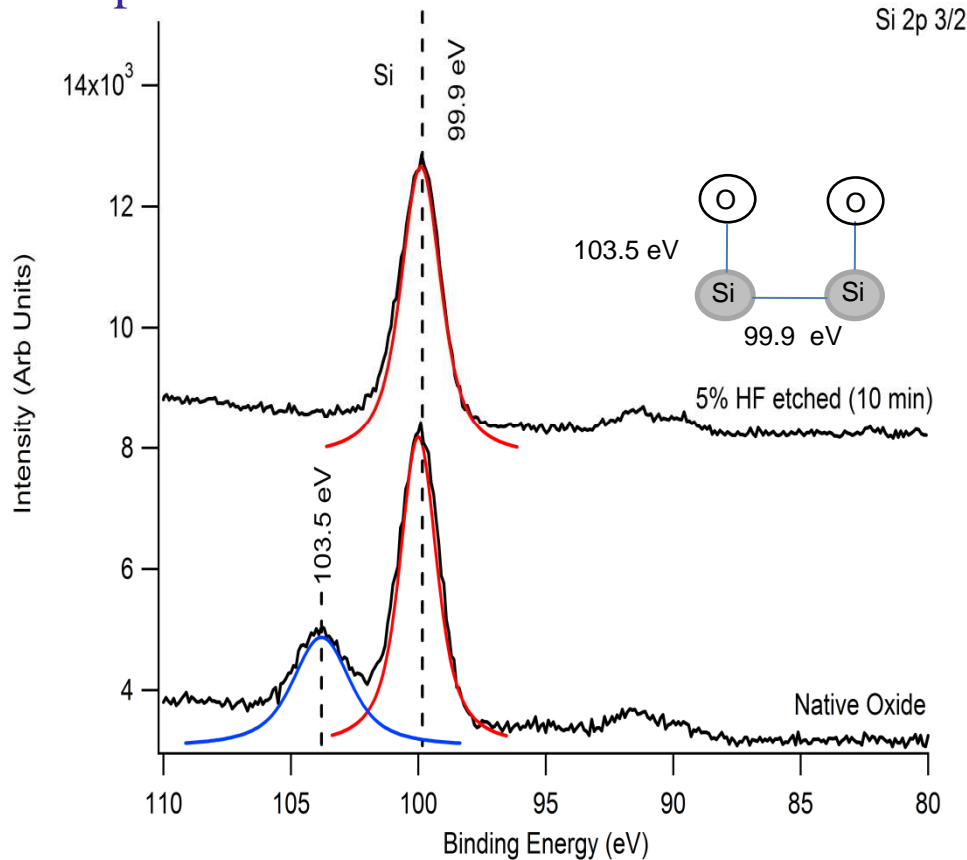
# Overview of the Project





# Si (100) Surface Characterization

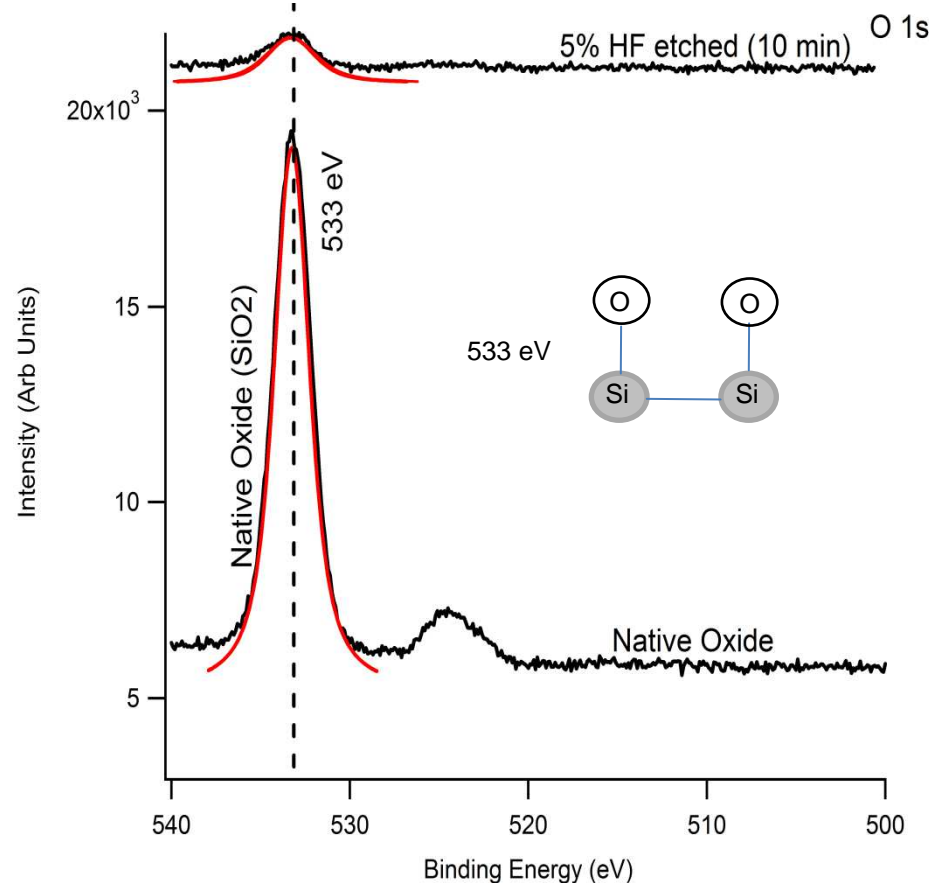
## Si 2p 3/2



Si 2p 3/2 = 2 main features  
103.5 eV = Native oxide ( $\text{SiO}_2$ )  
99.9 eV = Si

After etching 103.5 eV peak removed = Native oxide removed

## O 1s



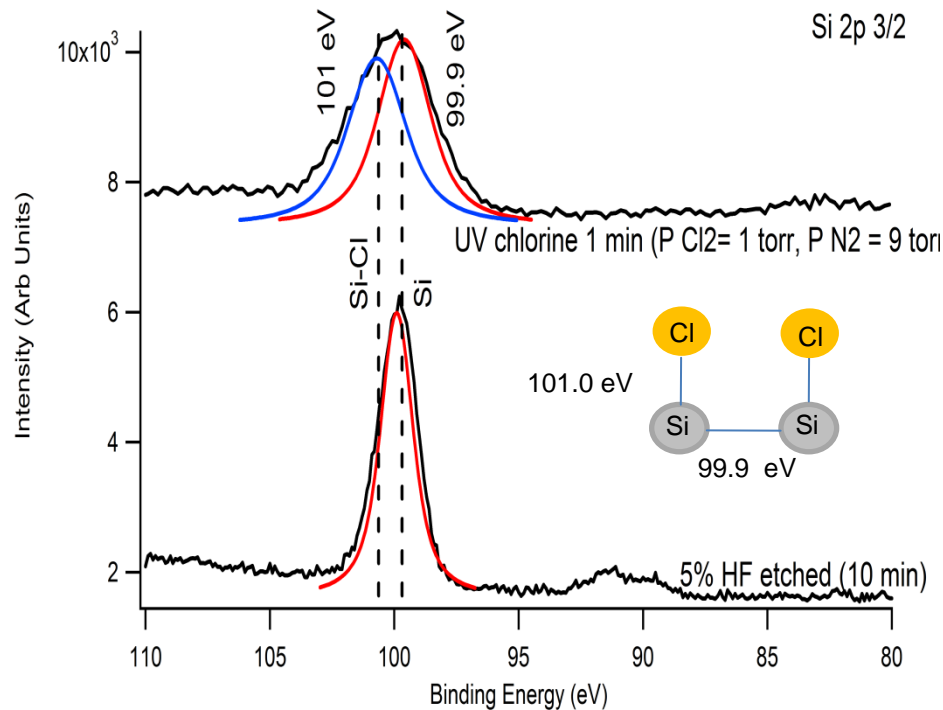
O 1s = Strong oxide signal present before HF etching (533 eV).

After HF etching oxide peak dramatically reduced

*Applied Surface Science (2007), 253(18), 7387-7392*

## Si 2p 3/2

# UV/Cl<sub>2</sub> on Si(100) Surfaces



UV/Cl<sub>2</sub> conditions:

$p_{Cl_2} = 1$  torr,  $p_{N_2} = 9$  torr

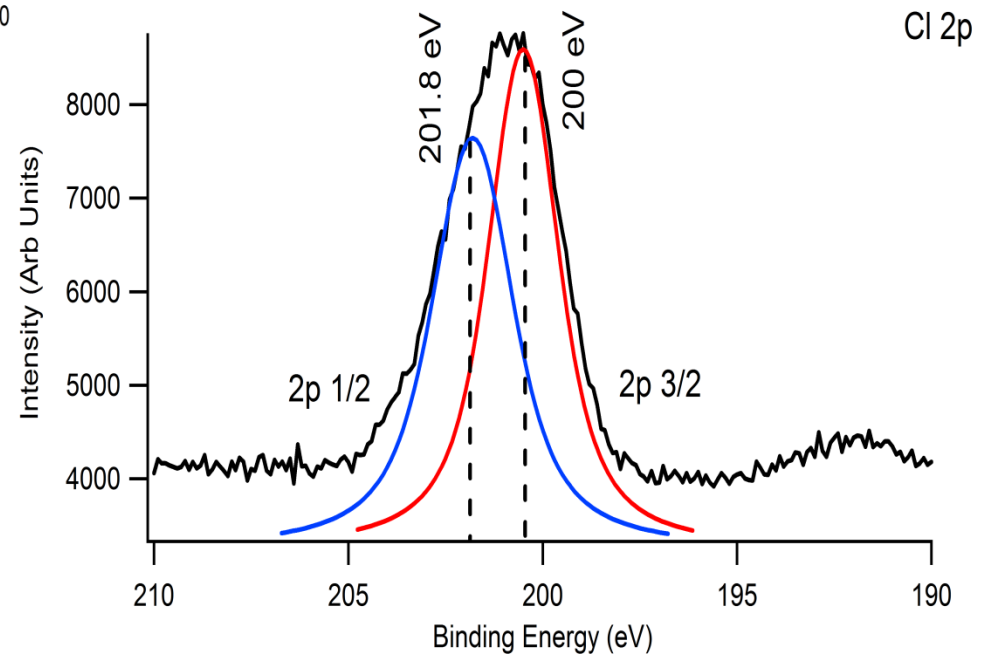
Exposed HF etched sample to mixture with 350 nm UV light for 1 min

Cl 2p spectrum shows presence of Cl on the HF etched Si substrate after exposure to UV/Cl<sub>2</sub>

200 eV = Cl 2p 3/2, 201.8 eV = Cl 2p 1/2.

Post Cl exposure 2 features are noticeable in Si 2p 3/2 spectrum  
99.9 eV = Si, 101 eV = Si-Cl

## Cl 2p



# Surface Patterning

## (i) Surface Preparation

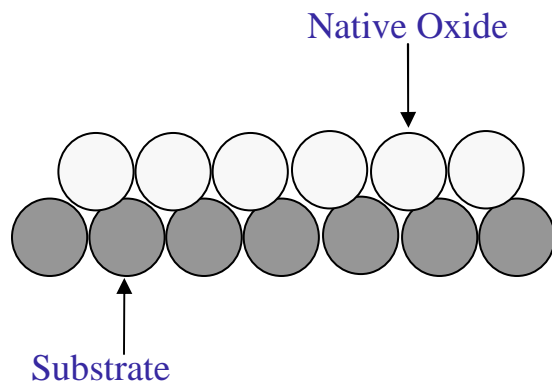
Cleaning performed by chemical etching.

Characterised via XPS, AFM, TPD.

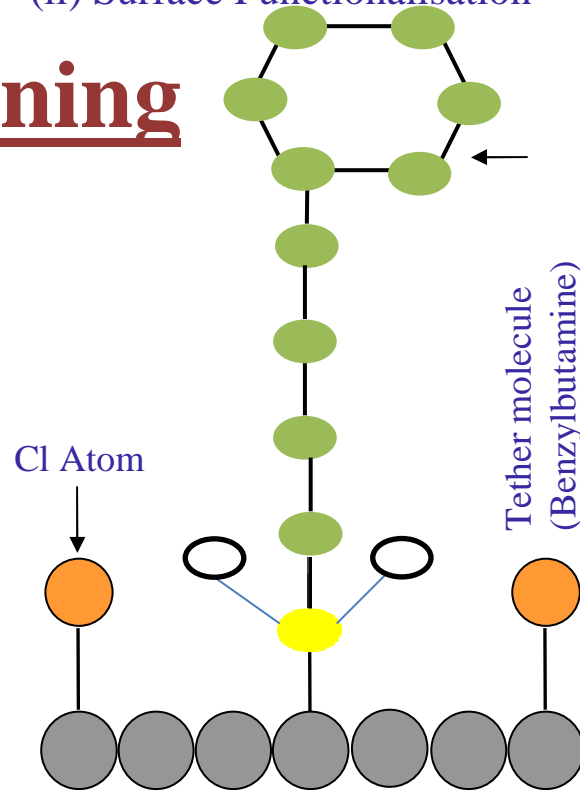
Possible Substrates for Use

Si, Ge, GaAs, InAs, InP, InSb

Tertiary Materials.



## (ii) Surface Functionalisation



Surface chemistry used to modify surface and to introduce patterning and tether molecules to attach lipid bilayer

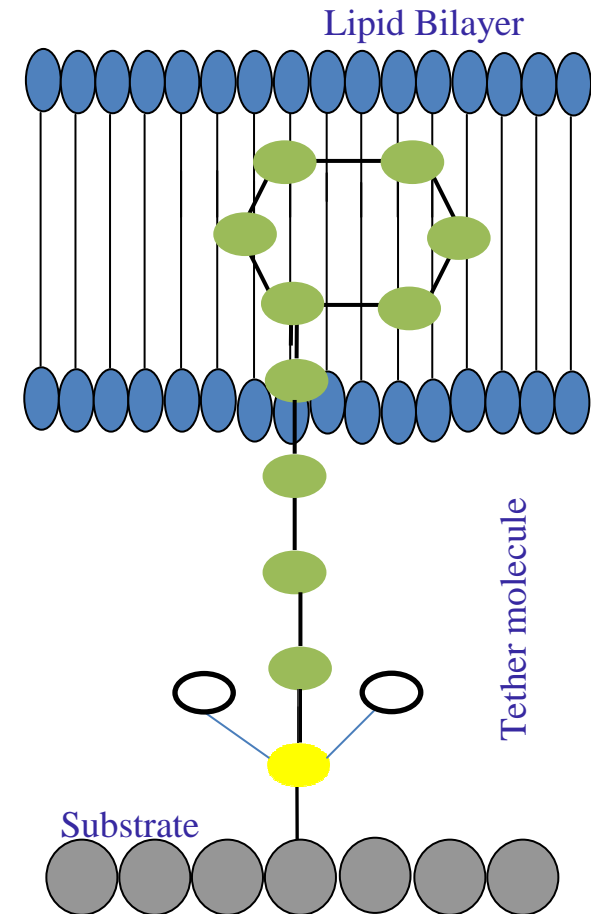
Types of Chemistry

Patterning Step: UV/Cl<sub>2</sub>, NH<sub>3</sub>

Tethers = Amines (dibutylamine, ethylamine), Benzene, Pyridine.

## (iii) Lipid Bilayer Addition

Attachment of lipid bilayer to surface.

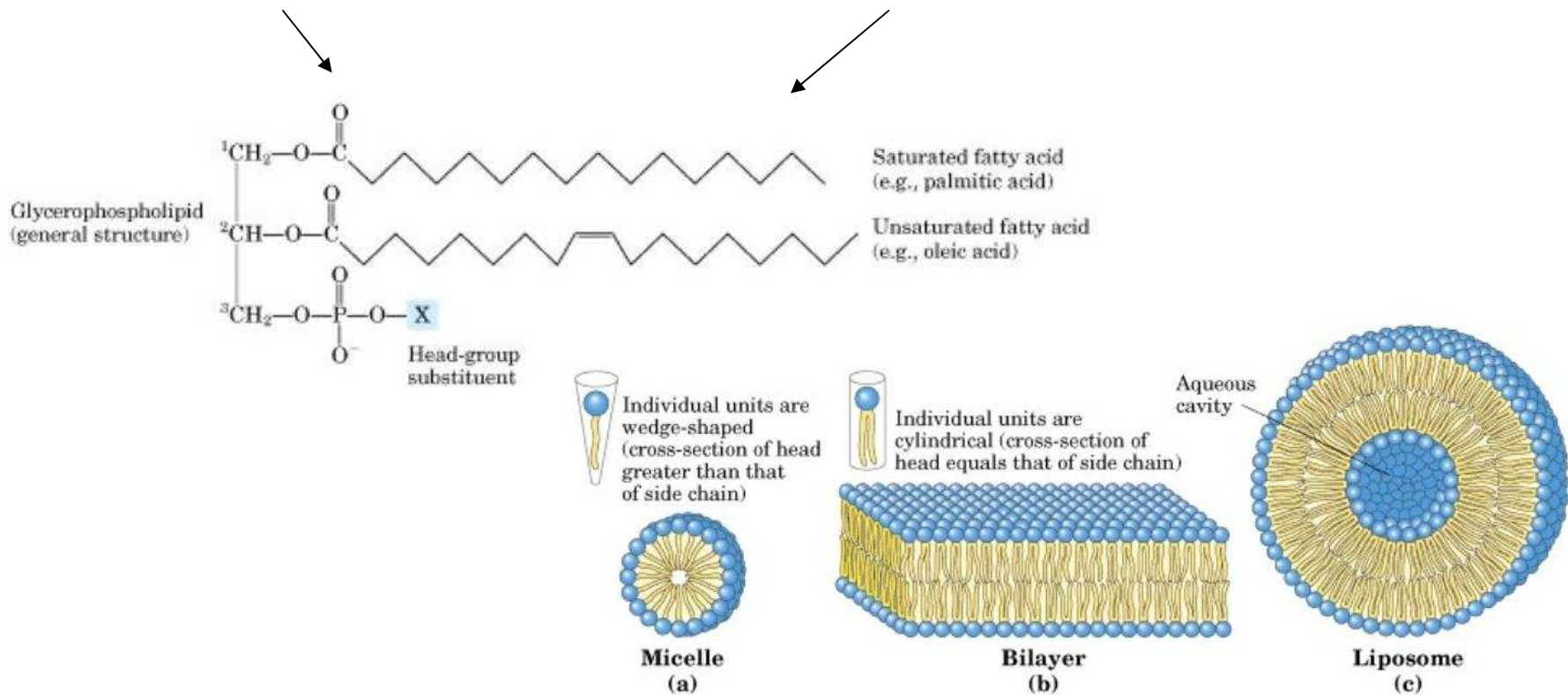


# Lipid Molecular Structure and Formations

- Lipids

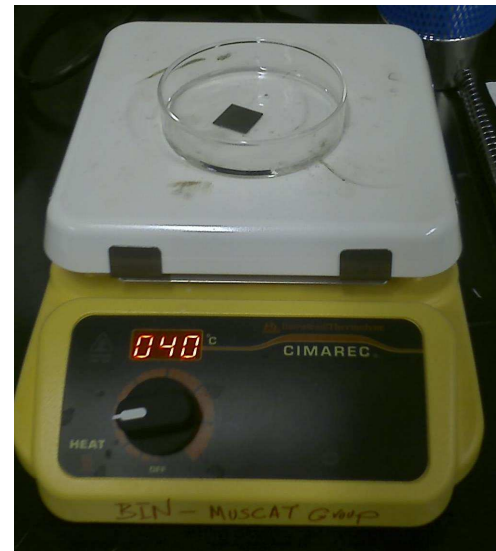
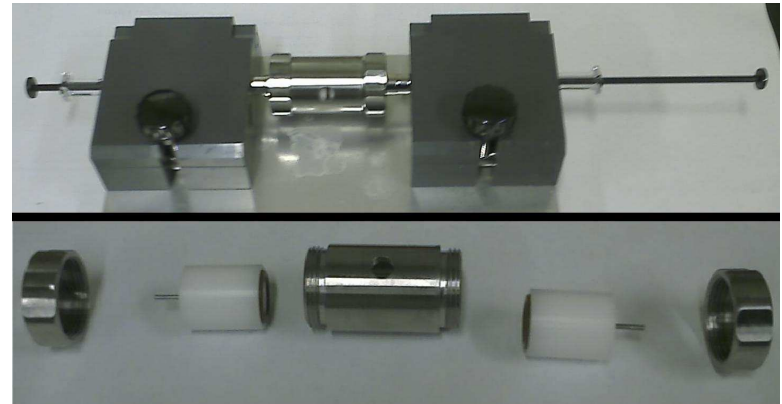
- Polar Head Group (Hydrophilic)

- Alkyl Chain (Hydrophobic)



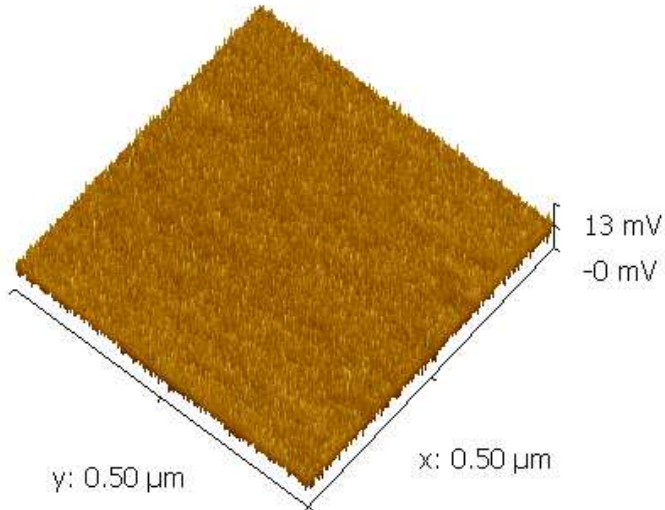
# Experimental Methods for Vesicle Formation

- Vesicle Formation
  - Freeze-thaw cycles
  - Extrusion
  - Sonication
- Vesicle Deposition and bilayer formation
  - 40  $\mu\text{L}$  vesicle solution for 2 cm x 2 cm silica surface
  - 2 hr incubation at 40  $^{\circ}\text{C}$

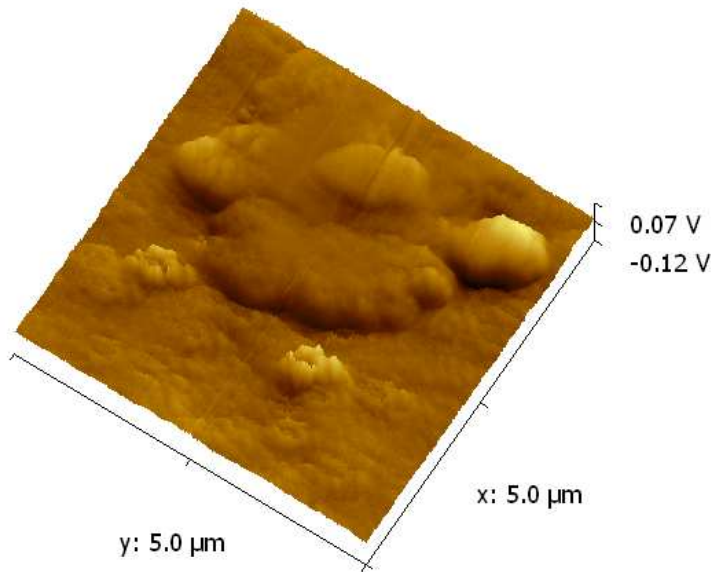


# Lipid Bilayer Formation

Continuous Lipid Bilayer



Discontinuous Lipid Bilayer

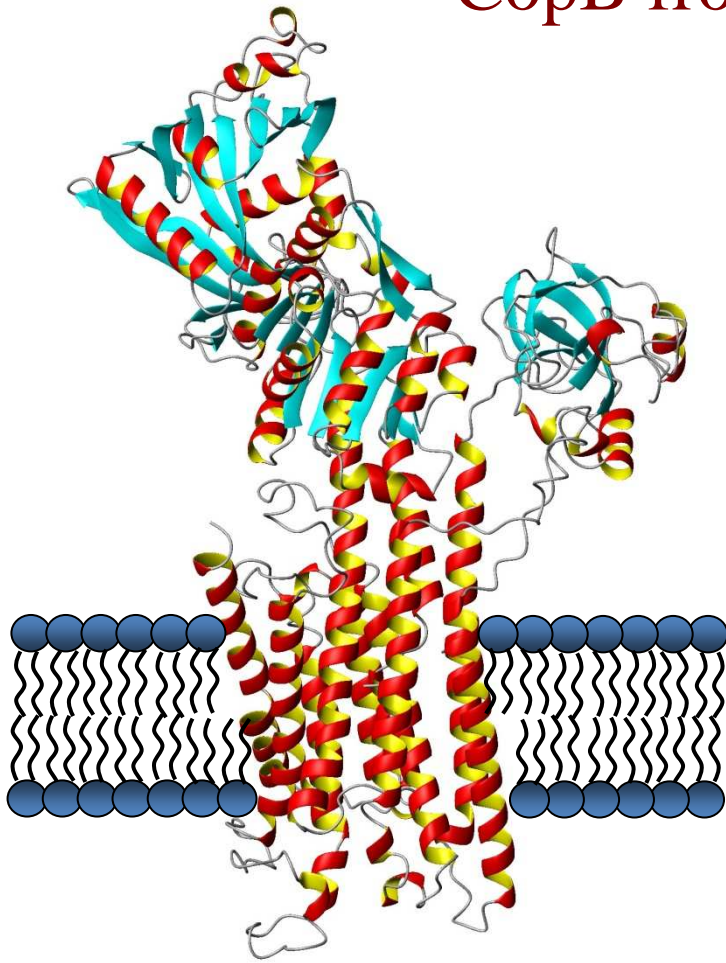


- Formation of bilayer occurs spontaneously
- Bilayer thickness is 3-4 nm
- AFM images depict piecewise uniformity



# Methods and Approach

## Metal Transport Proteins: CopB from *Archaeoglobus fulgidus*

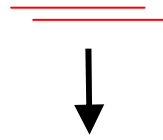


- Recombinant protein purified from *E. coli*
- Cu(II) transport activity in artificial membranes
- Energy source: Adenosine triphosphate (ATP)
- Enhanced stability at room temperature

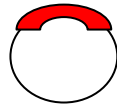
Homologous Ca(II) ATPase – PDB ID 1EUL

# Preparation of CopB

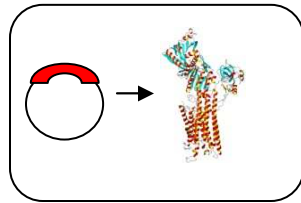
*copB* gene



*E. coli*  
expression  
plasmid



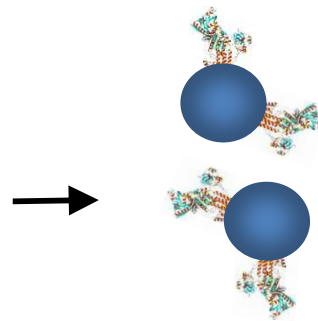
CopB protein  
expression  
in *E. coli*



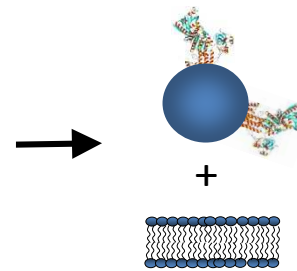
Affinity  
chromatography  
to isolate  
CopB protein



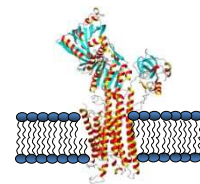
- The *copB* gene from *Archaeoglobus fulgidus* has been isolated using the polymerase chain reaction (PCR)
- The *copB* gene has been inserted into a plasmid for expression in *E. coli*
- CopB is being expressed in *E. coli* and purified using an affinity tag
- CopB containing vesicles will be fused with lipid bilayers



Purified CopB  
in vesicles



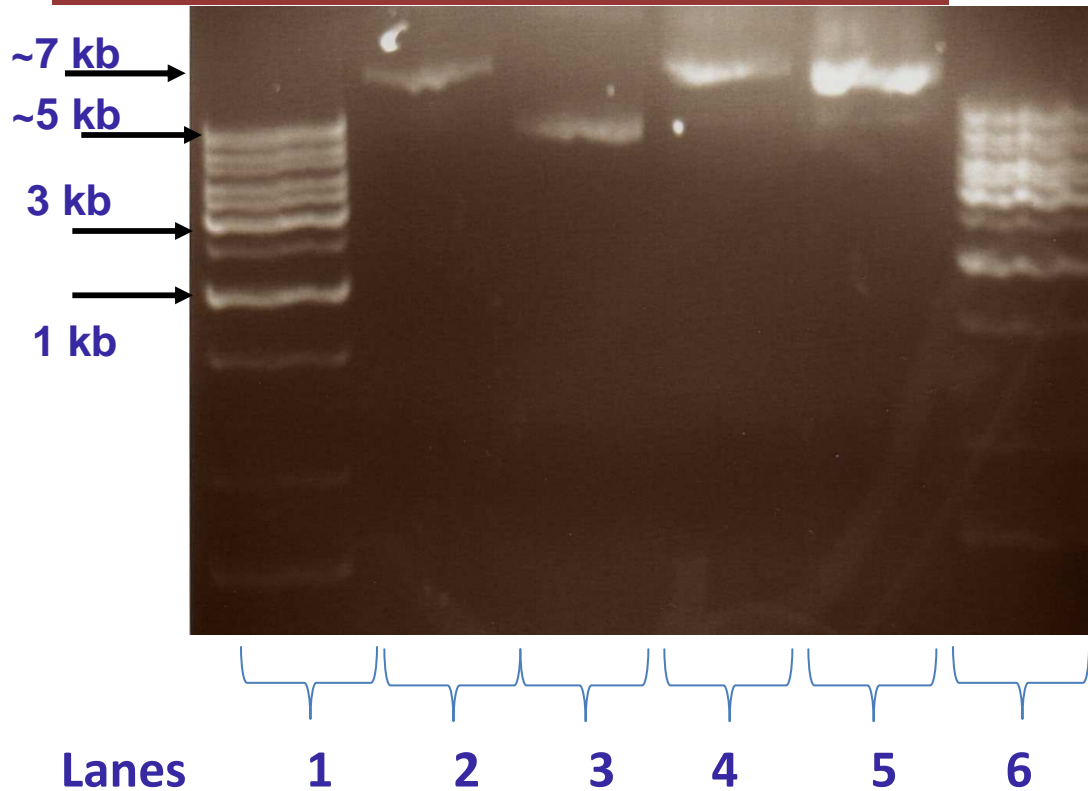
Fusion of vesicles  
and lipid bilayer



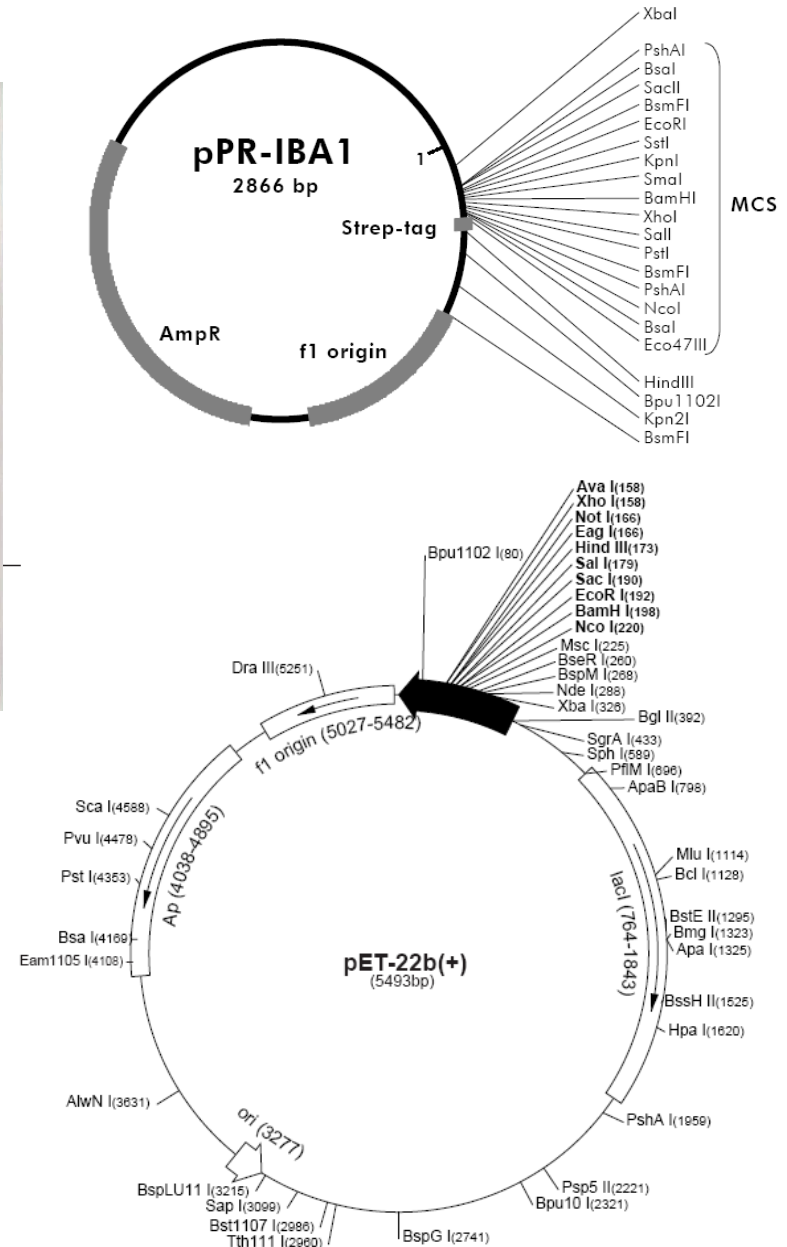
CopB  
incorporated in  
lipid bilayer



# Preparation of full length CopB plasmids (pET-22b, pPR-IBAI)



- Lane 2 – pET22b(+)-CopB without Tag (7kb).
- Lane 3 – pPR-IBAI-CopB with Strep Tag (5kb)
- Lane 4 – pET22b(+)-CopB with Strep Tag (7kb)
- Lane 5 – pET22b(+)-CopB with His tag (7kb)
- Lanes 1 & 6 GeneRuler 1kb DNA ladder



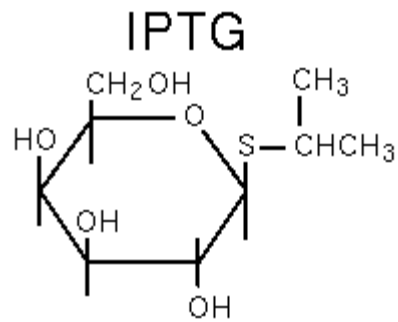
# Purification protocol for CopB

- Transformation of the plasmid/vector into ROSETTA competent cells (for unusual codons)
- Pre-culture in LB (Luria-Bertani) media with ampicillin.
- Culture in 1L LB media with ampicillin (dil 1:100), shaking at 37 ° C until O.D.(600 nm) =1.
- Induce overexpression with IPTG (0.5mM), allow cell growth overnight.
- Harvest cells at 10 000 rpm /10 min/4°C.
- 5g Frozen wet cells (ROSETTA) to be resuspended with 30 ml 'Buffer A' containing 25 mM Tris-HCl (pH 7.0), 100 mM sucrose, 1 mM PMSF (freshly added) and other protease inhibitor.
- Add lysozyme 10mg/ml incubate 30 min RT
- Break cells with French press (3 to 5) times, 12, 000 psi.
- Centrifuge at 9,000 rpm for 30 min at 4°C in rotor SL 50T in sorvall super T21 centrifuge.

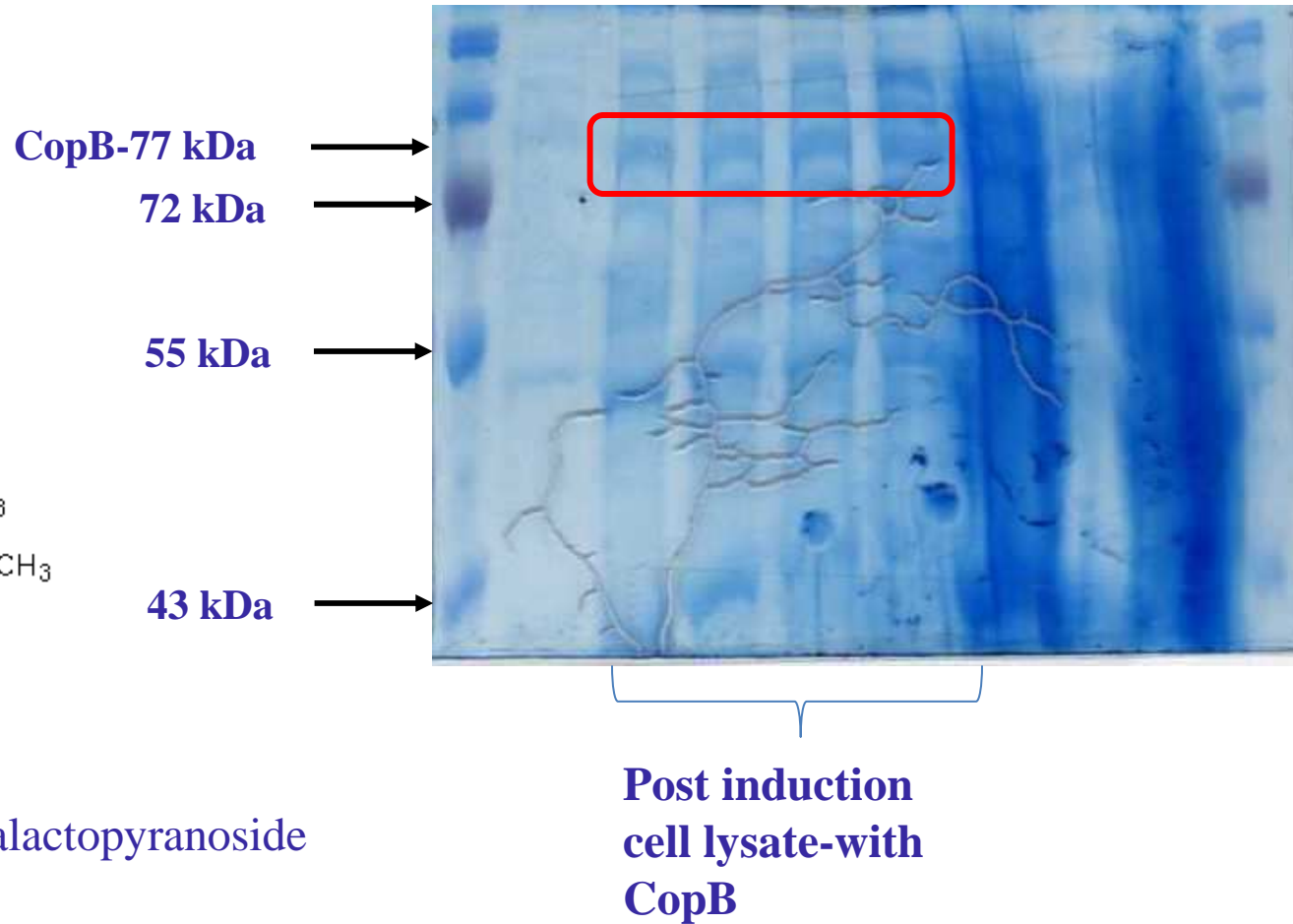
# Purification protocol for CopB

- Pour the supernatant into clean 26 ml Beckman ultracentrifuge tube. Fill the tube with “Buffer A” and centrifuge at 33,000 rpm in Beckman rotor 50.2Ti for 1 hr at 4°C in Beckman ultracentrifuge L8-70.
- Discard the supernatant. Pour 10 mls “Buffer A” into the centrifuge tube, resuspend by using glass rod.
- Transfer the membrane to the glass hand homogenizer (keep it in ice all the time). Wash the centrifuge tube once more with 1 ml of “Buffer A” and transfer to the homogenizer.
- Homogenize the protein by 5 strokes with Teflon coated piston in glass hand homogenizer.
- Transfer the protein to the 15 ml falcon tube.
- Estimate the protein by Bradford reagent with BSA as standard (see protocol for protein estimation).
- Store at -20°C until further use. Run sample on Strep/His Column

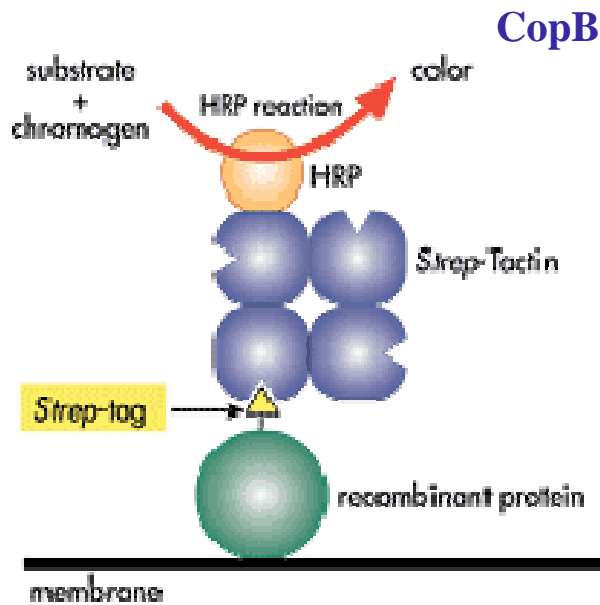
# Expression of CopB upon induction with IPTG



Isopropyl  $\beta$ -D-1-thiogalactopyranoside



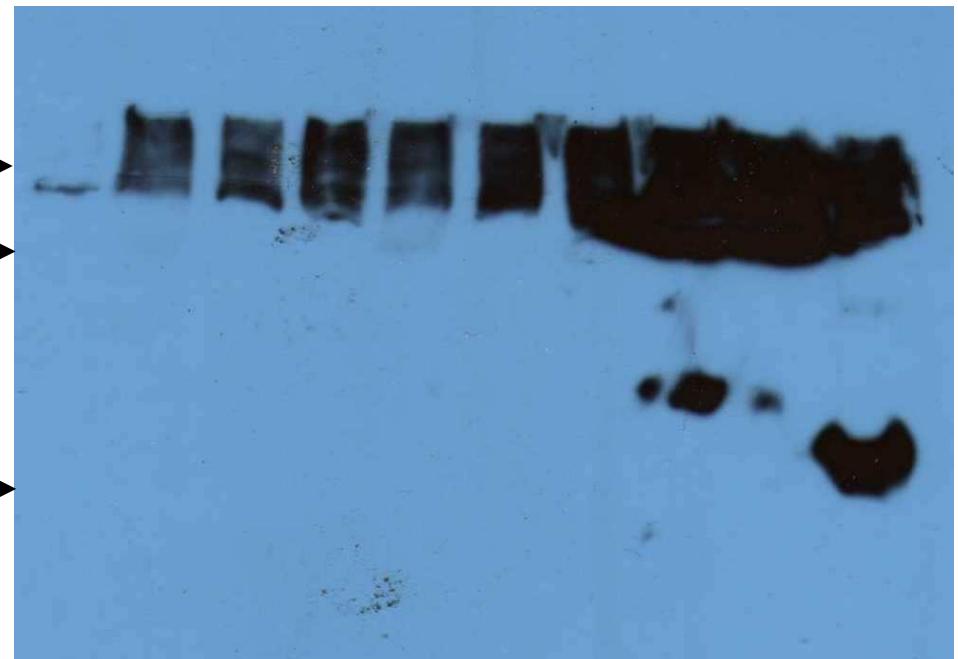
# Western blot detection of CopB solubilized in Detergent (DDM) using Strep-tactin HRP conjugate



CopB-77 kDa

45 kDa

10 kDa



Lanes

2-7

8 & 9

10

Lane 2 – 7 CopB with Strep-Tag (77 kDa).

Lane 8, 9 – Positive control CusB with Strep-Tag (45kDa)

Lane 10 – Positive control CusE with Strep-tag (10kDa)

# Future Directions

- Characterization of various potential substrates for lipid bilayer formation such as GaAs, Ge.
- Attachment of lipid bilayers to tethered semiconductor surfaces.
- Purification scheme has to be optimized so as facilitate the solubilization of protein in detergent.
- CopB with Poly Histidine tag is being expressed and will be subject to purification trials using Cobalt/Nickel affinity chromatography
- Homogenous transporter protein to be incorporated into bilayer and imaged using AFM.

# Acknowledgements

- Science Foundation Arizona
  - Strategic Research Group
- SRC/Sematech
  - Engineering Research Center for Environmentally Benign Semiconductor Manufacturing
- The University of Arizona Honors College
  - Undergraduate Research Grant Program

# Planarization Long Range Plan

February 2008



UNIVERSITY AT ALBANY  
State University of New York



*SRC/Sematech Engineering Research Center for Environmentally Benign Semiconductor Manufacturing*



# Team

- PIs:

- A. Philipossian (UA)
- D. Boning (MIT)
- S. Raghavan (UA)
- V. Manno (Tufts)
- C. Rogers (Tufts)
- R. White (Tufts)
- A. West (Columbia)

- Other Researchers:

- L. Borucki (Araca)
- Y. Zhuang (UA)
- F. Sudargho (UA)

- Other Researchers (cont'd):

- J. Cheng (UA)
- S. Theng (UA)
- E. Paul (Stockton College)

- Advisory Committee

- P. Fischer (Intel)
- M. Moinpour (Intel)
- L. Economikos (IBM)
- C. Spiro (Cabot)
- C. Borst (U at Albany)
- Y. Moon (AMD)

## Team (cont'd)

- Ph. D. Candidates:

- A. Muthukumaran (UA)
- Y. Sampurno (UA)
- T. Sun (UA)
- H. Lee (UA)
- X. Wei (UA)
- C. Gray (Tufts)
- J. Vlahakis (Tufts)
- W. Fan (MIT)
- K. Shattuck (Columbia)
- A. Meled (UA)

- M. S. Candidates:

- N. Braun (Tufts)
- D. Gauthier (Tufts)
- J. Johnson (MIT)

- Undergraduate Students:

- G. Steward (UA)
- R. Dittler (UA)
- Z. Li (MIT)

# Next Five Years

- Landscape:
  - Research, fundamental in nature yet industrially relevant, addressing the technological, economic and environmental challenges of planarizing:
    - Copper
    - Tantalum and other advanced barrier materials
    - Dielectrics (STI CMP with ceria slurries & FA – pads, and ILD CMP relating to barrier polish)
    - New materials and structures (relating to new memory devices)

# Next Five Years

- Gaps to be Filled:

- Processes & consumables for:

- Advanced processes and consumables for planarization
- Electrochemically assisted planarization
- Post-planarization cleaning and surface preparation

ALWAYS KEEP THE BIG PICTURE IN MIND

**... YIELD IS EVERYTHING ...**

environmental and economic losses resulting from lower yields  
are far greater than any gains realized through  
consumables reduction and incremental process tweaks

# Advanced Processes & Consumables for Planarization

- Focus:

- Basic scientific investigations of the controlling processes in planarization of advanced materials over several length scales and levels of complexity
- Development of validated, science-based descriptions that relate specific planarization process and material attributes (including material micro-structure) to measurable process outcomes

- **Specification and testing of environmentally-conscious process and material alternatives for rapid feedback into the planarization design process**

# Advanced Processes & Consumables for Planarization

- Objectives

- Real-time detection and modeling of pattern evolution

- Develop novel force-spectra endpoint detection methods by determining how various wafer and pad surface states during polish affect the frictional energy in particular frequency bands
- Relate these signals to details of the wafer topography evolution by integrating pattern evolution models with the above endpoint or diagnostic signal analysis

- Effect of pad grooving on process performance

- Empirical and numerical investigation of the effect of various pad designs (materials, groove shapes and dimensions) as well as different types of slurries on RR, COF and pad temperature for copper and tantalum CMP
- Identification and verification of optimal pad designs for technology transfer to 300-mm platforms

# Advanced Processes & Consumables for Planarization

- Objectives (continued)

- Wear phenomena and their effect on process performance
  - Isolate, quantify and model the processes that determine how nanoparticles, pads, diamonds, retaining rings and wafers interact with one another in representative systems and how these interactions evolve with extended use.
  - Develop methods to visualize and measure local wafer-pad mechanical interactions using confocal microscopy, UV-enhanced fluorescence, laser-induced fluorescence and micro-machined shear stress sensors
- Fundamental limits of topography control
  - Development & characterization of consumables to modulate removal rate selectivity, dishing and erosion for 'n + 1' and 'n + 2' technology nodes

# Advanced Processes & Consumables for Electrochemically Assisted Planarization

- Focus and Objectives:

- Development and implementation of a ‘full’ process that includes clearing of copper & planarization of the barrier (i.e. tantalum) layer. ‘Full’ process may include post-processing steps such as oxide planarization or buff steps.

- **Novel chemistries** to enhance and control electrochemical removal and passivation of copper, tantalum and ruthenium
- **Modeling and characterization** of tool, pad and wafer interactions for design and control (particularly endpoint detection) are needed to minimize process cost and environmental impact



# Advanced Processes & Consumables for Electrochemically Assisted Planarization

- Objectives

- **Cu – ECMP bath chemistries**

- Determination of planarization capabilities of electrolytes including optimization of operating conditions such as applied pressure, voltage treatment, and additive concentration
    - Develop a fundamental understanding of feature-scale planarization mechanisms, including mathematical models

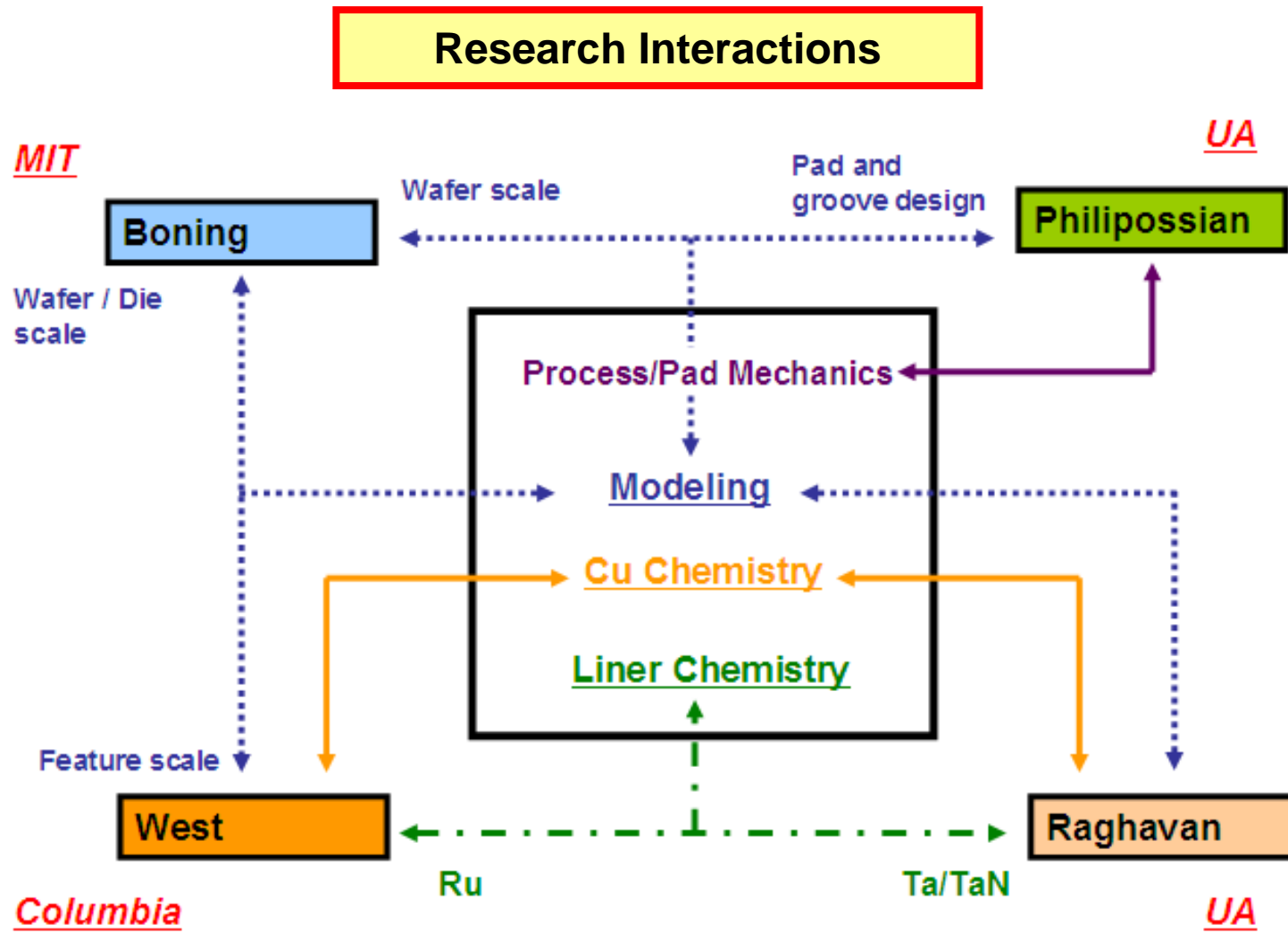
- **Ru – ECMP bath chemistries**

- Investigation of electrolytes, including studies of the effect of pH and voltage treatment on removal rates
    - Studies of chemistry optimization to enhance liner/Cu selectivity

- **Post – ECMP clean chemistries**

- Develop cleaning formulations for the removal of inhibitor films that may form by electro-oxidation on metal films
    - Develop strategies for the removal of scratches formed on metal films due to contact with pad electrode (anode)

# Advanced Processes & Consumables for Electrochemically Assisted Planarization



# Advanced Post-Planarization Cleaning Processes & Consumables

- Focus and Objectives:

- Fundamental study of the effects of brush (new and used) material and design on shear force, creep, rebound and cleaning efficiency of insulator and metal films

- **Novel surface mechanical testing methodologies** to perform cyclic and incremental brush deformation measurements before and after extended wear to understand failure mechanisms
- **Design and use of novel tribometers** to study the frictional forces in post-planarization scrubbing
- **Modeling and characterization** of brush, cleaning fluid and wafer interactions within the realm of nano-lubrication theories

# Low Environmental Impact Fabrication of Gate Stack Structures

*(Task Number: Proposed Project)*

## PI:

- Anthony Muscat, Chemical and Environmental Engineering, UA

## Graduate Students:

- Shariq Siddiqui, MS candidate, Chemical and Environmental Engineering, UA
- Fee Li Lie, PhD candidate, Chemical and Environmental Engineering, UA

## Undergraduate Students:

- Genevieve Max, Chemistry and Computer Science, UA

## Other Researchers:

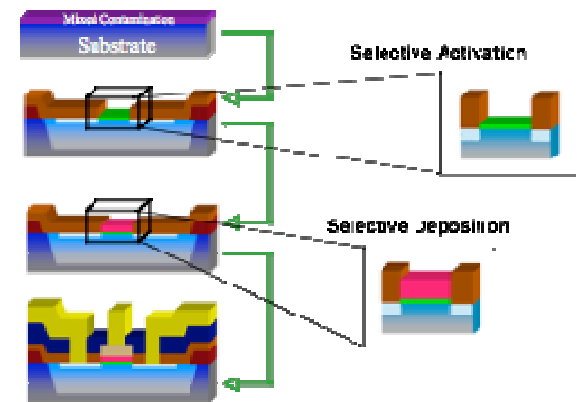
- Gary Fleming, Postdoctoral Fellow, Chemical and Environmental Engineering, UA

## Cost Share (other than core ERC funding):

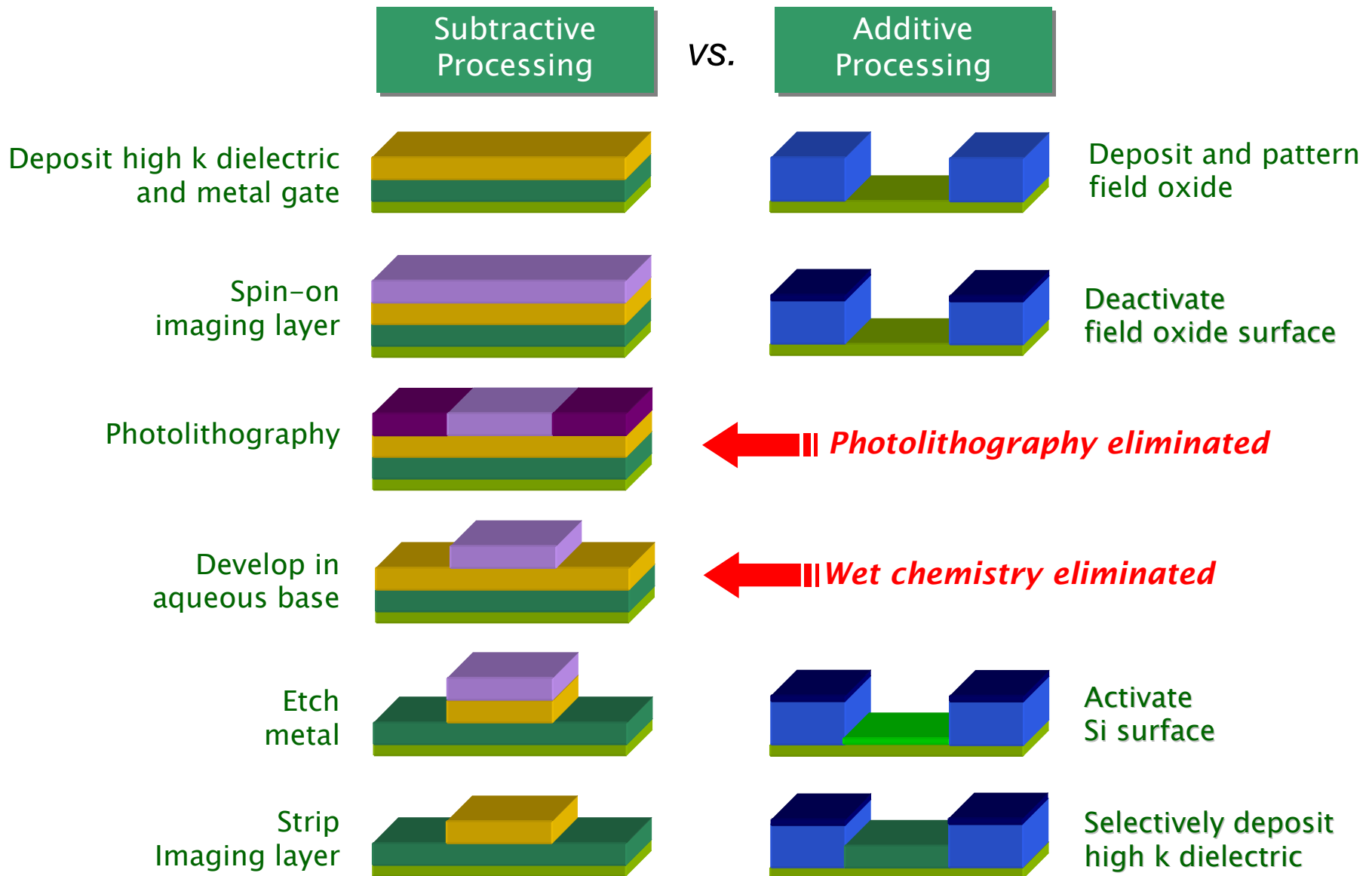
- \$25k from SEZ

# Objectives

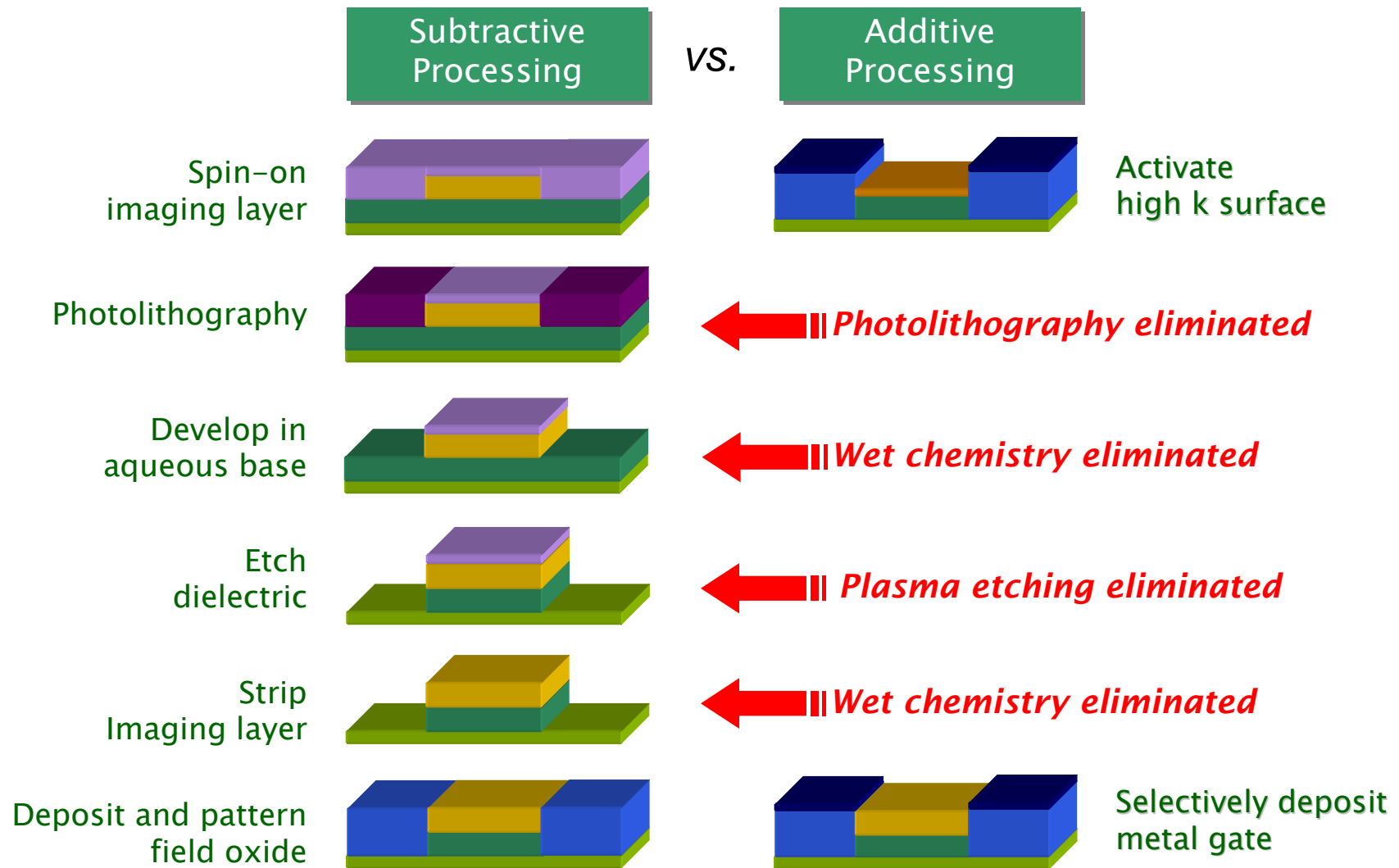
- **Develop low cost of ownership surface passivation and activation processes**
  - **Minimize water, energy, and materials use**
  - **Introduce cost effective processes into high-volume manufacturing**
- **Compare chemistries to clean and passivate advanced gate stack materials with minimal impact to high mobility substrates**
  - **Liquids leverage existing technology base**
  - **Gases provide ideal surface terminations**
- **Enable gate first process by selectively depositing high-k directly on Ge and III-V binary and ternary substrates**



# ESH Metrics and Impact: Self-aligned High k Gate Stack



# ESH Metrics and Impact: Self-aligned High k Gate Stack



Reduce processing steps & Minimize ESH impact

*SRC/SEMATECH Engineering Research Center for Environmentally Benign Semiconductor Manufacturing*

# Methods and Approach

1. Use gas phase chemistries to create ideal surface terminations
2. Generate fundamental data sets containing adsorption, desorption, and reaction rate parameters to compare liquid and gas phase processes
3. Build process models to transfer to tool and device companies in order to assess the viability of integrating new steps into existing manufacturing processes

---

## Current Projects

Ge(100) surface prep and high-k deposition

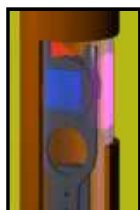
InAs(100) surface prep and high-k deposition

GaAs(100) surface prep

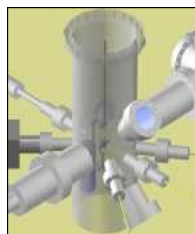
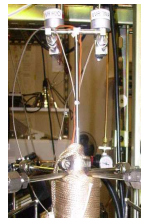


# Clustered Reactor Apparatus

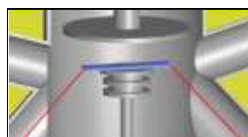
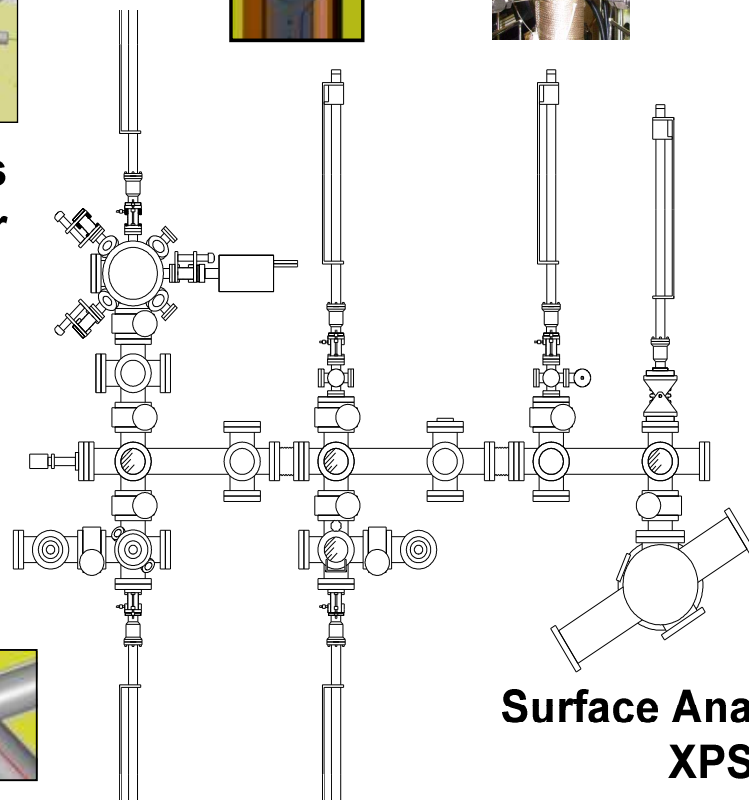
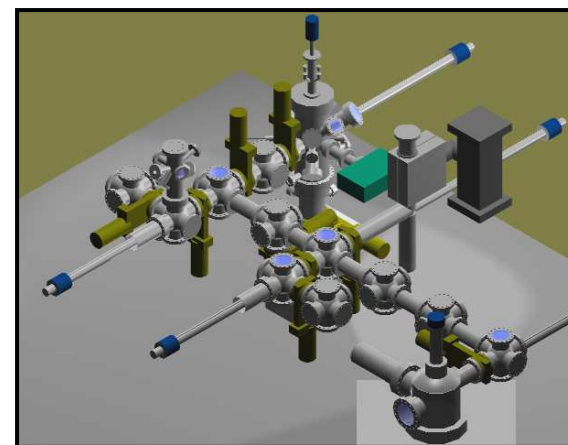
**Photoreactor**  
UV-Cl/NH<sub>3</sub>



**ALD Reactor**  
Al<sub>2</sub>O<sub>3</sub>, HfO<sub>2</sub>



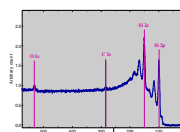
**TPD Analysis Chamber**



**Gas phase HF Reactor**

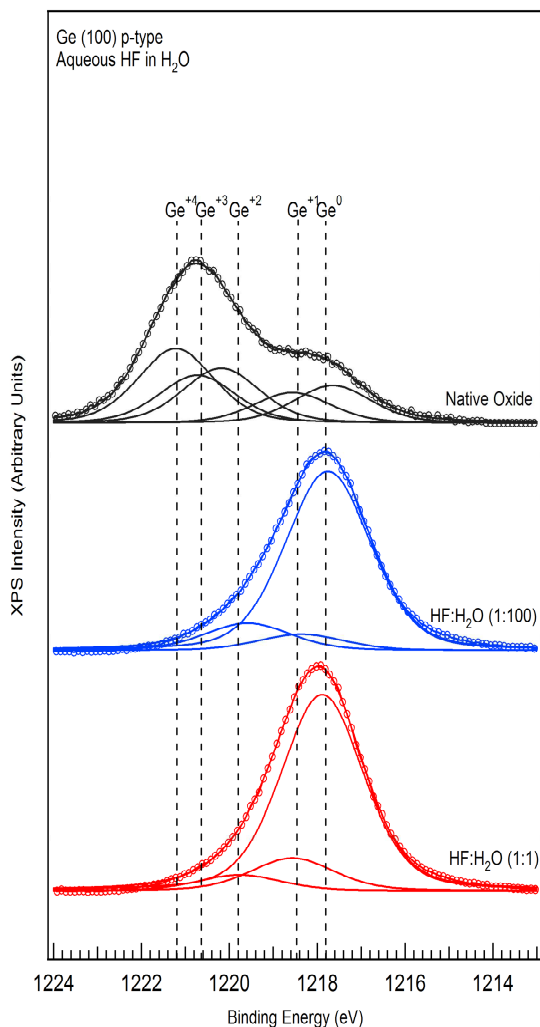
**Sample Loading**

**Surface Analysis Chamber**  
XPS - AES

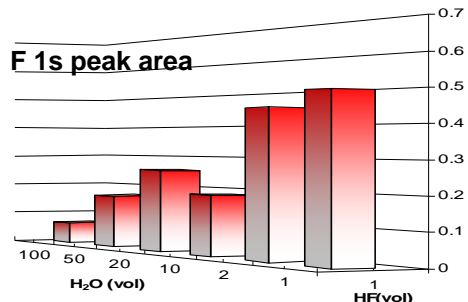
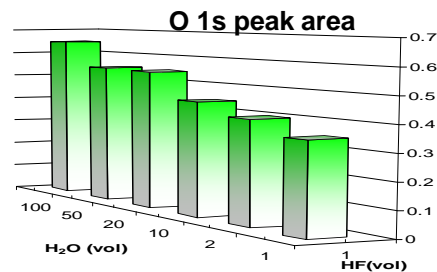
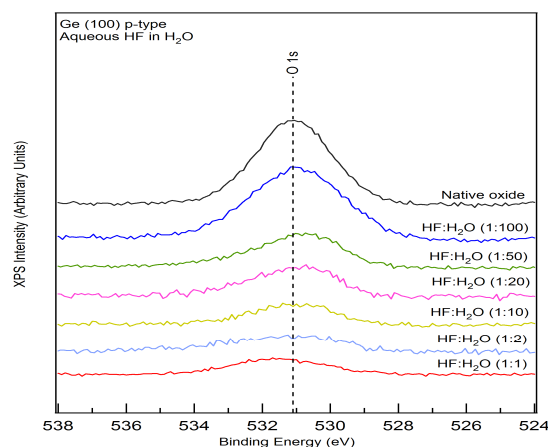


# Ge Oxide Removal: Liquid Phase HF

High Resolution XPS Ge 2p<sub>3/2</sub>

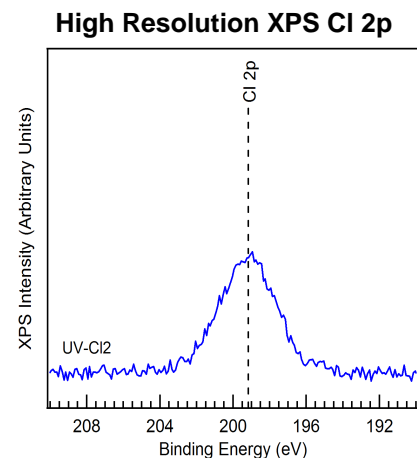
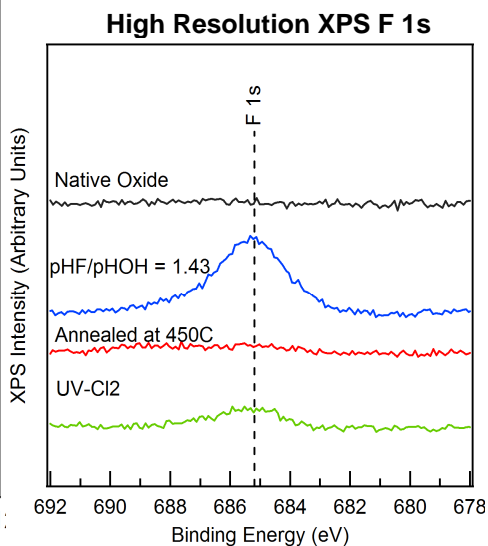
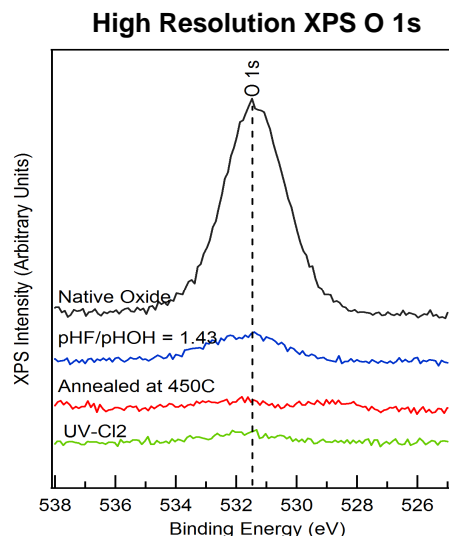
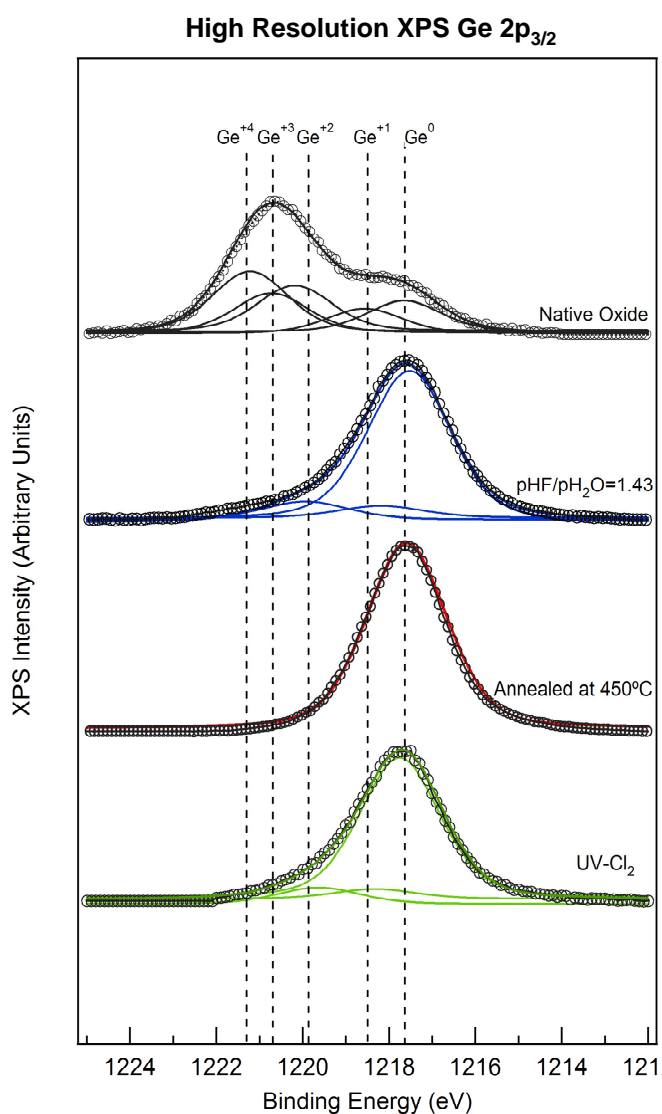


High Resolution XPS O 1s  
RT, etching time = 5 min



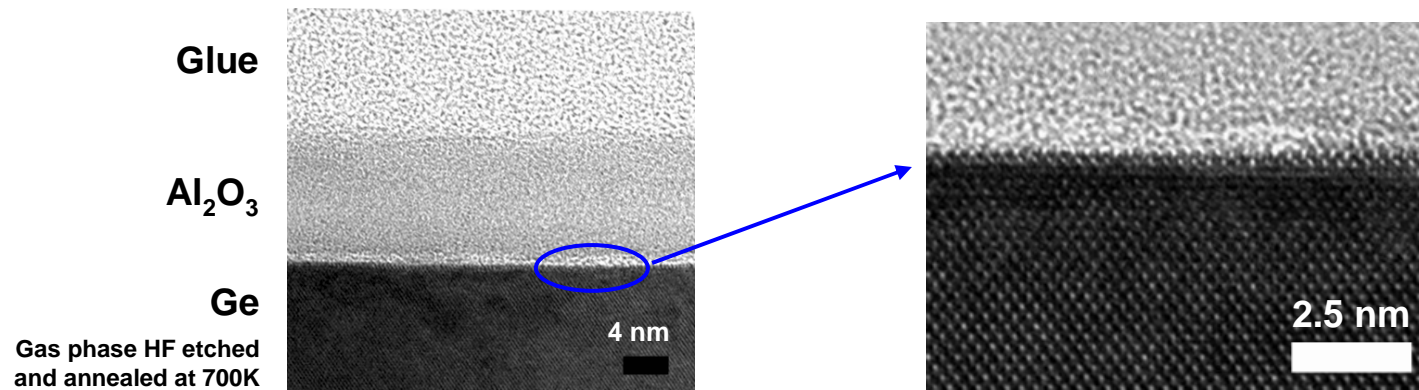
- Ge 2p<sub>3/2</sub> XPS peak showed GeO<sub>2</sub> and GeO are dominant native oxides
- Aqueous HF did not completely remove oxide layer
- O 1s peak gradually decreased and F 1s peak increased with increasing HF concentration
- Smallest O peak was obtained at HF:H<sub>2</sub>O (1:1) solution

# Ge Oxide Removal: Gas Phase HF & UV-Cl<sub>2</sub>



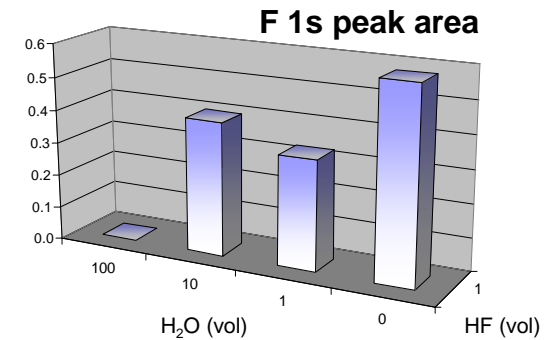
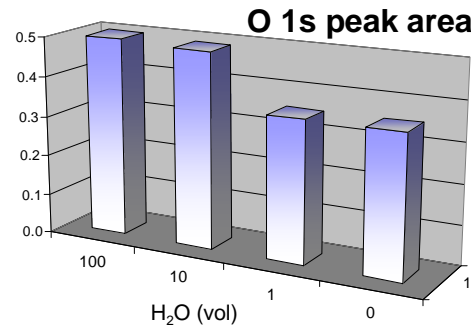
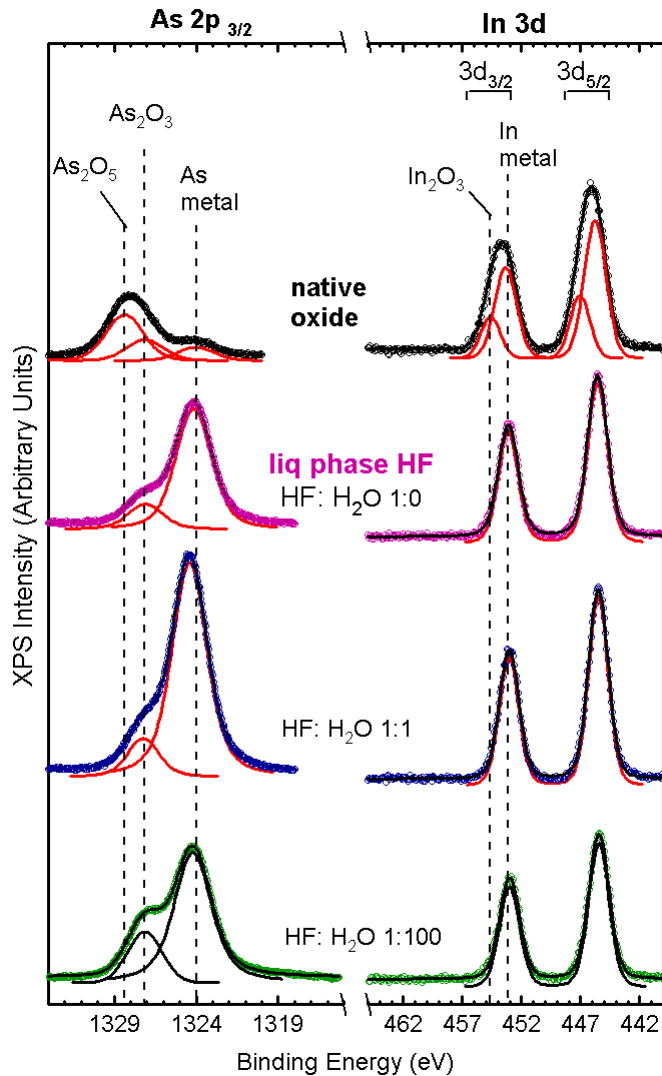
- Gas phase offers a way to create an idealized surface termination
- HF/vapor exhibited better removal of GeO<sub>x</sub> on Ge (100) than liquid
  - Removal of GeO<sub>2</sub> and Ge<sub>2</sub>O<sub>3</sub> controlled using partial pressures of HF and water
- Highest oxide removal was achieved at higher partial pressures of HF and H<sub>2</sub>O
- UV-Cl<sub>2</sub> replaced O and F on the surface
- Chlorine terminated surface is achieved after UV-Cl<sub>2</sub> process

# Direct Deposition of Al<sub>2</sub>O<sub>3</sub> on Ge(100)



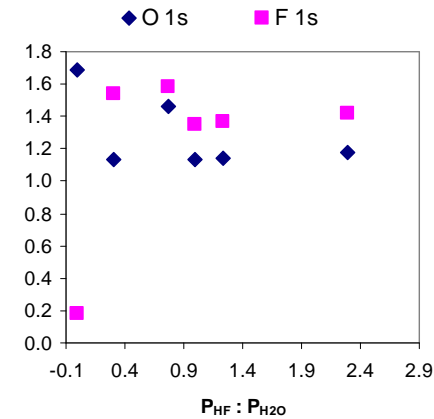
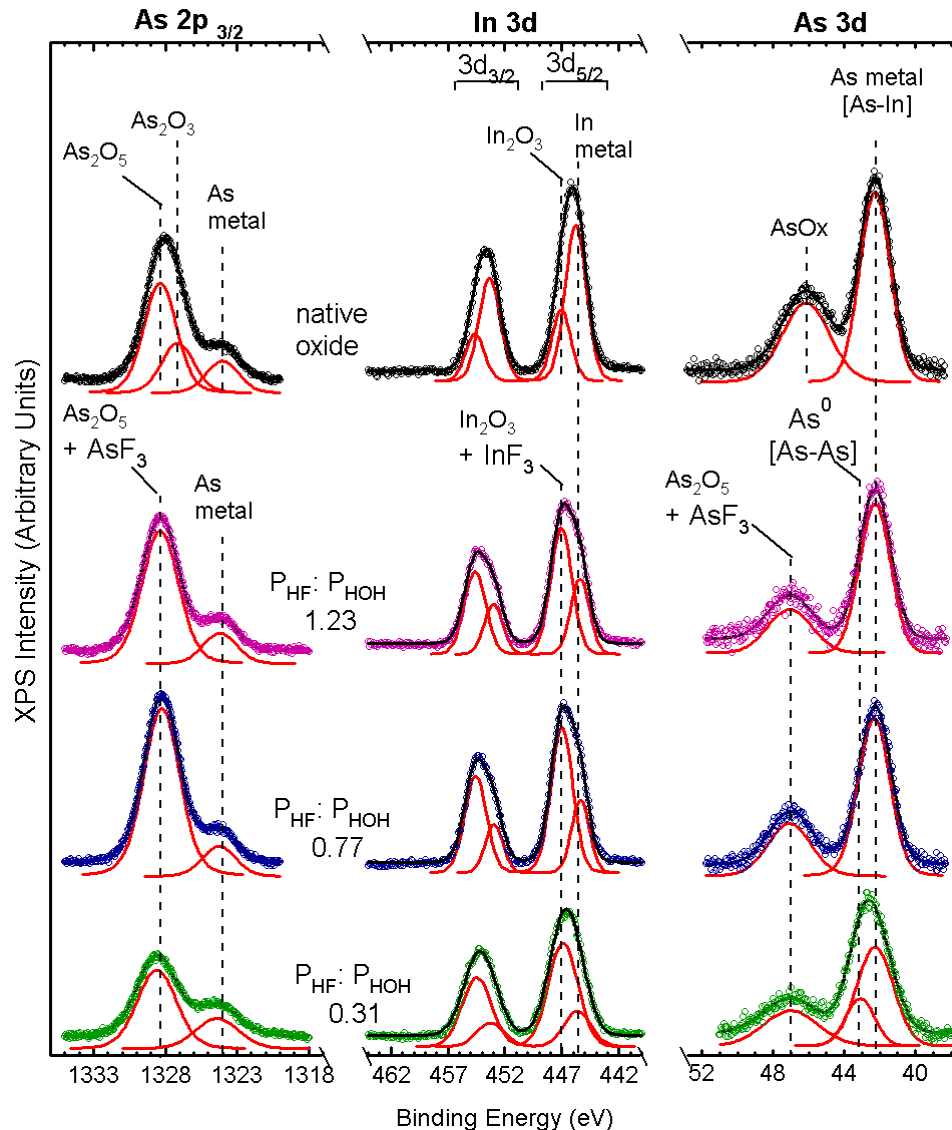
- H<sub>2</sub>O pulse followed by TMA pulse
- Obtain controlled growth of Al<sub>2</sub>O<sub>3</sub> on Ge using atomic layer deposition
- A 0.8 nm interfacial layer observed between Ge substrate and uniform a- Al<sub>2</sub>O<sub>3</sub>

# InAs Oxide Removal: Liquid Phase HF



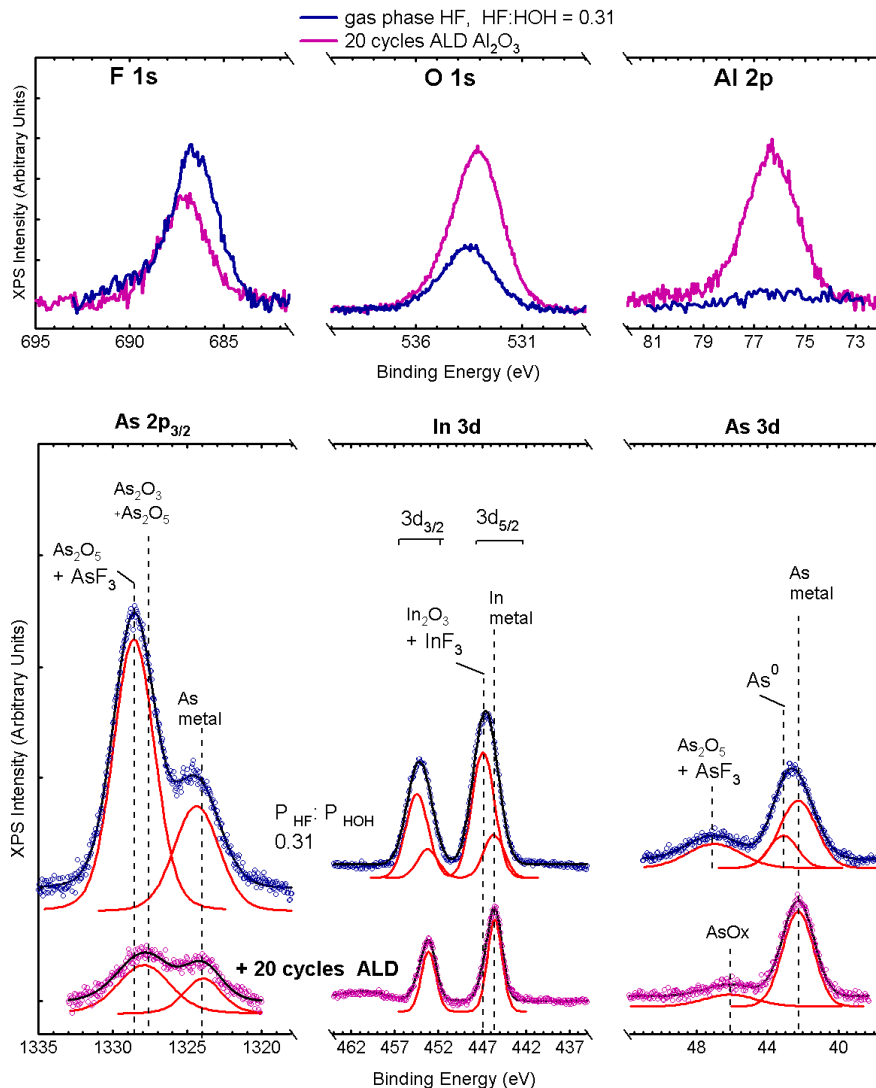
- Native oxide comprised of As<sub>2</sub>O<sub>3</sub>, As<sub>2</sub>O<sub>5</sub> and In<sub>2</sub>O<sub>3</sub>
- Selective etching of In<sub>2</sub>O<sub>3</sub> and As<sub>2</sub>O<sub>5</sub>
- Residual oxide consists of As<sub>2</sub>O<sub>3</sub>
- Higher HF concentration resulted in higher oxide removal
- As 3d spectra (not shown) of sample etched with HF:H<sub>2</sub>O 1:0 and 1:1 showed the presence of elemental As

# InAs Oxide Removal: Gas Phase HF



- Complete removal of As<sub>2</sub>O<sub>3</sub>
- Etching product consists of AsF<sub>3</sub> and InF<sub>3</sub>
- Lower HF concentration results in higher oxide removal and lower F residue
- Highest oxide removal achieved at P<sub>HF</sub>:P<sub>H<sub>2</sub>O</sub> 0.31 with elemental As observed

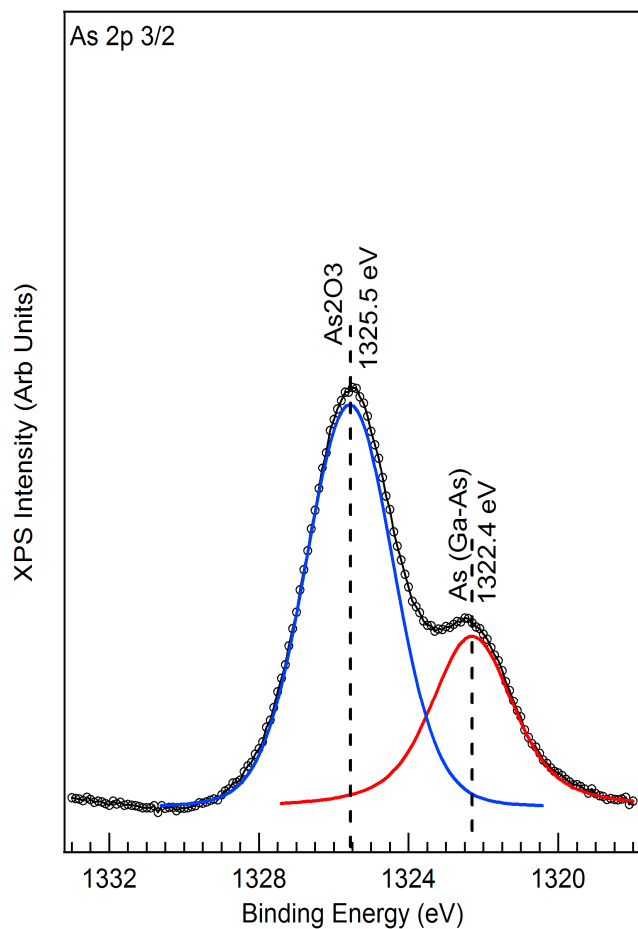
# InAs Atomic Layer Deposition of Al<sub>2</sub>O<sub>3</sub>



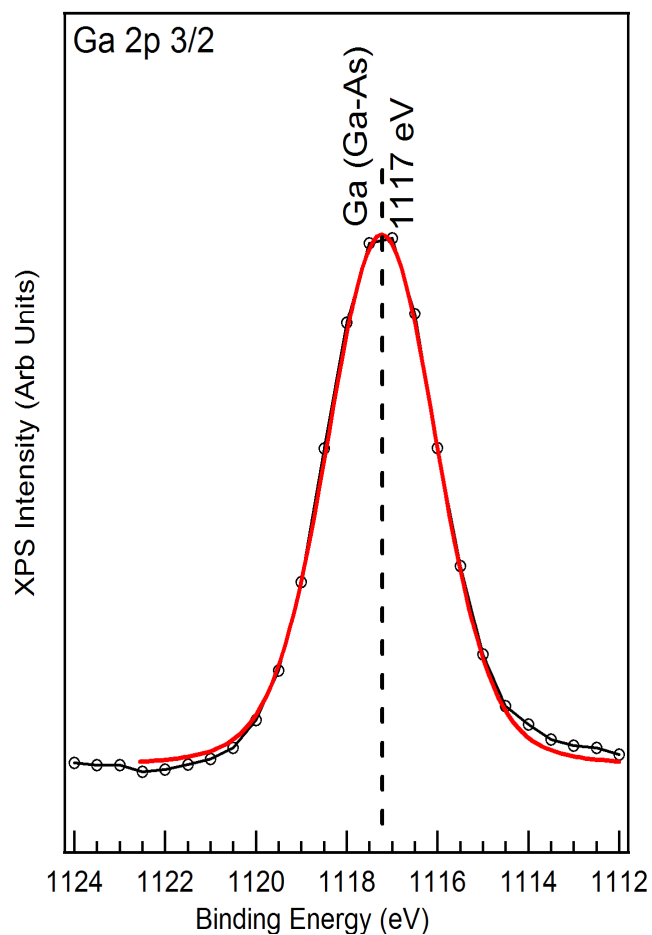
- Demonstrate atomic layer deposition (ALD) of Al<sub>2</sub>O<sub>3</sub> on gas phase etched InAs(100)
  - Precursors : Al(CH<sub>3</sub>)<sub>3</sub> and H<sub>2</sub>O
  - Growth rate 1.08 Å/cycle
- HR-XPS of Al<sub>2</sub>O<sub>3</sub> film shows interfacial reaction between surface species and ALD precursors
  - Removal of In<sub>2</sub>O<sub>3</sub> and InF<sub>3</sub>
  - Removal/conversion of elemental As and AsF<sub>3</sub> to As<sub>2</sub>O<sub>5</sub> and As<sub>2</sub>O<sub>3</sub>
  - Preferential bonding of O to Al

# GaAs Oxide Removal: Gas Phase HF

High Resolution XPS As 2p<sub>3/2</sub>



High Resolution XPS Ga 2p<sub>3/2</sub>



•No Ga oxides present in Native Oxide Scan.

•1322.4 eV = As (GaAs)

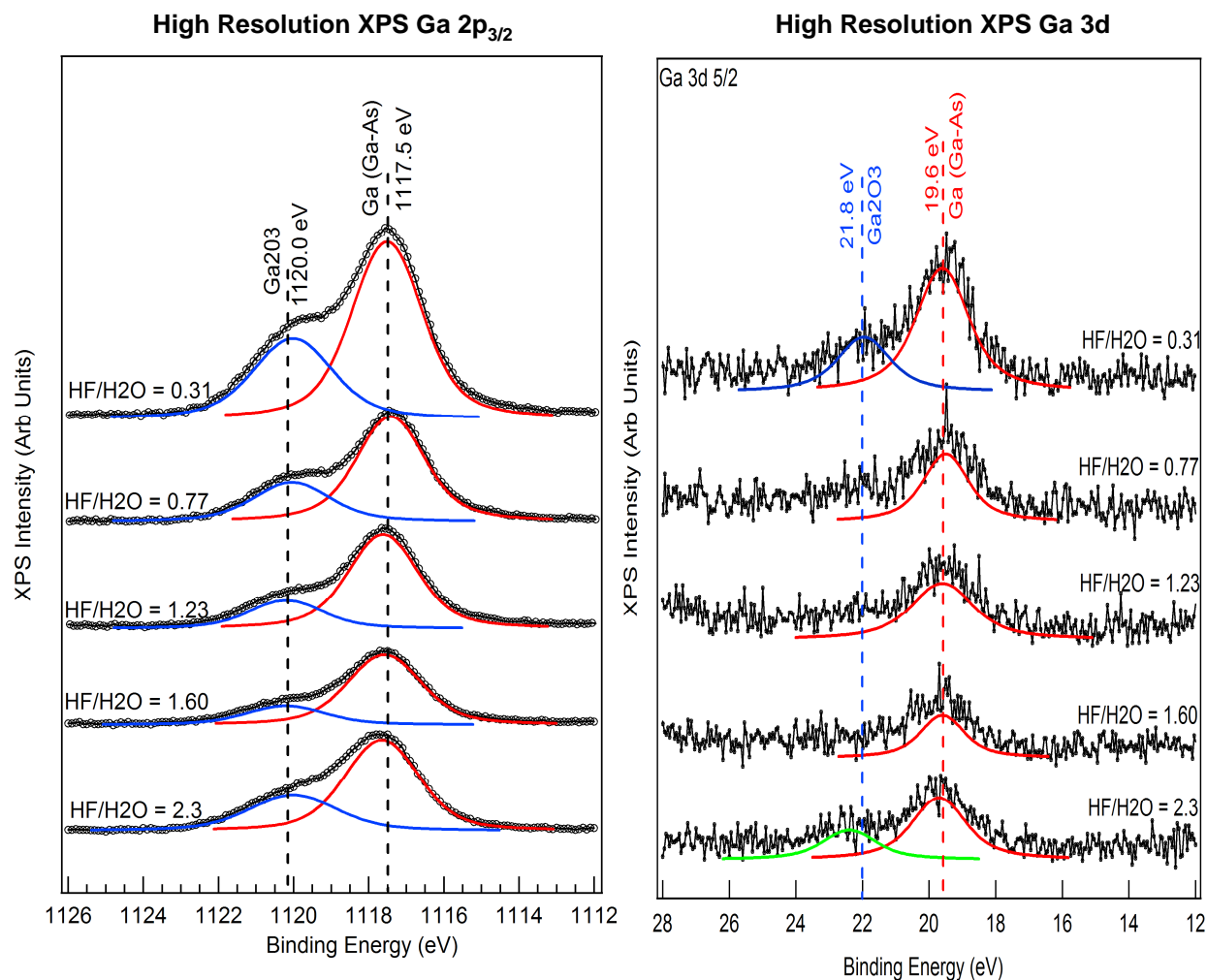
•1325.6 eV = As<sub>2</sub>O<sub>3</sub>

•No As<sub>2</sub>O<sub>5</sub> present in native oxide

*Surf. Interface Anal.* 2005; 37: 673–682



# GaAs Oxide Removal: Gas Phase HF



Surf. Interface Anal. 2005; 37: 673–682

- Ga 2p<sub>3/2</sub> shows presence of signals at 1117 eV (GaAs) and 1120 eV (Ga<sub>2</sub>O<sub>3</sub>)

- With increasing in  $p\text{HF}/p\text{H}_2\text{O}$  ratio = decrease in 1120 eV peak until a ratio 2.23 is reached.

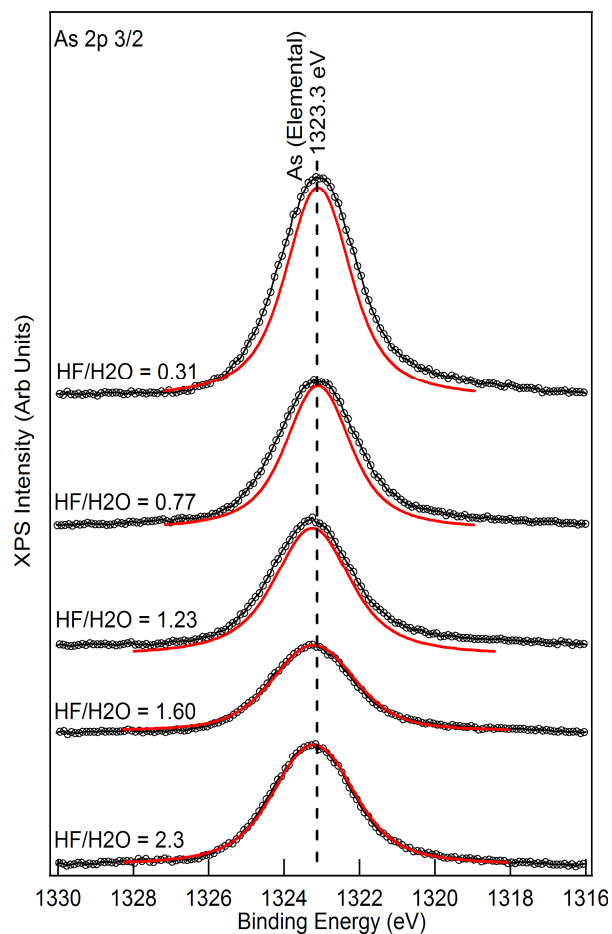
- Ga 3d bulk shows presence of signals at 19.6 eV (GaAs) and 21.8 eV (Ga<sub>2</sub>O<sub>3</sub>)

- With increasing in  $p\text{HF}/p\text{H}_2\text{O}$  ratio = decrease in 1120 eV peak until a ratio of 2.3 is reached.

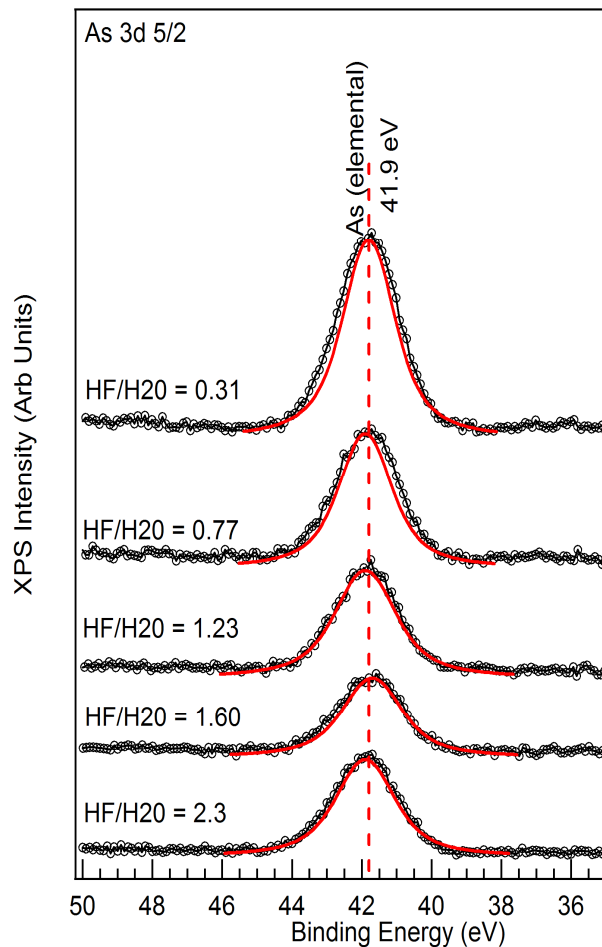
- At  $p\text{HF}/p\text{H}_2\text{O}$  ratio = 2.3 shift to high BE in 21.8 eV peak noticeable. Possibly due to the presence of Ga-F.

# GaAs Oxide Removal: Gas Phase HF

High Resolution XPS As 2p<sub>3/2</sub>



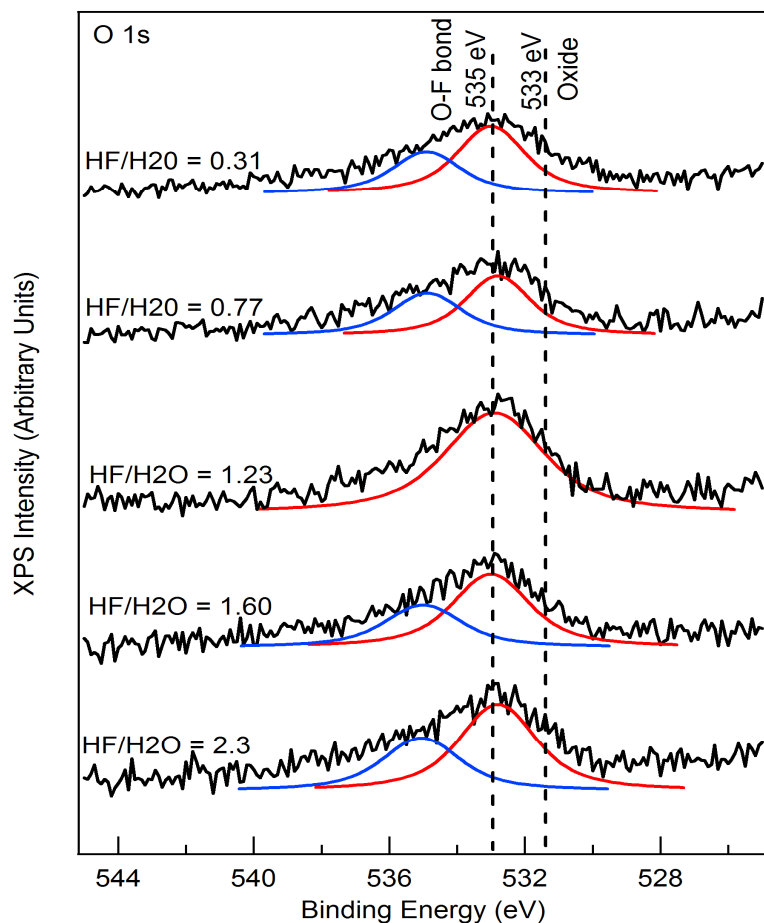
High Resolution XPS As 3d



- As 2p<sub>3/2</sub> = 1323 eV = As (elemental). As 3d<sub>5/2</sub> = 41.9 eV = As (elemental).
- No bulk or surface As oxides present. Gas-phase HF etching completely removes the oxides from the surface.

# GaAs Oxide Removal: Gas Phase HF

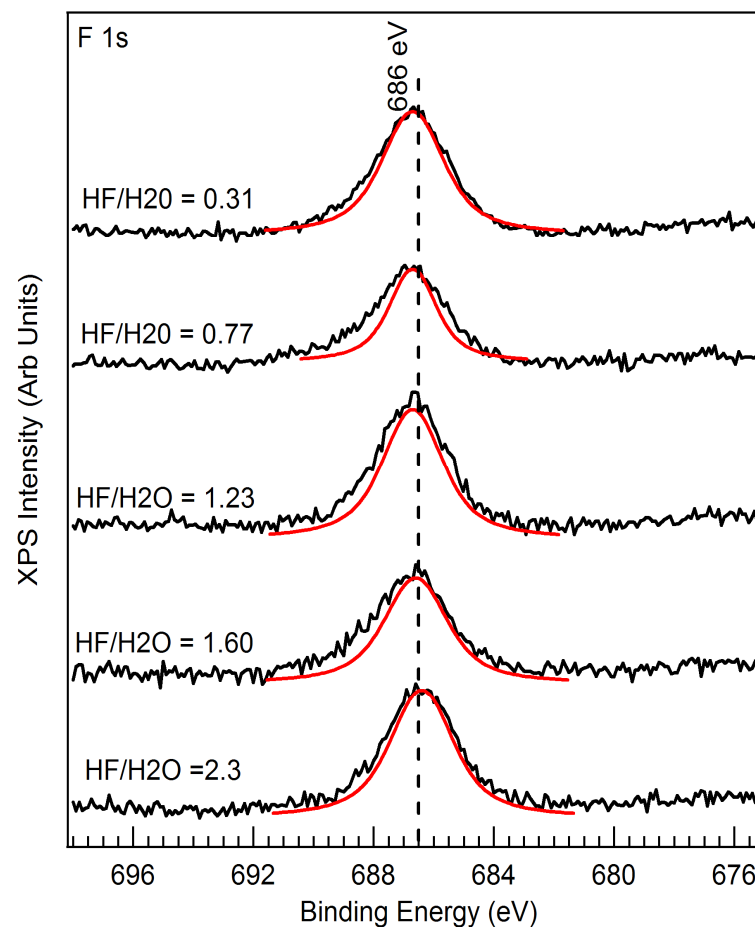
High Resolution XPS O 1s



O 1s (Oxide) = 533 eV

O-F = 535 eV

High Resolution XPS F 1s



Increase in HF/H<sub>2</sub>O ratio =  
Constant F on surface at 686 eV

# Industrial Interactions and Technology Transfer

- **Project updates to IMEC**
  - **Marc Meuris**
  - **Valentina Terzieva**
- **Project updates to SEZ**
  - **Harald Okorn-Schmidt**
  - **Jeremy Klitzke**

# Future Plans

## Next Year Plans

- **Compare native oxide removal from Ge and III-V using conventional and nonconventional liquid and gas phase processes**
- **Demonstrate atomic layer deposition of high k material on Ge and III-V materials**
- **Characterize high-k/substrate interface properties**

## Long-Term Plans

- **Correlate surface preparation method and interfacial properties of high k material/substrate to device electrical performance**

# New Planarization Proposal

## Effect of Retaining Ring Geometry on Slurry Flow and Pad Micro- and Macro-Texture

**Prof. Philipossian ...** 1 Ph.D. student for Year – 1, Year – 2 and Year – 3 at UA

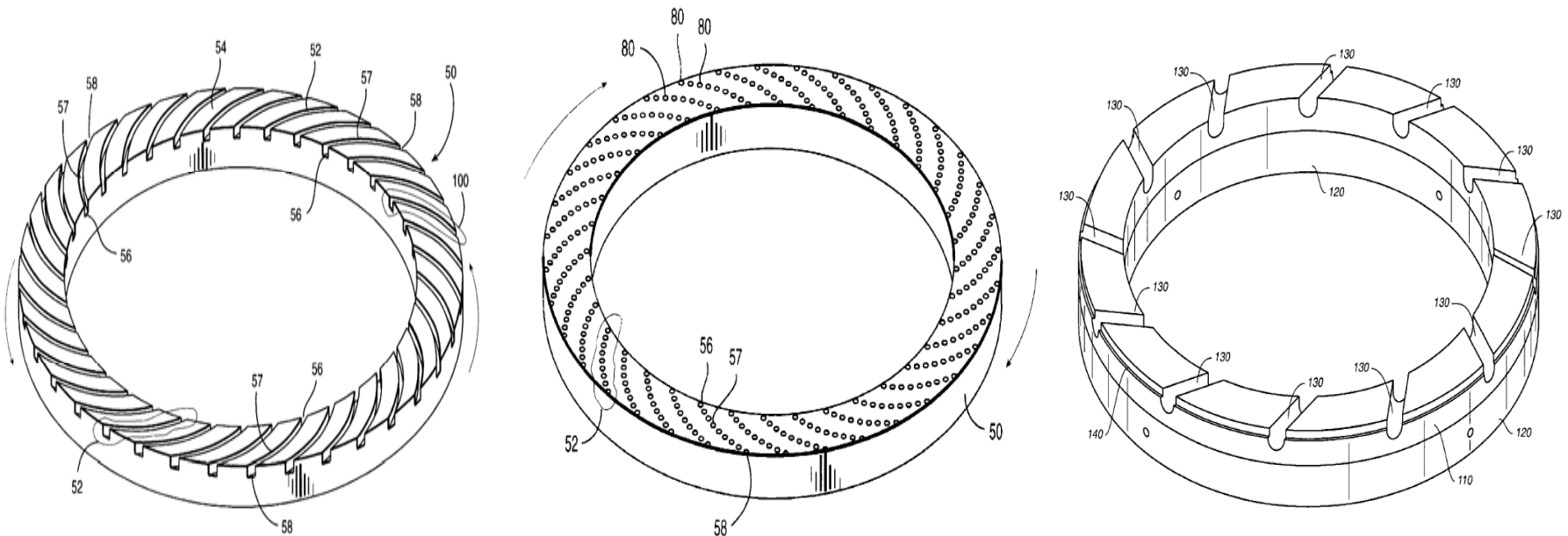
**Prof. Boning ...** 1 Ph.D. student for Year – 2 and Year – 3 at MIT (Year – 1 activities at MIT will leverage resources from already-funded ERC projects)



February 2008

# Problem Statement

- Slurry consumption continues to be one of the main drivers in CMP EHS and COO
- Patent literature claims that retaining rings with different geometric designs (like those shown below) can affect slurry transport in the pad-wafer region, however a systematic study of their slurry transport characteristics has not yet been undertaken



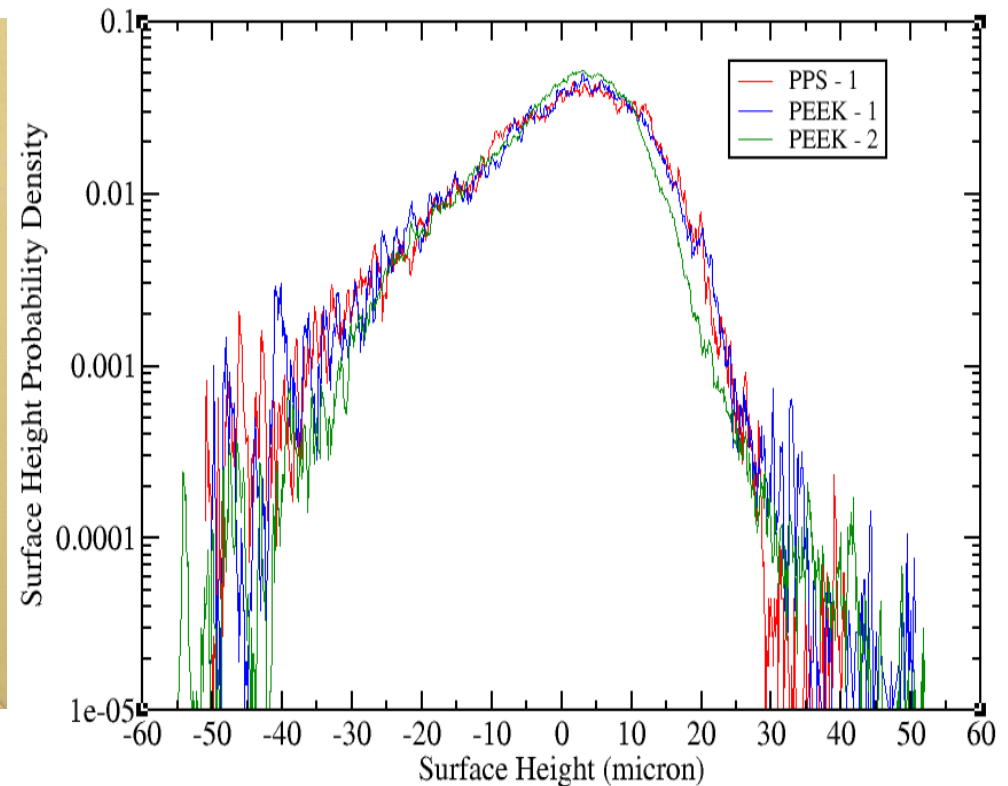
## Problem Statement (continued)

- There is evidence that retaining rings with different designs affect pad micro-texture differently
  - ✓ PEEK and PPS rings with Design – 1 result in wider pad asperity height distributions compared to a PEEK ring with Design – 2
  - ✓ This may suggest that planarity can be affected by ring geometry



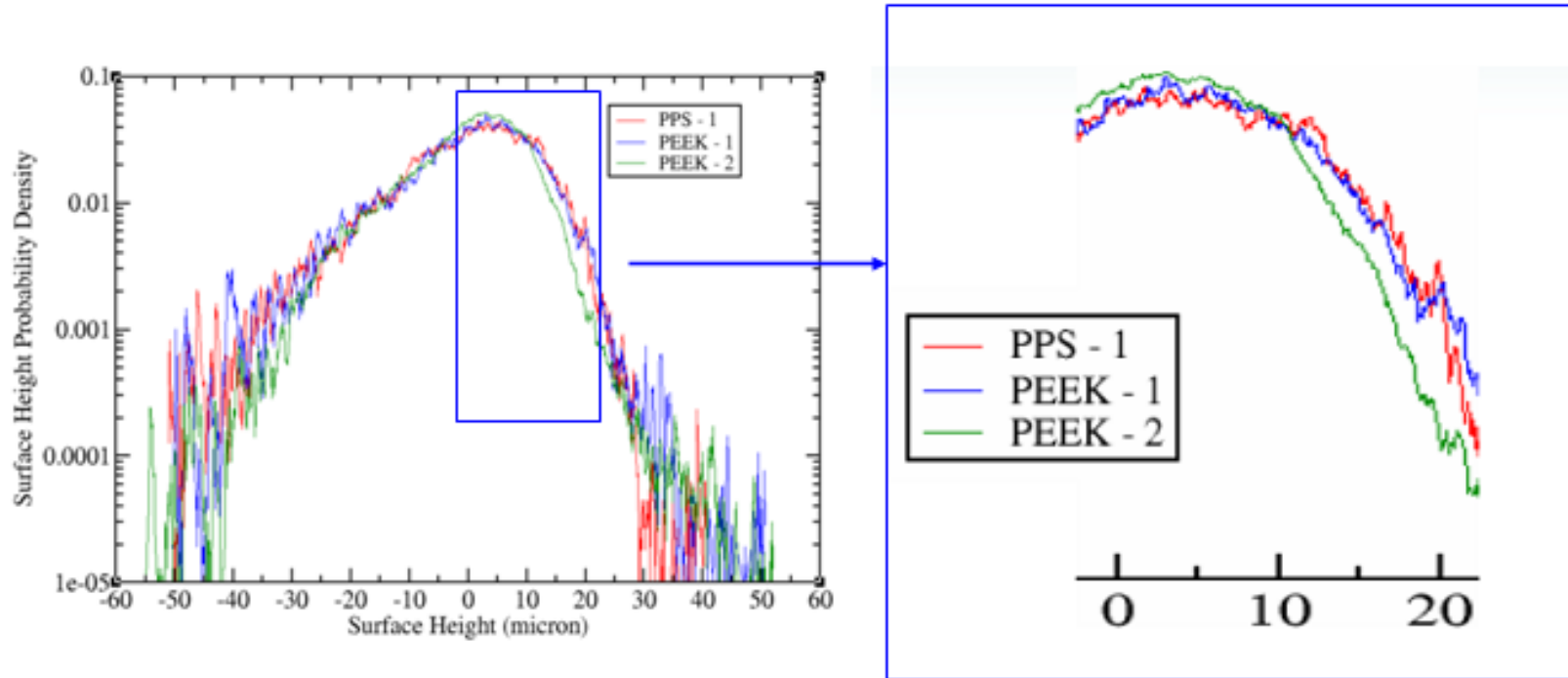
Design – 1

Design – 2





## Problem Statement (continued)



The PEEK – 2 ring achieves a narrower pad surface height distribution than the PPS – 1 and PEEK – 1 rings, suggesting that the slot design and the edge rounding plays significant roles in shaping the pad micro texture.

# Objective

- **Objective:**
  - ✓ Determine how slurry transport in the pad-wafer region is affected by various retaining ring slot angles, concentric pad groove designs, slurry flow rates and polisher kinematics
  - ✓ Determine how above ring geometric parameters affect pad asperity height distributions (i.e. micro-texture) and pad profile (i.e. macro-texture)
  - ✓ **Relate (experimentally and numerically) pad micro-texture and macro-texture to planarity**
  - ✓ Define novel retaining ring geometries that minimize slurry use yet provide superior polish performance

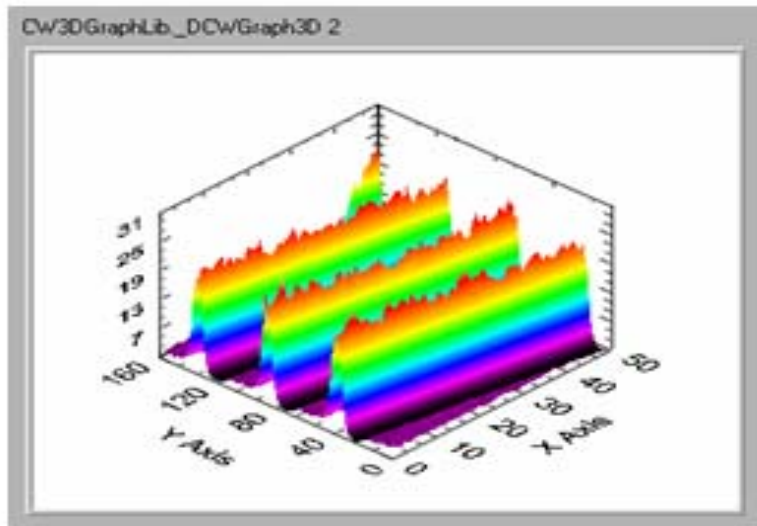
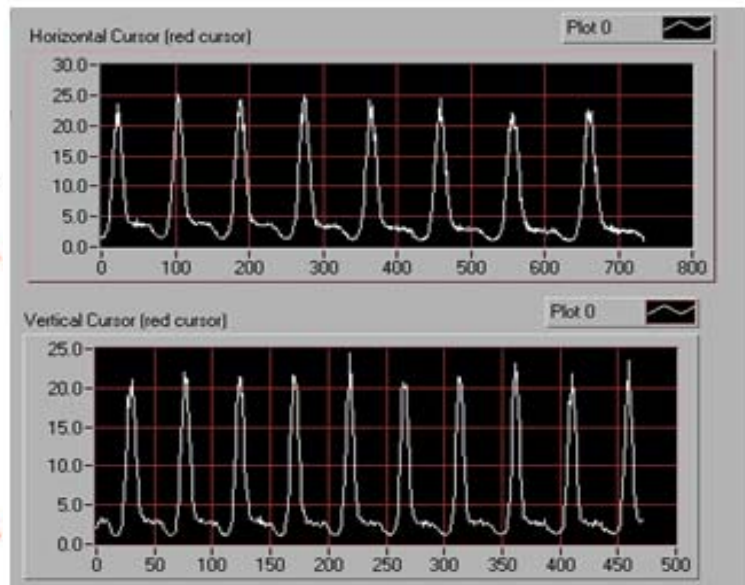
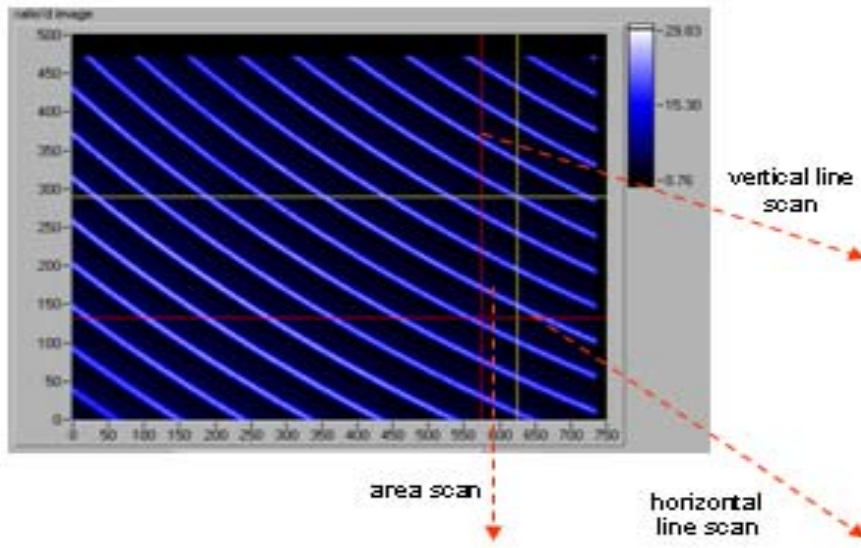
# Approach

- **General Approach:**

- ✓ **Work with a retaining ring manufacturer and a pad grooving outfit and make PEEK rings and pads with various designs**
- ✓ **Use dual emission UV-enhanced fluorescence (DEUVEF) on a 200-mm platform fitted with a special quartz wafer and retaining ring assembly to quantify slurry mean residence time and film thickness in the land areas as a function of ring, pad and process (see next page)**



# Approach (continued)

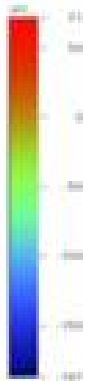
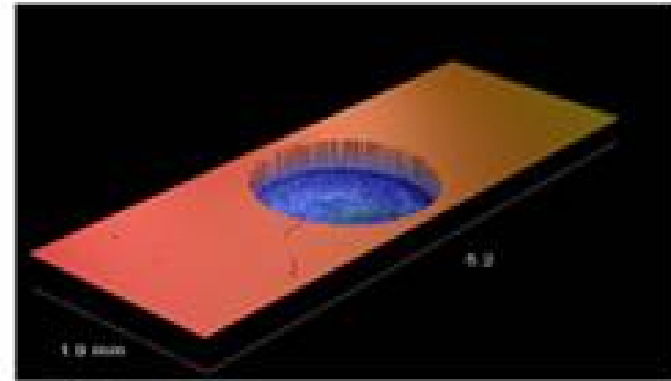
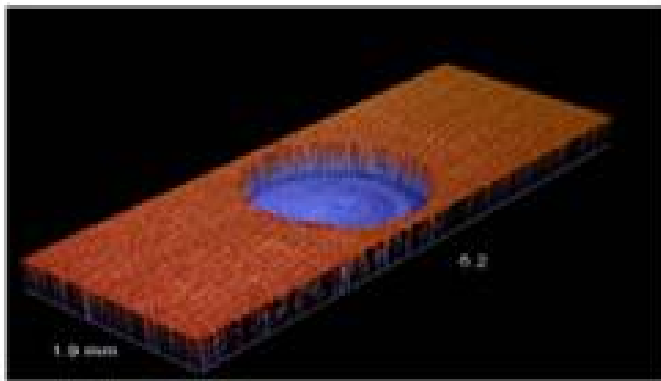


## Approach (continued)

- Perform land-area slurry film thickness tests and residence time distribution (RTD) tests (using slurry spiked with fluorescent dyes) with multiple types of pads and retaining rings at various:
  - ✓ Velocities
  - ✓ Flow rates
  - ✓ Pressures
- Analyze results using traditional RTD reactor design methodologies to determine mean residence time and dispersion number for each combination of parameters

## Approach (continued)

- Perform extended wear tests on each retaining ring (on 300-mm STI and copper processes)
  - ✓ Determine pad temperature, COF & variance of shear force as a function of wear time
  - ✓ Accurately determine wear rate using white light interferometry before (left) and after (right) the 6-hour wear test on shallow trenches machined on the land areas of the ring
  - ✓ Determine pad asperity height distribution using white light interferometry, and determine pad wear profile using micrometry



# Perceived Technical & EHS Benefits

- Understanding how retaining ring design can influence slurry transport in the wafer-pad region can aid IC makers in optimizing rings that can:
  - ✓ Significantly reduce overall slurry consumption
  - ✓ Facilitate slurry transport into the wafer-pad region and by-product transport out of the wafer-pad region
- Micro-scale and macro-scale pad-ring interactions in CMP are not well understood
- For a given down force, the ring-slurry-pad shear force is 2 – 3X that of the wafer-slurry-pad shear force (i.e. pads are more prone to wear as a result of contacting the ring than contacting the wafer), hence pad life can be enhanced through novel ring design as well

## Perceived Technical & EHS Benefits

- For 300 – mm processes, polyurethane pads and retaining rings are similarly priced and tend to get replaced during the same pit stops thus exacerbating COO and EHS issues
- Early evidence suggesting an effect on pad micro-texture by differently designed rings may be properly exploited to yield optimum pad micro-textures (critical for achieving die-level topography module target specs) through improved ring design
- For 450 – mm process (*circa* 2015), holding the wafer in place during planarization will be a formidable task thus placing tremendous mechanical (in the shear and normal directions), thermal and slurry fluid dynamics responsibilities on the retaining ring

$$\bar{T} = \bar{T}_p + \Delta\bar{T}_f$$



# Perceived Technical & EHS Benefits

- ‘Bracing’ for 450 – mm processes ... reaction temperature (i.e. true wafer surface temperature) increases significantly as wafer size is increased ... surface temperature of the retaining ring will increase even more due to higher COF

Mean asperity contact tip pressure (next page)

Polisher geometry factor

Fraction of heat conducted to pad

$$\Delta \bar{T}_f = \frac{2\zeta(r_w, c_w) \bar{P}_a}{\sqrt{\pi \rho C_p \kappa} P} \frac{\gamma_p}{V^{1/2} \mu_k P V}$$

Pad thermal properties

COF

$\zeta = 0.197 \text{ m}^{1/2}$  (100-mm)  
 $\zeta = 0.281 \text{ m}^{1/2}$  (200-mm)  
 $\zeta = 0.344 \text{ m}^{1/2}$  (300-mm)  
 $\zeta = 0.402 \text{ m}^{1/2}$  (450-mm)

$$\zeta(r_w, c_w) = \frac{2c_w^{1/2}}{3\pi r_w^2} \int_{c_w - r_w}^{c_w + r_w} R \left\{ 2 \cos^{-1} \left[ \frac{(R^2 + c_w^2 - r_w^2)}{(2Rc_w)} \right] \right\}^{3/2} dR$$

# New Planarization Proposal

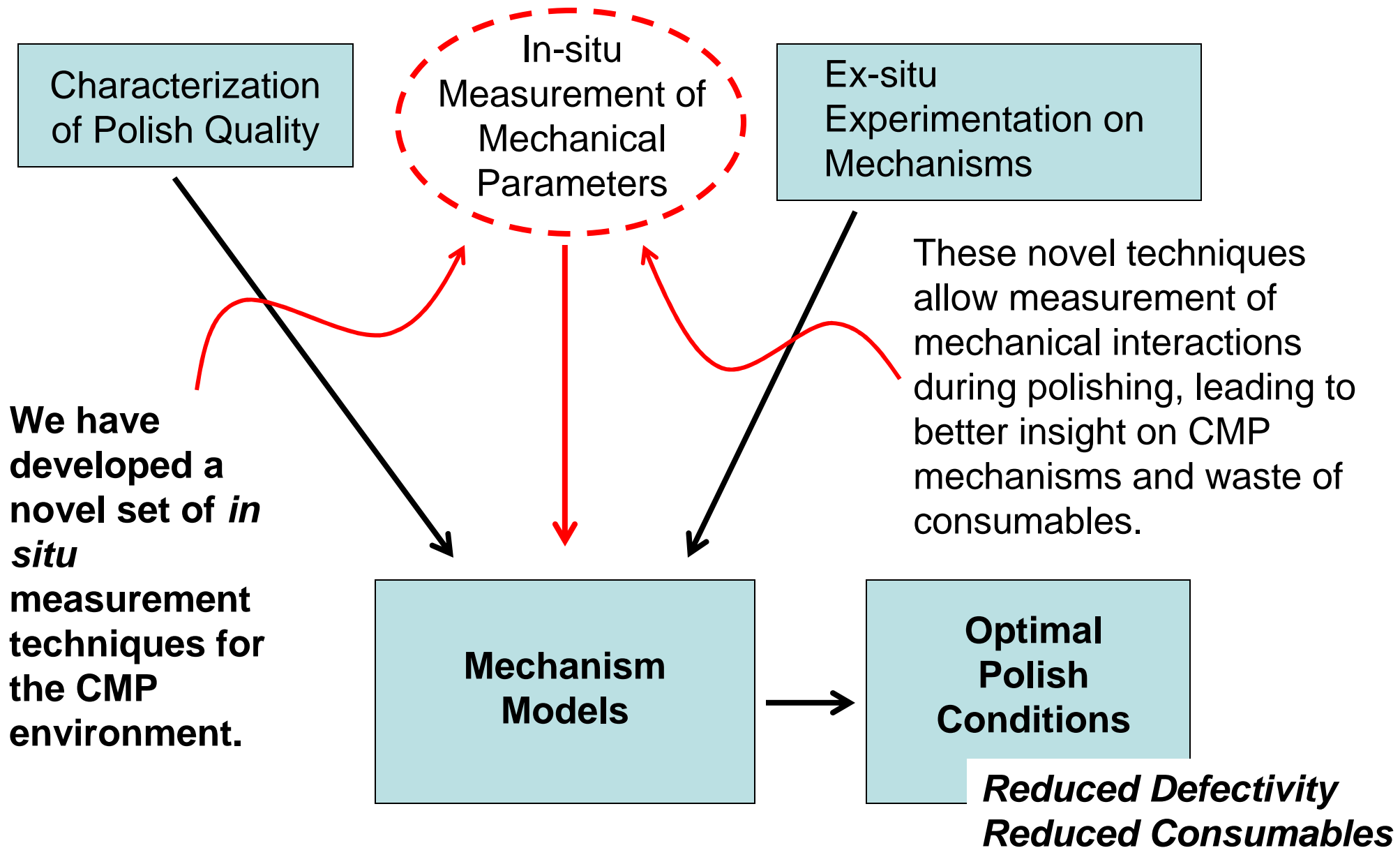
## Investigation of the Impact of Microscale Forces and Global Fluid Mechanics on Polish Defectivity and Consumable Use

Prof. Robert White, Prof. Chris Rogers,  
Prof. Vincent Manno



**February 2008**

# Concept



# Goals: Planarity

**Goal #1:** Reduce polish damage to fragile structures such as porous low-k dielectrics.

**Question #1:** Does reducing the microscale lateral forces by optimal choice of polish conditions, pad type, and conditioning reduce damage to fragile structures such as low-k dielectrics?

**Goal #2:** Reduce damage to patterned substrates .

**Question #2:** Point defects, scratches, dishing and erosion may be caused by mechanical expansion of the pad around nanoscale features. Thus, does increasing pad-wafer contact percentage by optimal conditioning and pad design reduce local normal forces, thereby reducing pad expansion around nanoscale features and reducing damage?

# Goals: Consumables

**Goal #3:** Reduce pad maintenance time and pad usage while maintaining polish quality.

**Question #3:** In production, pads may be changed early and often to avoid any possibility of loss of polish quality. Will in-process monitoring of microscale and macroscale forces, wafer attitude, and pad-wafer contact allow improved detection of pad end-of-life condition, resulting in reduced pad usage and tool down-time?

**Goal #4:** Reduce slurry consumption while maintaining polish quality.

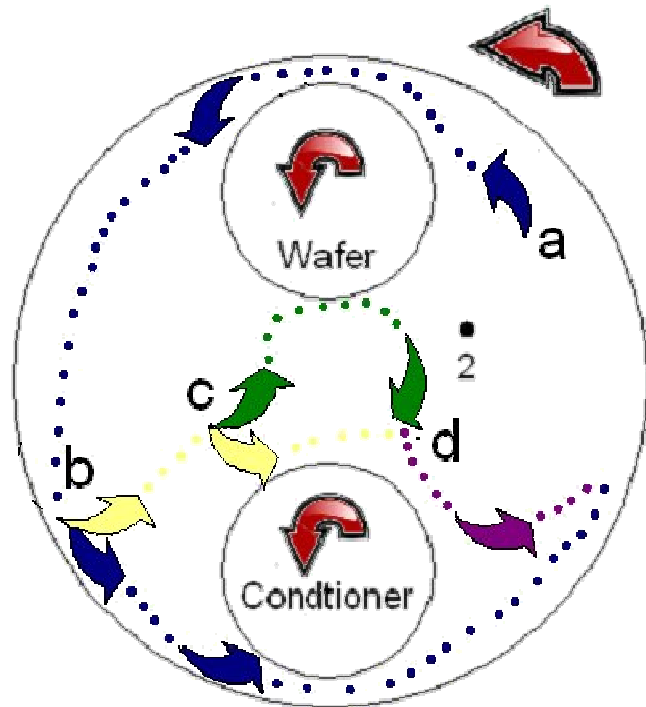
**Question #4:** Much of the slurry introduced to the pad may never interact with the wafer, and may be wasted. Can optimization of slurry introduction point, pad grooving, and rotation rate increase slurry usage, and therefore reduce the required slurry flow rate?

# Technical Approach: Platform

- **Deploy experimental techniques in a relevant system.**
  - Experimental techniques thus far have been developed and demonstrated on a small scale (75 mm substrate) polisher.
  - Deploy the techniques to a 200 mm polisher.
  - Move to dilute, colloidal silica slurries.
- **Use patterned substrates.**
  - Development work at Tufts thus far has focused on unpatterned substrates.
  - Move to patterned substrates to investigate mechanical and fluid effects near patterned structures:
    - Micron-scale patterns fabricated at Tufts.
    - Nano-scale patterns from industrial partners.

# Technical Approach: Global Flow

- Fluid visualization and particle tracking velocimetry (PTV).



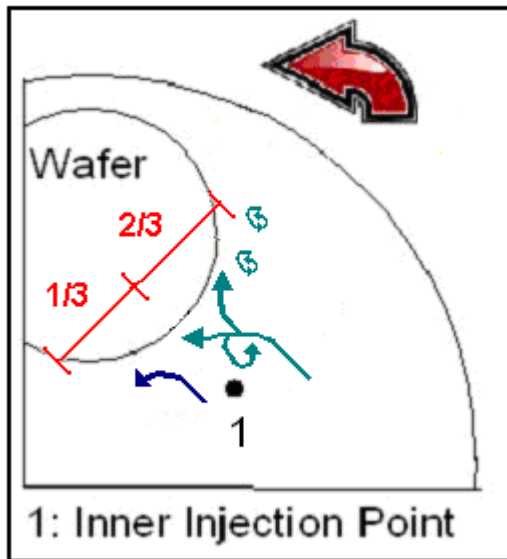
*Example of flow visualization analysis showing observed full-wafer slurry flow on the 75 mm polisher.*

## Questions to be investigated:

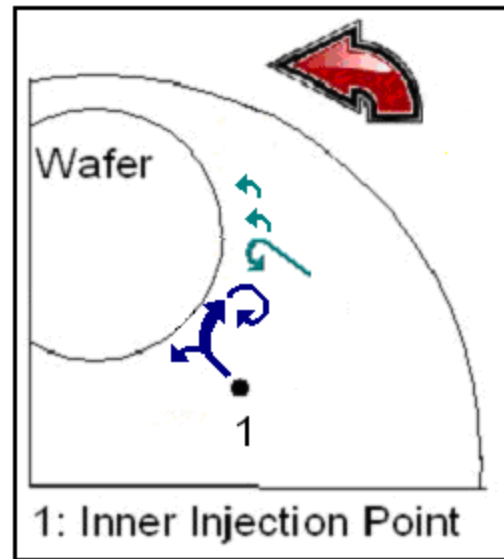
- How does pad grooving affect slurry flow over the entire polishing pad?
- How does asperity distribution on the pad due to pad design and conditioner geometry affect local and global slurry flow patterns?
- Is there a correlation between age of the active slurry and defectivity?
- Is there a correlation between local flow patterns at the wafer and defectivity?
- Can we change the process to reduce slurry waste while maintaining a high quality polish?

# Technical Approach: Global Flow

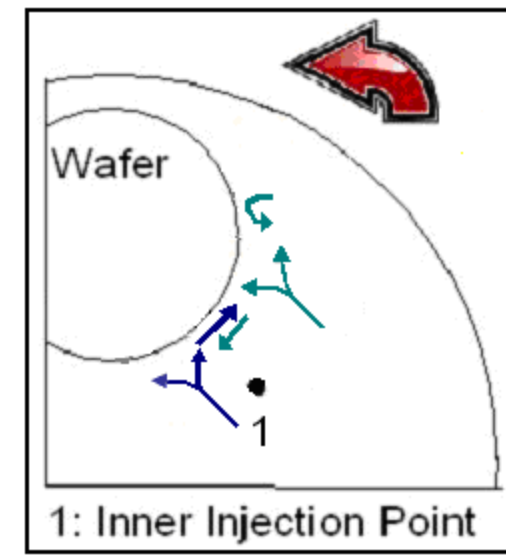
- Initial results using flow visualization show the impact of grooving on global slurry flow patterns.



Ungrooved FX9 pad:  
Old slurry dominates  
wafer bow wave.



XY Grooved FX9 Pad:  
New slurry dominates  
wafer bow wave.



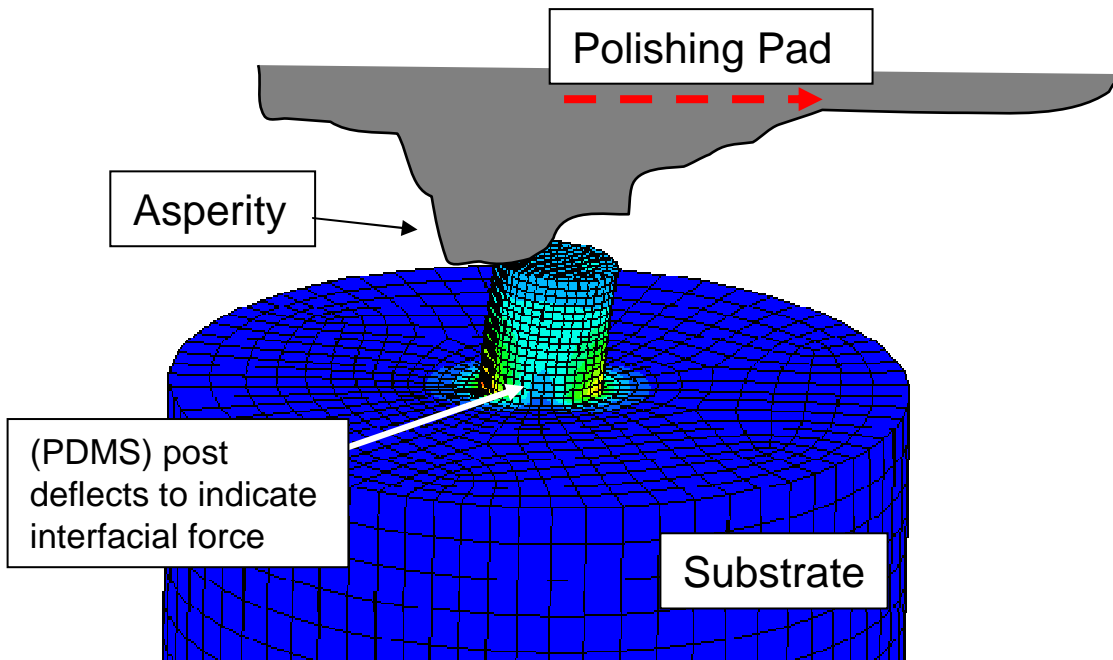
AC Grooved D100 Pad:  
Shearing of old and new  
slurry, mixing at bow wave.

- 1) Proposed: Flow visualization studies over the whole pad surface.
- 2) Proposed: Add particle tracking velocimetry (PTV) to quantify the velocity field.



# Technical Approach : MEMS Sensors

– MEMS lateral force sensors for asperity-level and feature-level forces.



*Diagram of a MEMS shear stress sensor, already demonstrated at Tufts on the 75 mm polisher, and capable of resolving forces in the 10-1000  $\mu\text{N}$  range at 30-100  $\mu\text{m}$  scale.*

Questions to be investigated:

-How does the geometry of patterns at the wafer surface influence microscale shear forces at the pad-wafer interface?

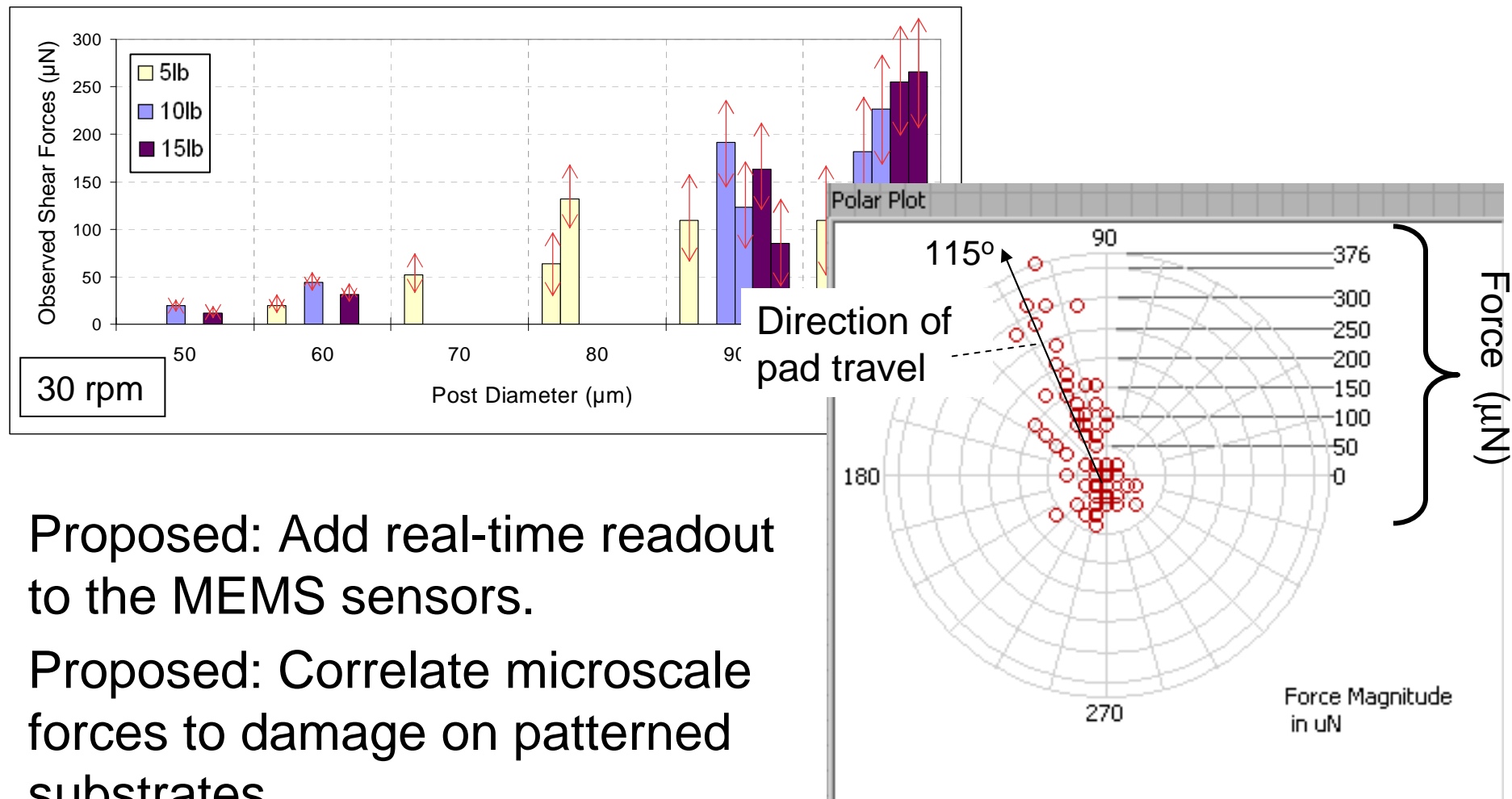
-How do changes in pad and conditioner geometry and material (including grooving) affect microscale shear forces?

-Is there a correlation between microscale shear forces and defectivity of patterned surfaces?

-Can we change the pad and/or conditioner to reduce pad waste while maintaining a high quality polish?

# Technical Approach : MEMS Sensors

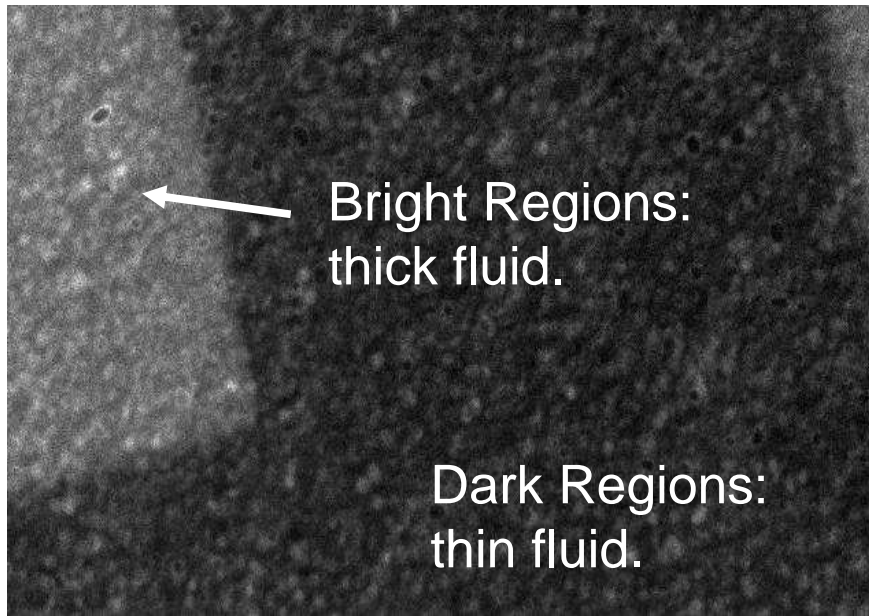
- Initial results show the ability to measure microNewton forces on micron-scale structures.



- 1) Proposed: Add real-time readout to the MEMS sensors.
- 2) Proposed: Correlate microscale forces to damage on patterned substrates.

# Technical Approach: DELIF

- Nanosecond dual enhanced laser induced fluorescence (DELIF) for fluid film thickness and pad-wafer contact.



*Image showing current DELIF capabilities on the 75 mm polisher. This is an image of a square well in a glass wafer during polish.*

## Questions to be investigated:

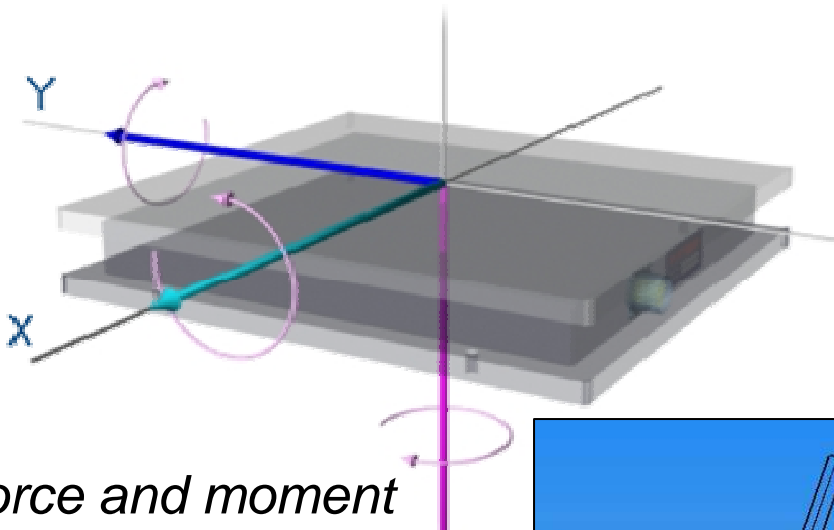
- How does pad-wafer contact/film thickness vary near the edges of a patterned structure on the surface?
- Is there a correlation between contact/film thickness and pad asperity distribution/pad grooving?
- Is there a correlation between contact/film thickness and conditioner geometry?
- Do these mechanisms correlate to observed polish defectivity?
- Can we change the process to maintain quality by reduced consumables?

# Technical Approach: Global Force

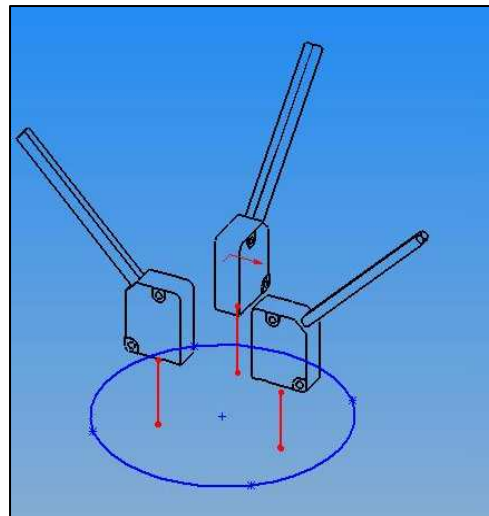
- Global wafer attitude (laser displacement sensors) and wafer-level forces.

## Questions to be investigated:

- How do the coefficient of friction (COF) and the force spectra change with pad type, conditioning, and slurry flow?
- How does the wafer attitude change with pad type, conditioning, and slurry flow?
- Is there a correlation between defectivity and force spectra and/or wafer pitch & roll?
- Can we change the pad, conditioner, and/or slurry flow pattern to reduce waste while maintaining a high quality polish?



*Force and moment plates are used to measure global forces. Three laser displacement sensors measure wafer attitude (pitch & roll) during processing.*



# Leverage

- **Collaborations:**
  - Philipossian: retaining ring fluid mechanics, pad-wafer contact, conditioner activity
  - Boning: modeling of polish of patterned substrates, model validation and providing model parameters
  - Stone (Harvard) and McKinley (MIT): thin film fluid modeling and experimental techniques
  - Paul (Stockton): chemi-mechanical process modeling
- **Experimental Techniques:**
  - DELIF, MEMS sensors, flow visualization, wafer attitude and global force measurement have already been demonstrated on a 75 mm scale model polisher
  - Techniques will be scaled up to a 200 mm polisher.
- **Industry Advisors:**
  - Cabot Microelectronics and Intel served as advisors on our previous project
  - Advanced Diamond is considering partnering by providing experimental conditioner geometries
  - Draper Laboratories has sponsored MS students with projects related to planarization
- **Patterned Substrates:**
  - Patterned substrates will be microfabricated at the Tufts Microfab
  - Tufts Microfab metrology tools will be used for evaluation of planarity on patterned substrates.

# **Biologically Inspired Nano-Manufacturing**

## **(BIN-M): Characterization**

### **PIs:**

- **Anthony Muscat, Chemical and Environmental Engineering, UA**
- **Megan McEvoy, Biochemistry and Molecular Biophysics, BIO5 Institute, UA**
- **Masud Mansuripur, College of Optical Sciences, UA**

### **Graduate Students:**

- **Amber Young, PhD candidate, College of Optical Sciences, UA**
- **Sam Jayakanthan, PhD candidate, Biochemistry and Molecular Biophysics, UA**
- **Shawn Miller, PhD candidate, College of Optical Sciences, UA**
- **Rahul Jain, PhD candidate, Chemical and Environmental Engineering, UA**

### **Undergraduate Student:**

- **Ben Mills, Chemical and Environmental Engineering, UA**

### **Other Researchers:**

- **Zhengtao Deng, Postdoctoral Fellow, ChEE & Optical Sciences, UA**
- **Babak Imangholi, Postdoctoral Fellow, ChEE & Optical Sciences, UA**
- **Gary Fleming, Postdoctoral Fellow, Chemical and Environmental Engineering, UA**

### **Cost Share (other than core ERC funding):**

- **\$825k Science Foundation Arizona, ASM, SEZ, Arizona TRIF**

# Project Objectives

- Minimize costs of materials, energy, and water to fabricate nanoscale devices using bio-based strategy
- Exploit homogeneity, mild reaction conditions, and specificity of active biological molecules
- Grow 3D structures to achieve scalable architecture
- Employ additive, bottom up patterning methods

# ESH Metrics and Impact

Sustainability metrics			
Process	Water l/bit/masking layer	Energy J/bit/masking layer	Materials g/bit/masking layer
Subtractive 32 nm*	$3.3 \times 10^{-10}$	$1.5 \times 10^{-12}$ EUV	$2.9 \times 10^{-16}$
Additive	$3.6 \times 10^{-13}$	$9.2 \times 10^{-17}$	$1.8 \times 10^{-19}$

\*D. Herr, Extending Charge-based Technology to its Ultimate Limits: Selected Research Challenges for Novel Materials and Assembly Methods. Presentation at the NSF/SRC EBSM Engineering Research Center Review Meeting: February 24, 2006.

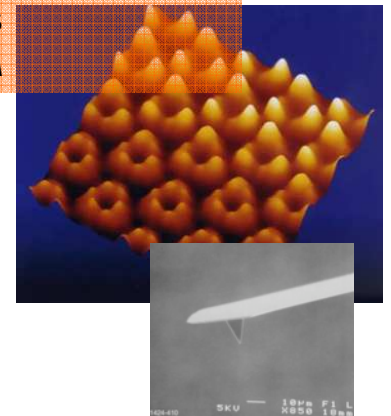


# Process Goal: Deposit Array of Metal Dots

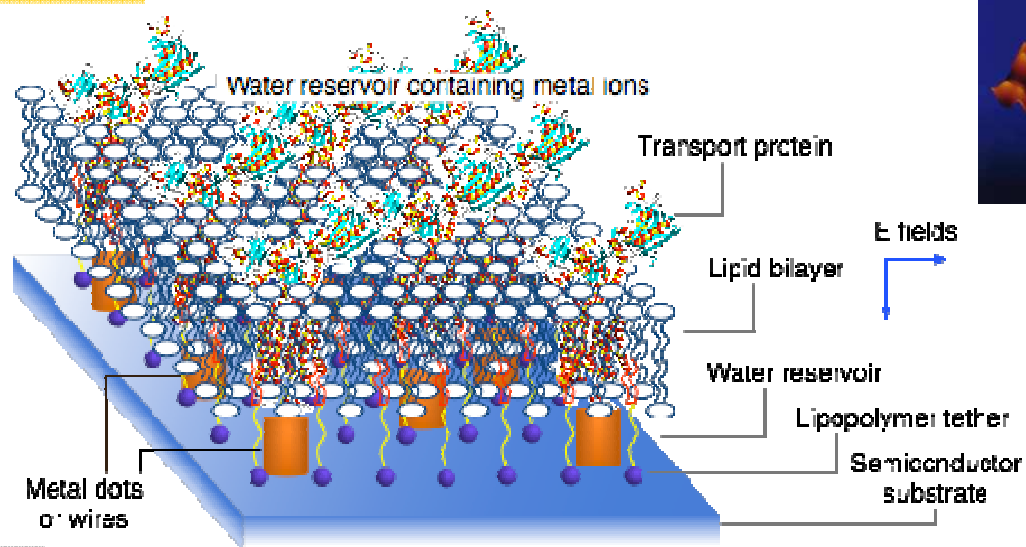
Biochemistry of metal transport proteins  
*Megan McEvoy/UA*



Characterize bio & inorganic structures using scanning probe and optical techniques  
*Masud Mansuripur/UA*



Selective deposition  
*Glen Wilk, Eric Shero, Christophe Pomaredo, Steve Marcus/ASM*



Pattern surfaces and build structures  
*Anthony Muscat/UA*



Semiconductor surface preparation  
*Harald Okorn-Schmidt, Zach Hatcher, Jeremy Klitzke/SEZ*



# Characterization

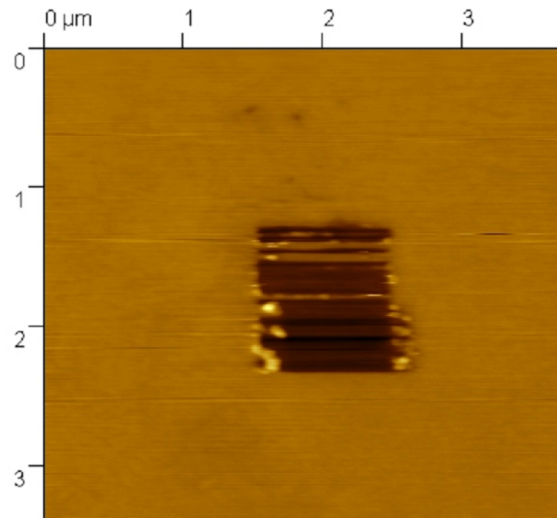
## **Lipid Bilayer**

- **Verify lipid membrane is a bilayer using patchclamp, AFM, impedance measurements and ellipsometry**
- **Examine large area coverage**
- **Investigate surface uniformity**

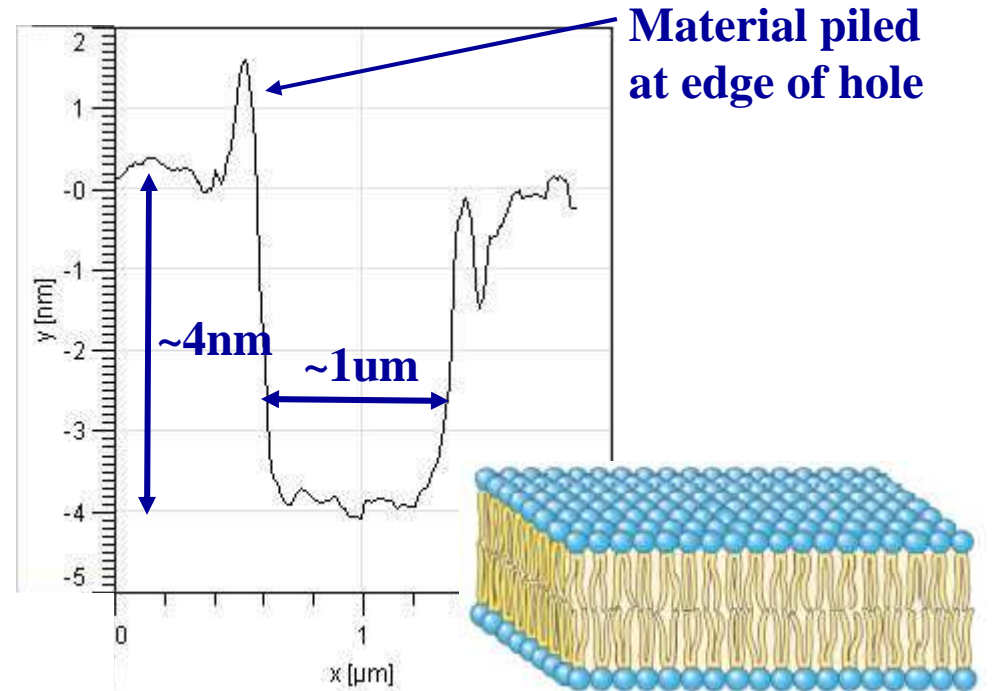
## **Proteins**

- **Explore fluorescence microscopy, fluorescence spectrometry and AFM as tools to characterize quantum-dot-tagged proteins**
- **Determine multi-color resolution of quantum-dot-tagged proteins in a lipid bilayer**

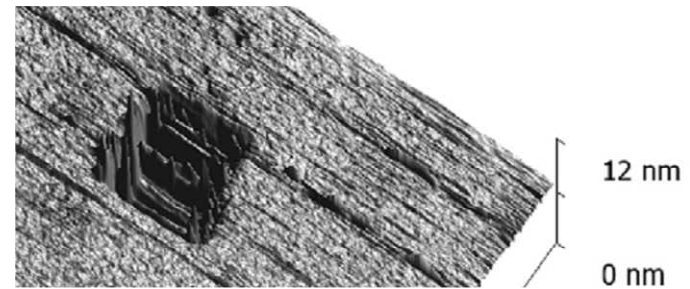
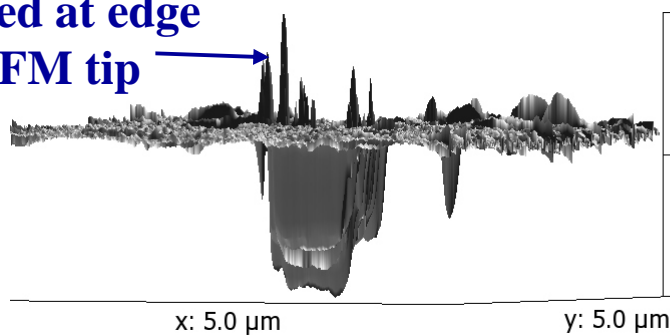
# AFM Characterization of Bilayer



**1 μm square hole dug in lipid membrane. Observe smooth bilayer surface. Note excess material piled at edge of hole.**

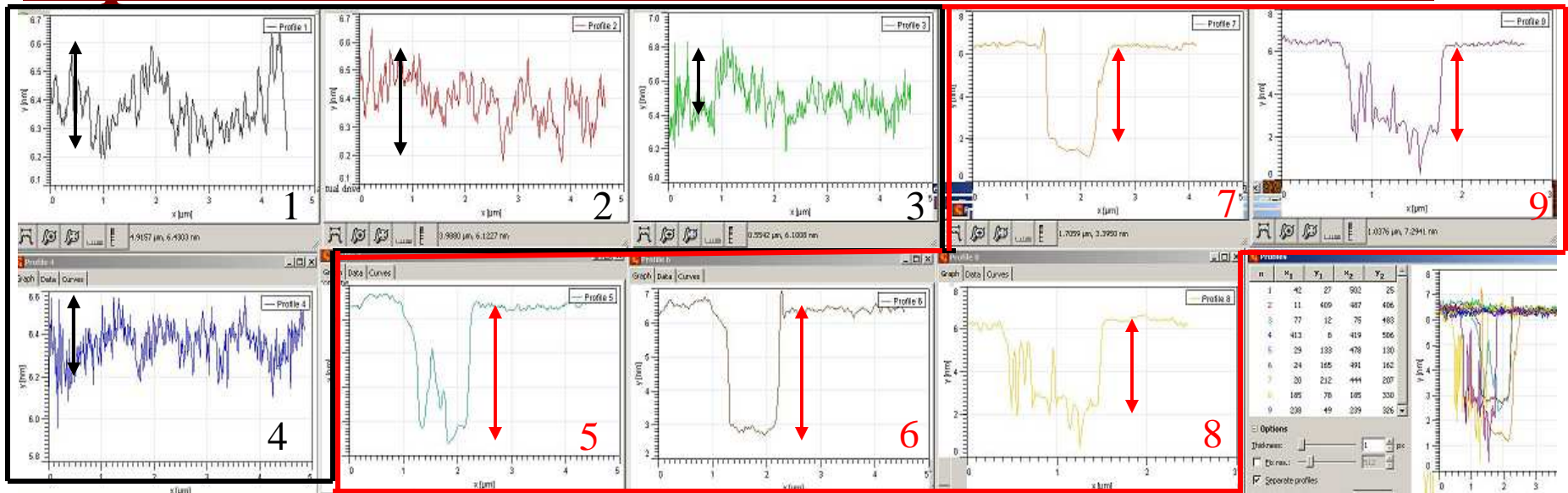


**Material piled at edge of hole by AFM tip**



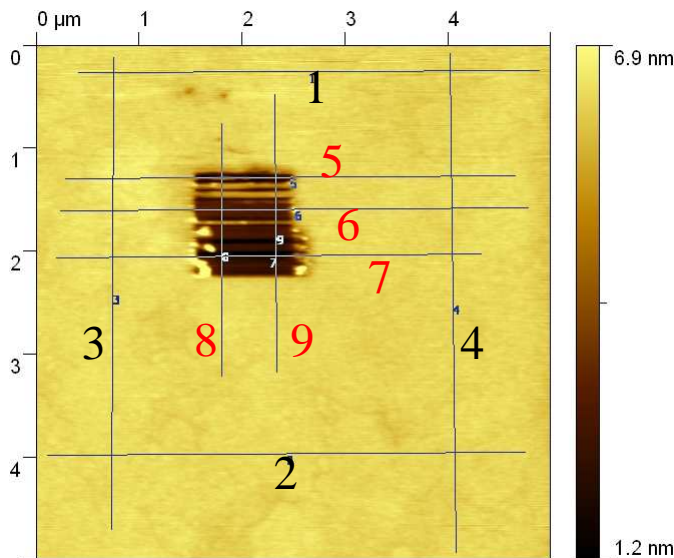
**3D representations of hole dug in bilayer**

# Lipid Membrane Surface Cross-Sections



↕ Represents 0.4nm variation

↕ Represents 4nm variation



## Observations:

- Some material remains in hole, but fairly uniform depth
- 3.5 nm depth is consistent with expected lipid bilayer thickness
- Variation in bilayer surface in regions far from hole  $\leq 0.4\text{nm}$

# Bilayer Electrical Properties

## **Challenge**

- Large area characterization of lipid membrane
- Patch clamp technique is limited to small areas

## **Conventional Solution**

- Impedance spectroscopy on conductive substrates is used to characterize large area lipid membranes
  - Insulating native oxide on the semiconductor impairs impedance measurement
  - Frequency dependence of semiconductor electrical property complicate impedance measurement

## **Our Novel Solution**

- Phase Sensitive Measurements with a Lock-in amplifier

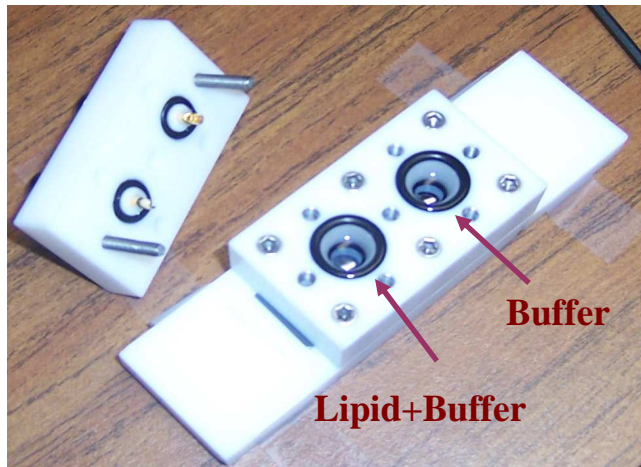
# Phase Sensitive Detection

## Basic Theory

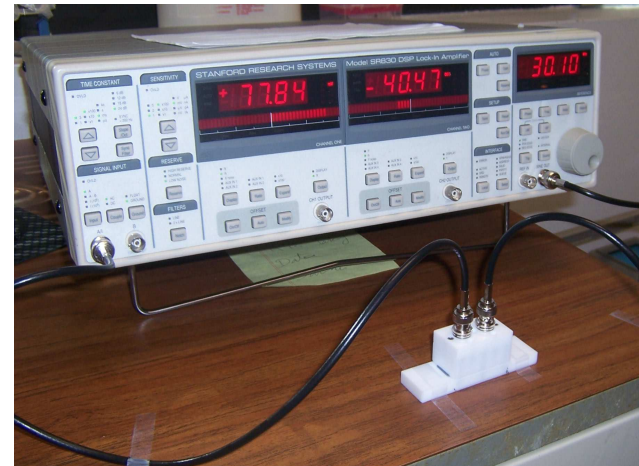
Phase vs. frequency of lipid bilayer is measured independent of semiconductor properties via differential phase measurement

$$\Delta\varphi = -\text{ArcTan}\left[\frac{R_L^2 X_C}{R R_L^2 + (R + R_L) X_C^2}\right]$$

$R_L$  &  $X_C$  represent lipid resistance and impedance,  $R$  is Lock-in input impedance



Test chambers



Labview controlled Lock-in amplifier



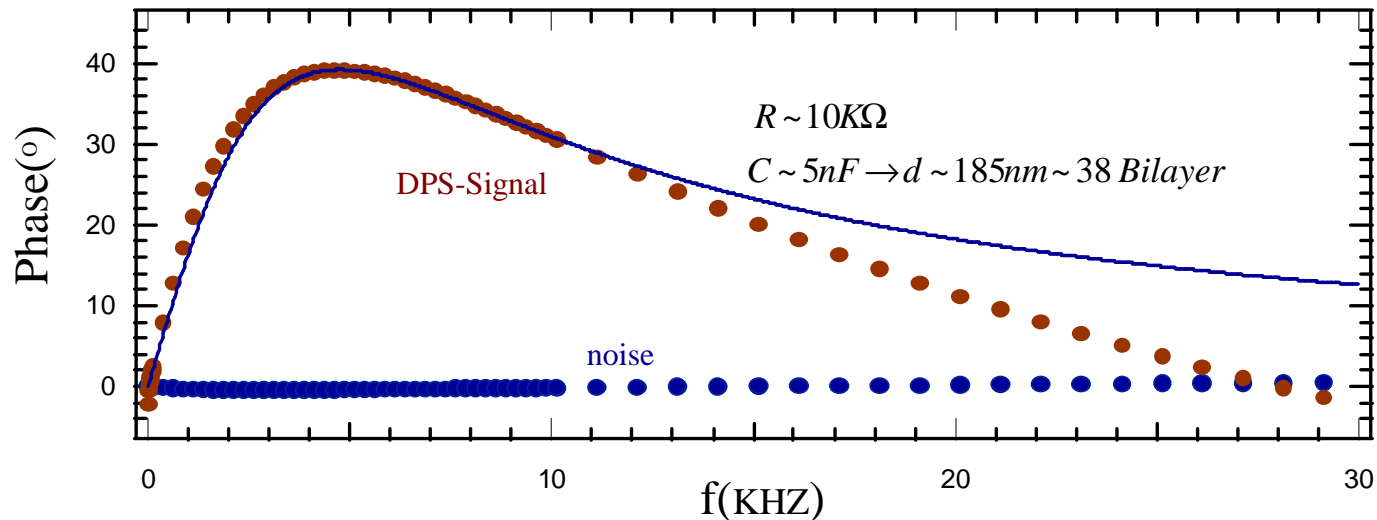
# Data Analysis and Discussion

## Calibration

Lock-in system is calibrated using electronic component

## Measurement

Phase change due to resistance and capacitance of Lipid is measured

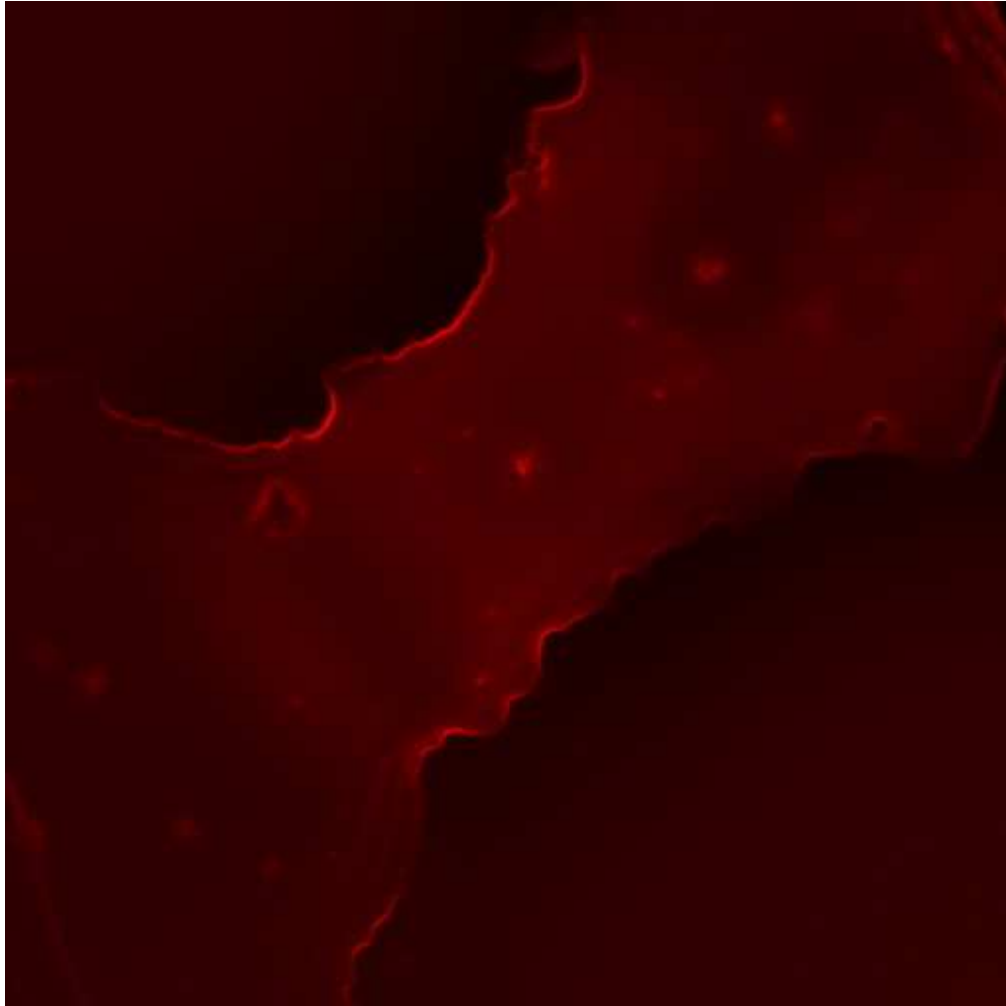


## Goal

Lipid resistance describes impermeability of the lipid membrane

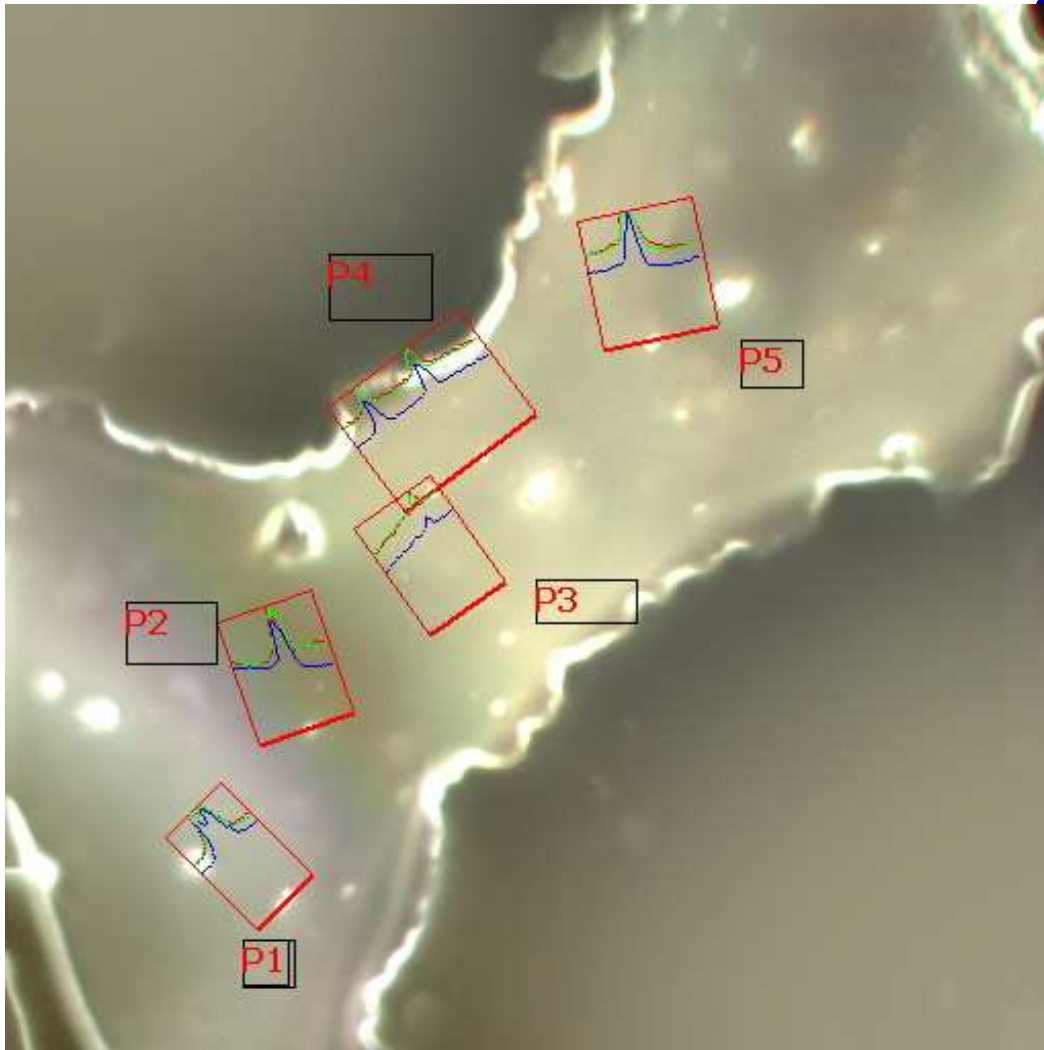
Lipid capacitance describes thickness and uniformity of the Lipid

# Single Filter Fluorescence Image



- **Sample: Red (605nm) and Green (540nm) Quantum dots on glass substrate**
- **Excitation: HBO filtered by 365nm filter with 20nm FWHM**
- **Emission Filter: 525nm**

# Combined Image



**Sample: Red (605nm)  
and Green (540nm)  
Quantum dots on glass  
substrate**

**Excitation: HBO  
filtered by 365nm filter  
with 20nm FWHM**

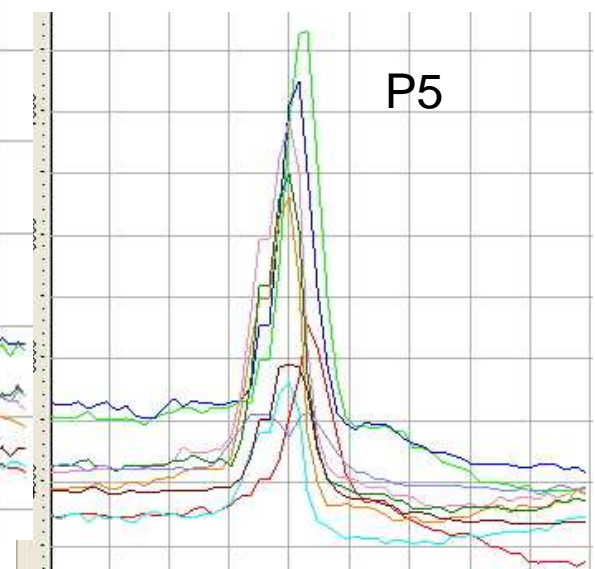
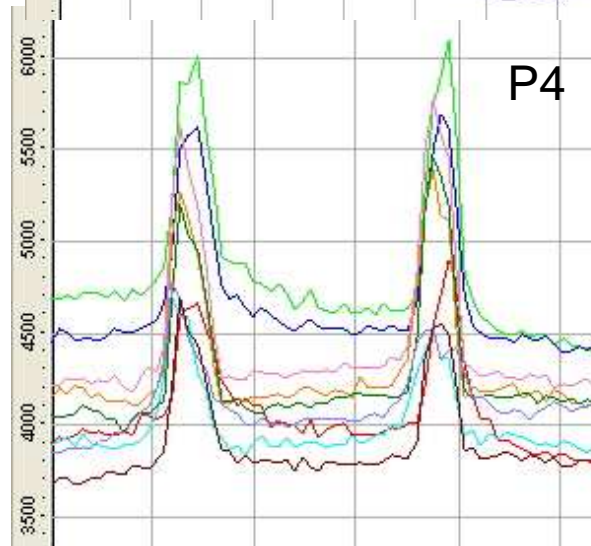
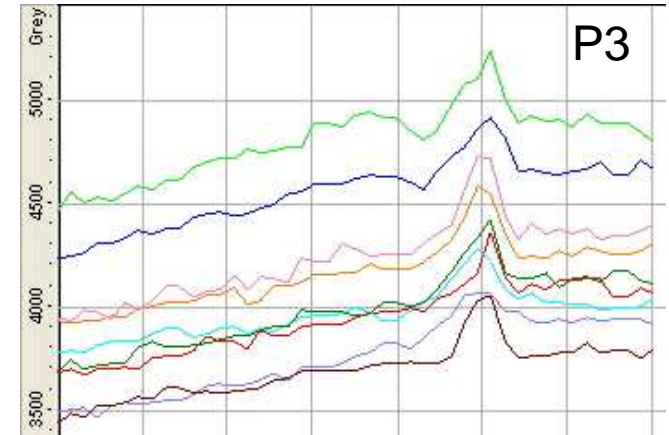
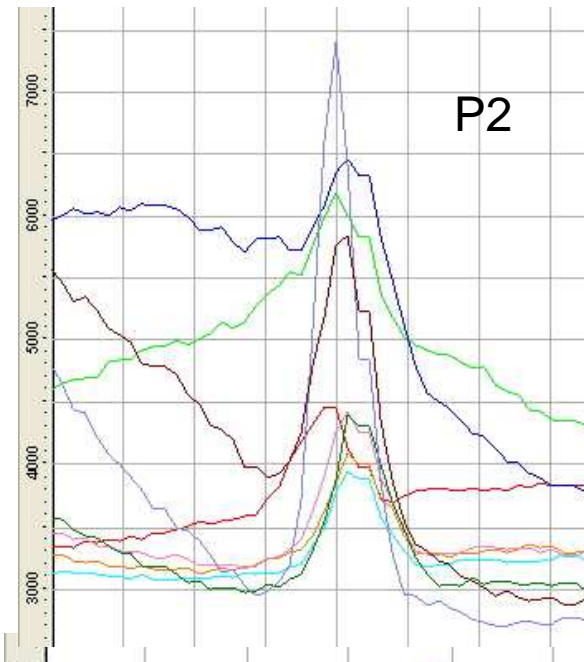
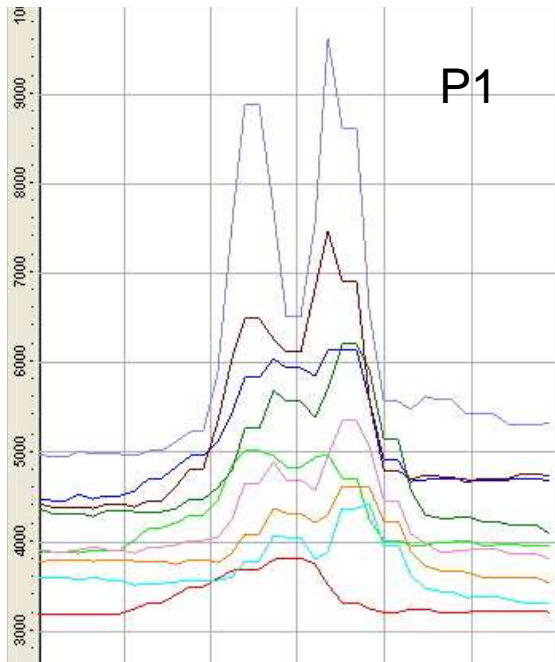
**9 Emission Filters**

- **525, 565, 595, 605,  
655, 705, 755, 800,  
850 nm (20 nm  
FWHM)**

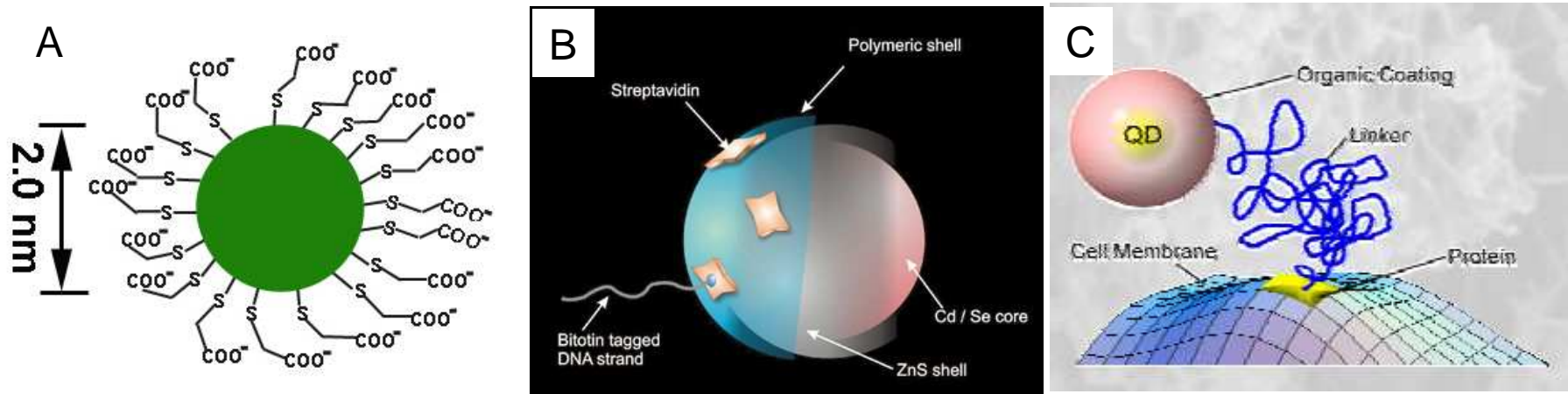
**Profiles drawn across  
points of interest**



# Profiles Referenced on Combined Image

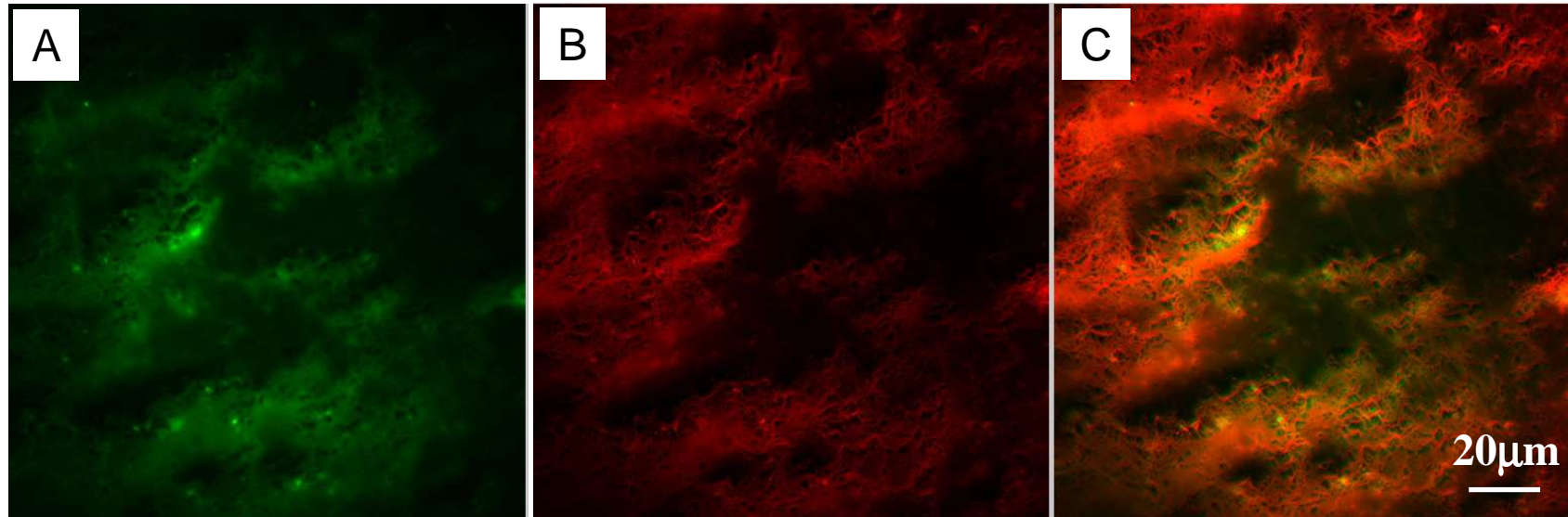


# Imaging of Proteins with Quantum Dots



- (A) Single quantum dot terminated with COOH groups
- (B) Functionalized quantum dot
- (C) Quantum dot attached to protein with linker

# Fluorescent Microscopy Study of Red CdTe QDs Labeled YFP



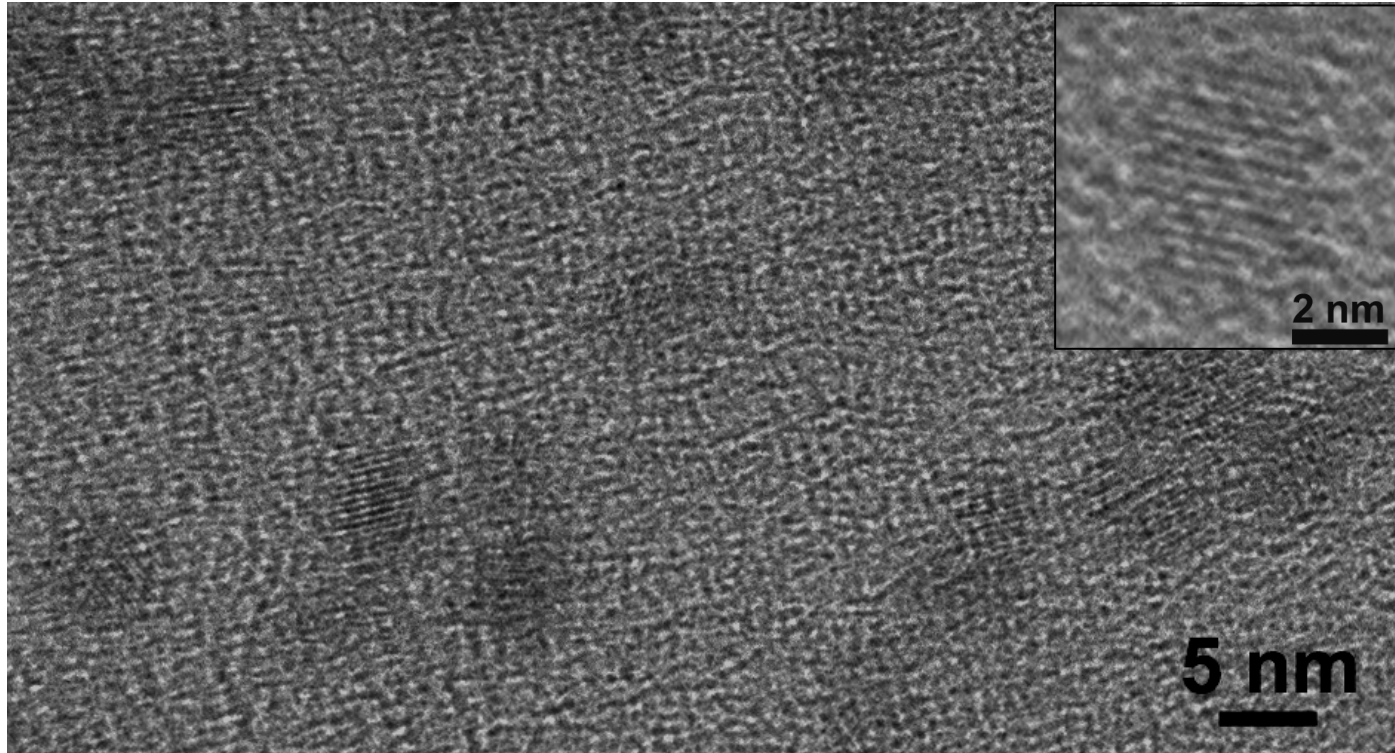
**(A) Image with filter  $525 \pm 10$  nm;**

**(B) Image with filter  $605 \pm 10$  nm;**

**Note: Pure CdTe QDs with emission peak at 600 nm;**  
**(C) Combined image of A and B.**  
**Pure YFP with emission peak at 528 nm**

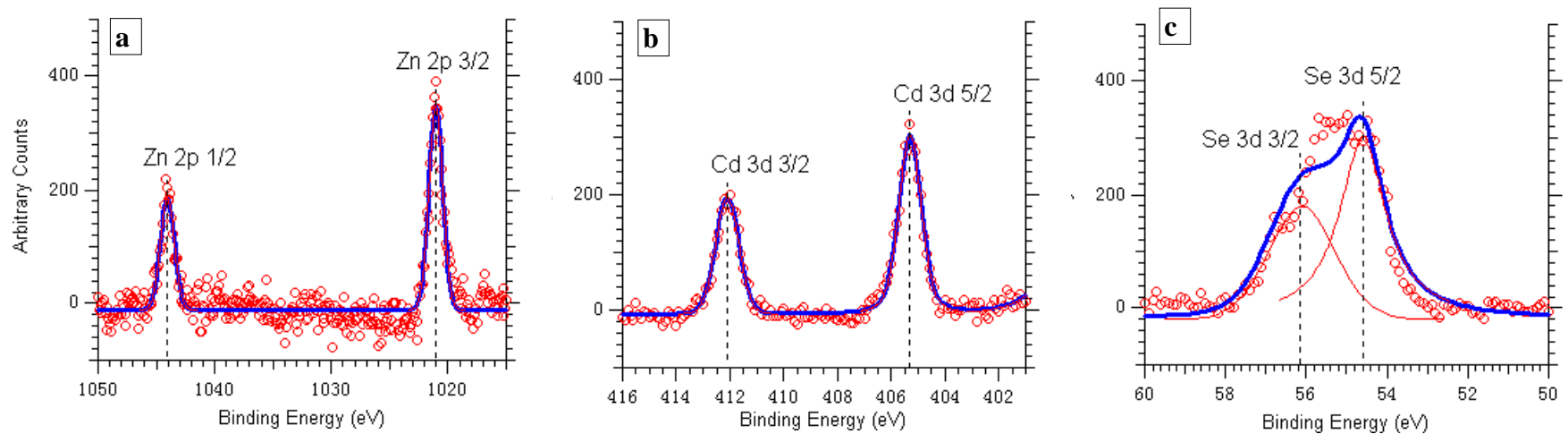


# TEM of QDs



Transmission electron microscopy image of thioglycolic acid capped CdTe quantum dots deposited on TEM grid

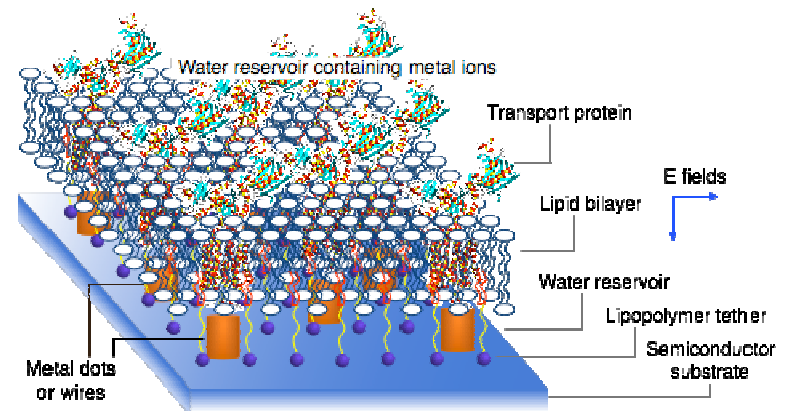
# XPS study of $Zn_xCd_{1-x}Se$ QDs



**High-resolution x-ray photoelectron spectra of  $Zn_xCd_{1-x}Se$  QDs samples with near bandgap emission peak at 490 nm: (a) Zn 2p<sub>3/2</sub> and Zn 2p<sub>1/2</sub> spectral lines; (b) Cd 3d<sub>3/2</sub> and Cd 3d<sub>5/2</sub> spectral lines; (c) Se 3d<sub>5/2</sub> and Se 3d<sub>3/2</sub> spectral lines.**

# Future Characterization Efforts

- Incorporate proteins in lipid bilayer
  - Verify presence of proteins in lipid bilayer with AFM, PSD and other imaging techniques including fluorescence microscopy
- Characterize protein-quantum dot pairs
- Activate and control quantum-dot-tagged-transport proteins in lipid bilayer
- Experiment with additive, bottom up patterning methods using quantum-dot-tagged proteins in lipid bilayer



# **HIGH-DOSE IMPLANT RESIST STRIPPING (HDIS) : ALTERNATIVES TO SUPER- HOT SPM SOLUTIONS**

Srini Raghavan

Materials Science and Engineering

University of Arizona

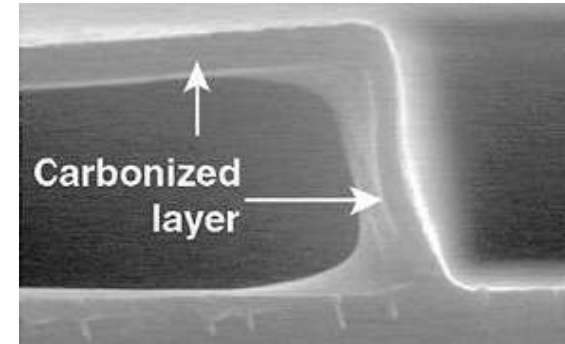
## High Dose, Low Energy Implants Used for Formation of Shallow Junctions

### **ION IMPLANTATION**

**( $> 10^{15}/\text{cm}^2$ )**

### **CREATES A CRUST**

### **LAYER ON RESISTS**



**Courtesy: FSI Intl**

- Crust is *dehydrogenated* resist in the form of amorphous carbon/graphite

➤ An efficient HDIS process needs to clean all resist (carbonized crust as well as underlying resist) and remove residues without causing substrate damage



## HDIS TECHNIQUES USING SPM

- **These techniques rely on making SPM as “hot” as possible ( $\geq 180^{\circ}\text{C}$ ) without losing oxidizing power**
- **Enhanced Sulfuric Acid (ESA) (SEZ)**
  - Hot SPM with proprietary additive
- **VIPR Process (FSI-International)**
  - *‘Freshly’ mixed SPM with catalyst*
- **Modified SPM (high temperature, *freshly mixed*) with Thermal Pretreatment (DNS)**
  - Oxidation power drops off dramatically with time

# ARE WE STUCK WITH SUPER-HOT SPM TO BREAK C-C BONDS IN THE CRUST LAYER?

## HOW DOES SPM WORK?

. Oxidation by  $\text{HSO}_5^-$  (peroxy monosulfate)?

$\text{H}_3\text{O}_2^+$  (hydroperoxonium ion or hydroxyl cation) ?

. Introduction of sulfonic acid groups on the surface amorphous/graphitic carbon crust ? (Note: one strategy for the breakdown/solubilization of carbon nanotubes (CNT) is the introduction of active sulfonic acid groups on the surface)

## ARE THERE SAFER ALTERNATIVES TO VERY HOT SPM?

## TWO REAGENTS HAVE BEEN FOUND USEFUL IN BREAKING DOWN ORGANIC COMPOUNDS IN SOLUTION

### I: **FENTON'S REAGENT**

- . H<sub>2</sub>O<sub>2</sub> plus certain metal ions which can exist in multiple oxidation rates (ex. iron, cobalt, manganese, tin) in bare or chelated form



OH\* is a strong oxidant

- . Typically ambient temperature; pH ~ 4 to 6

.

## II. **CATALYZED HYDROGEN PEROXIDE (CHP) or MODIFIED FENTON'S REAGENT**

- uses much higher concentration (2 to 25%) hydrogen peroxide
- Contains  $\text{OH}^*$  (oxidant),  $\text{HO}_2^*$  ( weak oxidant),  $\text{O}_2^{*-}$  (weak reductant and nucleophile),  $\text{HO}_2^-$  (strong nucleophile)
- Higher peroxide content provides a solvent effect

**Drawback: Rate of oxidation of C-C bonds by Fenton's reagent and CHP is lower than that of hot SPM**

## PROPOSED WORK

### Overall Objective

- Investigate the feasibility of disrupting carbonized crust on deep UV resist layers exposed to high dose ( $> 10^{15}/\text{cm}^2$ ) arsenic ions using **CHP reagents**

### *Specific Tasks and Deliverables*

- *Investigate suitable metal ion- hydrogen peroxide combinations and ratios for “attacking” the crust*
- *Obtain kinetic data with model amorphous carbon and graphite materials*
- *Evaluate the **removal of disrupted layer** and the underlying resist using conventional SPM*

## **INDUSTRIAL MENTORS**

- Joel Barnett, Sematech
- John Marsella, Air Products and Chemicals
- Jeff Butterbaugh, FSI-International

## **PERSONNEL NEEDED**

- . **One graduate (master's) student for two years**